Design, Synthesis and Biological evaluation of Verapamil analogues, Reversed Isoniazids and Hybrid efflux pump inhibitors against *Mycobacterium tuberculosis*

Malkeet Kumar

University of Cape Town

October 2015

Supervisor: Signed by candidate

Student: Signed by candidate

Design, Synthesis and Biological evaluation of Verapamil analogues, Reversed Isoniazids and Hybrid efflux pump inhibitors against *Mycobacterium tuberculosis*

A thesis submitted to the

University of Cape Town

in fulfilment of the requirements for the degree of

Doctor of Philosophy

by

Malkeet Kumar

Supervisor: Professor Kelly Chibale

Department of Chemistry,

University of Cape Town,

South Africa

Declaration

I know the meaning of plagiarism and declare that all of the work in the document, **"Design, synthesis and biological evaluation of verapamil analogues, reversed isoniazids and hybrid efflux pump inhibitors against *Mycobacterium tuberculosis*"**, is my own work and to the best of my knowledge has never been submitted for examination for any degree at any university. All sources of information are cited and fully referenced.

Malkeet Kumar Signed by candidate

Date 2nd October 2015 ……..

Acknowledgement

Firstly, I would like to thank my supervisor, Professor Kelly Chibale, for his assistance, guidance, support and infinite patience throughout my PhD project. The important lesson that he taught me during my PhD is value to the journey. His guidance helped me in acquiring the medicinal chemistry knowledge.

Secondly, I acknowledge the contribution of our collaborators at the University of Cape Town (Associate Professor Digby Warner and Dr. Krupa Naran), Saint Louis University (Dr. Peter Ruminski and Dr. Getahun Abate) and Stellenbosch University (Dr. Andile Ngwane and Prof. Paul van Helden).

Next, I would like to thank past and present members of the UCT Drug discovery and Development Centre (H3D), Chibale MedChem group and the Chemistry Department at UCT. A special thanks to Dr. Kawaljit Singh, Karis Moxley, Peter Cheuka and Shakeela Sayed for helping in my thesis write up and proofreading my drafts. I laud the important role played by Saroja Naicker and Elaine Rutherfoord-Jones, the administrative and support staff in the Department of Chemistry at UCT in making our work environment efficient and enjoyable.

I wish to thank Peter Roberts for recording NMR spectra as well as for training and supporting me in the use of the Varian (300 MHz) and Brucker (400 and 600 MHz) NMR spectrometers. The contribution of Gianpiero Benincasa (LRMS) and the Stellenbosch University MS Unit (HRMS) is also acknowledged.

Finally, I cannot thank enough my family and friends for their emotional support throughout my PhD journey. A special thanks to Dr. Taigh Anderson, Shankari Nair, Gurminder Kaur, Dr. Tzu-Shean Feng, Dr. Richard Gessner, Dr. Diego Gonzalez Cabrera, Dr. Claire Le Manach, and Dr. Tanya Paquet for providing wonderful moments in the lab and at various outings. Colleagues from various groups in the UCT department of chemistry are also thanked for their support and company.

Abstract

Tuberculosis (TB) is one of the major infectious diseases and epidemics in the world. It is responsible for severe morbidity and mortality rates, especially in poor and resource-deficient countries. According to the World Health Organization 2014 report, about one third of the world's population is infected with tuberculosis and about 10-15% is co-infected with HIV, which further complicates the TB epidemic. Tuberculosis claims 2-3 million lives every year and is one of the biggest social and financial burdens on many countries. The disease is treatable but has been hampered by the emergence of drug resistance in the causative bacterium, *Mycobacterium tuberculosis (Mtb)*.

Resistant strains of *Mtb* counter the efficacy of various anti-TB drugs *via* mechanisms that help it overcome the toxic and inhibitory effects of these drugs. These mechanisms include mutation, enzymatic drug degradation, target modification and drug efflux. Drug efflux by efflux pumps (EPs) is one of the major mechanisms responsible for the development of drug tolerance leading to the emergence of drug resistance. These efflux pumps are regulated by the house keeping proteins present in the cell membrane of *Mtb* and perform a pre-existing role of rescuing the *Mtb* from toxic agents. These EPs extrude structurally unrelated compounds from the cell including anti-TB drugs and reduce the drug concentration to sub-inhibitory levels and aid *Mtb* in developing resistance. Therefore, development of antimycobacterials that target EPs and reduce their activity can be a viable strategy to reduce the global TB burden and counter the emergence of resistance.

Many strategies have been used to counter the EP-mediated resistance in *Mtb*. In this study, two strategies were employed: (i) the development of efflux pump inhibitors (EPIs) *via* structural modification of a known efflux pump inhibitor, verapamil (VER), and the development of hybrid efflux pump inhibitors (HEPIs) incorporating a VER motif; and (ii) the development of antimycobacterial agents based on covalent linking or attachment of efflux pump inhibitor moieties to an anti-TB drug. These agents are termed reversed anti-TB agents and are based on isoniazid for this study.

For the development of potential EPIs, various structural modifications were carried out on the VER core structure in order to explore structure activity relationship (SAR) studies (**Figure 1**). Biological screening of synthesized compounds led to the identification of VER analogues with low cytotoxicity, and high potentiating potential. Some VER analogues showed high potentiating effects by exhibiting 4-, 8- and 32-fold reduction in the minimal inhibitory concentration (MIC) of the anti-TB drugs rifampicin (RIF), moxifloxacin (MOX) and bedaquiline (BDQ), respectively, and demonstrated reduced interactions with *Mtb*-specific T-cells relative to VER. The SAR 1 study identified the cyclohexyl substituted analogue **3.13n**, which showed low cytotoxicity against the THP-1 cell lines, *in vitro* potentiation of RIF when used in combination (4-fold reduction in the MIC_{90} of RIF), and increased the susceptibility of *Mtb* towards sub-inhibitory concentrations of RIF and INH in macrophages. The SAR 2 study revealed *N*-benzyl analogues (**3.13h** and **3.17a)** that exhibited potentiating effects on RIF *in vitro*, comparable to verapamil (4-fold reduction in the MIC_{90} of RIF) but at a lower concentration relative to VER. The benzyl analogue **3.13h** also showed lower *ex vivo* cytotoxicity than VER, both individually and in combination with various anti-TB drugs, and exhibited synergistic interaction with RIF. The SAR 3 study demonstrated that variation in the alkyl chain length between the basic nitrogen atom and stereogenic centre of VER was more tolerated than the chain length variation between this nitrogen atom and the dimethoxyphenyl group. The evaluation of frontrunner compounds in the ethidium bromide assay demonstrated that EP inhibition is one of the plausible mechanisms for the potentiating of various anti-TB drugs by VER analogues. A 2-4-fold potentiation of RIF *in vitro* was shown by rigid VER analogues but no significant effect was observed in macrophages and in the EB assay.

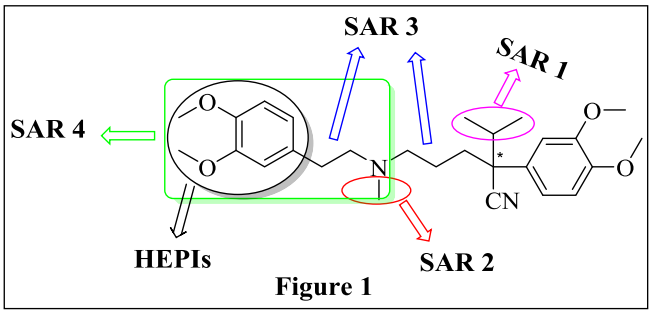

Figure 1

Within the context of HEPIs, a dimethoxyphenyl group of verapamil was replaced with various potential EPI moieties (**Figure 1**). A series of 11 HEPIs was designed and synthesized for biological evaluation. Among the synthesized HEPIs, four compounds (**4.57a**, **4.57b**, **4.59a** and **4.60b**) showed low cytotoxicity ($IC_{20} \geq 25$ µM) and a superior (4-fold) potentiating effect on RIF *in vitro* compared to verapamil. Two HEPIs (**4.59a** and **4.60b**) demonstrated high potency ($MIC_{90} \leq 5$ µM) and a potentiating effect (4-fold) on RIF *in vitro*

at a 100-fold lower concentration than VER. HEPIs **4.59a** and **4.60b** also exhibited a high potentiating effect on sub-inhibitory concentrations of RIF in macrophages along with low cytotoxicity against THP-1 cell lines. The EP inhibitory activity of **4.59a** and **4.60b** was confirmed by the inhibition of EB efflux in the EB assay.

Reversed anti-TB agents based on isoniazid, termed RINHs, were designed by covalently linking the anti-TB drug isoniazid with various potential EPI moieties *via* a three carbon alkyl chain linker (**Figure 2**). A total of 15 RINH agents were designed and synthesized. Antimycobacterial screening revealed that most of the RINHs were potent (MIC ≤ 10 μM) against a drug sensitive strain (H37Rv) of *Mtb* with a good selective index (SI ≥ 10). In addition to phenothiazine-based RINHs (**4.3a**, **4.3b** and **4.17b**), some compounds (**4.46**, **4.49** and **4.53**) containing non-tricyclic EPI moieties also showed excellent potency (MIC ≤ 1.25 μM) against the H37Rv strain of *Mtb*. The screening of potent RINH agents against resistant *Mtb* strains revealed eight compounds (**4.14a**, **4.17b**, **4.23a**, **4.23b**, **4.23c**, **4.46**, **4.49**, and **4.53**) with good to moderate potency (0.625 μM ≤ MIC_{99} ≤ 5 μM) against a low level INH mono-resistant (R5401) strain of *Mtb*. Most of these potent RINHs also exhibited encouraging potency against extremely drug resistant clinical isolates (X_60 and X_61; MIC ≤ 10 μM). The brief SAR study demonstrated the importance of the pyridyl nitrogen atom for antimycobacterial activity *in vitro* and in macrophages. The macrophage evaluation of a selected number of RINH agents also revealed potency against intracellular *Mtb,* while screening in an ethidium bromide assay revealed that RINH agents possess EP inhibitory activity.

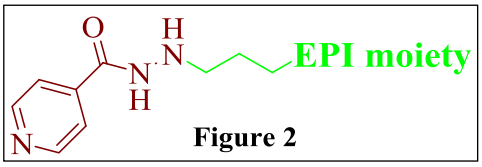

Figure 2

Abbreviations

TB	Tuberculosis
USA	United States of America
HIV	Human Immunodeficiency Virus
Mtb	Mycobacterium tuberculosis
EP	Efflux pump
EPI	Efflux Pump Inhibitor
HEPI	Hybrid Efflux Pump Inhibitor
VER	Verapamil
MIC	Minimum Inhibitory Concentration
RIF	Rifampicin
MOX	Moxifloxacin
BDQ	Bedaquiline
INH	Isoniazid
RINH	Reversed Isoniazid
MTBC	Mycobacterium Tuberculosis Complex
AIDS	Acquired Immune Deficiency Syndrome
WHO	World Health Organization
HBC	High Burden Country
SEAR	South East Asia Region
MDR	Multidrug resistant
XDR	Extremely drug resistant
TDR	Total Drug Resistant
DOT	Direct Observed Treatment
LTB	Latent Tuberculosis
DS-TB	Drug Sensitive Tuberculosis
DR-TB	Drug Resistant Tuberculosis

PZA	Pyrazinamide
ETB	Ethambutol
FQ	Fluoroquinolone
DNA	Deoxyribonucleic acid
CFZ	Clofazimine
FDA	Food and Drug Administration
BTZ	Benzothiazinones
ATP	Adenosine Triphosphate
ABC	ATP-Binding Cassette
RNA	Ribonucleic Acid
PDE-Is	Phosphodiesterase Inhibitors
QBP	Quinolone Binding Pocket
TET	Tetracycline
MFS	Major Facilitator Superfamily
MATE	Multidrug And Toxic compounds Extrusion family
SMR	Small Multidrug Resistance family
RND	Resistance Nodulation Division
PMF	Proton Motive Force
EB	Ethidium Bromide
CIP	Ciprofloxacin
CPZ	Chlorpromazine
THZ	Thioridazine
FICI	Fractional Inhibitory Concentration Index
FIC	Fractional Inhibitory Concentration
CCCP	Carbonyl Cyanide *m*-Chlorophenyl Hydrazone
TIM	Timcodar

DOX	Doxorubicin
CYPs	Cytochrome P450s
RATA	Reversed anti-TB Agents
RCQ	Reversed Chloroquine
CQ^S	Chloroquine sensitive
CQ^R	Chloroquine resistant
RAs	Reversal Agents
CNS	Central Nervous System
LDA	Lithium Diisopropyl Amide
n-BuLi	*n*-Butyl Lithium
TFA	Trifluoroacetic acid
DCE	Dichloroethane
DMF	Dimethylformamide
MS	Mass Spectroscopy
HPLC	High Performance Liquid Chromatography
NMR	Nuclear Magnetic Resonance
EC-ESI/MS	Electrochemical oxidation online with Electrospray Mass Spectrometry
DME	Dimethoxyethane
DBU	1,8-Diazabicyclo[5.4.0]undec-7-ene
NBS	N–Bromosuccinimide
LC	Liquid Chromatography
THF	Tetrahydrofuran
DMSO	Dimethylsulfoxide

DCM	Dichloromethane
ppm	Parts per million
SAR	Structure Activity Relationship
SI	Selectivity Index
TLC	Thin Layer Chromatography
UCT	University of Cape Town
SLU	Saint Louis University
MABA	Microplate Alamar Blue Assay
CFSE	Carboxyfluorescein Succinimidyl Ester
PBMC	Peripheral Blood Mononuclear Cells
BCG	Bacillus Chalmette Guerin
MFI	Mean Fluorescence Intensity
s	Singlet
d	Doublet
t	Triplet
dd	Doublet of doublets
td	Triplet of doublets
q	Quadruplet
quin	Quintet
br	Broad

Table of content

Chapter 1: Introduction

1.1 Chapter overview

This chapter introduces tuberculosis (TB) with respect to epidemiology, geographical distribution, and chemotherapy. Thereafter, it continues with the classification of anti-Tuberculosis drugs followed by a brief discussion on the associated main drug targets as well as the development of drug resistance.

1.2 Tuberculosis

Tuberculosis (TB) is a disease caused by the pathogen *Mycobacterium tuberculosis (Mtb),* which was discovered by Robert Koch in 1882. This pathogen belongs to the genus Mycobacterium, which consists of 85 species of which, only five (*M. tuberculosis, M. bovis, M. africanum, M. microtti, and M. canetti*) commonly infect humans. These bacteria are collectively referred to as *Mycobacterium tuberculosis* complex (MTBC). The word *Mycobacterium* is derived from two words, Myo and bacterium, where Myo is a Greek word meaning fungus and refers to the fashion in which *Mtb* grows when cultured on the surface of a liquid (**Figure 1.1**). The bacteria have a unique waxy cell wall coating consisting of mycolic acids, which allows the bacteria to stay dormant for extended periods of time. Tuberculosis is a contagious and airborne disease mostly affecting women and children.[1]

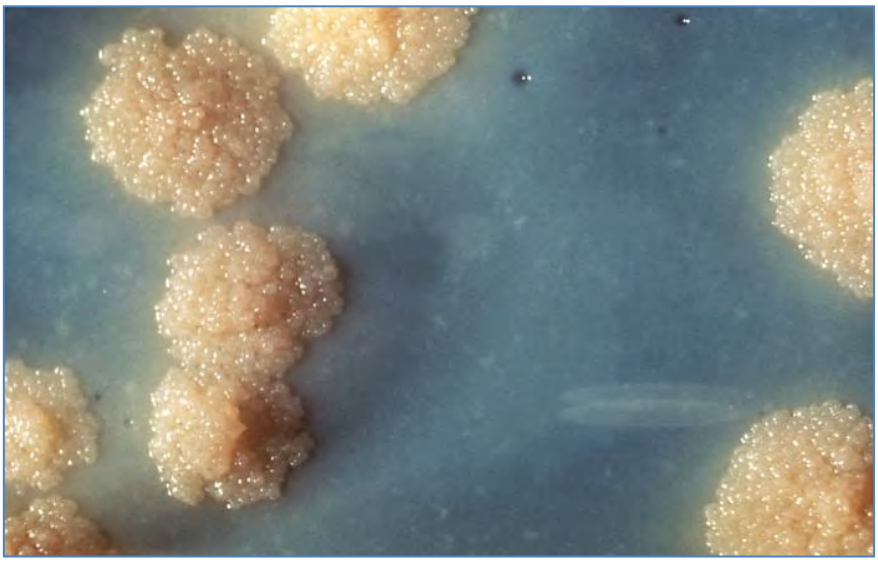

Figure 1.1: The foam like growth pattern of *M. tuberculosis*.[2]

1.3 Epidemiology of tuberculosis

Tuberculosis is one of the major epidemics causing morbidity and mortality in the world. TB is second only to Acquired Immune Deficiency Syndrome (AIDS) as the greatest killer worldwide. The origin of TB has been traced to ancient times dating back to about 3 million years ago.[3] This disease has claimed millions of lives especially in the early 18th and 19th century in Europe and North America. In the early 19th century, TB was known as the white plague and was said to be "the captain of all men of death". The severity of TB has continued with 9 million people getting infected and 1.5 million dying in 2014.[4] TB mainly affects the lungs but can also affect other parts of the body.[5]

1.4 Stages of *Mtb* infection

TB is considered a disease of the poor and is more severe in densely populated areas where hygiene standards are low, with 95% of the cases occurring in poor and developing countries.[4] It has been reported that one third of the world's population is infected with *Mtb*. However, only a small portion (5-10%) with weakened immune systems suffer from active TB (**Figure 1.2**).[6] The pathogen cannot be spread by people infected with latent TB as only the active form is contagious.

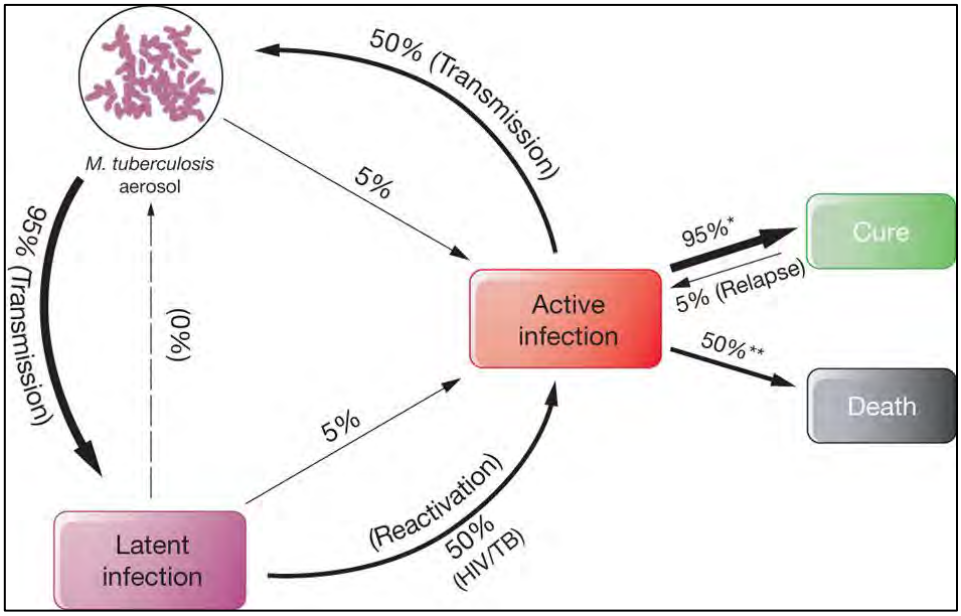

Figure1.2: Stages of *Mtb* infection.[7]

The synergy of TB with Human Immunodeficiency Virus (HIV) infections makes patients 15 times more susceptible to active TB compared to healthy individuals. This is due to the decrease in the CD4 cell count of these patients, which are responsible for signal responses of the immune system (**Figure 1.2**). As shown in **Figure 1.2**, drug susceptible TB can be treated

with an estimated 95% of patients recovering with a 5% possibility of a relapse (denoted by single asterisk) while untreated patients have a high mortality rate.

1.5 Global distribution of tuberculosis

The global distribution of TB is testimony to the above statements as it is more severe in developing and under developed countries (**Figure 1.3**, green regions, consultation countries, 89% of estimated TB cases)**.** According to the 2014 WHO global TB report, there were an estimated 11 million (uncertainty range 9-13 millions) prevalence cases and 9 million (uncertainty range 7-9 millions) incidences in 2013. The average prevalence per 100 000 sample population was 159, which is likely to be greater in high burden countries (HBCs) like India, China and African countries.

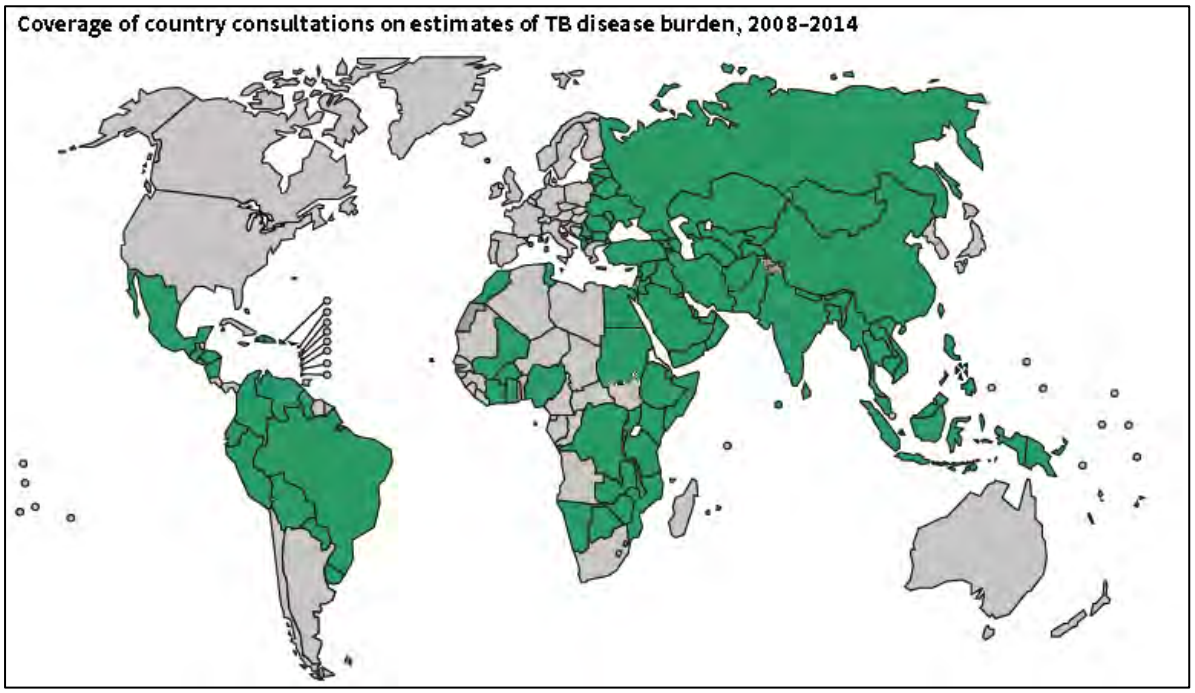

Figure 1.3: The Global distribution of TB, 2008-2014 (green regions, consultation countries, 89% of estimated TB cases).[4]

The South East Asia Region (SEAR) and western pacific regions accounted for the highest incidents (56% of the total TB cases in 2013) (**Figure 1.4**). On the other hand, India and China alone accounted for 35% of the new TB cases in 2013. Of the 9 million incident cases in 2013, women and children accounted for 37% and 6% cases, respectively. The six countries with the highest number of reported incidences in 2013 were India (2.0-2.3 million), China (0.9-1.1 million), Nigeria (340-880 thousand), Pakistan (370-650 thousand), Indonesia (410-520 thousand) and South Africa (410-520 thousand). The underdeveloped African region had one quarter of TB cases in 2013.

Of the 9 million incident cases in 2013, 1.2 million (approximately 13%) were co-infected with HIV. HIV co-infected patients are three times more likely to succumb to this disease compared to their HIV negative counterparts (11.4% versus 3.4%).[4] The synergy of *Mtb* and HIV reduce immunological responses and results in death if untreated.[8] A total of 1.5 million deaths were reported in 2013 with 360 thousand occurring in the HIV positive population. Of the 1.5 million deaths in 2013, 0.5 million were women. The co-infection of TB with HIV has increased the mortality rate among women and children in Africa and the SEAR. Approximately 70% of these deaths occur in the SEAR and Africa where the majority affected are women and children aged between 15 and 44 years. Nigeria and India alone accounted for one third of global mortality.

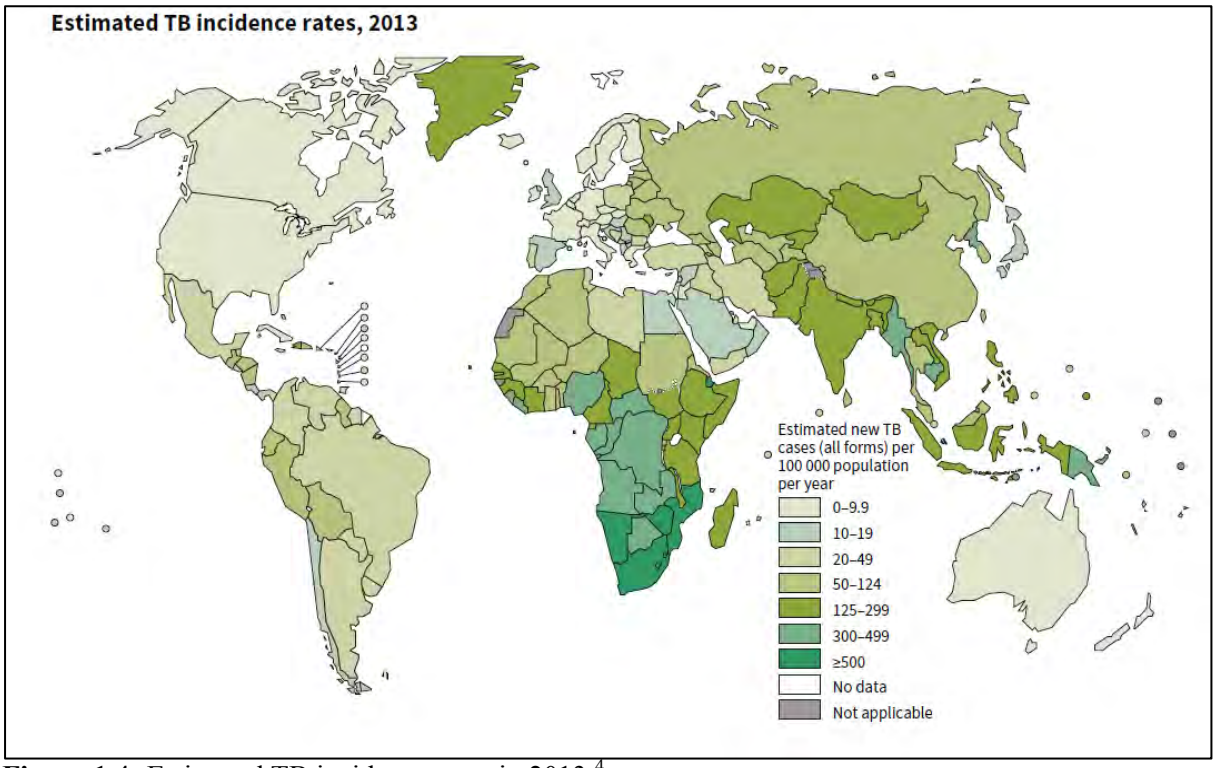

Figure 1.4: Estimated TB incidence rates in 2013.[4]

1.6 The role of drug resistance in TB epidemiology

HIV is not the only factor amplifying the TB epidemic. The development of resistance by *Mtb* leading to multidrug resistant TB (MDR-TB) and extremely drug resistant TB (XDR-TB) are upcoming challenges, which are threatening to destabilize control of this disease.[9,10] Current regimen guidelines recommend at least 20 months of treatment. However, such regimens are toxic, poorly tolerated, and inadequately effective, with cure rates as low as 36% and default rates as high as 50%.[11]

MDR-TB:- This is an infection caused by *Mtb* strains that have developed resistance to at least two of the most important first-line anti-TB drugs, rifampicin (RIF) and isoniazid (INH).

XDR-TB:- This is a less common form of drug resistant TB where *Mtb* becomes resistant to first line anti-TB drugs, INH and RIF, as well as drugs used for the treatment of MDR-TB i.e. second-line drugs including any fluoroquinolone, and at least one of the other three injectable anti-TB drugs amikacin, kanamycin, or capreomycin.[12,13] Recently few patients with resistance to a wider range of drugs have been reported with their infection termed as total drug resistant tuberculosis (TDR-TB).[14, 15]

The main factors favouring infection with these resistant strains are contact with infected patients, inhalation of M/XDR bacteria, and relapse of the TB treatment.[15] On the basis of reliable data available from 194 countries on MDR-TB, in 2011 there were an estimated 3.5% of new TB cases and 20.5% of old TB cases of MDR-TB. XDR-TB was recorded from 100 countries, on average 9% (uncertainty range 6.7 to 11.2%) of MDR cases were XDR-TB.[4] These resistant forms of TB are more fatal and challenging to treat. The inadequate facilities for diagnosis coupled with expensive and lengthy treatment durations make the situation worse.[16,17] In addition, these expensive treatments are at times not available at the required places.

1.7 Treatment of Tuberculosis

The initial treatment was launched in 1946 using streptomycin (STP).[18] The wonder drug isoniazid (INH) was introduced in treatment of TB in 1952 and proved to be a breakthrough in TB treatment. It has a very low minimum inhibitory concentration (MIC) and low toxicity. This drug helped in circumventing resistance to treatment by streptomycin and resulted in reduction of the dose required when used in combination therapy.[19,20]

The main objectives of TB treatment are to:

(i) Reduce TB mortality rate.
(ii) Minimise cases of relapse.
(iii) Block transmission of TB.
(iv) Prevent development of acquired resistance.

1.7.1 Tuberculosis Chemotherapy

Initial TB treatment was 18 months long using a drug regimen composed of anti-TB drugs, STP, INH and *para*-aminosalicylic acid.[21] Over time, various drugs have been developed and used in TB treatment. The main aim was to shorten the treatment duration and achieve efficacious treatment.[22] The current chemotherapy is administered as direct observed treatment (DOT) and has been divided into two phases, an intensive phase and a continuation phase. The intensive phase is the initial phase of two months where bacteria grows at a very high rate and are treated with a combination of rifampicin, isoniazid and pyrazinamide in combination with either ethambutol or streptomycin (**Figure 1.5**).

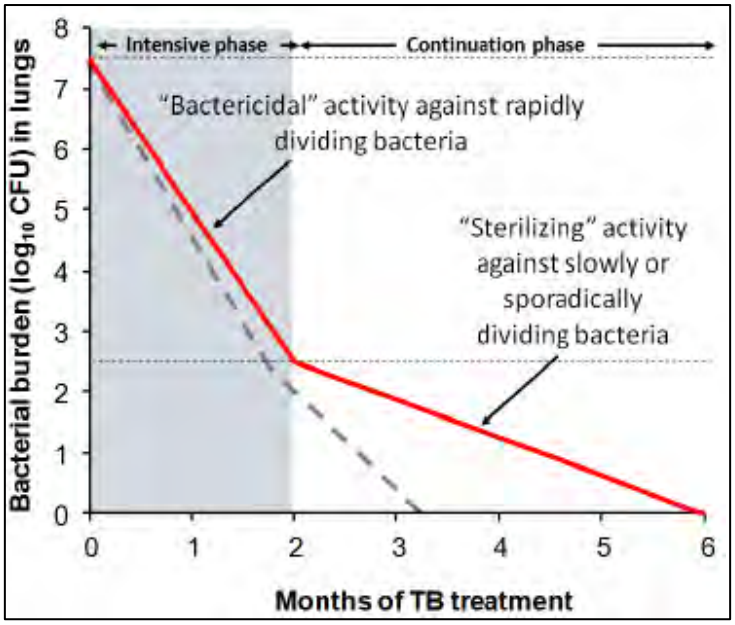

Figure 1.5: Mode of TB treatment.[23]

The second phase is a continuous phase of four months, where bacilli are in slow growing persister form (**Figure 1.5**), with a combination of rifampicin and isoniazid.[24–26] The actively multiplying bacteria are killed very quickly by the initial treatment phase. However, slow multiplying bacilli require longer treatment phases to eliminate all bacteria, which can require up to 6 months of treatment.

1.7.2 Challenges in Tuberculosis Chemotherapy

The treatment of tuberculosis faces many challenges even with the availability of many drugs in the drug armamentarium. The lengthy duration and complexity of treatment leads to high rates of relapse followed by failure of treatment.[27] Sometimes medical facilities are remote, inadequate, and too expensive for patients leading to high mortality rates, relapse of treatment, and development of resistant forms of *Mtb*.[28,29]

Development of resistance is one of the major challenges in the TB eradication campaign. The M/XDR-TB requires second line anti-TB drugs, which are less efficacious, more toxic, expensive and require longer periods of administration compared to first line anti-TB drugs.[30] The demand far outweighs the supply of these drugs, which makes availability a big problem particularly in poorer countries. These deficiencies result in high prevalence of resistant TB cases and higher mortality rates.[4]

The co-infection of HIV and TB poses a serious challenge causing high mortality rates.[4,31] The treatment of HIV-TB co-infections suffers from serious diagnostic and therapeutic shortcomings. These include drug-drug interactions, high pill burden causing adherence problems, toxicity overlap of anti-TB and antiviral drugs as well as immune reconstruction risk.[8,28,32]

Active tuberculosis results from activation of latent forms of tuberculosis (LTB) in most cases. Hence chemotherapeutic treatment of LTB may reduce the probability of reactivation and development of active TB. The current treatment method involves the use of INH over a period of 9 months where it has been noted that this course of treatment has a low success rate. The development of drugs against LTB, which have high efficacy, low toxicity and a shorter duration of treatment, will increase the success rate. This will play a very important role in the eradication of TB.[33,34]

In light of these challenges and requirements, new drugs are required with the following characteristics:[35]

(i) Shorter and simpler treatment
(ii) More effective, less toxic and less expensive drugs for resistant TB
(iii) No drug-drugs interactions.
(iv) Potent against latent and non-replicating *Mtb.*

1.8 Classification of anti-TB drugs

There are more than twenty anti-TB drugs, which are available for the treatment of infected individuals. These drugs have been categorized on the basis of their mode of administration, efficacy, potency, their use as line of defence, structural identity and past experiences during their use.[36] The groups are as follows:

Group 1. Oral: isoniazid, pyrazinamide, ethambutol, rifampicin/rifampin, rifapentine or rifabutin.

Group 2. Injectable aminoglycosides: kanamycin**,** streptomycin, amikacin, injectable poly-peptides: capreomycin, viomycin.

Group 3. Oral and injectable fluoroquinolones: ciprofloxacin, levofloxacin, moxifloxacin,ofloxacin, gatifloxacin.

Group 4. Oral: para-aminosalicylic acid, D-cycloserine, terizidone, ethionamide, prothionamide, thioacetazone.

Group 5. Clofazimine, linezolid, amoxicillin plus clavulanate, imipenem plus cilastatin (Ipm/Cln), clarithromycin.

1.8.1 First line anti-TB drugs

The first line anti-TB drugs are used as a front line defence against *Mtb* and employed for the treatment of drug sensitive tuberculosis (DS-TB). These mainly consist of group 1 drugs and streptomycin from group 2 and are administered orally except streptomycin, which is administered intravenously. These drugs were discovered during the 1950s and 60s and used for initial confrontation of TB, were very efficacious and proved to be an asset for TB patients. These were used as combination regimens for 6 months and showed greater than 95% cure rate when administered under DOT for DS-TB.[37]

Isoniazid (INH) (**Figure 1.7**) is one the most active drugs in current use. It was discovered in 1946. INH is bactericidal against fast replicating and bacteriostatic to slow-replicating *Mtb*, also known as persisters, hence included in the 6 months DOTs chemotherapy.[22] INH is a prodrug and is activated by a peroxidase enzyme KatG of *Mtb*, which converts INH to its active form, nicotinic acid, nitric radical (NO) along with different active species (**Figure 1.6**).[38,39] It acts on *Mtb* by inhibiting mycolyic acid, an important component in cell wall synthesis.[40]

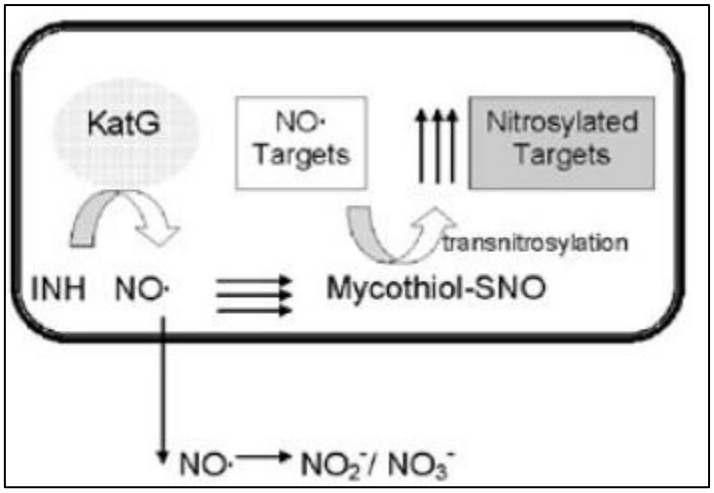

Figure1.6: Interaction of NO with mycothiol.[39]

One of its mechanisms of action is the interaction of the INH activated product with mycothiol of *Mtb* to produce *S*-nitromycothiol, which in turn affects the biosynthesis of many intracellular molecules (**Figure 1.6**). In the absence of mycothiol, NO gets effluxed and quenched in the medium to the corresponding nitrate or nitrite anion. One side effect due to overdose of INH is peripheral neuritis as it leads to quantitative reduction in vitamin B6 through urine excretions.[41,42]

Pyrazinamide (PZA) (**Figure 1.7**) is another important member of DOTS chemotherapy. PZA is also a prodrug and is activated by the enzyme pyrazinamidase coded by the pncA gene of *Mtb* into its active form pyrazinoic acid. PZA shortened the complex chemotherapy from nine months to six months when added to the drug regimen in the 1980s.[43] PZA accumulates in *Mtb* by disrupting the energetics and membrane transport leading to bactericidal activity. Its potency against non-replicating bacteria has added an advantage to chemotherapy leading to the shortening of treatment duration.[44] The combination of PZA with rifampicin can also be used for treatment of persisters and latent TB.[45]

Ethambutol (ETB) (**Figure 1.7**) is another important member of current chemotherapy. It is bactericidal against fast multiplying *Mtb* but bacteriostatic against slow growing bacilli. ETB targets the cell wall synthesis of *Mtb* similar to INH. However, it does so *via* a different mechanism. ETB disturbs biosynthesis of arabinogalactan by targeting arabinosyl transferase, which is responsible for arabinogalactan biosynthesis, an essential requirement for cell wall synthesis.[46,47] The synergy with other frontline drugs and low toxicity of ETB makes it a suitable candidate as a member of first line chemotherapy.

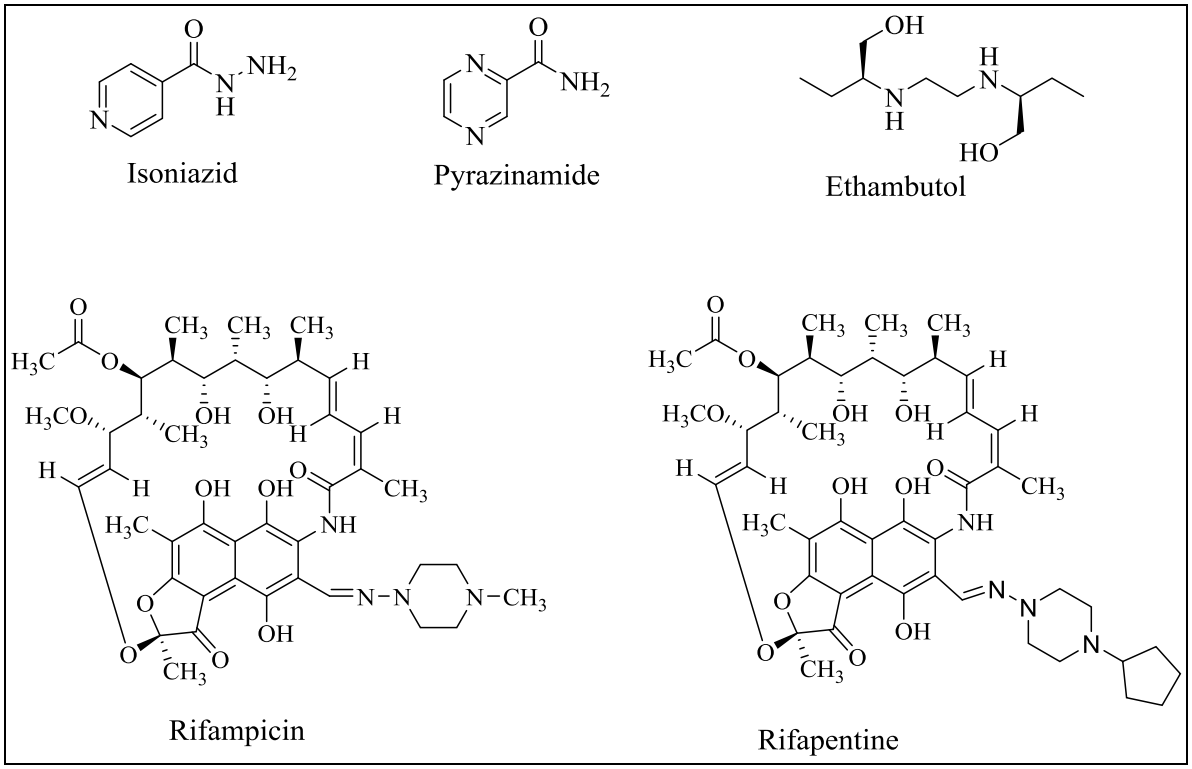

Figure 1.7: First line anti-TB drugs.

Another cornerstone of the front line drug regimen is rifampicin (RIF) (**Figure 1.7**).[48] RIF is the most potent sterilizing agent in DOTs and keeps on killing the persisters throughout the course of chemotherapy.[49] The inclusion of the highly potent RIF in DOTS reduced the dose frequency.[50,51] Recent studies have revealed that RIF monotherapy or its combination with PZA for 3-4 months is equally effective as 9-12 months of INH monotherapy for latent TB infection.[52,53] RIF targets the ß-subunit of DNA dependent RNA polymerase, which is an essential product of *rpoB* gene.[54] The cyclopentyl substituted analogue of RIF called Rifapentin (RIP) (**Figure 1.7**) has been developed from the rifamycin class. It has shown encouraging results in recent evaluation in combination and individual studies against LTB infection and active TB in HIV negative patients.[55] RIP has shown potential to reduce cost and increase the adherence to chemotherapy treatment because as a once a week dose of RIP and INH has shown the same efficacy as twice a week dose of RIF and INH in the continuation phase of pulmonary tuberculosis.[26] RIP is a very strong contender to replace rifampicin from the DOTs chemotherapy. However, complete evaluation of its efficacy and pharmacokinetics still needs to be done.[56]

1.8.2 Second line anti-TB drugs

Second line anti-TB drugs are a second line defence against tuberculosis infection and used against resistant strains of TB (M/XDR TB) where first line anti-TB drugs are ineffective.[57] The second line drugs are both oral and injectable, which include drugs from group 2, 3 and 4.[37]

Fluoroquinolones (FQs) (**Figure 1.8**) are an emerging class of drugs for TB treatment due to their good pharmacokinetic profile and good potency against *Mtb*, particularly against resistant *Mtb*. These FQ drugs are repurposed drugs for TB and have shown good activity against both extracellular rapidly multiplying bacteria as well as intracellular, non-multiplying bacteria. These drugs are efficacious and well distributed throughout the body and cells.[58] FQ drugs have been suggested for the treatment of MDR-TB by the WHO,[37] and categorised as second line anti-TB drugs. They were also assessed as first line regimens after showing reduction in the duration of TB treatment in the murine model.[59] These drugs are currently used as anti-TB agents in the treatment of MDR-TB.

Moxifloxacin (MOX) and Gatifloxacin (Gfx) (**Figure 1.8**) are new and very potent FQ anti-TB drugs with similar efficacy.[60,61] MOX and Gfx seem to have potential to shorten the treatment duration of TB as they have shown high bactericidal activity with low MIC and high efficacy.[62,63] They are currently undergoing phase 3 clinical trials for evaluation of the possibility of shortening the treatment duration of DS-TB from 6 months to 4 months by substituting Gfx for ethambutol or MOX for ethambutol or isoniazid.[64,65] MOX has recently been approved for the treatment of respiratory and other infections. It is also included in the WHO guidelines for treatment of drug-resistant TB in combination with other drugs although it has not been approved by any other regulatory authority.[66]

Ofloxacin and its levo isomers levofloxacin, and ciprofloxacin (**Figure 1.8**) are old FQ drugs, which are repurposed for the treatment of TB and have shown potency against *Mtb*.[67] Levofloxacin is the most potent among these drugs and has shown an excellent safety and tolerance profile.[68] All the FQ drugs target the DNA gyrase enzyme of *Mtb* and inhibit the DNA replication process.[69] Having a common target, cross resistance has been observed between the different FQ drugs and hence administration of more than one FQ drug to one patient has not been advised. There is a growing concern about the development of acquired

FQ resistance in undiagnosed TB patients due to the extensive use of these drugs for other infectious diseases or when FQ is the only active drug in a failing TB regimen.[70]

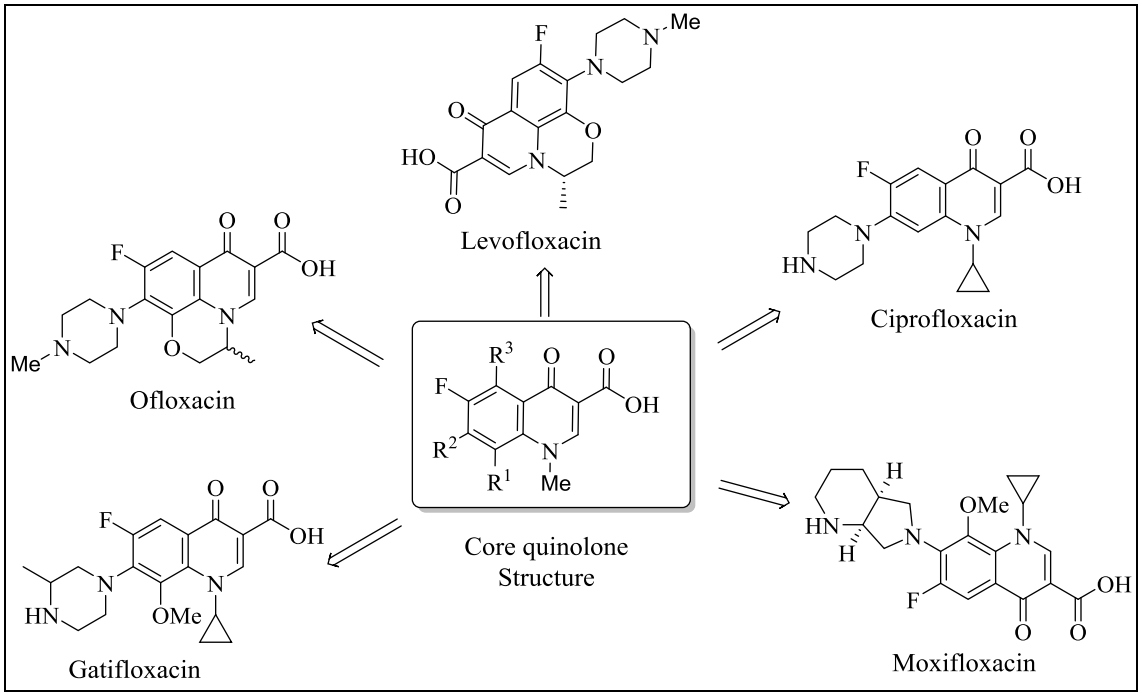

Figure 1.8: Fluoroquinolone drugs.

Drugs of group 2 are injectable aminoglycosides and polypeptides and are the second most important drugs after FQ drugs in the treatment of MDR-TB. Streptomycin was the first discovered aminoglycoside in the early 1940s and proved to be the first breakthrough in TB treatment. Streptomycin was replaced by ethambutol in first line chemotherapy due to its poor toxicity profile and oral absorption. Later members of this group include kanamycin and amikacin. Group 2 also includes members of the polypeptide family,[71,72] capreomycin and viomycin. An unexpected pattern of cross resistance has been observed among group 2 drugs belonging to different families. This can be attributed to the fact that these drugs all target the 30 ribosomal unit, which affects polypeptide synthesis leading to the inhibition of translation.

Group 4 drugs are used for the treatment of MDR and XDR-TB. Some of these drugs have been used as first line drugs in the past. Toxicity, lower potency, and higher cost led to their replacement by the current first line drugs. For example, 4-aminosalicylic acid and ethionamide (**Figure 1.9**) were discovered in the 1950s after streptomycin, and used in TB treatment but later on replaced by rifamycin, ethambutol and pyrazinamide.[73]

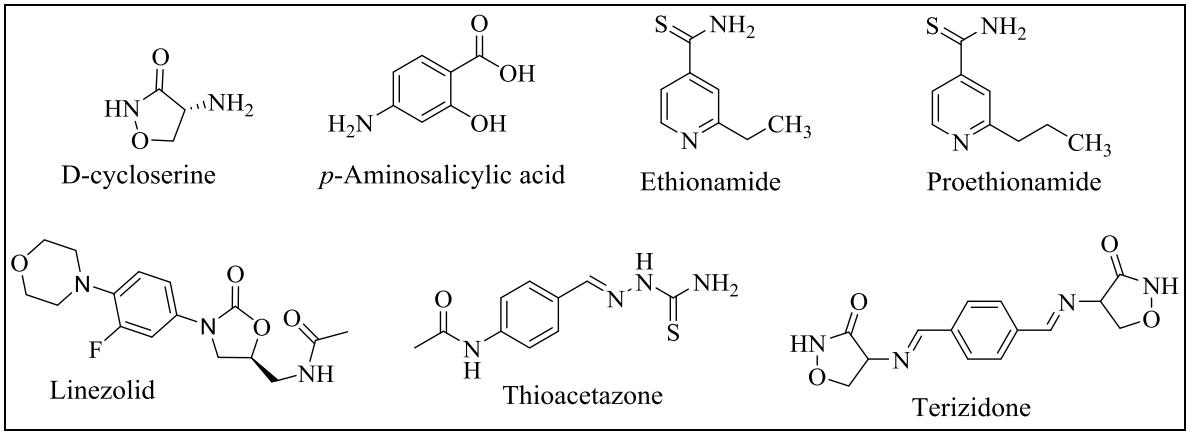

Figure 1.9: Group 4 anti-TB drugs.

Thiacetazone (**Figure 1.9**) has similar properties to ethambutol, thereby controlling the development of resistance against frontline drugs (INH and RIF) in a treatment regimen. However, it is not recommended for frequent use due to severe skin reactions reported, especially in patients with HIV co-infections. It is only used in some parts of Africa in the treatment of DS-TB as it is a cheaper alternative.[74]

Group 5 drugs are classified as third line anti-TB agents and used against XDR-TB, when other drugs become ineffective. The efficacy and role of these drugs is poorly understood, therefore they are not recommended for general use. Clofazimine (CFZ) (**Figure 1.10**) is considered as an important prospective drug for the shortening of the drug resistant TB (DR-TB) regimen as it has shown good efficacy and low toxicity in a murine model.[75,76] A CFZ containing drug regimen was reported to show a 80% cure rate of DR-TB in nine months, a relatively short treatment duration compared to the standard treatment regimen.[77,78]

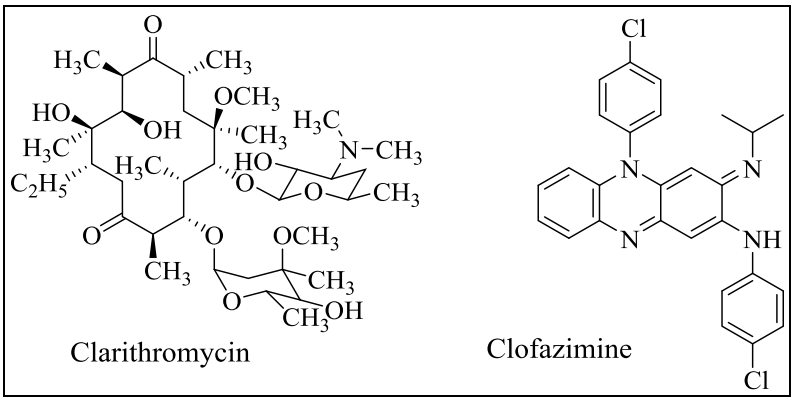

Figure 1.10: Two of group 5 anti-TB drugs.

Linezolid (**Figure 1.9**) is used for the treatment of XDR-TB, albeit a high rate of adverse effects has been a major concern. Nevertheless the side effects are absent at lower dosage levels.[79]

1.9 Tuberculosis drug Pipeline

The TB drug pipeline is a set of drug candidates in developmental stages. The pipeline typically includes four stages: discovery, pre-clinical, clinical trial and marketing. This includes completely new drugs, variants of existing drugs and new applications of existing drugs. It also highlights the advancement, achievement and potential of success of drug candidates for chemotherapy. The current drugs for tuberculosis are inefficient to overcome many inherent and emerging challenges of treatment due to resistance and long treatment durations. As already mentioned, drug resistance occurs due to reasons such as gene mutations and selection, drug-efflux mechanisms or due to drug modifying enzymes. Therefore, to combat the emerging challenges, new drugs, novel drug combinations, and drugs with novel targets are required.

Information compiled by the Stop TB Partnership Working Group on New Drugs has shown a steady increase in the global TB drug pipeline over the past few years (**Figure 1.11**).[80] There are approximately 26 projects and 19 compounds in the current global portfolio, among which 10 compounds are in different stages of clinical development and 9 compounds are in preclinical development.[81]

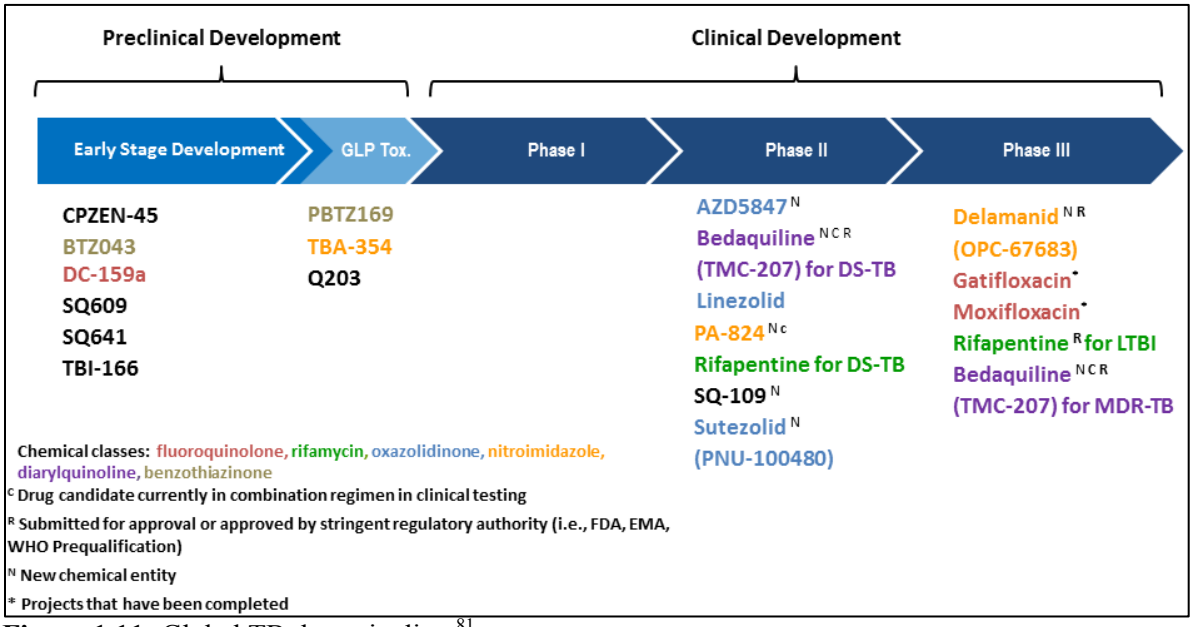

Figure 1.11: Global TB drug pipeline.[81]

1.9.1 Clinical candidates

Among 10 compounds in clinical development, four are in phase 3 evaluation. Two other compounds (Gfx and MOX) from the FQ class have already completed phase 3 clinical trials for development of a new regimen for drug sensitive TB (DS-TB) to shorten the treatment duration (Section **1.8.2**).

Delamanid also known as **OPC-67683** and **PA-824** (**Figure 1.12**) are from the nitroimidazole class. **OPC-67683** has been submitted for registration to regulatory authorities such as the Food and Drug Administration (FDA), European Medicine Agency (EMA) and World Health Organisation (WHO). In addition to good *in vitro* and *in vivo* activity against DS-TB and DR-TB,[82] it has shown similar early bactericidal activity (EBA) as RIF over 14 days. Delamanid has displayed a reduced mortality rate among MDR and XDR TB patients, when treated with it along with the standard regimen for six months.[83] **PA-824** has shown good potency against both DS and DR strains of TB both *in vitro* and *in vivo* experiments. It was also effective against non-replicating bacteria under anaerobic conditions. In addition, it is well tolerated on daily dosing and has suitable pharmacokinetics for daily administration. It was reported that the combination of **PA-824** with PZA and MOX has the potential to shorten the duration of treatment of DS and MDR-TB. As discussed earlier, RIP (Section **1.8.1**) has shown potency against LTB infection and is currently in phase 3 clinical trials for the inclusion of this drug in the TB treatment regimen.[84]

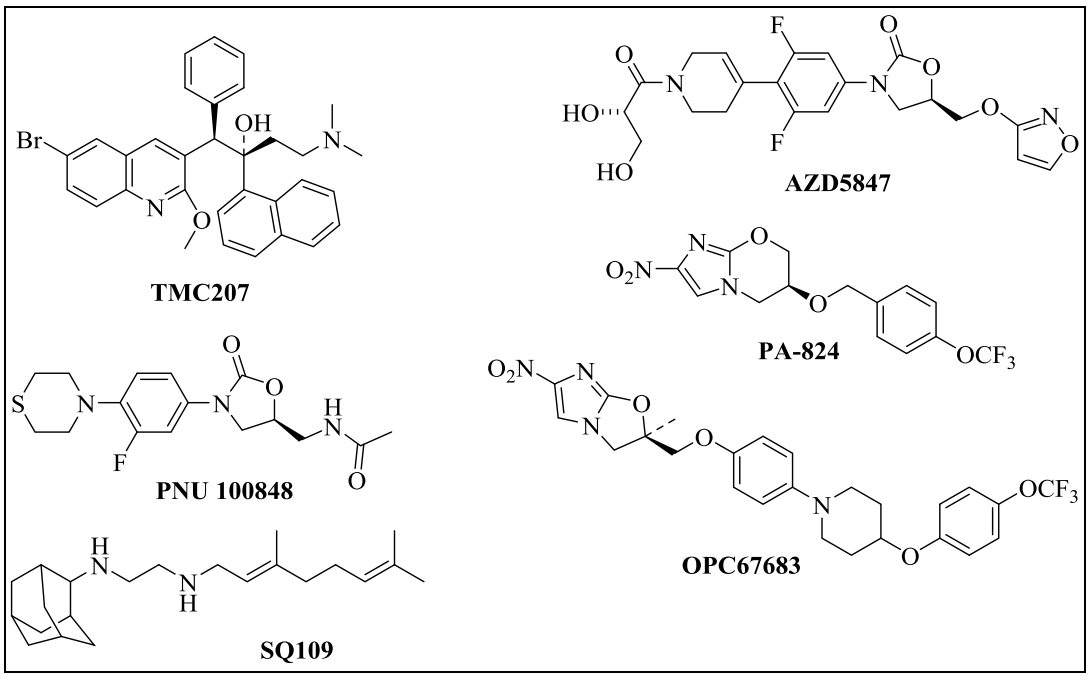

Figure 1.12: Clinical candidates in the TB drug pipeline.

The family of oxazolidinones (**Figure 1.12**) currently has three members in advanced stages of development namely, Linezolid, Sutezolid **(PNU 100480)** and **AZD5874**. Sutezolid and **AZD5874** have been developed following reports of toxicity and adverse effects of linezolid (section **1.7.2**). Both these compounds have shown promising *in vitro* activity and efficacy in murine models.[85,86] They are currently in the phase 2 stage of development.

SQ-109: (**Figure 1.12**) is a synthetic diamine derivative of ethambutol with a novel mechanism of action. It has shown good *in vitro* and *in vivo* activity against both DS and DR *Mtb.* The *in vitro* synergistic results with **TMC207**, **PNU100480**, INH and RIF make it a suitable candidate for a new drug regimen for MDR-TB and DS-TB.[87] It has also shown an additive effect when used in combination with EMB and STP.[88] It was also found to be safe, tolerable, and having suitable pharmacokinetics for evaluation in phase 2 of clinical development for different combination regimens with or without RIF.

TMC207: (**Figure 1.12**) is the first TB drug to be approved in over 40 years.[89] It had been recommended that this drug be accelerated for approval by FDA for treatment of MDR-TB. This drug belongs to the diarylquinoline class, and is currently in phase 2 clinical development for the treatment of DS TB and in phase 3 clinical development for MDR-TB. In addition to its effectiveness against DS and DR *Mtb*,[90] it is also potent against replicating and dormant *Mtb*.[91] The long half-life of BDQ and synergistic interaction with PZA make it a suitable candidate in intermittent drug regimens.[92]

1.9.2 Preclinical candidates

As mentioned earlier, there are approximately 26 projects with a number of compounds in discovery, preclinical and clinical development stages for TB treatment. In addition, there are 14 candidates in lead optimization and 12 in the screening stages of development.[81] However, there is a gap between late preclinical development and phase 1 trials, which needs to be addressed so that continuity in clinical trials can be maintained and any attrition can be countered. These developments are focused on addressing two main challenges in TB drug therapy: drug resistance and drug persistence. To effectively address these challenges, novel combinations of drugs with novel mechanisms, which are also equipotent against DS and DR-TB (including MDR and XDR TB) are under way. These novel combinations should have minimal interaction with metabolic enzymes such as cytochrome P450s so that the

regimens can be used for the treatment of HIV co-infected patients.[80] Among the 9 compounds in preclinical development 5 possess new chemical identities, 2 are from the benzothiazone class and one each from the fluoroquinolones and nitroimidazole classes (**Figure 1.13**). The biological profiles of some of these compounds are summarised below:

CAPZEN-45: (**Figure 1.13**) is a lipo-nucleoside antibiotic which is isolated from *Streptomyces sp*. It has shown *in vitro* activity with MIC = 3.13-12.5 μM (DS-*Mtb*); MIC = 6.25-12.5 μM, (DR-*Mtb*) and good potency against replicating as well as non-replicating *Mtb*. Animal studies in mice revealed its efficacy against both DS and XDR-TB infections.[93]

SQ609: (**Figure 1.13**) is a dipiperidine compound with good *in vitro* and *in vivo* activity against *Mtb.*[94] It exhibited an *in vitro* MIC of 7.8 μM and low mammalian toxicity with desirable lipophilicity and solubility characteristics (LogP <4.0). It also showed 90% inhibition of intracellular growth of *Mtb* in infected macrophages and mice.[84] An extended therapeutic effect of two weeks was observed in murine models, suggesting that it is well tolerated and not eliminated immediately after termination of dosages.[95]

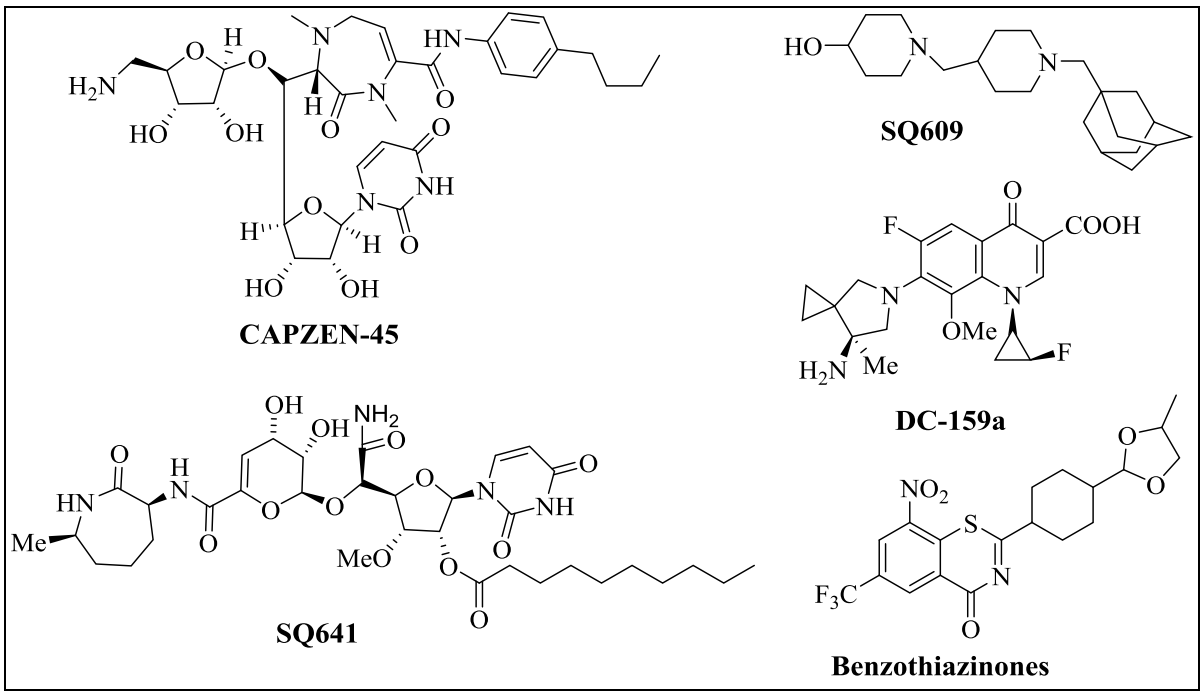

Figure 1.13: Preclinical candidates in TB drug pipeline.

SQ641 (**Figure 1.13**) is an analogue of the naturally occurring nucleoside capuramycin from the culture filtrate of *Streptomyces griseus*. It has shown *in vitro* activity against *Mtb* (MIC = 1.0 μg/ml) and a greater bactericidal rate compared to many anti-TB drugs including INH and

RIF.[96] It has shown synergistic interactions and an enhanced killing rate when used in combination with STP, INH, RIF and EMB. However, **SQ641** has very limited solubility in water and high susceptibility to PgP-mediated efflux pumps. These limitations led to modest potency against intracellular *Mtb* and poor *in vivo* activity.[97] However, by associating **SQ641** with water soluble vitamin E (α-tocopheryl polyethylene glycol 1000 succinate-TPGS), a significant increase in activity against *Mtb* in the mouse model of tuberculosis was observed.[98]

DC-159a (**Figure 1.13**) is a highly potent FQ analogue active against both DS and DR-TB. It is one of the most active FQ drugs against quinolone resistant strains (MIC = 0.5 μM) and drug susceptible isolates (MIC = 0.6 μg/ml).[99] It has a similar pharmacokinetics profile to MOX but showed greater activity in the initial as well as continuation phases of the treatment in a murine model.[100] Thus, **DC-159a** is a suitable prospective member of a drug regimen combination against DS and FQ resistant *Mtb*.

Benzothiazinones (BTZ) (**Figure 1.13**) are a new developing class of anti-TB agents and have shown the most promising anti-TB potencies as they inhibit *Mtb* in the nanomolar (MIC = 2.3 nM) range, both *in vivo* and in *ex vivo* models of TB.[101] **BTZ043** and **PBTZ169** are two of the most potent BTZ derivatives currently in preclinical development. **BTZ043** is relatively less efficacious in animal model compared to its *in vitro* potency (MIC = 1.0 nM), due to its hydrophobic nature. Subsequent Structure Activity Relationship (SAR) studies furnished the piperidine analogue, **PBTZ169**, which has improved solubility required for inclusion in the treatment regimens for DS and DR-TB. Both analogues inhibit cell wall synthesis. As such cross resistance has been observed although **PBTZ169** proved to be less susceptible to nitroreductase NfnB than **BTZ043.** NfnB nitroreductase is responsible for reduction of the nitro group of BTZ. **PBTZ169** showed *in vivo* bactericidal activity equivalent to INH and greater than **BTZ043**. The synergism was observed between **PBTZ169** and BDQ in *in vivo* murine models. These drugs showed superior efficacy in drug regimens, when included with BDQ and PZA, to the standard triple therapy of INH, RIF and PZA in the chronic model of TB. The compatibility with other drugs shows promise for the development of novel combinations including **PZA169**.[102]

1.10 Main anti-TB drug targets and development of resistance

Every anti-TB drug kills *Mtb* by blocking specific biological pathways or targets having an important contribution to the survival of bacteria. In this section, an overview of some important drug targets will be presented followed by a discussion of factors leading to the development of resistance in *Mtb* against specific drugs.

The main drug targets (**Figure 1.14**) with corresponding drugs are classified as follow:

1. Cell wall biosynthesis (INH, EMB, BTZ03, PBTZ169, DNB1, SQ109, SQ641)
2. Cell membrane (PZA)
3. Folate synthesis (*p*-aminoglycoside)
4. Transcription (rifampicin)
5. Translation (aminoglycoside)
6. DNA metabolism (Fluorquinolones)

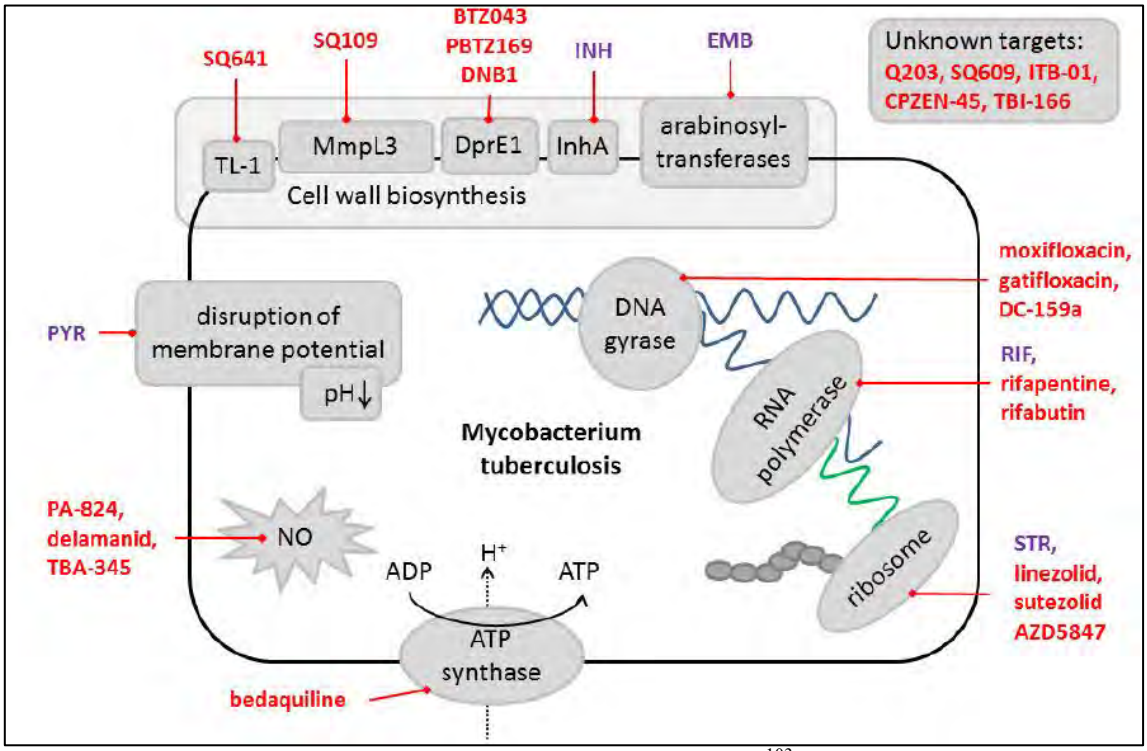

Figure 1.14: Different drug targets in *Mycobacterium tuberculosis*.[103]

1.10.1 Inhibitors of cell wall synthesis

The cell wall of *Mtb* is an important component for its survival, especially within constrained conditions such as those inside of human macrophages. The cell wall of *Mtb* consists of covalently linked macromolecule peptidoglycan, arabinogalactan and mycolic acids. The biosynthesis of these cell wall macromolecules is a complex biological process and includes various enzymes. The potency of current anti-TB drugs such as INH, EMB and D-cycloserine is due to the targeting one of these biological processes. The additional advantage of targeting cell wall enzymes is the absence of homology within mammalian cells.[104]

The table **1.1** presents an overview of various drugs targeting various cell wall targets and cause of resistance in *Mtb* against these drugs:

Table 1.1: Drugs targeting cell wall synthesis and case of resistance.

Pathway	Drugs class or drug/s	Target and mechanism of action	Cause of resistance
Mycolic acid synthesis	INH	Activated form of INH binds to the NADPH dependent carrier protein reductase *InhA* responsible for fatty acid elongation.[105]	**1**. Mutation in KatG and *InhA* causes high and low levels of resistance respectively.[106] **2.** Active efflux pumps contribute for low level of resistance.[107]
Arabinogalactan biosynthesis	EMB	Disrupts arabinogalactan synthesis required for the formation of the cell wall by inhibiting the enzyme arabinosyl transferase.[108]	Mutation in the regions of gene embB encoding the enzyme arabinosyl transferase.[109]

Pathway	Drugs class or drug/s	Target and mechanism of action	Cause of resistance
Arabinose synthesis	Benzothiazin-ones: BTZ043 and PBTZ 169. DNB1	Binds to the subunit of enzyme decaprenylphosphoryl-b-o-ribose 2′-epimerase (DprE1) responsible for biosynthesis of decaprenylphosphoryl arabinose an important component of cell wall.[101]	The mutation in *MSMEG*_6503 leading to overexpression of nitroreductase enzyme NfnB, responsible for inactivation of drugs results in the development of resistance.[110]
Mycolic acid incorporation in cell wall	SQ109	This drug binds to the protein *MmpL3* resulting in inhibition of ATP powered mycolate translocation[88]; hence disturbing cell wall mycolate synthesis and decreasing cell wall biosynthesis.[111,112]	Considered to be the upregulation of gene ahpC however, the complete mechanism of resistance is yet to be proven.[113]
Biosynthesis of peptidoglycan	SQ641	It blocks the enzyme translocase 1 (TL1)[114] required for peptidoglycan biosynthesis.[115]	Overexpression of PgP protein coding for efflux pumps.[98]

1.10.2 DNA metabolism, transcription and translation

DNA replication and transcription are the most important biological processes involved in multiplication and protein synthesis required for survival of bacteria. There are numerous targets, which can be targeted by drugs for bactericidal activity and one of the targets is thymidin monophosphate (TMP) kinase. TMP kinase is an ideal drug target in *Mtb* as it differs from its counterpart in mammalian cell lines.[116] The table **1.2** presents an overview of various drugs and their targets during DNA metabolism, transcription and translation as well as the cause of resistance in *Mtb* against these drugs.

Table 1.2: Drugs targeting DNA metabolism, transcription and translation and cause of resistance.

Pathway	Drug class or drug/s	Target and mechanism of action	Cause of resistance
Inhibition of DNA biosynthesis	Fluoroquinolones; Gfx, MOX, and DC159a	Inhibition of Topoisomerase II (DNA gyrase) required for DNA supercoiling[117]	1.Mutation at position 90 and 94 of gyrase A[118,119] 2. ABC transporters (efflux pumps).[120,121]
Inhibition of RNA biosynthesis	Rifamycins: RIF, RIP and Rifabutin	By binding with ß-subunit of *rpoB* gene that codes for ß-subunit of RNA polymerase responsible for elongation of mRNA.[122]	1. Mutation in the *rpoB* gene specially in codon 507-533 causes 95% of resistance. 2.The low level of resistance is also caused by efflux pumps.[123]
Protein synthesis	Aminoglycosides: STP	It binds to the 30S unit of ribosome at ribosomal protein S12 and 16S rRNA and inhibits the initiation of translation[124] in protein synthesis	Mutation in genes rpsl and rrs encode for ribosomal protein S12 and 16S rRNA.[125,126]
Protein synthesis	Oxazolidinone: Linezolid, sutezolid and AZD5847	It bind to the A site of peptidyl transferase (PTC) responsible for enzymatic function of ribosomes during the translation process of protein biosynthesis	Resistance is less frequent but arises due to the 1. Mutation in 23S rRNA.[86] 2. Efflux pumps.[121]

PA824 and **OPC-67638:** are nitroimidazole drugs and inhibit mycolic acid synthesis in replicating bacteria and inhibit ATP synthesis in non-replicating *Mtb.*[127] The nitroimidazoles are prodrugs and require activation by a nitroreductase.[128] The main mechanism of resistance arises due to the mutation in the gene coding for the enzyme deazaflavin (cofactor 420).[129]

Pyrazinamide (PZA): is a prodrug activated by the enzyme pyrazinamidase/nicotinamidase (PZase) encoded by the *pncA*[130] gene and converted to pyrazinoic acid. It gets effluxed out by efflux pumps but gets reabsorbed in the acidic pH. PZA acts on *Mtb* by inhibiting membrane transport arising from disturbing the membrane energetics[131] (**Figure 1.15**). The most common cause of resistance to pyrazinamide, is a mutation in the gene pncA, which decreases the probability of activation.[132] Other mechanisms of resistance have also been proposed such as a mutation in the unidentified regulatory gene or a mutation leading to up regulation of efflux pumps. These have been suggested since some PZA resistant mutants are lacking the mutation in the pncA gene.[133]

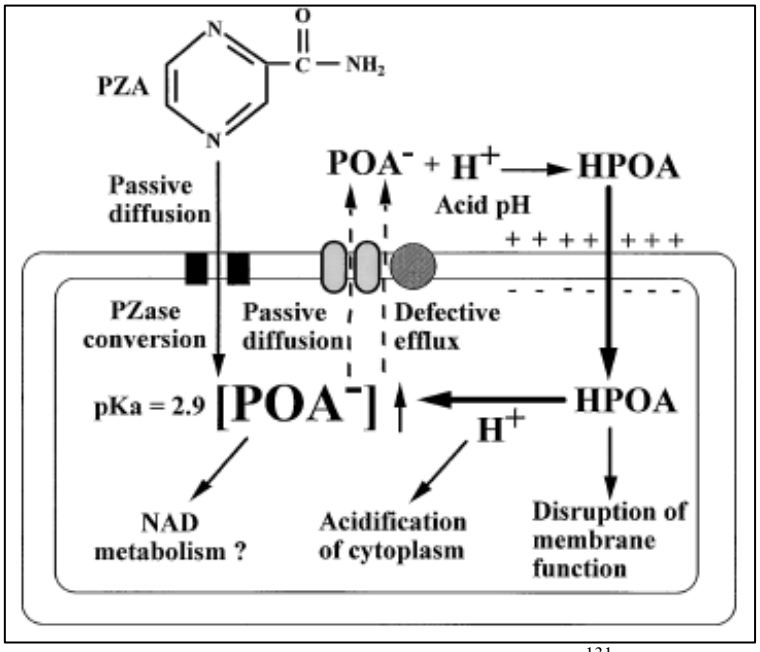

Figure 1.15: Mode of action of Pyrazinamide (PZA),[131] POA = Pyrazonic acid, HPOA = protonated POA, NAD = nicotinamide adenine dinucleotide.

Bedaquiline **(TMC207)** is a new antibacterial drug with a novel mode of action.[134] It targets the c subunit of ATP synthase, hence decreasing the intracellular adenosine triphosphate (ATP) concentration.[90] It is highly selective since human ATP synthase is 20, 000 times less sensitive than *Mtb* ATP synthase.[135] The mechanism of resistance to BDQ is not well

established. However, 15 of 53 isolated mutants have shown the mutation in the *apE* gene responsible for encoding c part of the F0 and F1 subunit of the ATP synthase. This suggests the possibility of alternative mechanisms of action.[136]

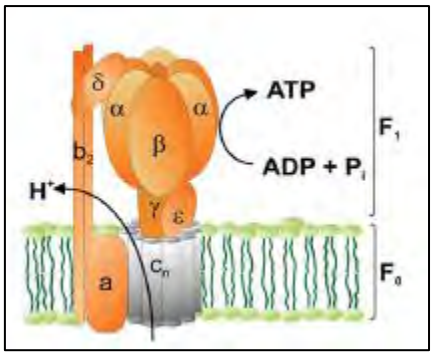

Figure 1.16: ATP synthase and the proton-conducting subunit c. (A) Schematic view of ATP synthase subunits. The bacterial enzyme consists of a membrane-bound F0 part (subunits $\alpha_3\beta_3\gamma\delta\varepsilon$) for conduction of protons, and a hydrophilic F1 part (subunits $\alpha_3\beta_3\gamma\delta\varepsilon$) responsible for synthesis of ATP. The oligomeric subunit c (AtpE) is shown in gray.[148]

1.11 Adjunctive chemotherapy

Adjunctive chemotherapy is an addition to primary or main chemotherapy. Adjunctive agents are incorporated to enhance or maximize the effectiveness of primary or main agents. The concept of adjunctive immunotherapy is well explored in tuberculosis and has shown encouraging results with potential for further development as a tool to combat the growing threats of MDR and XDR-TB. The use of interleukin 2, interferon *g*, and interleukin 7 immunotherapeutic agents as adjuncts to drug treatment presents a bright future outlook for adjunctive immunotherapy.[137]

Various chemical agents can also be employed as adjunctive chemotherapeutic agents to achieve enhanced results.[138,139] The use of various therapeutic agents like anti-diabetic drugs as adjunctive agents has also shown encouraging results.[140] Moreover, the use of metformin, a well known anti-diabetic agent, as an adjunctive agent has shown enhancement in efficacy of conventional TB drugs in mouse models.[141] The observed shortening of treatment duration by phosphodiesterase inhibitors (PDE-Is) in mice is a motivation to evaluate such inhibitors in humans.[142] An additional class of compounds, which can also be used for adjunctive chemotherapy are the efflux pump inhibitors or chemosensitizers. This is due to the fact that the efflux of drugs has been one of the underlying mechanisms for the emergence of resistance in *Mtb* and has been highlighted in section **1.9**. Therefore the inhibition of these

efflux pumps has the potential to overcome the emerging resistance.[143] In addition, MDR clinical isolates exhibiting efflux pump (EP)-mediated resistance can be made more sensitive to the relevant antibiotics. These adjunctives may also present an alternative option to decrease the cytotoxicity of the second-line antibiotics when used in combination therapy. The development of various efflux pump inhibitor (EPIs) has been accelerated recently due to the achievement of better efficacy and potency *in vitro* and in animal models when EPIs are used as adjunctives.[144] Verapamil is a well known FDA approved calcium channel blocker and is an efflux pump inhibitor. It has shown acceleration of both bactericidal and bacteriostatic activity of standard TB drugs *in vitro,* in macrophages,[145] and in mouse models. The development of adjunctive agents presents an opportunity for overcoming the emerging resistance, which can potentially lead to reduction in treatment relapse and shortening of treatment duration. These adjunctive agents can also be used to reduce the probability of development of resistance in newly developed drugs like BDQ and FQ class of drugs[146] and give new life to old anti-TB agents that were put aside due to various pharmacological challenges of cytotoxicity and resistance.[147]

1.12 Conclusion

The high epidemiology of tuberculosis and emerging resistance against various anti-TB agents suggest that the development of new antimycobacterial agents remains a key priority. The importance of efflux pump-mediated resistance has highlighted the requirement for the development of new antimycobacterial agents, which can counter the efflux pump and efflux pump-mediated resistance.

This project therefore seeks to contribute to these aspects, and is an attempt to identify new agents effective against these efflux pumps and overcome efflux pump-mediated resistance. Chapter two provides a brief discussion of efflux pumps and various approaches to counter the resistance mediated by efflux pumps.

References:

(1) Kenneth Todar. *Mycobacterium tuberculosis* and Tuberculosis_http://textbookofbacteriology.net/tuberculosis.html_2012 pg:1 -4.

(2) http://en.wikipedia.org/wiki/*Mycobacterium_tuberculosis*#/media/File:TB_Culture.jpg (Last seen 03 Apr 2015).

(3) Daniel, T. M. The History of Tuberculosis. *Respir. Med.* **2006**, *100*, 1862–1870.

(4) *Global Tuberculosis Report 2014*; 2014; p. 171.

(5) Riley, R. L. The Contagiosity of Tuberculosis. *Schweiz. Med. Wochenschr.* **1983**, *113*, 75–79.

(6) Borgdorff, M. W.; Sebek, M.; Geskus, R. B.; Kremer, K.; Kalisvaart, N.; van Soolingen, D. The Incubation Period Distribution of Tuberculosis Estimated with a Molecular Epidemiological Approach. *Int. J. Epidemiol.* **2011**, *40*, 964–970.

(7) Koul, A.; Arnoult, E.; Lounis, N.; Guillemont, J.; Andries, K. The Challenge of New Drug Discovery for Tuberculosis. *Nature* **2011**, *469*, 483–490.

(8) Pawlowski, A.; Jansson, M.; Sköld, M.; Rottenberg, M. E.; Källenius, G. Tuberculosis and HIV Co-Infection. *PLoS Pathog.* **2012**, *8*, e1002464.

(9) Centers for Disease Control and Prevention. Emergence of *Mycobacterium tuberculosis* with Extensive Resistance to Second-Line Drugs Worldwide. *MMWR Morb Mortal Wkly Rep,* **2006**, *55*, 301–305.

(10) Korenromp, E. L.; Glaziou, P.; Fitzpatrick, C.; Floyd, K.; Hosseini, M.; Raviglione, M.; Atun, R.; Williams, B. Implementing the Global Plan to Stop TB, 2011-2015--Optimizing Allocations and the Global Fund's Contribution: A Scenario Projections Study. *PLoS One* **2012**, *7*, e38816.

(11) "Totally Drug-Resistant TB ": A WHO Consultation on the Diagnostic Definition and Treatment Options. *By WHO* **2012**, 21–22.

(12) Zignol, M.; van Gemert, W.; Falzon, D.; Sismanidis, C.; Glaziou, P.; Floyd, K.; Raviglione, M. Surveillance of Anti-Tuberculosis Drug Resistance in the World: An Updated Analysis, 2007-2010. *Bull. World Health Organ.* **2012**, *90*, 111–119D.

(13) Van Ingen, J.; de Lange, W. C.; Boeree, M. J.; Iseman, M. D.; Daley, C. L.; Heifets, L. B.; Böttger, E. C.; van Soolingen, D. XDR Tuberculosis. *Lancet. Infect. Dis.* **2011**, *11*, 585.

(14) Velayati, A. A.; Masjedi, M. R.; Farnia, P.; Tabarsi, P.; Ghanavi, J.; Ziazarifi, A. H.; Hoffner, S. E. Emergence of New Forms of Totally Drug-Resistant Tuberculosis Bacilli: Super Extensively Drug-Resistant Tuberculosis or Totally Drug-Resistant Strains in Iran. *Chest* **2009**, *136*, 420–425.

(15) Udwadia, Z. F.; Amale, R. A.; Ajbani, K. K.; Rodrigues, C. Totally Drug-Resistant Tuberculosis in India. *Clin. Infect. Dis.* **2012**, *54*, 579–581.

(16) Caminero, J. A.; Sotgiu, G.; Zumla, A.; Migliori, G. B. Best Drug Treatment for Multidrug-Resistant and Extensively Drug-Resistant Tuberculosis. *Lancet. Infect. Dis.* **2010**, *10*, 621–629.

(17) Rieder H.L.; Lauritsen J.M.; Naranbat N.; Katamba A.; Laticevschi D. Mabaera B.;. Quantitative Differences in Sputum Smear Microscopy Results for Acid-Fast Bacilli by Age and Sex in Four Countries. *Int. J. Tuberc. Lung Dis.* **2009**, *13*, 1393–1398.

(18) Streptomycin Treatment of Pulmonary Tuberculosis. *Br. Med. J.* **1948**, *2*, 769–782.

(19) Treatment of Pulmonary Tuberculosis with Isoniazid; an Interim Report to the Medical Research Council by Their Tuberculosis Chemotherapy Trials Committee. *Br. Med. J.* **1952**, *2*, 735–746.

(20) Isoniazid in the Treatment of Pulmonary Tuberculosis; Second Report to the Medical Research Council by Their Tuberculosis Chemotherapy Trials Committee. *Br. Med. J.* **1953**, *1*, 521–536.

(21) Nuermberger, E. L.; Spigelman, M. K.; Yew, W. W. Current Development and Future Prospects in Chemotherapy of Tuberculosis. *Respirology* **2010**, *15*, 764–778.

(22) Mitchison, D.; Davies, G. The Chemotherapy of Tuberculosis : Past, Present and Future. *Int. J. Tuberc. Lung Dis.* **2013**, *16*, 724–732.

(23) Ordonez, A. A.; Maiga, M.; Gupta, S.; Weinstein, E. a.; Bishai, W. R.; Jain, S. K. Novel Adjunctive Therapies for the Treatment of Tuberculosis. *Curr. Mol. Med.* **2014**, *14*, 385–395.

(24) Hang, Y.; Yew, W. W.; Barer, M. R. Targeting Persisters for Tuberculosis Control. *Antimicrob. Agents Chemother.* **2012**, *56*, 2223–2230.

(25) Chang, K. C.; Leung, C. C.; Yew, W. W.; Chan, S. L.; Tam, C. M. Dosing Schedules of 6-Month Regimens and Relapse for Pulmonary Tuberculosis. *Am. J. Respir. Crit. Care Med.* **2006**, *174*, 1153–1158.

(26) Benator, D.; Bhattacharya, M.; Bozeman L.; Burman, W.; Cantazaro, A.; Chaisson, R.; Gordin, F.; Horsburgh, C. R.; Horton, J.; Khan, A.; Lahart, C.; Metchock, B.; Pachucki, C.; Stanton, L.; Vernon, A.; Villarino, M. E.; Wang, Y. C.; Weiner, M.; Weis, S.; Tuberculosis Trials Consortium.. Rifapentine and Isoniazid Once a Week versus Rifampicin and Isoniazid Twice a Week for Treatment of Drug-Susceptible Pulmonary Tuberculosis in HIV-Negative Patients : A Randomised Clinical Trial. *Lancet (London, England)* **2002**, *360*, 528–534.

(27) Volmink, J.; Garner, P. Directly Observed Therapy for Treating Tuberculosis. *Cochrane Database Syst Rev* **2007**, CD003343.

(28) Van den Boogaard, J.; Kibiki, G. S.; Kisanga, E. R.; Boeree, M. J.; Aarnoutse, R. E.

New Drugs against Tuberculosis: Problems, Progress, and Evaluation of Agents in Clinical Development. *Antimicrob. Agents Chemother.* **2009**, *53*, 849–862.

(29) Chan, E. D. Current Medical Treatment for Tuberculosis. *BMJ* **2002**, *325*, 1282–1286.

(30) Iseman, M. D. Treatment of Multidrug-Resistant Tuberculosis. *N. Engl. J. Med.* **1993**, *329*, 784–791.

(31) Getahun, H.; Gunneberg, C.; Granich, R.; Nunn, P. HIV Infection-Associated Tuberculosis: The Epidemiology and the Response. *Clin. Infect. Dis.* **2010**, *50 Suppl 3*, S201–S207.

(32) Narita, M.; Ashkin, D.; Hollender, E. S.; Pitchenik, A. E. Paradoxical Worsening of Tuberculosis Following Antiretroviral Therapy in Patients with AIDS. *Am. J. Respir. Crit. Care Med.* **1998**, *158*, 157–161.

(33) Dick Menzies, Hamdan Al Jahdali, and B. A. O. Recent Developments in Treatment of Latent Tuberculosis Infection. *Indian J. Med. Res.* **2011**, *133*, 257–266.

(34) World Health Organization. *Guidelines on the Management of Latent Tuberculosis Infection*; 2010.

(35) Ginsberg, A. "Drugs in Development for Tuberculosis." *Drugs* **2010**, *70*, 2201–2214.

(36) World Health Organization. *Treatment of Tuberculosis: Guidelines-4th Edition*; 2010; p. 147.

(37) Zumla, A.; Nahid, P.; Cole, S. T. Advances in the Development of New Tuberculosis Drugs and Treatment Regimens. *Nat. Rev. Drug Discov.* **2013**, *12*, 388–404.

(38) Heym, B.; Zhang, Y.; Poulet, S.; Young, D.; Cole, S. T. Characterization of the katG Gene Encoding a Catalase- Peroxidase Required for the Isoniazid Susceptibility of *Mycobacterium tuberculosis*. *J. Bacteriol.***1993**, *175*, 4255–4259.

(39) (a) Miesel, L.; Rozwarski, D. A.; Sacchettini, J. C.; Jacobs, W. R. Mechanisms for Isoniazid Action and Resistance. *Novartis Found. Symp.* **1998**, *217*, 209–220; discussion 220–221. (b) Barry, C. E.; Slayden, R. A.; Mdluli, K. Mechanisms of Isoniazid Resistance in *Mycobacterium tuberculosis*. *Drug Resist. Updat.* **1998**, *1*, 128–134.

(40) Timmins, G. S.; Deretic, V. Mechanisms of Action of Isoniazid. *Mol. Microbiol.* **2006**, *62*, 1220–1227.

(41) Biehl, J. P.; Vilter, R. W. Effects of Isoniazid on Pyridoxine Metabolism. *J. Am. Med. Assoc.* **1954**, *156*, 1549–1552.

(42) Van der Watt, J. J.; Harrison, T. B.; Benatar, M.; Heckmann, J. M. Polyneuropathy, Anti-Tuberculosis Treatment and the Role of Pyridoxine in the HIV/AIDS Era: A Systematic Review. *Int. J. Tuberc. Lung Dis.* **2011**, *15*, 722–728.

(43) Mitchison, D. A. The Action of Antituberculosis Drugs in Short-Course Chemotherapy. *Tubercle* **1985**, *66*, 219–225.

(44) Zhang, Y.; Wade, M. M.; Scorpio, A.; Zhang, H.; Sun, Z. Mode of Action of Pyrazinamide: Disruption of *Mycobacterium tuberculosis* Membrane Transport and Energetics by Pyrazinoic Acid. *J. Antimicrob. Chemother.* **2003**, *52*, 790–795.

(45) Targeted Tuberculin Testing and Treatment of Latent Tuberculosis Infection. American Thoracic Society. *MMWR. Recomm. Rep.* **2000**, *49*, 1–51.

(46) Alderwick, L. J.; Seidel, M.; Sahm, H.; Besra, G. S.; Eggeling, L. Identification of a Novel Arabinofuranosyltransferase (AftA) Involved in Cell Wall Arabinan Biosynthesis in *Mycobacterium tuberculosis*. *J. Biol. Chem.* **2006**, *281*, 15653–15661.

(47) Lee, R. E.; Mikusovb, K.; Brennan, P. J.; Besra, G. S. Synthesis of the Mycobacterial Arabinose Donor Development of a Basic Arabinosyl-Transferase Assay , and Identification of Ethambutol as an Arabinosyl Transferase Inhibitor. *J. Am. Chem. Soc*. **1995**, 11829–11832.

(48) Burman, W. J.; Gallicano, K.; Peloquin, C. Comparative Pharmacokinetics and Pharmacodynamics of the Rifamycin Antibacterials. *Clin. Pharmacokinet.* **2001**, *40*, 327–341.

(49) Kolyva, A. S.; Karakousis, P. C. *Understanding Tuberculosis - New Approaches to Fighting Against Drug Resistance*; Cardona, P.-J., Ed.; InTech, 2012.

(50) Observed, D.; Regimen, C.; Cohn, D. L.; Catlin, B. J.; Peterson, K. L.; Franklyn, N. J.; Sbarbaro, J. A. A 62-Dose , 6-Month Therapy for Pulmonary and Extrapulmonary Tuberculosis. *Ann. Intern Med*. **1990**, 407–416.

(51) Dutt, A. K.; Jones, L.; Stead, W. W. Short-Course Chemotherapy of Tuberculosis with Largely Twice-Weekly Isoniazid-Rifampin. *Chest* **1979**, *75*, 441–447.

(52) Gordin, F.; Chaisson, R. E.; Matts, J. P.; Miller, C.; de Lourdes Garcia, M.; Hafner, R.; Valdespino, J. L.; Coberly, J.; Schechter, M.; Klukowicz, A. J.; Barry, M. A.; O'Brien, R. J. Rifampin and Pyrazinamide vs Isoniazid for Prevention of Tuberculosis in HIV-Infected Persons: An International Randomized Trial. Terry Beirn Community Programs for Clinical Research on AIDS, the Adult AIDS Clinical Trials Group, the Pan American Health O. *JAMA* **2000**, *283*, 1445–1450.

(53) Stagg, H. R.; Zenner, D.; Harris, R. J.; Muñoz, L.; Lipman, M. C.; Abubakar, I. Treatment of Latent Tuberculosis Infection: A Network Meta-Analysis. *Ann. Intern. Med.* **2014**, *161*, 419–428.

(54) Wehrli, W.; Knüsel, F.; Schmid, K.; Staehelin, M. Interaction of Rifamycin with Bacterial RNA Polymerase. *Proc. Natl. Acad. Sci. U. S. A.* **1968**, *61*, 667–673.

(55) Horne, D. J.; Spitters, C.; Narita, M. Experience with Rifabutin Replacing Rifampin in the Treatment of Tuberculosis. *Int. J. Tuberc. Lung Dis.* **2011**, *15*, 1485–1489, i.

(56) Sharma, S. K.; Sharma, A.; Kadhiravan, T.; Tharyan, P. Rifamycins (rifampicin, Rifabutin and Rifapentine) Compared to Isoniazid for Preventing Tuberculosis in HIV-Negative People at Risk of Active TB. *Cochrane database Syst. Rev.* **2013**, *7*, CD007545.

(57) Global Report on Surveillanceresponse. *Multidrug and Extensively Drug-Resistant TB (M/XDR-TB) 2010*; 2010.

(58) Gillespie, S. H.; Kennedy, N. Fluoroquinolones: A New Treatment for Tuberculosis? *Int. J. Tuberc. Lung Dis.* **1998**, *2*, 265–271.

(59) Nuermberger, E. L.; Yoshimatsu, T.; Tyagi, S.; O'Brien, R. J.; Vernon, A. N.; Chaisson, R. E.; Bishai, W. R.; Grosset, J. H. Moxifloxacin-Containing Regimen Greatly Reduces Time to Culture Conversion in Murine Tuberculosis. *Am. J. Respir. Crit. Care Med.* **2004**, *169*, 421–426.

(60) Choice of anti-TB drugs used to treat MDR-TB. https://drtbnetwork.org/35-choice-anti-tb-drugs-used-treat-mdr-tb. (Last visited 15 april 2015).

(61) Berning, S. E. The Role of Fluoroquinolones in Tuberculosis Today. *Drugs* **2001**, *61*, 9–18.

(62) Grossman, R. F.; Hsueh, P.-R.; Gillespie, S. H.; Blasi, F. Community-Acquired Pneumonia and Tuberculosis: Differential Diagnosis and the Use of Fluoroquinolones. *Int. J. Infect. Dis.* **2014**, *18*, 14–21.

(63) Laurenzi, M.; Ginsberg, A.; M. Spigelman. Challenges Associated with Current and Future TB Treatment. *Infect. Disord. - Drug Targets* **2007**, *7*, 105–119.

(64) Alvirez-freites, E. J.; Carter, J. L.; Cynamon, M. H.; Minassian, B.; Conf, I.; Agents, A. In Vitro and In Vivo Activities of Gatifloxacin against *Mycobacterium tuberculosis*. *Antimicrobial agents and chemotherapy*. **2002**, *46*, 1022–1025.

(65) Ma, Z.; Lienhardt, C.; McIlleron, H.; Nunn, A. J.; Wang, X. Global Tuberculosis Drug Development Pipeline: The Need and the Reality. *Lancet* **2010**, *375*, 2100–2109.

(66) Results of Phase 3 Clinical Trial of New Tuberculosis Drug Regimen Published in New England Journal of Medicine - http://www.tballiance.org/newscenter/view-brief.php?id=1106#sthash.5s7KBg9E.dpuf.

(67) Berning, S. E. The Role of Fluoroquinolones in Tuberculosis Today. *Drugs* **2001**, *61*, 9–18.

(68) Ginsburg, A.; Grosset, J.; Bishai, W. Fluoroquinolones, Tuberculosis, and Resistance. *Lancet Infect. Dis.* **2003**, *3*, 432–442.

(69) Hooper, D. C. Mode of Action of Fluoroquinolones. *Drugs* **1999**, *58*, 6–10.

(70) Lalloo, U. G.; Ambaram, A. New Antituberculous Drugs in Development. *Curr. HIV/AIDS Rep.* **2010**, *7*, 143–151.

(71) Tsukamura, M.; Mizuno, S. Cross-Resistant Relationships among the Aminoglucoside Antibiotics in *Mycobacterium tuberculosis*. *J. Gen. Microbiol.* **1975**, *88*, 269–274.

(72) Almeida Da Silva, P. E. A.; Palomino, J. C. Molecular Basis and Mechanisms of Drug Resistance in *Mycobacterium tuberculosis*: Classical and New Drugs. *J. Antimicrob. Chemother.* **2011**, *66*, 1417–1430.

(73) Mitchison, D. A. Role of Individual Drugs in the Chemotherapy of Tuberculosis. *Int. J. Tuberc. Lung Dis.* **2000**, *4*, 796–806.

(74) Rieder, H. L.; Arnadottir, T.; Trébucq, A.; Enarson, D. A. Tuberculosis Treatment: Dangerous Regimens? *Int. J. Tuberc. Lung Dis.* **2001**, *5*, 1–3.

(75) Dey, T.; Brigden, G.; Cox, H.; Shubber, Z.; Cooke, G.; Ford, N. Outcomes of Clofazimine for the Treatment of Drug-Resistant Tuberculosis: A Systematic Review and Meta-Analysis. *J. Antimicrob. Chemother.* **2013**, *68*, 284–293.

(76) Jagannath, C.; Reddy, M. V; Kailasam, S.; O'Sullivan, J. F.; Gangadharam, P. R. Chemotherapeutic Activity of Clofazimine and Its Analogues against *Mycobacterium tuberculosis*. In Vitro, Intracellular, and in Vivo Studies. *Am. J. Respir. Crit. Care Med.* **1995**, *151*, 1083–1086.

(77) Van Deun, A.; Maug, A. K. J.; Salim, M. A. H.; Das, P. K.; Sarker, M. R.; Daru, P.; Rieder, H. L. Short, Highly Effective, and Inexpensive Standardized Treatment of Multidrug-Resistant Tuberculosis. *Am. J. Respir. Crit. Care Med.* **2010**, *182*, 684–692.

(78) Mitnick, C.; Horsburgh, C. R. Encouraging News for Multidrug-Resistant Tuberculosis Treatment. *Am. J. Respir. Crit. Care Med.* **2010**, *182*, 1337–1338.

(79) Lee, M.; Lee, J.; Carroll, M. W.; Choi, H.; Min, S.; Song, T.; Via, L. E.; Goldfeder, L. C.; Kang, E.; Jin, B.; Park, H.; Kwak, H.; Kim, H.; Jeon, H. S.; Jeong, I.; Joh, J. S.; Chen, R. Y.; Olivier, K. N.; Shaw, P. A; Follmann, D.; Song, S. D.; Lee, J. K.; Lee, D.; Kim, C. T.; Dartois, V.; Park, S. K.; Cho, S. N.; Barry, C. E. Linezolid for Treatment of Chronic Extensively Drug-Resistant Tuberculosis. *N. Engl. J. Med.* **2012**, *367*, 1508–1518.

(80) Ma, Z.; Lienhardt, C. Toward an Optimized Therapy for Tuberculosis? Drugs in Clinical Trials and in Preclinical Development. *Clin. Chest Med.* **2009**, *30*, 755–768, ix.

(81) Stop TB Partnership Working Group On New TB Drugs: http://www.newtbdrugs.org/pipeline.php_Aug 2014.

(82) Matsumoto, M.; Hashizume, H.; Tomishige, T.; Kawasaki, M.; Tsubouchi, H.; Sasaki, H.; Shimokawa, Y.; Komatsu, M. OPC-67683, a Nitro-Dihydro-Imidazooxazole Derivative with Promising Action against Tuberculosis in Vitro and in Mice. *PLoS Med.* **2006**, *3*, e466.

(83) Skripconoka, V.; Danilovits, M.; Pehme, L.; Tomson, T.; Skenders, G.; Kummik, T.; Cirule, A.; Leimane, V.; Kurve, A.; Levina, K.; Geiter, L. J.; Manissero, D.; Wells, C.

D. Delamanid Improves Outcomes and Reduces Mortality in Multidrug-Resistant Tuberculosis. *Eur. Respir. J.* **2013**, *41*, 1393–1400.

(84) Palomino, J.; Martin, A. Tuberculosis Clinical Trial Update and the Current Anti-Tuberculosis Drug Portfolio. *Curr. Med. Chem.* **2013**, *20*, 3785–3796.

(85) Williams, K. N.; Stover, C. K.; Zhu, T.; Tasneen, R.; Tyagi, S.; Grosset, J. H.; Nuermberger, E. Promising Antituberculosis Activity of the Oxazolidinone PNU-100480 Relative to that of Linezolid in a Murine Model. *Antimicrob. Agents Chemother.* **2009**, *53*, 1314–1319.

(86) Shaw, K. J.; Barbachyn, M. R. The Oxazolidinones: Past, Present, and Future. *Ann. N. Y. Acad. Sci.* **2011**, *1241*, 48–70.

(87) Nikonenko, B. V; Protopopova, M.; Samala, R.; Einck, L.; Nacy, C. A. Drug Therapy of Experimental Tuberculosis (TB): Improved Outcome by Combining SQ109, a New Diamine Antibiotic, with Existing TB Drugs. *Antimicrob. Agents Chemother.* **2007**, *51*, 1563–1565.

(88) Sacksteder, K.; Protopopova, M. Discovery and Development of SQ109: A New Antitubercular Drug with a Novel Mechanism of Action. *Future Microbiol.* **2012**, *7*, 823–837.

(89) Mahajan, R. Bedaquiline: First FDA-Approved Tuberculosis Drug in 40 Years. *Int. J. Appl. basic Med. Res.* **2013**, *3*, 1–2.

(90) Andries, K.; Verhasselt, P.; Guillemont, J.; Göhlmann, H. W. H.; Neefs, J.; Winkler, H.; Van Gestel, J.; Timmerman, P.; Zhu, M.; Lee, E.; Williams, P.; de Chaffoy, D.; Huitric, E.; Hoffner, S.; Cambau, E.; Truffot-Pernot, C.; Lounis, N.; Jarlier, V. A Diarylquinoline Drug Active on the ATP Synthase of *Mycobacterium tuberculosis*. *Science* **2005**, *307*, 223–227.

(91) Koul, A.; Vranckx, L.; Dendouga, N.; Balemans, W.; Van den Wyngaert, I.; Vergauwen, K.; Göhlmann, H. W. H.; Willebrords, R.; Poncelet, A.; Guillemont, J.; Bald, D.; Andries, K. Diarylquinolines Are Bactericidal for Dormant Mycobacteria as a Result of Disturbed ATP Homeostasis. *J. Biol. Chem.* **2008**, *283*, 25273–25280.

(92) Matteelli, A.; Carvalho, A. C.; Dooley, K. E.; Kritski, A. TMC207: The First Compound of a New Class of Potent Anti-Tuberculosis Drugs. *Future Microbiol.* **2010**, *5*, 849–858.

(93) Engohang-Ndong, J. Antimycobacterial Drugs Currently in Phase II Clinical Trials and Preclinical Phase for Tuberculosis Treatment. *Expert Opin. Investig. Drugs* **2012**, *21*, 1789–1800.

(94) Bogatcheva, E.; Hanrahan, C.; Chen, P.; Gearhart, J.; Sacksteder, K.; Einck, L.; Nacy, C.; Protopopova, M. Discovery of Dipiperidines as New Antitubercular Agents. *Bioorg. Med. Chem. Lett.* **2010**, *20*, 201–205.

(95) Bogatcheva, E.; Hanrahan, C.; Nikonenko, B.; de los Santos, G.; Reddy, V.; Chen, P.;

Barbosa, F.; Einck, L.; Nacy, C.; Protopopova, M. Identification of SQ609 as a Lead Compound from a Library of Dipiperidines. *Bioorg. Med. Chem. Lett.* **2011**, *21*, 5353–5357.

(96) Reddy, V. M.; Einck, L.; Nacy, C. A. In Vitro Antimycobacterial Activities of Capuramycin Analogues. *Antimicrob. Agents Chemother.* **2008**, *52*, 719–721.

(97) Koga, T.; Fukuoka, T.; Doi, N.; Harasaki, T.; Inoue, H.; Hotoda, H.; Kakuta, M.; Muramatsu, Y.; Yamamura, N.; Hoshi, M.; Hirota, T. Activity of Capuramycin Analogues against *Mycobacterium tuberculosis*, Mycobacterium Avium and Mycobacterium Intracellulare in Vitro and in Vivo. *J. Antimicrob. Chemother.* **2004**, *54*, 755–760.

(98) Nikonenko, B. V; Reddy, V. M.; Protopopova, M.; Bogatcheva, E.; Einck, L.; Nacy, C. A. Activity of SQ641, a Capuramycin Analog, in a Murine Model of Tuberculosis. *Antimicrob. Agents Chemother.* **2009**, *53*, 3138–3139.

(99) Disratthakit, A.; Doi, N. In Vitro Activities of DC-159a, a Novel Fluoroquinolone, against Mycobacterium Species. *Antimicrob. Agents Chemother.* **2010**, *54*, 2684–2686.

(100) Ahmad, Z.; Minkowski, A.; Peloquin, C. A.; Williams, K. N.; Mdluli, K. E.; Grosset, J. H.; Nuermberger, E. L. Activity of the Fluoroquinolone DC-159a in the Initial and Continuation Phases of Treatment of Murine Tuberculosis. *Antimicrob. Agents Chemother.* **2011**, *55*, 1781–1783.

(101) Makarov, V.; Manina, G.; Mikusova, K.; Möllmann, U.; Ryabova, O.; Saint-Joanis, B.; Dhar, N.; Pasca, M. R.; Buroni, S.; Lucarelli, A. P.; Milano, A.; De Rossi, E.; Belanova, M.; Bobovska, A.; Dianiskova, P.; Kordulakova, J.; Sala, C.; Fullam, E.; Schneider, P.; McKinney, J. D.; Brodin, P.; Christophe, T.; Waddell, S.; Butcher, P.; Albrethsen, J.; Rosenkrands, I.; Brosch, R.; Nandi, V.; Bharath, S.; Gaonkar, S.; Shandil, R. K.; Balasubramanian, V.; Balganesh, T.; Tyagi, S.; Grosset, J.; Riccardi, G.; Cole, S. T. Benzothiazinones Kill *Mycobacterium tuberculosis* by Blocking Arabinan Synthesis. *Science* **2009**, *324*, 801–804.

(102) Makarov, V.; Lechartier, B.; Zhang, M.; Neres, J.; van der Sar, A. M.; Raadsen, S. A; Hartkoorn, R. C.; Ryabova, O. B.; Vocat, A.; Decosterd, L. a; Widmer, N.; Buclin, T.; Bitter, W.; Andries, K.; Pojer, F.; Dyson, P. J.; Cole, S. T. Towards a New Combination Therapy for Tuberculosis with next Generation Benzothiazinones. *EMBO Mol. Med.* **2014**, *6*, 372–383.

(103) Rudolph, A. Antitubercular Benzothiazinones: Synthesis, Activity, Properties and SAR. Dissertation; Martin-Luther-Universität Halle-Wittenberg **2014**.

(104) Mdluli, K.; Spigelman, M. Novel Targets for Tuberculosis Drug Discovery. *Curr. Opin. Pharmacol.* **2006**, *6*, 459–467.

(105) Que, A.; Marrakchi, H.; Lane, G. InhA , a Target of the Antituberculous Drug Isoniazid , Is Involved in a Mycobacterial Fatty Acid Elongation System , FAS-II. *Microbiology.* **2000**, 289–296.

(106) Zhang, Y.; Yew, W. W. Mechanisms of Drug Resistance in *Mycobacterium tuberculosis*. *Int. J. Tuberc. Lung Dis.* **2009**, *13*, 1320–1330.

(107) Machado, D.; Couto, I.; Perdigão, J.; Rodrigues, L.; Portugal, I.; Baptista, P.; Veigas, B.; Amaral, L.; Viveiros, M. Contribution of Efflux to the Emergence of Isoniazid and Multidrug Resistance in *Mycobacterium tuberculosis*. *PLoS One* **2012**, *7*, e34538.

(108) Belanger, A.; Besra, G. The embAB Genes of Mycobacterium Avium Encode an Arabinosyl Transferase Involved in Cell Wall Arabinan Biosynthesis That Is the Target for the Antimycobacterial. *Proc. Natl. Acad. Sci. USA* **1996**, *93*, 11919–11924.

(109) Telenti, A.; Philipp, W. J.; Sreevatsan, S.; Bernasconi, C.; Stockbauer, K. E.; Wieles, B.; Musser, J. M.; Jacobs, W. R. The Emb Operon, a Gene Cluster of *Mycobacterium tuberculosis* Involved in Resistance to Ethambutol. *Nat. Med.* **1997**, *3*, 567–570.

(110) Ribeiro, A. L. D. J. L.; Degiacomi, G.; Ewann, F.; Buroni, S.; Incandela, M. L.; Chiarelli, L. R.; Mori, G.; Kim, J.; Contreras-Dominguez, M.; Park, Y. S.; Han, S. J.; Brodin, P.; Valentini, G.; Rizzi, M.; Riccardi, G.; Pasca, M. R. Analogous Mechanisms of Resistance to Benzothiazinones and Dinitrobenzamides in Mycobacterium Smegmatis. *PLoS One* **2011**, *6*, e26675.

(111) Tahlan, K.; Wilson, R.; Kastrinsky, D. B.; Arora, K.; Nair, V.; Fischer, E.; Barnes, S. W. SQ109 Targets MmpL3 , a Membrane Transporter of Trehalose Monomycolate Involved in Mycolic Acid Donation to the Cell Wall Core of *Mycobacterium tuberculosis*. *Antimicrob. Agents and Chemother.* **2012**, 1797–1809.

(112) Li, K.; Schurig-Briccio, L. A.; Feng, X.; Upadhyay, A.; Pujari, V.; Lechartier, B.; Fontes, F. L.; Yang, H.; Rao, G.; Zhu, W.; Gulati, A.; No, J. H.; Cintra, G.; Bogue, S.; Liu, Y.; Molohon, K.; Orlean, P.; Mitchell, D. A.; Freitas-Junior, L.; Ren, F.; Sun, H.; Jiang, T.; Li, Y.; Guo, R.; Cole, S. T.; Gennis, R. B.; Crick, D. C.; Oldfield, E. Multitarget Drug Discovery for Tuberculosis and Other Infectious Diseases. *J. Med. Chem.* **2014**, *57*, 3126–3139.

(113) Jia, L.; Coward, L.; Gorman, G. Pharmacoproteomic Effects of Isoniazid, Ethambutol, and N-Geranyl-N′-(2-Adamantyl) Ethane-1, 2-Diamine (SQ109) on *Mycobacterium tuberculosis* H37Rv. *J. Pharmacol. Exp. Ther.* **2005**, *315*, 905–911.

(114) Bugg, T. D. H.; Lloyd, A. J.; Roper, D. I. Phospho-MurNAc-Pentapeptide Translocase (MraY) as a Target for Antibacterial Agents and Antibacterial Proteins. *Infect. Disord. Drug Targets* **2006**, *6*, 85–106.

(115) Kimura, K.; Bugg, T. D. H. Recent Advances in Antimicrobial Nucleoside Antibiotics Targeting Cell Wall Biosynthesis. *Nat. Prod. Rep.* **2003**, *20*, 252–273.

(116) Haouz, A.; Vanheusden, V.; Munier-Lehmann, H.; Froeyen, M.; Herdewijn, P.; Van Calenbergh, S.; Delarue, M. Enzymatic and Structural Analysis of Inhibitors Designed against *Mycobacterium tuberculosis* Thymidylate Kinase. New Insights into the Phosphoryl Transfer Mechanism. *J. Biol. Chem.* **2003**, *278*, 4963–4971.

(117) Khisimuzi Mdlul.; Zhenkun Ma. *Mycobacterium tuberculosis* DNA Gyrase as a Target

for Drug Discovery. *Infect. Disord. - Drug Targets* **2007**, *7*, 159–168.

(118) Takiff, H. E.; Salazar, L.; Guerrero, C.; Philipp, W.; Huang, W. M.; Kreiswirth, B.; Cole, S. T.; Jacobs, W. R.; Telenti, A. Cloning and Nucleotide Sequence of *Mycobacterium tuberculosis* gyrA and gyrB Genes and Detection of Quinolone Resistance Mutations. *Antimicrob. Agents Chemother* **1994**, *38*, 773–780.

(119) Piton, J.; Petrella, S.; Delarue, M.; André-Leroux, G.; Jarlier, V.; Aubry, A.; Mayer, C. Structural Insights into the Quinolone Resistance Mechanism of *Mycobacterium tuberculosis* DNA Gyrase. *PLoS One* **2010**, *5*, e12245.

(120) Aldred, K.; Kerns, R.; Osheroff, N. Mechanism of Quinolone Action and Resistance. *Biochemistry* **2014**.

(121) Escribano, I.; Rodríguez, J. C.; Llorca, B.; García-Pachon, E.; Ruiz, M.; Royo, G. Importance of the Efflux Pump Systems in the Resistance of *Mycobacterium tuberculosis* to Fluoroquinolones and Linezolid. *Chemotherapy* **2007**, *53*, 397–401.

(122) Blanchard, J. S. Molecular Mechanisms of Drug Resistance in *Mycobacterium tuberculosis*. *Annu. Rev. Biochem.* **1996**, *65*, 215–239.

(123) Piddock, L. Accumulation of Rifampicin by Mycobacterium Aurum, Mycobacterium Smegmatis and *Mycobacterium tuberculosis*. *J. Antimicrob. Chemother.* **2000**, 159–165.

(124) Davies, J.; Gorini, L.; Davis, B. D. Misreading of RNA Codewords Induced by Aminoglycoside Antibiotics. *Mol. Pharmacol.* **1965**, *1*, 93–106.

(125) Honore, N.; Marchal, G.; Cole, S. T. Novel Mutation in 16S rRNA Associated with Streptomycin Dependence in *Mycobacterium tuberculosis*. *Antimicrob. Agents Chemother.* **1995**, *39*, 769–770.

(126) Honoré, N.; Cole, S. T. Streptomycin Resistance in Mycobacteria. *Antimicrob. Agents Chemother.* **1994**, *38*, 238–242.

(127) Manjunatha, U.; Boshoff, H. I. M.; Barry, C. E. The Mechanism of Action of PA-824. *Commun. Integr. Biol.* **2014**, *2*, 215–218.

(128) Stover, C. K.; Warrener, P.; VanDevanter, D. R.; Sherman, D. R.; Arain, T. M.; Langhorne, M. H.; Anderson, S. W.; Towell, J. A.; Yuan, Y.; McMurray, D. N.; Kreiswirth, B. N.; Barry, C. E.; Baker, W. R. A Small-Molecule Nitroimidazopyran Drug Candidate for the Treatment of Tuberculosis. *Nature* **2000**, *405*, 962–966.

(129) Manjunatha, U. H.; Boshoff, H.; Dowd, C. S.; Zhang, L.; Albert, T. J.; Norton, J. E.; Daniels, L.; Dick, T.; Pang, S. S.; Barry, C. E. Identification of a Nitroimidazo-Oxazine-Specific Protein Involved in PA-824 Resistance in *Mycobacterium tuberculosis*. *Proc. Natl. Acad. Sci. U. S. A.* **2006**, *103*, 431–436.

(130) Scorpio, A.; Zhang, Y. Mutations in pncA, a Gene Encoding Pyrazinamidase/nicotinamidase, Cause Resistance to the Antituberculous Drug

Pyrazinamide in Tubercle Bacillus. *Nat. Med.* **1996**, *2*, 662–667.

(131) Zhang, Y.; Mitchison, D. The Curious Characteristics of Pyrazinamide: A Review. *Int. J. Tuberc. Lung Dis.* **2003**, *7*, 6–21.

(132) Juréen, P.; Werngren, J.; Toro, J.-C.; Hoffner, S. Pyrazinamide Resistance and pncA Gene Mutations in *Mycobacterium tuberculosis*. *Antimicrob. Agents Chemother.* **2008**, *52*, 1852–1854.

(133) Cheng, S. J.; Thibert, L.; Sanchez, T.; Heifets, L.; Zhang, Y. pncA Mutations as a Major Mechanism of Pyrazinamide Resistance in *Mycobacterium tuberculosis*: Spread of a Monoresistant Strain in Quebec, Canada. *Antimicrob. Agents Chemother.* **2000**, *44*, 528–532.

(134) Cox, E.; Laessig, K. FDA Approval of Bedaquiline — The Benefit–Risk Balance for Drug-Resistant Tuberculosis. *The New England journal of medicine* **2014**, 2014–2016.

(135) Haagsma, A. C.; Abdillahi-Ibrahim, R.; Wagner, M. J.; Krab, K.; Vergauwen, K.; Guillemont, J.; Andries, K.; Lill, H.; Koul, A.; Bald, D. Selectivity of TMC207 towards Mycobacterial ATP Synthase Compared with That towards the Eukaryotic Homologue. *Antimicrob. Agents Chemother.* **2009**, *53*, 1290–1292.

(136) Huitric, E.; Verhasselt, P.; Koul, A.; Andries, K.; Hoffner, S.; Andersson, D. I. Rates and Mechanisms of Resistance Development in *Mycobacterium tuberculosis* to a Novel Diarylquinoline ATP Synthase Inhibitor. *Antimicrob. Agents Chemother.* **2010**, *54*, 1022–1028.

(137) Uhlin, M.; Andersson, J.; Zumla, A.; Maeurer, M. Adjunct Immunotherapies for Tuberculosis. *J. Infect. Dis.* **2012**, *205 Suppl* , S325–S334.

(138) Alzeer, A. H.; FitzGerald, J. M. Corticosteroids and Tuberculosis: Risks and Use as Adjunct Therapy. *Tuber. Lung Dis.* **1993**, *74*, 6–11.

(139) Senderovitz, T.; Viskum, K. Corticosteroids and Tuberculosis. *Respir. Med.* **1994**, *88*, 561–565.

(140) Http://www.a-star.edu.sg/Media/News/Press-Releases/ID/3740/Anti-diabetic-drug-springs-new-hope-for-tuberculosis-patients.aspx. Anti-Diabetic Drug Springs New Hope for Tuberculosis Patients. **2014**.

(141) Singhal, A.; Jie, L.; Kumar, P.; Hong, G. S.; Leow, M. K.-S.; Paleja, B.; Tsenova, L.; Kurepina, N.; Chen, J.; Zolezzi, F.; Kreiswirth, B.; Poidinger, M.; Chee, C.; Kaplan, G.; Wang, Y. T.; De Libero, G. Metformin as Adjunct Antituberculosis Therapy. *Sci. Transl. Med.* **2014**, *6*, 263ra159–ra263ra159.

(142) Maiga, M.; Ammerman, N. C.; Maiga, M. C.; Tounkara, A.; Siddiqui, S.; Polis, M.; Murphy, R.; Bishai, W. R. Adjuvant Host-Directed Therapy with Types 3 and 5 but Not Type 4 Phosphodiesterase Inhibitors Shortens the Duration of Tuberculosis Treatment. *J. Infect. Dis.* **2013**, *208*, 512–519.

(143) Ughachukwu, P.; Unekwe, P. Efflux Pump-Mediated Resistance in Chemotherapy. *Ann. Med. Health Sci. Res.* **2012**, *2*, 191–198.

(144) Bambeke, F.; Pages, J.-M.; Lee, V. Inhibitors of Bacterial Efflux Pumps as Adjuvants in Antibiotic Treatments and Diagnostic Tools for Detection of Resistance by Efflux. *Recent Pat. Antiinfect. Drug Discov.* **2006**, *1*, 157–175.

(145) Adams, K. N.; Szumowski, J. D.; Ramakrishnan, L. Verapamil, and Its Metabolite Norverapamil, Inhibit Macrophage-Induced, Bacterial Efflux Pump-Mediated Tolerance to Multiple Anti-Tubercular Drugs. *J. Infect. Dis.* **2014**, *210*, 456–466.

(146) Gupta, S.; Cohen, K. A.; Winglee, K.; Maiga, M.; Diarra, B.; Bishai, W. R. Efflux Inhibition with Verapamil Potentiates Bedaquiline in *Mycobacterium tuberculosis*. *Antimicrob. Agents Chemother.* **2014**, *58*, 574–576.

(147) Martins, M. Is Adjuvant Therapy a Potential Road for Fighting *Mycobacterium tuberculosis* Resistance? *Expert Rev. Anti. Infect. Ther.* **2012**, *10*, 1225–1227.

(148) Balemans, W.; Vranckx, L.; Lounis, N.; Pop, O.; Guillemont, J.; Vergauwen, K.; Mol, S.; Gilissen, R.; Motte, M.; Lançois, D.; De Bolle, M.; Bonroy, K.; Lill, H.; Andries, K.; Bald, D.; Koul, A. Novel Antibiotics Targeting Respiratory ATP Synthesis in Gram-Positive Pathogenic Bacteria. *Antimicrob. Agents Chemother.* **2012**, *56*, 4131–4139.

Chapter 2: Efflux pumps and Efflux pump inhibitors-An approach to Anti-Tuberculosis Drug Discovery

2.1 Introduction

This chapter presents a brief overview of efflux pumps and various strategies to overcome efflux pump-mediated resistance. A discussion of efflux pumps (EPs) and efflux pump inhibitors (EPIs) is also included followed by a description of various efflux pump inhibitors evaluated against *Mycobacterium tuberculosis*. The chapter concludes with a description of different methods used in this study to potentially counter EP-mediated resistance in TB.

2.2 Resistance in *Mycobacterium tuberculosis*

The phenomenon of resistance in *Mtb* is as old as its discovery. *Mtb* responds to the stress of the inhibiting drug by developing resistance. This resistance in *Mtb* is developed by different mechanisms and can be divided into two types; acquired and intrinsic resistance.

Acquired resistance is developed with time as *Mtb* becomes less susceptible to the drug's inhibitory activity. The acquired resistance in *Mtb* is generated by spontaneous mutation in a specific target gene, causing *Mtb* resistance to a specific drug. Resistance in *Mtb* does not emerge by horizontal gene transfer as is the case with other bacteria due to the absence of plasmids in *Mtb*.[1]

The modification of drug targets (**Figure 2.1**) by gene mutation is the most common form of acquired resistance in *Mtb*. For example alteration of the *tlyA* gene causes resistance against aminoglycosides like capreomycin and viomycin in *Mtb*.[2] The *tlyA* gene is known to code for the enzyme 2'-*O*-methyltransferase enzyme, which is responsible for the methylation of 16S and 23S ribosomal RNA at nucleotide C1409 and C1920, respectively. The mutation of this gene disturbs the methylation of ribosomes affecting the susceptibility of the ribosomes to selected drugs.[3]

The second example is the alteration in DNA encoded proteins causing FQ resistance. The mutation in *gyrA* and *gyrB* genes encoding for DNA gyrase leads to changes in the structure of the quinolone binding pocket (QBP) resulting in reduction of its affinity for FQ drugs.[4]

Intrinsic resistance is a phenotypic property of *Mtb* to resist the activity of a drug through its inherent structural or functional characteristics. The other term used for this type of resistance is insensitivity as this causes *Mtb* to remain insensitive to some drugs. Intrinsic resistance mainly causes restricted influx of drugs due to the highly impermeable cell wall, which is composed of mycolic acids and reduced intracellular accumulation due to putative EPs (**Figure 2.1**).[5]

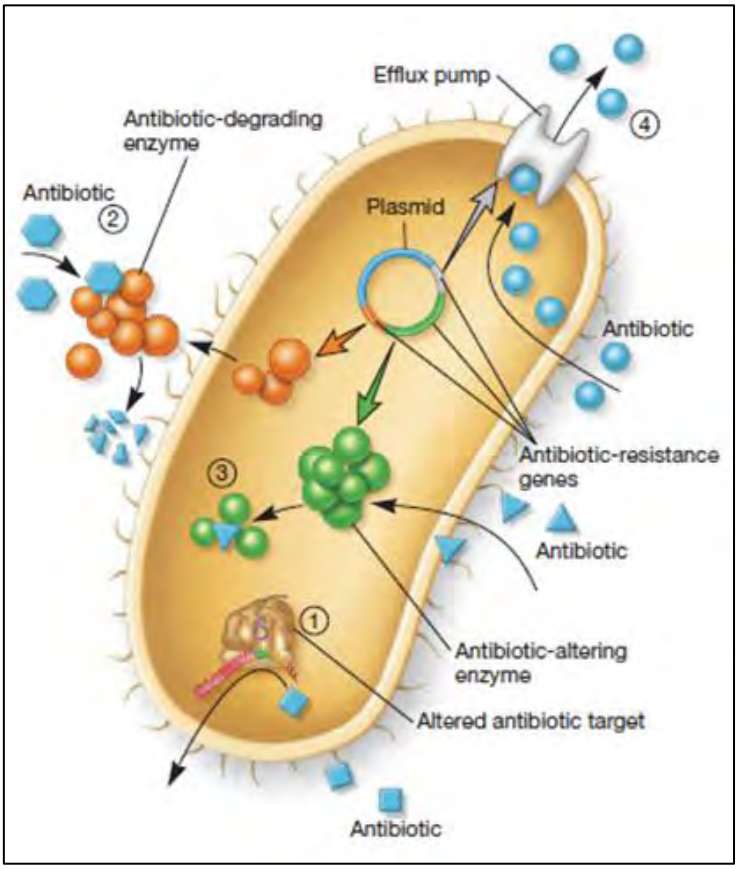

Figure 2.1: Mechanism of resistance in *Mtb*: 1) Modification of drug target; 2) Degradation of drug; 3) Inactivation of drug; 4) Efflux pump.[6]

Cell wall impermeability is the first line of defence of *Mtb* and restricts the entrance of drugs thereby protecting the *Mtb* from the inhibitory activity of the drugs. The *Mtb* cell wall is composed of covalently linked peptidoglycan, arabinogalactan and mycolic acid molecules.[7] The first two components resist the entrance of hydrophobic drugs like RIF and FQs while the mycolic acid resists the influx of both hydrophobic and hydrophilic drugs like INH and PYZ.

Efflux pumps (EPs) (**Figure 2.1**) synergise with cell wall impermeability to provide additional resistance to anti-TB drugs in *Mtb*. This leads to a reduction in the intracellular concentration to sub optimal levels with attendant reduction in the potency of drugs.[8] These EPs are encoded by different *Mtb* genes leading to resistance to FQs, erythromycin (ERY) and tetracycline (TET). The EPs also contribute toward the low level resistance to INH, RIF and other drugs.[9] The EP mechanism of resistance is also a main contributor to resistance in cancer chemotherapy.[10] This topic will be discussed in sections **2.3.**

2.2.1 Mechanism of intrinsic resistance in *Mycobacterium tuberculosis*

Intrinsic resistance cannot be explained completely on the basis of cell wall permeability and EPs, but other aspects have to be considered (**Figure 2.1**). [11,12,13] These include:

a) Enzymatic degradation of drugs.
b) Drug inactivation.
c) Target mimicry.

The resistance towards a particular antimycobacterial agent arises either due to a single or a combination of these mechanisms.

2.2.1.1 Enzymatic degradation of drugs

Enzyme degradation is another method used by *Mtb* to avoid the antibacterial activity of drugs by directly degrading them to non-effective forms. The degradation is usually carried out by various enzymes encountered during transportation of the drugs to their intended targets. This mode of resistance is well studied in the case of β-lactams. The β-lactamase enzyme hydrolyses the β-lactam ring and makes the drug ineffective.[14] This is the main reason for the resistance against β-lactam drugs like ampicillin, amoxicillin, and imipenem in *Mtb.*

2.2.1.2 Inactivation of drugs

The ability of *Mtb* to inactivate anti-TB drugs *via* direct chemical modification is also responsible for resistance against various drugs. For example, the recent findings of resistance against aminoglycosides has been attributed to the modification caused by various acetyltransferases.[15] *In vitro* studies showed that multiple amino groups were acetylated by acetyl-coenzyme, which acts as acetyl donors, making the drugs ineffective.[16]

2.2.1.3 Target mimicry

Molecular mimicry of certain drug targets is another mechanism of intrinsic resistance in *Mtb*. This defence tactic can be explained using the example of the failure of certain FQ drugs due to the resistance caused by the MfpA protein.[11] The FQs act on bacteria by inhibiting the transcription, replication, and repair of DNA by interfering with DNA gyrase. The MfpA protein has many similarities with DNA in respect of shape, size, and electronic nature, and is considered to acts as a DNA mimic.[17] Due to these similarities, MfpA is able to bind to the DNA gyrase inhibiting its normal activity and thereby rescuing it from the activity of the FQ drugs.[11]

2.3 Efflux pump mechanism

EPs are expressed in all living cells, including gram positive and negative bacteria. *Mtb* expresses the largest number of putative EPs in comparison to its genome. These EPs are encoded and regulated by housekeeping genes of *Mtb*.[18] A pre-existing role for EPs is known, as the protection of bacillus from low level intracellular concentrations of toxic substances and metabolites by extruding them out of the cell, for example saving *Mtb* from dyes, bile salts and fatty acids (**Figure 2.2**) in the host's body. EPs are also very important in maintaining homeostasis and physiological balance of *Mtb* growth in the host environment.[19]

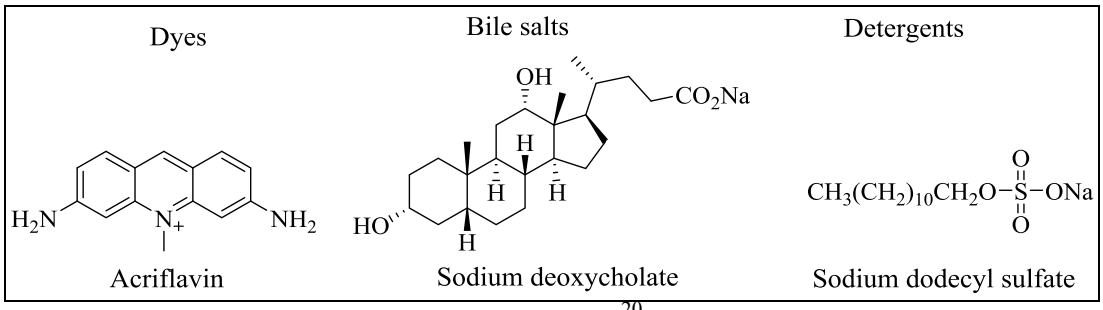

Figure 2.2: Some non-antibiotic Efflux pump substrates.[20]

EP-mediated resistance may have evolved due to the overexpression of EPs or alteration in the EP expressing proteins leading to more efficient EPs. The resistance caused by EPs can be considered as an "accidental and opportunistic" side effect of the transport of unidentified physiological substrates in bacterial and mycobacterial species.[9] Some EPs are substrate specific while others transport functionally dissimilar compounds (including drugs from different classes),[21] and hence are also called multidrug transporters or multidrug EPs.

These EPs reduce the intracellular concentration of various antibacterial agents, resulting in

the survival of bacteria. The EPs assist *Mtb* to survive in the presence of an anti-TB drug until resistance is acquired leading to the development of resistant clones.

2.3.1 Classification of efflux pumps

EPs are classified into different classes and families on the basis of their energetics and structural characteristics. Primarily, EPs are classified into primary and secondary transporters.[19,20]

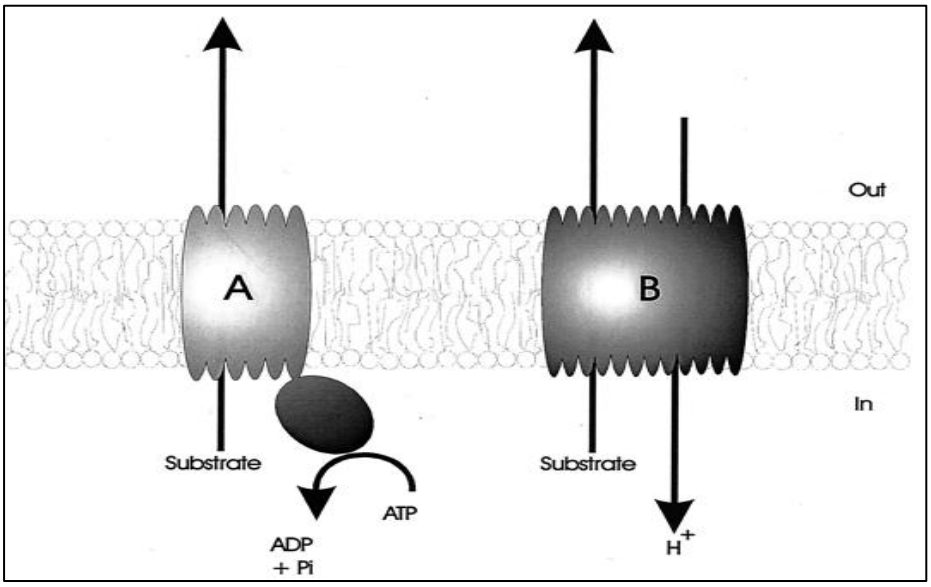

Figure 2.3: Schematic representation of the two major classes of multidrug transporters. (A) ABC-type multidrug transporters are driven by energy generated from ATP hydrolysis. (B) Secondary multidrug transporters manage the extrusion *via* coupling the exchange of substrate with protons or sodium ions.[21]

Primary transporters are energised by adenosine triphosphate (ATP) hydrolysis **(Figure 2.3)** and named as ATP-binding cassette (ABC) family. These EPs are responsible for the transport of many toxins, metabolites and drugs.[22] The ABC cytoplasmic domain is divided into two pairs, one ATP binding domain and a hydrophobic trans domain.[23] The nucleotide binding domains are highly homologous and consist of Walker A and Walker B motifs, regular for all ATP binding proteins and an ABC transporter specific signature motif.[24] In *Mtb*, 2.5% of the entire genome encodes for the ABC transporters and comprises 37 completely and incompletely identified ABC transporters.[25] These ABC transporters confer low level resistance to many drugs (summarised in Table **2.1**) including INH, FQs, β-lactams, STP, chloramphenicol, vancomycin and tetracycline.[25–28] A recently characterized ABC transporter is known to contribute towards the efflux of many substrates including

novobiocins, pyrazolones, biarylpiperazines, bisanilinopyrimidines, pyrroles, and pyridones resulting in the increase in their corresponding MIC values by four to eight fold.[29]

Secondary transporters are multidrug transporters, which work on a proton or sodium driven energy gradient **(Figure 2.3)**. Secondary transporters are subdivided into four families on the basis of size and similarities in their protein structure. These are; a) Major facilitator superfamily (MFS); b) Multidrug and toxic compounds extrusion family (MATE); c) Small multidrug resistance family (SMR); and d) Resistance nodulation division (RND)

The MFS is the largest characterized family of secondary transporters. The MFS transporters are involved in symport, uniport, and antiport of various substrates like sugars, Kreb cycle intermediates, phosphate esters, oligosaccharides and antibiotics in bacteria.[30] Bioinformatics tools have identified 20 EP genes in *Mtb* encoding for MFS drug transporters.[31] MFS efflux protein can be divided into the domains of 12 or 14 transmembrane segments (TMS). Most transporters are substrate specific while six are non-specific and MDR transporters.[32] Various EPs from the MFS family confer resistance to aminoglycosides, tetracycline, FQs, INH, RIF, KAN, and erythromycin (Table **2.1**) **(Figure 2.3)**.

MATE-EPs are responsible for extrusion of various toxic compounds such as metabolites and xenobiotic organic cations,[33] and have been found in various kinds of bacteria mainly in *Vibrio cholerate* (VcrM; VcmA),[34] *Bacterioides thetaiotaomicron* (BexA), *Haemophilus* (HmrM), and *Staphylococcus aureus* (MepA).[35] MATE transporters function on energy driven from the sodium gradient **(Figure 2.3)**. The presence of MATE EPs is not reported for *Mtb* and hence no contribution towards resistance of any anti-TB drugs has been reported (Table **2.1**).[36]

SMR is the smallest known family of secondary bacterial transporters. The SMR transporter proteins consist of approximately 100-140 amino acids in the form of four α-helices. The SMR transporters are driven by a proton motive force (PMF),[37,38] and are responsible for extruding a wide variety of substrates like sugars, peptides, complex carbohydrates, drugs, and metals in various ionic states.[39] The contribution of SMR transporters to *Mtb* drug resistance is very minimal as only one multidrug transporter (Mmr) is known to confer resistance in *Mtb* and extruding drugs like tetracycline, acriflavine, ethidium bromide and erythromycin (Table **2.1**) **(Figure 2.3)**.[40]

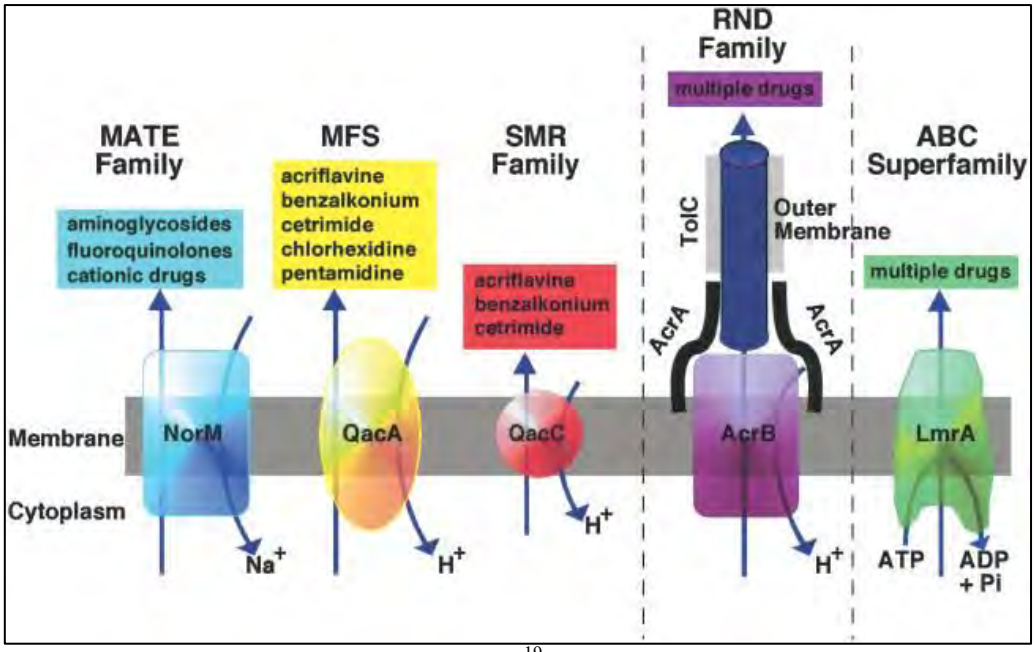

Figure 2.4: Comparison of various families of EPs.[19]

RND transporters are the most studied transporters in gram negative bacteria where they play a crucial role in resistance. The RND transporters consist of polypeptide chains with approximately 700-1300 amino acids. These transporters operate on PMF energy, and exclude a wide range of substrates including neutral, positively or negatively charged molecules, hydrophobic, and hydrophilic compounds **(Figure 2.3)**.[18,19] Approximately 15 transmembrane putative EP proteins in *Mtb* are predicted from the RND family and named as MmpL (Mycobacterial membrane protein, Large), since they are only found in *Mtb*.[41]

Table 2.1: List of efflux pump genes, transporters and corresponding drug substrates in *Mtb* (adapted from Louw G.E. *et al*,[9] Viveiros, Martins, Rodrigues *et* al[42] and Rahul *et. al*.[43])

Family	Efflux Pump	Drug Substrates	Reference
ABC	*pstB*	INH, RIF, EMB, CIP	44
ABC	Rv2686c-Rv2687c-Rv2688c	FQs	27
ABC	drrA-drrB-drrC	STP, TET, EMB, CIP	26
ABC	Rv1747	INH	25
ABC	Rv0194	β-lactam, STP, TET, CIP, VAN	28
ABC	Rv1456c-Rv1457v-Rv1458c	One of first line drug INH, RIF, STP, EMB	45
MFS	Rv1258c	INH, RIF, EMB, OFL	46–48
MFS	Rv1877	TET, KAN, ERY	49
MFS	Rv1634	FQs	50
MFS	P55	TET, RIF, Aminoglycosides	51–54
MFS	Rv2333c	TET	55
SMR	Mmr	EB, ERY	40
RND	MpL7	INH	56–59

FQs: Fluoroquinolones; INH: Isoniazid; EMB: Ethambutol; CIP: Ciprofloxacin; STP: Streptomycin; TET: Tetracycline; VA: Viomycin; OFL: Ofloxacin; ERY: Erythromycin; KAN: Kanamycin; EB: Ethidium bromide.

2.3.2 Efflux pumps in macrophages

Mtb in the host body resides in a complex environment of granulomas consisting of macrophages and different immune cells such as T-cells, B-cells, CD4, and CD8 cells. It has been shown that the presence of granulomas reduces the replication and metabolic activities of *Mtb* and sequesters it into a dormant state.[60,61] The slow growing *Mtb* lesions in granulomas initiates different defence mechanisms to counter the immune and drug stress. The induction and regulation of several EPs has been reported as one of the defence

mechanisms post macrophage infection.[52,62–64] Adams and co-workers have shown that induction of EPs immediately after macrophage infection is one of the primary defence mechanisms employed by *Mtb*.[65] The tolerance developed during the non-replicating dormant phase while residing in the macrophage has been reported to be retained in bacteria even after the resumption to growth phase. The EP-mediated resistance during the macrophage invasion leads to acquired and higher levels of resistance.[66,67] Many EPs are known to contribute to the resistance of drugs *in vitro* (Table **2.1**) and during macrophage residence. *Rv1258c* is a well known EP of *Mtb* and mainly targets RIF.[47] The overexpression of *Rv1258c* has been observed during macrophage invasion at sub-inhibitory concentrations of RIF. The hypersensitivity of *Rv1258c* increases the RIF MIC by three times while corresponding mutants shows 2 to 2.5 fold reduction in MIC. This EP dependent tolerance was also shown to be retained in the growth phase.[65]

2.4 Strategies to counter efflux pump mediated resistance

As pointed out in section **2.3**, active EPs are well known mechanisms for resistance in bacteria. These pumps present attractive prospects for the development of anti-TB agents targeting EPs to counter the development of resistance. There are many methods to counter EP-related mechanisms of resistance. These include bypassing EPs as well as their biological and pharmacological inhibition.

Bypassing EPs is an attractive strategy to counter EP-mediated resistance, and has been widely employed during the development of various FQ drugs. The molecular mechanisms of recognising the substrates for EPs in bacteria are still not completely understood. However, structural modification has shown reduction of efflux of antibacterials belonging to a specific family. The third and fourth generation FQs are less susceptible to EPs as compared to first and second generation FQs.[68,69] Thus, optimization of the structure of a drug class might provide a potent antimycobacterial with less susceptibility to EPs.

The biological inhibition of proteins regulated by EPs through neutralizing specific proteins is an emerging approach and presents an opportunity to counter EP-mediated resistance. The translation step of the EP proteins can be targeted using antisense therapy, in which antisense oligonucleotide or small interfering ribonucleic acid (RNA) are selectively used to prevent the transcription of the gene coding for the EPs. The well explored example is the inhibition

of AcrAB EPs in *E. coli.* Deletion of the corresponding gene leads to restoration of susceptibility to FQs in *E coli*.[70] There is always the possibility that this approach can be expanded to other EPs.

The development of pharmacological efflux pump inhibitors (EPIs) is the most widely explored strategy to counter EP-mediated resistance. These EPIs are developed as adjunctive agents and are intended to be used in combination with the known antibacterial agents, which are expected to be the substrates of EPs. The EPIs are used as competitive and non-competitive inhibitors of EPs to overcome the EP-mediated drug resistance. The concept of efflux pump inhibitors is discussed in detail in the following section.

2.5 Efflux pump inhibitors (EPIs)

A decline in anti-infective research has been observed in the past decade resulting in very few anti-infective molecules getting through the drug pipeline. To overcome this drawback in drug development, and pace down the development of resistance in *Mtb* and other bacteria, different strategies need to be employed. The development of novel molecules, which can overcome the resistance mechanisms involving genetic mutations, various enzymes, and EPs is an alternative approach to counter the increasing disease burden.[71] Drug efflux is a common theme known to affect the efficacy of old and new drugs. Hence the approach of developing antibacterial agents to overcome drug efflux can offer new opportunities to combat antibacterial resistance emerging across a wide spectrum of drugs in clinical use. Bacterial EPIs are novel "non-antimicrobial" agents, which have shown potential to shorten TB treatment and shown promise to successfully treat MDR TB.[72] As mentioned earlier, (Section **2.3**), drug tolerance due to EPs is considered one of the major contributing factors to *Mtb* persistence, leading to the emergence of other forms of resistance. Therefore, the development of EPIs presents enormous potential for a breakthrough in drug development.[73]

The mechanism of action of EPIs is not well understood. It has been indicated that an EPI may block EPs by binding directly to the EP in a competitive or non-competitive manner or may form complexes with the antibacterial agent and facilitate the influx and inhibit the efflux of drugs.[74]

2.5.1 Efflux pump inhibitors: proof-of-concept

The mechanism of antibiotic efflux was first discovered in 1980 when it was suggested as one of the factors for tetracycline resistance in enterobacteria.[75] However, EP proteins have been characterised and found to have low homology with human proteins. This makes them suitable targets for drug development.[76]

The concept of using efflux pump inhibitors to accumulate desired antibacterial agents also exists in nature and has been observed in several *Berberis plants* (*Berberis repen*, *B. aquifola*, and *B. fremontii*). In addition to berberine (**Figure 2.5**), which is an antibacterial and substrate to the Nor MDR EPs, *Berberis* plants also synthesize 5'-methoxyhydnocarpin (5'-MHC) (**Figure 2.5**), which inhibits the EP and shows the potentiating effect for berberine in bacteria.[77] This finding led to the evaluation of 5'-MHC as an EPI for a variety of drugs in different bacteria. It was found that 5'-MHC also inhibits efflux of berberine in *Staphylococcous aureus* by inhibiting the *Nor-A* MDR-EP, which also confers resistance to quinolone drugs.[78,79]

The discovery of an EPI from plants intensified the discovery and identification of various EPIs from plants and other natural product sources. The screening of purified natural products from various plants yielded a number of EPIs acting against different EPs of gram positive bacteria.

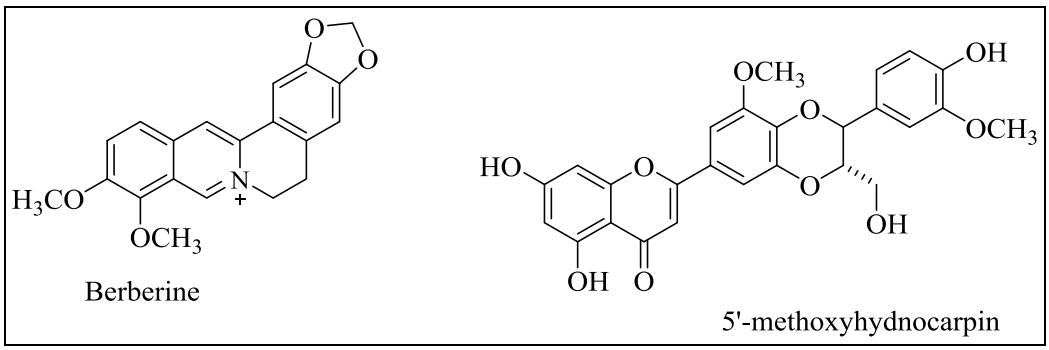

Figure 2.5: Berberine and its EPI 5'-MHC in *Berberis* plants.[77]

The development of EPIs as a strategy to potentiate drugs is not new and has been studied for several decades, highlighting the importance of EPIs in the treatment of diseases. Microcide and Daiichi pharmaceutical started a comprehensive development of EPIs against multiple homologous tripartite RND-EPs (MexAB-OprM, MexCD-OprJ, MexEF-OprN, and MexXY-OprM) in gram negative bacteria *Pseudomonas aeruginos* to potentiate levofloxacin. A

sample strategy led to the identification of a broad spectrum EP inhibitor, **MC-210,110** (**Figure 2.6**) which is also known to inhibit similar RND-EPs in other gram negative bacteria.[80] It was also shown that the selection frequency of FQ-resistant bacteria can be reduced *via* reducing bacterial tolerance due to EPs. In addition, the reduction of both EP-based and target-based resistance was observed in the presence of **MC-207,110**. Hence, the concept of reversing resistance and slowing down its development by use of EPIs was validated.[81–83]

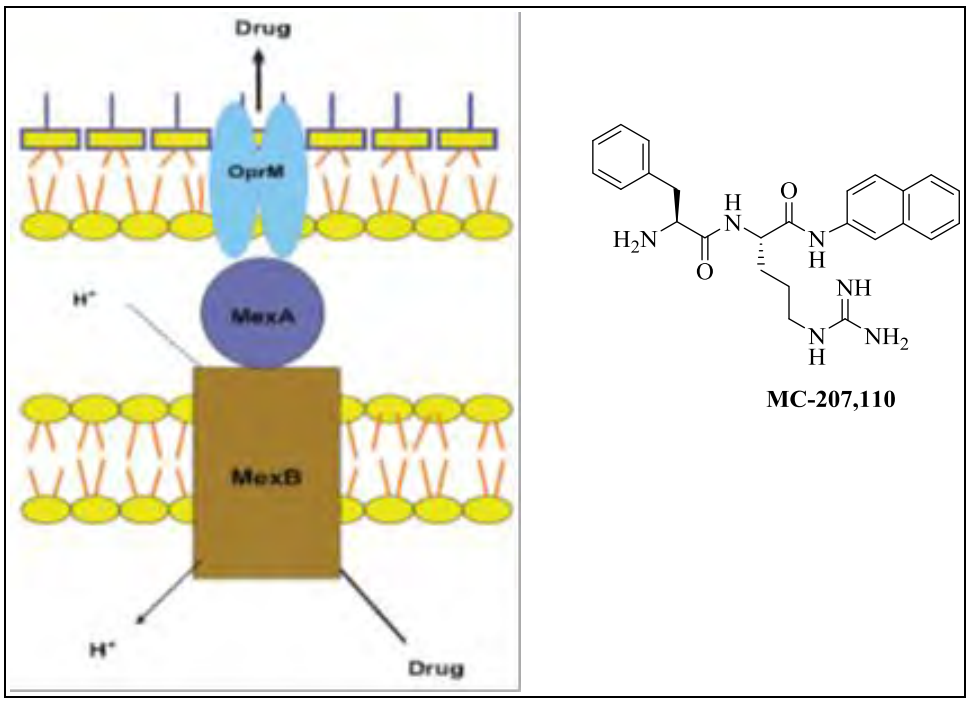

Figure 2.6: MexAB-OprM in *Pesudomonas aeuroginosa* and **MC-207,110**.[84]

The success of **MC-207,110** inspired the development of a range of EPIs with many pharmaceutical companies initiating numerous development programmes.[85]

2.5.2 Ideal characteristics of an EPI:

i) It should potentiate multiple substrates of EPs.
ii) It should not potentiate non-EP substrates.
iii) It should not show any effects in the strains lacking EPs.
iv) It should decrease the extrusion and increase the accumulation of EP substrates.
v) It should not affect the ion gradient in bacteria.

2.5.3 Efflux pump inhibitors in *Mycobacterium tuberculosis*

EPs have been shown to reduce the inhibitory concentration of many anti-TB drugs *in vitro,* in macrophages, and in mouse models.[8,86,87] The encouraging success from the development of EPIs for other bacteria has also inspired the quest to develop EPIs in *Mtb.* The screening of known bacterial EPIs in *Mtb* has led to the identification of many potential EPIs (**Figure 2.7)** shown to also be effective in *Mtb*.

Phenothiazine analogues, chlorpromazine (CPZ) and thioridazine (THZ) (**Figure 2.7**), have shown EP inhibition activity in *Mtb*. CPZ showed potential to inhibit *Mtb* growth directly *in vitro* (MIC_{50} = 6-12 mg/L) but its anti-psychotic side effect led to its structural modification giving rise to THZ.[88] This drug (MIC_{50} = 2.5 mg/L) is the most potent antimycobacterial among all the phenothiazine analogues and is considered as a non-antibiotic helper compound, which synergizes its mode of action with other drugs to facilitate better antibiotic activity for the co-administered drugs.[89] THZ exerts a synergistic effect by antagonising the mechanism responsible for low drug potency. Moreover, THZ is effective against *Mtb* infected human macrophages, and *in vivo Mtb* in mice with multiple targets. Hence, THZ shows good prospects as a molecule with dual action being an EPI and having good antimycobacterial activity. THZ is currently considered for the treatment of MDR and XDR-TB.[90,91]

The isoflavonoid compound biochanin A (**Figure 2.7**) has shown EP inhibition in *Mycobacterium smegmatis* (*M. smeg*) in an *M. smeg* mc^2 asssay. Biochain A exhibited weak antimycobacterial activity but 4-8 fold reduction in the MIC_{50} of ethidium bromide (EB) in an ethidium bromide assay. The synergism with EB (Fractional inhibitory concentration index = 0.25) was also observed.[92]

Piperine (Pip) (**Figure 2.7**) has shown a two-fold potentiating effect on RIF when tested in combination in *Mtb*.[93] Pip also restricts the emergence of resistance against RIF in *Mtb* up to a clinically achievable concentration of 2 mg/ml. In addition, accumulation of EB in the presence of Pip and interaction with binding sites of putative EPs substantiates the efflux pump inhibition property of piperine.[94]

Farsenol (**Figure 2.7**) is a 15-carbon isoprenoid, which also exhibited EP inhibition in *M. smeg*. In addition to better synergistic interaction (FICI = 0.375), compared to CPZ (FICI = 0.75), it has shown a 2-8 fold potentiation of EB.[95]

Reserpine (RSP) (**Figure 2.7**) is a plant alkaloid, an antihypertensive, and a well known inhibitor of ATP-dependent EPs in bacteria.[96] It has been found to possess potentiating effects on FQ drugs in many bacteria including *Mtb*.[97,98] RSP is the second most potent EPI after CPZ and has shown potentiation of various drugs at sub-inhibitory concentrations in *Staphylococcus aureus*. RSP showed an 8-128 fold potentiation of β-lactams in *S. auerus*.[99] The importance of RSP is highlighted by its ability to potentiate INH in *M. smeg* by inhibiting the EP coded by the mmL7 gene.[56]

Timcodar (TIM) (**Figure 2.7**) is a well characterized mammalian EP inhibitor. It has moderate *in vitro* potency (MIC_{90} = 18.7 μg/ml) against *Mtb*. TIM also exhibited a pronounced adjunctive effect with anti-TB drugs *in vitro*, in macrophages, and in an *in vivo* mouse model. A drug synergy was exhibited with RIF, BDQ and MOX in H37Rv infected THP-1 macrophages while an additive effect was observed with PA-824, LZD, INH and CFZ. In the *in vivo* mouse model, a combination of TIM and RIF showed a ten-fold reduction in bacilli load compared to RIF alone with improved efficacy. A faster sterilization effect was also observed in mice treated with a combination of TIM-RIF-INH as compared to a combination of RIF-INH.[100]

Carbonyl cyanide *m*-chlorophenyl hydrazone (CCCP) (**Figure 2.7**) is a protonophore and potentiates antimycobacterial drugs by dissipation of proton movie force (PMF) of the bacterial membrane. It has been shown to inhibit the EP encoded by the *mml7* gene in *M. smeg.* and potentiates INH.[56]

Verapamil (**Figure 2.7**) is a well known calcium channel antagonist, which has been repurposed as an EPI for different EPs as an adjunctive TB agent. It has also shown inhibition of broad spectrum MDR bacterial EPs *in vitro* as well as in experimental models of infection.[65,101] Verapamil has been found to reverse the resistance due to EPs and restore activity of first-line anti-TB drugs in mice infected with a MDR *Mtb* strain.[86]

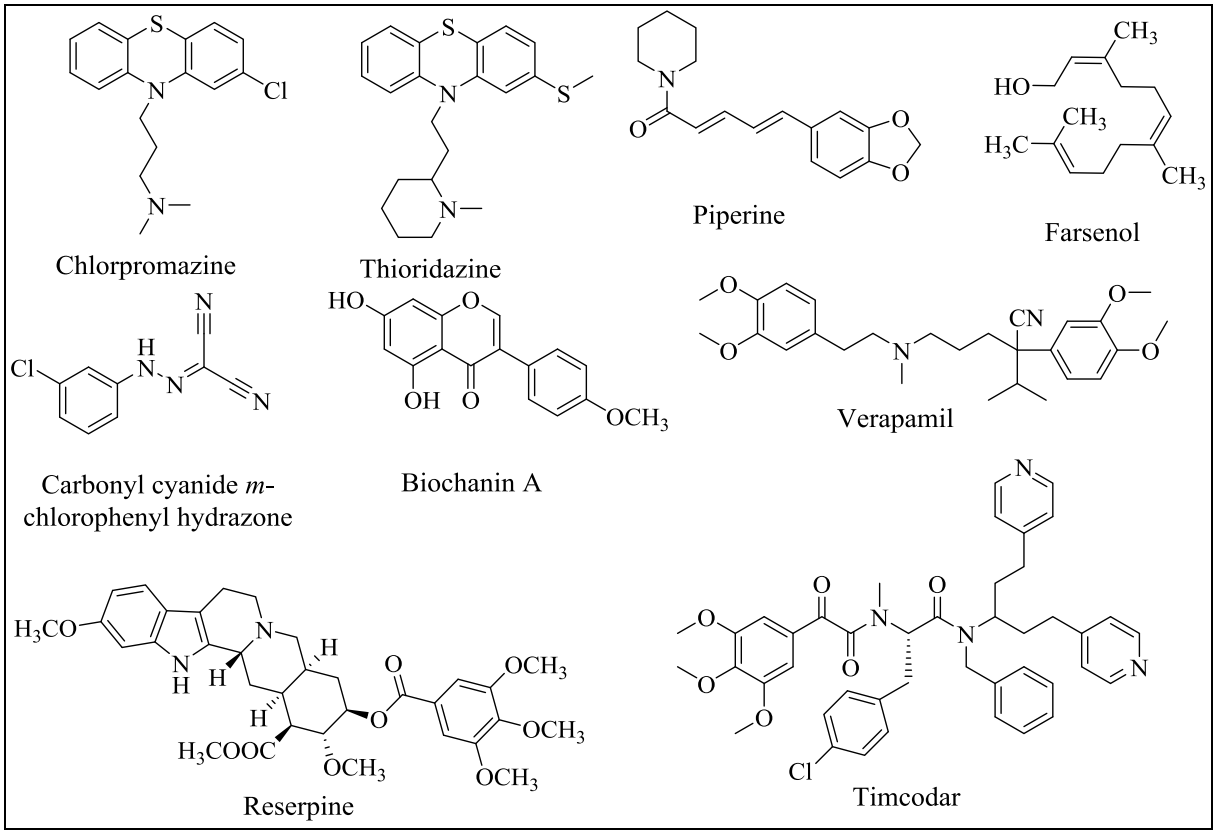

Figure 2.7: Representative compounds which have shown efflux pump inhibition in *Mtb*.

2.5.4 Efflux pump inhibition in *Mtb*-infected macrophages

Mtb resides intracellularly in macrophages especially in the case of pulmonary TB. Therefore, prospective anti-TB drugs are expected to show their bactericidal activity at the intracellular sites where *Mtb* is sequestered.[102] As already pointed out in section **2.3.2**, various MDR EPs are invoked after macrophage invasion by *Mtb* and are responsible for the establishment of high levels of acquired resistance. Hence, an antimycobacterial agent with capabilities to kill *Mtb* in macrophages or potentiates killing in combination with known anti-TB drugs in macrophages will mitigate the problem of drug resistance. On the basis of this, the development of drugs, which can promote intracellular killing of *Mtb via* inhibition of EPs presents good prospects to counter the development of resistance in *Mtb*.

The EPIs known to disturb the ion gradient in bacteria have shown the most promising modulation effect in *Mtb* infected macrophages. Thioridazine (THZ), and verapamil are two such compounds. As already mentioned, THZ has shown both antimycobacterial and EP inhibition properties.[103] Verapamil has specifically exhibited EPI properties and synergistic effects both *in vitro* and in macrophages with first and second line anti-TB drugs as well as with some newly developed drugs.[65]

Figure 2.8 shows the stepwise mode of action of EPIs in macrophages. A phagosome is formed by the macrophage after invagination of *Mtb.* The *Mtb*-containing phagosome, then fuses with the lysosome and forms phagolysosome.[104] Inside the phagolysosome, the Ca^+ and K^+ concentration gets reduced due to their extrusion by EPs from the cytoplasm to the macrophage resulting in non-acidic conditions, which do not allow the activation of hydrolytic enzymes. Therefore, *Mtb* survives and results in the development of persister and resistant forms of *Mtb*. The presence of an EPI like THZ inhibits the EP and accumulates the Ca^+ and K^+ inside the phagolysosome. The accumulation of ions causes the activation of V-ATPase to maintain osmolarity, and proton ions start accumulating in the phagolysosome and causing an acidic pH. The acidic pH activates the hydrolase, resulting in the degradation of the *Mtb*.[104]

2.6 Drug discovery strategies applied in this study to counter efflux pumps

All the EPIs with potentiating effects in *Mtb* are associated with unwanted side effects. Hence there is not a single EPI in clinical development. The encouraging *in vitro*, *ex-vivo* and *in vivo* results shown by various EPIs have revitalized the importance and potential of the development of new EPIs. The EPIs devoid of the side effects are required for successful development to counter the emergence of drug resistance.

Three approaches are employed in this study towards new chemical entities to counter EP-mediated resistance, as follows:

1) Development of verapamil analogues (repositioning).
2) Development of reversed anti-TB agents.
3) Development of hybrid efflux pump inhibitors.

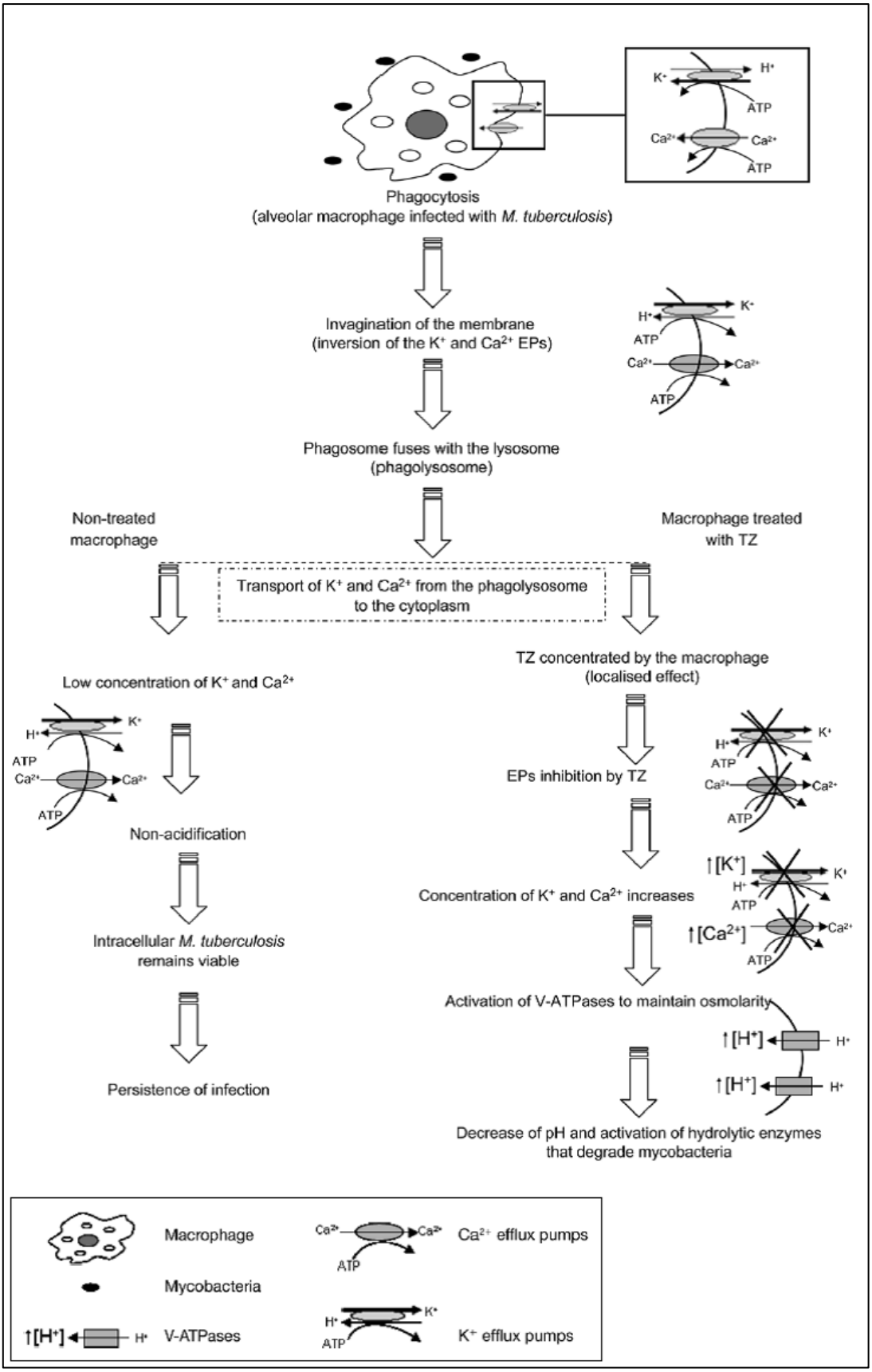

Figure 2.8: The effect of thioridazine on killing of alveolar macrophages infected with *M. tuberculosis*.[104]

2.6.1 Repositioning of verapamil

2.6.1.1 Introduction

Drug repurposing and repositioning of existing antimicrobials and other drugs for non-infectious indications are common approaches used to fast-track drug discovery and development. Drug repurposing is defined as the investigation of existing drugs (which may or may not be in clinical use) for new uses. This does not involve structural modification of the original drug. On the other hand, drug repositioning refers to the structural modification of known drugs (which, also, may or may not be in clinical use) to improve their activity and effectiveness. The application of these approaches may lead to the development of new efflux pump inhibitors (EPIs) for the treatment of tuberculosis.

Verapamil (VER) belongs to the phenylalkylamine prototype and is a well known calcium channel antagonist. It is currently used for the clinical treatment of angina and hypertension. This compound has also been used in the prevention of migraine headaches. VER is a class four antiarrhythmic, and was approved by the FDA in 1982. VER has also been repurposed for different indications, such as oncolytic adenovirus co-infected with cancer, peyronies, Huntington's disease (HD), hypertrophic cardiomyopathy, diabetes, bipolar disorder, and different types of cancers.[105–108] Many studies, including phase 3 randomized clinical trials, have shown the possibility of developing VER as a chemosensitizer in different types of cancers.[109]

2.6.1.2 Verapamil as a MDR modulator in cancer

VER has also proven to be an inhibitor of permeability glycoprotein (Pgp), which is an ATP-binding cassette transporter that affects the cellular accumulation of antiviral, anticancer and anti-TB drugs.[110] In the recent past, VER has been repurposed as a chemosensitizer for different diseases, especially for cancer and tuberculosis.[109,111] In cancer, the use of VER as a MDR reversal agent progressed up to phase 3 clinical trials.[112–114] However, VER is associated with various cardiovascular activities, which are major hurdles in its development as a multi-drug resistance (MDR) modulator. The *R*-enantiomer of VER possesses lower cardiovascular activity in addition to equipotent MDR modulating activity compared to the *S*-enantiomer. Hence, the *R*-isomer was also tested in clinical trials with encouraging results.[115] *Nor*-VER also showed potentiation similar to VER along with lower cytotoxicity than VER. Towards the development of more selective MDR modulators, various analogues of VER

were synthesized, which are summarised below:

LU48895 (**Figure 2.9**) was synthesised by replacing the dimethoxyphenylethyl motif of VER with an aliphatic chain. This new compound showed a two-fold higher potentiation of doxorubicin (DOX) compared to VER, along with a four-fold reduction in cytotoxicity.[116]

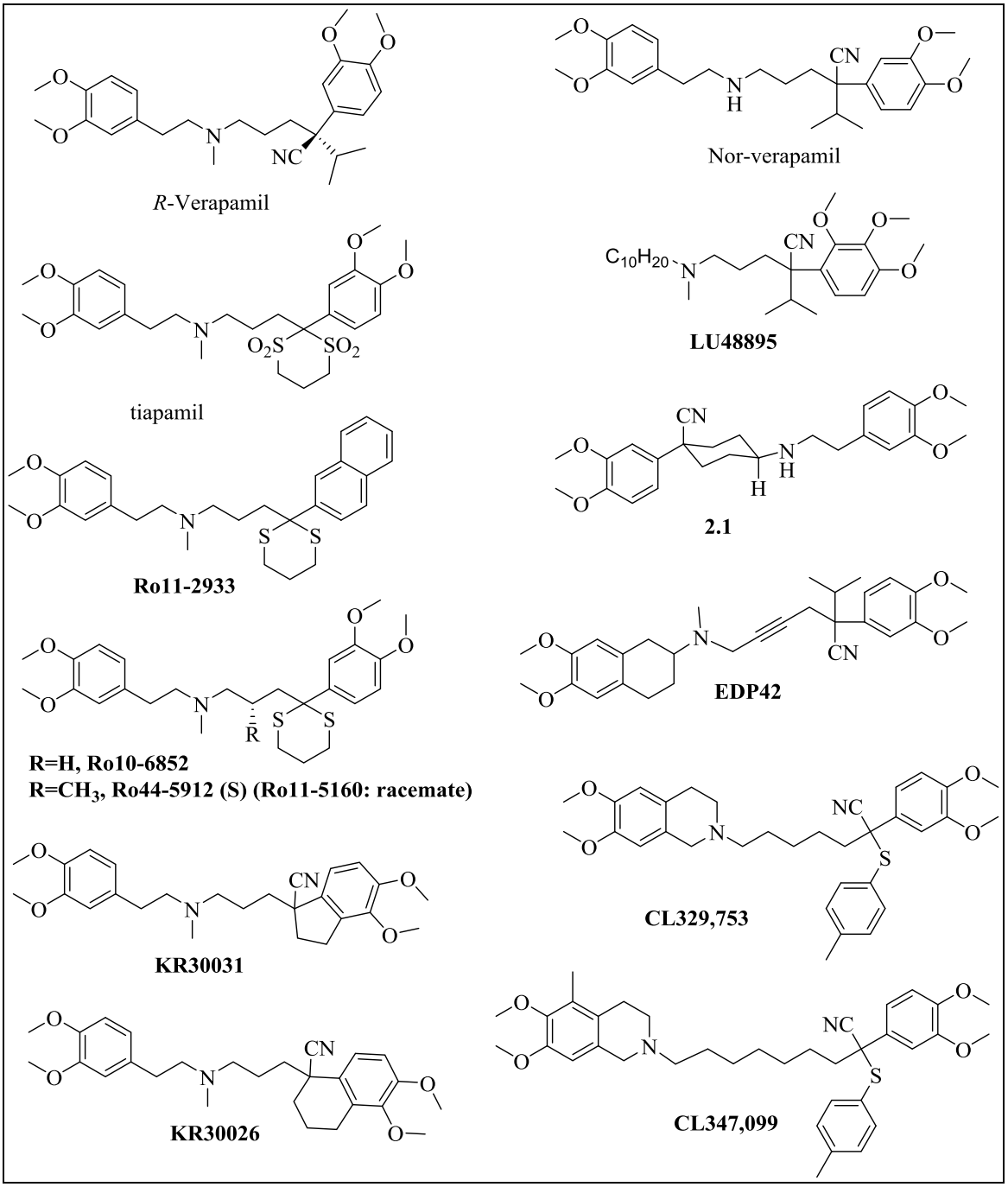

Figure 2.9: Verapamil related MDR modulators for cancer.

The tiapamil-related analogues of VER (**Figure 2.9**) were developed to reverse the Pgp-mediated MDR in cancer cell lines.[117] Many tiapamil analogues, including **Ro10-6852,**

Ro11-5160 and **Ro11-2933** (**Figure 2.9**), showed significantly higher activity in reversing resistance than VER in some selected cell lines. The *S*-enantiomer of **Ro-5160** (**Figure 2.9**) possesses slightly better potency than the R-enantiomer and was, therefore, selected for further studies and development.[118]

Another series of analogues was synthesized by replacing the isopropyl group with various thioethers and changing the amine substituents. This led to the identification of potent molecules such as **CL 329,753**, and **CL 347,099** (**Figure 2.9**) with good pharmacological profiles. These drugs reversed MDR by a ten-fold higher margin than VER and were 70 times less potent as calcium channel antagonists.[119] Similar results were also observed with another series of MDR modulators among which **KR30026** and **KR30031** (**Figure 2.9**) were the most potent analogues with good pharmacological properties.[120] **KR30031** was comparatively less cytotoxic than **KR30026** and 70 times less cytotoxic than VER. Further studies showed that ***R*-KR30031** was two-fold less cytotoxic as a cardiovascular antagonist but equipotent to ***S*-KR30031** as a MDR reversal agent.[121] *In vivo* evaluation in a mouse model showed a 7 times increase in bioavailability of the cancer drug, paclitaxel, when co-administered with **KR30031**.[122]

A large set of VER analogues with reduced molecular flexibility were developed as calcium channel antagonists, and these also showed excellent MDR reversal activity against erythroleukemia cell lines *in vitro*.[123,124] In addition to comparable MDR reversal activity with VER, some analogues also showed reduced to negligible calcium channel antagonism. For example, **EDP42** and **2.1** (**Figure 2.9**) were inactive as cardiovascular agents.[125]

2.6.1.3 Development of verapamil in tuberculosis

As already mentioned, verapamil has also been repurposed as a chemosensitizer in tuberculosis. It has shown encouraging results both *in vitro* and in *in vivo* mouse models of tuberculosis. These encouraging results have led to the recommendation of clinical evaluation of VER in humans in combination with different drug regimens.[126] The various developments of VER in TB as an EPI are briefly discussed below:

VER restored a significant amount of *in vitro* susceptibility to RIF mono-resistant as well as MDR strains of *Mtb*.[127,128] The potentiating effect of VER has also been observed in the case

of STP, INH and clofazimine.[129,130] VER also exhibited a modulation effect with new developing drugs. For instance, an 8-16 fold reduction in the MIC of BDQ was observed in different clinical isolates irrespective of the resistance pattern. A combination of suboptimal concentrations of BDQ and VER in a mouse model has shown equivalent efficacy as the human bioequivalent of BDQ. Therefore, a combination regimen of VER and BDQ presents an attractive drug regimen with the potential to reduce the toxic effects of BDQ and shorten the treatment duration.[131]VER reduced the load of bacilli in mice infected with MDR-TB and restored susceptibility to first line anti-TB drugs (INH, RIF, PYZ) when used as an adjunctive agent.[132] VER also accelerated the bactericidal activity of the standard TB regimen (INH + PYZ + RIF) and achieved persistent sterilization.[133]

In addition to various *in vitro* and *in vivo* studies in mouse models, a model of *Mycobacterium marinum* (*Mm*) in zebrafish was employed by Ramakrishnan and co-workers for the evaluation of VER individually, and in combination with known anti-TB drugs in *Mycobacteria*-infected macrophages.[134] VER showed inhibition of specifically induced efflux pumps after the invasion of macrophages by the mycobacteria. This resulted in reduced intracellular growth of *Mtb*. VER in combination with INH and RIF showed reduced *Mm* survival rate by 15.6 and 9.2 fold, respectively.

VER has also showed intracellular potency in *Mtb* infected THP-1 macrophage cell lines and potentiating effects on multiple drugs. VER impaired the growth of both RIF sensitive and RIF resistant *Mtb* strains in macrophages and reduced RIF survival by 1.4 fold, and inhibited the tolerance against MOX.[86]

2.6.1.4 Solutions to pharmacological concerns of verapamil

There are some serious concerns regarding VER being used as an adjunctive agent in TB chemotherapy. The most prominent issues are the cardiovascular related properties of VER and the high susceptibility toward cytochrome P450, mainly CYP3A4, leading to reduced bioavailability of VER. CYP3A4 is induced by RIF and reduces the bioavailability of VER through rapid metabolism resulting in various metabolites (**Figure 2.10**).[135] Therefore, it is less common to use VER in combination with RIF. Higher doses or replacement of RIF with rifabutin may be an alternative to overcome these problems because rifabutin does not induce CYP 450s to the same extent as RIF.[133]

It has been observed that the potency of VER is independent of its enantiomeric forms. However, cardiovascular activity is dependent on its stereochemistry. As already mentioned, the *R*-enantiomer has reduced cardiovascular properties but equivalent potentiating ability as *S*-VER or the racemic mixture. Therefore, the *R*-enantiomer of VER presents an opportunity to substitute VER as a potentiating agent with attendant reduction in calcium channel antagonism. The metabolite of VER, *Nor*-VER, has also shown comparable potentiating effects to VER along with reduced calcium channel antagonism and presents a possible alternative.[86]

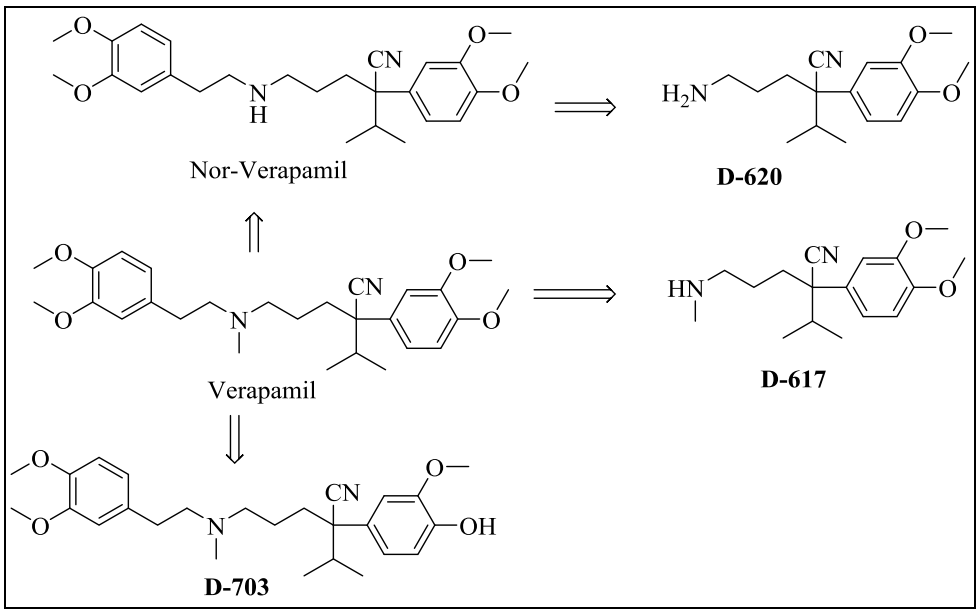

Figure 2.10: Major metabolites of verapamil.[136]

Structural modification of VER is another strategy, which can be employed to identify analogues with the desired pharmacological properties and devoid of unwanted side effects. This strategy delivered promising results in cancer studies, as discussed in section **2.6.1.2**. *However, to our knowledge, there are no literature reports on the structural modification of VER towards identification of chemosensitizers that can reverse drug resistance in Mtb against existing and emerging anti-TB drugs.*

Hence, structure activity relationship studies have been performed in this PhD study towards identifying VER analogues with superior potentiating effects in combination with existing and emerging anti-TB drugs, and which are devoid of undesirable side effects.

2.6.2 Reversed anti-TB agents

2.6.2.1 Introduction

Reversed anti-TB agents (RATAs) are dual action hybrid molecules in which an EPI moiety is covalently linked to a complete anti-TB drug or its molecular framework. These RATAs are designed to reverse the EP-mediated resistance to the corresponding linked anti-TB drugs in the hybrid molecule. The RATAs may present an alternative solution to the various challenges presented by the probable combination therapy of EPIs and anti-TB drugs. These challenges include the requirement of synergy of pharmacokinetic and physiochemical properties of structurally unrelated co-administered compounds, and balancing drug-drug interactions and other dosing related challenges. A strategic design and development of RATAs for various properties may present a solution to the challenges related to physical combination therapy of an EPI and anti-TB drug.

2.6.2.2 Concept of dual action hybrid molecules

The concept of hybrid molecules or dual action drugs is a well-explored strategy to counter the development of drug resistance in various diseases.[137] In a hybrid molecule, two pharmacological molecules or their structural motifs with different functional domains are linked in a single molecular entity in such a way that the resulting molecule can deliver enhanced pharmacological properties. The linking structural motifs are either complete molecules or molecular frameworks consisting of structural features thought to be responsible for the observed pharmacological activity of the original compounds.

The constituents of hybrid molecules are selected in such a way that their desired pharmacological features can be maintained after the fusion to produce hybrid molecules. The linkers used to couple the native molecule/pharmacophoric units can be labile or biologically cleavable, like prodrugs, or they can be stable entities. These linkers are also designed to incorporate various desired pharmacokinetics and physiochemical properties into the hybrid molecule and can be selected *via* various screening methods including modelling and synergistic evaluation of molecules by checker board assays.[138,139] These linkers may cleave hydrolytically or enzymatically *in vivo* to release individual compounds. The site directed delivery of a pharmacological molecule can also be achieved by designing the linkers to be cleaved at desired sites.[140] In addition to these advantages, there are some benefits of administering a hybrid molecule rather than a cocktail of drugs, which is

discussed in the following section.

2.6.2.3 Advantages of hybrid molecules

a) Low cost and reduction in pill burden: The administration of a cocktail of drugs is much more expensive than mono-therapy and presents a higher risk of relapse. Therefore, hybrid drugs present alternative approaches to overcome this challenge. [141,142]

b) Broad spectrum of activity: Hybrid molecules can be designed to manage multiple targets for broad spectrum activity.[143] The multi targeting hybrid can show sensitivity in different resistant strains as well as different bacterial species. This advantage can be illustrated by the following example of AU-FQ hybrid molecule.

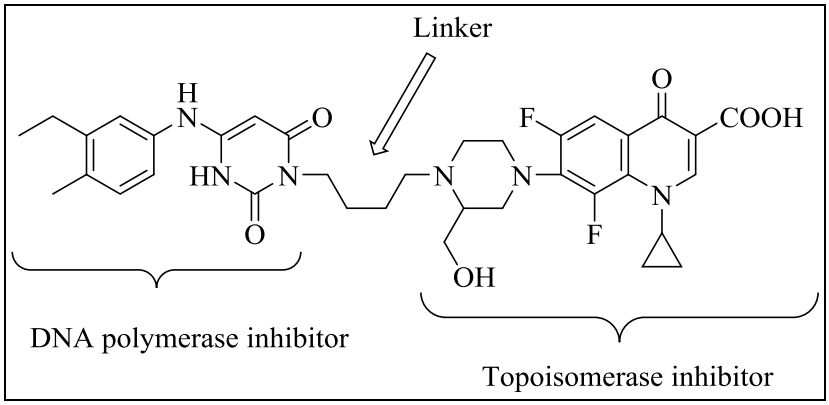

Figure 2.11: Hybrid (AU-FQ) of DNA polymerase and topoisomerase inhibitor

The hybrid molecule (AU-FQ) (**Figure 2.11**) of 6-(3-ethyl-4-methylanilino)uracil unit (AU), a known potent inhibitor of DNA polymerase III in Gram positive bacterium *Bacillus subtilis*, and a fluoroquinolone (FQ) unit known to inhibit bacterial DNA topoisomerase, shows good potencies in Gram positive bacteria (*S. aureus*) and moderate activity in Gram negative bacteria (*E. coli*).[144] In addition to broad spectrum activity against the infection caused by Gram negative and Gram positive bacteria, this hybrid molecule also delayed the development of resistance against two linked antibacterial agents.

c) Enhanced potency and synergy. As mentioned earlier, linkers can be tailored to reduce the toxicity of linking moieties (as in the case of non-toxic prodrug linkers). These linkers can be designed to mask the cytotoxic site of constituent molecules in a transient manner. These prodrug linkers are then cleaved at a site of action and show good prospects for the delivery of a cytotoxic antibacterial agent with enhanced safety and selectivity.[140,145] Therefore, hybrid molecules designed with appropriate linkers may exhibit low cytotoxicity with higher

potency, synergy and safety as compared to their constituent agents.

An example of the above mentioned application of a prodrug is the hybrid molecule developed by Albrecht and co-workers, in which a FQ drug was linked to a β-lactam antibiotic (**Figure 2.12**).[146,147] The most promising analogue was a hybrid of third generation FQ (fleroxacin) and third generation cephalosporin (desacetylceforaxime) linked *via* an ester prodrug (**Figure 2.12**). This analogue showed potent *in vitro* and *in vivo* activity against varieties of gram negative (*E. coli*; MIC = 0.125 μg/ml) and gram positive (*S. aureus*; MIC = 1.0 μg/ml) bacteria.[147]

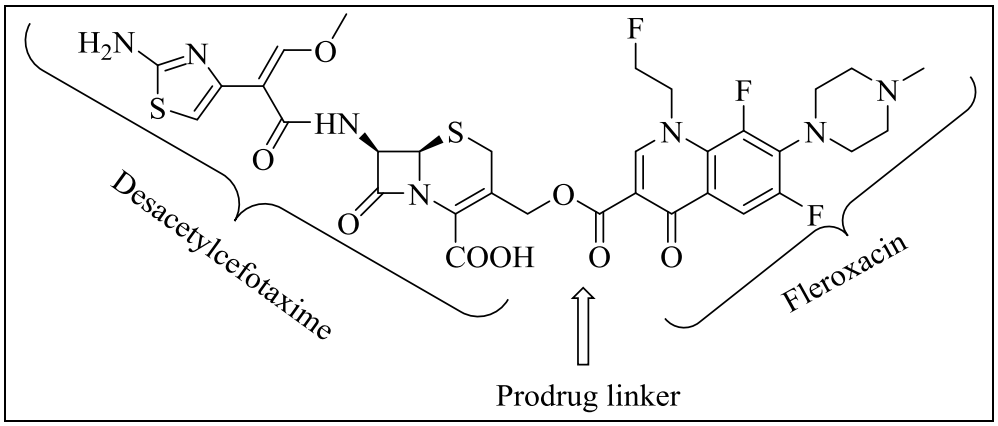

Figure 2.12: Hybrid molecule developed by Albrecht and co-workers with prodrug linkers.[147]

d) Reduction in development of acquired resistance: Hybrid molecules can also be designed to counter the development of acquired resistance. The Oxazolidinone-quinolone hybrid and FQ-aminoglycoside hybrids (**Figure 2.13**) are ideal examples.[148,149]

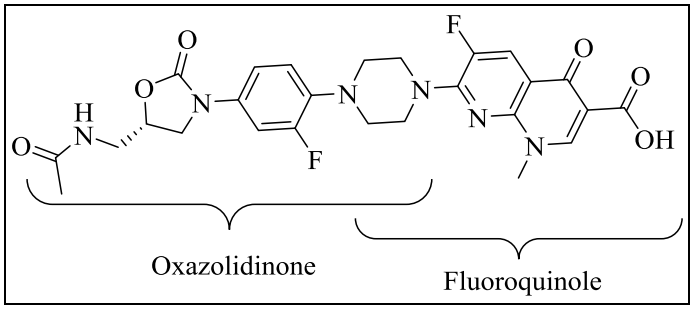

Figure 2.13: Oxazolidinone and fluoroquinolone hybrid.

The hybrid molecule shown in **Figure 2.13** has demonstrated a dual mode of action and strong inhibition of protein synthesis by inhibiting both targets i.e. DNA gyrase and topoisomerase IV in Gram positive and Gram negative bacteria. It showed a 4-16 fold higher potency than linezolid and overcame all the clinically resistant Gram positive bacteria.[148]

Other examples of dual action drugs (Section **2.6.2.2)** with potential to counter the emergence of acquired resistance are reversed chloroquine (RCQs) agents. These RCQs are hybrids of chloroquine (CQ) and a chemosensitizer. This concept will be briefly discussed in the next section.

2.6.2.4 Reversed chloroquine concept

As mentioned earlier, reversed chloroquine (RCQ)-like molecules are one of the illustrative examples of dual action hybrid molecules in which a chemosensitizer and an anti-malarial drug, CQ has been covalently linked.[151] These RCQ molecules were designed to counter the emerging resistance in the human malaria parasite *Plasmodium falciparum* due to mutation in the *pfcrt* gene. This gene codes for the *P. falciparum* chloroquine resistance transporter (PfCRT) protein located in the digestive vacuole (DV),[152–154] which is responsible for the regulation and expression of various transporters of drugs or metabolites. The mutation in the *pfcrt* gene causes over expression of PfCRT-regulated EPs which leads to a reduction in the accumulation of CQ inside the DV.[155]

The reversion of EP-mediated resistance in this parasite was observed by well known chemosensitizers like verapamil and desipramine. Therefore, hybrids of CQ and various chemosensitizers were developed with the aim of reducing cytotoxicity, cost and increasing drug accumulation required for an effective dose (**Figure 2.14**).[156–158]

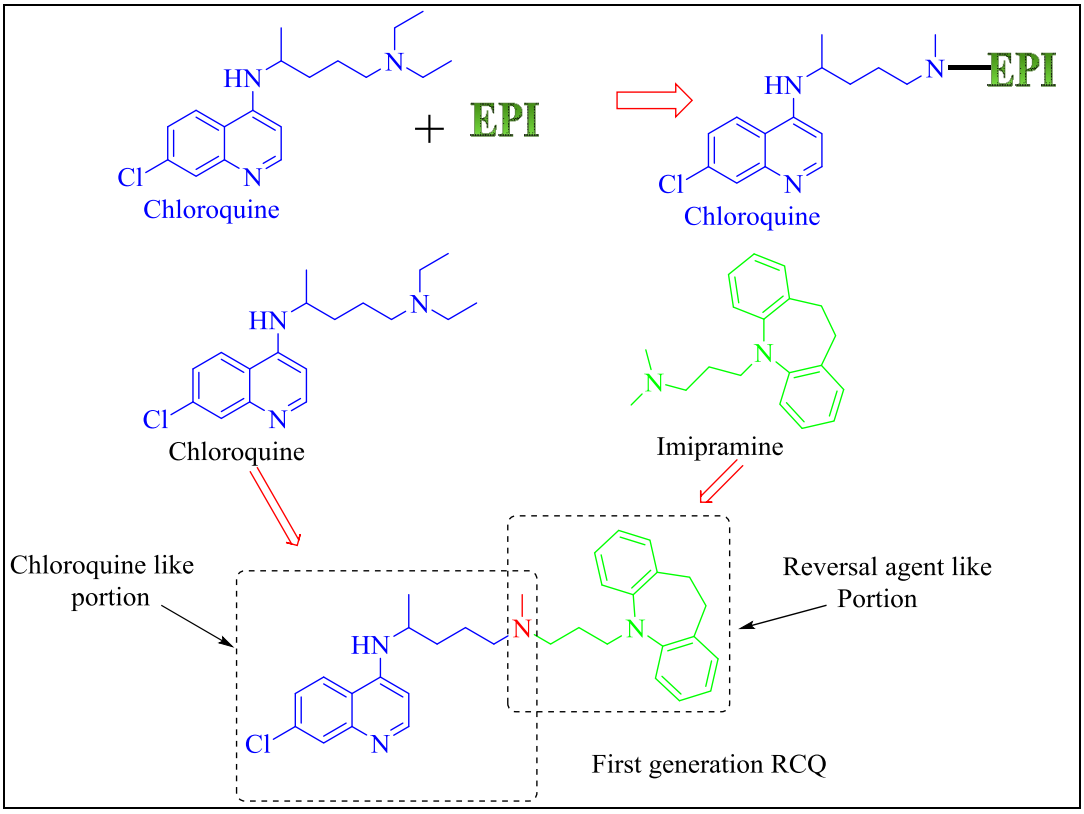

Figure 2.14: First generation RCQ.

The prototype RCQ (**Figure 2.14**) showed a lower IC_{50} value than CQ against both CQ sensitive (CQ^S) and CQ resistant (CQ^R) strains of *P. falciparum*. The good viability and potency of RCQs, *in vitro* and *in vivo* against CQ^S and CQ^R strains demonstrated a proof-of-concept of reversing resistance by RCQ-like molecules. Therefore, various RCQ molecules were developed with various reversal agents (RAs) to optimize the various pharmacological properties.[151]

The success of prototype RCQs led to the development of many second generation RCQ molecules (**Figure 2.15)** with improved pharmacological properties.[159,160]

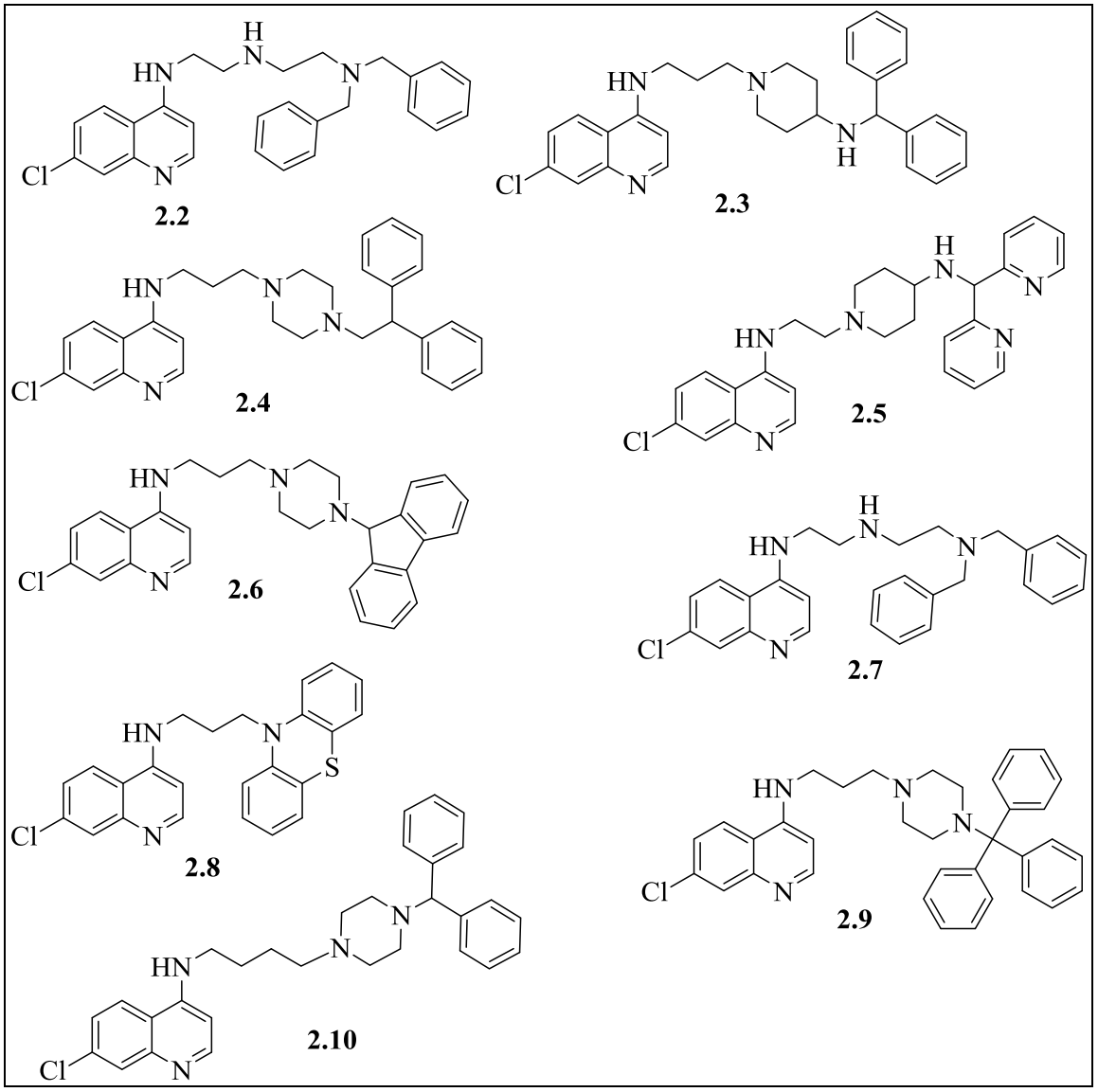

Figure 2.15: Some second generation RCQ molecules.

The various RAs for RCQs were selected on the basis of the pharmacophore identified by *Bhattacharjee et al* (**Figure 2.15**).[161] This pharmacophore is characterised by "two aromatic hydrophobic sites and a hydrogen bond acceptor site, preferably at a side chain nitrogen atom". Therefore, various RAs with open structures i.e. removing the tricyclic nature of imipramine molecule with the expectation of removing central nervous system (CNS) related properties, were selected. The new RCQs were more effective with better pharmacokinetics and pharmacodynamics properties. The RCQ molecule **2.5** showed excellent *in vivo* activity after oral administration, low ClogP values and no obvious cytotoxicity.[159]

2.6.2.5 Dual action antibacterial agents

As explained earlier, EPs are one of the major contributors to MDR resistance in bacteria. Therefore, the potential of dual-action hybrid-like RCQ molecules was also explored for the development of antibacterial agents by Prof. Kim Lewis for the treatment of infection caused by MDR bacterial pathogens. One such example of a dual action antibacterial is the hybrid of an antibacterial biberine and an EPI **INF55**. The berberine is known as a NorA-EP substrate and **INF55** (5-nitro-2-phenylindole) has been identified as inhibitor of NorA-EP. These were covalently linked *via* a non-cleavable methylene spacer to form the **SS14** hybrid (**Figure 2.16**).[162]

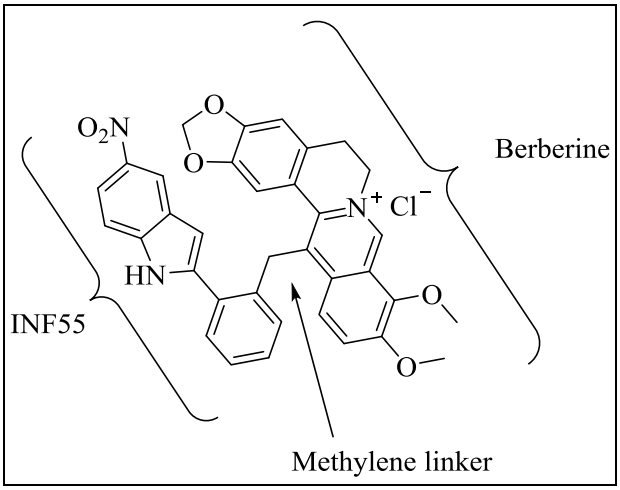

Figure 2.16: Dual action anti-bacterial hybrid **SS14**.[162]

SS14 hybrid was more active than the equivalent combination of biberine and **INF55**, and showed enhanced accumulation of biberine in bacteria. **SS14** indicated the viability of the concept of dual action-based antibacterial drugs by incorporating a bacterial EPI and an anti-bacterial agent.[139,163]

2.6.2.6 Design of dual action reversed anti-TB agents

The promising results shown by RCQ molecules and the antibacterial hybrid **SS14** demonstrates the potential to exploit this innovative approach to design novel anti-TB agents for potential treatment of MDR-TB and XDR-TB.

It has been explained that many anti-TB drugs are substrates of EPs including RIF, INH and STP.[9,42,43] Therefore, the development of dual action hybrid anti-TB agents by covalently linking an EPI and an anti-TB drug is a viable strategy to potentially counter EP-mediated resistance. The reversal agents used in the development of various RCQs also include some

bacterial resistance reversal agents.[164] These reversal agents have shown potentiation of anti-TB drugs in *Mtb* when used in combination.

In this study, these dual action hybrids are referred to as reversed anti-TB agents (RATAs) which are expected to reverse the resistance of corresponding anti-TB drugs in resistant strains of *Mtb*. These reversed anti-TB agents were designed by replacing the CQ moiety in RCQ molecules with various anti-TB drug moieties (**Figure 2.17**).

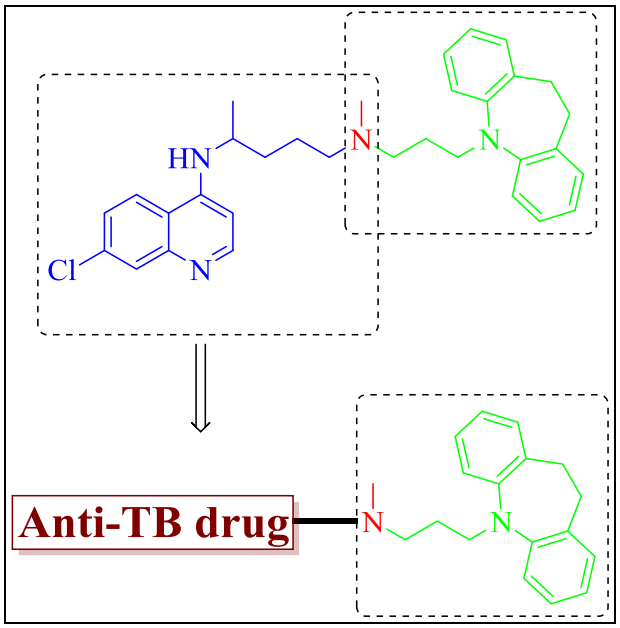

Figure 2.17: Design of reversed anti-TB agents based on the RCQ concept.

In this project, the anti-TB drug isoniazid was covalently linked to various chemosensitizers or EPIs moieties *via* a three carbon alkyl chain (**Figure 2.17**). This approach was employed to develop first generation RATAs towards establishing proof-of-principle.

2.6.3 Hybrid efflux pump inhibitors

2.6.3.1 Introduction

As described earlier (Section **2.6.2.2**), hybrid molecules are synthesised by covalently linking two or more chemical entities with different functional characteristics. In the recent past, the strategy of hybridization was also applied to EPIs with an enhanced potentiation effect. A typical example is the development of an anticancer drug modulator against Pgp.

2.6.3.2 Hybrid efflux pump inhibitors for cancer chemotherapy

Hybrid efflux pump inhibitors (HEPIs) are designed by covalently linking two chemosensitizer or their pharmacophoric subunits. The two units or their motifs are joined in such a way that the structural and functional requirements of a chemosensitizer are not disturbed, such as lipophilicity and the presence of a basic nitrogen.[165]

In order to construct an EPI with enhanced potentiating potential and potentially reduced unwanted side effects, the VER template was used to develop hybrid efflux pump inhibitors by replacing the dimethoxyphenyl group with aromatic phamacophoric units of various chemosensitizers (**Figure 2.18**).

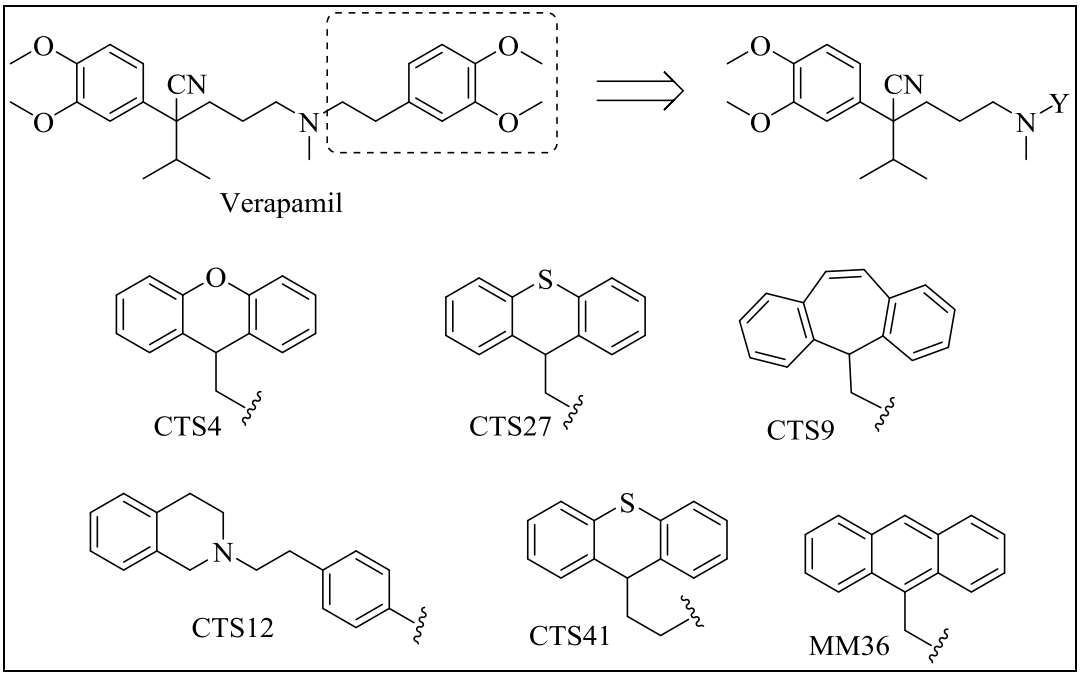

Figure 2.18: Hybrid efflux pump inhibitor developed for cancer chemotherapy.

Many HEPIs, as shown in **figure 2.18,** have been synthesised for cancer chemotherapy. These compounds were evaluated against the human leukaemia cell line K-562/doxR with

increased Pgp expression and AM-l blast cells. Among these, MM36, CTS27 and CTS41 were the most potent modulators, compared to VER, and displayed good MDR-reversal activity.[165] In comparison to VER, these compounds also had a reduced effect on cardiovascular activity in the order MM36 > CTS27 > CTS41 was devoid of cardiovascular activity. Hence, these analogues were selected for further clinical evaluation.[166]

In this study, a brief investigation of the replacement of the dimethoxyphenyl group of VER with a pharmacophoric framework of various chemosensitizers was conducted towards the identification of an EPI with better potentiating potential and which is devoid of undesirable properties found in VER.

2.7 Research question

The research question that this study aimed to answer was whether it would be possible to develop a potential efflux pump inhibitor by structural modification of verapamil, and an antimycobacterial agent from the reversed anti-TB approach as well as a hybrid chemosensitizer for maximum potentiation of anti-TB drug activity in MDR strains

2.8 Specific aims and objectives:

- To design and synthesise verapamil analogues and hybrid efflux pump inhibitors for structure activity relationship studies as potential efflux pump inhibitors, which can potentiate various anti-TB drugs in drug sensitive and drug resistant strains of *Mtb*.
- To pharmacologically evaluate verapamil analogues and hybrid efflux pump inhibitors *in vitro* individually and in combination with various anti-TB drugs.
- To evaluate potent, less cytotoxic verapamil analogues in *Mtb*-infected macrophages, individually and in combination with various anti-TB drugs.
- To design and synthesise a series of reversed anti-TB (isoniazid) molecules as potential antimycobacterial agents able to circumvent drug resistance.
- To pharmacologically evaluate synthesised reversed isoniazids against DS and DR *Mtb* in *in vitro* for antimycobacterial activity, and potent molecules in macrophages for intracellular potency against *Mtb*.

References:

(1) Ramaswamy, S.; Musser, J. Molecular Genetic Basis of Antimicrobial Agent Resistance in

Mycobacterium tuberculosis: 1998 Update. *Tuber. Lung Dis.* **1998**, *79*, 3–29.

(2) Maus, C. E.; Plikaytis, B. B.; Shinnick, T. M. Mutation of tlyA Confers Capreomycin Resistance in *Mycobacterium tuberculosis*. *Antimicrob. Agents Chemother.* **2005**, *49*, 571–577.

(3) Monshupanee, T.; Johansen, S. K.; Dahlberg, A. E.; Douthwaite, S. Capreomycin Susceptibility Is Increased by TlyA-Directed 2'-O-Methylation on Both Ribosomal Subunits. *Mol. Microbiol.* **2012**, *85*, 1194–1203.

(4) Piton, J.; Petrella, S.; Delarue, M.; André-Leroux, G.; Jarlier, V.; Aubry, A.; Mayer, C. Structural Insights into the Quinolone Resistance Mechanism of *Mycobacterium tuberculosis* DNA Gyrase. *PLoS One* **2010**, *5*, e12245.

(5) Jarlier, V.; Nikaido, H. Mycobacterial Cell Wall: Structure and Role in Natural Resistance to Antibiotics. *FEMS Microbiol. Lett.* **1994**, *123*, 11–18.

(6) https://www.studyblue.com/?closeForm=false#flashcard/view/2189544 (last seen 24th march 2015).

(7) Brennan, P. Structure, Function, and Biogenesis of the Cell Wall of *Mycobacterium tuberculosis*. *Tuberculosis* **2003**, *83*, 91–97.

(8) Szumowski, J. D.; Adams, K. N.; Edelstein, P. H.; Ramakrishnan, L. Antimicrobial Efflux Pumps and *Mycobacterium tuberculosis* Drug Tolerance: Evolutionary Considerations. *Curr. Top. Microbiol. Immunol.* **2013**, *374*, 81–108.

(9) Louw, G. E.; Warren, R. M.; Gey van Pittius, N. C.; McEvoy, C. R. E.; Van Helden, P. D.; Victor, T. C. A Balancing Act: Efflux/influx in Mycobacterial Drug Resistance. *Antimicrob. Agents Chemother.* **2009**, *53*, 3181–3189.

(10) Rang HP, Dale MM, Ritter JM. *More PK. Pharmacology. 5th Ed*; 2004; p. 631.

(11) Nguyen, L.; Pieters, J. Mycobacterial Subversion of Chemotherapeutic Reagents and Host Defense Tactics: Challenges in Tuberculosis Drug Development. *Annu. Rev. Pharmacol. Toxicol.* **2009**, *49*, 427–453.

(12) Cox, G.; Wright, G. D. Intrinsic Antibiotic Resistance: Mechanisms, Origins, Challenges and Solutions. *Int. J. Med. Microbiol.* **2013**, *303*, 287–292.

(13) Alekshun, M. N.; Levy, S. B. Molecular Mechanisms of Antibacterial Multidrug Resistance. *Cell* **2007**, *128*, 1037–1050.

(14) Chambers, H. F.; Moreau, D.; Yajko, D.; Miick, C.; Wagner, C.; Hackbarth, C.;

Kocago, S.; Rosenberg, E.; Hadley, W. K. Can Penicillins and Other SS -Lactam Antibiotics Be Used To Treat Tuberculosis . *Antimicrob. Agents Chemother.* **1995**, *39*, 2620–2624.

(15) Zaunbrecher, M. A.; Sikes, R. D.; Metchock, B.; Shinnick, T. M.; Posey, J. E. Overexpression of the Chromosomally Encoded Aminoglycoside Acetyltransferase Eis Confers Kanamycin Resistance in *Mycobacterium tuberculosis*. *Proc. Natl. Acad. Sci. U. S. A.* **2009**, *106*, 20004–20009.

(16) Chen, W.; Biswas, T. Unusual Regioversatility of Acetyltransferase Eis, A Cause of Drug Resistance in XDR-TB. *Proc. Natl. Acad. Sci. U. S. A.* **2011**, *108*, 1–5.

(17) Li, G.; Zhang, J.; Guo, Q.; Jiang, Y.; Wei, J.; Zhao, L.; Zhao, X.; Lu, J.; Wan, K. Efflux Pump Gene Expression in Multidrug-Resistant *Mycobacterium tuberculosis* Clinical Isolates. *PLoS One* **2015**, *10*, e0119013.

(18) Poole, K. Efflux-Mediated Antimicrobial Resistance. *J. Antimicrob. Chemother.* **2005**, *56*, 20–51.

(19) Piddock, L. J. V. Clinically Relevant Chromosomally Encoded Multidrug Resistance Efflux Pumps in Bacteria. *Clin. Microbiol. Rev.* **2006**, *19*, 382–402.

(20) Nikaido, H.; Pagès, J.-M. Broad-Specificity Efflux Pumps and Their Role in Multidrug Resistance of Gram-Negative Bacteria. *FEMS Microbiol. Rev.* **2012**, *36*, 340–363.

(21) Putman, M.; Hendrik, W. Molecular Properties of Bacterial Multidrug Transporters. *Microbiol. Mol. Biol. Rev.* **2000**, *64*, 672–693.

(22) Paulsen, I. T.; Lewis, K. Microbial Multidrug Efflux: Introduction. *J. Mol. Microbiol. Biotechnol.* **2001**, *3*, 143–144.

(23) Higgins, C. F. ABC Transporters: Physiology, Structure and Mechanism – an Overview. *Res. Microbiol.* **2001**, *152*, 205–210.

(24) Kerr, I. D. Structure and Association of ATP-Binding Cassette Transporter Nucleotide-Binding Domains. *Biochim. Biophys. Acta - Biomembr.* **2002**, *1561*, 47–64.

(25) Braibant, M.; Gilot, P. The ATP Binding Cassette (ABC) Transport Systems of *Mycobacterium tuberculosis*. *FEMS Microbiol. Rev.* **2000**, *24*.

(26) Choudhuri, B.; Bhakta, S.; Barik, R.; Basu, J. Overexpression and Functional Characterization of an ABC (ATP-Binding Cassette) Transporter Encoded by the Genes drrA and drrB of *Mycobacterium tuberculosis*. *Biochem. J* **2002**, *285*, 279–285.

(27) Pasca, M. R.; Guglierame, P.; Arcesi, F.; Bellinzoni, M.; De Rossi, E.; Riccardi, G. Rv2686c-Rv2687c-Rv2688c, an ABC Fluoroquinolone Efflux Pump in *Mycobacterium tuberculosis*. *Antimicrob. Agents Chemother.* **2004**, *48*, 3175–3178.

(28) Danilchanka, O.; Mailaender, C.; Niederweis, M. Identification of a Novel Multidrug Efflux Pump of *Mycobacterium tuberculosis*. *Antimicrob. Agents Chemother.* **2008**,

52, 2503–2511.

(29) Balganesh, M.; Kuruppath, S.; Marcel, N.; Sharma, S.; Nair, A.; Sharma, U. Rv1218c, an ABC Transporter of *Mycobacterium tuberculosis* with Implications in Drug Discovery. *Antimicrob. Agents Chemother.* **2010**, *54*, 5167–5172.

(30) Law, C. J.; Maloney, P. C.; Wang, D.-N. Ins and Outs of Major Facilitator Superfamily Antiporters. *Annu. Rev. Microbiol.* **2008**, *62*, 289–305.

(31) Saier, M. H.; Yen, M. R.; Noto, K.; Tamang, D. G.; Elkan, C. The Transporter Classification Database: Recent Advances. *Nucleic Acids Res.* **2009**, *37*, D274–D278.

(32) Pao, S.; Paulsen, I.; Saier, M. Major Facilitator Superfamily. *Microbiol. Mol. ...* **1998**, *62*, 1–34.

(33) Omote, H.; Hiasa, M.; Matsumoto, T.; Otsuka, M.; Moriyama, Y. The MATE Proteins as Fundamental Transporters of Metabolic and Xenobiotic Organic Cations. *Trends Pharmacol. Sci.* **2006**, *27*, 587–593.

(34) Otsuka, M.; Yasuda, M.; Morita, Y. Identification of Essential Amino Acid Residues of the NorM Na+/multidrug Antiporter in Vibrio Parahaemolyticus. *J. Bacteriol.* **2005**, *187*, 1552–1558.

(35) McAleese, F.; Petersen, P.; Ruzin, A.; Dunman, P. M.; Murphy, E.; Projan, S. J.; Bradford, P. A. A Novel MATE Family Efflux Pump Contributes to the Reduced Susceptibility of Laboratory-Derived Staphylococcus Aureus Mutants to Tigecycline. *Antimicrob. Agents Chemother.* **2005**, *49*, 1865–1871.

(36) Li, X.-Z.; Nikaido, H. Efflux-Mediated Drug Resistance in Bacteria. *Drugs* **2004**, *64*, 159–204.

(37) Littlejohn, T. Substrate Specificity and Energetics of Antiseptic and Disinfectant Resistance in Staphylococcus Aureus. *FEMS Microbiol. Lett.* **1992**, *95*, 259–265.

(38) Grinius, L.; Goldberg, E. Bacterial Multidrug Resistance Is due to a Single Membrane Protein Which Functions as a Drug Pump. *J. Biol. Chem.* **1994**, *269*, 29998–30004.

(39) Paulsen, I. T.; Skurray, R. A.; Tam, R.; Saier, M. H.; Turner, R. J.; Weiner, J. H.; Goldberg, E. B.; Grinius, L. L. The SMR Family: A Novel Family of Multidrug Efflux Proteins Involved with the Efflux of Lipophilic Drugs. *Mol. Microbiol.* **1996**, *19*, 1167–1175.

(40) Rossi, E. De; Branzoni, M.; Cantoni, R. Mmr, a *Mycobacterium tuberculosis* Gene Conferring Resistance to Small Cationic Dyes and Inhibitors. *J. Bacteriol.* **1998**, *180*, 6068–6071.

(41) Da Silva, P. E. A.; Von Groll, A.; Martin, A.; Palomino, J. C. Efflux as a Mechanism for Drug Resistance in *Mycobacterium tuberculosis*. *FEMS Immunol. Med. Microbiol.* **2011**, *63*, 1–9.

(42) Viveiros, M.; Martins, M.; Rodrigues, L.; Machado, D.; Couto, I.; Ainsa, J.; Amaral, L. Inhibitors of Mycobacterial Efflux Pumps as Potential Boosters for Anti-Tubercular Drugs. *Expert Rev. Anti. Infect. Ther.* **2012**, *10*, 983–998.

(43) Pal, R.; Fatima, Z.; Hameed, S. Efflux Pumps in Drug Resistance of *Mycobacterium tuberculosis*: A Panoramic View. *Int. J. Curr. Microbiol. App. Sci* **2014**, *3*, 528–546.

(44) Bhatt, K. Evidence That Phosphate Specific Transporter Is Amplified in a Fluoroquinolone Resistant Mycobacterium Smegmatis. *Eur. J. Biochem* **2000**, *4032*, 4028–4033.

(45) Hao, P.; Shi-Liang, Z.; Ju, L.; Ya-Xin, D.; Biao, H.; Xu, W.; Min-Tao, H.; Shou-Gang, K.; Ke, W. The Role of ABC Efflux Pump, Rv1456c-Rv1457c-Rv1458c, from *Mycobacterium tuberculosis* Clinical Isolates in China. *Folia Microbiol. (Praha).* **2011**, *56*, 549–553.

(46) Aínsa, J.; Blokpoel, M.; Otal, I. Molecular Cloning and Characterization of Tap, a Putative Multidrug Efflux Pump Present in Mycobacterium Fortuitum and *Mycobacterium tuberculosis*. *J. Bacteriol.* **1998**, *180*, 5836–5843.

(47) Siddiqi, N.; Das, R.; Pathak, N.; Banerjee, S.; Ahmed, N.; Katoch, V. M.; Hasnain, S. E. *Mycobacterium tuberculosis* Isolate with a Distinct Genomic Identity Overexpresses a Tap-like Efflux Pump. *Infection* **2004**, *32*, 109–111.

(48) Ramón-García, S.; Mick, V.; Dainese, E.; Martín, C.; Thompson, C. J.; De Rossi, E.; Manganelli, R.; Aínsa, J. A. Functional and Genetic Characterization of the Tap Efflux Pump in Mycobacterium Bovis BCG. *Antimicrob. Agents Chemother.* **2012**, *56*, 2074–2083.

(49) Li, X.-Z.; Zhang, L.; Nikaido, H. Efflux Pump-Mediated Intrinsic Drug Resistance in Mycobacterium Smegmatis. *Antimicrob. Agents Chemother.* **2004**, *48*, 2415–2423.

(50) Rossi, E. De; Arrigo, P.; Bellinzoni, M. The Multidrug Transporters Belonging to Major Facilitator Superfamily in *Mycobacterium tuberculosis*. *Mol. Med.* **2002**, *8*, 714–724.

(51) Silva, P. E.; Bigi, F.; Santangelo, M. P.; Romano, M. I.; Martín, C.; Cataldi, A; Aínsa, J. A. Characterization of P55, a Multidrug Efflux Pump in Mycobacterium Bovis and *Mycobacterium tuberculosis*. *Antimicrob. Agents Chemother.* **2001**, *45*, 800–804.

(52) Ramón-García, S.; Martín, C.; Thompson, C. J.; Aínsa, J. A. Role of the *Mycobacterium tuberculosis* P55 Efflux Pump in Intrinsic Drug Resistance, Oxidative Stress Responses, and Growth. *Antimicrob. Agents Chemother.* **2009**, *53*, 3675–3682.

(53) Bianco, M.; Blanco, F. Role of P27-P55 Operon from *Mycobacterium tuberculosis* in the Resistance to Toxic Compounds. *BMC Infect. Dis.* **2011**.

(54) Farrow, M. F.; Rubin, E. J. Function of a Mycobacterial Major Facilitator Superfamily Pump Requires a Membrane-Associated Lipoprotein. *J. Bacteriol.* **2008**, *190*, 1783–1791.

(55) Ramón-García, S.; Martín, C.; De Rossi, E.; Aínsa, J. A. Contribution of the Rv2333c Efflux Pump (the Stp Protein) from *Mycobacterium tuberculosis* to Intrinsic Antibiotic Resistance in Mycobacterium Bovis BCG. *J. Antimicrob. Chemother.* **2007**, *59*, 544–547.

(56) Pasca, M. R.; Guglierame, P.; De Rossi, E.; Zara, F.; Riccardi, G. mmpL7 Gene of *Mycobacterium tuberculosis* Is Responsible for Isoniazid Efflux in Mycobacterium Smegmatis. *Antimicrob. Agents Chemother.* **2005**, *49*, 4775–4777.

(57) Domenech, P.; Reed, M.; Barry, C. Contribution of the *Mycobacterium tuberculosis* MmpL Protein Family to Virulence and Drug Resistance. *Infect. Immun.* **2005**, *73*, 3492–3501.

(58) Camacho, L. R.; Constant, P.; Raynaud, C.; Laneelle, M. A; Triccas, J. A; Gicquel, B.; Daffe, M.; Guilhot, C. Analysis of the Phthiocerol Dimycocerosate Locus of *Mycobacterium tuberculosis*. Evidence That This Lipid Is Involved in the Cell Wall Permeability Barrier. *J. Biol. Chem.* **2001**, *276*, 19845–19854.

(59) Rodrigues, L.; Machado, D.; Couto, I.; Amaral, L.; Viveiros, M. Contribution of Efflux Activity to Isoniazid Resistance in the *Mycobacterium tuberculosis* Complex. *Infect. Genet. Evol.* **2012**, *12*, 695–700.

(60) Barry, C. E.; Boshoff, H. I.; Dartois, V.; Dick, T.; Ehrt, S.; Flynn, J.; Schnappinger, D.; Wilkinson, R. J.; Young, D. The Spectrum of Latent Tuberculosis: Rethinking the Biology and Intervention Strategies. *Nat. Rev. Microbiol.* **2009**, *7*, 845–855.

(61) Connolly, L. E.; Edelstein, P. H.; Ramakrishnan, L. Why Is Long-Term Therapy Required to Cure Tuberculosis? *PLoS Med.* **2007**, *4*, e120.

(62) Fontán, P. A; Aris, V.; Alvarez, M. E.; Ghanny, S.; Cheng, J.; Soteropoulos, P.; Trevani, A.; Pine, R.; Smith, I. *Mycobacterium tuberculosis* Sigma Factor E Regulon Modulates the Host Inflammatory Response. *J. Infect. Dis.* **2008**, *198*, 877–885.

(63) Morris, R. P.; Nguyen, L.; Gatfield, J.; Visconti, K.; Nguyen, K.; Schnappinger, D.; Ehrt, S.; Liu, Y.; Heifets, L.; Pieters, J.; Schoolnik, G.; Thompson, C. J. Ancestral Antibiotic Resistance in *Mycobacterium tuberculosis*. *Proc. Natl. Acad. Sci. U. S. A.* **2005**, *102*, 12200–12205.

(64) Nguyen, L.; Thompson, C. J. Foundations of Antibiotic Resistance in Bacterial Physiology: The Mycobacterial Paradigm. *Trends Microbiol.* **2006**, *14*, 304–312.

(65) Adams, K. N.; Takaki, K.; Connolly, L. E.; Wiedenhoft, H.; Winglee, K.; Humbert, O.; Edelstein, P. H.; Cosma, C. L.; Ramakrishnan, L. Drug Tolerance in Replicating Mycobacteria Mediated by a Macrophage-Induced Efflux Mechanism. *Cell* **2011**, *145*, 39–53.

(66) Schmalstieg, A. M.; Srivastava, S.; Belkaya, S.; Deshpande, D.; Meek, C.; Leff, R.; van Oers, N. S. C.; Gumbo, T. The Antibiotic Resistance Arrow of Time: Efflux Pump Induction Is a General First Step in the Evolution of Mycobacterial Drug Resistance.

Antimicrob. Agents Chemother. **2012**, *56*, 4806–4815.

(67) Quinn, T.; O'Mahony, R.; Baird, A.; Drudy, D.; Whyte, P.; Fanning, S. Multi-Drug Resistance in Salmonella Enterica: Efflux Mechanisms and Their Relationships with the Development of Chromosomal Resistance Gene Clusters. *Curr. Drug Targets* **2006**, *7*, 849–860.

(68) Hooper, D. Mechanisms of Action and Resistance of Older and Newer Fluoroquinolones. *Clin. Infect. Dis.* **2000**, *2696*, 24–28.

(69) Bambeke, F.; Pages, J.-M.; Lee, V. Inhibitors of Bacterial Efflux Pumps as Adjuvants in Antibiotic Treatments and Diagnostic Tools for Detection of Resistance by Efflux. *Recent Pat. Antiinfect. Drug Discov.* **2006**, *1*, 157–175.

(70) Oethinger, M.; Kern, W. Ineffectiveness of Topoisomerase Mutations in Mediating Clinically Significant Fluoroquinolone Resistance inEscherichia Coli in the Absence of the AcrAB Efflux Pump. *Antimicrob. Agents Chemother.* **2000**, *44*, 10–13.

(71) Martins, M. Is Adjuvant Therapy a Potential Road for Fighting *Mycobacterium tuberculosis* Resistance? *Expert Rev. Anti. Infect. Ther.* **2012**, *10*, 1225–1227.

(72) Amaral, L.; Engi, H.; Viveiros, M.; Molnar, J. Comparison of Multidrug Resistant Efflux Pumps of Cancer and Bacterial Cells with Respect to the Same Inhibitory Agents. *In Vivo (Brooklyn).* **2007**, *244*, 237–244.

(73) Lomovskaya, O.; Bostian, K. A. Practical Applications and Feasibility of Efflux Pump Inhibitors in the Clinic--a Vision for Applied Use. *Biochem. Pharmacol.* **2006**, *71*, 910–918.

(74) Zloh, M.; Kaatz, G. W.; Gibbons, S. Inhibitors of Multidrug Resistance (MDR) Have Affinity for MDR Substrates. *Bioorg. Med. Chem. Lett.* **2004**, *14*, 881–885.

(75) Levy, S. B. Active Efflux Mechanisms for Antimicrobial Resistance. *Antimicrob. Agents Chemother.* **1992**, *36*, 695–703.

(76) Gupta, A.; Reddy, V. jefA (Rv2459), a Drug Efflux Gene in *Mycobacterium tuberculosis* Confers Resistance to Isoniazid & Ethambutol. *Indian J Med Res* **2010**, 176–188.

(77) Stermitz, F.; Lorenz, P. Synergy in a Medicinal Plant: Antimicrobial Action of Berberine Potentiated by 5′-Methoxyhydnocarpin, a Multidrug Pump Inhibitor. *Proc. Natl. Acad. Sci* **2000**.

(78) Ng, E. Y.; Trucksis, M.; Hooper, D. C. Quinolone Resistance Mediated by norA: Physiologic Characterization and Relationship to flqB, a Quinolone Resistance Locus on the Staphylococcus Aureus Chromosome. *Antimicrob. Agents Chemother.* **1994**, *38*, 1345–1355.

(79) Neyfakh, A. A.; Borsch, C. M.; Kaatz, G. W. Fluoroquinolone Resistance Protein NorA of Staphylococcus Aureus Is a Multidrug Efflux Transporter. *Antimicrob. Agents*

Chemother. **1993**, *37*, 128–129.

(80) Lomovskaya, O.; Warren, M. S.; Lee, A.; Galazzo, J.; Fronko, R.; Lee, M.; Blais, J.; Cho, D.; Chamberland, S.; Renau, T.; Leger, R.; Hecker, S.; Watkins, W.; Hoshino, K.; Ishida, H.; Lee, V. J. Identification and Characterization of Inhibitors of Multidrug Resistance Efflux Pumps in Pseudomonas Aeruginosa: Novel Agents for Combination Therapy. *Antimicrob. Agents Chemother.* **2001**, *45*, 105–116.

(81) Lomovskaya, O.; Watkins, W. Inhibition of Efflux Pumps as a Novel Approach to Combat Drug Resistance in Bacteria Real-Time PCR Bioinformatics and Data. *J. Mol. Microbiol. Biotechnol* **2001**, *3*, 225–236.

(82) Pagès, J.-M.; Masi, M.; Barbe, J. Inhibitors of Efflux Pumps in Gram-Negative Bacteria. *Trends Mol. Med.* **2005**, *11*, 382–389.

(83) Kaatz, G. W. Bacterial Efflux Pump Inhibition. *Curr. Opin. Investig. Drugs* **2005**, *6*, 191–198.

(84) Askoura, M.; Mottawea, W.; Abujamel, T.; Taher, I. Efflux Pump Inhibitors (EPIs) as New Antimicrobial Agents against Pseudomonas Aeruginosa. *Libyan J. Med.* **2011**, *6*, 1–8.

(85) Ryan, B. M.; Dougherty, T. J.; Beaulieu, D.; Chuang, J.; Dougherty, B. a; Barrett, J. F. Efflux in Bacteria: What Do We Really Know about It? *Expert Opin. Investig. Drugs* **2001**, *10*, 1409–1422.

(86) Adams, K. N.; Szumowski, J. D.; Ramakrishnan, L. Verapamil, and Its Metabolite Norverapamil, Inhibit Macrophage-Induced, Bacterial Efflux Pump-Mediated Tolerance to Multiple Anti-Tubercular Drugs. *J. Infect. Dis.* **2014**, *210*, 456–466.

(87) Adams, K. N.; Takaki, K.; Connolly, L. E.; Wiedenhoft, H.; Winglee, K.; Humbert, O.; Edelstein, P. H.; Cosma, C. L.; Ramakrishnan, L. Drug Tolerance in Replicating Mycobacteria Mediated by a Macrophage-Induced Efflux Mechanism. *Cell* **2011**, *145*, 39–53.

(88) Martins, M.; Schelz, Z.; Martins, A.; Molnar, J.; Hajös, G.; Riedl, Z.; Viveiros, M.; Yalcin, I.; Aki-Sener, E.; Amaral, L. In Vitro and Ex Vivo Activity of Thioridazine Derivatives against *Mycobacterium tuberculosis*. *Int. J. Antimicrob. Agents* **2007**, *29*, 338–340.

(89) Salie, S.; Hsu, N.-J.; Semenya, D.; Jardine, A.; Jacobs, M. Novel Non-Neuroleptic Phenothiazines Inhibit *Mycobacterium tuberculosis* Replication. *J. Antimicrob. Chemother.* **2014**, *69*, 1551–1558.

(90) Amaral, L.; Molnar, J. Therapy of XDR TB with Thioridazine a Drug Beyond Patent Protection but Eligible for Patent "As New Use." *Recent Pat. Antiinfect. Drug Discov.* **2010**, *5*, 109–114.

(91) Amaral, L.; Viveiros, M.; Molnar, J.; Kristiansen, J. E. Effective Therapy with the Neuroleptic Thioridazine as an Adjunct to Second Line of Defence Drugs, and the

Potential That Thioridazine Offers for New Patents That Cover a Variety of "New Uses". *Recent Pat. Antiinfect. Drug Discov.* **2011**, *6*, 84–87.

(92) Lechner, D.; Gibbons, S.; Bucar, F. Plant Phenolic Compounds as Ethidium Bromide Efflux Inhibitors in Mycobacterium Smegmatis. *J. Antimicrob. Chemother.* **2008**, *62*, 345–348.

(93) Jin, J.; Zhang, J.; Guo, N.; Feng, H.; Li, L.; Liang, J.; Sun, K.; Wu, X.; Wang, X.; Liu, M.; Deng, X.; Yu, L. The Plant Alkaloid Piperine as a Potential Inhibitor of Ethidium Bromide Efflux in Mycobacterium Smegmatis. *J. Med. Microbiol.* **2011**, *60*, 223–229.

(94) Sharma, S.; Kumar, M.; Nargotra, a.; Koul, S.; Khan, I. A. Piperine as an Inhibitor of Rv1258c, a Putative Multidrug Efflux Pump of *Mycobacterium tuberculosis*. *J. Antimicrob. Chemother.* **2010**, *65*, 1694–1701.

(95) Jin, J.; Zhang, J.-Y.; Guo, N.; Sheng, H.; Li, L.; Liang, J.-C.; Wang, X.-L.; Li, Y.; Liu, M.-Y.; Wu, X.-P.; Yu, L. Farnesol, a Potential Efflux Pump Inhibitor in Mycobacterium Smegmatis. *Molecules* **2010**, *15*, 7750–7762.

(96) Stavri, M.; Piddock, L. J. V; Gibbons, S. Bacterial Efflux Pump Inhibitors from Natural Sources. *J. Antimicrob. Chemother.* **2007**, *59*, 1247–1260.

(97) Huang, T.-S.; Kunin, C. M.; Wang, H.-M.; Yan, B.-S.; Huang, S.-P.; Chen, Y.-S.; Lee, S. S.-J.; Syu, W.-J. Inhibition of the *Mycobacterium tuberculosis* Reserpine-Sensitive Efflux Pump Augments Intracellular Concentrations of Ciprofloxacin and Enhances Susceptibility of Some Clinical Isolates. *J. Formos. Med. Assoc.* **2013**, *112*, 789–794.

(98) Garvey, M.; Piddock, L. The Efflux Pump Inhibitor Reserpine Selects Multidrug-Resistant Streptococcus Pneumoniae Strains That Overexpress the ABC Transporters PatA and PatB. *Antimicrob. Agents Chemother.* **2008**, *52*, 1677–1685.

(99) Ahmed, R. Effect Of Different Efflux Inhibitors On β-Lactams Resistance In Multidrug Resistant Staphylococcus Aureus. *Egypt. J. Med. Microbiol.* **2007**, *16*, 429–436.

(100) Grossman, T. H.; Shoen, C. M.; Jones, S. M.; Jones, P. L.; Cynamon, M. H.; Locher, C. P. The Efflux Pump Inhibitor Timcodar Improves the Potency of Antimycobacterial Agents. *Antimicrob. Agents Chemother.* **2015**, *59*, 1534–1541.

(101) Gupta, S.; Cohen, K. A.; Winglee, K.; Maiga, M.; Diarra, B.; Bishai, W. R. Efflux Inhibition with Verapamil Potentiates Bedaquiline in *Mycobacterium tuberculosis*. *Antimicrob. Agents Chemother.* **2014**, *58*, 574–576.

(102) Parasa, V. R.; Rahman, M. J.; Ngyuen Hoang, A. T.; Svensson, M.; Brighenti, S.; Lerm, M. Modeling *Mycobacterium tuberculosis* Early Granuloma Formation in Experimental Human Lung Tissue. *Dis. Model. Mech.* **2014**, *7*, 281–288.

(103) Amaral, L.; Kristiansen, J. E.; Viveiros, M.; Atouguia, J. Activity of Phenothiazines against Antibiotic-Resistant *Mycobacterium tuberculosis*: A Review Supporting Further Studies That May Elucidate the Potential Use of Thioridazine as Anti-

Tuberculosis Therapy. *J. Antimicrob. Chemother.* **2001**, *47*, 505–511.

(104) Martins, M.; Viveiros, M.; Couto, I.; Amaral, L. Targeting Human Macrophages for Enhanced Killing of Intracellular XDR-TB and MDR-TB. *Int. J. Tuberc. Lung Dis.* **2009**, *13*, 569–573.

(105) Koski, A.; Raki, M.; Nokisalmi, P.; Liikanen, I.; Kangasniemi, L.; Joensuu, T.; Kanerva, A.; Pesonen, S.; Alemany, R.; Hemminki, A. Verapamil Results in Increased Blood Levels of Oncolytic Adenovirus in Treatment of Patients with Advanced Cancer. *Mol. Ther.* **2012**, *20*, 221–229.

(106) Levine, L.; Estrada, C. Intralesional Verapamil for the Treatment of Peyronie's Disease: A Review. *Int. J. Impot. Res.* **2002**, 324–328.

(107) Udelson, J.; Bonow, R.; O'gara, P. Verapamil Prevents Silent Myocardial Perfusion Abnormalities during Exercise in Asymptomatic Patients with Hypertrophic Cardiomyopathy. *Circulation* **1989**, 1052–1061.

(108) Figueredo, A.; Arnold, A.; Goodyear, M.; Findlay, B.; Neville, A.; Normandeau, R.; Jones, A. Addition of Verapamil and Tamoxifen to the Initial Chemotherapy of Small Cell Lung Cancer a Phase I/II Study. *Cancer* **1990**, *65*, 1895–1902.

(109) Dalton, W.; Crowley, J.; Salmon, S. Phase III Randomized Study of Oral Verapamil as a Chemosensitizer to Reverse Drug Resistance in Patients with Refractory Myeloma. A Southwest Oncology Group Study. *Cancer* **1995**, *75*, 815–820.

(110) Jones, K.; Bray, P.; Khoo, S.; Davey, R. P-Glycoprotein and Transporter MRP1 Reduce HIV Protease Inhibitor Uptake in CD4 Cells: Potential for Accelerated Viral Drug Resistance? *AIDS* **2001**.

(111) Lehnert, B. M.; Dalton, W. S.; Roe, D.; Emerson, S.; Salmon, S. E. Synergistic Inhibition by Verapamil and Quinine of P-Glycoprotein-Mediated Multidrug Resistance in a Human Myeloma Cell Line Model. *Blood* **2015**, *77*, 348–354.

(112) Tsuruo, T.; Iida, H.; Tsukagoshi, S.; Sakurai, Y. Overcoming of Vincristine Resistance in P388 Leukemia in Vivo and in Vitro through Enhanced Cytotoxicity of Vincristine and Vinblastine by Verapamil. *Cancer Res.* **1981**, 1967–1972.

(113) Belpomme, D.; Gauthier, S.; Pujade-Lauraine, E.; Facchini, T.; Goudier, M. J.; Krakowski, I.; Netter-Pinon, G.; Frenay, M.; Gousset, C.; Marié, F. N.; Benmiloud, M.; Sturtz, F. Verapamil Increases the Survival of Patients with Anthracycline-Resistant Metastatic Breast Carcinoma. *Ann. Oncol.* **2000**, *11*, 1471–1476.

(114) Warhurst, D. Polymorphism in the Plasmodium Falciparum Chloroquine-Resistance Transporter Protein Links Verapamil Enhancement of Chloroquine Sensitivity with the. *Malar. J.* **2003**, *2*, 31.

(115) Bates, S.; Wilson, W.; Fojo, A.; Alvarez, M. Clinical Reversal of Multidrug Resistance. *Oncologist* **1996**, 269–275.

(116) Toffoli, G.; Simone, F.; Corona, G. Structure-Activity Relationship of Verapamil Analogs and Reversal of Multidrug Resistance. *Biochem. Phamracology* **1995**, *50*, 1245–1255.

(117) Eliason, J.; Ramuz, H.; Yoshikubo, T. Novel Dithiane Analogues of Tiapamil with High Activity to Overcome Multidrug Resistance in Vitro. *Biochem. Pharmacol.* **1995**, *50*.

(118) Eliason, J. F.; Sawada, R.; Tsukaguchi, T.; Kobayashi, K.; Ichihara, S.; Konishi, C.; Horii, I.; Kuruma, I.; Ramuz, H. The Dithiane Ro 44-5912 Enhances Vinblastine Sensitivity of Drug Resistant and Parental KB Lines in Vivo. *Eur. J. Cancer* **1995**, *31*, 2354–2361.

(119) Berger, D.; Citarella, R. Novel Multidrug Resistance Reversal Agents. *J. Med. Chem.* **1999**, 2145–2161.

(120) Choi, S. U.; Lee, B. H.; Kim, K. H.; Choi, E. J.; Park, S. H.; Shin, H. S.; Yoo, S. E.; Jung, N. P.; Lee, C. O. Novel Multidrug-Resistance Modulators, KR-30026 and KR-30031, in Cancer Cells. *Anticancer Res. 17*, 4577–4582.

(121) Lee, B. H.; Lee, C. O.; Kwon, M.-J.; Yi, K. Y.; Yoo, S.-E.; Choi, S.-U. Differential Effects of the Optical Isomers of KR30031 on Cardiotoxicity and on Multidrug Resistance Reversal Activity. *Anticancer. Drugs* **2003**, *14*, 175–181.

(122) Woo, J. S.; Lee, C. H.; Shim, C. K.; Hwang, S. Enhanced Oral Bioavailability of Paclitaxel by Coadministration of the P-Glycoprotein Inhibitor KR30031. *Pharmaceutical research* **2003**, *20*, 24–30.

(123) Dei, S.; Romanelli, M. N.; Scapecchi, S.; Teodori, E.; Chiarini, A.; Gualtieri, F. Verapamil Analogues with Restricted Molecular Flexibility. *J. Med. Chem.* **1991**, *34*, 2219–2225.

(124) Teodori, E.; Dei, S.; Romanelli, M.; Scapecchi, S.; Gualtieri, F.; Budriesi, R.; Chiarini, A.; Lemoine, H.; Mannhold, R. Synthesis and Pharmacological Evaluation of Verapamil Analogs with Restricted Molecular Flexibility. *Eur. J. Med. Chem.* **1994**, *29*, 139–148.

(125) Pereira, E.; Teodori, E.; Dei, S.; Gualtieri, F.; Garnier-Suillerot, A. Reversal of Multidrug Resistance by Verapamil Analogues. *Biochem. Pharmacol.* **1995**, *50*, 451–457.

(126) http://www.dddmag.com/news/2013/08/adding-verapamil-speeds-tb-treatment (Last visited 28 April 2015).

(127) Singh, M.; Jadaun, G. P. S.; Srivastava, K.; Chauhan, V.; Mishra, R.; Gupta, K.; Nair, S. Effect of Efflux Pump Inhibitors on Drug Susceptibility of Ofloxacin Resistant *Mycobacterium tuberculosis* Isolates. *Indian J Med Res* **2011**, 535–540.

(128) Demitto, F. D. O.; do Amaral, R. C. R.; Maltempe, F. G.; Siqueira, V. L. D.; Scodro, R. B. D. L.; Lopes, M. A.; Caleffi-Ferracioli, K. R.; Canezin, P. H.; Cardoso, R. F. In

Vitro Activity of Rifampicin and Verapamil Combination in Multidrug-Resistant *Mycobacterium tuberculosis*. *PLoS One* **2015**, *10*, e0116545.

(129) Spies, F. S.; da Silva, P. E. A.; Ribeiro, M. O.; Rossetti, M. L.; Zaha, A. Identification of Mutations Related to Streptomycin Resistance in Clinical Isolates of *Mycobacterium tuberculosis* and Possible Involvement of Efflux Mechanism. *Antimicrob. Agents Chemother.* **2008**, *52*, 2947–2949.

(130) Machado, D.; Couto, I.; Perdigão, J.; Rodrigues, L.; Portugal, I.; Baptista, P.; Veigas, B.; Amaral, L.; Viveiros, M. Contribution of Efflux to the Emergence of Isoniazid and Multidrug Resistance in *Mycobacterium tuberculosis*. *PLoS One* **2012**, *7*, e34538.

(131) Gupta, S.; Tyagi, S.; Bishai, W. R. Verapamil Increases the Bactericidal Activity of Bedaquiline against *Mycobacterium tuberculosis* in a Mouse Model. *Antimicrob. Agents Chemother.* **2015**, *59*, 673–676.

(132) Louw, G. E.; Warren, R. M.; Gey van Pittius, N. C.; Leon, R.; Jimenez, A.; Hernandez-Pando, R.; McEvoy, C. R. E.; Grobbelaar, M.; Murray, M.; van Helden, P. D.; Victor, T. C. Rifampicin Reduces Susceptibility to Ofloxacin in Rifampicin-Resistant *Mycobacterium tuberculosis* through Efflux. *Am. J. Respir. Crit. Care Med.* **2011**, *184*, 269–276.

(133) Gupta, S.; Tyagi, S.; Almeida, D. V; Maiga, M. C.; Ammerman, N. C.; Bishai, W. R. Acceleration of Tuberculosis Treatment by Adjunctive Therapy with Verapamil as an Efflux Inhibitor. *Am. J. Respir. Crit. Care Med.* **2013**, *188*, 600–607.

(134) Berg, R. D.; Ramakrishnan, L. Insights into Tuberculosis from the Zebrafish Model. *Trends Mol. Med.* **2012**, *18*, 689–690.

(135) Barbarash, R. A.; Fischer, J. H.; Batenhorst, L. Near-total Reduction in Verapamil Bioavailability by Rifampin*. *Chest* **1988**.

(136) Pauli-magnus, C.; Richter, O. V. O. N.; Burk, O.; Ziegler, A.; Mettang, T.; Eichelbaum, M.; Fromm, M. F.; Fischer-bosch-institute, M.; Pharmacology, C.; Germany, C. P.; R, O. Characterization of the Major Metabolites of Verapamil as Substrates and Inhibitors of P-Glycoprotein 1. *Pharmacology* **2000**, *293*, 376–382.

(137) Meunier, B. Hybrid Molecules with a Dual Mode of Action: Dream or Reality? *Acc. Chem. Res.* **2008**, *41*, 69–77.

(138) Van Bambeke, F.; Glupczynski, Y.; Plésiat, P.; Pechère, J. C.; Tulkens, P. M. Antibiotic Efflux Pumps in Prokaryotic Cells: Occurrence, Impact on Resistance and Strategies for the Future of Antimicrobial Therapy. *J. Antimicrob. Chemother.* **2003**, *51*, 1055–1065.

(139) Bremner, J.; Ambrus, J.; Samosorn, S. Dual Action-Based Approaches to Antibacterial Agents. *Curr. Med. Chem.* **2007**, *14*, 1459–1477.

(140) Wermuth, C.; Ganellin, C. Glossary of Terms Used in Medicinal Chemistry (IUPAC

Recommendations 1998). *Pure Appl. ...* **1998**, *70*, 1129–1143.

(141) Barbachyn, M. R. Chapter 17 – Recent Advances in the Discovery of Hybrid Antibacterial Agents. *Annu. Rep. Med. Chem.* **2008**, *43*, 281–290.

(142) Morphy, R.; Rankovic, Z. Designed Multiple Ligands. An Emerging Drug Discovery Paradigm. *J. Med. Chem.* **2005**, *48*, 6523–6543.

(143) Charifson, P. S.; Grillot, A.; Grossman, T. H.; Parsons, J. D.; Badia, M.; Bellon, S.; Deininger, D. D.; Drumm, J. E.; Gross, C. H.; LeTiran, A.; Liao, Y.; Mani, N.; Nicolau, D. P.; Perola, E.; Ronkin, S.; Shannon, D.; Swenson, L. L.; Tang, Q.; Tessier, P. R.; Tian, S.; Trudeau, M.; Wang, T.; Wei, Y.; Zhang, H.; Stamos, D. Novel Dual-Targeting Benzimidazole Urea Inhibitors of DNA Gyrase and Topoisomerase IV Possessing Potent Antibacterial Activity: Intelligent Design and Evolution through the Judicious Use of Structure-Guided Design and Structure-Activity Relationships. *J. Med. Chem.* **2008**, *51*, 5243–5263.

(144) Zhi, C.; Long, Z.; Manikowski, A.; Comstock, J.; Xu, W.; Brown, N. C.; Tarantino, P. M.; Holm, K. A.; Dix, E. J.; Wright, G. E.; Barnes, M. H.; Butler, M. M.; Foster, K. A.; LaMarr, W. A.; Bachand, B.; Bethell, R.; Cadilhac, C.; Charron, S.; Lamothe, S.; Motorina, I.; Storer, R. Hybrid Antibacterials. DNA Polymerase-Topoisomerase Inhibitors. *J. Med. Chem.* **2006**, *49*, 1455–1465.

(145) Yoon, K. J.; Qi, J.; Remack, J. S.; Virga, K. G.; Hatfield, M. J.; Potter, P. M.; Lee, R. E.; Danks, M. K. Development of an Etoposide Prodrug for Dual Prodrug-Enzyme Antitumor Therapy. *Mol. Cancer Ther.* **2006**, *5*, 1577–1584.

(146) Albrecht, H. A.; Beskid, G.; Christenson, J. G.; Deitcher, K. H.; Georgopapadakou, N. H.; Keith, D. D.; Konzelmann, F. M.; Pruess, D. L.; Chen Wei, C. Dual-Action Cephalosporins Incorporating a 3'-Tertiary-Amine-Linked Quinolone. *J. Med. Chem.* **1994**, *37*, 400–407.

(147) Beskid, G.; Albrecht, H. A.; Fallat, V.; Keith, D. D.; Lipschitz, E. R.; McGarry, C. M.; McGarry, D. H.; Rossman, P.; Siebelist, J. In Vitro and in Vivo Activity of Carbamate-Linked Dual-Action Antibacterial Ro 24-4383. *Chemotherapy* **1991**, *37*, 310–317.

(148) Hubschwerlen, C.; Specklin, J.-L.; Sigwalt, C.; Schroeder, S.; Locher, H. H. Design, Synthesis and Biological Evaluation of Oxazolidinone–Quinolone Hybrids. *Bioorg. Med. Chem.* **2003**, *11*, 2313–2319.

(149) Pokrovskaya, V.; Belakhov, V.; Hainrichson, M.; Yaron, S.; Baasov, T. Design, Synthesis, and Evaluation of Novel Fluoroquinolone-Aminoglycoside Hybrid Antibiotics. *J. Med. Chem.* **2009**, *52*, 2243–2254.

(150) Frantz, S. The Trouble with Making Combination Drugs. *Nat. Rev. Drug Discov.* **2006**, *5*, 881–882.

(151) Burgess, S. J.; Selzer, A.; Kelly, J. X.; Smilkstein, M. J.; Riscoe, M. K.; Peyton, D. H. A Chloroquine-like Molecule Designed to Reverse Resistance in Plasmodium

Falciparum. *J. Med. Chem.* **2006**, *49*, 5623–5625.

(152) Zhang, H.; Paguio, M.; Roepe, P. D. The Antimalarial Drug Resistance Protein Plasmodium Falciparum Chloroquine Resistance Transporter Binds Chloroquine. *Biochemistry* **2004**, *43*, 8290–8296.

(153) Bennett, T. Drug Resistance-Associated pfCRT Mutations Confer Decreased Plasmodium Falciparum Digestive Vacuolar pH. *Mol. Biochem. Parasitol.* **2004**, *133*, 99–114.

(154) Martin, R. E.; Kirk, K. The Malaria Parasite's Chloroquine Resistance Transporter Is a Member of the Drug/metabolite Transporter Superfamily. *Mol. Biol. Evol.* **2004**, *21*, 1938–1949.

(155) Krogstad, D. J.; Gluzman, I. Y.; Kyle, D. E.; Oduola, A. M.; Martin, S. K.; Milhous, W. K.; Schlesinger, P. H. Efflux of Chloroquine from Plasmodium Falciparum: Mechanism of Chloroquine Resistance. *Science* **1987**, *238*, 1283–1285.

(156) Martin, S. K.; Oduola, A. M.; Milhous, W. K. Reversal of Chloroquine Resistance in Plasmodium Falciparum by Verapamil. *Science* **1987**, *235*, 899–901.

(157) Van Schalkwyk, D. A; Walden, J. C.; Smith, P. J. Reversal of Chloroquine Resistance in Plasmodium Falciparum Using Combinations of Chemosensitizers. *Antimicrob. Agents Chemother.* **2001**, *45*, 3171–3174.

(158) Millet, J.; Torrentino-Madamet, M.; Alibert, S.; Rogier, C.; Santelli-Rouvier, C.; Mosnier, J.; Baret, E.; Barbe, J.; Parzy, D.; Pradines, B. Dihydroethanoanthracene Derivatives as in Vitro Malarial Chloroquine Resistance Reversal Agents. *Antimicrob. Agents Chemother.* **2004**, *48*, 2753–2756.

(159) H. Peyton, D. Reversed Chloroquine Molecules as a Strategy to Overcome Resistance in Malaria. *Curr. Top. Med. Chem.* **2012**, *12*, 400–407.

(160) Burgess, S. J.; Kelly, J. X.; Shomloo, S.; Wittlin, S.; Brun, R.; Liebmann, K.; Peyton, D. H. Synthesis, Structure-Activity Relationship, and Mode-of-Action Studies of Antimalarial Reversed Chloroquine Compounds. *J. Med. Chem.* **2010**, *53*, 6477–6489.

(161) Bhattacharjee, A. K.; Kyle, D. E.; Vennerstrom, J. L.; Milhous, W. K. A 3D QSAR Pharmacophore Model and Quantum Chemical Structure-Activity Analysis of Chloroquine(CQ)-Resistance Reversal. *J. Chem. Inf. Model.* **2002**, *42*, 1212–1220.

(162) Ball, A. R.; Casadei, G.; Samosorn, S.; Bremner, J. B.; Ausubel, F. M.; Moy, T. I.; Lewis, K. Conjugating Berberine to a Multidrug Efflux Pump Inhibitor Creates an Effective Antimicrobial. *ACS Chem. Biol.* **2006**, *1*, 594–600.

(163) Bremner, J. B.; Kelso, M. J. Synthesis of Berberine-Efflux Pump Inhibitor Hybrid Antibacterials. *Synth. Commun.* **2010**, *40*, 3561–3568.

(164) H. Peyton, David; Burgess, S. Quinoline Derivatives and Uses Thereof, *United States Patent Application 20110257160*. **2011**.

(165) Teodori, E.; Dei, S.; Quidu, P.; Budriesi, R.; Chiarini, A.; Garnier-Suillerot, A.; Gualtieri, F.; Manetti, D.; Romanelli, M. N.; Scapecchi, S. Design, Synthesis, and in Vitro Activity of Catamphiphilic Reverters of Multidrug Resistance: Discovery of a Selective, Highly Efficacious Chemosensitizer with Potency in the Nanomolar Range. *J. Med. Chem.* **1999**, *42*, 1687–1697.

(166) Biscardi, M.; Teodori, E.; Caporale, R.; Budriesi, R.; Balestri, F.; Scappini, B.; Gavazzi, S.; Grossi, A. Multidrug Reverting Activity toward Leukemia Cells in a Group of New Verapamil Analogues with Low Cardiovascular Activity. *Leuk. Res.* **2006**, *30*, 1–8.

Chapter 3: Design, synthesis and characterization of verapamil analogues as potential efflux pump Inhibitors

3.1 Introduction

This chapter presents an account of the design, synthesis, and characterization of various verapamil analogues as potential efflux pump inhibitors. These inhibitors have the potential to counter the efflux pump (EP)-mediated resistance that DS and DR strains of *Mtb* have developed against various anti-TB drugs.

3.2 Verapamil and related analogues

As outlined in chapter **2**, section **2.6.1**, verapamil (VER) is an encouraging and viable template for the development of efflux pump inhibitors (EPIs). It has been clinically widely used for a number of years and, therefore, repositioning of this compound presents the advantage of a fast-track development process based on prior knowledge of various properties that need to be manipulated to make analogues with favourable pharmacological profiles. The various VER related MDR modulators for cancer mentioned in section **2.6.1.2** also serve as a guide to indicate which pharmacological functionalities can be incorporated to improve the various properties of VER as a chemosensitizer.

3.2.1 Rationale

As discussed in section **2.6.1**, VER, a well known calcium channel blocker, has also been shown to inhibit *Mtb* efflux pumps *in vitro*, *ex vivo,* and in mouse models of tuberculosis.[1] VER is also known to enhance the sensitivity of various resistant cancer cell lines towards chemotherapy through inhibition of Pgp-related EPs. It has also been reported that the inhibition of Pgp-related EPs may increase drug accumulation in cellular layers of pulmonary granulomas, and increase the efficacy of various drugs.[2] However, inhibition of Pgp by VER may be accompanied by altered cytokine secretion, enhanced apoptosis, and reduction in the *Mtb*-specific T-cells. These disadvantageous properties are the bottleneck, which must be overcome in order to reposition VER as a MDR modulator in TB treatment.

Structural modifications of VER have shown promising improvements in its pharmacological properties against cancer. This approach can also be employed to develop VER analogues as EPIs to chemosensitize resistant strains of *Mtb.* It is important to note that a synergy between

the immune system of the human body and the action of antimycobacterial agents is required for enhanced drug activity. Hence, structural modifications of VER should not lead to the development of new analogues with unfavourable properties that may limit the application in clinical stages by negatively impacting on the human host immune system.

In order to synthesize new VER analogues for SAR studies, the guidelines proposed by Bhattarjee *et. al.*[3] for achieving chemosensitization in the reversal of CQ-resistance in *Plasmodium falciparum* were considered. In this regard, it has been reported that high lipophilicity and the presence of an amino group, which can be protonated under acidic conditions, are favourable features for a chemosensitizer.[4] Indeed various studies have found that the lipophilic terminus of verapamil (**Figure 3.1,** SAR 1) is important for its EP inhibition properties.[3,5] Therefore, our SAR1 studies focused on investigating the effects of replacing the *iso*-propyl moiety with various alkyl groups with equivalent or enhanced lipophilicity.

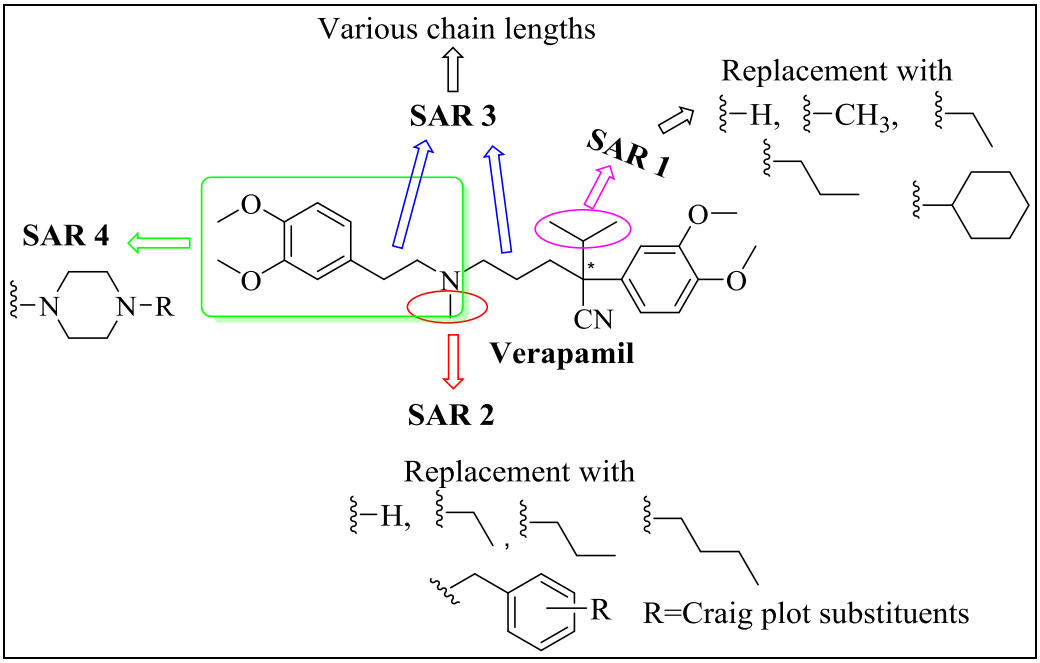

Figure 3.1: Designing of various SAR studies on verapamil to develop potential EPIs to potentiate various anti-TB drugs

The basic nitrogen of VER acts as a proton acceptor and is a structural requirement for the chemosensitization property. It has also been reported that spatial arrangements of the molecule, and weak polar interactions produced by the phenyl groups due to their π orbitals, affect VER's efflux pump inhibitory properties in cancer.[6] Thus a part of SAR 2 has been

designed to explore the effect of lipophilicity and polar interactions of π orbitals, by replacing the methyl group on the basic nitrogen with various benzyl groups. The potent analogues of VER with a benzyl substituent on the nitrogen can also provide the option of exploring Craig plot substituents on the aromatic rings to potentially develop analogues with enhanced efflux pump inhibition properties.[7] Additional analogues of VER were designed by replacing the methyl group on the nitrogen with various alkyl groups to investigate the effect of these changes on activity (**Figure 3.1**, SAR 2).

SAR 3 (**Figure 3.1**) involves the modification of the alkyl chain lengths between nitrogen and each hydrophobic dimethoxyphenyl ring, and assessing the effect of various VER spatial arrangements.

SAR 4 (**Figure 3.1**) was designed by replacing the 2-(3,4-dimethoxyphenyl)ethan-1-amino part of the VER with various piperazinyl moieties. These analogues were used to investigate the effect of incorporating additional protonatable nitrogens and substituted aromatic moieties.

3.2.2 Chemical synthesis

3.2.2.1 Retrosynthetic analysis

Scheme **3.1** shows the retrosynthetic analysis of target VER analogues, which can be envisioned from coupling of intermediates **3.2** and **3.6**. The intermediate **3.2** with desired substituents on nitrogen were envisioned from Boc-deprotection of the *N*-Boc-protected intermediate **3.3**, which can be obtained by alkylation of Boc protected amine **3.4**, which would in turn be obtained by Boc protection of starting amine **3.5**. The alkylation of intermediate **3.6** was envisioned from sequential alkylation of nitriles **3.7** and **3.8**.

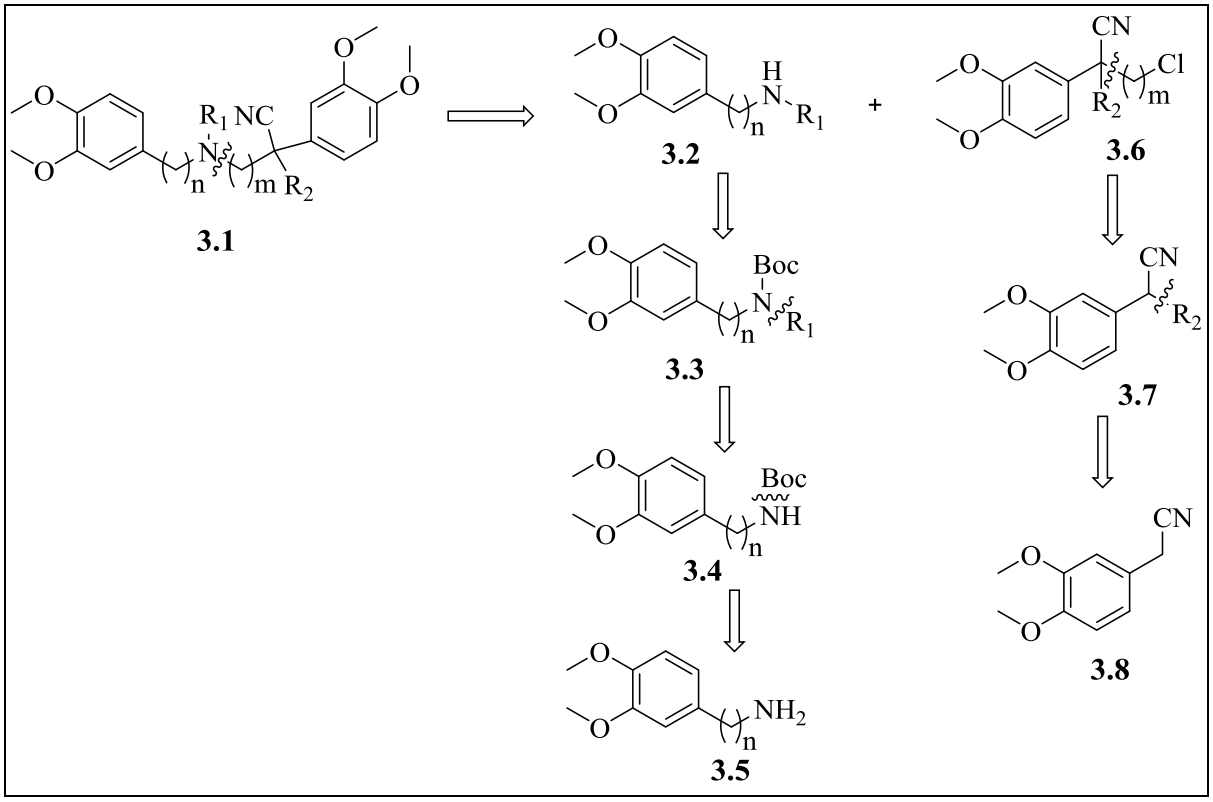

Scheme 3.1: Retrosynthetic analysis of verapamil analogues.

3.2.2.2 Synthesis of 2-(3,4-dimethoxyphenyl)acetonitrile intermediates (3.6)

The synthesis of 2-(3,4-dimethoxyphenyl)acetonitrile intermediates **3.6** was achieved using a method described by Zhongxu *et. al.*[8] with some modifications. As outlined in scheme **3.2**, the synthesis of intermediate **3.7** was achieved in moderate yield (Table **3.1**) *via* alkylation of commercially available 2-(3,4-dimethoxyphenyl)acetonitrile **3.8**, with various alkyl halides in THF in the presence of *n*-butyllithium at 0 °C, under an atmosphere of nitrogen. This intermediate was further reacted with commercially available 1-bromo-3-chloropropane/1,2-dibromoethane using lithium diisopropyl amide (LDA) in dry THF under an atmosphere of nitrogen at -78 °C, to afford **3.6** in moderate to good yields (Table **3.1**).

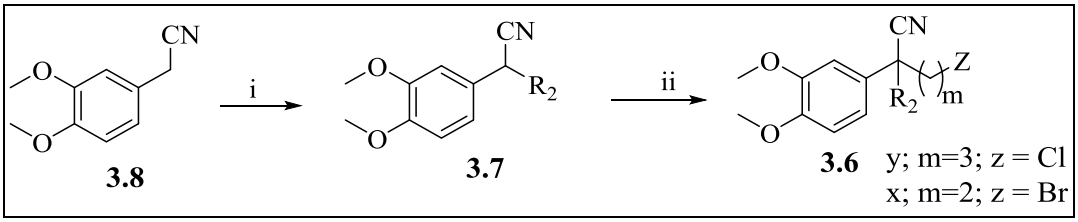

Scheme 3.2: *Reagents and reaction conditions:* (i) Bromoalkane (1.5 eq.), *n*-BuLi (1.1 eq.), THF, 0 °C to 25 °C, 1.5-2 h; (ii) 1-Bromo-3-chloropropane/1,2-dibromoethane (1.5 eq.), LDA (1.2 eq.), THF, -78 °C to 25 °C, 1-2 h.

Table 3.1: Yields of isolated intermediates **3.7** and **3.6**.

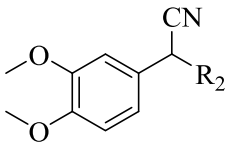

3.7

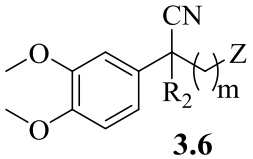

3.6

x; m=2; z = Br
y; m=3; z = Cl

Entry	R_2	3.7 Yield %	3.6y Yield %	3.6x Yield %
a	$-CH(CH_3)_2$	69	81	76
b	$-H$	*	41	*
c	$-CH_3$	46	66	*
d	$-CH_2CH_3$	48	68	*
e	$-CH_2CH_2CH_3$	53	65	*
f	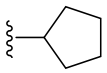	60	46	*
g	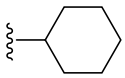	50	43	*

*Compound not synthesised.

3.2.2.4 Synthesis of 2-(3,4-dimethoxyphenyl)amine intermediates (3.2)

The 2-(3,4-dimethoxyphenyl)amine intermediates **3.2** were synthesized from various commercially available 3,4-dimethoxyphenylamines **3.5** (Scheme **3.3**). The controlled alkylation of amines is not feasible with straight forward alkylation methods due to an increase in the nucleophilic character of the substituted amine, which reacts further to form various side products.[10]

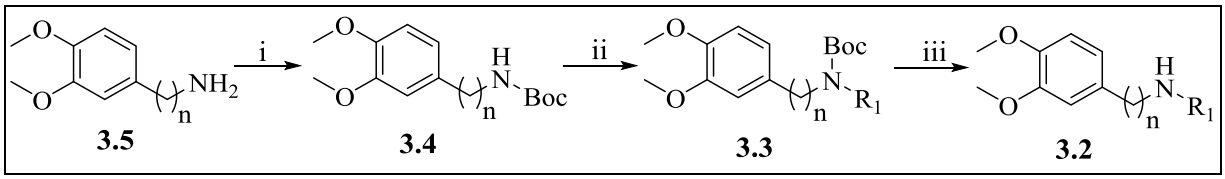

Scheme 3.5: *Reagents and reaction conditions:* (i) Boc_2O (1.2 eq.), DCM, Et_3N (1.5 eq.), 0 °C, 20 min; (ii) Alkyl halide (1.3 eq.), NaH (1.5), DMF, 0 °C, 6-8 h; (iii) TFA (10 eq.), Amberlyst A-21, DCM, 25 °C, 1-2 h.

To overcome this challenge and obtain the desired mono-alkylated intermediate, the nucleophilicity of nitrogen is reduced with the use of a protecting group. In this method, the amines were protected with *di-tert*-butyl dicarbonate [$(Boc)_2O$] in DCM at 0 °C in the presence of triethylamine, to obtain intermediates **3.4** (Scheme **3.3**).[11] These intermediates were subjected to reaction with various alkyl halides in DMF in the presence of NaH at 0 °C to produce **3.3**. The subsequent deprotection of **3.3** with TFA in DCM and neutralization with amberlyst A-21 produced intermediate **3.2** in good yield (Table **3.2**).

Table 3.2: Yields of isolated intermediates **3.3**, **3.4** and **3.5.**

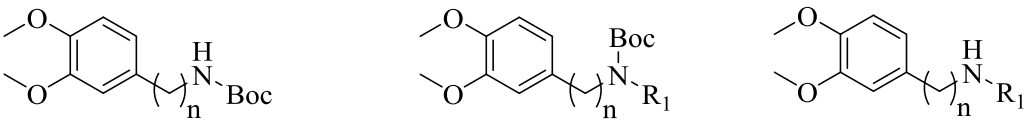

3.4 **3.3** **3.2**

Entry	n	Yield %	Entry	R_1	n	3.3 Yield %	3.2 Yield %
3.4a	0	67	**a**	$-CH_3$	0	65	67
3.4b	1	85	**b**	$-CH_3$	1	60	85
3.4c	2	94	**c**	$-CH_2CH_3$	2	54	87
			d	$-CH_2CH_2CH_3$	2	84	90

3.2.2.5 Mechanism for Boc-deprotection

Boc-deprotection of the amine can be achieved by various methods, which include basic deprotection with strong to weak bases, like potassium hydroxide and carbonates, or acidic deprotection with TFA and acetic acid (Scheme **3.4**).

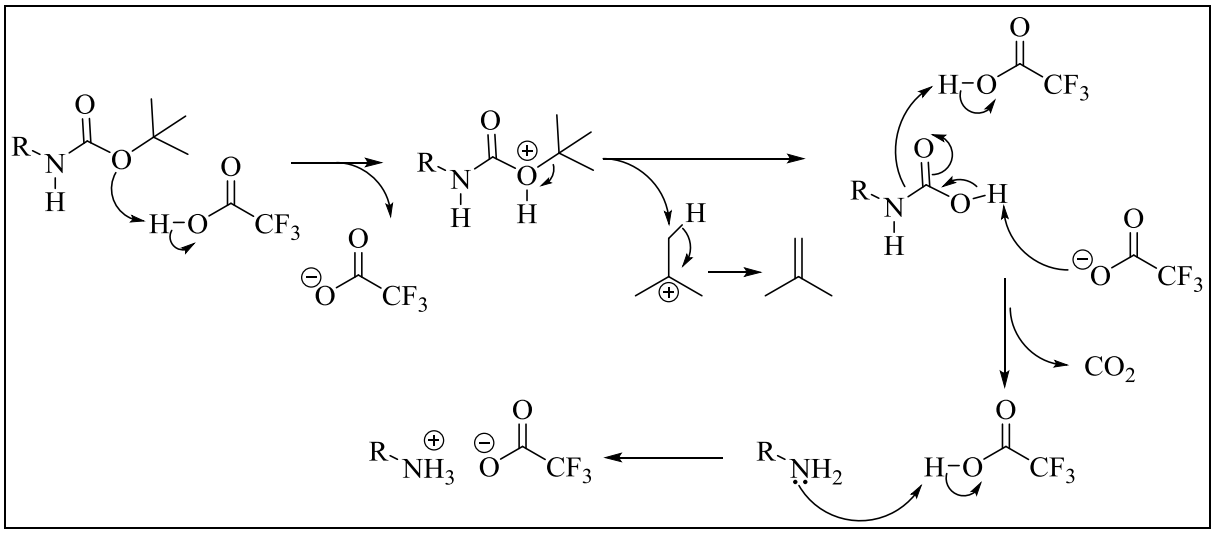

Scheme 3.4: Proposed mechanism of Boc-deprotection.

Boc deprotection mediated by acid requires an excess of acid. The first step in the deprotection is the protonation of the protected amine, followed by the release of the *tert*-butyl carbocation and deprotected amine. Within an acidic medium, the deprotected amine abstracts a proton from TFA and forms the trifluoroacetate salt,[12] which can be neutralized with various bases to obtain the free amine. The polymer-bound basic resin can be used to avoid the aqueous workup.

3.2.2.6 Synthesis of verapamil analogues (3.13)

The target verapamil analogues of SAR 1, 2, and 3 were obtained by coupling the previously synthesised intermediates **3.2** and **3.6** (Schemes **3.5** and **3.2)** in the presence of potassium carbonate in DMF at 80 °C. The target compounds **3.13** were obtained in low to moderate yields (Scheme **3.5** Table **3.3**).

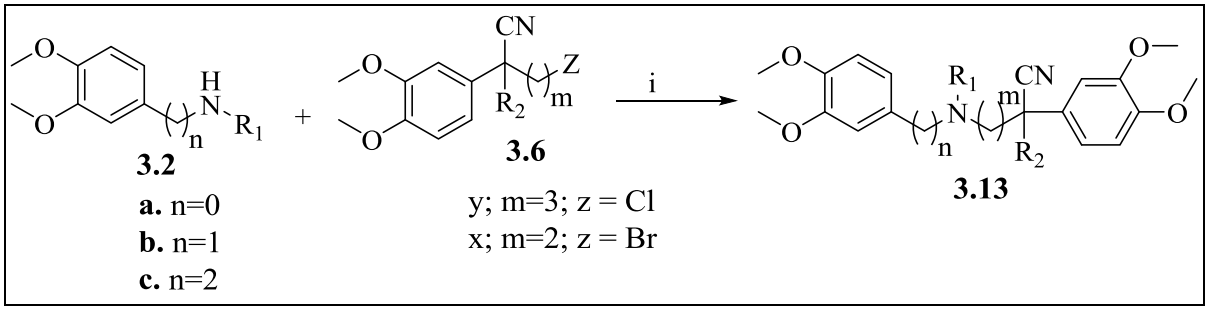

Scheme 3.5: *Reagents and reaction conditions:* (i) K_2CO_3 (2 eq.), DMF, 80 °C, 12 h.

In order to incorporate a cyclopropyl substituent on the nitrogen, a copper-promoted coupling reaction of the amine with a boronic acid, reported by Chan and Larn,[13] and further modified by Sebastien *et al*.,[13] was used to synthesize the desired target molecule **3.13o** (Scheme **3.6**). A mixture of **3.13e**, and an equimolar amount of cyclopropyl boronic acid and 2,2'-bipyridine were refluxed in dichloroethane (DCE) for two hours in the presence of sodium carbonate to obtain the desired compound **3.13o** in low yield **(**Table **3.3)**.

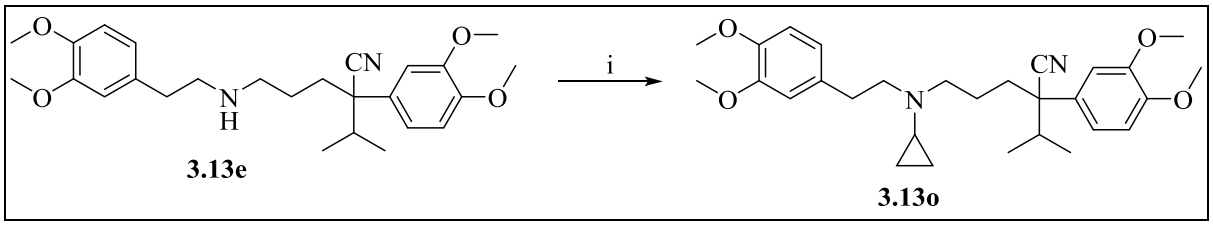

Scheme 3.6: *Reagents and reaction conditions:* (i) Cyclopropylboronic acid (2 eq.), $Cu(OAc)_2$ (1 eq.), Bipy (1 eq.), Na_2CO_3 (2 eq.), DCE , reflux (90 °C), 2 h.

Table 3.3: Yields of isolated target compounds **3.13**.

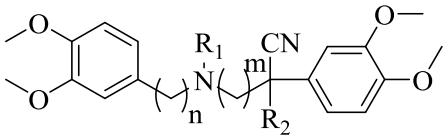

3.13

Compound	n	m	R^1	R^2	Yield %
3.13a	0	3	$-CH_3$	$-CH(CH)_3$	29
3.13b	1	3	$-CH_3$	$-CH(CH_3)_2$	34
3.13c	1	2	$-CH_3$	$-CH(CH_3)_2$	29
3.13d	2	2	$-CH_3$	$-CH(CH_3)_2$	40
3.13e	2	3	$-H$	$-CH(CH_3)_2$	37
3.13f	2	3	$-CH_2CH_3$	$-CH(CH_3)_2$	37
3.13g	2	3	$-CH_2CH_2CH_3$	$-CH(CH_3)_2$	17
3.13h	2	3	$-CH_2Ph$	$-CH(CH_3)_2$	26
3.13i	2	3	$-CH_3$	$-H$	32
3.13j	2	3	$-CH_3$	$-CH_3$	49
3.13k	2	3	$-CH_3$	$-CH_2CH_3$	49
3.13l	2	3	$-CH_3$	$-CH_2CH_2CH_3$	53
3.13m	2	3	$-CH_3$	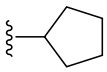	36
3.13n	2	3	$-CH_3$	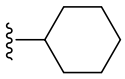	32
3.13o	2	3		$-CH(CH_3)_2$	19

3.2.2.7 Characterization of representative verapamil analogue from SAR 1

The verapamil analogues were characterized using ^{1}H-NMR, ^{13}C-NMR and mass spectroscopy (MS). The purity of compounds was checked using high performance liquid chromatography (HPLC) and more than 95% purity was recorded for all the analogues.

The ^{1}H-NMR chemical shifts were assigned with the aid of ^{1}H-^{1}H COSY and ^{1}H-^{13}C NOSY spectroscopy. The ^{1}H-NMR spectrum of the verapamil analogue **3.13k,** having an ethyl substituent at the stereogenic centre, is shown in **figure 3.3**. The key signals in the ^{1}H-NMR

spectrum are a triplet resonating at δ 0.92 ppm corresponding to the three methyl protons H-2' and the presence of multiplets in the aliphatic region between δ 1.80-1.95 ppm, corresponding to methylene protons H-1', which confirmed the presence of the ethyl group.

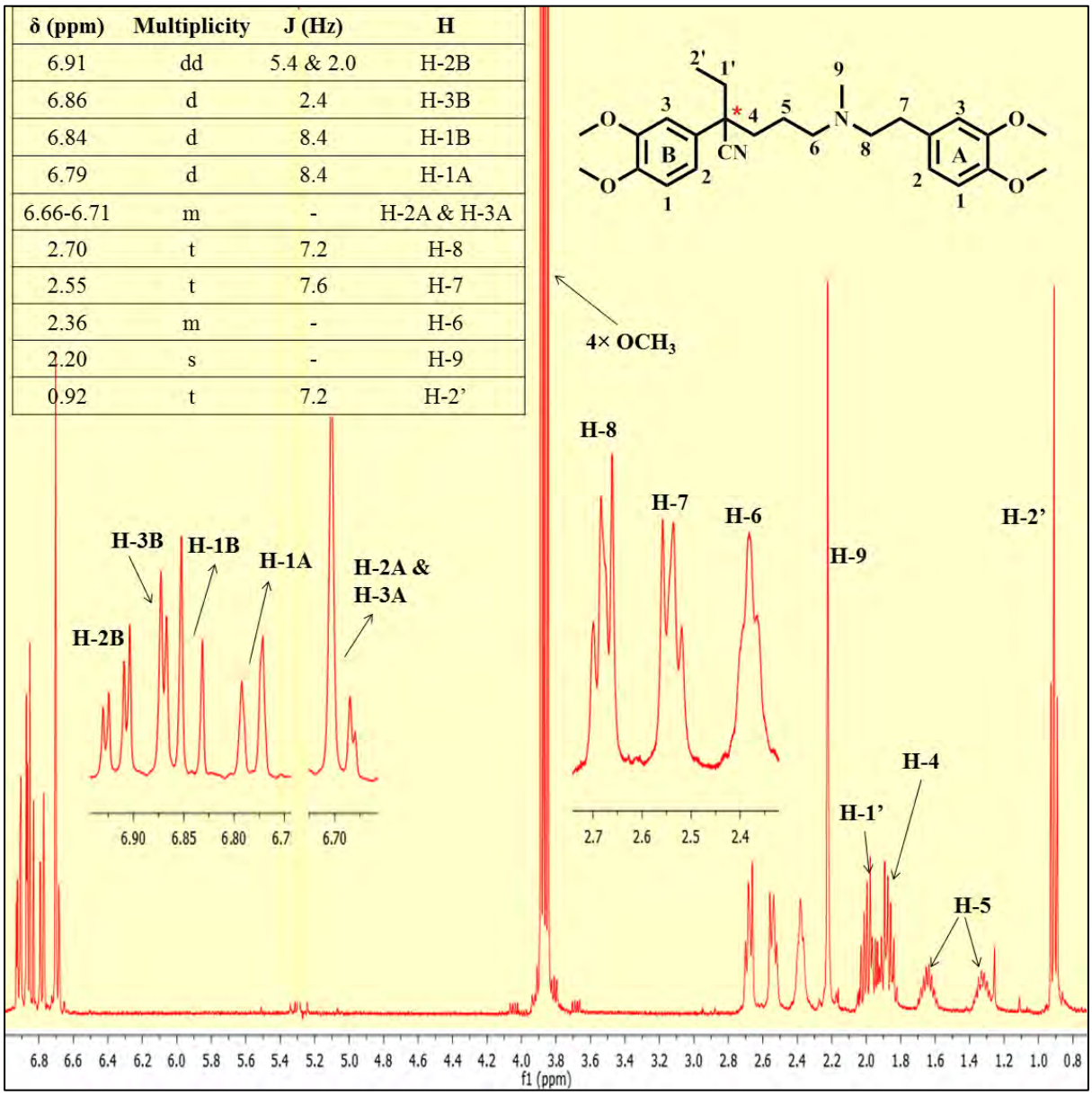

Figure 3.3: ^{1}H-NMR spectrum of verapamil analogue **3.13k** in $CDCl_3$ at 400 MHz.

The aromatic region of the ^{1}H-NMR spectrum contains signals corresponding to the six aromatic protons of **3.13k**. These signals appeared as one doublet of doublet at 6.91 ppm corresponding to H-2B, one doublet with a coupling constant of J = 2.4 Hz representing H-3B, two doublets with an equal coupling constant of J = 8.4 Hz corresponding to H-1B and H-1A, and a multiplet in the range of 6.71-6.66 ppm corresponding H-2A and H-3A. These aromatic signals were found to exist in the ^{1}H-NMR spectrum of all the VER analogues as no

modification of the phenyl rings were carried out during the synthesis of the VER analogues in this study.

An anomalous splitting pattern for protons (H-4 and H-5), adjacent to the stereogenic centre was observed. The methylene protons H-5 appeared as two separate, one proton multiplets at δ 1.33 and 1.63 ppm. The methylene protons H-4 also resonated as broad multiplets at δ 1.88 ppm. Speculatively, this may be attributed to through space coupling or could be indicative of the diastereotopic nature of these protons in **3.13k**. An additional set of two triplets, one multiplet and one singlet were also observed at δ 2.70, 2.55, 2.36 and 2.20 ppm corresponding to H-8, H-7, H-6 and H-9 protons, respectively.

The ^{13}C-NMR spectrum (**Figure 3.4**) of compound **3.13k** showed 22 non-equivalent signals, whose total intensity correlated with the 26 carbons of compound **3.13k**. The key signals to support the presence of the ethyl group at the stereogenic centre are the appearance of two signals corresponding to methyl and methylene carbons at δ 9.66 and 33.19 ppm, respectively.

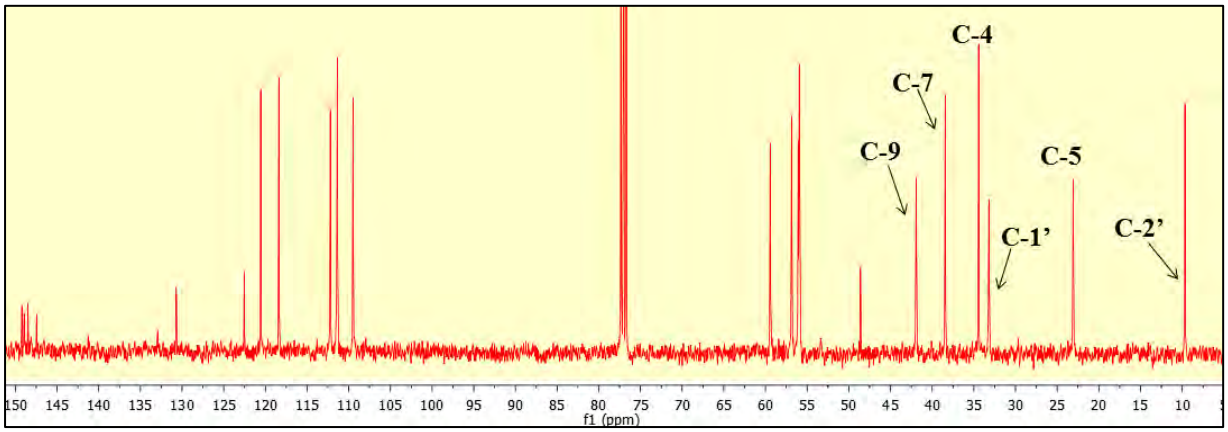

Figure 3.4: ^{13}C-NMR spectrum of verapamil analogue **3.13k** in $CDCl_3$ at 101 MHz.

3.2.2.8 Synthesis of piperazine analogues of verapamil (3.15)

The piperazinyl analogues of verapamil, according to SAR 4 (**Figure 3.1**), were synthesised by reaction of intermediate **3.6c** with various commercially available piperazinyls **3.14** in DMF in the presence of potassium carbonate at 80 °C (Scheme **3.7**) to afford target compounds **3.15** in poor to moderate yield (Table **3.4**).

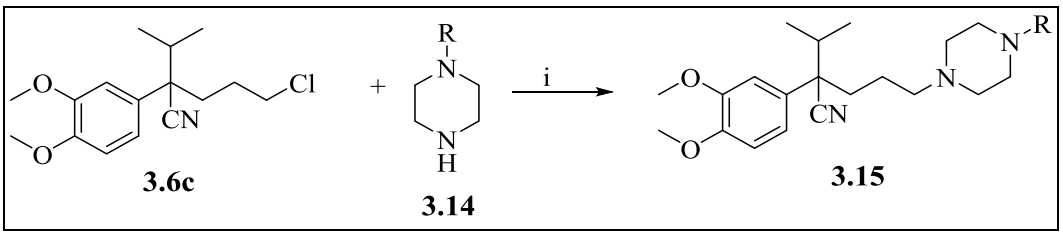

Scheme 3.7: *Reagents and condition:* (i) K_2CO_3 (2.5 eq.), DMF, 80 °C, 12 h.

Table 3.4: Yields of isolated target compounds **3.15**.

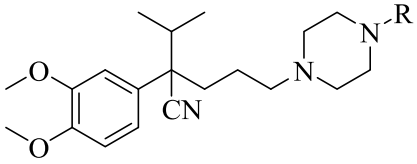

3.15

Compound	R	Yield %	Compound	R	Yield %
3.15a		60	**3.15g**	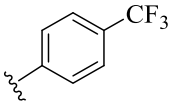	37
3.15b	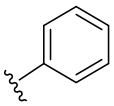	49	**3.15h**	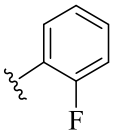	37
3.15c	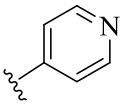	24	**3.15i**	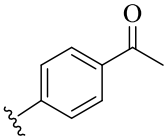	28
3.15d	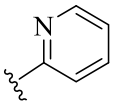	58	**3.15j**	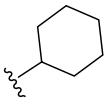	32
3.15e	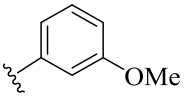	47	**3.15k**	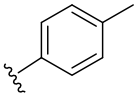	35
3.15f	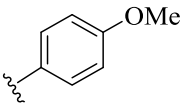	28	**3.15l**	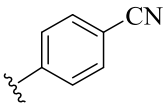	30

3.2.2.9 Characterization of piperazine analogue of verapamil 3.15i

The structural confirmations of piperazinyl analogues of VER were achieved with the aid of various spectroscopic techniques (^{1}H-NMR, ^{13}C-NMR and mass spectroscopy). The purity of compounds was checked with the aid of HPLC, which showed more than 95% purity for all the analogues. Electrospray ionization (ESI) mass spectroscopy showed pseudomolecular ion peaks as *m/z* [M+H], corresponding to the required masses of the analogues **3.15**. Figures **3.5** and **3.6** show the ^{1}H-NMR and ^{13}C-NMR spectra of a representative piperazinyl analogue of verapamil, **3.15i**. The piperazine motif attached to the verapamil substructure was confirmed with the appearance of two broad triplets at δ 3.36 and 2.51 ppm with an identical coupling constant of J = 4.8 Hz, corresponding to H-8 and H-7 protons, respectively.

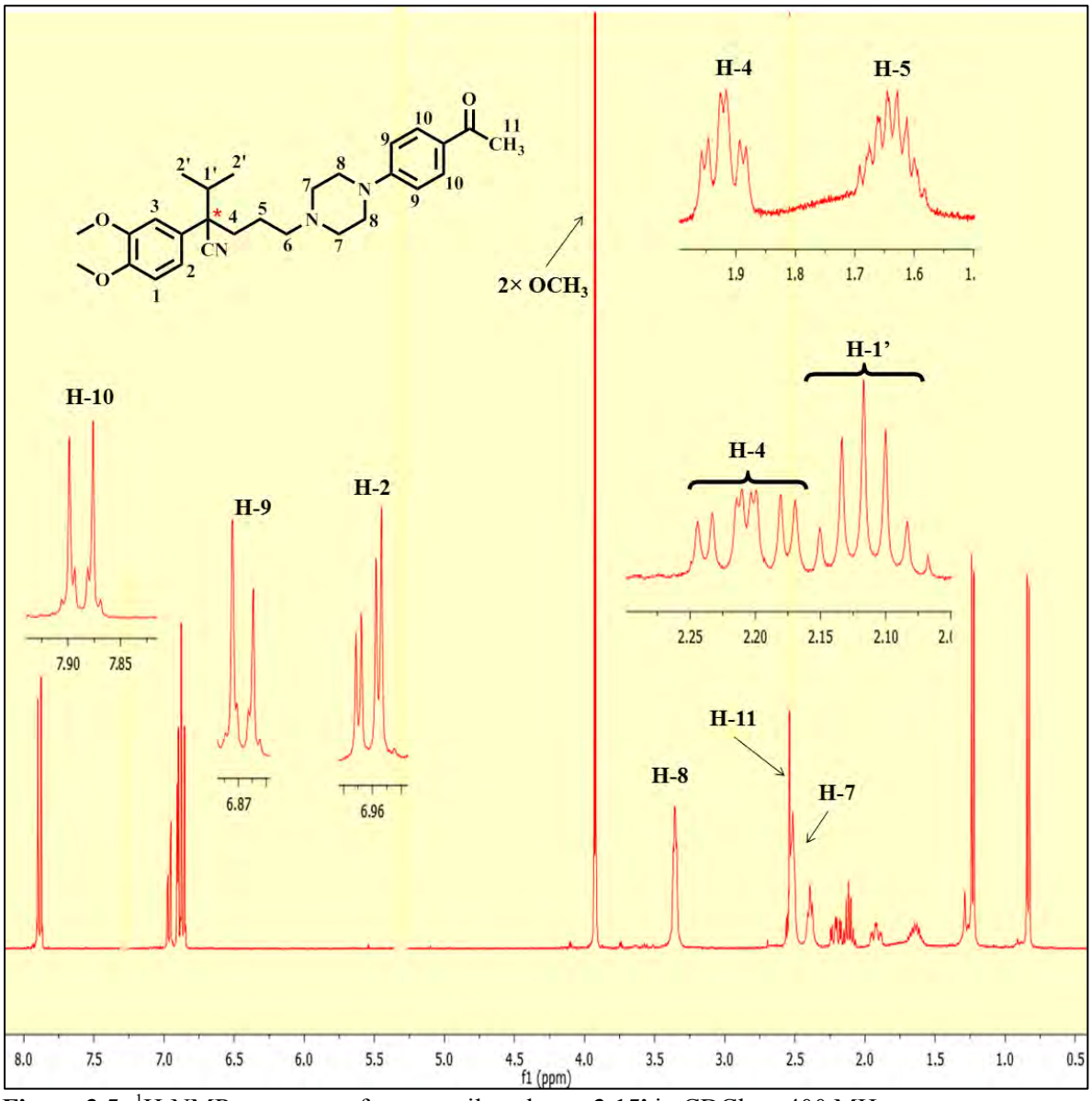

Figure 3.5: ^{1}H-NMR spectrum of verapamil analogue **3.15i** in $CDCl_3$ at 400 MHz.

In addition to the expected number of aromatic protons, the splitting pattern of aromatic signals varied according to the substituent on the phenyl group of the piperazinyl moiety. In the case of **3.15i**, two doublets at δ 6.87 and 7.88 ppm with an identical coupling constant of *J*= 8.8 Hz were observed, corresponding to H-9 and H-10 protons, respectively. Among other key signals, three multiplets were observed for H-1', H-4, and H-5 protons in the region δ 2.30-1.60 ppm. The diastereotopic nature of these protons could account for these anomalous splitting patterns.

The ^{13}C-NMR spectrum showed 24 non-equivalent signals corresponding to the 28 carbons of compound **3.15i** (**Figure 3.6**). The presence of the characteristic carbonyl carbon peak at δ 196.4 ppm confirms the synthesis of the desired derivative. Additional key signals appeared at δ 52.6, 42.2, and 26.0 ppm corresponding to C-8, C-7 and C-11 carbons of the piperazine moiety, respectively.

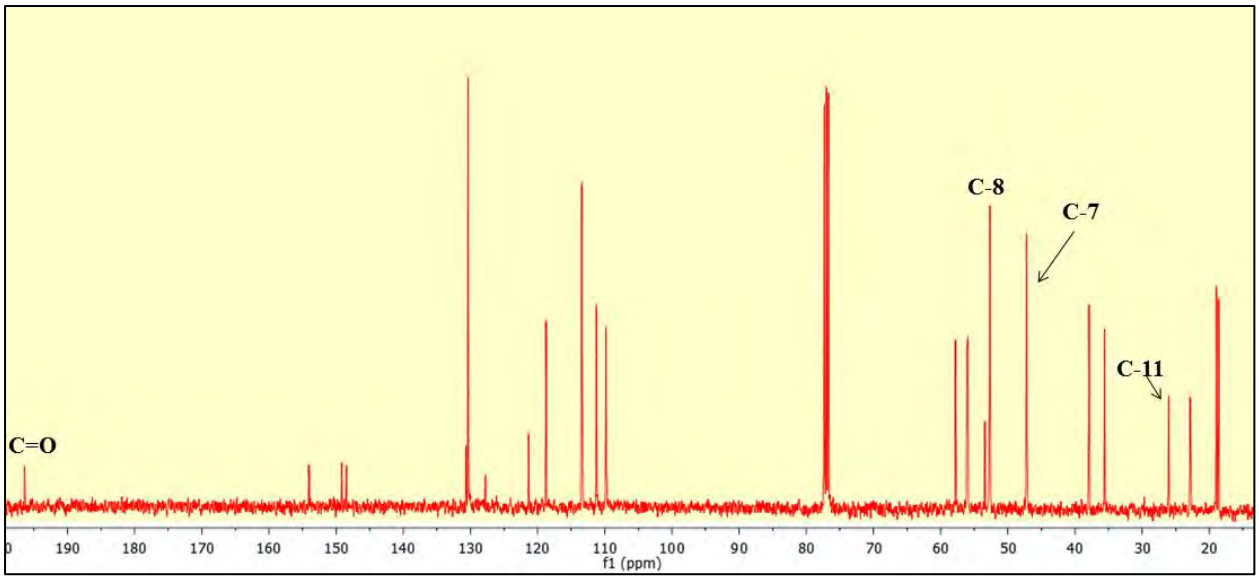

Figure 3.6: ^{13}C-NMR spectrum of verapamil analogue **3.15i** in $CDCl_3$ at 101 MHz.

3.2.2.10 Synthesis of *N*-benzylated verapamil analogues (3.17)

The synthesis of verapamil analogues **3.17** (Scheme **3.8**), with various benzyl substituents on the basic nitrogen, began with the synthesis of *Nor*-verapamil **3.13e** (Section **3.2.2.6**). *Nor*-verapamil **3.13e** was then reacted with various benzyl halides in DMF using potassium carbonate at 80 °C (Scheme **3.8**) to obtain target compounds **3.17** in low to moderate yields (Table **3.5**).

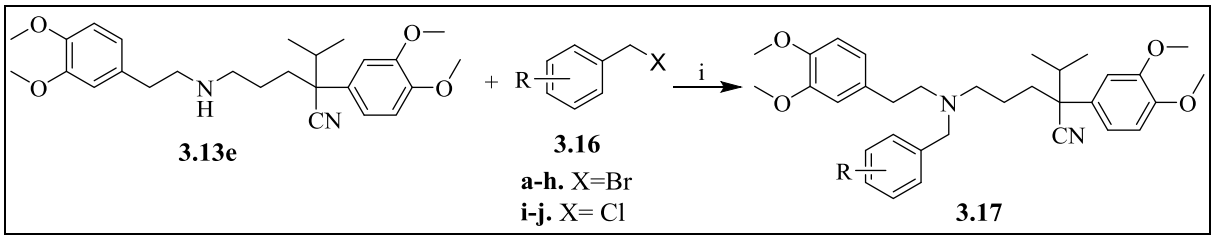

Scheme 3.8: *Reagents and condition:* (i) K_2CO_3 (2.5 eq.), DMF, 80 °C, 8 h.

Table 3.5: Isolated yields of target compounds **3.17**.

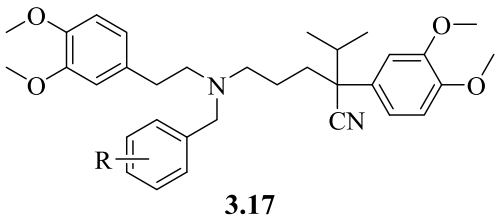

3.17

Compound	R	Yield (%)
3.17a	4-CH_3	28
3.17b	4-Cl	21
3.17c	2-CN	58
3.17d	3-OCH_3	20
3.17e	3-CF_3	33
3.17f	2-OCF_3	28
3.17g	4-OCF_3	34
3.17h	4-SCH_3	61
3.17i	4-CN	21
317j	3-$COCH_3$	27

3.2.2.11 Synthesis of rigid verapamil analogues

3.2.2.11.1 Rationale

As described in chapter **2**, section **2.6.2.1**, the spatial arrangements of VER play an important role in the modulation of Pgp-mediated resistance.[6] A number of VER analogues with restricted flexibility have been developed and have shown reversal of resistance to 4'-*O*-tetrahydropyranyl Adriamycin, comparable to the activity of VER against a K562 erythroleukemia cell line but with reduced calcium channel antagonism.[14–16] Therefore, the design of rigid VER analogues and investigating their potentiating properties on anti-TB drugs against *Mtb* may lead to the identification and development of potent chemosensitizers devoid of calcium channel blocking properties. In this study, two reported VER analogues, **EDP42** and **MKVR1** (**Figure 3.11**),[16] with reduced rotational degree of freedom were synthesised to investigate the effect of rigidity on the activity of anti-TB drugs against *Mtb*.

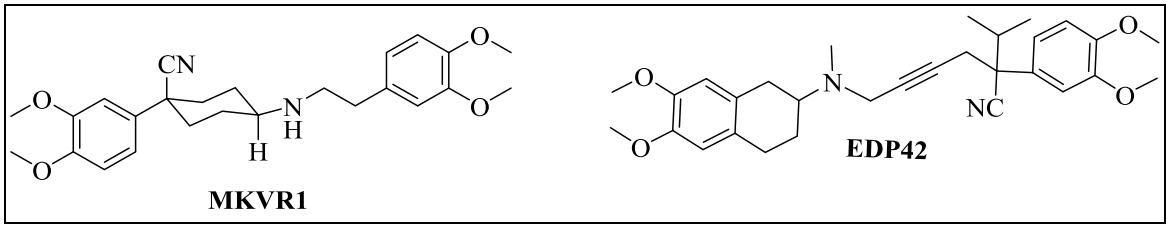

Figure 3.11: Rigid VER analogues with reduced calcium channel antagonism.

3.2.2.11.2 Synthesis of verapamil analogue MKVR1

The synthesis of **MKVR1** was preceded by the synthesis of the cyclohexyl precursor **3.20** by using a method established previously (Scheme **3.9**).[17] The synthesis of **3.20** commenced with the reaction of commercially available 2-(3,4-dimethoxyphenyl)acetonitrile **3.8**, with methylacrylate using an organic base triton-B in *tertiary*-butyl alcohol, resulting in the intermediate **3.18**. This compound was cyclized in the presence of sodium hydride in dimethoxy ethane (DME) under a nitrogen atmosphere at 70 °C to produce **3.19** in 65% yield. Subsequent decarboxylation of **3.19** by refluxing in 10% aqueous sulphuric acid for 10 hours produced the cyclohexanone intermediate **3.20** in 54% yield.

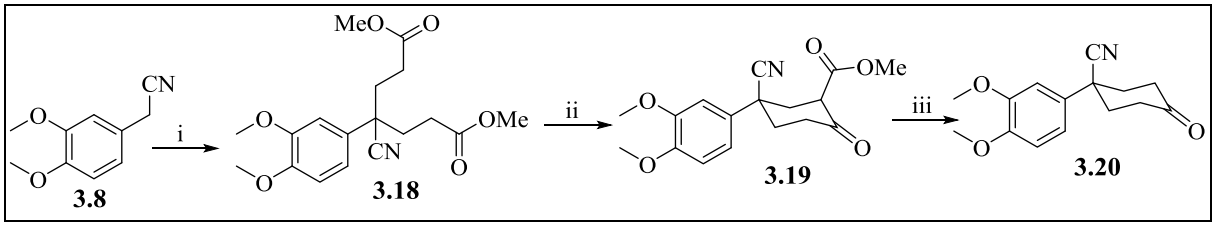

Scheme 3.9: *Reagents and reaction conditions:* (i) Triton B (0.22 eq.), methyl acrylate (3.2 eq.), *t*-BuOH, reflux (90 °C), 18 h; (ii) NaH (1.55 eq.), DME, 70 °C, 1 h; (iii) H_2SO_4 10%, reflux (95 °C), 10 h.

3.2.2.11.2.1 Synthesis of (R,Z)-4-((3,4-dimethoxyphenethyl)imino)-1-(3,4-dimethoxyphenyl) cyclohexane-1-carbonitrile

The synthesis of the target compound **3.22 (MKVR1)** commenced with reductive amination of the cyclohexanone intermediate **3.20** with 2-(3,4-dimethoxyphenyl)ethan-1-amine **3.5** (Scheme **3.10**) to obtain imine **3.21.** This intermediate **3.21** was reduced *in situ* without further purification to obtain target compound **3.22** in moderate yield (Table **3.6**). This method stereoselectively produced the target compound as a *cis* isomer, which was confirmed by ^{1}H-NMR as discussed in the following section.

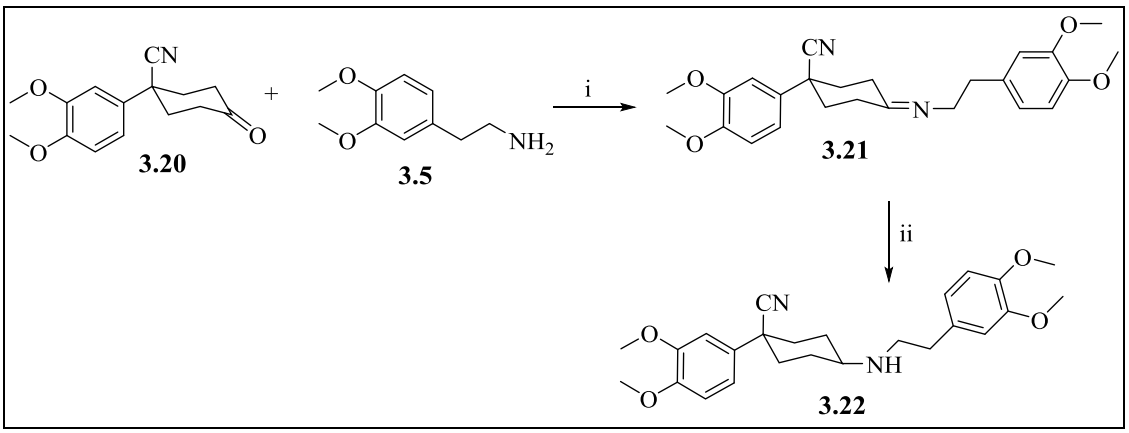

Scheme 3.10: *Reagents and reaction conditions:* (d) (i) *para*-toluene sulfonic acid (*p*-TSA), toluene, reflux, 45 h (ii) $NaBH_4$ (1.1 eq.), MeOH, reflux, 0.5 h.

Table 3.6: Percentage yields of intermediates (**3.18**, **3.19,** and **3.20)** and target compound **3.22**.

Compounds	Yield (%)	m.p (°C)
3.18	72	60-62
3.19	65	118–120
3.20	60	109-112
3.22	22	59–61

3.2.2.11.2.2 Characterization of target compound 3.22

The target compound **3.22** was characterized using ^{1}H-NMR and ^{13}C-NMR spectroscopy as well as LC-MS. The LC-MS chromatogram showed more than 99% purity of **3.22** and a pseudomolecular ion mass peak of *m/z* 425.2 [M+H]. The ^{1}H-NMR spectrum (**Figure 3.7**) correlates with the reported spectrum of **3.22**.[17] The characteristic signals include four multiplets in the range of δ 2.25-1.68 ppm, corresponding to the eight hydrogens (H-4, H-5,

H-6 and H-7) of the cyclohexyl moiety. A triplet of triplets was observed at δ 2.60 ppm with coupling constants of J = 11.2 and 3.4 Hz for H-8, thus confirming its axial orientation and the *cis* conformation of the molecule with respect to the nitrile group.

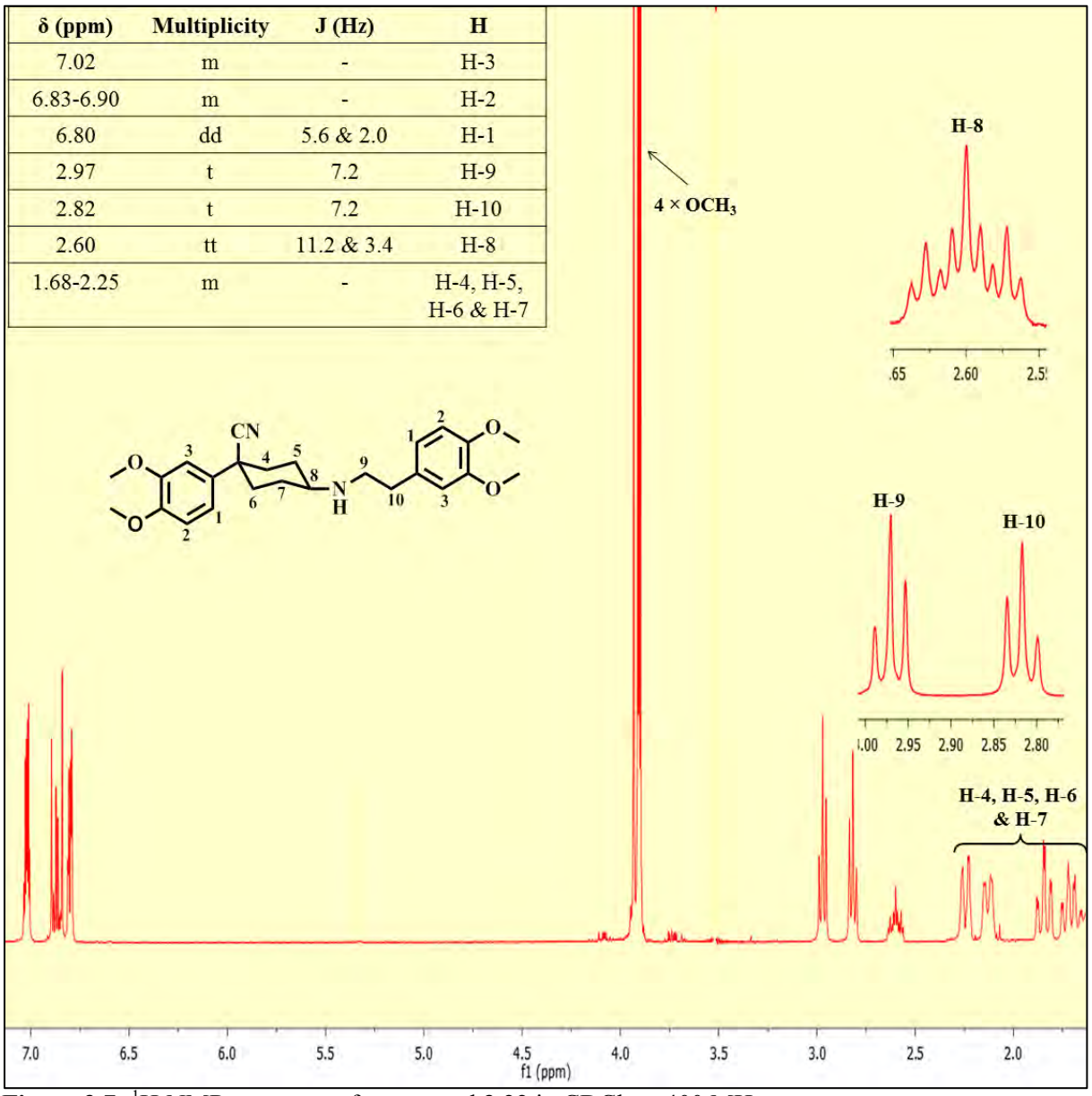

Figure 3.7: ^{1}H-NMR spectrum of compound **3.22** in $CDCl_3$ at 400 MHz.

The ^{13}C-NMR spectrum of the target compound **3.22** (**Figure 3.8**) showed 25 non-equivalent signals with some signals resonating for two carbons and correlated with the spectrum reported by Romanelli *et. al*.[17] The characteristic signals corresponding to the cyclohexyl carbons C-5 to C-7 were observed in the aliphatic region.

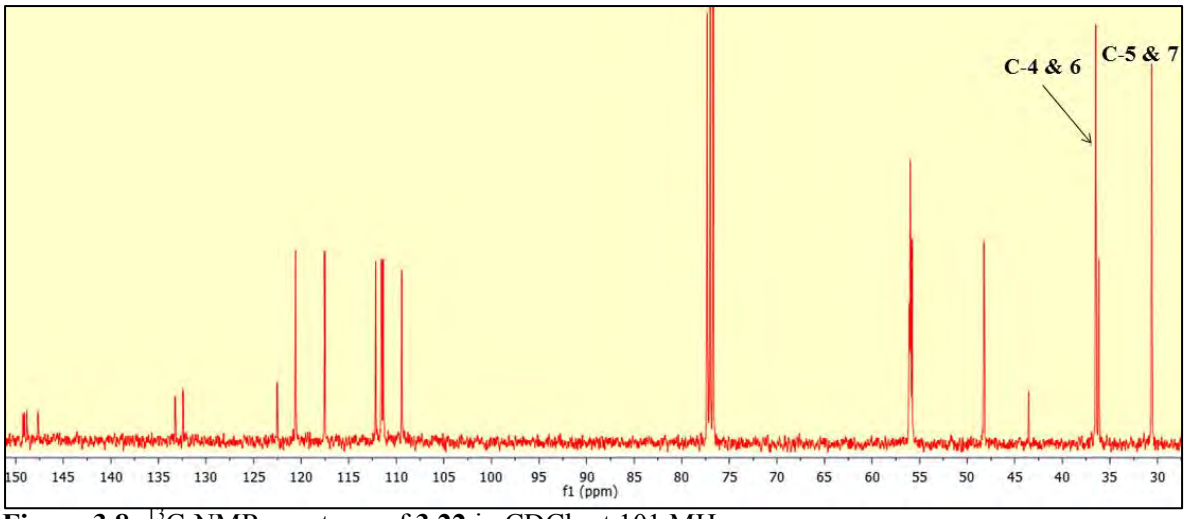

Figure 3.8: ^{13}C-NMR spectrum of **3.22** in $CDCl_3$ at 101 MHz.

3.2.2.11.3 Synthesis of verapamil analogue EDP42

3.2.2.11.3.1 Synthesis of 6,7-dimethoxy-3,4-dihydronaphthalen-2(1H)-one

The synthesis of the rigid verapamil analogue **EDP42** was preceded by the synthesis of a key precursor, 6,7-dimethoxy-3,4-dihydronaphthalen-2(1H)-one **3.28**. Scheme **3.11** presents the outline of the synthesis of **3.28** from 6,7-dimethoxy-3,4-dihydronaphthalen-1(1H)-one **3.23**. The synthesis was achieved through the reduction of **3.23** with sodium borohydride in ethanol, followed by acid-catalysed dehydration by refluxing intermediate **3.24** in the presence of *para*-toluene sulfonic acid (*p*-TSA) in toluene to obtain the alkene intermediate **3.25**. The synthesis of **3.28** from intermediate **3.25** was envisioned by epoxidation of **3.25** in the presence of *meta*-chloroperbenzoic acid (*m*-CPBA) in DCM at 0 to 25 °C, followed by a 1,2-oxygen shift to afford the desired 6,7-dimethoxy-3,4-dihydronaphthalen-2(1H)-one **3.28**.

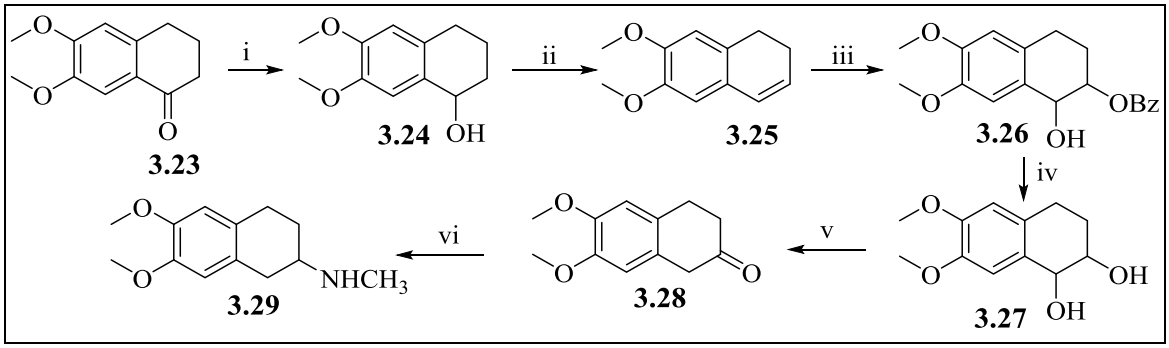

Scheme 3.11: *Reagents and reaction conditions*: (i) $NaBH_4$ (2 eq.), EtOH, 25 °C, 10 h; (ii) *p*-TsOH (0.1), toluene, reflux (115 °C), 2 h; (iii) *m*-CPBA (1.1 eq.), DCM, 0-25 °C, 1 h; (iv) 2M NaOH, MeOH, reflux, 2 h; (v) BF_3 (cat.), diethyl ether, 0-25 °C, 2 h; (vi) NH_2CH_3 (5.5 eq.), $NaCNBH_3$ (3 eq.), EtOH, $NaHCO_3$, 25 °C, 24 h.

It is known that tetralines with electron-donating substituents on aromatic rings are very

sensitive to epoxidation with *m*-CPBA, which leads to many side products.[18] Therefore, the reaction of the alkene intermediate **3.25** with *m*-CPBA produced many side products, with α-hydroxy benzoate ester **3.26** as the major product. This intermediate was converted to **3.28** by sodium hydroxide-mediated basic hydrolysis, followed by acid-catalysed dehydration with boron trifluoro etherate in diethyl ether. The reductive amination of **3.28** with methylamine in the presence of sodium cyanoborohydride in ethanol furnished the desired advanced intermediate **3.29**.

3.2.2.11.3.2 The mechanism of acid-catalysed regioselective dehydration

It is known that both epoxide isomerization and diol dehydration proceed through a common pathway of the enol intermediate (Scheme **3.12**). The tautomerization of the enol intermediate produces the desired 6,7-dimethoxy-3,4-dihydronaphthalen-2(1H)-one.[18,19]

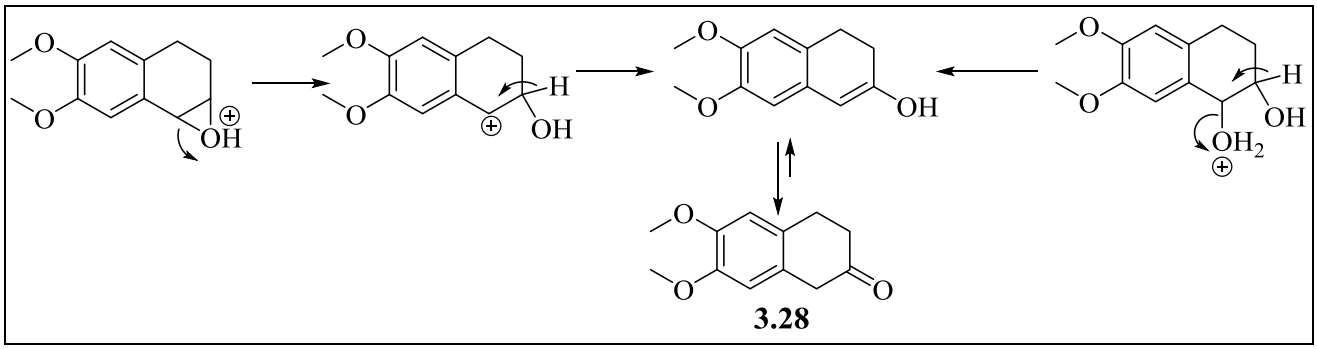

Scheme 3.12: Proposed mechanistic pathway for diol-dehydration and epoxide isomerization.

3.2.2.11.3.3 Synthesis of target compound EDP42

The target compound **EDP42** was obtained through a multicomponent Mannich reaction of **3.30**, **3.29** and formaldehyde in 40% aqueous ethanol in the presence of copper sulfate as a catalyst under slightly basic conditions (pH = 8) (Scheme **3.13**). A Mannich base is expected to be formed by the reaction of **3.29** and formaldehyde, and subsequent addition of alkyne **3.30** to this base leads to the formation of **EDP42**.

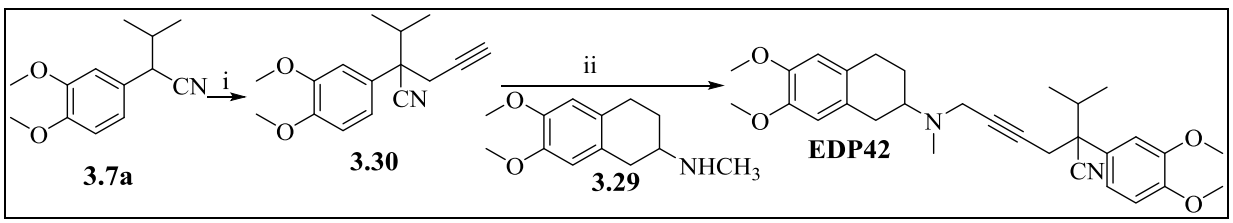

Scheme 3.13: *Reagents and reaction conditions*: (i) Propargylbromide (1.5 eq.), *n*-BuLi (1.1 eq.), THF, 0-25 °C, 1 h, (55%); (ii) CH_2O (40% in water) (1.1 eq.), $CuSO_4$ (cat.), EtOH/H_2O (1:1), reflux (85 °C), 24 h, (20%).

3.2.2.11.3.4 Characterization of EDP42

The LCMS chromatogram of **EDP42** showed 99% purity of the compound and a pseudomolecular ion mass peak of *m/z* 491.3 [M+H]. The ^{1}H-NMR spectrum (**Figure 3.9**) correlates well with that reported.[20]

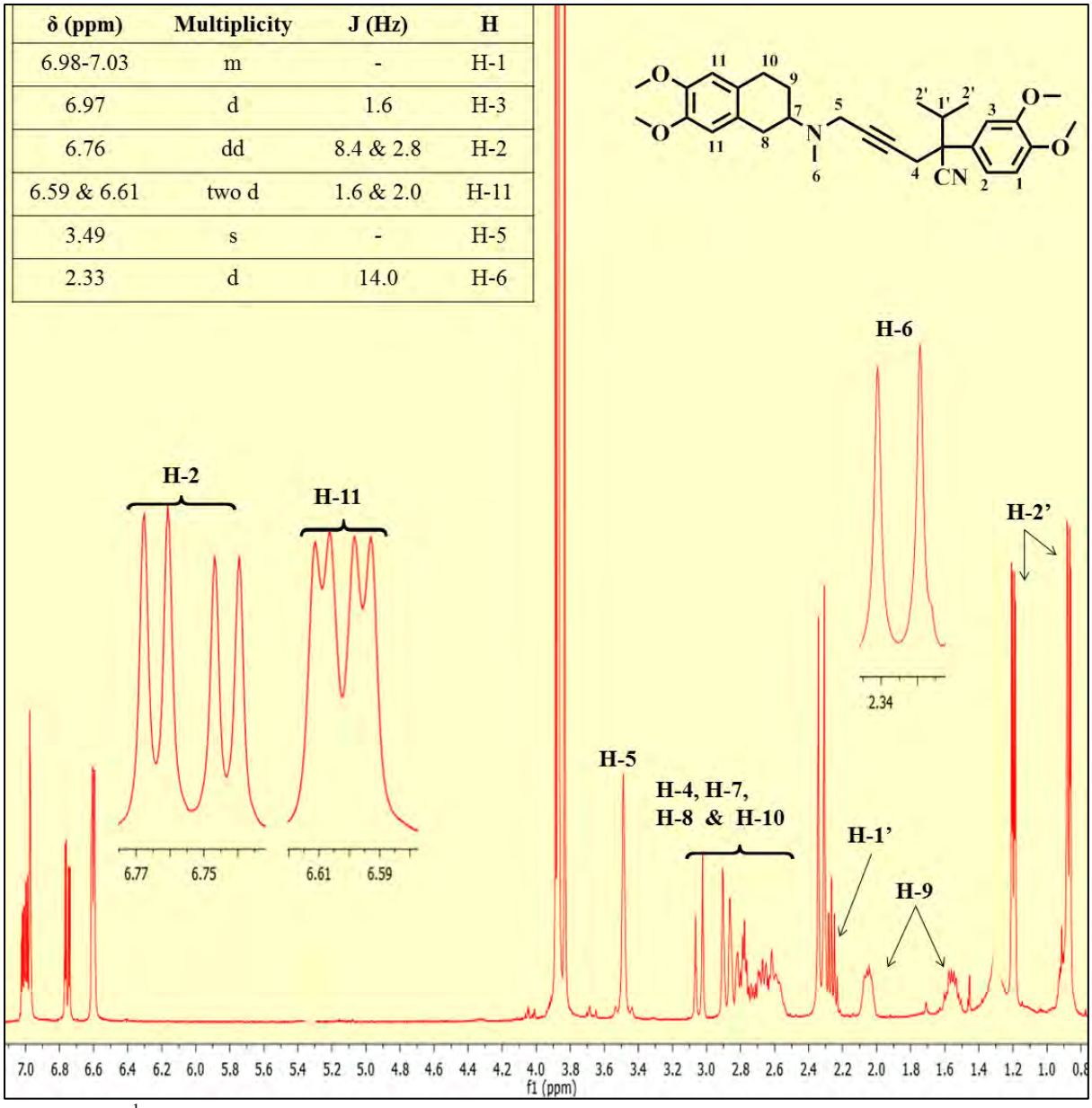

Figure 3.9: ^{1}H-NMR spectrum of **EDP42** in $CDCl_3$ at 400 MHz.

The characteristic signals include a singlet at δ 3.49 ppm, and a doublet at δ 2.33 ppm, corresponding to H-5, and H-6 protons, respectively. Other characteristic signals are two doublets at δ 6.59 and 6.61 ppm with coupling constants of J = 1.6 and 2.0 Hz, corresponding to the two aromatic protons H-11 of the 6,7-dimethoxy-3,4-dihydronaphthalen-2(1H)-one substructure. The splitting of H-11 may be attributed to the long range coupling of benzylic

protons H-10/H-8.[21,22] All the remaining aliphatic protons appeared as multiplets scattered in the aliphatic region due to the diastereotopic nature of the compound. The presence of the lipophilic head of verapamil was confirmed by the presence of aromatic signals, and aliphatic signals as one multiplet (δ 2.26 ppm), and two doublets of doublets (δ 0.87, and 1.2 ppm) corresponding to H-1' and H-2' protons, respectively.

The ^{13}C-NMR spectrum (**Figure 3.10**) correlated well with ^{1}H-NMR spectral data and showed 26 singlets corresponding to the expected 30 carbons of the compound **EDP42**. The characteristic signals are two low intensity peaks at δ 79.8 and 80.1 ppm, corresponding to the quaternary carbons of the alkyne. The additional key signals at δ 57.6 and 43.4 ppm corresponded to C-5 and C-7 carbons, respectively.

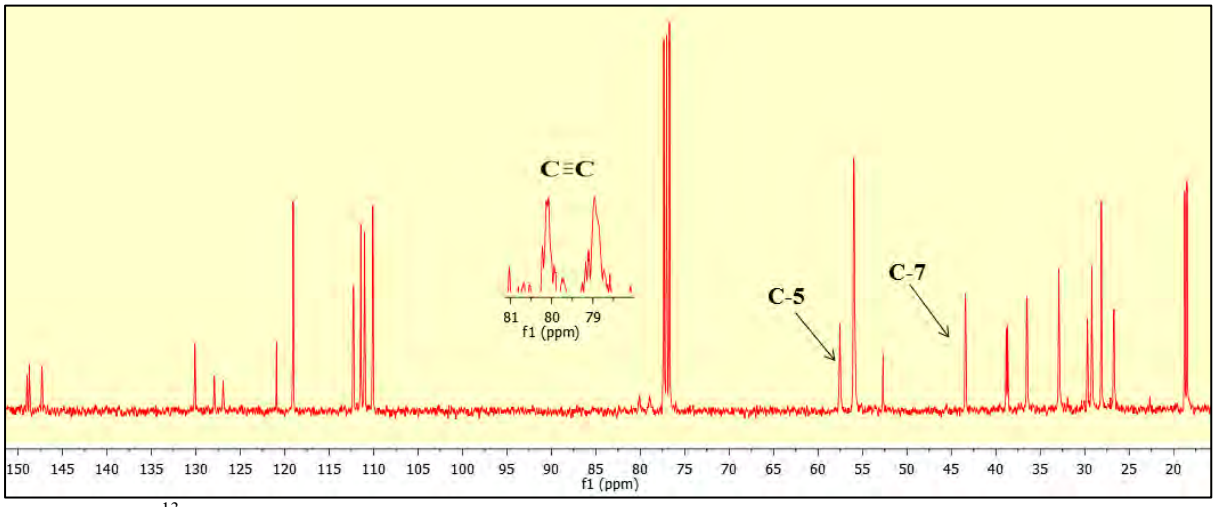

Figure 3.10: ^{13}C-NMR spectrum of **EDP42** in $CDCl_3$ at 101 MHz.

3.3 Conclusion

The design, synthesis and characterization of various verapamil analogues was successfully carried out. The spectroscopic data confirmed the structures of the expected compounds. The biological evaluation of the synthesized analogues will be presented and discussed in chapter **5** of this thesis.

Reference:

(1) Adams, K. N.; Szumowski, J. D.; Ramakrishnan, L. Verapamil, and Its Metabolite Norverapamil, Inhibit Macrophage-Induced, Bacterial Efflux Pump-Mediated Tolerance to Multiple Anti-Tubercular Drugs. *J. Infect. Dis.* **2014**, *210*, 456–466.

(2) Dartois, V.; Barry, C. E. A Medicinal Chemists' Guide to the Unique Difficulties of Lead Optimization for Tuberculosis. *Bioorg. Med. Chem. Lett.* **2013**, *23*, 4741–4750.

(3) Bhattacharjee, A. K.; Kyle, D. E.; Vennerstrom, J. L.; Milhous, W. K. A 3D QSAR Pharmacophore Model and Quantum Chemical Structure-Activity Analysis of Chloroquine(CQ)-Resistance Reversal. *J. Chem. Inf. Model.* **2002**, *42*, 1212–1220.

(4) Teodori, E.; Dei, S.; Quidu, P.; Budriesi, R.; Chiarini, A.; Garnier-Suillerot, A.; Gualtieri, F.; Manetti, D.; Romanelli, M. N.; Scapecchi, S. Design, Synthesis, and in Vitro Activity of Catamphiphilic Reverters of Multidrug Resistance: Discovery of a Selective, Highly Efficacious Chemosensitizer with Potency in the Nanomolar Range. *J. Med. Chem.* **1999**, *42*, 1687–1697.

(5) Loe, D. W.; Oleschuk, C. J.; Deeley, R. G.; Cole, S. P. Structure-Activity Studies of Verapamil Analogs That Modulate Transport of Leukotriene C(4) and Reduced Glutathione by Multidrug Resistance Protein MRP1. *Biochem. Biophys. Res. Commun.* **2000**, *275*, 795–803.

(6) Grossi, A.; Biscardi, M. Reversal of MDR by Verapamil Analogues. *Hematology* **2004**, *9*, 47–56.

(7) Singh, K.; Kumar, M.; Pavadai, E.; Naran, K.; Warner, D. F.; Ruminski, P. G.; Chibale, K. Synthesis of New Verapamil Analogues and Their Evaluation in Combination with Rifampicin against *Mycobacterium tuberculosis* and Molecular Docking Studies in the Binding Site of Efflux Protein Rv1258c. *Bioorg. Med. Chem. Lett.* **2014**, *24*, 2985–2990.

(8) Zhongxu Ren, Bo-Liang Deng, Jennifer Riggs-Sauthier, M. H. Oligomer-Calcium Channel Blocker Conjugates. PCT/ US 2008/ 010385.

(9) *Encyclopedia of Reagents for Organic Synthesis*; John Wiley & Sons, Ltd: Chichester, 2001.

(10) Salvatore, R. N.; Yoon, C. H.; Jung, K. W. Synthesis of Secondary Amines. *Tetrahedron* **2001**, *57*, 7785–7811.

(11) Greene, T. W.; Wuts, P. G. M. *Protective Groups in Organic Synthesis*; John Wiley & Sons, Inc.: New York, USA, **1999**.

(12) Ashworth, I. W.; Cox, B. G.; Meyrick, B. Kinetics and Mechanism of N-Boc Cleavage: Evidence of a Second-Order Dependence upon Acid Concentration. *J. Org. Chem.* **2010**, *75*, 8117–8125.

(13) Lam, P. Y.; Clark, C. G.; Saubern, S.; Adams, J.; Winters, M. P.; Chan, D. M. .; Combs, A. New Aryl/heteroaryl C-N Bond Cross-Coupling Reactions via Arylboronic Acid/cupric Acetate Arylation. *Tetrahedron Lett.* **1998**, *39*, 2941–2944.

(14) Dei, S.; Romanelli, M. N.; Scapecchi, S.; Teodori, E.; Gualtieri, F.; Chiarini, A.; Voigt, W.; Lemoine, H. Verapamil Analogs with Restricted Molecular Flexibility: Synthesis and Pharmacological Evaluation of the Four Isomers of .alpha.-[1-[3-[N-[1-[2-(3,4-Dimethoxyphenyl)ethyl]]-N-Methylamino]cyclohexyl]]-.alpha.-Isopropyl-3,4-Dimethoxybenzeneacetonitrile. *J. Med. Chem.* **1993**, *36*, 439–445.

(15) E Teodori, S Dei, MN Romanelli, S Scapecchi, F Gualtieri, R Budriesi, A Chiarini, H Lemoine, R. M. Synthesis and Pharmacological Evaluation of Verapamil Analogs with Restricted Molecular Flexibility. *Eur. J. Med. Chem.* **1994**, *29*, 139–148.

(16) Pereira, E.; Teodori, E.; Dei, S.; Gualtieri, F.; Garnier-Suillerot, A. Reversal of Multidrug Resistance by Verapamil Analogues. *Biochem. Pharmacol.* **1995**, *50*, 451–457.

(17) Dei, S.; Romanelli, M. N.; Scapecchi, S.; Teodori, E.; Chiarini, A; Gualtieri, F. Verapamil Analogues with Restricted Molecular Flexibility. *J. Med. Chem.* **1991**, *34*, 2219–2225.

(18) Jensen, B. L.; Slobodzian, S. V. A Concise Synthesis of 1-Substituted-2-Tetralones by Selective Diol Dehydration Leading to Ketone Transposition. *Tetrahedron Lett.* **2000**, *41*, 6029–6033.

(19) Prasomsri, T.; Galiasso Tailleur, R. E.; Alvarez, W. E.; Sooknoi, T.; Resasco, D. E. Conversion of 1- and 2-Tetralone Over HY Zeolite. *Catal. Letters* **2010**, *135*, 226–232.

(20) Teodori, E.; Dei, S.; Romanelli, M.; Scapecchi, S.; Gualtieri, F.; Budriesi, R.; Chiarini, A.; Lemoine, H.; Mannhold, R. Synthesis and Pharmacological Evaluation of Verapamil Analogs with Restricted Molecular Flexibility. *Eur. J. Med. Chem.* **1994**, *29*, 139–148.

(21) Barfield, M.; Chakrabarti, B. Long-Range Proton Spin-Spin Coupling. *Chem. Rev.* **1969**, *69*.

(22) Jint, P.; Wildman, T. A. Conformational Behavior of 1-Tetralone, 1-Benzosuberone, Dibenzosuberone, and Some Structurally Related Aryl Ketones from NMR Spectroscopy. *J. Phys. Chem.* **1991**, *95*, 20–25.

Chapter 4: Design, synthesis and characterization of Reversed isoniazid anti-TB agents and Hybrid efflux pump inhibitors

4.1 Introduction

In this chapter, the design, synthesis, and characterization of various reversed isoniazid (RINH) anti-TB agents and hybrid efflux pump inhibitors (HEPIs) is presented. As discussed in chapter **2**, efflux pumps (EPs) of *Mycobacterium tuberculosis (Mtb)* are one of the major factors contributing to the development of low to higher levels of drug resistance in this microorganism. The development of EPIs and the structural modification of various classes of drugs are some of the methods which have been successfully employed to counter EP-mediated resistance.[1–3]

4.2 Background

As discussed in chapter **2**, efflux pumps (EPs) are one of the major causes of resistance. These EPs reduce intracellular concentrations to sub-inhibitory levels, which leads to the emergence of resistance in *Mtb* and various agents causing different infections. Isoniazid (INH) is also known to be a substrate of EPs, which reduce the intracellular concentration and potency of this drug against *Mtb*.[4] The evaluation of various EPIs in combination with INH against sensitive and resistant strains of *Mtb* has shown enhanced potency and efficacy of INH both *in vitro* and in mouse models of tuberculosis.[5]

In the past, a comprehensive structure activity relationship study of isoniazid has shown that the potentiating agent linked to it enhances the antimycobacterial activity. The linking moieties leading to increased lipophilicity and Schiff bases have also shown a positive effect on the potency of INH as well as enhanced efficacy as compared to isoniazid alone.[6,7] Therefore, development of dual-action hybrid molecules as exemplified by reversed anti-TB agents presents an attractive strategy to overcoming INH resistance in *Mtb*. The development of reversed isoniazid (RINH) anti-TB agents could also be used as a strategy to overcome the challenges presented by the administration of INH and EPIs. In addition to efflux pump inhibition properties, some EPIs are also known to have antimycobacterial activity with their own specific mechanisms of action. Therefore, the reversed isoniazid anti-TB agents developed by covalently linking INH and an EPI or EPI moiety may show enhanced antimycobacterial activity with synergy of two different mechanisms targeting *Mtb*.[8,9]

In addition to various other methods used for the development of new EPIs, the concept of hybridization presents a good prospective as this strategy is well explored in cancer research with promising results.[10,11] Therefore, development of novel efflux pump inhibitors (EPIs) is a viable strategy to counter the emergence of EP-mediated resistance in *Mtb*.[12,13] In this regard, hybrid efflux pump inhibitors (HEPIs) have been produced following the covalent attachment of aromatic moieties/molecular frame works of one EPI to another (such as verapamil) *via* appropriate linkers.

Although many hybrid and dual-action drugs, including numerous highly active molecules, have been explored in the recent past, hybrid molecules are not yet used as anti-TB drugs. Therefore, the exploration of the RINH and HEPI strategy may lead to the development of a novel antimycobacterial and EPI with a novel mechanism of action and good pharmacological profile.

4.3 Reversed isoniazid anti-TB agents

4.3.1 Rationale

As mentioned in chapter **2**, the strategy for the development of reversed anti-TB agents has been derived from the concept of hybrid strategies explored in malaria drug discovery, which led to the development of chloroquine-based reversed agents, also known as reversed chloroquine (RCQ) agents (**Figure 4.1**).[14,15] These RCQs have achieved better potency and efficacy against sensitive and resistant strains of *Plasmodium falciparum,* both *in vitro* and *in vivo.* These RCQs have shown a number of advantages compared to the parent drug (CQ) in terms of potency, efficacy and dose lowering.

In this work, various EPIs were covalently linked to isoniazid to develop first generation RINH anti-TB agents (**Figure 4.1**). The development of first generation RINH agents can potentially provide a "proof-of-concept" and possibly lead to the development of a reversed antimycobacterial agent in the future.

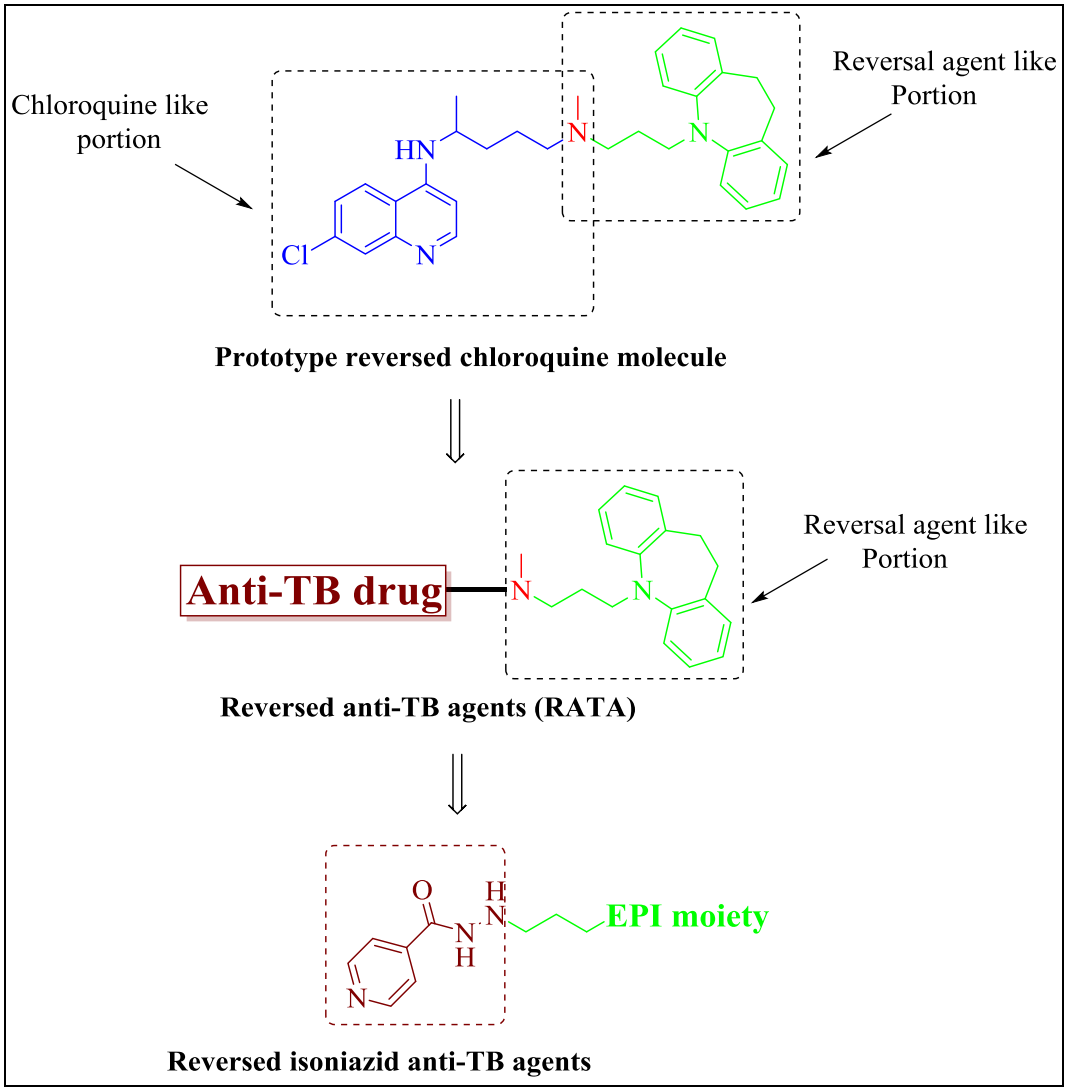

Figure 4.1: The design of RATAs and RINH anti-TB agents based on the RCQ concept. CQ moiety can be replaced with various anti-TB drugs and can be linked with various EPIs/EPI moieties to generate RATAs. In this study, INH has been linked with various EPIs/EPI moieties to design first generation RINHs.

4.3.2 Selection of EPI moieties for the synthesis of RINH agents

4.3.2.1 Tricyclic efflux pump inhibitor moieties

The EPIs or EPI moieties were selected from various journal articles published by Peyton and co-workers on RCQs.[16,17] Some EPIs and EPI moieties used in the development of RCQs had also shown chemosensitization of resistant *Mtb* in combination with various anti-TB drugs.[18] Therefore, RINH agents developed with these EPIs and EPI moieties are hypothesized to show enhanced antimycobacterial activity.

As discussed in chapter **2**, tricyclic molecules, such as phenothiazines, dibenzazepines and their analogues, are also known for their ability to reverse efflux pump-mediated resistance in *Mtb*. These chromophores are used for various indications and are well explored for different pharmacological properties such as antibacterial and antimalarial action.[13,19] These various findings can be useful in designing RINH agents with good pharmacological properties. The phenothiazine analogues, such as thioridazine, have shown stereospecific antibacterial activity over CNS activity. The racemic (+/-) thioridazine showed strong antimycobacterial activity but (-) thioridazine is devoid of CNS effects.[9] Therefore, various phenothiazine (**Figure 4.2**, series A, B and C, D) and dibenzazepine analogues (**Figure 4.2**, RINH-E) were selected for initial exploration.[20]

4.3.2.2 Design of RINH agents with tricyclic EPI moieties

All the EPI moieties were linked to isoniazid *via* a three carbon chain linker (**Figure 4.2**).

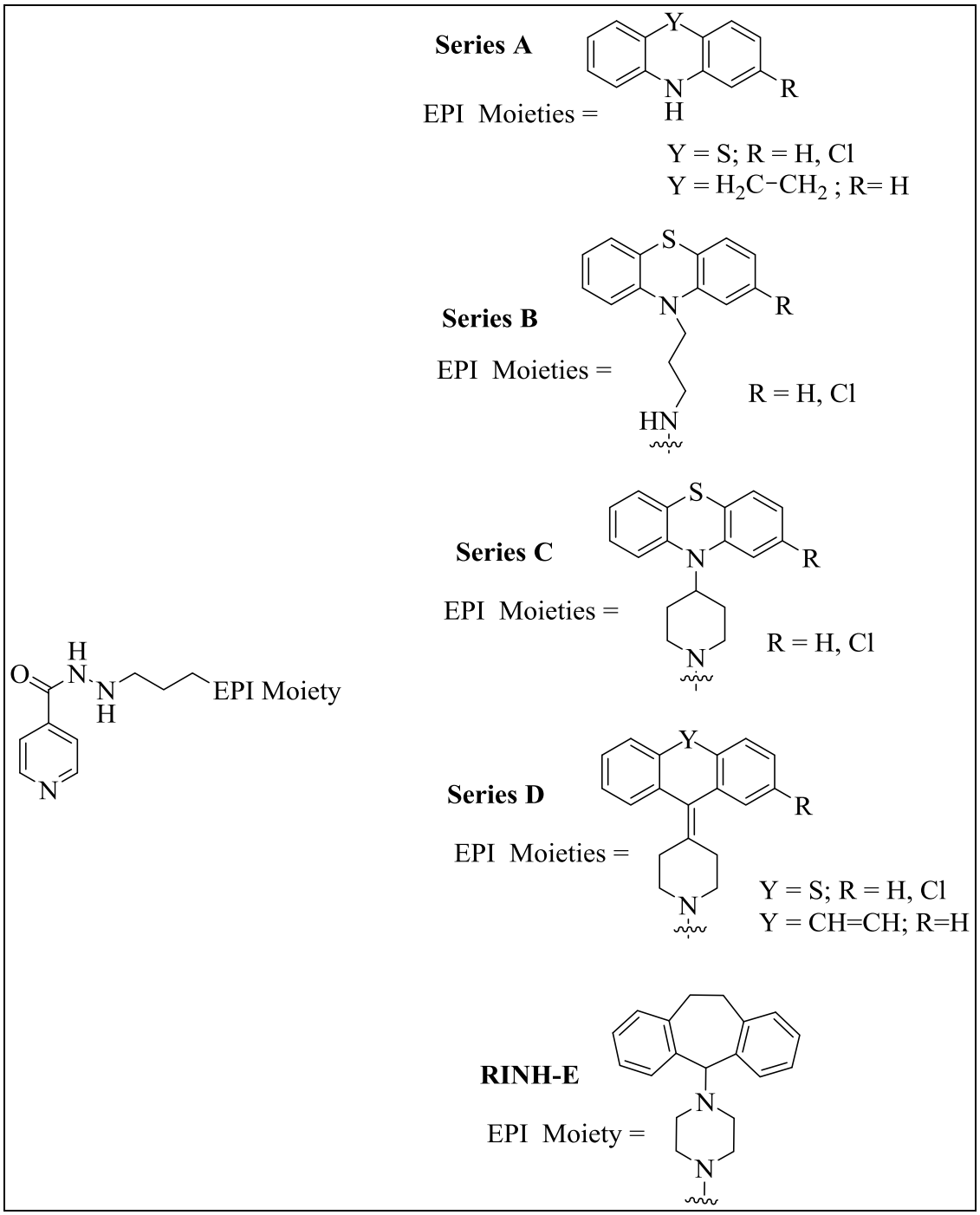

Figure 4.2: Design of first generation RINH anti-TB agents with tricyclic EPI/EPI moieties containing a phenothiazine/dibenzazepine nucleus.

4.3.3 Synthesis of RINHs with tricyclic EPIs

4.3.3.1 Synthesis of RINH anti-TB agents of series A (4.3)

The synthesis of target compounds of series A was a two-step procedure (Scheme **4.1**). This commenced with the alkylation of commercially available phenothiazines **4.1** to obtain **4.2 (a** and **b)**, according to a procedure reported by Kubota *et. al*.[21] In the procedure for **4.2** (**a** and **b**), 1.5 equivalents of 1-bromo-3-chloropropane and 2.5 equivalents of sodium hydride and one equivalent of the appropriate phenothiazine were stirred in DMF at room temperature (25 °C) for 4 to 6 hours in an atmosphere of nitrogen. Addition of an excess of sodium hydride did not result in completion of the reaction in the case of unsubstituted phenothiazine **4.2a**. However, the reaction involving 2-chlorophenothiazine **4.2b** went to completion (Scheme **4.1**). For the synthesis of intermediate **4.2c**, commercially available iminodibenzyl **4.1c** was reacted with 1-bromo-3-chloropropane in the presence of excess sodium amide in toluene under reflux. The synthesis of target compounds **4.3 (a** and **b)** was achieved by the coupling of intermediate **4.2 (a** and **b)** with an equimolar amount of isoniazid using sodium hydride in DMF at 25 °C. The target compound **4.3 (a** and **b)** were produced as minor products while major product **4.4** was formed by further alkylation of **4.3**. The target compound **4.3c** with an iminodibenzyl moiety as an EPI chromophore was obtained by refluxing a mixture of intermediate **4.2c** and isoniazid in *iso*-propanol in the presence of excess triethylamine (4 equivalents). The reaction did not go to completion even with longer reflux times and a low yield was obtained (Table **4.1**) with the recovery of the intermediate **4.2c**.

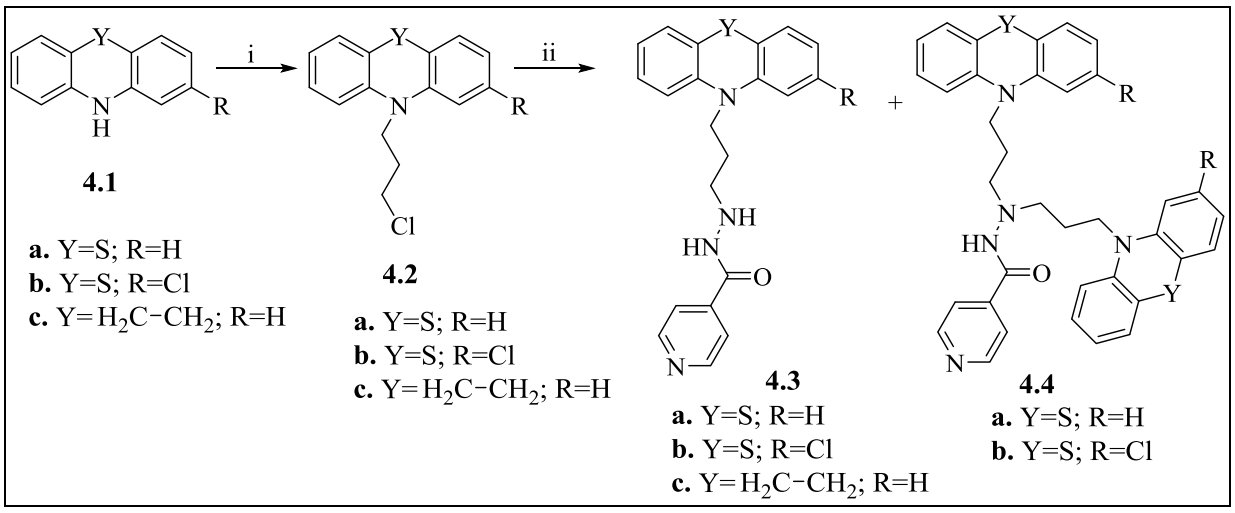

Scheme 4.1: *Reagents and reaction conditions*: (i) 1-Bromo-3-chloropropane (1 eq.), NaH (1 eq.), DMF, 25 °C, 4-6 h (**4.2a** and **4.2b**); 1-Bromo-3-chloropropane (2 eq.), $NaNH_2$ (2.5 eq.), toluene, reflux (115 °C), 12 h, (**4.2c**); (ii) Isoniazid (1.2 eq.), NaH (1.2 eq.), DMF, 25 °C, 5-6 h, (**4.3a** and **4.3b**); Isoniazid (4 eq.), Et_3N (4 eq.), *iso*-propanol, reflux (95 °C), 12 h, (**4.3c)**.

Table 4.1: Yields and melting points (m.p.) of isolated intermediate **4.2**, target compound **4.3**, and by-product **4.4**.

Compounds	Yield %	m.p. (°C)
4.2a	63	61
4.2b	75	66
4.2c	40	*
4.3a	18	*
4.3b	24	*
4.3c	15	*
4.4a	27	*
4.4b	26	*

*Compound isolated as an oil.

4.3.3.2 Synthesis of RINH anti-TB agents of series B

4.3.3.2.1 Synthesis of alkylated intermediates of phenothiazine (4.6)

Synthesis of intermediates **4.6 (a** and **b)** followed a three-step procedure (Scheme **4.2**), which commenced with the alkylation of commercially available phenothiazines **4.1** to obtain **4.2,** as described previously in scheme **4.1**. Intermediate **4.2** was further reacted with 3-aminopropanol in the presence of potassium carbonate in DMF at 80 °C to obtain **4.5** in moderate yield (Table **4.2**). A by-product was also formed by further alkylation of **4.5** with **4.2**. The intermediate **4.5** was *N*-protected in DCM in the presence of triethylamine and a slight excess of *di-tert*-butyl carbonate (1.2 equivalents) at room temperature (25 °C) to afford **4.6** in quantitative yield (Table **4.2**).

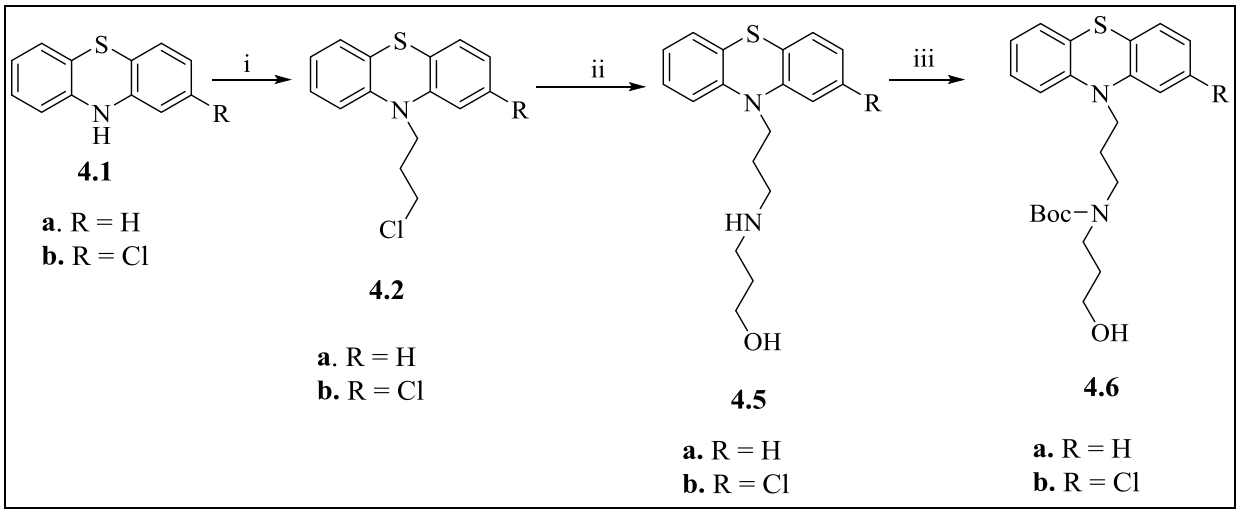

Scheme 4.2:*Reagents and reaction conditions*: (i) 1-Bromo-3-chloropropane (1 eq.), NaH (1 eq.), DMF, 0-25 °C, 11-12 h; (ii) 3-Aminopropanol (1.5 eq.), K_2CO_3 (1.3 eq.), DMF, 80 °C, 10-12 h; (iii) $(Boc)_2O$ (1.1 eq.), Et_3N (1.1 eq.), DCM, 25 °C, 30-40 min.

Table 4.2: Yields and melting points of isolated intermediate (**4.5** and **4.6)**.

Compound	Yield %	m.p. (°C)
4.5a	65	100-103
4.5b	68	61-64
4.6a	95	*
4.6b	93	*

*Compound isolated as an oil

4.3.3.2.2 Synthesis of target compounds of series B *via* the Appel reaction (4.10)

4.3.3.2.2.1 The Appel reaction

The Appel reaction was named after Rolf Appel. It is a facile method of converting an alkyl alcohol to an alkyl halide under mild reaction conditions using tetrahalomethane and triphenylphosphine (Scheme **4.3**).[22]

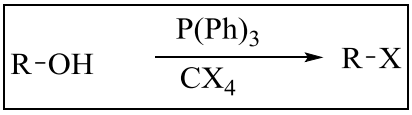

Scheme 4.3: The Appel reaction.

The mechanism of the reaction is shown in scheme **4.4**. The reaction is initiated by the formation of a carbanion generated for the reaction between triphenyl phosphine and tetrahalomethane, followed by alkoxide ion formation by abstraction of the hydroxyl proton by the carbanion. An alkoxide ion subsequently reacts with the phosphonium salt releasing the halide ion. The nucleophilic substitution reaction takes place by the attack of a halide ion on the electrophilic carbon of the resulting complex leading to the formation of an alkyl halide and triphenylphophine oxide.

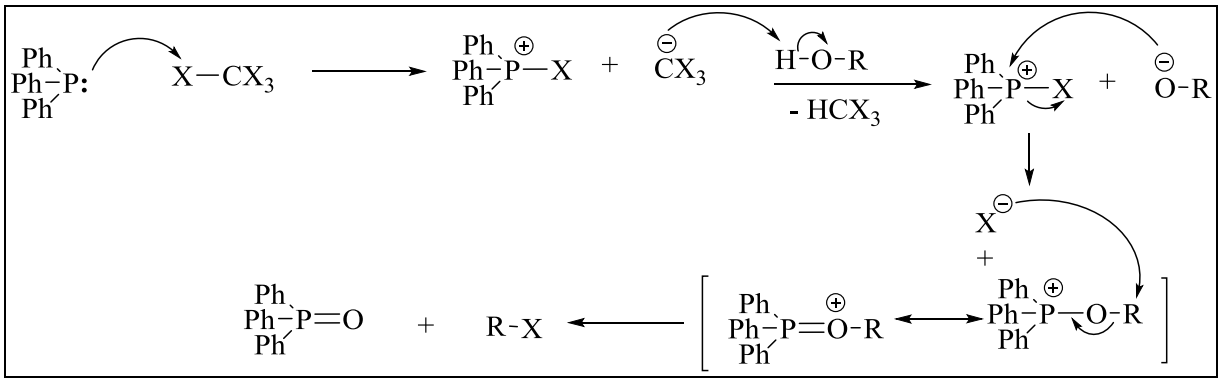

Scheme 4.4: Proposed mechanism of the Appel reaction.

4.3.3.2.2.2 Synthesis of target compounds (4.10)

The synthesis of target molecules of series B from intermediate **4.6** was achieved in three steps outlined in scheme **4.5**. Firstly, the hydroxyl group of intermediate **4.6** was converted to a bromide *via* the above-mentioned Appel reaction. An excess of carbon tetrabromide (1.5 equivalents) and triphenylphosphine (1.5 equivalents) were used in DCM at room temperature (25 °C) to obtain intermediate **4.7** in good yields (Table **4.4**). The product **4.7** appeared less-polar on TLC than the triphenylphosphine oxide formed in the reaction, and was easily purified by flash chromatography.

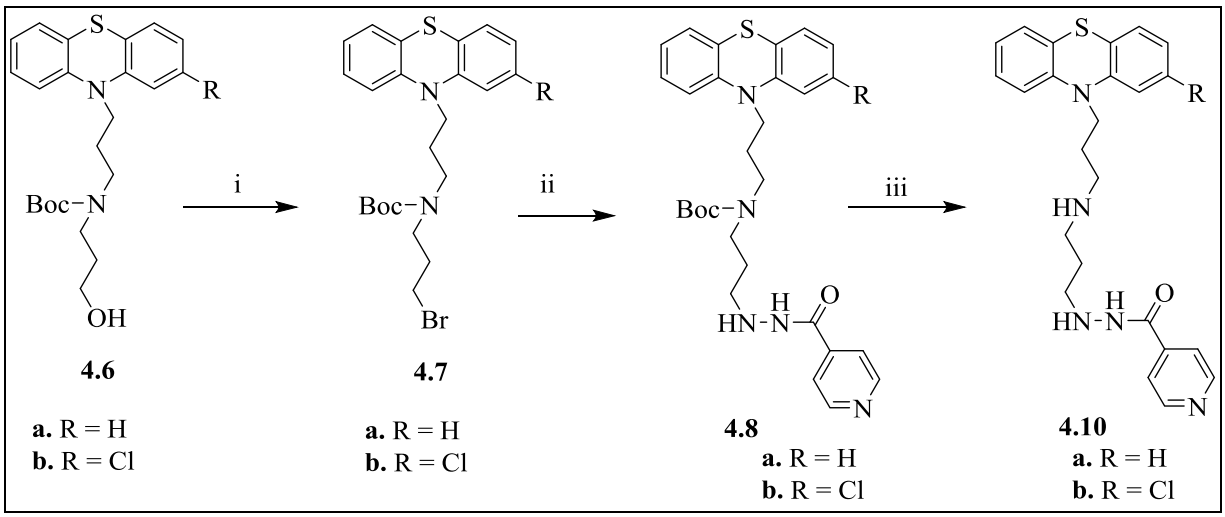

Scheme 4.5: *Reagents and reaction conditions*: (i) Ph_3P (1.5 eq.), CBr_4 (1.5 eq.), DCM, 25 °C, 1.5-2 h; (ii) Isoniazid (5 eq.), Et_3N (3 eq.), DMF, 55 °C, 12 h; (iii) TFA/DCM (10% v/v), 25 °C, $NaHCO_3$, 1-1.5 h.

The bromide intermediate **4.7** was then reacted with isoniazid (Scheme **4.5**). This reaction proved to be challenging and often resulted in low yields of **4.8** and was accompanied by double alkylation to give **4.9a** as a by-product (Scheme **4.6**). Attempts to further optimize the reaction yield for **4.8** were made by exploring combinations of various bases in different solvents at variable temperatures (Table **4.3**). The reaction of **4.7a** with isoniazid in the presence of NaH in DMF did not afford the desired hybrid molecule but led to the formation of **4.9a** as major product (Scheme **4.6**). The use of potassium carbonate in DMF with equimolar amounts of reactants (**4.7a** and isoniazid) at 80 °C showed no reaction as indicated by TLC. The reaction, with a combination of triethylamine (1 to 5 equivalents) in various organic solvents at room temperature (25 °C), did not give any indication of progress as evidenced by TLC while heating under reflux led to target product formation in very low yield (5%), with excess side product (**4.9a)** formation. The final attempt was made by using 5

equivalents of isoniazid and 3 equivalents of triethylamine in DMF and heating at 55 °C for 12 hour. This resulted in an improved yield (35%) of **4.8a**. The target compound was obtained by removal of the Boc group from *N*-Boc-protected intermediate **4.8a** using 10% TFA in DCM (by volume) followed by neutralization with a saturated solution of sodium bicarbonate.

Table 4.3: Various reaction conditions explored for synthesis of **4.8a.**

Entry.	Reaction conditions	Observation
1	INH, NaH (1:1), DMF, 25 °C, 30 mint	**4.9** as only product
2	INH, K_2CO_3(1:2.5), DMF, 25-80 °C, 6-12h	No reaction
3	INH, TEA (1:2.3), THF, 25-66 °C,1-6h	No reaction
4	INH, TEA (1:5), Toluene, reflux, 1-6h	**4.9** as major product
5	INH, TEA (1:3), DMF, 55 °C, 12 h	**4.8a** in 35% yield

4.3.3.2.3 Reaction of 4.7 with isoniazid

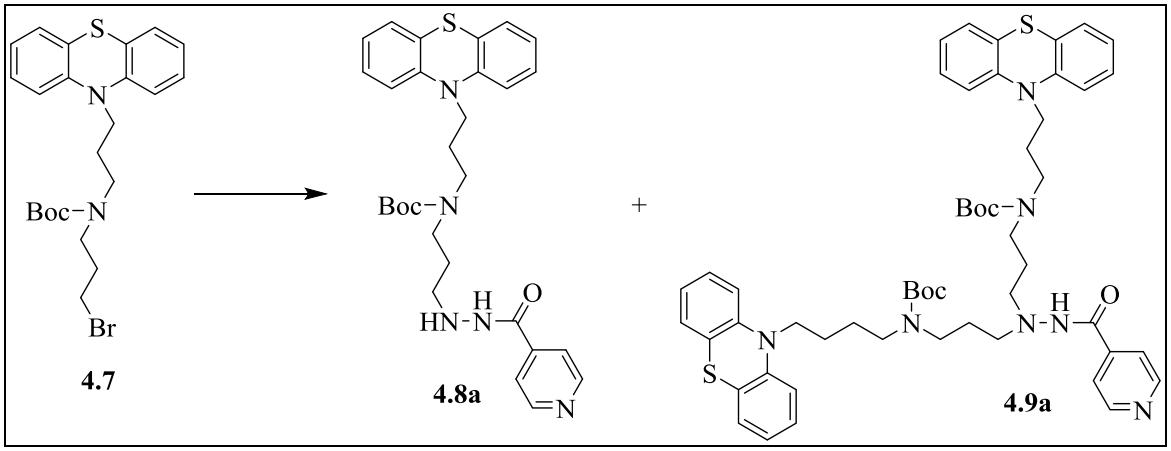

Scheme 4.6: Alkylation of isoniazid with bromide intermediate **4.7** accompanied with the formation of by-product **4.9a**.

Table 4.4: Yields and melting points of isolated intermediates (**4.7** and **4.8**) and target compound **4.10**.

Compound	Yield%	m.p. (°C)
4.7a	82	*
4.7b	88	*
4.8a	35	55-57
4.8b	30	63-65
4.10a	66	48-50
4.10b	83	61-64

*Compound was isolated as an oil.

4.3.3.2.4 Characterization of target compound 4.10a

The target molecule **4.10a** was fully characterized using ^{1}H-NMR and ^{13}C-NMR spectroscopy as well as LC-MS. The LC-MS chromatogram showed 99% purity and a pseudomolecular ion mass peak of *m/z* 434.2 [M+H], which is expected for compound **4.10a**. NMR spectra were recorded in deuterated DMSO. Among the key signals identified in the ^{1}H-NMR spectrum (**Figure 4.3**) are two doublets corresponding to four isoniazid moiety protons H-12 and H-11 resonating downfield at δ 8.72 and 7.71 ppm, respectively, which confirmed the successful attachment of the isoniazid motif to the molecule. The coupling constants (J = 4.4 and 6.0 Hz) are less than the expected value and may be attributed to the distortion signals caused by the overlapping of NH signals with the signal of aromatic protons.

δ (ppm)	Multiplicity	J (Hz)	H
8.72	d	4.4	H-12
7.71	d	6.0	H-11
7.19	m	-	H-1 & H-3
7.06	d	8.0	H-4
6.96	t	8.4	H-2
3.99	t	6.8	H-5
3.04	m	-	H-7 & H-8
2.89	t	6.4	H-10
2.06	quin	6.8	H-6
1.73	quin	6.8	H-9

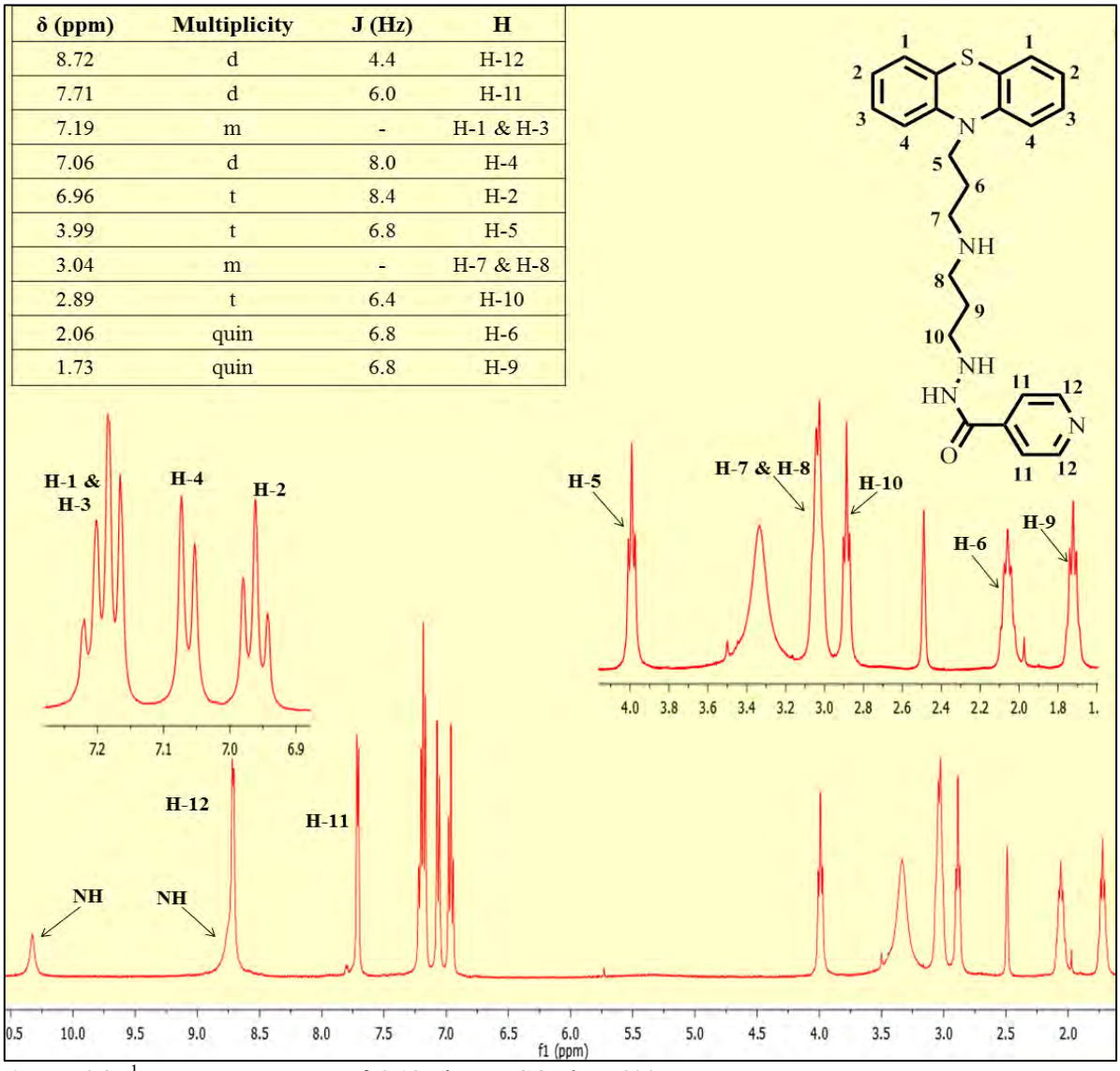

Figure 4.3: ^{1}H-NMR spectrum of **4.10a** in DMSO-d_6 at 400 MHz.

Other key signals in the downfield aromatic region are representative of a phenothiazine nucleus and resonate in the range from δ 7.22 to 6.93 ppm. These signals include a multiplet (overlapping triplet and doublet) at δ 7.19 ppm (corresponding to H-1 and H-3), a doublet at δ 7.06 ppm (corresponding to H-4) and a triplet at δ 6.96 ppm (corresponding to H-2). Two broad signals at δ 10.32 and 8.78 ppm are observed for two N-H protons. The upfield region contains the representative signals of expected aliphatic protons, which include two triplets at δ 3.99 and 2.89 ppm, two quintets at δ 2.06 and 1.73 ppm and one multiplet at δ 3.04 ppm corresponding to H-5, H-10, H-6, H-9, H-7 and H-8 protons, respectively. The multiplet at δ 3.04 ppm and corresponding to H-7 and H-8 is the result of an overlap of two triplets corresponding to the two methylene protons adjacent to nitrogen as they have similar electronic environments.

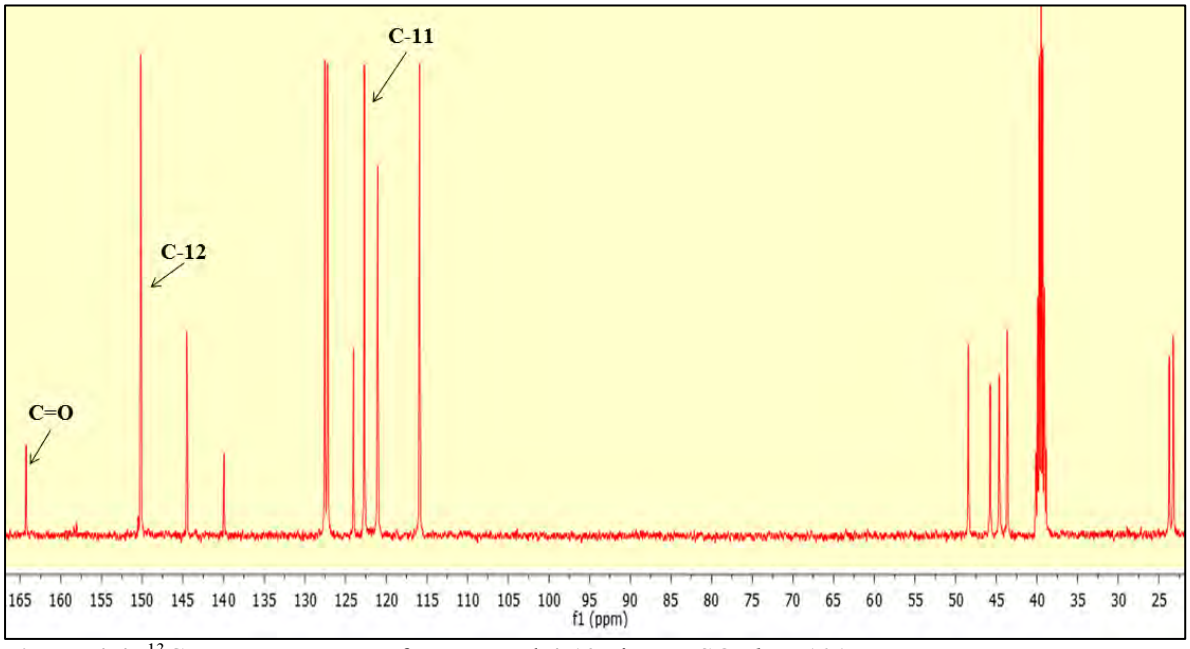

Figure 4.4: ^{13}C-NMR spectrum of compound **4.10a** in DMSO-d_6 at 101 MHz.

The ^{13}C-NMR spectrum of **4.10a** showed 16 distinct signals corresponding to 24 carbons as some signal intensities are equivalent to two carbons. The characteristic signals include those for the carbonyl carbon and two isoniazid carbons C-12 and C-11 at δ 164.3, 150.2, and 122.7 Hz, respectively.

4.3.3.3 Synthesis of RINH anti-TB agents of series C

4.3.3.3.1 Synthesis of phenothiazine-piperidine intermediate (4.15)

The synthesis of the piperidine-based phenothiazine intermediate **4.15** is outlined in scheme **4.7** and commenced with the preparation of scaffold **4.13** by Boc-protection of commercially available 4-hydroxyl piperidine **4.11** and subsequent mesylation using methane sulfonyl chloride in DCM at 0 °C in the presence of triethylamine to afford **4.13** in 95% yield (Scheme **4.7**). This intermediate was then reacted with phenothiazine (**4.1a** and **4.1b**). The adopted protocol described in a patent using sodium hydride in DMSO successfully delivered the intermediate **4.14**.[23] This was achieved by the treatment of phenothiazine with an equimolar amount of NaH at 70 °C in DMF with stirring for 50 minutes, followed by the addition of compound **4.13** at 100 °C and further stirring for 24 hours. The reaction was monitored over 24 hours by HPLC as both the reactant and product were found to have the same retention factor on TLC, regardless of the solvent system used. Complete consumption of phenothiazine could not be achieved even at high temperatures and after a long reaction time of 24 hours. The reaction was accompanied by the formation of many coloured impurities, which were removed by column chromatography to leave a light pink solid product **4.14** in moderate yield (Table **4.5**). This compound showed various colour changes (pink, red, and brown) in the presence of light due to the photosensitive nature of the phenothiazine nucleus. Boc-deprotection of **4.14** was conducted using TFA in DCM (50% v/v) with excess TFA being removed with 1*N*-NaOH to afford **4.15a** and **4.15b** in 30 and 32% yield, respectively, over three steps.

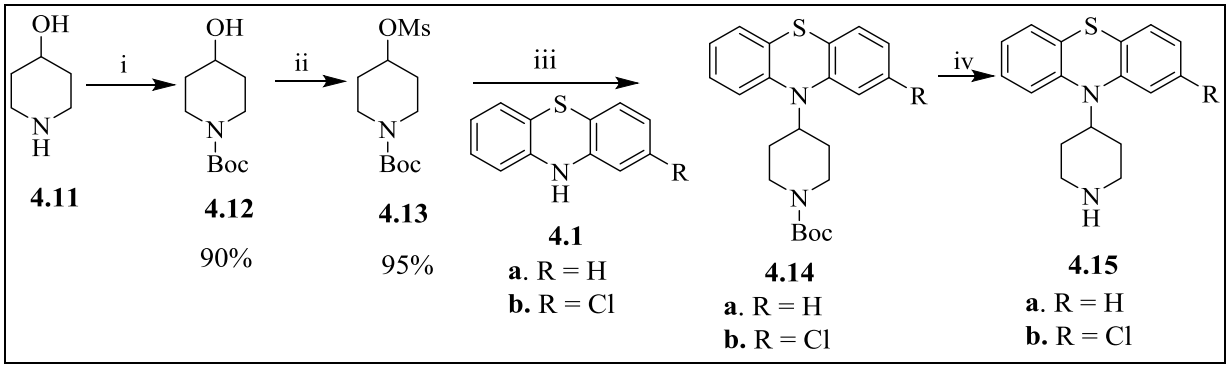

Scheme 4.7: *Reagents and reaction conditions*: (i) $(Boc)_2O$ (1.3 eq.), Et_3N (1.3 eq.), DCM, 0-25 °C, 1.5 h; (ii) Methanesulfonyl chloride (1.2 eq.), Et_3N (1.2 eq.), DCM, 0-25 °C, 6 h; (iii) NaH (1 eq.), DMSO, 25-70 °C, 50 min-24 h; (iv) TFA (50% v/v in DCM), 1*N*-NaOH, 1-1.5 h.

Table 4.5: Yields and melting points of isolated intermediate (**4.14** and **4.15**).

Compound	Yield %	m.p. (°C)
4.14a	30	120-122
4.14b	32	157-158
4.15a	87	100-103
4.15b	95	131-133

4.3.3.3.2 Synthesis of target compounds of series C (4.17)

The synthesis of target molecules **4.17** from the key intermediate **4.15** commenced with the alkylation of **4.15** with 1-bromo-3-chloropropane in toluene in the presence of triethylamine (Scheme **4.8**). The final step involves *N*-alkylation of isoniazid with intermediate **4.16**. A modified method, reported by Hoover and co-workers, for the alkylation of various acyl hydrazones was used.[24] A mixture of four equivalents of isoniazid and triethylamine relative to **4.16** were refluxed in *iso*-propanol, which delivered **4.17** in moderate yield (Table **4.6**).

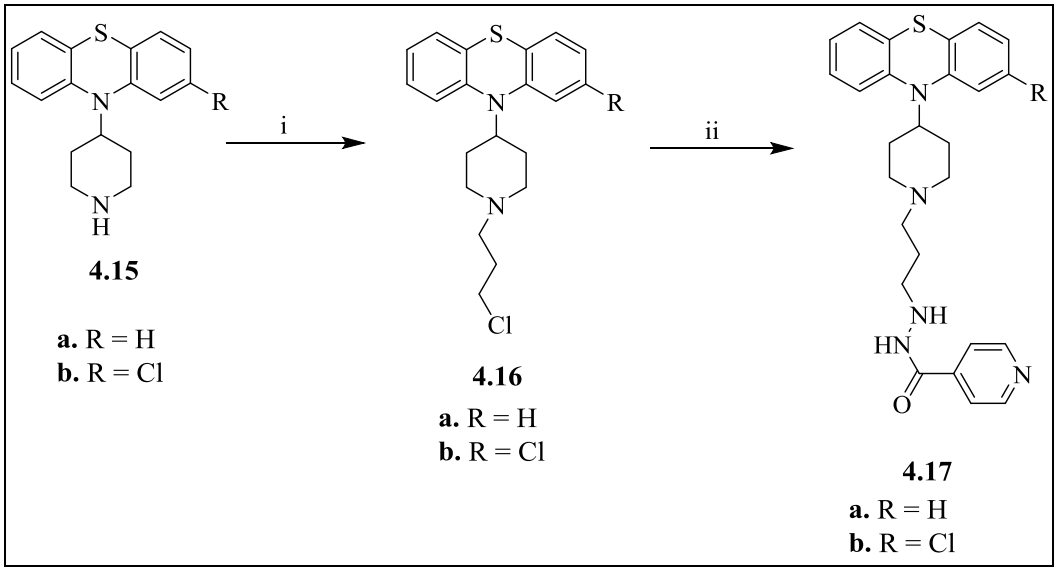

4.15

a. R = H
b. R = Cl

4.16

a. R = H
b. R = Cl

4.17

a. R = H
b. R = Cl

Scheme 4.8: *Reagents and reaction conditions*: (i) 1-Bromo-3-chloropropane (2 eq.), Et_3N (2.5 eq.), toluene, 65 °C, 6-8 h; (ii) Isoniazid (4 eq.), Et_3N (4 eq.), *iso*-propanol, reflux (95 °C), 10-12h.

Table 4.6: Yields and melting points of isolated intermediate **4.16** and target compound **4.17.**

Compound	Yield %	m.p. (°C)
4.16a	75	*
4.16b	72	*
4.17a	30	54-56
4.17b	32	85-87

*Compound isolated as an oil.

4.3.3.3.3 Characterization of target compound 4.17b.

The targeted compounds **4.17a** and **4.17b** were characterized by ^{1}H-NMR and ^{13}C-NMR spectroscopy as well as LC-MS. The LC-MS chromatogram showed 99.9% purity of the compound and a pseudomolecular ion mass peak of *m/z* 494.1 [M+H] for **4.17b**. Figures **4.5** and **4.6** show the ^{1}H-NMR and ^{13}C-NMR spectra of the representative compound **4.17b**.

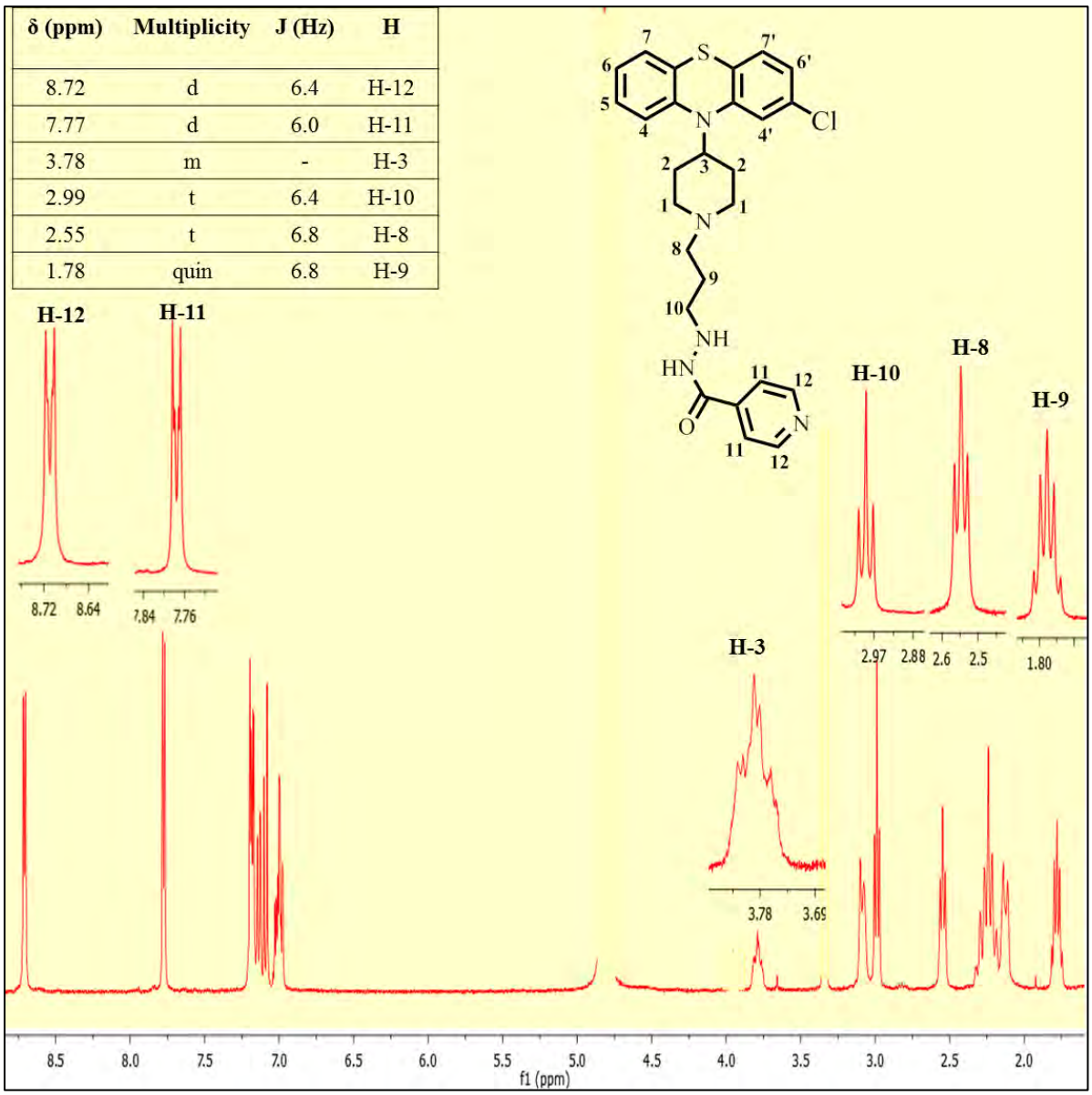

Figure 4.5: ^{1}H-NMR spectrum of **4.17b** in CD_3OD at 400MHz.

The presence of all the signals corresponding to the isoniazid moiety, aliphatic chain and intermediate **4.15b** confirmed that the desired coupling of **4.15b** and isoniazid had occurred. Two doublets at δ 8.72 and 7.77 ppm, corresponding to H-11 and H-12, confirmed the presence of an attached isoniazid moiety. The additional signals were a group of multiplets between δ 6.70 and 7.40 ppm and corresponded to the 2-chlorophenothiazine nucleus. The

upfield region from δ 3.90 to 1.60 ppm, containing two triplets and one quintet at δ 2.99, 2.55 and 1.78 ppm, respectively, accounted for the attached propyl linker in addition to the signals corresponding to the piperidine ring.

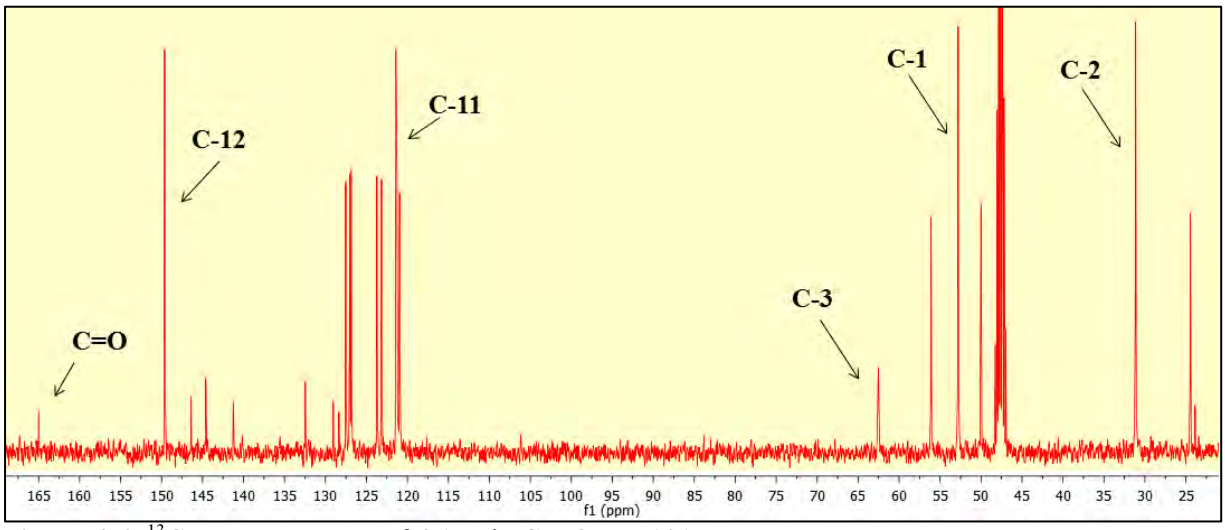

Figure 4.6: ^{13}C-NMR spectrum of **4.17b** in CD_3OD at 101 MHz.

A total of 22 distinct signals were observed in the ^{13}C-NMR spectrum corresponding to 26 carbons of **4.17b**. Among these, some signals showed intensities equivalent to two carbons. The characteristic signals arise from isoniazid ring carbons C-12 and C-11 and one accounted for a carbonyl carbon. Additional signals in the aliphatic region were also observed corresponding to C-1, C-2 and C-3.

4.3.3.4 Synthesis of RINH anti-TB agents of series D using the McMurry reaction (4.23)

4.3.3.4.1 The McMurry reaction

Named after John E. McMurry, the McMurry reaction is a reaction used to couple two carbonyl compounds to form an alkene using the titanium chloride reagents ($TiCl_3$ or $TiCl_4$) and a reducing agent such as zinc (Scheme **4.9**).[25]

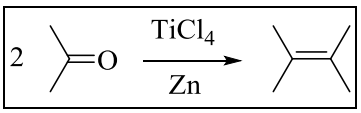

Scheme 4.9: McMurry reaction.

This reaction can be related to the pinacolate coupling as it also proceeds *via* a reductive coupling reaction. The various titanium-based reagents have been developed for this reaction and originally, $TiCl_3$ coupled with lithium aluminium hydride was used. The use of $TiCl_3$ and $TiCl_4$ along with reducing agents like potassium, zinc and magnesium has been extensive in practice.[26]

The mechanism of the reaction can be divided into two parts: (i) formation of pinacolate and (ii) deoxygenation of pinacolate to generate an alkene (Scheme **4.10**).[27]

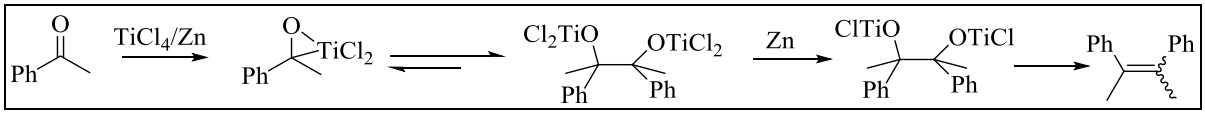

Scheme 4.10: Proposed mechanism of McMurry reaction.

It has been proposed that it is the low valent titanium generated *via in situ* reduction of Ti(III) or Ti(IV) in the presence of reducing agents like zinc, which co-ordinates to the carbonyl oxygen and forms pinacolate at room temperature (25 °C). This pinacolate then gets reduced to produce the alkene under reflux (Scheme **4.10**).

4.3.3.4.2 Synthesis of xanthone-piperidinoneylide intermediate (4.21)

The synthesis of intermediate **4.21** is outlined in scheme **4.11** and began with the *N*-Boc-protection of commercially available piperidinone hydrochloride **4.18** in DCM in the presence of triethylamine and a catalytic amount of 4-dimethylaminopyridine (DMAP) at room temperature (25 °C) to obtain **4.19** in good yield (Table **4.7**). The key intermediate **4.21** was synthesised by coupling **4.19** with commercially available ketones **4.20** using the above-mentioned McMurry reaction.[28,29]

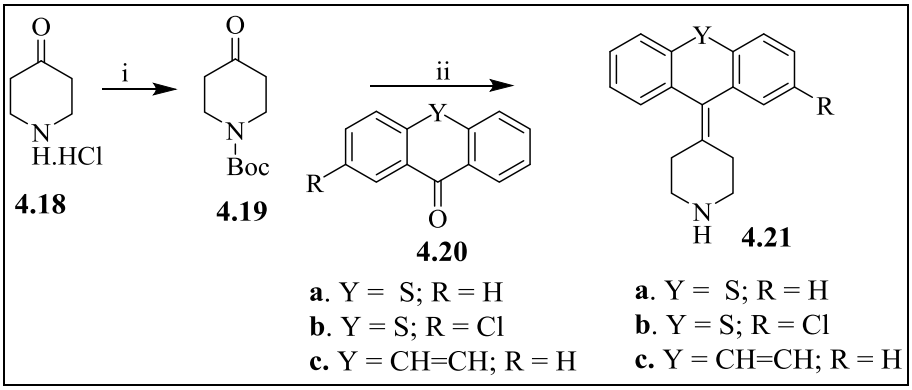

Scheme 4.11: *Reagents and reaction conditions*: (i) $(Boc)_2O$ (1.3 eq.), Et_3N (1.5 eq.), DMAP (0.01 eq.), DCM, 0-25 °C, 6 h; (ii) Zn (4.5 eq.), $TiCl_4$ (1M in toluene) (2 eq.), 1,4-dioxane, 60 °C-reflux, 10-12 h.

An excess of zinc (4 equivalents) and titanium(IV) chloride (2 equivalents) was stirred for 24 hours at 40 °C under an atmosphere of nitrogen to reduce the titanium from Ti(IV) to Ti(II). The addition of a solution of two ketones **4.20** and **4.19** in dioxane to the mixture of zinc and titanium produced the desired alkene **4.21** after refluxing for an additional two hours.

Table 4.7: Yields and melting points of isolated intermediate (**4.19** and **4.21**).

Compound	Yield %	m.p. (°C)
4.19	95	75-78
4.21a	43	188-190
4.21b	40	216-218
4.21c	55	250-252

4.3.3.4.3 Synthesis of target compounds of series D

The synthesis of target compounds of series D from intermediate **4.21** was achieved *via* alkylation of **4.21** with 1-bromo-3-chloropropane in toluene at 65 °C in the presence of triethylamine (Scheme **4.12**) to obtain **4.22** in moderate yield (Table **4.8**). The final product **4.23** was obtained using the previously described method (Section **4.3.3.2**) of refluxing a mixture of **4.22** and four equivalents each of triethylamine and isoniazid in *iso*-propanol for 10-12 hours.

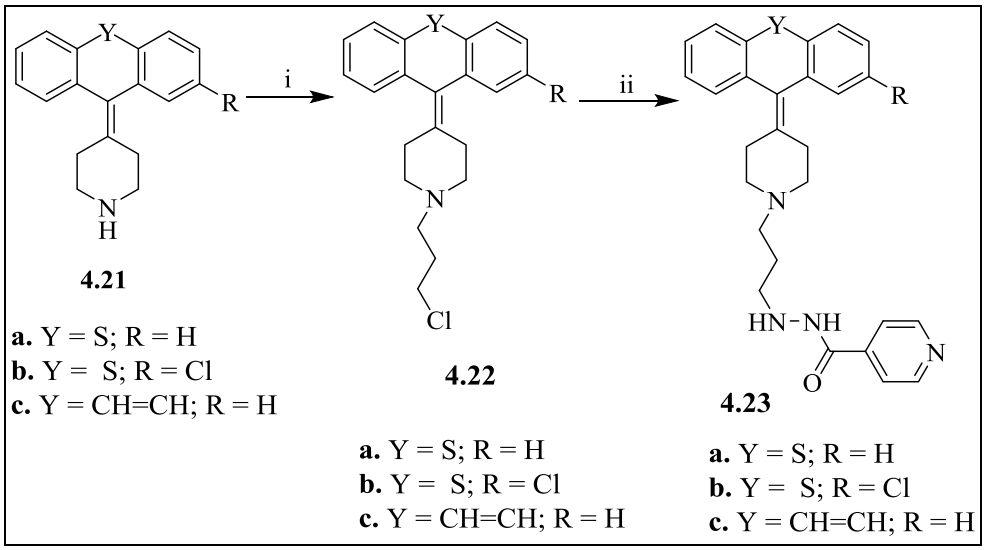

Scheme 4.12: *Reagents and reaction conditions*: (i) 1-Bromo-3-chloropropane (2 eq.), Et_3N (2.5 eq.), toluene, 65 °C, 6-8 h; (ii) Isoniazid (4 eq.), Et_3N (4 eq.), *iso*-propanol, reflux (95 °C), 10-12 h.

Table 4.8: Yields and melting points of isolated intermediate (**4.22)** and target compound (**4.23**).

Compounds	Yield %	m.p. (°C)
4.22a	65	136-138
4.22b	60	*
4.22c	56	*
4.23a	37	105-107
4.23b	32	99-102
4.23c	40	120-122

*Compound isolated as an oil.

4.3.3.4.4 Characterization of target compound 4.23c

The target compounds **4.23** (**a-c**) were characterized by ^{1}H-NMR and ^{13}C-NMR spectroscopy as well as LC-MS. Figures **4.7** and **4.8** represent the ^{1}H-NMR and ^{13}C-NMR spectra of representative compound **4.23c**, respectively. The presence of all the signals corresponding to isoniazid, aliphatic chain and intermediate **4.22c** confirmed that the desired coupling of **4.23c** and isoniazid had occurred. Two doublets at δ 8.72 and 7.76 ppm confirmed the presence of the isoniazid ring. The additional signals between δ 6.75 and 7.50 ppm corresponded to aromatic protons H-3, H-4, H-5 and H-6. In addition to piperidine protons (H-1 and H-2), the upfield region from δ 3.70 to 1.71 ppm also contain two triplets and one quintet at δ 2.98, 2.59 and 1.77 ppm, respectively, accounting for the attached carbon chain.

The ^{13}C-NMR spectrum also supported the expected structure of **4.23c**. A total of 17 distinct signals were observed corresponding to 29 carbons of **4.23c**. The characteristic signals include those for the carbonyl carbon and the isoniazid ring carbons C-13 and C-12. Signals corresponding to piperidine carbons C-1 and C-2, and three carbon linker chain C-9, C-10 and C-11 are also observed.

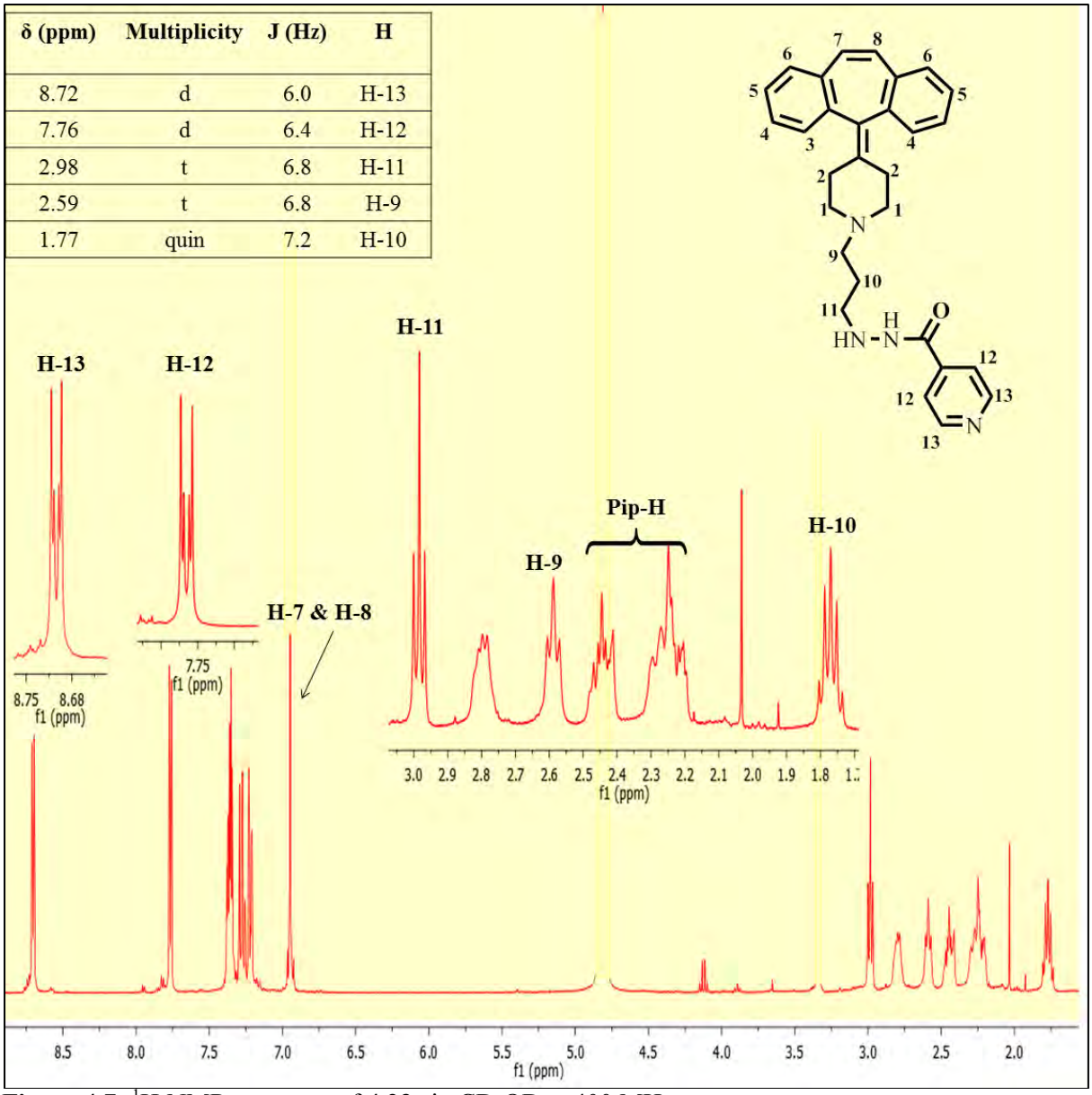

Figure 4.7: ^{1}H-NMR spectrum of **4.23c** in CD_3OD at 400 MHz.

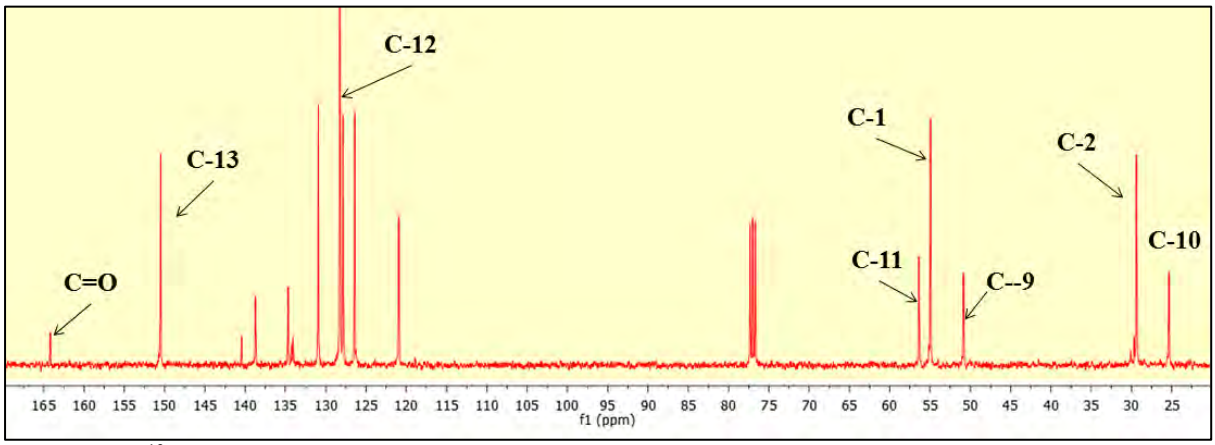

Figure 4.8: ^{13}C-NMR spectrum of **4.23c** in CD_3OD at 101 MHz.

4.3.3.5 Synthesis of RINH-E (4.27)

The synthesis of target compound **4.27** (Scheme **4.13**) commenced with the reaction of commercially available dibenzosuberyl chloride **4.24** and piperazine in the presence of 1,8-diazabicyclo[5.4.0]undec-7-ene (DBU) and molecular sieves of 4 A° under an atmosphere of argon to afford intermediate **4.25** in moderate yield (Table **4.9**). This intermediate was alkylated with 1-bromo-3-chloropropane in toluene in the presence of triethylamine at 65 °C to afford **4.26** in good yield. The final product **4.27** was obtained by refluxing a mixture of **4.26** and four equivalents each of isoniazid and triethylamine in *iso*-propanol.

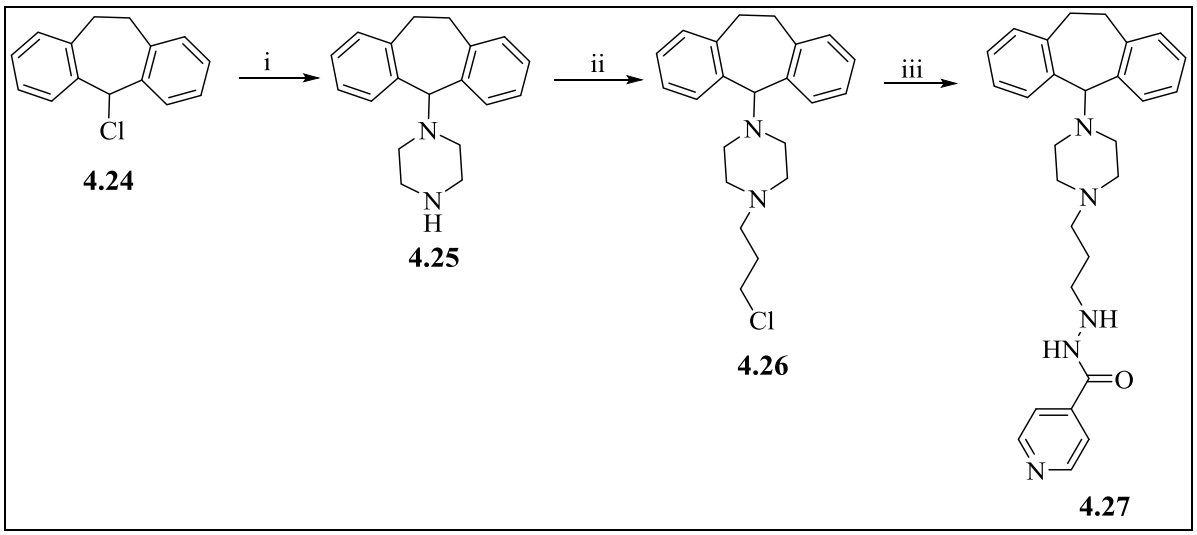

Scheme 4.13: *Reagents and reaction conditions*: (i) Piperazine (1.1 eq.), DBU (0.25 eq.), MS-4 A°, 0-25 °C, toluene, 12 h; (ii) 1-Bromo-3-chloropropane (2 eq.), Et_3N (2.5 eq.), toluene, 65 °C, 8 h; (iii) Isoniazid (4 eq.), Et_3N (4 eq.), *iso*-propanol, reflux (95 °C), 12 h.

Table 4.9: Yield and melting point of isolated intermediates (**4.25** and **4.26)** and target compound **4.27**.

Compounds	Yield %	m.p. (°C)
4.25	67	246-246
4.26	72	*
4.27	42	155-157

*Compound isolated as an oil.

4.3.3.6 Benzhydrazide-based reversed anti-TB agents

4.3.3.7.1 Rationale

The synthesised RINH anti-TB agents **4.3** (**Figure 4.9**) showed good *in vitro* potency against the *Mtb* H37Rv strain (MIC_{99} = 0.625 μM). To investigate the contribution of the pyridyl motif to the antimycobacterial and EPI activities of these compounds, this motif was replaced with a phenyl group.

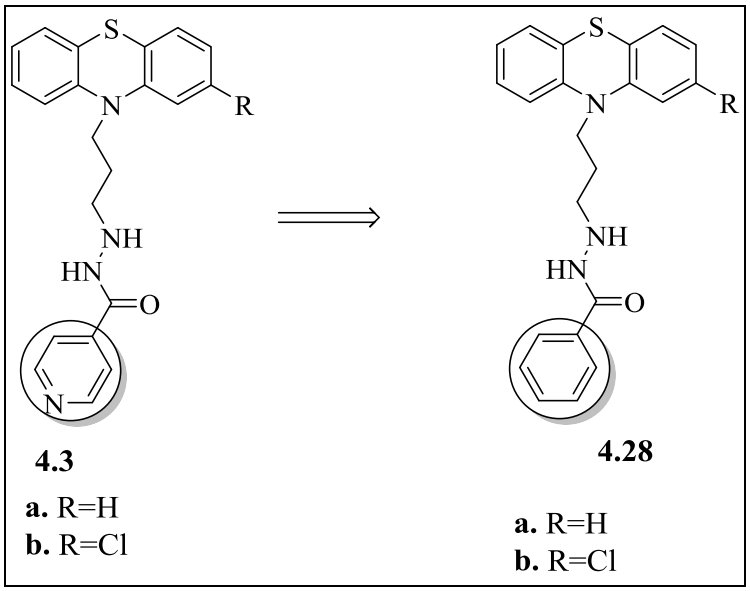

Figure 4.9: The design of benzoylhydrazine-based RATAs based on the phenothiazine core.

4.3.3.7.2 Synthesis of benzhydrazide -based RATAs (4.28)

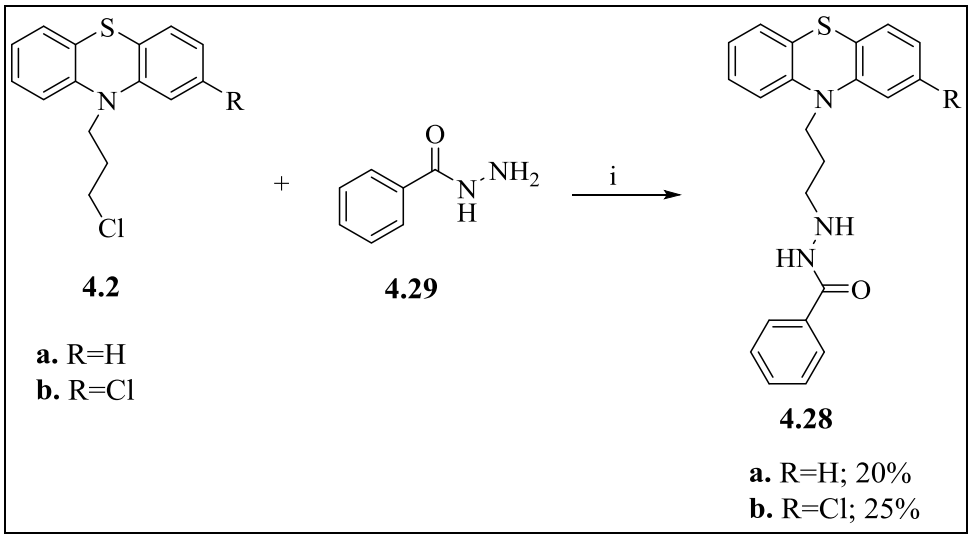

Scheme 4.14: *Reagents and reaction conditions*: (i) Et_3N, *iso*-propanol, reflux (95 °C), 10-12 h (20-25%).

The synthesis of benzhydrazide-based hybrid molecules commenced with the previously described intermediate **4.2** (Scheme **4.1**). The target molecule was obtained in low yield by

refluxing intermediate **4.2** and four equivalents of benzoylhydrazine and triethylamine in *iso*-propanol (Scheme **4.14**).

4.3.4 RINH anti-TB agents with non-tricyclic efflux pump inhibitor moieties

4.3.4.1 Rationale

The non-tricyclic EPI moieties found in cancer MDR modulators (**Figure 4.10**) were also considered for inclusion in RINHs. These non-tricyclic moieties have previously been explored for their multi drug resistance (MDR) reversion activity in cancer.[20] For example dihydropyridines (DHP) showed excellent MDR modulation against cancer cell lines and displayed a reduced affinity for the calcium channel. In addition, the potent DHP dexniguldipine was also evaluated in phase II clinical trials. The analogue **PAK-104P** was the most active against Pgp and MRP-dependent MDR. The quinine related compounds were also explored for MDR reversion activity and various compounds exemplified by **MS-209** were developed.[20]

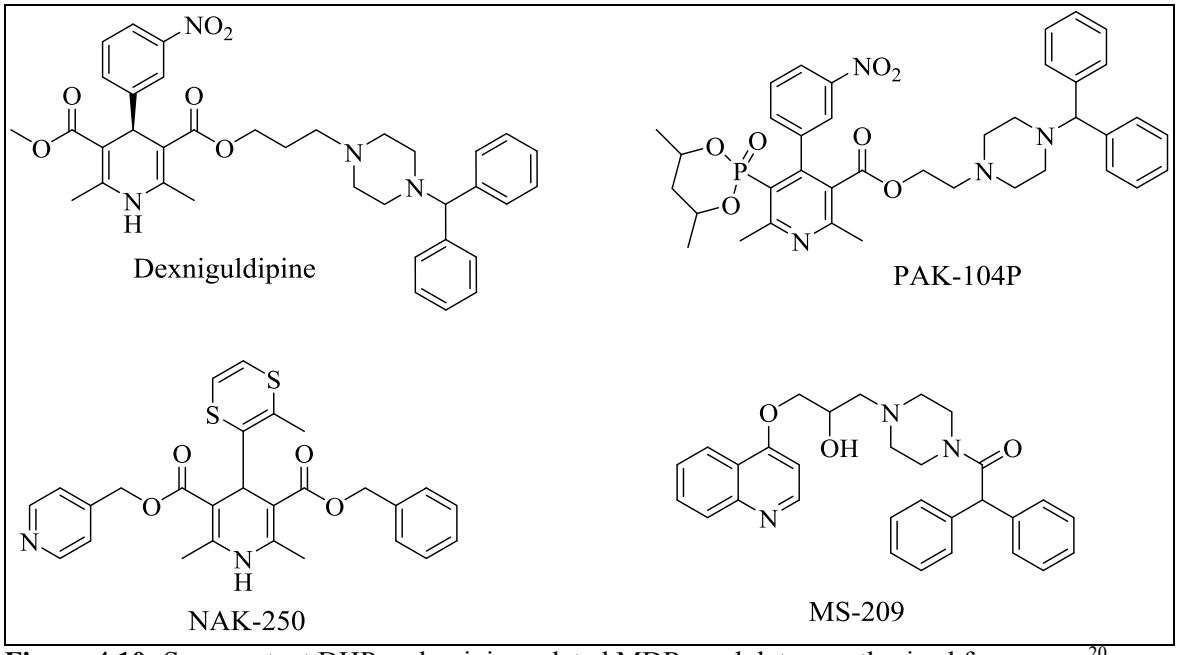

Figure 4.10: Some potent DHP and quinine related MDR modulator synthesized for cancer.[20]

On the basis of the excellent results obtained in reversion of resistance in cancer, some of these structural motifs were selected for incorporation into RINHs (**Figure 4.11**).

4.3.4.2 Design of RINH agents with non-tricyclic EPIs

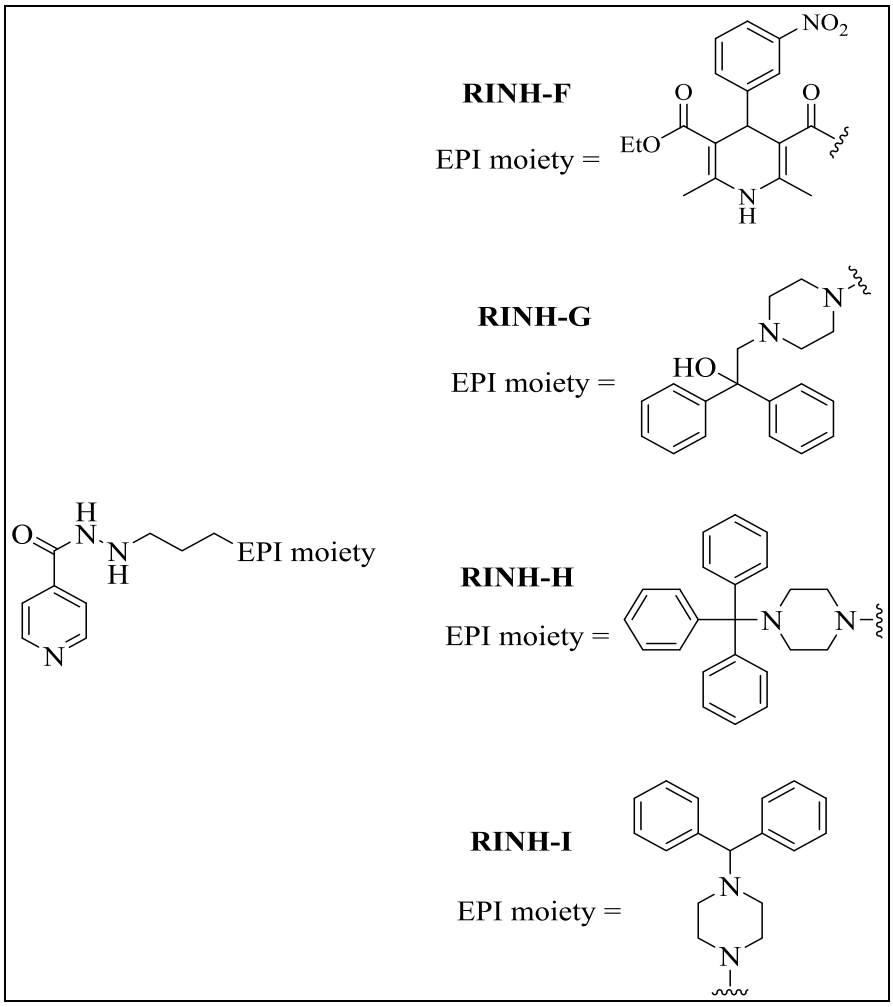

Figure 4.11: RINH agents with non-tricyclic EPI moieties.

4.3.4.3 Synthesis of dihydropyridine based RINH-F using the Hantzsch reaction

4.3.4.3.1 The Hantzsch reaction

The Hantzsch reaction is a multi-component reaction of a non-enolizable aldehyde (formaldehyde or benzaldehyde), a β-ketoester (ethyl acetoacetate) and a nitrogen donor (ammonium acetate or ammonia) to obtain a dihydropyridine (DHP) (Scheme **4.15**). The reaction was first reported and named after Arthur Rudolf Hantzsch. The product obtained as a DHP dicarboxylate is also called the Hantzsch compound. The acid form of these DHP can be easily obtained using basic hydrolysis.

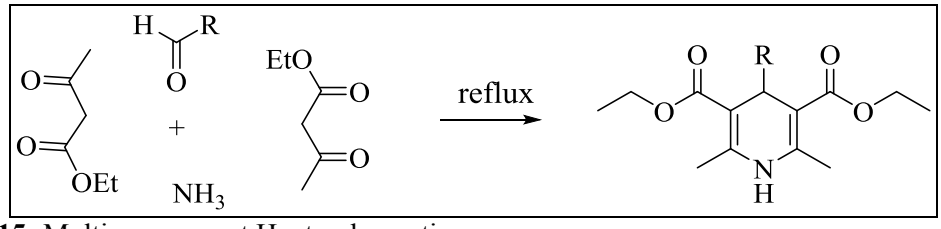

Scheme 4.15: Multi-component Hantzsch reaction.

The multistep mechanism of this reaction is outlined in scheme **4.16 (a-c)**. The reaction can be divided in two separate parts. The first part can be visualized as a condensation of the aldehyde and β-ketoester to form one of the key intermediates **I**. This condensation takes place *via* the Knoevenagel condensation reaction (Scheme **4.16a)**.

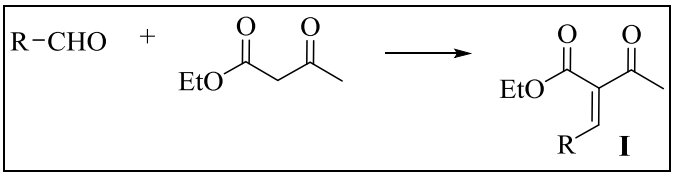

Scheme 4.16a: The formation of first key intermediate by condensation of the β-ketoester and non-enolizable aldehyde.

The second part of the reaction can be considered to be the formation of the ester amine by the condensation of an amine and a second equivalent of the β-ketoester (Scheme **4.16b**) to form intermediate **II**.

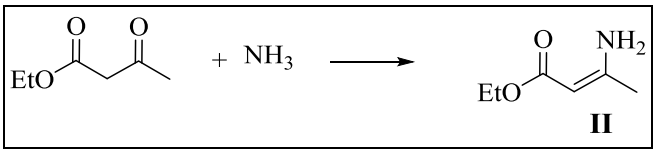

Scheme 4.16b: The formation of second key intermediate by condensation of the β-ketoester and an amine.

The condensation of these two intermediates **I** and **II** furnishes the dihydropyridine. This condensation follows a multistep mechanistic pathway.

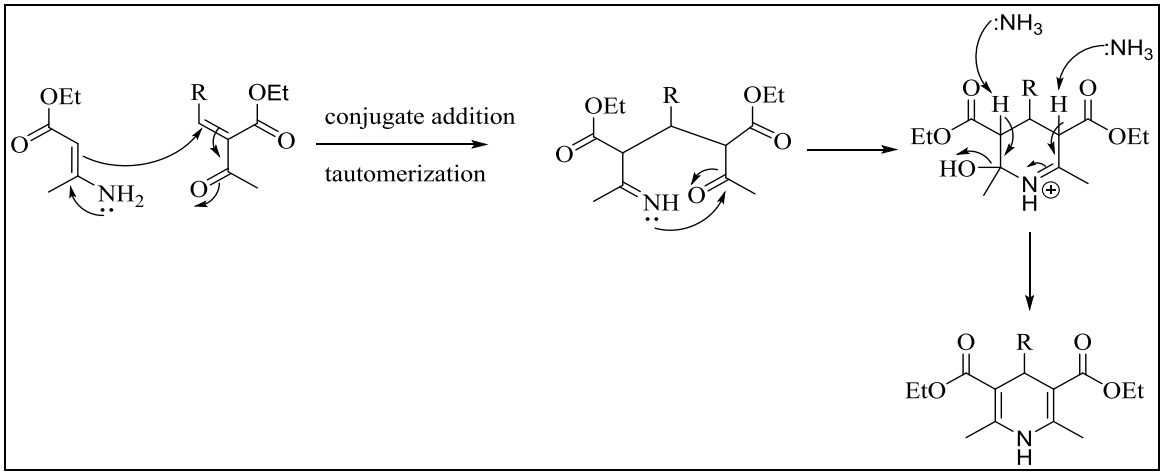

Scheme 4.16c: The mechanism of condensation of two intermediates (**I** and **II**) in the Hantzsch reaction.

First, a transient state is formed by the conjugate addition and tautomerism of the two above

mentioned intermediates. The resulting intermediate product then further rearranges after intramolecular condensation in the presence of ammonia to produce the dihydropyridine (Scheme **4.16c**).

4.3.4.3.2 Synthesis of dihydropyridine (4.32)

The synthesis of RINH-F includes the synthesis of the key precursor dihydropyridine (DHP) and its coupling with isoniazid. The synthesis of DHP commenced with the reaction of ethyl acetoacetate **4.29** and ammonium acetate to afford **4.30**. This intermediate was subsequently reacted with ethyl acetoacetate **4.29** and 2-nitro benzaldehyde **4.31** in the presence of a catalytic amount of acetic acid in ethanol (Scheme **4.17**) to afford **4.32** in good yield.

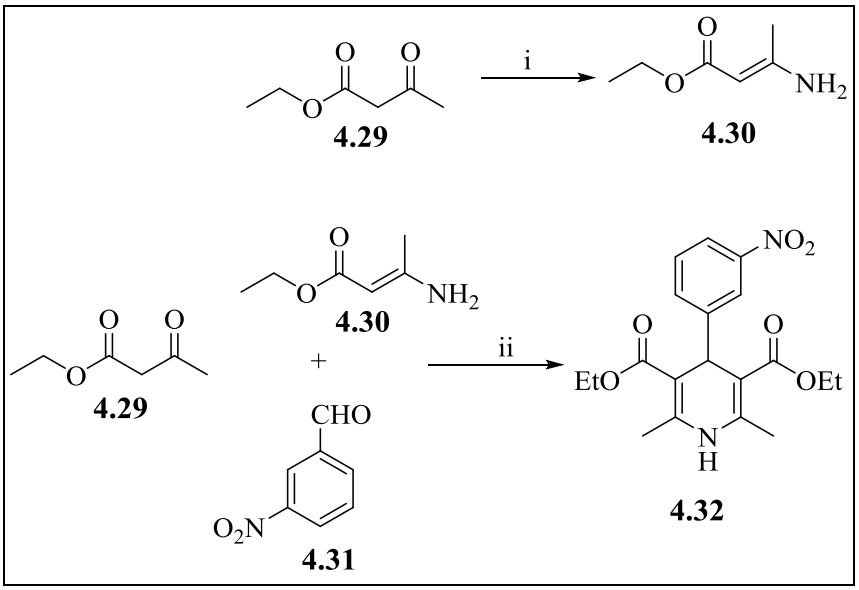

Scheme 4.17: *Reagents and reaction conditions*: (i) NH_4OAc (5.5 eq.), MeOH, 25 °C, 12 h, 95%; (ii) CH_3COOH (cat), EtOH, reflux (85 °C), 24 h, 90%.

4.3.4.3.3 Synthesis of target compound (4.36)

The asymmetric hydrolysis of ester groups of DHPs cannot be achieved *via* direct acidic or basic hydrolysis.[30] Firstly, the DHP was *N*-protected with ethyl chloroacetate in THF using sodium hydride in an atmosphere of nitrogen at room temperature (25 °C). Next, an anion was generated at 0 °C before the addition of ethyl chloroacetate and transfer to room temperature (25 °C). Thereafter, the asymmetric DHP was obtained by the method optimized by Masaru Iwanami and co-workers.[30] The reaction of DHP **4.32** with dimethylaminoethanol in benzene in the presence of sodium furnished a mixture of symmetric and asymmetric esters, which afforded a good yield of the asymmetric ester after purification (Scheme **4.18**). Subsequent deprotection with dilute hydrochloric acid (1*N*) afforded unsubstituted DHP **4.35**

in good yield (Table **4.10**). The target compound **4.36** was finally obtained by the coupling of the unsymmetric DHP **4.35** with commercially available isoniazid in DMF using coupling reagents 1-ethyl-3-(3-dimethylaminopropyl)carbodiimide (EDCI) and hydroxybenzotriazole (HOBt). The target compound was obtained in a low yield of 36% (Table **4.10**).

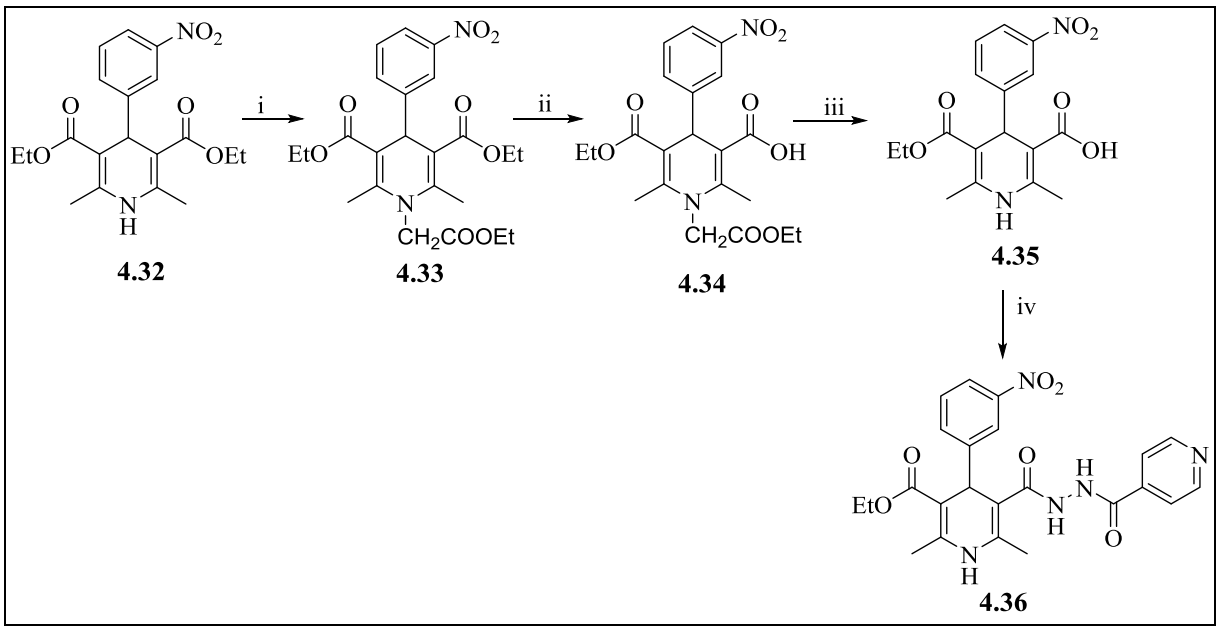

Scheme 4.18: *Reagents and reaction conditions*: (i) $ClCH_2COOEt$ (1.5 eq.), NaH (1.5 eq.), THF, 0-25 °C; (ii) $(Me)_2NCH(OH)CH_3$ (1.1 eq.), Na (1 eq.), H_2O, Benzene, 25 °C; (iii) 1*N* HCl, acetone, 25 °C; (iv) Isoniazid (1 eq.), EDCI (2.5 eq.), HOBt (2.5 eq.), DMF, 25 °C.

Table 4.10: Yields and melting points of isolated intermediate (**4.33-4.35)** and target compound **4.36.**

Compounds	Yield%	m.p. (°C)
4.33	68	188-189
4.34	28	175-176
4.35	23	157-159
4.36	36	172-174

4.3.4.3.4 Characterization of target molecule RINH-F (4.36)

The characterization of target compound **4.36** was accomplished using ^{1}H-NMR, ^{13}C-NMR and mass spectroscopy (MS). The HPLC chromatogram showed 97% purity and MS confirmed the molecular mass of **4.36** (a pseudomolecular ion mass peak of *m/z* 466.3 [M+H]). Figures **4.11** and **4.12** represent the ^{1}H-NMR and ^{13}C-NMR spectra of **4.36**, respectively. The ^{1}H-NMR spectrum confirmed the expected structure of target compound

4.36. The characteristic signals include two doublets at δ 8.74 and 7.76 ppm, which correspond to isoniazid protons H-9 and H-10 thus confirming the presence of the isoniazid moiety.

δ (ppm)	Multiplicity	J (Hz)	H
8.74	d	6.0	H-10
8.05	t	2.0	H-4
8.02	ddd	11.6, 3.6 & 1.2	H-1
7.76	d	6.0	H-9
7.70	d	8.0	H-3
7.57	t	8.4	H-2
4.99	s	-	H-8
4.01	m	-	H-5
1.15	t	6.8	H-6

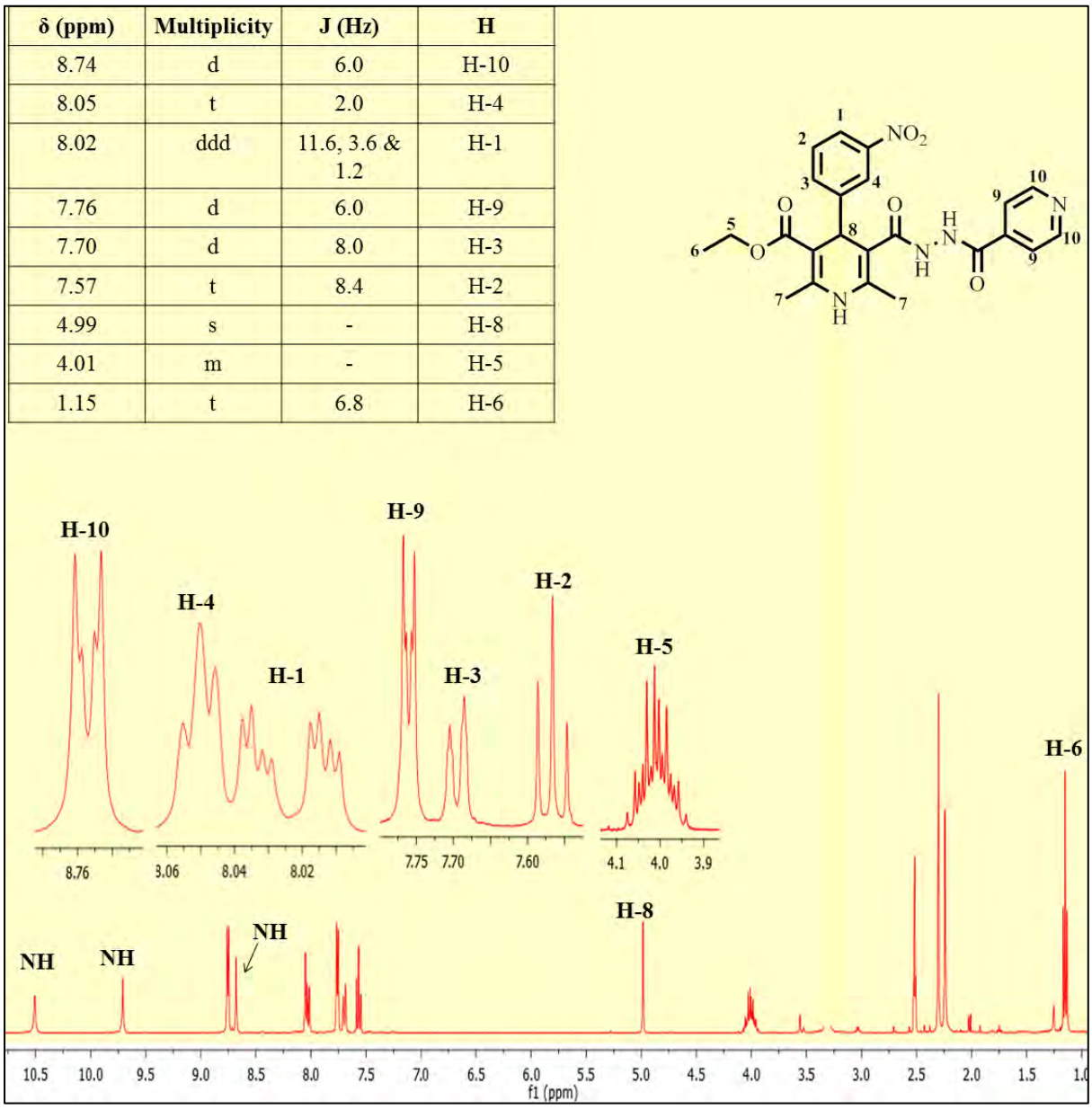

Figure 4.11: ^{1}H-NMR spectrum of **4.36** in DMSO-d_6 at 400 MHz.

Additional signals in aromatic regions confirmed the presence of the DHP moiety in the target compound. These signals include a triplet, a doublet of doublet of doublet, a broad doublet and a well-defined triplet at δ 8.05, 8.02, 7.70 and 7.57 ppm corresponding to H-4, H-1, H-3, and H-2 protons, respectively. The upfield aliphatic region showed three signals corresponding to six methyl protons H-7 and five ethyl protons (H-5 and H-6) on the DHP moiety.

The ^{13}C-NMR spectrum also supported the expected structure of **4.36**. The characteristic signals include three peaks between δ 164-167 ppm, which confirm the presence of three carbonyl carbons of **4.36**. Additional signals were also observed at δ 150.8 and 121.8 ppm, which correspond to the ring carbons C-9 and C-10 of the isoniazid moiety.

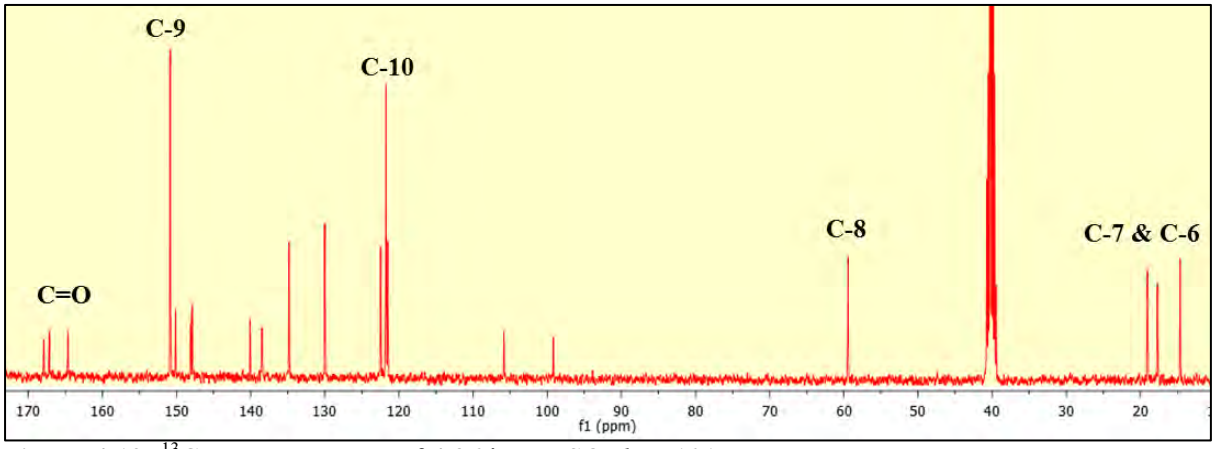

Figure 4.12: ^{13}C-NMR spectrum of **4.36** in DMSO-d_6 at 101 MHz.

4.3.4.4 Synthesis of RINH-G (4.46)

4.3.4.4.1 Synthesis of piperazine intermediate (4.41)

The synthesis of target molecule **4.46** included the synthesis of an important piperazine precursor **4.41** as shown in scheme **4.19**. The intermediate **4.39** was successfully produced in good yield by the reaction of 2-chloroacetophenone **4.37** and benzylpiperazine **4.38** using triethylamine in dichloromethane (DCM). The subsequent reaction of this intermediate with phenylmagnesium bromide proved to be challenging and could not be achieved with a good yield of **4.40** in various solvents (THF, diethyl ether, toluene and dioxane) at variable temperatures (0 °C to reflux).

The LC-MS showed conversion of only 40% of intermediate **4.39** to product **4.40**. The difference in retention factors on TLC between **4.39** and **4.40** was less than 0.1 in various solvent systems, and this presented purification challenges. The low yield has also been reported by Zaugg and co-workers for this type of reactions.[31] Removal of the benzyl group of **4.40** using a crude mixture was also accompanied by the formation of various by-products, which further intensified the difficulty in purification. Therefore, to obtain a high yield and avoid laborious purification, an alternative pathway was pursued (Scheme **4.20**), which successfully delivered the desired precursor **4.41**.

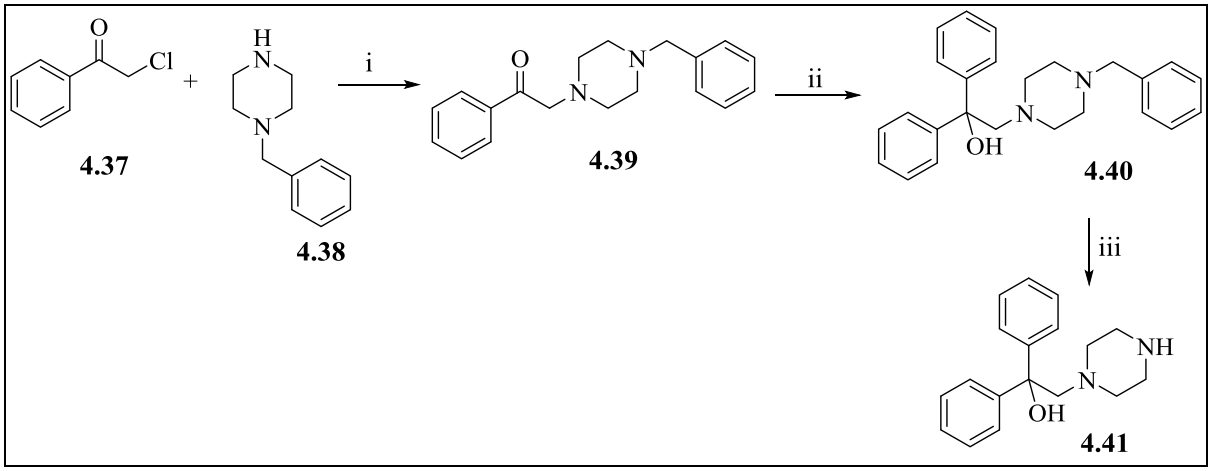

Scheme 4.19: *Reagents and reaction conditions*: (i) Et_3N (1.1 eq.), DCM, 0-25 °C, 1 h; (ii) PhMgBr (1.1 eq.), THF, 25 °C-reflux (70 °C), 12 h; (iii) Trifluoroacetic acid, reflux (85 °C), 12 h.

The synthesis of intermediate **4.41** with the alternative route commenced with the treatment of commercially available diphenylethene **4.42** with 1.1 equivalents of *N*-bromosuccinimide (NBS) in a mixture of acetone and water (5:1), which afforded intermediate **4.43** in 90% yield (Table **4.11)** (Scheme **4.20**).[32] This intermediate was then reacted with 1-Boc-piperazine in DMSO in the presence of cesium carbonate to afford **4.44** in 40% yield with recovery of starting material. Removal of the Boc group from **4.44** was accomplished by treating with TFA in DCM, resulting in a high yield of **4.41**.

To obtain target compound **4.46,** intermediate **4.41** was alkylated by reaction with 1-bromo-3-chloropropane in toluene using triethylamine at 65 °C to obtain intermediate **4.45**. The subsequent reaction of this intermediate with isoniazid in the presence of excess triethylamine in *iso*-propanol under reflux delivered the target molecule **4.46** in 35% yield (Scheme **4.20**).

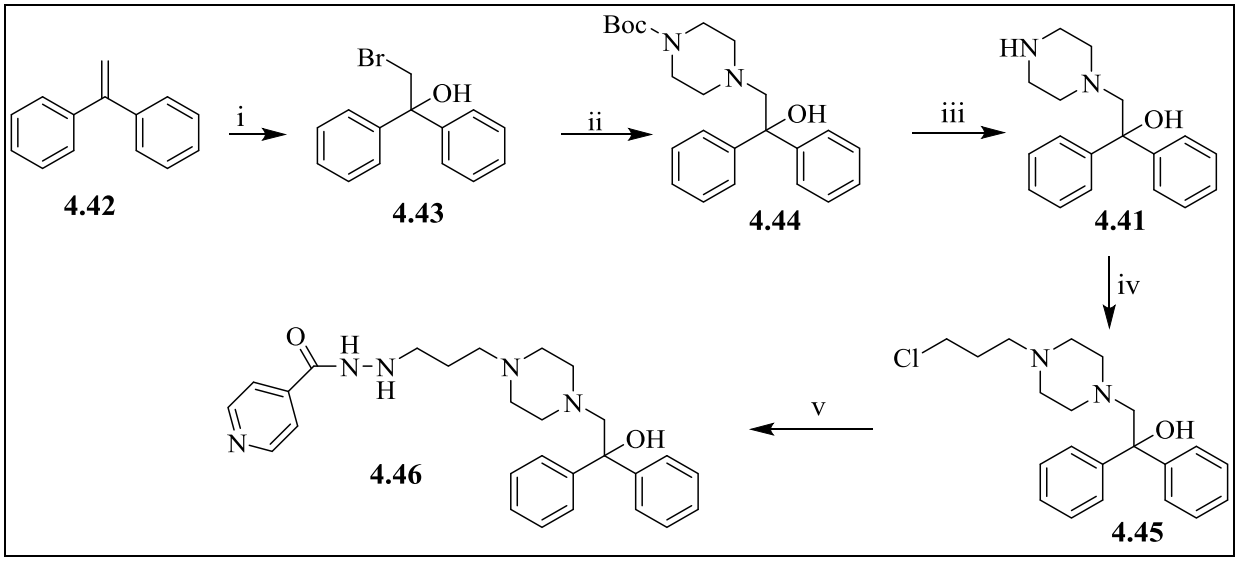

Scheme 4.20: *Reagents and reaction conditions:* (i) NBS (1.1 eq.), H_2O, Acetone, 25 °C, 2 h; (ii) 1-Boc-piperazine (1.1 eq.), DMSO, $CsCO_3$ (2 eq.), 60 °C, 8 h; (iii) TFA (10 eq.), DCM, 25 °C, 1 h; (iv) 1-Bromo-3-chloropropane (2 eq.), Et_3N (2.5 eq.), toluene, 65 °C, 8 h; (v) Isoniazid (4 eq.), Et_3N (4 eq.), *iso*-propanol, reflux (95 °C), 12 h.

Table 4.11: Yields and melting points of isolated intermediates (**4.41** and **4.43-4.45)** and target compound **4.46**.

Compound	Yield %	m.p. (°C)
4.43	90	70-72
4.44	40	100-102
4.41	96	66
4.45	72	77-79
4.46	35	115-117

4.3.4.4.2 Characterization of target compound 4.46

Target compound **4.46** was characterized using ^{1}H- and ^{13}C-NMR spectroscopy as well as LC-MS. The LC-MS chromatogram showed 97% purity of the compound and a pseudomolecular ion mass peak of *m/z* 460.3 [M+H], as expected for the target compound **4.46**. Figure **4.13** and **4.14** represent the ^{1}H-NMR and ^{13}C-NMR spectra of **4.46**, respectively. The appearance of two doublets at δ 8.75 and 7.63 ppm corresponding to four isoniazid protons H-11 and H-10 confirmed the presence of an isoniazid moiety in **4.46**. A typical pattern of two phenyl moieties also appeared as one doublet, one triplet and one triplet of triplet corresponding to H-1, H-2 and H-3 phenyl protons, respectively. A broad singlet at δ 5.10 ppm and a sharp singlet at δ 3.27 ppm were also observed. These correspond to the OH

proton and the H-4 protons, respectively. The confirmatory signals for the three carbon alkyl linker appeared as two triplets and one quintet at δ 2.99, 2.56 and 1.76 corresponding to H-7, H-9 and H-8 protons, respectively. The second triplet at δ 2.56 appeared to be overlapping with the broad singlet representing eight piperazine protons.

δ (ppm)	Multiplicity	J (Hz)	H
8.75	d	6.0	H-11
7.63	d	6.0	H-10
7.50	d	8.4	H-1
7.32	t	8.0	H-2
7.21	tt	7.6 & 1.2	H-3
5.10	s	-	OH
3.27	s	-	H-4
2.99	t	6.4	H-9
1.76	quin	6.0	H-8

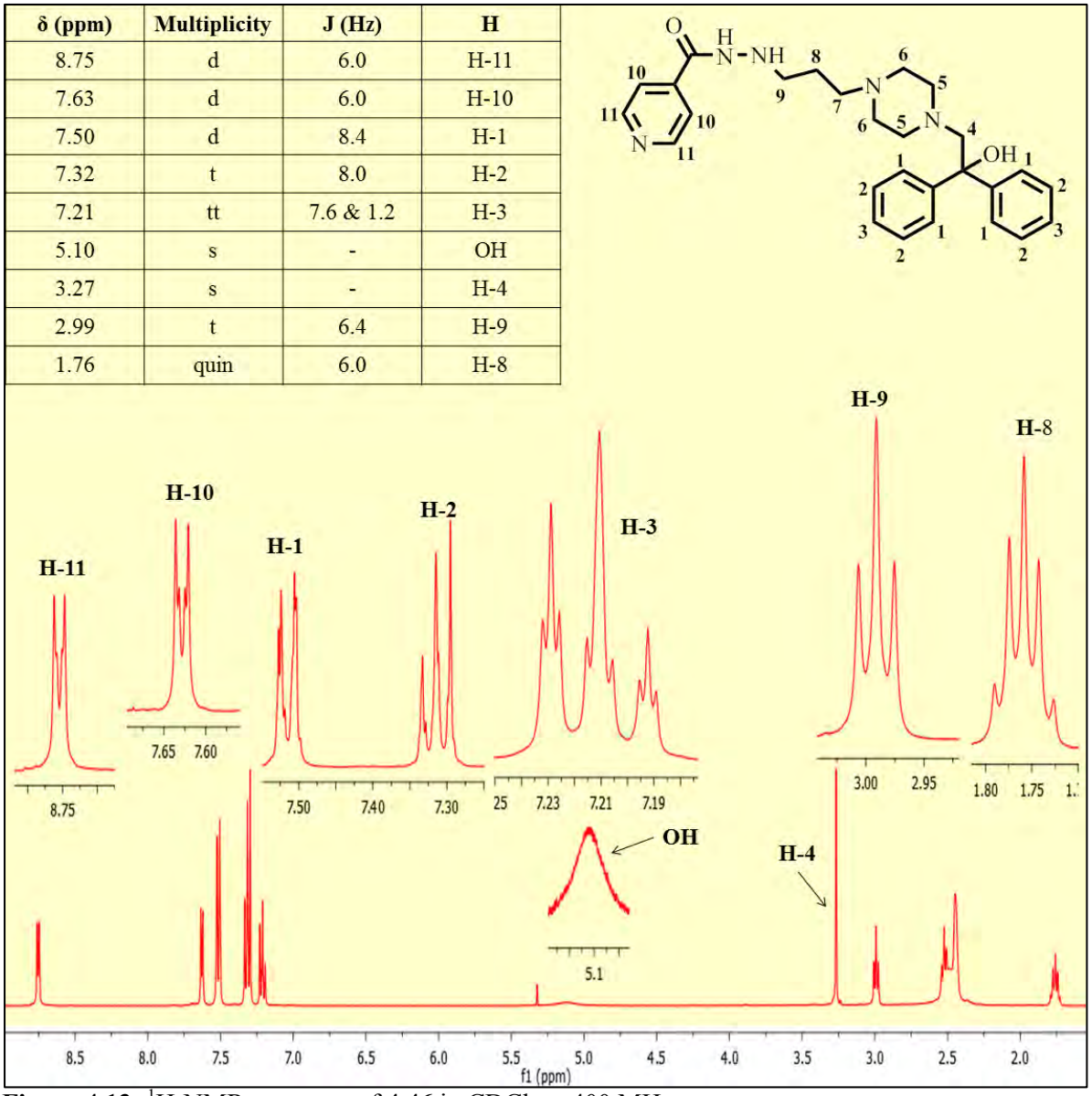

Figure 4.13: ^{1}H-NMR spectrum of **4.46** in $CDCl_3$ at 400 MHz.

The ^{13}C-NMR spectrum showed 15 distinct singlets corresponding to 27 carbons of **4.46** as some signal intensities being equivalent to two and four carbons. The characteristic signals included peaks at δ 164.3, 150.6 and 120.9 ppm corresponding to a carbonyl carbon and isoniazid ring carbons C-11 and C-10, respectively. Additional signals appeared in the upfield aliphatic region corresponding to the propyl linker and piperazine ring carbons C-5 to C-9, including C-4.

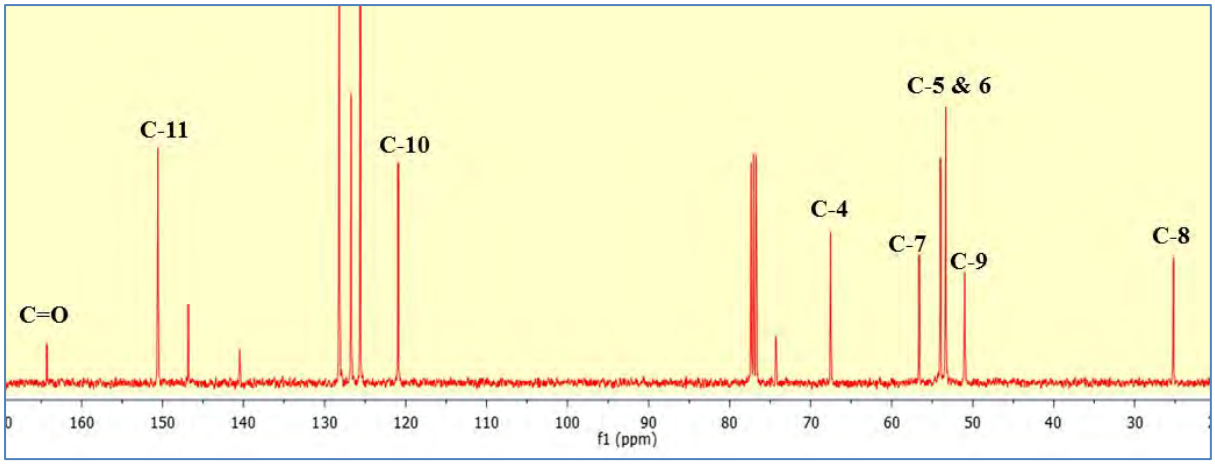

Figure 4.14: ^{13}C-NMR spectrum of **4.46** in $CDCl_3$ at 101 MHz.

4.3.4.5 Synthesis of RINH-H (4.50)

The synthesis of the target molecule **4.50** was achieved *via* a straight forward three step synthesis (Scheme **4.21**) and commenced with the reaction of commercially available tritylbromide **4.47** with an excess of piperazine at room temperature (25 °C) for one hour in DCM to afford **4.48** in 70% yield. The intermediate **4.48** was then alkylated with 1-bromo-3-chloropropane in toluene using triethylamine to afford the advanced intermediate **4.49**. The desired compound **4.50** was obtained by reacting **4.49** with isoniazid in *iso*-propanol using an excess of isoniazid and triethylamine (Table **4.12**).

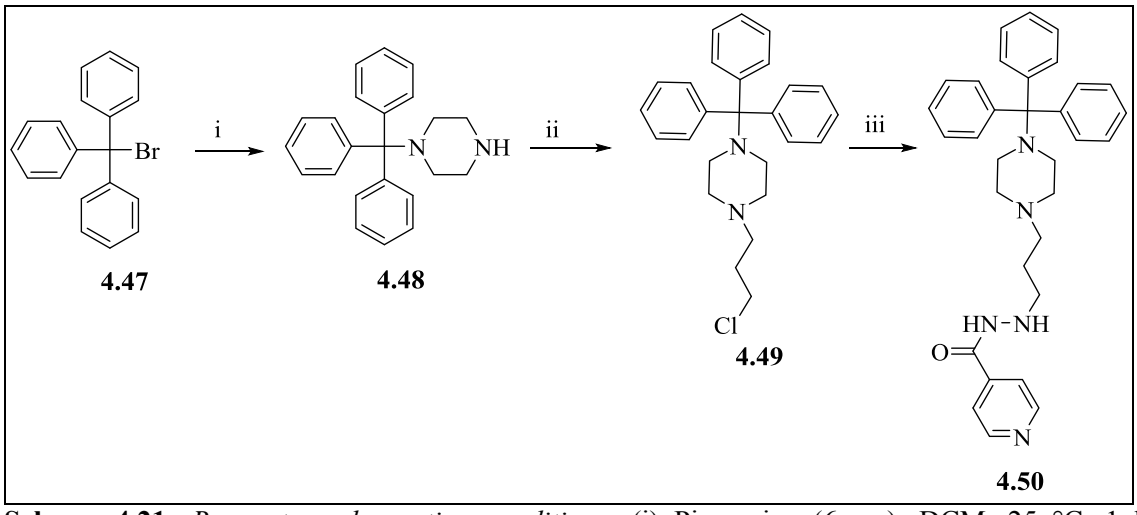

Scheme 4.21: *Reagents and reaction conditions:* (i) Piperazine (6 eq.), DCM, 25 °C, 1 h; (ii) 1-Bromo-3-chloropropane (2 eq.), Et_3N92.5 eq.), toluene, 65 °C, 8 h; (iii) Isoniazid (4 eq.), *iso*-propanol, Et_3N (4 eq.), 95 °C, 12 h.

Table 4.12: Yields and melting points of isolated intermediate (**4.48** and **4.49)** and target compound **4.50**.

Compound	Yield %	m.p. (°C)
4.48	70	94-96
4.49	62	114-116
4.50	40	199-200

4.3.4.6 Synthesis of RINH-I (4.54)

The synthesis of the target compound commenced with the reaction of commercially available diphenyl bromomethane **4.51** with piperazine to obtain intermediate **4.52** in good yield (Scheme **4.22**). This intermediate was then reacted with 1-bromo-3-chloropropane in toluene in the presence of triethylamine at 65 °C to afford **4.53** in high yield. The target compound **4.54** was obtained in low yield (Table **4.13**) by reaction of **4.53** with an excess of isoniazid and triethylamine in *iso*-propanol under reflux.

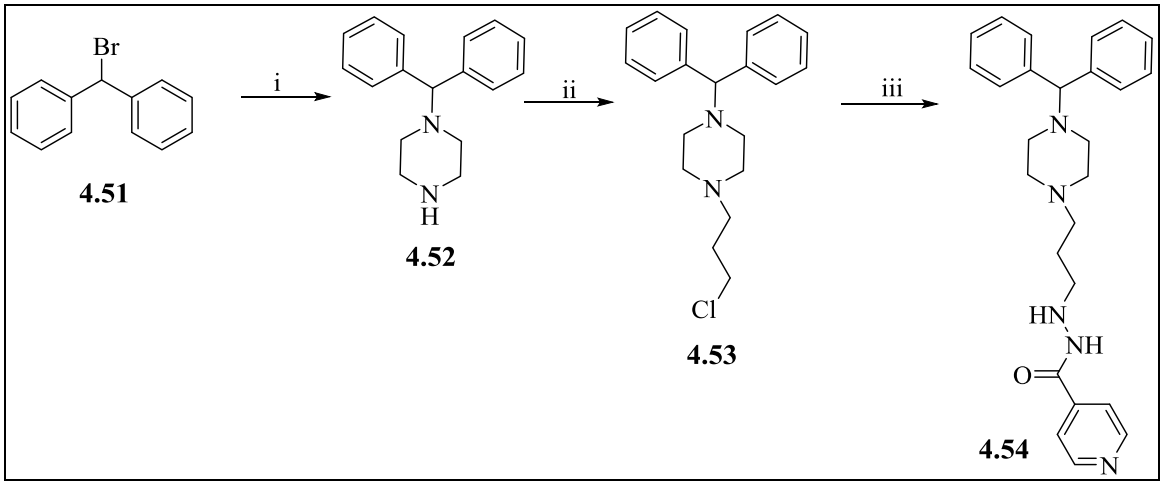

Scheme 4.22: *Reagents and reaction conditions*: (i) Piperazine (2 eq.), K_2CO_3 (1 eq.), NaI (0.2 eq.), acetonitrile, reflux (90 °C), 8 h; (ii) 1-Bromo-3-chloropropane (2 eq.), Et_3N (2.5 eq.), toluene, 65 °C, 8 h; (iii) Isoniazid (4 eq.), Et_3N (4 eq.), *iso*-propanol, reflux (95 °C), 10 h.

Table 4.13: Yields and melting points of intermediates (**4.52** and **4.53)** and target compound **4.54.**

Compound	Yield %	m.p. (°C)
4.52	65	70-72
4.53	90	*
4.54	42	55-57

*Compound isolated as an oil.

4.4 Hybrid efflux pump inhibitors

4.4.1 Rationale

The rationale behind the design of HEPIs is based on SAR studies of known EPIs, which have revealed the importance of an aromatic moiety and a basic nitrogen atom appropriately spaced *via* an alkyl chain linker. It was hypothesised that replacement of one or both aromatic moieties of verapamil might produce novel EPIs with potentially superior potency profiles to that of verapamil.[10,11]

During the course of writing this PhD thesis, an article describing a related but different concept appeared in the literature.[33] This concept is based on the chemical modification of thioridazine (THZ) in such a way that the phenothiazine core was replaced by bicyclic and tricyclic flat structures while keeping the *N*-methyl piperidine moiety of THZ intact. Among the various reported HEPIs, **H-1**, **H-2**, **H-3**, and **H-4** (**Figure 4.15**) displayed the most promising results.

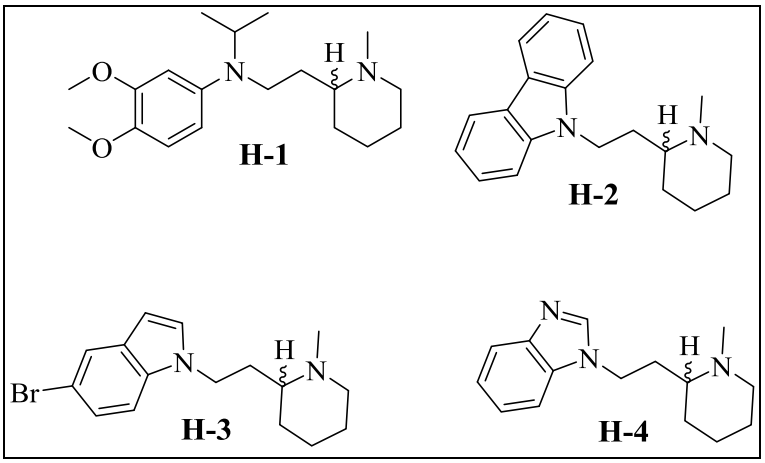

Figure 4.15: The reported HEPIs with EPI properties.[33]

In addition to low antimycobacterial activity (*M. smegmatis* mc^{2}155 and H37Rv; MIC ≥ 128 μg/mL) and low cytotoxicity against a human monocyte cell line (IC_{50} ≥ 84.8 μg/mL), all these compounds (**H-1**, **H-2**, **H-3**, and **H-4**; **Figure 4.15**) showed comparable or superior inhibition of EB efflux in *M. smegmatis* cells and H37Rv strain of *Mtb*. A combination screening of these compounds with anti-TB drugs, INH, RIF, amikacin (AMK), and ofloxacin (OFX) *in vitro* demonstrated their synergistic and potentiating effect, with the exception of **H-4**, which was inactive in the combination assay. However, all the compounds were reported to potentiate sub-inhibitory concentrations of INH and RIF in macrophages at a concentration lower than their cytotoxic concentrations.[33] Compound **H-3** was selected for

further development as it exhibited superior synergistic interactions (FIC ≤ 0.25) with various anti-TB drugs (INH, RIF, AMK and OFX) in combination against *Mtb* H37Rv strain.

In the present preliminary study, the dimethoxyphenyl moiety of verapamil is replaced with other known bacterial EPI moieties (**Figure 4.16**).

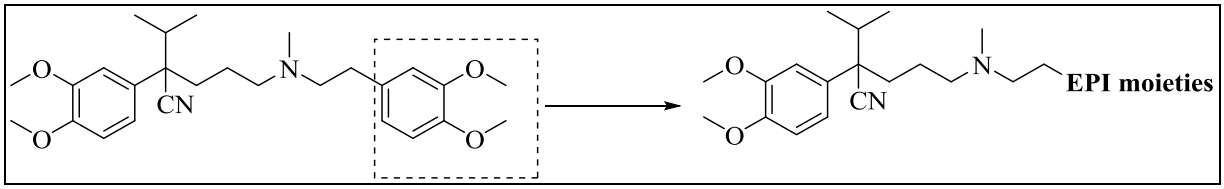

Figure 4.16: Design of hybrid efflux pump inhibitors of verapamil template. A dimethoxyphenyl moiety has been replaced with various EPIs/EPI moieties for the development of HEPIs.

4.4.2 Synthesis of hybrid efflux pump inhibitors

The synthesis of hybrid efflux pump inhibitors involved reaction of the verapamil sub-structure intermediate **4.56** with various commercially available EPIs or EPI moieties synthesised in section **4.3.3**.

4.4.2.1 Synthesis of verapamil substructure motif (4.56)

The synthesis of the key intermediate **4.56** is outlined in scheme **4.23**, and commenced with the synthesis of intermediate **3.6c**, using methods described in chapter **3** (Section **3.2.2.2**). In the process, commercially available 2-(3,4-dimethoxyphenyl)acetonitrile **3.8** was reacted with *iso*-propyl bromide, according to an established method,[34] followed by reaction with 1-bromo-3-chloropropane in THF in the presence of LDA to afford intermediate **3.6c**. This intermediate was further reacted with 2-(methylamine)ethanol in DMF using potassium carbonate at 80 °C to obtain intermediate **4.55**, which, upon reaction with an excess of thionyl chloride (1.5 equivalents) at room temperature (25 °C), produced **4.56** in high yield.

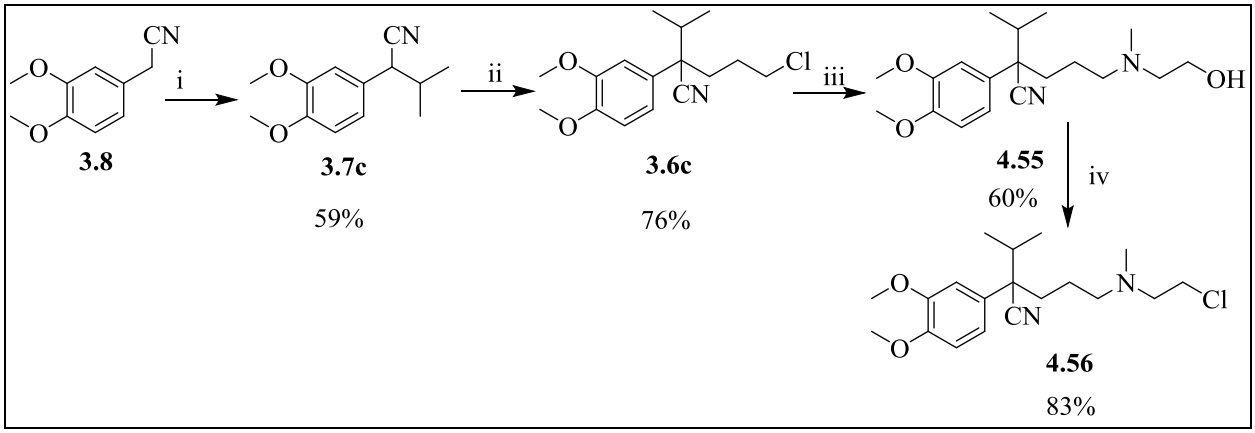

Scheme 4.23: *Reagents and reaction conditions:* (i) 2-Bromopropane (1.5 eq.), *n*-BuLi (1.1 eq.), THF, 0-25 °C, 2 h; (ii) 1-Bromo-3-chloropropane (1.5 eq.), LDA (1.2 eq.), THF, -78-25 °C, 2 h; (iii) 2-(methylamino)ethan-1-ol (1 eq.), K_2CO_3 (1.7 eq.), DMF, 80 °C, 12 h; (iv) $SOCl_2$ (10 eq.), DCM, 25 °C, 14 h.

4.4.2.2 Synthesis of hybrid efflux pump inhibitors

The desired HEPIs (**4.57-4.61** and **4.63**) were obtained in poor to moderate yields by the coupling of intermediate **4.56** with various EPI moieties synthesised in section **4.3.3** using different reaction conditions (Scheme **4.24**).

The piperazine and piperidine-containing EPI moieties (**4.15**, **4.21**, **4.25**, and **4.51**) were reacted with **4.56** in DMF using potassium carbonate at 80 °C to obtain target compounds **4.58-4.61** in low to moderate yields (Table **4.14**).

The diphenylmethylamine **4.62** was reacted with **4.56** in ethanol in the presence of potassium carbonate at reflux temperature to afford **4.63** in low yield (Table **4.14**).

The HEPIs **4.57a** and **4.57b** were obtained in poor yield by reacting **4.56** with phenothiazine **4.1a**, and 2-chlorophenothiazine **4.1b**, respectively, in DMF using sodium hydride at room temperature (25 °C). The target compound **4.57c** was obtained by refluxing **4.56** with dibenzazepine **4.1c** in the presence of sodium amide in toluene, which produced the desired compound **4.57c** (Table **4.14**).

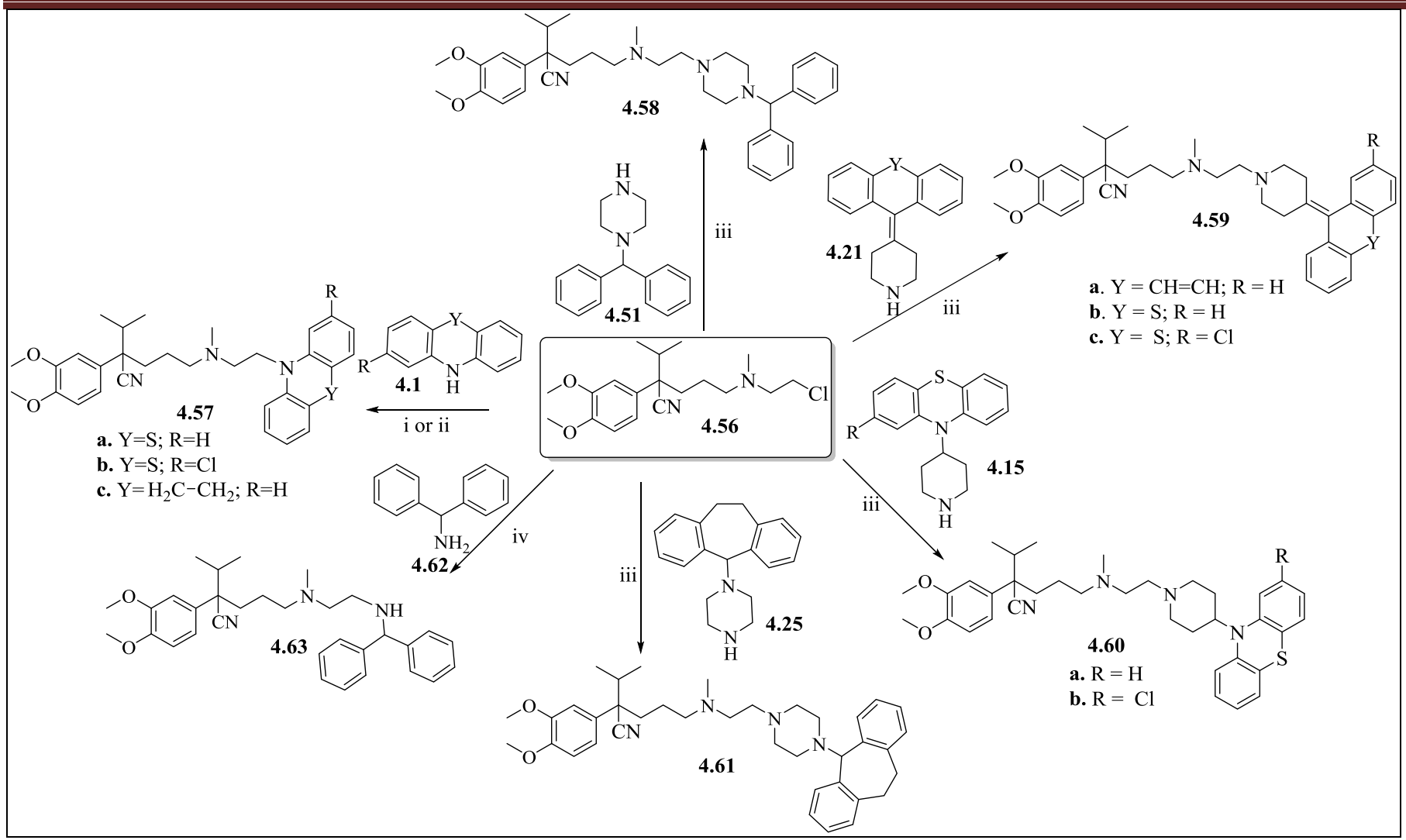

Scheme 4.24: *Reagents and reaction conditions:* (i) NaH (1 eq.), DMF, 25 °C, 6-8 h; (ii) $NaNH_2$ (1.5 eq.), toluene, reflux (115 °C), 12 h; (iii) K_2CO_3 (2 eq.), DMF, 80 °C, 8-12 h; (iv) K_2CO_3 (1 eq.), EtOH, reflux (85 °C), 12 h.

Table 4.14: Yield and melting points target compounds indicated in scheme **4.24**.

Compound	Yield %	m.p. (°C)
4.57a	16	*
4.57b	29	*
4.57c	24	*
4.58	57	*
4.59a	24	70-72
4.59b	20	60-62
4.59c	36	85-87
4.60a	25	35-37
4.60b	21	50-52
4.61	34	60-61
4.63	30	*

*Compound obtained as an oil.

4.4.2.3. Characterization of HEPIs

HEPIs **4.57-4.61** and **4.63** were characterized with the aid of ^{1}H-NMR, ^{13}C-NMR, NOSY and COSY spectroscopy as well as LC-MS.

4.4.2.3.1 Characterization of 4.63

An expected pseudomolecular ion peak of m/z 500.6 [M+H] was observed, which corresponds to **4.63**. Figures **4.16** and **4.17** represent the ^{1}H-NMR and ^{13}C-NMR spectra of **4.63**. The number of protons in the aromatic region was equal to the expected number of aromatic protons of **4.63**. A doublet and two triplets at δ 7.40, 7.32 and 7.24 ppm corresponding to H-12, H-13 and H-14 protons, respectively, were observed. These signals were further split through long range couplings, albeit secondary couplings were not well resolved. In addition, a doublet of doublets, one multiplet and a doublet corresponding to H-2, H-3 and H-1 protons of the 3,4-dimethoxy phenyl group of **4.63** were also observed at δ 7.02, 6.99 and 6.95 ppm, respectively.

The signals observed in the aliphatic region of the molecule correlated well with the expected protons of **4.63**. Two unresolved triplets corresponding to H-11 and H-10 protons appeared as multiplets at δ 2.65 and 2.61 ppm. Additionally, one multiplet, two singlets and two doublets at δ 2.49, 4.84, 2.21, 1.99 and 0.77 ppm, corresponding to H-8, H-15 and H-9, and H-5 protons, respectively, were also observed. An anomalous pattern of signals was observed corresponding to protons adjacent to the stereogenic centre. This pattern appeared as three

multiplets integrating for one proton each (H-6 and H-7), and a multiplet integrating for two protons (H-4 and H-6). This anomalous pattern may be attributed to the diastereotopic nature of these protons.

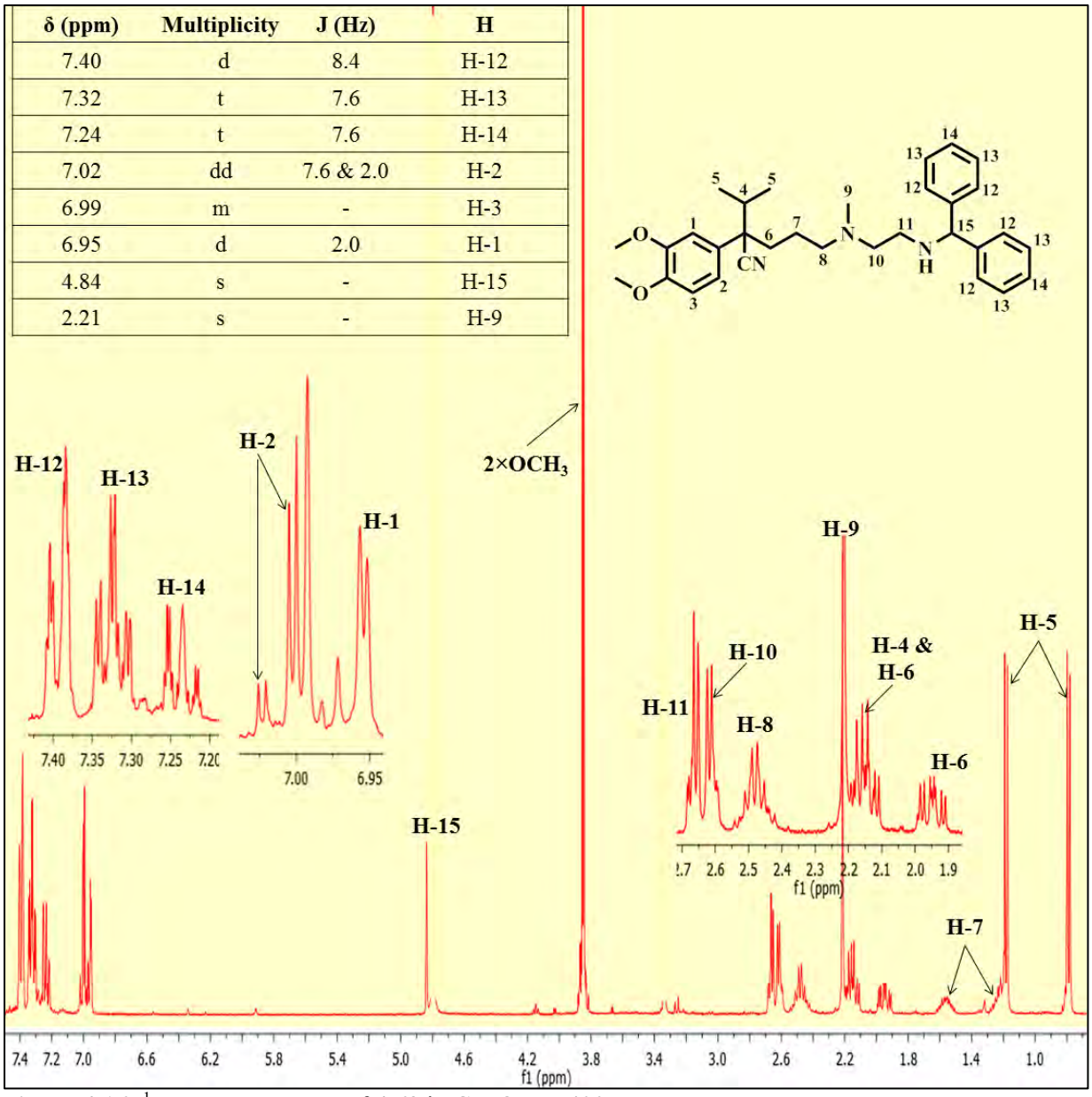

Figure 4.16: ^{1}H-NMR spectrum of **4.63** in CD_3OD at 400 MHz.

The ^{13}C-NMR spectra of **4.63** showed 23 distinct signals corresponding to 32 carbons of **4.63**. Some signals showed intensity equal to two or four carbons. The aliphatic region contains signals corresponding to all the aliphatic carbons, including C-15, C-6, C-7 and C-5.

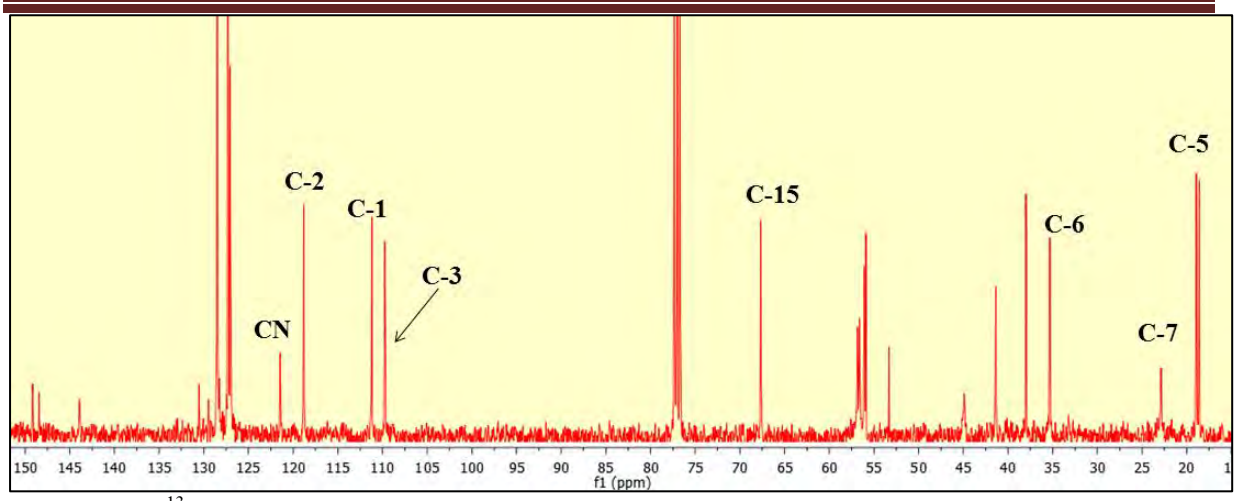

Figure 4.17: ^{13}C-NMR spectrum of **4.63** in CD_3OD at 101 MHz.

4.4.2.3.2 Characterization of HEPI-4.59c

Figures **4.18** and **4.19** represent the ^{1}H-NMR and ^{13}C-NMR spectra of **4.59c**, respectively. The LCMS chromatogram showed a purity of 97% and a pseudomolecular ion mass peak of *m/z* 630.2 [M+H]. The aromatic region of the ^{1}H-NMR spectrum showed signals corresponding to the protons expected for **4.59c**. Two doublets, one multiplet and one triplet were observed at δ 7.50, 7.34 and 7.24 ppm, respectively, corresponding to protons of a 2-chlorophenothiazine nucleus. Three multiplets were observed in the range of δ 2.55-2.33 ppm, corresponding to eight protons of the piperidine moiety (H-12 and H-13) of **4.59c**.

The ^{13}C-NMR spectrum of **4.59c** showed 32 distinct signals corresponding to 37 carbons with some signals showing intensity equal to two or four carbons of **4.59c** and correlated well with the ^{1}H-NMR spectrum. In addition to the signals corresponding to the all the aromatic and nitrile carbons in the aromatic region, two signals also appeared corresponding to two alkene carbons. The aliphatic region also showed two signals for C-12 and C-13 carbons.

δ (ppm)	Multiplicity	J (Hz)	H
7.50	two d	7.8	H-17 & H-17'
7.34	m	-	H-14', H-16' & H-14
7.24	t	7.8	H-15 & H-16
2.55-2.11	m	-	H-12 & H-13
2.20	s	-	H-9

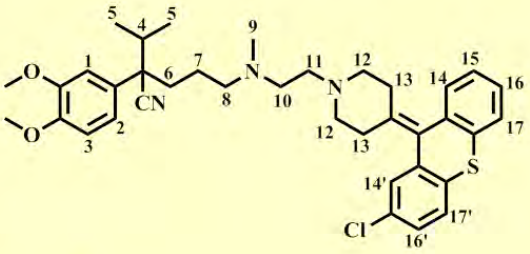

Figure 4.18: ^{1}H-NMR spectrum of **4.59c** in CD_3OD at 400 MHz.

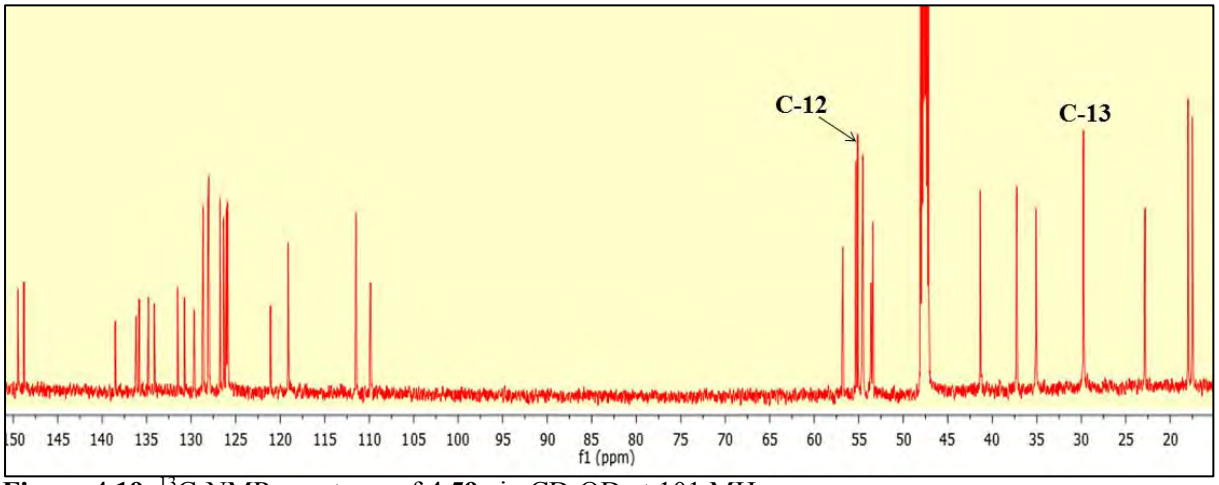

Figure 4.19: ^{13}C-NMR spectrum of **4.59c** in CD_3OD at 101 MHz.

4.5 Conclusion

The synthesis of various designed RINHs and HEPIs was accomplished *via* a range of synthetic protocols. They were characterized using various analytical and spectroscopic techniques, which confirmed the structures of the expected compounds. The biological evaluation of the synthesised analogues will be discussed in chapter **5** of this thesis.

References:

(1) Hooper, D. Mechanisms of Action and Resistance of Older and Newer Fluoroquinolones. *Clin. Infect. Dis.* **2000**, *2696*, 24–28.

(2) Bambeke, F.; Pages, J.-M.; Lee, V. Inhibitors of Bacterial Efflux Pumps as Adjuvants in Antibiotic Treatments and Diagnostic Tools for Detection of Resistance by Efflux. *Recent Pat. Antiinfect. Drug Discov.* **2006**, *1*, 157–175.

(3) Hubschwerlen, C.; Specklin, J.-L.; Sigwalt, C.; Schroeder, S.; Locher, H. H. Design, Synthesis and Biological Evaluation of Oxazolidinone–Quinolone Hybrids. *Bioorg. Med. Chem.* **2003**, *11*, 2313–2319.

(4) Viveiros, M.; Martins, M.; Rodrigues, L.; Machado, D.; Couto, I.; Ainsa, J.; Amaral, L. Inhibitors of Mycobacterial Efflux Pumps as Potential Boosters for Anti-Tubercular Drugs. *Expert Rev. Anti. Infect. Ther.* **2012**, *10*, 983–998.

(5) Adams, K. N.; Szumowski, J. D.; Ramakrishnan, L. Verapamil, and Its Metabolite Norverapamil, Inhibit Macrophage-Induced, Bacterial Efflux Pump-Mediated Tolerance to Multiple Anti-Tubercular Drugs. *J. Infect. Dis.* **2014**, *210*, 456–466.

(6) Vinsova, J.; Imramovsky, A.; Jampilek, J.; Monreal, J.; Dolezal, M. Recent Advances on Isoniazide Derivatives. *Antiinfect. Agents Med. Chem.* **2008**, *7*, 12–31.

(7) Jardosh, H. H.; Patel, M. P. Design and Synthesis of Biquinolone-Isoniazid Hybrids as a New Class of Antitubercular and Antimicrobial Agents. *Eur. J. Med. Chem.* **2013**, *65*, 348–359.

(8) Molnar, a. Antiplasmid Effect of Promethazine in Mixed Bacterial Cultures. *Int. J. Antimicrob. Agents* **2003**, *22*, 217–222.

(9) Wainwright, M. The Evolution of Antimycobacterial Agents from Non- Antibiotics. *Anticancer research* **2012**, 32, 2947-2957

(10) Biscardi, M.; Teodori, E.; Caporale, R.; Budriesi, R.; Balestri, F.; Scappini, B.; Gavazzi, S.; Grossi, A. Multidrug Reverting Activity toward Leukemia Cells in a Group of New Verapamil Analogues with Low Cardiovascular Activity. *Leuk. Res.* **2006**, *30*, 1–8.

(11) Teodori, E.; Dei, S.; Quidu, P.; Budriesi, R.; Chiarini, A.; Garnier-Suillerot, A.; Gualtieri, F.; Manetti, D.; Romanelli, M. N.; Scapecchi, S. Design, Synthesis, and in Vitro Activity of Catamphiphilic Reverters of Multidrug Resistance: Discovery of a Selective, Highly Efficacious Chemosensitizer with Potency in the Nanomolar Range. *J. Med. Chem.* **1999**, *42*, 1687–1697.

(12) Rodrigues, L.; Machado, D.; Couto, I.; Amaral, L.; Viveiros, M. Contribution of Efflux Activity to Isoniazid Resistance in the *Mycobacterium tuberculosis* Complex. *Infect. Genet. Evol.* **2012**, *12*, 695–700.

(13) Rodrigues, L.; Aínsa, J. A.; Amaral, L.; Viveiros, M. Inhibition of Drug Efflux in Mycobacteria with Phenothiazines and Other Putative Efflux Inhibitors. *Recent Pat. Antiinfect. Drug Discov.* **2011**, *6*, 118–127.

(14) Burgess, S. J.; Selzer, A.; Kelly, J. X.; Smilkstein, M. J.; Riscoe, M. K.; Peyton, D. H. A Chloroquine-like Molecule Designed to Reverse Resistance in Plasmodium Falciparum. *J. Med. Chem.* **2006**, *49*, 5623–5625.

(15) Peyton, D. H. Reversed Chloroquine Molecules as a Strategy to Overcome Resistance in Malaria. *Curr. Top. Med. Chem.* **2012**, *12*, 400–407.

(16) H. Peyton, D. Reversed Chloroquine Molecules as a Strategy to Overcome Resistance in Malaria. *Curr. Top. Med. Chem.* **2012**, *12*, 400–407.

(17) Burgess, S. J.; Kelly, J. X.; Shomloo, S.; Wittlin, S.; Brun, R.; Liebmann, K.; Peyton, D. H. Synthesis, Structure-Activity Relationship, and Mode-of-Action Studies of Antimalarial Reversed Chloroquine Compounds. *J. Med. Chem.* **2010**, *53*, 6477–6489.

(18) H. Peyton, David; Burgess, S. Quinoline Derivativer and Uses Thereof, *United States Patent Application 20110257160*. **2011**.

(19) Marquez, B. Bacterial Efflux Systems and Efflux Pumps Inhibitors. *Biochimie* **2005**, *87*, 1137–1147.

(20) Teodori, E.; Dei, S.; Scapecchi, S.; Gualtieri, F. The Medicinal Chemistry of Multidrug Resistance (MDR) Reversing Drugs. *Farm.* **2002**, *57*, 385–415.

(21) Kubota, K.; Kurebayashi, H.; Miyachi, H.; Tobe, M.; Onishi, M.; Isobe, Y. Synthesis and Structure-Activity Relationships of Phenothiazine Carboxylic Acids Having Pyrimidine-Dione as Novel Histamine H(1) Antagonists. *Bioorg. Med. Chem. Lett.* **2009**, *19*, 2766–2771.

(22) Appel, R. Tertiary Phosphane/Tetrachloromethane, a Versatile Reagent for Chlorination, Dehydration, and P-N Linkage. *Angew. Chemie Int. Ed. English* **1975**, *14*, 801–811.

(23) Lera R. M. De; Michael Y. B.; Junying Z.; Robert G. A.; Kevin D. M.; Qingbei Z. Tricyclic heterocycle derivatives as histamine h3 antagonists. *PCT/US2009/051257; WO2010/011653 A1*.

(24) Hoover, J. M.; Dipasquale, A.; Mayer, J. M.; Michael, F. E. Platinum-Catalyzed Intramolecular Hydrohydrazination: Evidence for Alkene Insertion into a Pt-N Bond. *J. Am. Chem. Soc.* **2010**, *132*, 5043–5053.

(25) McMurry, J. E.; Fleming, M. P. New Method for the Reductive Coupling of Carbonyls to Olefins. Synthesis of .beta.-Carotene. *J. Am. Chem. Soc.* **1974**, *96*, 4708–4709.

(26) *Encyclopedia of Reagents for Organic Synthesis*; John Wiley & Sons, Ltd: Chichester, UK, 2001.

(27) Ephritikhine, M.; Moléculaire, S. D. C.; Ura, C.; Saclay, C. E. A.; Yvette, G. A New Look at the McMurry Reaction. *Chem. Commun.* **1998**, 2549–2554.

(28) Duan, X.; Zeng, J.; Lü, J.-W.; Zhang, Z.-B. Insights into the General and Efficient Cross McMurry Reactions between Ketones. *J. Org. Chem.* **2006**, *71*, 9873–9876.

(29) Mukaiyama, T.; Sato, T.; Hanna, J. Reductive Coupling of Carbonyl Compounds to Pinacols and Olefins by Using $TiCl_4$ and Zn. *Chem. Lett.* **1973**, 1041–1044.

(30) Iwanami, M.; Shibanuma, T.; Fujimoto, M.; Kawai, R.; Tamazawa, K.; Takenaka, T.; Takahashi, K.; Murakami, M. Synthesis of New Water-Soluble Dihydropyridine Vasodilators. *Chem. Pharm. Bull. (Tokyo).* **1979**, *27*, 1426–1440.

(31) Zaugg, H. E.; Michaels, R. J.; Glenn, H. J.; Swett, L. R.; Freifelder, M.; Stone, G. R.; Weston, A. W. Tertiary Carbinols of the Piperazine Series. I. *J. Am. Chem. Soc.* **1958**, *80*, 2763–2768.

(32) Yu, L.; Ren, L.; Yi, R.; Wu, Y.; Chen, T.; Guo, R. Palladium-Catalyzed Reaction of Olefins with PhI(OAc)2-TBAB System: An Efficient and Highly Selective Bisfunctionalization Strategy. *Synlett* **2011**, *2011*, 579–581.

(33) Pieroni, M.; Machado, D.; Azzali, E.; Santos Costa, S.; Couto, I.; Costantino, G.; Viveiros, M. Rational Design and Synthesis of Thioridazine Analogues as Enhancers of the Antituberculosis Therapy. *J. Med. Chem.* **2015**, *58*, 5842–5853.

(34) Zhongxu Ren, Bo-Liang Deng, Jennifer Riggs-Sauthier, M. H. Oligomer-Calcium Channel Blocker Conjugates. PCT/ US 2008/ 010385.

Chapter 5: Antimycobacterial activity of verapamil analogues, reversed isoniazid anti-TB agents and hybrid efflux pump inhibitors

5.1 Introduction

This chapter describes the biological results of various compounds synthesized in chapters **3**, and **4**. The chapter begins with a description of the various assays and screening cascade used followed by the results and their discussion in three different sections.

5.2 Assays for Antimycobacterial testing

All *in vitro* screening was performed in Associate Professor Digby Warner's laboratory by Dr. Krupa Naran of the MRC/NHLS/UCT Molecular Mycobacteriology Research Unit, Division of Medical Microbiology, University of Cape Town (UCT), South Africa. The macrophage studies were conducted at two independent laboratories; Department of Internal Medicine, Division of Infectious Diseases, Allergy and Immunology, Saint Louis University (SLU), USA and Assoc. Prof. Digby Warner's laboratory at UCT.

5.2.1 Chequerboard synergy assay

The synthesized compounds were evaluated against the *Mtb* H37Rv strain individually as well as in combination with various anti-TB drugs, both *in vitro* and *ex vivo*. The individual screening was aimed at investigating the antimycobacterial potency while combination screening was conducted in order to evaluate the potentiating effect of VER analogues on anti-TB drugs against *Mtb*.

The combination screening against the H37Rv strain of *Mtb* was performed in a 96-well plate format using Microplate Alamar Blue Assay (MABA). An adaptation of the broth microdilution method was used, in which the antimicrobial agent (compound A) and the EPI (compound B), were 2-fold serially diluted across and down the plate, respectively (**Figure 5.1**).[1] The fluorometric method was used to monitor the growth of *Mtb* in the 96-well plate. The growth of *Mtb* is indicated by the change in colour of the well from blue to pink, and the lowest concentration of antimycobacterial agent that prevent this colour change is considered as minimum inhibitory concentration (MIC). The first horizontal row is drug only (from A3 to A11) while second column is the efflux pump inhibitor (EPI) only (from B2 to H2) and A2 well of the plate is 'no drug' control. The first and last column was assigned for minimum

and maximum inhibition control as no drug was added to the first column and a very high concentration of drug (Rifampicin > MIC_{99}) in last column was added.

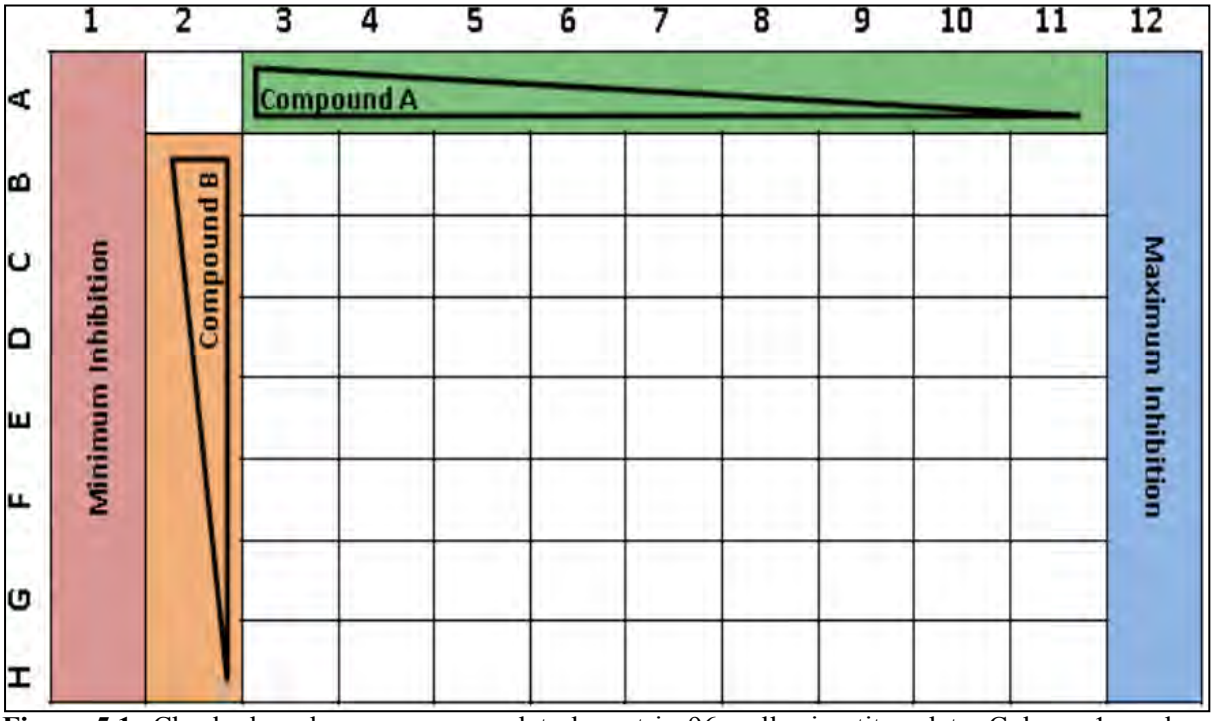

Figure 5.1: Checkerboard synergy assay plate layout in 96-well microtitre plate. Column 1 used as minimum inhibition control (no drug/EPI) and column 12 used as maximum inhibition control (rifampicin). The drug (compound A) was 2-fold serially diluted across the plate (column 3 – 11) and the EPI (compound B) was 2-fold serially diluted down the plate (row B – H). Well A2 serves as the "no drug" control.

The Fractional Inhibitory Concentration Index (FICI) values of the combination of the EPI and the anti-TB drug is a sum of the Fractional Inhibitory Concentration (FIC) of each of the agents tested in combination:[2]

$$FIC(A) = \frac{\text{MIC of compound A in combination with compound B}}{\text{MIC of compound A}}$$

$$FIC(B) = \frac{\text{MIC of compound B in combination with compound A}}{\text{MIC of compound B}}$$

$$FICI(AB) = FIC(A) + FIC(B)$$

The FICI values are used to define synergistic, additive, and antagonist interactions between the agents used in the combination testing. By definition, a FICI value of ≤ 0.5 indicates synergy, a value FICI = 4.0 indicates antagonism while FICI values between 0.5 to 4.0 points to an additive effect.[3] The experimental details related to this assay are given in the experimental section.

5.2.2 *Ex vivo* assay for cytotoxicity and intracellular inhibition

The macrophage evaluation of VER analogues was performed in order to investigate the potentiating effect of synthesized EPI candidates on various anti-TB drugs against intracellular *Mtb*. The human monocyte cell lines (THP-1) were used to screen VER analogues for cytotoxicity prior to evaluation in macrophages. The experimental details for cytotoxicity and macrophage assays are captured in the experimental section. A strict screening cut off of IC_{20} > 10 μM was used as a criteria to shortlist the verapamil analogues for further testing on intracellular *Mtb*.

A checkerboard assay as described in section **5.2.1** was also used for the toxicity evaluation of EPI-anti-TB drug combinations. The EPIs with an *in vitro* MIC_{90} in combination with RIF lower than the toxicity against THP-1 cell lines (IC_{20}) were analysed in *ex vivo* checkerboard synergy assays with RIF and BDQ in Assoc. Prof. Digby Warner's laboratory. The laboratory at SLU also evaluated the selected analogues for intracellular inhibition in macrophages individually and in combination with sub-inhibitory concentrations of RIF and INH.

5.2.3 *Mtb*-specific T-cell assay

Since VER is also a known autophagy inducer, the effect of VER and selected analogues on *Mtb*-specific T-cells was investigated. An assay consisting of carboxyfluorescein succinimidyl ester (CFSE) labelled peripheral blood mononuclear cells (PBMC) infected with Bacillus Chalmette Guerin (BCG) was used. The number of proliferated and IFN-ɣ producing T-cells was measured using a flow cytometer.[4] The experimental details are described in the experimental section.

5.2.4 Ethidium bromide assay

As described in chapter **2**, ethidium bromide (EB) (**Figure 5.2**) is a well known substrate of efflux pumps.[5] Therefore, a semi-automated flow cytometry-based method using EB-stained BCG was employed for the determination of efflux pump inhibition potential of the various VER analogues.[6] Efflux pump inhibitors (EPIs) are expected to increase the intracellular accumulation of EB in BCG micro growth dilution assays. A mean fluorescence intensity (MFI) was recorded with and without the EPI in the EB containing BCG micro growth dilution assay. The EP inhibition capability of various VER analogues was indicated by recorded intensity. The detailed description of the method employed has been provided in the experimental section (Chapter **7**).[7]

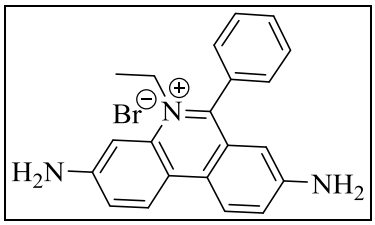

Figure 5.2: Ethidium bromide.

5.3 Screening cascades for verapamil analogues:

As mentioned in section **5.2**, VER analogues were screened at two separate laboratories. Therefore, two screening cascades were adopted, which are described below:

5.3.1 Screening cascade for *in vitro Mtb* and *ex vivo* cytotoxicity evaluation

The Warner laboratory at UCT performed various *in vitro* and *ex vivo* experiments with the aim of exploring VER analogues for their potentiating effect as well as the development of novel EPIs devoid of cytotoxicity. These analogues were screened *via* cascade 1 (**Figure 5.3**).

All the VER analogues were first screened against the H37Rv strain of *Mtb* for their individual antimycobacterial activities. Classically EPIs are expected to show low potency on their own but exhibit potentiating effects on drugs when used in combination. Therefore, VER analogues with low potency ($MIC_{90} \geq 50$ μM) were further evaluated in combination with the front line anti-TB drug rifampicin (RIF). The various parameters recorded during combination screening are fold reduction in RIF MIC_{90}, FICI values, and the MIC_{90} of analogues in combination with RIF.

The most important parameter is fold-reduction in the RIF MIC_{90}, which indicates the potentiation of RIF by analogues against *Mtb*. As explained in chapter **2**, two to four fold reductions in the MIC_{90} of an anti-TB agent, which are susceptible to EPs can be caused by the efflux pump inhibition property of chemosensitizers used in combination.[8] Another parameter is the MIC_{90} values of analogues in combination with RIF. This indicates the concentration of analogues required to achieve the respective potentiation of RIF. An EPI showing potentiation of an anti-TB drug at a low concentration is desired as high concentration may lead to various cytotoxic and unwanted effects on host human cells.

Another important parameter is the FICI value. As mentioned earlier in section **5.2.1**, FICI

values are used to identify the type of interaction (synergistic, additive or antagonist) between VER analogues and RIF when used in combination.

The analogues potentiating RIF by four-fold were further evaluated in combination with BDQ and MOX against H37Rv. Those showing potentiating effects on the chosen drugs were further selected for *ex vivo* cytotoxicity evaluation against THP-1 cell lines. Less cytotoxic analogues (IC_{20} > *in vitro* MIC_{90} in combination with BDQ) were evaluated for cytotoxicity in combination with BDQ against THP-1 cell lines. Analogues demonstrating a low cytotoxicity profile in combination with BDQ (IC_{20} in combination with BDQ > *in vitro* MIC_{90} in combination with BDQ) were screened in macrophages in combination with BDQ and with other front line anti-TB drugs (BDQ and MOX).

5.3.2 The screening cascade for macrophage and T-cell inhibition testing

An approach to develop novel EPIs which are less cytotoxic and devoid of interaction with the *Mtb*-specific T-cells was undertaken by the SLU laboratory of Dr. Getahun Abate.

The analogues exhibiting low cytotoxicity against THP-1 cell lines were first evaluated for individual antimycobacterial activity on intracellular *Mtb* in macrophages. Macrophages infected with BCG and *Mtb* were used in this study. BCG is a less virulent strain of *Mtb* and is easier to work with. Therefore, less cytotoxic analogues were screened against BCG-infected macrophages followed by evaluation of potent analogues (inhibition ≥ 30%) against *Mtb* infected macrophages. Those analogues showing comparable intracellular inhibition to VER (inhibition ≥ 30%) were further evaluated in the T-cell assay. The analogues with minimum interaction with *Mtb*-specific T-cells were further tested in combination with RIF and INH against *Mtb* in infected macrophages after evaluation in the ethidium bromide assay.

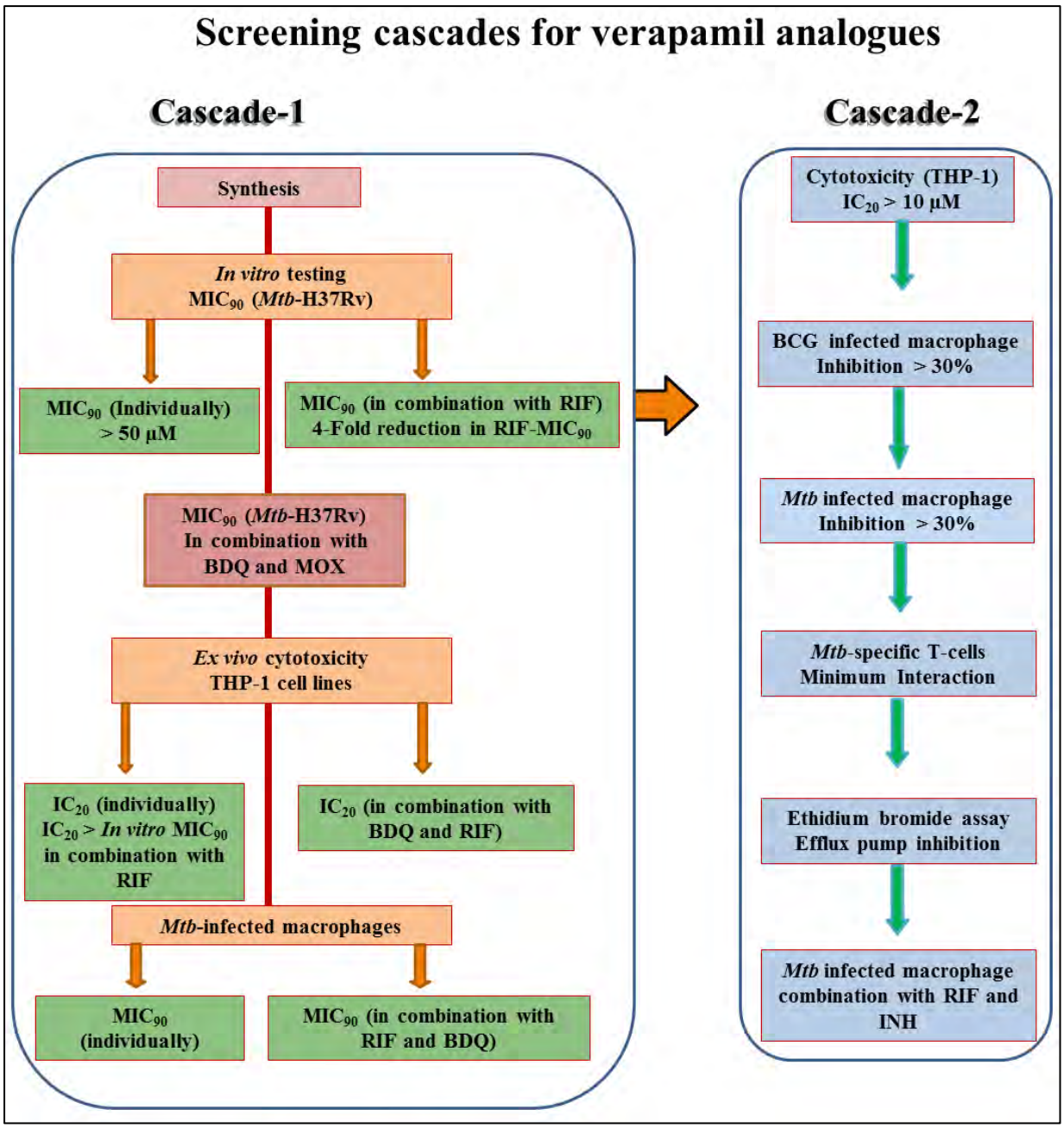

Figure 5.3: The screening cascades for verapamil analogues: Cascade 1 was used by the laboratory at UCT and cascade 2 was used by the laboratory at SLU for antimycobacterial evaluation of VER analogues *in vitro* and *ex vivo*.

5.4 Antimycobacterial activities of VER analogues

5.4.1 Antimycobacterial activities of VER analogues 3.13a-o

The synthesized VER analogues according to SAR 1, SAR 2, SAR 3 and SAR 4 (Chapter **3**), were screened *via* cascade 1 (**Figure 5.3**). Generally speaking, most of the VER analogues showed low *in vitro* potency against the H37Rv strain of *Mtb* (MIC_{90} > 50 μM) (Table **5.1**). The exceptions were, analogues **3.13m-o**, which exhibited superior antimycobacterial activity relative to VER, with **3.13n** being the most potent analogue (MIC_{90} = 62.5 μM) (Table **5.1**). Furthermore, all the analogues (**3.13)** were screened in combination with RIF to investigate their potentiating effects (fold reduction in the RIF MIC_{90}) and synergistic indications (FICI ≤ 0.5) (Table **5.1**).[4] The initial concentration of analogues used in combination was half of their individual MIC_{90}. This was in order to avoid any inhibitory effect of the analogues on the viability of *Mtb*. VER reduced the RIF MIC_{90} by four-fold and exhibited synergistic interactions (FICI = 0.5) at a concentration of 125 μM (Table **5.1**).

VER analogues (**3.13i-n)** synthesized by replacing an *iso*-propyl moiety at the stereogenic centre with various substituents (SAR 1), showed variable effects on the susceptibility of *Mtb* to RIF. The unsubstituted (**3.13i)**, methyl-substituted (**3.13j)**, and cyclopentyl-substituted (**3.13m)** analogues decreased the RIF MIC_{90} by two-fold. However, a four-fold reduction in the RIF MIC_{90} was observed with ethyl **(3.13k**), propyl **(3.13l)** and cyclohexyl **(3.13n)** substituted analogues (Table **5.1**). All these analogues exhibited FICI values in the range of 0.75 to 1.25, indicating an additive effect (0.5 < FICI ≤ 4.0) with RIF. Among these analogues, **3.13n** reduced the RIF MIC_{90} by four-fold at half (62.5 μM) the concentration of VER (125 μM) (Table **5.1**).

The derivatives **3.13e-h** and **3.13o** synthesized by varying substituents on the nitrogen (SAR 3) demonstrated varying potentiating effects on RIF (Table **5.1**). *Nor*-VER (**3.13e)** a known metabolite of VER, exhibited a two-fold reduction in the RIF MIC_{90} but did not exhibit synergistic interactions (FICI = 0.56). The *N*-ethyl (**3.13f**) and *N*-propyl (**3.13g**) substituted analogues did not exhibit any reduction in the RIF MIC_{90} (Table **5.1**). The VER analogue with a benzyl substituent on nitrogen, **3.13h** showed a four-fold reduction in the RIF MIC_{90} with a synergistic interaction (FICI = 0.3) at a four-fold lesser concentration (31.25 μM) as compared to VER (125 μM) (Table **5.1**).

[*]**Table 5.1:** *In vitro* combination activity of VER analogues (SAR 1 SAR 2 and SAR 3) with RIF against *Mtb*.

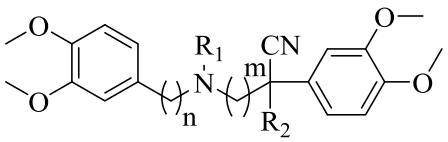

3.13a-o

[a]Comp	R^1	R^2	n	m	MIC_{90} (µM)			Fold reduction of RIF MIC	FICI
					[b]Anal	Anal (in combination with RIF)	[e]RIF (in combination with Anal)		
VER	$-CH_3$	$-CH(CH_3)_2$	2	3	500	125	0.002	4	0.5
3.13a	$-CH_3$	$-CH(CH_3)_2$	0	3	>1000	[c]ND	0.008	[d]NC	[f]ND
3.13b	$-CH_3$	$-CH(CH_3)_2$	1	3	>1000	[c]ND	0.008	[d]NC	[f]ND
3.13c	$-CH_3$	$-CH(CH_3)_2$	1	2	500	250	0.002	4	0.75
3.13d	$-CH_3$	$-CH(CH_3)_2$	2	2	1000	125	0.002	4	0.56
3.13e	$-H$	$-CH(CH_3)_2$	2	3	500	31.25	0.004	2	0.56
3.13f	$-CH_2CH_3$	$-CH(CH_3)_2$	2	3	1000	[c]ND	0.008	[d]NC	[f]ND
3.13g	$-(CH_2)_2CH_3$	$-CH(CH_3)_2$	2	3	500	[c]ND	0.008	[d]NC	[f]ND
3.13h	$-CH_2Ph$	$-CH(CH_3)_2$	2	3	1000	31.25	0.002	4	0.3
3.13i	$-CH_3$	$-H$	2	3	1000	500	0.004	2	1.0
3.13j	$-CH_3$	$-CH_3$	2	3	1000	500	0.004	2	1.0
3.13k	$-CH_3$	$-CH_2CH_3$	2	3	1000	250	0.002	4	0.75
3.13l	$-CH_3$	$-(CH_2)_2CH_3$	2	3	500	125	0.002	4	0.75
3.13m	$-CH_3$	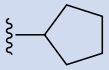	2	3	125	62.5	0.004	2	1.0
3.13n	$-CH_3$	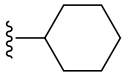	2	3	62.5	62.5	0.002	4	1.25
3.13o		$-CH(CH_3)_2$	2	3	125	31.25	0.004	2	0.75

[a]Comp: Compound; [b]Anal.: Analogue; [c]ND: Not determined as RIF MIC_{90} in combination was equal to individual RIF MIC_{90} and effect of analogues could not be observed; [d]NC: No change in RIF MIC_{90} in combination with analogue; [e]RIF MIC_{90} = 0.008 µM; [f]ND: Not possible to calculate as FIC of analogue could not be determined; *Data are representative of 3 replicate assays;.

VER analogues, **3.13a-d** were synthesized by varying the carbon chain length between the nitrogen atom and the two phenyl moieties. Among these analogues, **3.13a** and **3.13b** did not show any effect on the susceptibility of *Mtb* to RIF. On the other hand, analogues **3.13c** and **3.13d** reduced the RIF MIC_{90} by four-fold and exhibited an additive effect with RIF (FICI > 0.5).

5.4.2 Antimycobacterial activities of VER analogues 3.15a-l

The analogues **3.15a-l** (Table **5.2**) were synthesized by replacing the aminoethyl aromatic group of VER with various piperazinyl moieties. The positive control, VER, used in this batch reduced the RIF MIC_{90} by two-fold. The two-fold difference in potentiation of RIF by VER in comparison to section **5.4.1** (Table **5.1**) can be accounted for by the experimental conditions and the slow growing nature of *Mtb*. This variation in the antimycobacterial MIC_{90} of VER against the H37Rv laboratory strain of *Mtb* has been widely observed.

The piperazinyl analogues **3.15a-l** exhibited varying effects on the susceptibility of *Mtb* to RIF. While most piperazinyl analogues exhibited low potency (MIC_{90} > 50 μM) (Table **5.2**), derivatives, **3.15h** and **3.15j** were found to be the most potent analogues exhibiting MIC_{90} values of 62.5 and 125 μM respectively (Table **5.2**). The majority of the analogues reduced the RIF MIC_{90} by two-fold just like VER except **3.15a**, **3.15h** and **3.15j**, which did not show any effect on the susceptibility of *Mtb* to RIF (Table **5.2**). However, none of these analogues exhibited synergistic interactions with RIF. Among the analogues which reduced the RIF MIC_{90} by two-fold, **3.15b**, **3.15e**, and **3.13l** showed potentiating effects at concentrations of 62.5, 31.25 and 62.5 μM, respectively. These effects were two to four-fold lower than the concentration effect of VER required for a similar level of potentiation of RIF. Other analogues **3.15c**, **3.15d**, **3.15f**, **3.15g,** and **3.15k** exhibited potentiation at a concentration of 125 μM similar to VER (Table **5.2**). **3.15a-l** exhibited an additive effect when used in combination with RIF ($0.6 \leq FICI \leq 1.0$) (Table **5.2**)

*__Table 5.2:__ Antimycobacterial activity of verapamil analogues **3.15**.

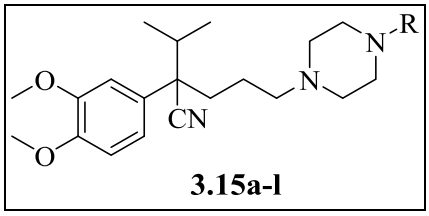

3.15a-l

Compound	R	MIC$_{90}$ (µM) H37Rv			Fold reduction in RIF MIC$_{90}$	FICI
		[a]Anal	Anal (in combination with RIF)	[b]RIF (in combination with Anal)		
VER		500	125	0.002	2	0.5
3.15a	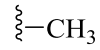	>1000	[c]ND	0.004	[d]NC	[e]ND
3.15b	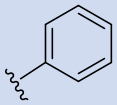	250	62.5	0.002	2	0.75
3.15c	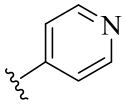	250	125	0.002	2	1.0
3.15d	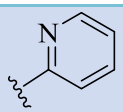	250	125	0.002	2	0.75
3.15e	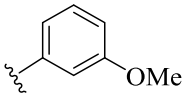	250	31.25	0.002	2	0.6
3.15f	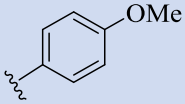	250	125	0.002	2	0.75
3.15g	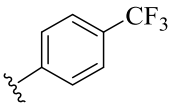	>1000	[c]ND	0.002	2	[e]ND
3.15h	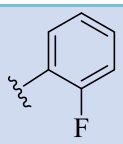	62.5	[c]ND	0.004	[d]NC	[e]ND
3.15i	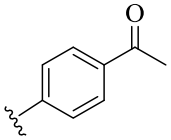	500	250	0.002	2	0.75
3.15j	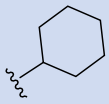	125	[c]ND	0.004	[d]NC	[e]ND

Compound	R	MIC$_{90}$ (µM) H37Rv			Fold reduction in RIF MIC$_{90}$	FICI
		[a]Anal	Anal (in combination with RIF)	[b]RIF (in combination with Anal)		
3.15k	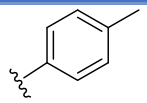	250	125	0.002	2	0.75
3.15l	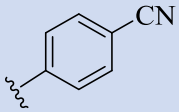	>1000	62.5	0.002	2	[e]ND

[a]Anal.: Analogue; [b]RIF MIC$_{90}$ = 0.004 µM: [c]ND: Not determined as RIF MIC$_{90}$ in combination was equal to individual RIF MIC$_{90}$ and effect of analogues could not be observed; [d]NC: No change in RIF MIC$_{90}$ in combination with analogue; [e]ND: Not determined as FIC of analogue could not be determined; *Data are representative of 3 replicate assays**.**

5.4.3 Antimycobacterial activities of VER analogues 3.17a-j

The favourable potentiating effect on RIF by the benzyl analogue, **3.13h** at a low concentration of 31.25 µM with a synergistic effect (FICI = 0.3) led to the synthesis of various VER analogues **3.17(a-j)** with various substituents on the benzyl group.

All the analogues showed poor antimycobacterial activity (MIC > 50 µM). Among these analogues, the 4-CH_3 substituted benzyl analogue, **3.17a** showed a 4-fold reduction in the RIF MIC$_{90}$ and exhibited synergistic interactions (FICI = 0.5) (Table **5.3**). However, substituted benzyl analogues 3-OCH_3 (**3.17d**), 4-OCF_3 (**3.17g**), 4-SCH_3 (**3.17h**) and 3-$COCH_3$ (**3.17j**) also displayed a two-fold reduction in the RIF MIC$_{90}$ but did not produce a synergistic interaction (Table **5.3**).

***Table 5.3:** Antimycobacterial activity of analogues **3.17a-j**.

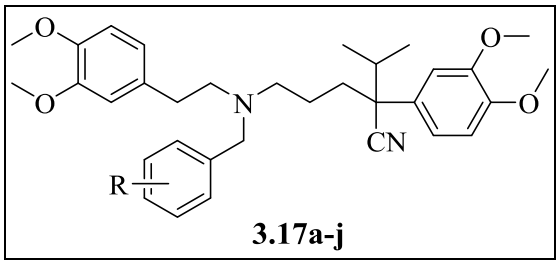

3.17a-j

Compound	R	MIC_{90} (µM)			Fold reduction in RIF MIC	FICI
		[a]Anal.	Anal (in comb with RIF)	[b]RIF(in comb with Anal)		
VER	[c]NA	500	125	0.001	4	0.5
3.13h	H	1000	31.25	0.001	4	0.3
3.17a	4-CH_3	500	125	0.001	4	0.5
3.17b	4-Cl	>1000	[d]ND	0.004	[e]NC	[f]ND
3.17c	2-CN	>1000	[d]ND	0.004	[e]NC	[f]ND
3.17d	3-OCH_3	>1000	62.5	0.002	2	[f]ND
3.17e	3-CF_3	>1000	[d]ND	0.004	[e]NC	[f]ND
3.17f	2-OCF_3	>1000	[d]ND	0.004	[e]NC	[f]ND
3.17g	4-OCF_3	500	250	0.002	2	1.0
3.17h	4-SCH_3	>1000	31.25	0.002	2	[f]ND
3.17i	4-CN	>1000	[d]ND	0.004	[e]NC	[f]ND
3.17j	3-$COCH_3$	>1000	62.5	0.002	2	[f]ND

[a]Anal.: Analogue; Comb: Combination; [b]RIF MIC_{90} = 0.004 µM; [c]NA: Not applicable; [d]NC: Not determined as RIF MIC_{90} in combination was equal to individual RIF MIC_{90} and effect of analogues could not be observed; [d]NC: No change in RIF MIC_{90}; [f]ND: Not determined as FIC of analogue could not be determined; *Data are representative of 3 replicate assays**.**

5.4.4 Structure activity relationship studies of VER analogues (3.13a-o, 3.15a-l and 3.17a-j)

A conclusive SAR cannot be deduced from the various antimycobacterial evaluations due to limited structural explorations. However, localised SAR studies can be interpreted. The lipophilic aromatic substituents on the basic nitrogen did not affect the potentiating effect of

VER on RIF while aliphatic substituents led to loss in potentiating properties. This observation was further supported by *in vitro* combination results of benzyl containing analogues **3.17**. Further structure activity relationships among various substituents on the benzyl group (**3.17a-j**), cannot be delineated as data on more analogues is needed for in-depth analysis.

Aliphatic substituents at the stereogenic centre (**3.13i-n**) were more tolerated than on the basic nitrogen (**3.13e-h** and **3.13o**). This was evidenced by the fact that all analogues with various aliphatic substituents at this position showed results comparable to VER with respect to potentiation of RIF against *Mtb* (Table **5.1**). In addition, variation in chain length between the stereogenic centre (**3.13c** and **3.13d**) and the nitrogen atom did not reduce the ability of analogues to increase the susceptibility of *Mtb* to RIF, while a change in chain length between the dimethoxy phenyl group (**3.13a-c**) and nitrogen led to complete loss of potentiating properties.

5.4.5 Combination evaluation of selected VER analogues (3.13h, 3.13k, 3.13l, and 3.15c) with bedaquiline and moxifloxacin

As discussed in section **5.4.1**, analogues **3.13h**, **3.13k**, **3.13l**, and **3.15c** increased the susceptibility of *Mtb* to RIF comparable to VER (Tables **5.1** and **5.2**).[9] These analogues were shortlisted for further investigation in combination with newer anti-TB drugs (BDQ and MOX). The analogues were evaluated *in vitro* against the H37Rv strain of *Mtb* individually and in combination with bedaquiline (BDQ) and moxifloxacin (MOX) using the checkerboard assay. The reported *in vitro* MIC_{90} values of BDQ and MOX against the H37Rv strain of *Mtb* are 1.12 and 0.56 μM, respectively (Table **5.4**).[10,11] Both VER and *Nor*-VER reduced the MIC_{90} of BDQ and MOX significantly (4-8 fold) but did not produce synergistic interactions (FICI > 0.5) (Table **5.4**). However, VER analogues increased the susceptibility of H37Rv to BDQ and MOX and exhibited synergistic interactions (Table **5.4**).

A varying effect on potentiation of BDQ and MOX by analogues was observed. A maximum of 16- and 32-fold reduction in the BDQ MIC_{90} was observed with **3.13h** and **3.13l**, respectively, along with synergistic interactions (FICI < 0.4) (Table **5.4**). However, only a maximum of an 8-fold reduction in the MIC_{90} of MOX could be achieved by **3.13k** and **3.13l** along with synergistic interactions (FICI = 0.49) (Table **5.4**).

*__Table 5.4:__ Antimycobacterial activity of VER analogues in combination with BDQ and MOX

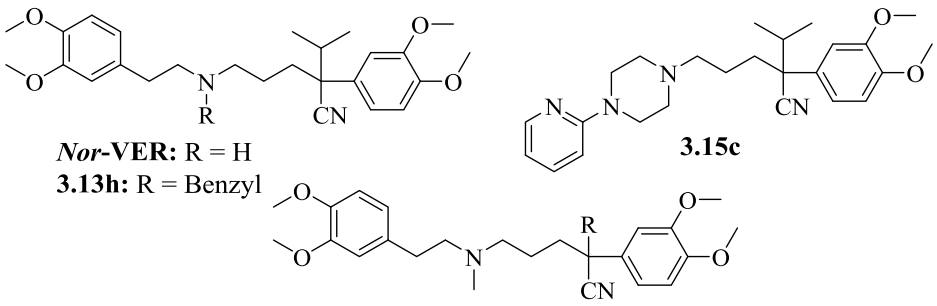

***Nor*-VER:** R = H
3.13h: R = Benzyl

3.15c

VER: R = $CH(CH_3)_2$
3.13k: R = CH_2CH_3
3.13l: R = $CH_2CH_2CH_3$

[a]Anal	[b]MIC_{90} (μM)	[c]BDQ			[d]MOX		
		MIC_{90} (μM) in combination with Anal	Fold reduction in MIC_{90}	FICI	MIC_{90} (μM) in combination with Anal	Fold reduction in MIC_{90}	FICI
VER	500	0.14	8	0.25	0.14	4	1.0
***Nor*-VER**	500	0.28	4	0.38	0.07	8	0.75
3.13h	1000	0.07	16	0.38	0.14	2	1.0
3.13k	1000	0.14	8	0.25	0.035	8	0.49
3.13l	500	0.035	32	0.25	0.035	8	0.49
3.15c	500	0.28	4	0.38	0.14	2	0.75

[a]Anal : Analogue; [b]MIC_{90} of analogues against H37Rv strain of *Mtb*; [c]BDQ MIC_{90} = 1.12 μM, [d]MOX MIC_{90} = 0.56 μM; *Data is representative of 3 replicate assays.

5.4.6 Selection of non-cytotoxic VER analogues

VER analogues, which demonstrated comparable activity to VER with respect to increasing the susceptibility of *Mtb* to various drugs, and showing synergistic interaction with RIF, were evaluated for their cytotoxicity against THP-1 monocyte cell lines. All the selected analogues displayed higher cytotoxicity than VER (IC_{20} = 125 μM) except **3.13h** and **3.17a** ($IC_{20} \geq 250$ μM) (Table **5.5**). Additionally, the IC_{20} values of these analogues were two-fold higher than their concentration required for the four-fold potentiation of RIF *in vitro* (Table **5.5**). On this basis, these compounds were selected for further cytotoxicity evaluation in combination with RIF and BDQ against THP-1 cell lines. VER and *Nor*-VER were used as the controls. RIF and BDQ were selected on the basis of their superior interaction with VER analogues (Table **5.1** and **5.4**). Among the two potential analogues, **3.13h** was found to be less cytotoxic ($IC_{20} \leq 250$ μM) in combination with RIF and BDQ as compared to VER (IC_{20} = 125 μM) (Table

5.5). Analogue **3.13h** was two-fold less cytotoxic in combination with RIF than VER with RIF, and four-fold less cytotoxic in combination with BDQ than VER with BDQ (Table **5.5**).

*__Table 5.5:__ *Ex vivo* combinatorial cytotoxicity of selected VER analogues (**3.13h**, **3.13k**, **3.13l**, **3.15c**, and **3.17a**)

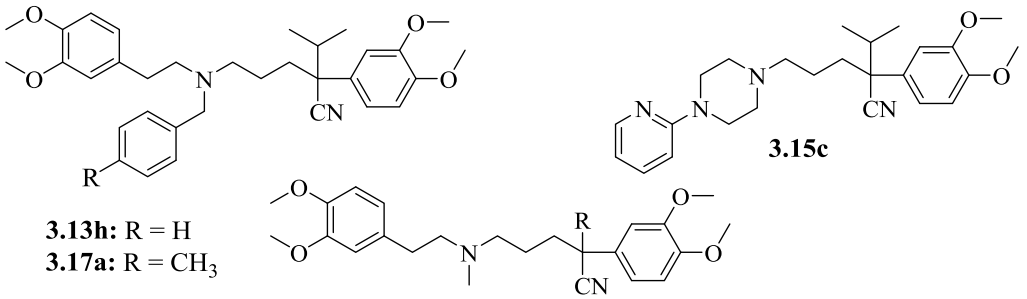

3.13h: R = H
3.17a: R = CH_3

3.15c

VER: R = $CH(CH_3)_2$
3.13k: R = CH_2CH_3
3.13l: R = $CH_2CH_2CH_3$

[a]Anal	IC_{20} (µM)	IC_{20} (µM) in combination with RIF	IC_{20} (µM) in combination with BDQ
VER	125	125	<62.5
***Nor*-VER**	<62.5	<62.5	<62.5
3.13h	250	<250	500
3.13k	<62.5	ND	ND
3.13l	<62.5	ND	ND
3.15c	<62.5	ND	ND
3.17a	500	500	ND

[a]Anal: Analogue; BDQ IC_{20} = 56.2 µM; RIF IC_{20} = 0.4 µM; *Data are representative of 2 replicate assays.

5.4.7 Intracellular evaluation of VER analogues in macrophages: A comparative study

As explained in chapter **2**, VER has attractive prospects for repurposing and repositioning as an EPI. In this section, a comparative study of selected VER analogues with VER is presented, with respect to intracellular potency against *Mtb*, interaction with *Mtb*-specific T-cells, EP inhibition and potentiating effects on INH as well as RIF against intracellular *Mtb* in macrophages.

The aim of this study was to identify new VER analogues, which are devoid of various undesirable effects such as cytotoxicity and interaction with *Mtb*-specific T-cells. A screening cascade **2**, described in section **5.3.2** was adopted for these studies.

5.4.7.1 *Ex vivo* cytotoxicity and intracellular inhibition

As described in chapter **2**, EP-induction is one of the major defence mechanisms adopted by *Mtb* after macrophage residence. Therefore, a moderate inhibition of *Mtb* in macrophages by EPIs has been reported and was also observed for VER (**Figure 5.4**).[12] Thus, all VER analogues described in section **5.4.5**, and **3.13n** were investigated for their intracellular potency against BCG after cytotoxicity screening against THP-1 cell lines. VER showed concentration dependent inhibition of BCG and *Mtb* in macrophages.

Among the analogues tested against BCG in macrophages, only **3.13h**, **3.13l**, and **3.13n** showed comparable inhibition to VER (Table **5.6**) at equivalent concentrations below their IC_{20} values. The analogue **3.13n** showed the best profile with moderate inhibition at 2.5 μM. Potent analogues **3.13h**, **3.13l** and **3.13n** were further tested for potency against intracellular *Mtb* at a concentration of 2.5 μM. Retention in activity was observed with **3.13n**, which showed the highest inhibition (**Figure 5.4**). The analogues were further evaluated for their effect on expansion of *Mtb*-specific T-cells along with VER. VER and **3.13l** significantly inhibited the proliferation of *Mtb* specific T-cells (**Figure 5.4**), while **3.13h** and **3.13n** did not exhibit any effect on *Mtb* specific T-cells at a concentration of 2.5 μM (**Figure 5.4**).

Table 5.6: *Ex vivo* cytotoxicity and intracellular antimycobacterial assessment of selected VER analogues

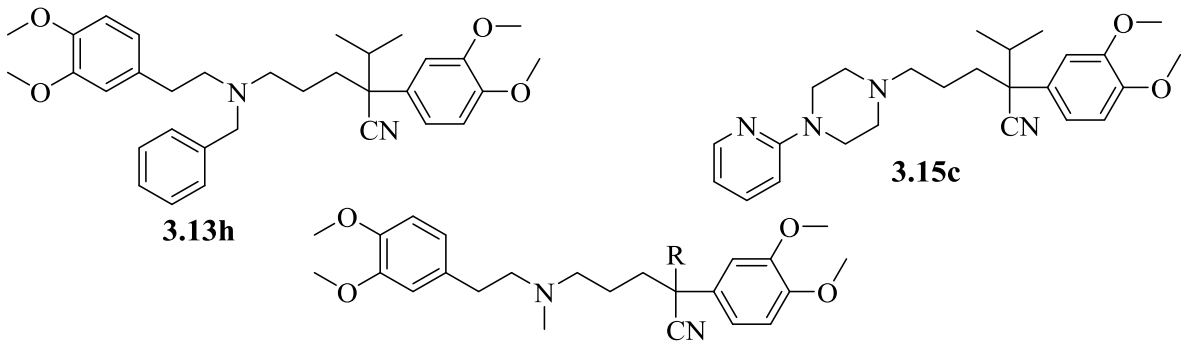

VER: R = $CH(CH_3)_2$
3.13k: R = CH_2CH_3
3.13l: R = $CH_2CH_2CH_3$
3.13n: R = C_6H_{13}

Analogues	IC_{20}(μM) THP-1	Maximum % Inhibition*
VER	>100	50
3.13h	>90	40
3.13k	>20	25
3.13l	>25	35
3.13n	<5	30
3.15c	>30	0

*Maximum intracellular growth inhibition of BCG in macrophages at concentration lower than IC_{20}

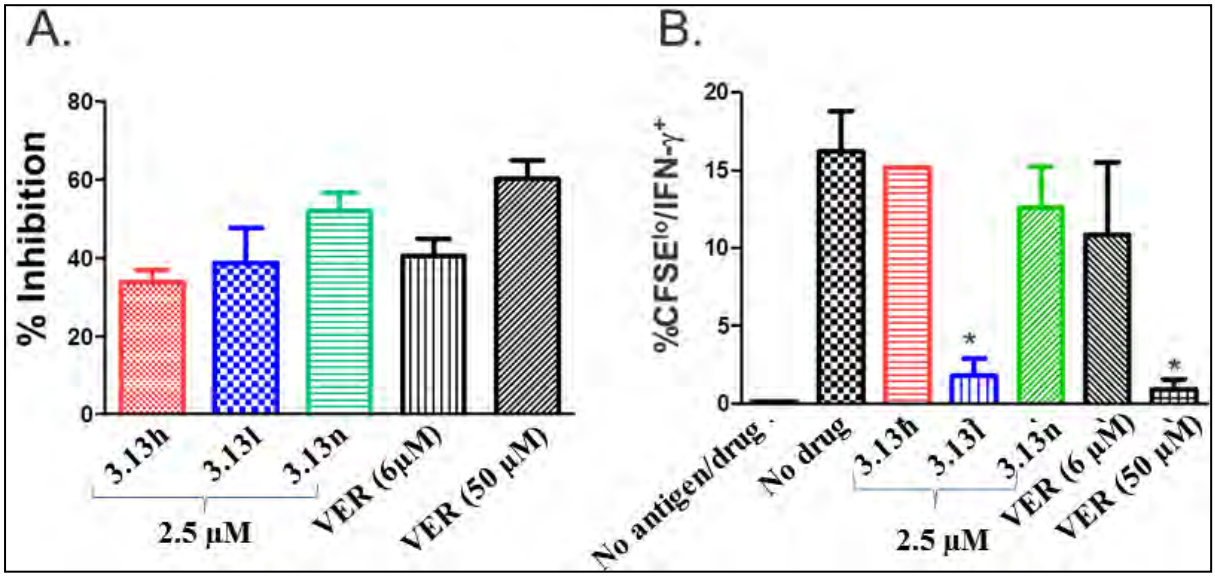

Figure 5.4: (A) Antimycobacterial activity of VER analogues on intracellular *Mtb* in macrophages at concentration of 2.5 μM along with VER at 6 and 50 μM; (B) Effect of VER analogues on proliferation of *Mtb*-specific T-cells in CFSE-labelled assay at 2.5 μM along with VER at 6 and 50 μM.

5.4.7.2 EP inhibition of VER analogues 3.13n and 3.131h

The EP inhibitory activity of VER analogues, **3.13h** and **3.13n**, was investigated in a modified EB-stained BCG assay. *Mtb* is known to extrude EB using EPs thereby reducing its intracellular concentration, which is monitored by a fluorescence activity measurement. EPIs are expected to increase the intracellular concentration thereby maintaining the fluorescence intensity.

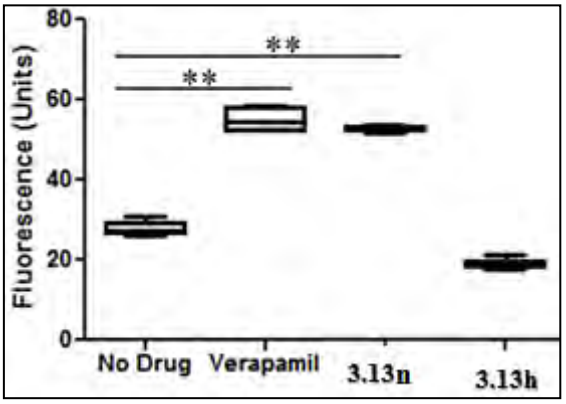

Figure 5.5: EP inhibitory indication by EB assay, inhibition of EB efflux leading to an increase in fluorescence intensity: (a) **3.13n** inhibited the efflux of EB at 40 μM comparable to VER at 100 μM; (b) **3.13h** failed to show any significant effect upto a concentration of 100 μM.

Compound **3.13n** at a concentration of 40 μM exhibited comparable fluorescence intensity to VER at 100 μM (**Figure 5.5**). This suggested that the EP inhibition may be a key mechanism of potentiation of RIF and INH in *Mtb* infected macrophages. On the other hand, compound **3.13h** did not exhibit any effect on the efflux of EB even upto a concentration of 100 μM, indicating the possibility that this analogue could be exerting its potentiation effect *via* a different mechanism.

5.4.7.3 Combination evaluation of 3.13n with INH and RIF against *Mtb* in macrophages

The frontrunner analogue **3.13n**, with the desired properties of low cytotoxicity, high potency against intracellular *Mtb* and absence of interaction with *Mtb*-specific T-cells was evaluated against *Mtb* in macrophages in combination with sub-inhibitory concentrations of INH and RIF. A concentration of 2.5 μM enhanced the potency of sub-inhibitory concentrations of INH and RIF against *Mtb* in macrophages (**Figure 5.6**).

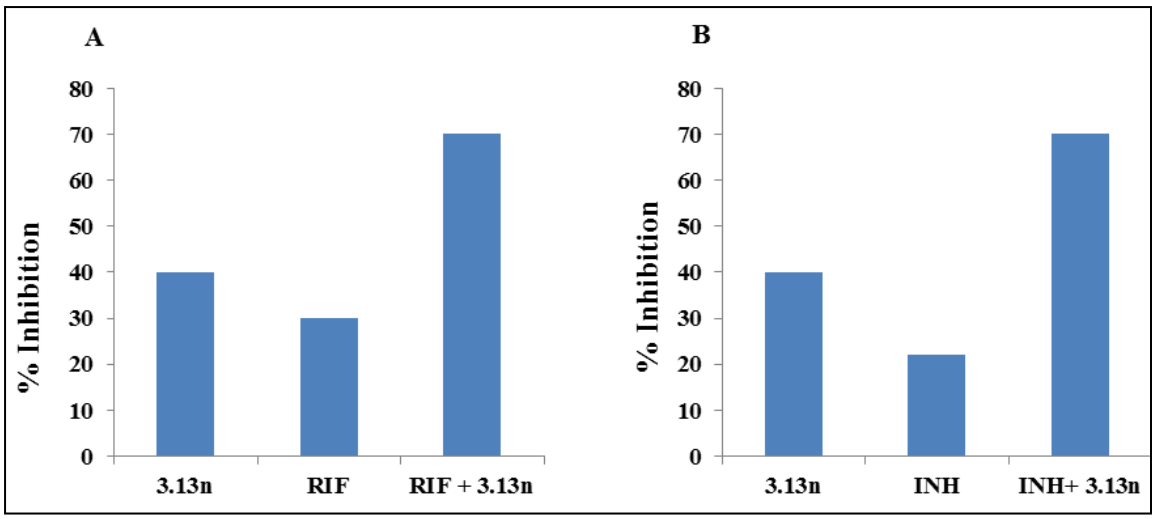

Figure 5.6: Intracellular potentiation of RIF and INH. (A) Potentiation of sub-inhibitory concentration of RIF by **3.13n** at a concentration of 2.5 µM; (B) Potentiation of sub-inhibitory concentration of INH by **3.13n** at a concentration of 2.5 µM.

5.4.8 Antimycobacterial evaluation of rigid VER analogues

Two synthesized rigid VER analogues (Chapter **3**) were tested *via* cascade 1 and cascade 2.

As expected, both analogues (**EDP42** and **MKVR1**) showed low antimycobacterial activity ($MIC_{90} \geq 250$ µM) (Table **5.7**). A four-fold reduction in the RIF MIC_{90} was observed with **MKVR1** and was comparable to VER, while **EDP42** increased the susceptibility of *Mtb* to RIF by two-fold. A high concentration of 500 µM was required for four-fold potentiation of RIF by **MKVR1**.

EDP42 was also found to have low cytotoxicity individually (IC_{20} = 500 µM) and in combination with RIF (IC_{20} = 125 µM) which is comparable to VER (Table **5.7**). The EB assay indicated that **EDP42** reduced the susceptibility of EB to EPs, leading to an increase in the fluorescence intensity, which was comparable to **3.13n** (**Figure 5.7**). However, negligible fluorescence intensity in the presence of **MKVR1** indicated that the analogue was devoid of any effect on EB susceptibility to EPs.

*__Table 5.7:__ Combination results of rigid VER analogues **EDP42** and **MKVR1**

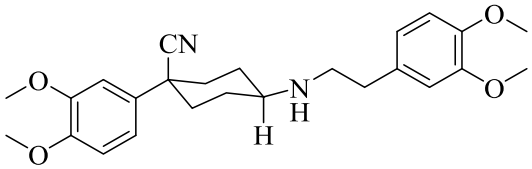

MKVR1

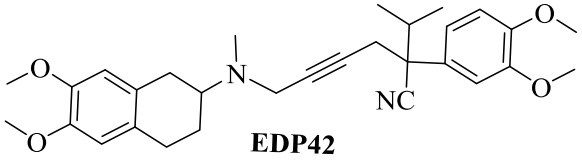

EDP42

[a]Anal	MIC_{90} (µM) H37Rv			Fold-reduction in RIF MIC_{90}	FICI	IC_{20} (µM) THP-1 cell lines	
	Anal	Anal in comb with RIF	[b]RIF in comb with Anal			Anal	Anal in comb with RIF
VER	500	125	0.001	4	0.5	125	125
MKVR1	1000	500	0.001	4	0.8	[c]ND	[c]ND
EDP42	250	125	0.002	2	0.6	500	125

[a]Anal: Analogue; [b]RIF MIC_{90} = 0.004; Comb: Combination; [c]ND: A very high concentration of analogue is required for reduction in RIF MIC_{90}, therefore not evaluated further; *Data are representative of 3 biological replicates.

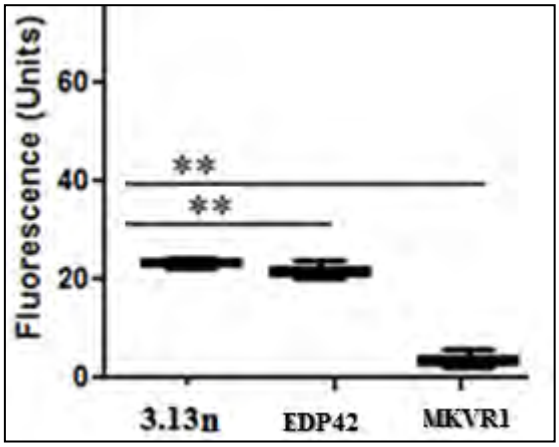

Figure 5.7: EP inhibition indication of **MKVR1** and **EDP42** with **3.13n** at 20 µM in EB assay. **EDP42** significantly limited the efflux of EB while **MKVR1** did not exhibit any effect.

A previous report on **EDP42** indicating its negligible calcium channel antagonism,[13] and superior *in vitro* potentiation to **MKVR1** at a low concentration prompted further testing in combination with sub-inhibitory concentrations of INH and RIF against intracellular *Mtb* in macrophages. However, no significant effect on the potency of sub-inhibitory concentrations of RIF and INH was observed in the presence of **EDP42** up to a maximum tested concentration of 40 µM (**Figure 5.8**)

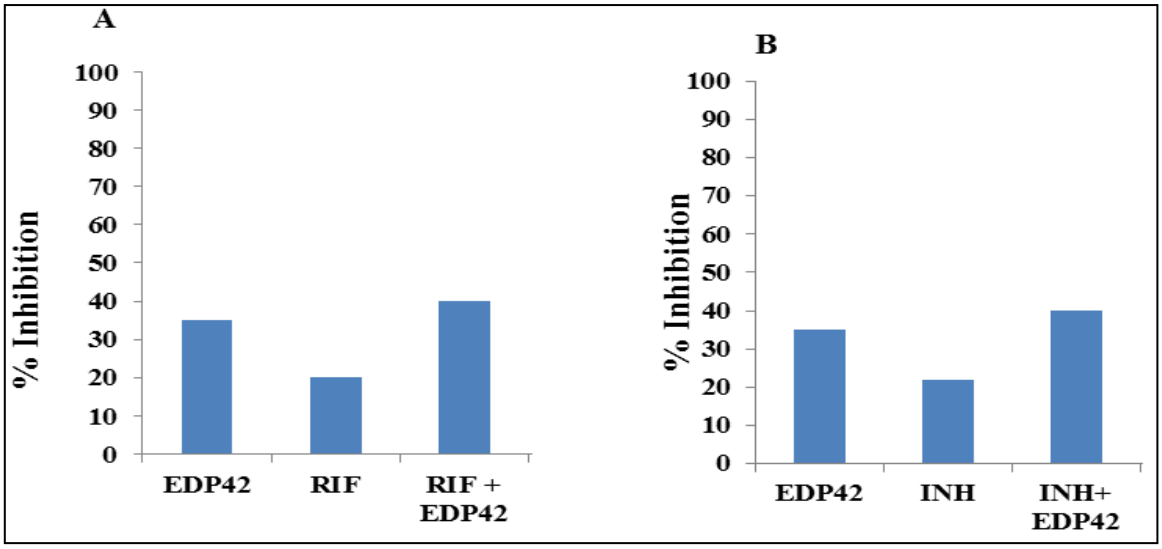

Figure 5.8: Potentiation of RIF and INH by **EDP42**. (A) Potentiation of sub-inhibitory concentration of RIF by **EDP42**; (B) Potentiation of sub-inhibitory concentration of INH by **EDP42**.

5.4.9 Discussion

A total of 40 VER analogues (**3.13**, **3.15** and **3.17**) were designed, synthesized and evaluated *in vitro* and (selectively) *ex vivo* for their potential to inhibit EPs as well as potentiating effect on various anti-TB drugs (Table **5.1-5.7**). The promising analogues were also investigated for their effect on proliferation of *Mtb*-specific T-cells (Table **5.6** and **Figure 5.4**).

Antimycobacterial evaluation of the analogues in combination with RIF revealed 27 analogues with the potential to increase the susceptibility of *Mtb* to RIF. Among these analogues, 17 analogues showed a reduction in the RIF MIC_{90} comparable or superior to VER. Out of these analogues 10 exhibited potentiating effects at lower concentrations than the required concentration of VER for equivalent reduction in the RIF MIC_{90} (Table **5.1-5.3**).

Additionally, two analogues **3.13h** and **3.17a** also exhibited a synergistic interaction with RIF, and **3.13h** showed superior synergistic interactions (FICI = 0.3) compared to VER (FICI = 0.5) (Table **5.1**). Selected analogues also showed potentiation of MOX and BDQ in combination and a 32-fold reduction in the BDQ MIC_{90} was achieved (Table **5.4**).

Ex vivo cytotoxicity evaluation (THP-1 cell lines) revealed two VER analogues (**3.13h** and **3.17a)** with lower cytotoxicity than VER. The benzyl analogues **3.13h** displayed lower cytotoxicity compared to VER and *Nor*-VER both individually and in combination with RIF and BDQ (Table **5.5**).

The macrophage evaluation of analogues exhibiting low cytotoxicity against THP-1 cell lines revealed three analogues, which showed potency against intracellular *Mtb* comparable to VER (Table **5.6**). Among these analogues, two did not show any effect on *Mtb*-specific immunity. However, only one analogue potentiated the sub-inhibitory concentration of RIF and INH in macrophages when used in combination (Figure **5.4**).

The rigid VER analogues reported to be devoid of calcium channel blocking antagonism did not show promising results against TB compared to indications in cancer. A potentiation of two- and four-fold was not accompanied by the synergistic interaction (Table **5.7**). The rigid VER analogues also failed to show any potentiation activity on RIF and INH against intracellular *Mtb* in macrophages (Figure **5.8**). These observations may be indicative of the involvement of various EPs for efflux of anti-TB drugs which may be different from the ones responsible for the reduction of intracellular concentrations of anti-cancer agents.

5.4.10 Conclusion

The various biological results suggest that the strategy of structural modification of verapamil has the potential to deliver an EPI with an improved pharmacological profile. The identification of VER analogues **3.13h**, **3.13k**, **3.13l**, and **3.13n** (Table **5.1**) with potentiating effects on RIF, BDQ, and MOX *in vitro*, including antimycobacterial potency in macrophages, and lower interaction with *Mtb*-specific T-cells compared to VER demonstrated the viability of the approach. Furthermore, potentiation of sub-inhibitory concentrations of RIF and INH in macrophages as well as inhibition of EB efflux in the EB assay by analogue **3.13n** confirms the efflux pump inhibition activity.[14] The increase in susceptibility of *Mtb* towards the new drugs, BDQ and MOX, in the presence of analogues (**3.13h**, **3.13k**, **3.13l**, and **3.13n**, Table **5.1**) demonstrate the possibility of developing adjunctive agents which can aid in overcoming the emergence of resistance against newly developed antimycobacterial agents. However, further studies are required on compound **3.13n** to generate analogues with potential to advance further in the drug development process. In addition, screening against EP over expressing strains, and in macrophages infected with RIF and INH resistant strains of *Mtb* can add more precise indications of EP inhibitory activity of potential analogues.[14] Furthermore, the metabolic stability and evaluation of calcium channel antagonism in a calcium channel assay may further add value to the pharmacological profile of these analogues.

5.5 Reversed isoniazid anti-TB agents

In this section, a summary of various biological activities of reversed isoniazid anti-TB agents against various strains of *Mtb* is presented. All *in vitro* antimycobacterial assays were performed at Stellenbosch University in the laboratory of Prof. P. Van Helden. Evaluation against intracellular *Mtb* in macrophages was conducted at SLU in the laboratory of Dr. Getahun Abate.

Antimycobacterial activity of reversed isoniazid (RINH) anti-TB agents was evaluated against drug sensitive (H37Rv) and various drug resistant strains of *Mtb* (Table **5.8**) using the BACTEC 460 system.[4] The primary screening was performed against the drug sensitive strain of *Mtb* (H37Rv). Potent compounds ($MIC_{99} \leq 10$ μM) were evaluated for cytotoxicity against the THP-1 cell line. Compounds exhibiting high selectivity indices ($SI \geq 10$) were selected for testing against various low to high level isoniazid mono-resistant strains of *Mtb* and various clinical isolates to investigate reversal of resistance and the possibility of cross-resistance.

Short listed RINH agents were further tested for intracellular *Mtb* inhibition in macrophages and EP inhibitory activity in the EB assay.

5.5.1 Classification, genotyping and susceptibility status of clinical isolates

Three isoniazid mono-resistant strains (R5401, R72, and R4965) and four XDR clinical isolates (TT135, X_3, X_60 and X_61) were used to investigate the potency and cross resistance of RINH agents (Table **5.8**). Isoniazid was used as a positive control.

Any clinical isolate that is resistant to 0.73 μM but sensitive to 2.92 μM of INH is regarded as a low level INH resistant strain (e.g. R5401), but resistance at $MIC_{99} \geq 2.91$ μM of INH is regarded as high level INH resistance as in strains R72 and R4965. These isolates have the following mutations: R72 (*inhA* promoter and *katG*); R4965 (*katG*); and R5401 (*inhA* promoter). These mutations are responsible for low to high levels of INH resistance. Controls used include INH (2.92 and 0.73 μM), rifampicin, and solvent (DMSO). These strains were susceptible towards rifampicin at a concentration of 0.0012 μM, which is an indication of the isoniazid mono-resistance nature of these isolates.

The classification, genotyping and susceptibility status of the various XDR clinical isolates used to investigate the potency of RINH agents are summarised in table **5.8**.

Table 5.8: *Mtb* clinical isolates classification, genotyping and susceptibility status:

Clinical isolate	Genotype	Resistance profile	Susceptibility status
TT135	Atypical Beijing	H;R;ET;S;A;C;O;M;	XDR
X_3	Beijing	H;R;E;K;S;C;O;	XDR
X_60	Beijing	H;R;E;A;ET;O;S;C;K	XDR
X_61	Beijing	H;R;ET;A;O;K;S;	XDR

H: isoniazid; R: rifampicin; E: ethionamide; ET: ethambutol; S: streptomycin; A: amikacin; C: capreomycin; O: ofloxacin; M: moxifloxacin.

5.5.2 Antimycobacterial activity of RINH agents

Based on the sequence mentioned in section **5.5**, all the synthesized RINH agents (Chapter **4**) were first tested against a drug sensitive strain of *Mtb* (H37Rv), followed by cytotoxicity evaluation against THP-1 or CHO cell lines.

All the RINH agents were found to be active against the H37Rv strain of *Mtb* (MIC_{99} < 10 µM) except **4.36** (MIC_{99} > 10 µM) (Table **5.9**). Among the active compounds **4.3a**, **4.3b**, **4.3c**, **4.17b** and **4.23b** were found to be the most potent ($MIC_{99} \leq 1$ µM).

All potent RINH compounds showed low cytotoxicity ($IC_{50} \geq 10$ µM) against tested cell lines (THP-1 or CHO) except **4.3b** and **4.10b** ($IC_{50} \leq 5$ µM) (Table **5.9**). The compounds exhibiting a high selectivity index (SI ≥ 10) were further subjected to testing against *Mtb* strains having low to high levels of INH mono-resistance as mentioned in section **5.5.1**.

All the selected compounds were found to be inactive up to the highest tested concentration (10 µM) against the high level INH-resistant strains (R72 and R4965) while compounds **4.23a**, **4.23b**, **4.23c**, **4.46**, **4.49** and **4.53**, exhibited some potency (MIC_{99} < 10 µM) against a low level isoniazid resistant strain (R5401) (Table **5.9**). All these compounds were further

evaluated against various clinical isolates (Table **5.8**). Most of these RINH agents were found to be inactive against clinical isolates TT135 and X_3 (MIC > 10 μM), while some potency was observed against X_61 and X_60 (MIC < 10 μM) (Table **5.9**). All the tested compounds showed potency against strain X_61 (MIC_{99} < 10 μM) except **4.17b** (MIC_{99} > 10 μM), while only one compound, **4.49** was found to be active against the X_60 strain (MIC_{99} < 10 μM) (Table **5.9**).

Reversed anti-TB agents **4.28a** and **4.28b**, synthesized by replacing the isoniazid moiety with benzhydrazide, did not display any activity up to the highest tested concentration of 10 μM. (Table **5.9**). The low antimycobacterial activity of compounds **4.28a** and **4.28b** (MIC > 10 μM) as compared to RINH agents **4.3a** and **4.3b** (MIC ≤ 1 μM) highlighted the importance of the nitrogen in the pyridyl moiety of the latter for potency against *Mtb*.

5.5.3 Structure activity relationship

Generally, it was observed that the 2-chloro-substituted phenothiazine-based RINH agents (**4.17b** and **4.23b**, Table **5.9**) exhibited superior antimycobacterial activity relative to unsubstituted phenothiazine-based counterparts with the exception of **4.3b** and **4.10b** (Table **5.9**). The compound **4.10b** and its unsubstituted counterpart **4.10a** were equipotent while **4.3b** was found to be less potent than the corresponding unsubstituted RINH agent **4.3a** (Table **5.9**). The nitrogen atom in the pyridyl moiety of RINH agents is important for antimycobacterial activity and a drastic loss in antimycobacterial activity was observed with its absence in **4.28 (a** and **b)** (Table **5.9**).

The importance of a sulphur atom of the phenothiazine nucleus in compounds **4.3a** and **4.3b** (Table **5.9**) for antimycobacterial potency was also demonstrated by replacing it with a two carbon alkyl moiety in **4.3c** (Table **5.9**), which causes a four-fold reduction in potency against *Mtb* (H37Rv).

The antimycobacterial results of **4.3**, **4.10**, and **4.17** revealed that addition of a piperidine moiety to the 2-chlorophenothiazine RINH agent **4.3b**, did not affect the antimycobacterial activity while incorporation of aminopropyl moiety reduced the potency against the H37Rv strain of *Mtb* (MIC_{99} changed from 1.0 to 5.0 μM, Table **5.9**). The incorporation of both of these moieties reduced the *Mtb* potency of phenothiazine compound **4.3a** (MIC_{99} changed

from 0.625 to 5.0 μM, Table **5.9**). However, an increase in potency against resistant strains (R5401 and X_61) was observed (MIC ≤ 10 μM) with the introduction of the piperidine moiety in **4.3a**.

Furthermore, the removal of a nitrogen atom from the phenothiazine nucleus of **4.17** and introduction of a ylidine bond (**4.23a** and **4.23b**) increased the antimycobacterial potency against the drug sensitive and resistant strains. However, varying effects were observed against the INH mono-resistant strain. No change in the MIC_{99} value was observed with unsubstituted phenothiazine-based RINH agent **4.23a** while increase in potency of the 2-chlorosubstituted phenothiazine containing compound **4.23b** was observed (MIC_{99} changed from 1.0 μM to 0.625 μM, Table **5.9**)

Most of the synthesized tricyclic (**4.23c**, **4.27** and **4.49**) as well bicyclic (**4.46** and **4.53**) EPI containing RINH agents also showed good potency (MIC_{99} ≤ 5 μM, Table **5.9**) against the H37Rv strain of *Mtb*. Most of these compounds exhibited good to moderate potency against the R5401 strain of *Mtb* except **4.27** and DHP-based compound **4.36**, which were inactive up to the highest tested concentration (10 μM). Among the potent compounds, bicyclic (**4.46** and **4.53**) and non-fused tricyclic **4.49** moiety containing RINH agents were the most potent.

In general, both tricyclic-(phenothiazine and non-phenothiazine-based) and bicyclic-based EPI containing RINH agents showed good to moderate potency against sensitive (H37Rv) and INH mono-resistant strains of *Mtb*. In addition, the piperidine group bonded *via* N-C and ylidine bonds to phenothiazine nucleus enhanced the activity of the phenothiazine-based RINH agents against the R5401 strain of *Mtb* and retained potency against the H37Rv strain. A minor reduction in activity of unsubstituted phenothiazine-based RINH agents was observed.

Table 5.9: Antimycobacterial activity results of RINH agents and RATAs.

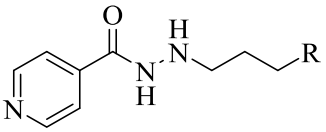

4.3-4.53

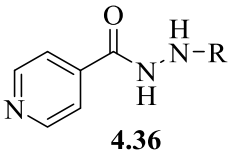

4.36

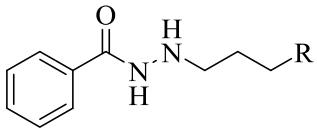

4.28

Compounds	R	MIC$_{99}$ (µM)				IC$_{50}$ (µM)	
		H37Rv	R5401	X_61	X_60	CHO Cell lines	THP-1 Cell lines
INH		0.25	>0.73 <2.91	<10	>10	>100	127
VER + INH (1:1)		5.0	<0.625	<5.0	>10	27.4	42
4.3a	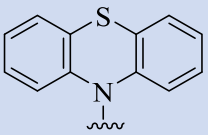	0.25	>10	[a]ND	[a]ND	[b]ND	27
4.3b	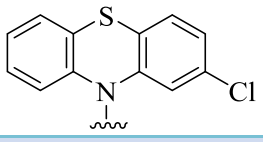	1.0	>10	[a]ND	[a]ND	[b]ND	2.4
4.3c	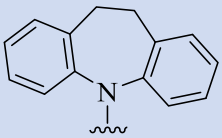	1.0	>10	[a]ND	[a]ND	[b]ND	32.0
4.10a	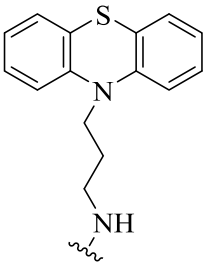	5.0	>10	[a]ND	[a]ND	[b]ND	111.2
4.10b		5.0	>10	[a]ND	[a]ND	[b]ND	5

Compounds	R	MIC_{99} (µM)				IC_{50} (µM)	
		H37Rv	R5401	X_61	X_60	CHO Cell lines	THP-1 Cell lines
4.17a	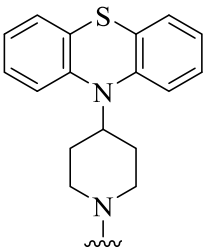	5.0	2.5	<5	>10	122	109
4.17b	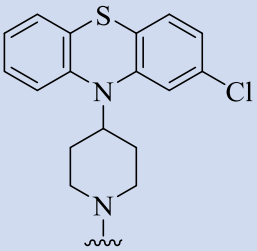	1.0	1.0	>10	>10	37.4	29
4.23a	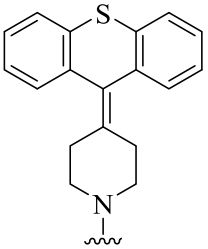	1.25	2.5	<10	>10	152	[c]ND
4.23b	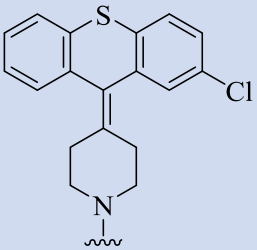	0.625	0.625	<10	>10	296	[c]ND
4.23c	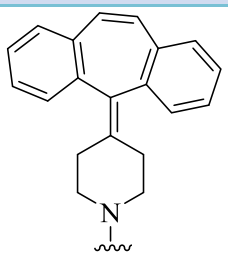	1.25	2.5	<10	>10	148	[c]ND
4.27	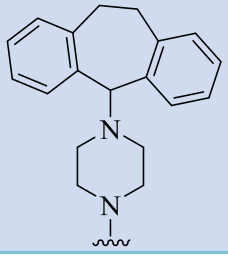	5.0	>10	[a]ND	[a]ND	[b]ND	84

Compounds	R	MIC$_{99}$ (µM)				IC$_{50}$ (µM)	
		H37Rv	R5401	X_61	X_60	CHO Cell lines	THP-1 Cell lines
4.46	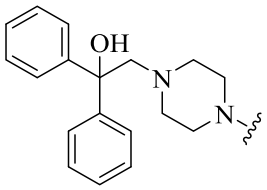	1.25	1.25	<10	>10	>174	[c]ND
4.49	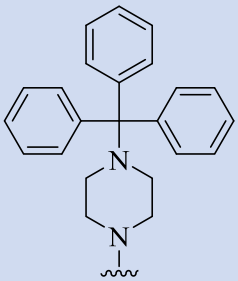	1.25	1.25	<10	<10	97.6	[c]ND
4.53	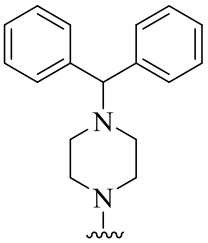	5.0	2.5	<10	>10	48.1	173
4.36	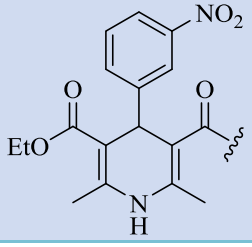	>10	[d]ND	[d]ND	[d]ND	[d]ND	[d]ND
4.28a	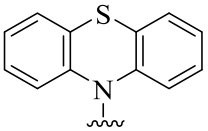	>10	[d]ND	[d]ND	[d]ND	[d]ND	[d]ND
4.28b	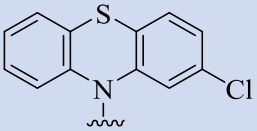	>10	[d]ND	[d]ND	[d]ND	[d]ND	[d]ND

[a]ND: Not determined as MIC$_{99}$ > 10 µM against R5401 strain of *Mtb*; [b]ND: Not determined as cytotoxicity has been evaluated against THP-1 cell lines; [c]ND - Not determined as cytotoxicity has been evaluated against CHO cell lines; [d]ND: Not determined as MIC$_{99}$ > 10 µM against H37Rv strain of *Mtb*.

5.5.4 *In vitro* activities of equimolar mixtures

A selected number of equimolar mixtures (1:1) of INH and chemosensitizer/EPI moiety were also tested *in vitro* (Table **5.10**). This was done in order to investigate whether or not covalently linking an EPI/EPI moiety to an anti-TB drug was advantageous over administration of the combination in equimolar amounts. A sequence of testing similar to that employed for RINH agents was used. Firstly, evaluation was performed against the drug sensitive H37Rv strain of *Mtb* followed by INH mono-resistant strains and lastly clinical isolates. A combination of VER and INH in equimolar amounts was also used to investigate the effect of VER on the *in vitro* susceptibility of various *Mtb* strains towards INH.

All the equimolar (1:1) mixtures of isoniazid and EPI/EPI moiety proved to be highly active against the H37Rv strain of *Mtb* ($MIC_{99} \leq 5$ μM) and displayed low cytotoxicity against THP-1 cell lines ($IC_{50} > 10$ μM and SI > 10) (Table **5.10**). The exception was equimolar mixtures (1:1) of VER/INH and **4.17ax**, which exhibited a low selectivity index of 8.4 and 0.08, respectively (Table **5.10**). Shortlisted mixtures were then tested against low to high level isoniazid mono-resistant strains of *Mtb* (R5401, R72 and R4965).

All the mixtures were inactive against isoniazid mono-resistant strains up to a maximum tested concentration of 10 μM. However, the mixture of VER and INH exhibited an MIC_{99} of 0.625 μM (Table **5.10**) against low level INH resistant strain (R5401). This correlates with various reports of the chemosensitization of INH by VER.[15] An $MIC_{99} < 5$ was also observed against the X_61 strain of *Mtb* by an equimolar (1:1) mixture of VER and INH but failed to show any potency against other clinical isolates.

A comparison of antimycobacterial activities of RINH agents and equimolar mixtures revealed the advantages of covalently linking the EPI moieties with INH over administration as physical mixtures. Generally, equimolar mixtures were found to be more potent than corresponding hybrid compounds against the H37Rv. However, equimolar mixtures failed to retain potency against INH mono-resistant and XDR strains while RINH agents retained the H37Rv potency against the R5401 (MIC ≤ 2.5 μM), and also exhibited some potency against the XDR strain (X_61) of *Mtb* ($MIC_{99} < 10$ μM). For example, equimolar mixtures **4.17**(**ax** and **bx**, Table **5.10**) were more potent than the corresponding hybrids **4.17** (Table **5.9**) against the H37Rv while they failed to show any activity against any of the resistant strains of *Mtb*.

On the other hand, hybrid **4.17** retained potency against R5401 and one of the compounds **4.17a** also showed some activity against the resistant strain (X_61).

A similar pattern was also observed with bicyclic hybrid **4.53** as it exhibited potency against the H37Rv (MIC_{99} = 5.0 µM), R5401 (MIC_{99} = 2.5 µM) and X_61 (MIC_{99} < 10 µM) while the corresponding equimolar mixture was more potent against the H37Rv (MIC_{99} = 0.5 µM) but did not show any potency against R5401 and X_61 (MIC_{99} > 10 µM).

Table 5.10: Antimycobacterial activity of equimolar mixtures of selected EPI/EPI moieties and isoniazid.

INH + EPI 1:1					
Mixture Code	**EPI**	**MIC_{99} (µM)**			**IC_{50} (µM)**
		H37Rv	**R5401**	**X_61**	**THP-1 Cell lines**
VER + INH 1:1		5.0	0.625	<5	42
4.10ax	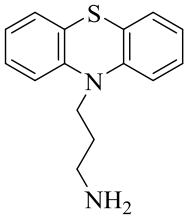	1.0	>10	ND	15.82
4.10bx	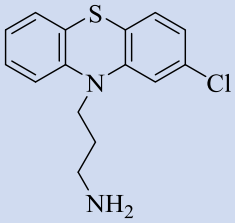	0.5	>10	ND	18.32
4.17ax	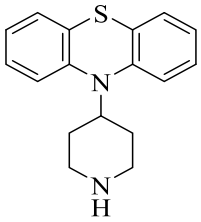	0.5	>10	ND	29.92
4.17bx	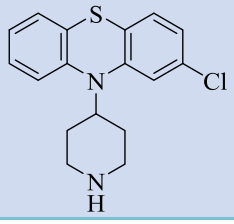	1.0	>10	ND	29.88

INH + EPI 1:1					
Mixture Code	**EPI**	**MIC_{99} (µM)**			**IC_{50} (µM)**
		H37Rv	**R5401**	**X_61**	**THP-1 Cell lines**
4.27x	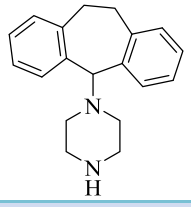	0.5	>10	ND	0.04
4.53x	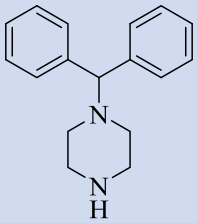	0.5	>10	ND	44.92

5.5.5 Antimycobacterial activities of selected intermediates (EPI moieties and benzhydrazide)

A selected number of EPI/EPI moieties (intermediates) and benzhydrazide were also evaluated against H37Rv for their *in vitro* activity and found to be inactive at the highest tested concentration (10 µM) (Table **5.11**). However, most of the tested EPI/EPI moieties showed varying levels of cytotoxicity against CHO cell lines. The EPI moieties **4.21a**, **4.41** and benzhydrazide showed low cytotoxicity (IC_{50} > 50 µM) while EPI moieties **4.47** and **MKN-62** were found to be more cytotoxic (IC_{50} < 10 µM) (Table **5.11**).

Table 5.11: *In vitro* activities of selected EPI/EP-moieties:

Intermediate	Structure	MIC_{99} (µM) H37Rv	IC_{50} (µM) CHO cell line
4.21a	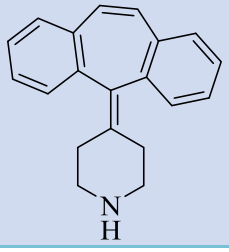	>10	65.2
4.41	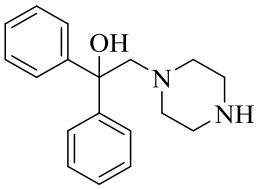	>10	284
4.47	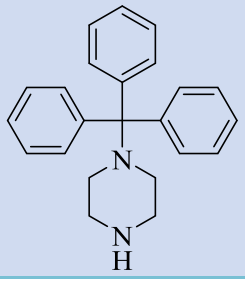	>10	6.52
4.29	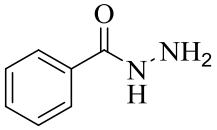	>10	>734
MKN-62	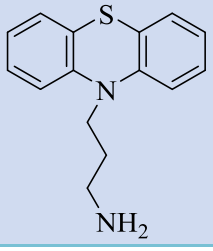	>10	22.9
MKN-63	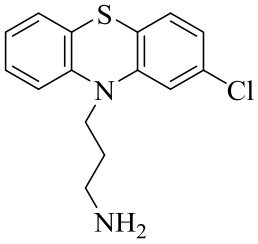	>10	7.9

5.5.6 Macrophage evaluation of RINH agents

Potent RINH agents were shortlisted after the screening of initial compounds against the H37Rv strain of *Mtb*. These shortlisted compounds (**4.3a**, **43.b**, **4.3c**, **4.17b**, **4.28a** and **4.28b**) were re-evaluated for cytotoxicity against THP-1 cell lines followed by testing against intracellular *Mtb* in macrophages at concentrations lower than IC_{20} value. Thereafter, potent analogues were tested for EP inhibition activity in the EB assay.

5.5.6.1 *Ex vivo* cytotoxicity and antimycobacterial evaluation of RINH agents

INH and chlorpromazine (CPZ) were used as controls for the comparison of antimycobacterial and EPI-like properties in macrophages. CPZ showed concentration-dependent inhibition of intracellular *Mtb* in macrophages with maximum inhibition being achieved at 40 μM while INH was highly potent (MIC_{90} = 0.015 μM) (Table **5.12**). All the compounds inhibited (>90%) the growth of intracellular *Mtb* in macrophages (Table **5.12**) at concentrations lower than their IC_{20} values (MIC_{90} < 3 μM). On the other hand, **4.28a** and **4.28b** only exhibited a maximum of 40% inhibition at the highest tested concentration of 26.6 and 12.2 μM, respectively (Table **5.12**). This further confirmed the importance of the nitrogen atom in the pyridyl moiety of RINH agents for antimycobacterial activity both *in vitro* and in macrophages.

Table 5.12: *Ex vivo* antimycobacterial activity of selected RINH agents (**4.3a**, **4.3b**, **4.3c**, **4.17b**, **4.28a** and **4.28b**):

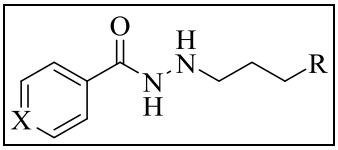

Comp	R	X	IC_{20} (µM) THP-1 cell line	% Inhibition of BCG in macrophages	IC (µM)
CPZ		-	>300	>90	31.4
INH		-	>40	>90	0.015
4.3a	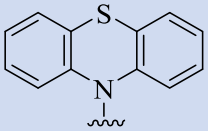	N	>40	>90	2.65
4.3b	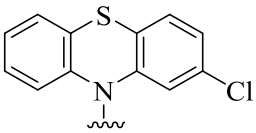	N	>10	>90	2.44
4.3c	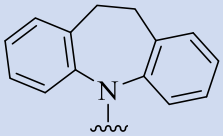	N	>40	>90	13.42
4.17b	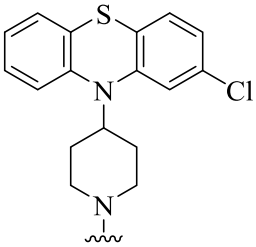	N	1.0	>90	1.0
4.28a	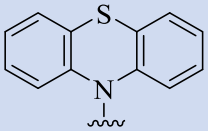	C	>40	40	26.6
4.28b	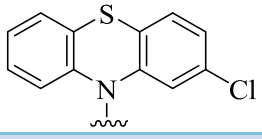	C	>40	40	12.2

Comp: compound; IC: inhibitor concentration corresponding to maximum inhibition of BCG in macrophages.

5.5.6.2 Efflux pump inhibition activity of RINH agents

All the short listed compounds (Table **5.12**) were also evaluated for their EP inhibition activity in the EB assay. The recorded mean fluorescence intensity signifies the concentration of EB present in the BCG-EB assay. Therefore, a higher intensity indicates superior inhibition of EPs responsible for efflux of EB in BCG.

All the compounds were tested in the EB assay at 20 μM except **4.17b**, which was tested at 10 μM due to its low IC_{20} value against the THP-1 cell lines. Most of the RINH compounds inhibited the efflux of EB to a greater degree than CPZ. Among these, compounds **4.28a**, **4.28b**, **4.17b** and **4.3b** were more efficient than CPZ at inhibiting EB efflux. Low intensity was exhibited by **4.57a** and INH, which indicated the lower efficacy towards inhibition of EB efflux than CPZ (**Figure 5.9**). These observations highlighted the dual action of RINH agents as inhibitors of efflux pumps (as suggested by the EB assay, **Figure 5.9**) and antimycobacterial agents per se (demonstrated by *in vitro* and macrophage antimycobacterial data in table **5.9** and **5.12**).

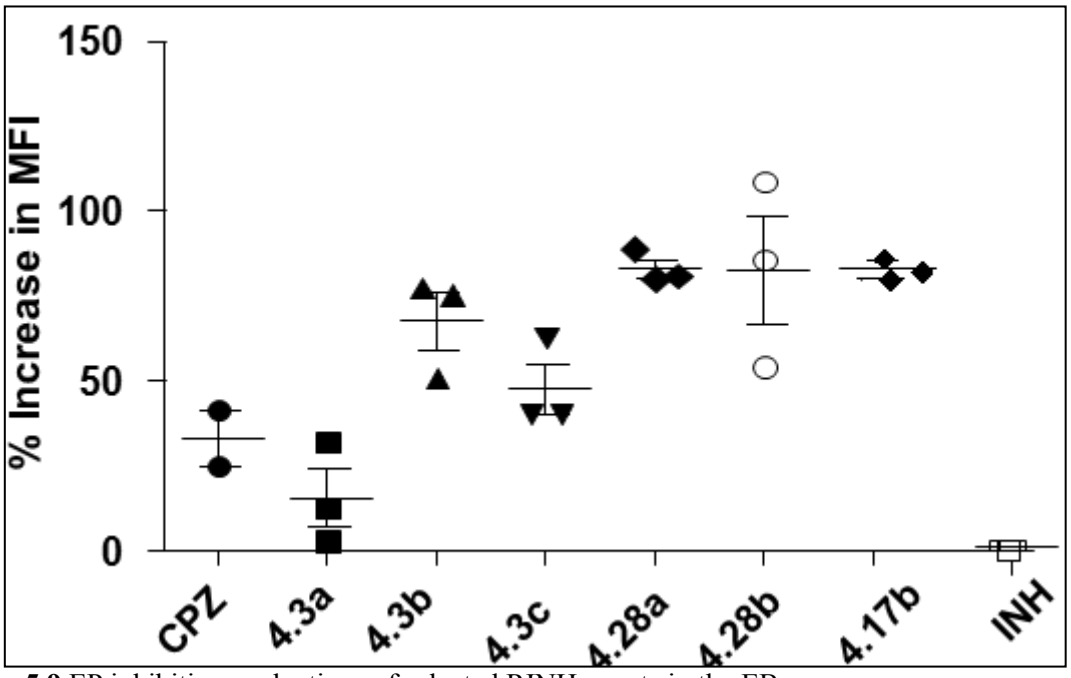

Figure 5.9 EP inhibition evaluations of selected RINH agents in the EB assay.

5.5.7 Discussion and conclusion

A total of 15 RINH agents and two benzhydrazide-based anti-TB agents were synthesized and evaluated against *Mtb in vitro* and *ex vivo* (Table **5.9**).

Antimycobacterial results showed that RINH agents containing a 2-chloro substituted phenothiazine moiety (**4.3b**, **4.10b**, **4.17b** and **4.23b**) exhibited greater potency than unsubstituted analogues (**4.3a**, **4.10a**, **4.17a** and **4.23a**) (Table **5.9**). An enhanced antimycobacterial activity in resistant strains was achieved by linking both tricyclic as well as non-tricyclic EPI moieties to INH *via* a three carbon alkyl chain linker (Table **5.9**). Superior antimycobacterial activity was exhibited by RINH agents (Table **5.9**) compared to their equimolar (1:1) mixtures (Table **5.10**), revealing the advantage of covalently linking the EPI moieties. The importance of the pyridyl nitrogen atom was validated as its replacement with a carbon atom led to loss of antimycobacterial activity both *in vitro* and in macrophages (Table **5.9** and **5.12**).

The macrophage and EB evaluation indicated the dual action nature of the RINH agents. All the shortlisted RINH compounds inhibited the efflux of EB in the ethidium bromide assay and displayed good potency against intracellular *Mtb* in macrophages (Table **5.12**). The pyridyl nitrogen was also found to be essential for intracellular growth inhibition of *Mtb* by RINH compounds while the EP inhibition activity of the EPI moiety was retained even in the absence of the pyridyl nitrogen atom in reversed anti-TB agents **4.28a** and **4.28b** (Table **5.9** and **Figure 5.9**).

5.5.8 Conclusion

In this study, the potency of RINH agents against the sensitive and resistant (INH mono-resistant and XDR) strains demonstrated the viability of the reversed anti-TB agent strategy for the development of antimycobacterials targeting EPs. The potent compounds (**4.17a**, **4.23a**, **4.23b**, **4.23c**, **4.46**, **4.49**, and **4.53**, Table **5.9**) require further evaluation in macrophage assay, *Mtb*-specific T-cell assay, metabolic stability studies and *in vivo* PK studies for advanced development of these compounds. The efficacy of hybrid compounds against resistant strains over the ineffectiveness of equimolar mixtures against these strains provided a "proof-of-principle" with respect to the advantage of covalently linking an EPI to an anti-TB agent over administration as a physical mixture. In addition to phenothiazine-based RINH

agents, demonstration of good to moderate potency by tricyclic (iminodibenzyl **4.3c**, cyproheptadine **4.23c** and trityl **4.49**) and bicyclic EPI (diphenylmethane **4.49)** based compounds further expanded the set of EPI motifs, which can be explored for further development of other classes of RINH agents. The brief SAR studies also revealed the effect of introduction of various structural motifs, including piperidine, aminoalkyl linker, and ylidine bond, into RINH agents. The deletion of the nitrogen atom from the pyridyl moiety of RINH agents **4.3**(**a** and **b**) demonstrated its importance for antimycobacterial activity.

To conclude, we believe that dual action RINH agents have potential for development as antimycobacterial agents effective against MDR and XDR strains of *Mtb*.

5.6 Hybrid efflux pump inhibitors

In this section, a summary of various biological activities of hybrid efflux pump inhibitors (HEPIs) against various strains of *Mtb* is presented. All HEPIs were evaluated against *Mtb in vitro* for their potential to sensitize the first line anti-TB drug RIF. A sequence of testing as described in cascade 1 (**Figure 5.3**) for VER analogues (Section **5.3.1**) was followed. VER was used as a positive control.

5.6.1 Antimycobacterial activity of hybrid efflux pump inhibitors

Firstly, HEPIs were evaluated for their cytotoxicity against THP-1 cell lines with the aim of screening then in macrophages. A strict cut off limit ($IC_{20} \geq 10$ μM) was employed for short listing the non-toxic compounds. Most of the HEPIs showed high toxicity ($IC_{20} < 10$ μM) except **4.57a**, **4.57b**, **4.59a** and **4.60b** (Table **5.13**). Among these, **4.57a** and **4.57b** were the least cytotoxic and exhibited $IC_{20} > 50$ μM, while **4.59a** and **4.60b** showed IC_{20} values in the range of 12.5 and 50 μM. These HEPIs were further evaluated *in vitro* against the replicating H37Rv strain of *Mtb* as individual agents and in combination with rifampicin (RIF) for their potentiating effect. As expected, a very low potency (MIC_{90} = 250 μM) was observed for **4.57a** and **4.57b**. On the other hand, high potency (MIC_{90} of 2.5 and 5.0 μM) was displayed by **4.59a** and **4.60b**, respectively (Table **5.13**).

In addition to the varying potency, these HEPIs also increased the susceptibility of *Mtb* towards RIF and reduced the RIF MIC_{90} by four-fold in combination, which is two-fold higher than the potentiation shown by VER (2-fold reduction in RIF MIC_{90}) (Table **5.13**). HEPIs **4.57a** and **4.57b** reduced the RIF MIC_{90} by two-fold at a lower concentration than that required for VER (125 μM) to achieve the same reduction. Moreover, much lower concentrations of **4.59a** and **4.60b** (1.25 μM) were required for four-fold potentiation of RIF. In addition to potentiation of RIF, three HEPIs (**4.57a**, **4.57b** and **4.60b**) showed a synergistic interaction with RIF (FICI ≤ 0.5) while **4.59a** exhibited an additive effect (FICI = 0.75) (Table **5.13**).

Table 5.13: Antimycobacterial activity of HEPIs in combination with RIF against *Mtb* (H37Rv).

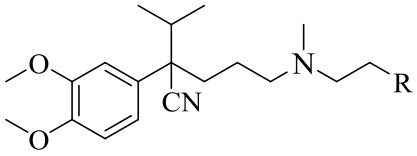

[a]Comp	R	IC_{20} (µM) THP-1 cell lines	MIC_{90} (µM)			Fold reduction in RIF MIC_{90}	FICI
			HEPI	HEPI in comb with RIF	RIF in comb with HEPI		
VER		>50	500	125	0.002	2	0.5
4.57a	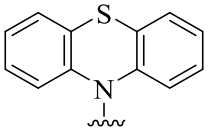	>50	250	62.5	0.001	4	0.3
4.57b	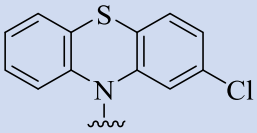	>50	250	62.5	0.001	4	0.4
4.57c	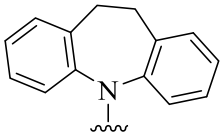	<6.25	[b]ND	[b]ND	[b]ND	[b]ND	[b]ND
4.58	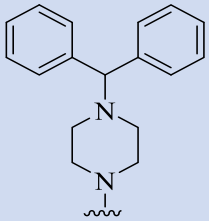	<6.25	[b]ND	[b]ND	[b]ND	[b]ND	[b]ND
4.59a	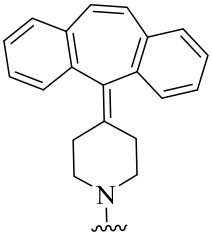	>25 <50	2.5	1.25	0.001	4	0.75
4.59b	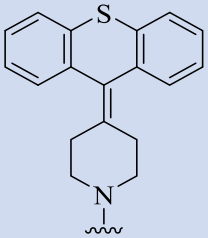	<10	[b]ND	[b]ND	[b]ND	[b]ND	[b]ND

[a]Comp	R	IC_{20} (µM) THP-1 cell lines	MIC_{90} (µM)			Fold reduction in RIF MIC_{90}	FICI
			HEPI	HEPI in comb with RIF	RIF in comb with HEPI		
4.59c	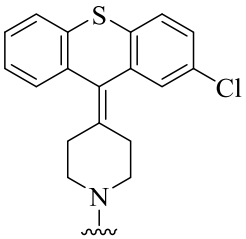	<10	[b]ND	[b]ND	[b]ND	[b]ND	[b]ND
4.60a	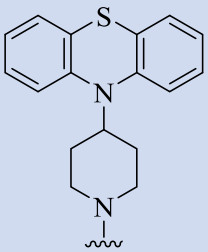	<10	[b]ND	[b]ND	[b]ND	[b]ND	[b]ND
4.60b	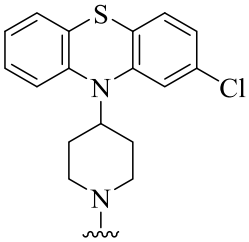	>12.5 <25	5.0	1.25	0.001	4	0.5
4.61	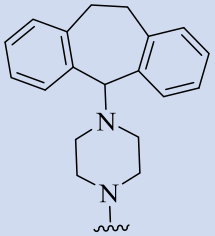	<6.25	[b]ND	[b]ND	[b]ND	[b]ND	[b]ND
4.63	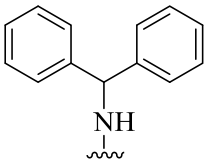	<10	[b]ND	[b]ND	[b]ND	[b]ND	[b]ND

[a]Comp: Compound; Comb: combination; [b]ND: Not determined as toxicity against THP-1 cell line is high (IC_{20} <10 µM), therefore not selected for further evaluations. RIF MIC_{90} = 0.004 µM.

5.6.2 Intracellular evaluation of HEPIs in macrophages

The good *in vitro* potentiating potential of selected HEPIs (**4.57a**, **4.57b**, **4.59a** and **4.60b**) led to their further evaluation against intracellular *Mtb* in macrophages and efflux pump inhibitory activity in the ethidium bromide assay.

5.6.2.1 Antimycobacterial activity of HEPIs against BCG and *Mtb* in macrophages

A sequence of testing similar to that shown in cascade 2 was followed for this study. The selected HEPIs were first evaluated against intracellular BCG followed by testing potent HEPIs against intracellular *Mtb*.

Since EPIs are expected to increase the susceptibility of *Mtb* in macrophages by countering the EP-mediated tolerance, this was confirmed by three of the four selected HEPIs, which showed greater than 40% inhibition of BCG in macrophages (**Figure 5.10**). HEPIs **4.59a** and **4.60b** displayed the highest potency by inhibiting intracellular BCG by more than 60%. However, **4.57a** did not exhibit significant inhibition of BCG in macrophages. The potent HEPIs (**4.57b**, **4.59a** and **4.60b**) were shortlisted for further evaluation against intracellular *Mtb* in macrophages.

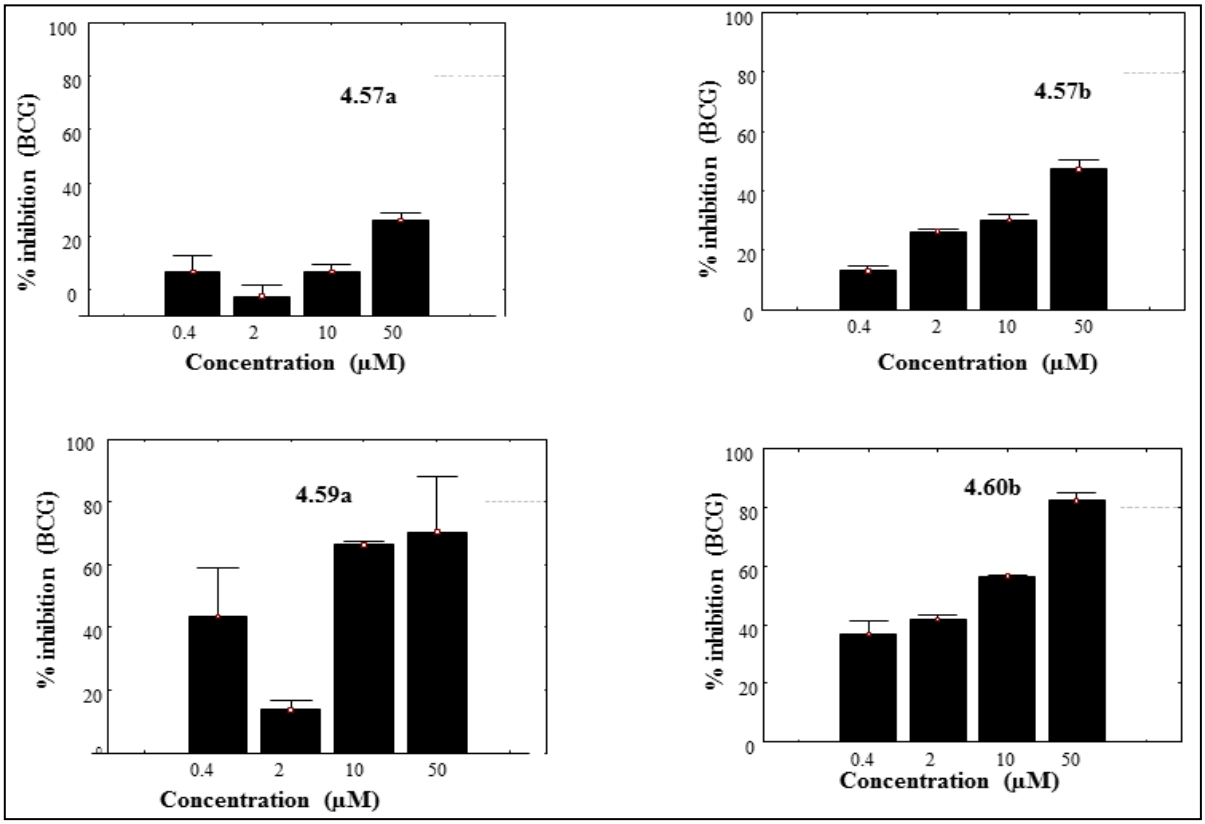

Figure 5.10: Antimycobacterial activity of HEPIs (**4.57a**, **4.57b**, **4.59a** and **4.60b**) against intracellular BCG in macrophages at 0.4, 2, 10 and 50 µM concentrations.

All the tested HEPIs retained potency and displayed more than 40% inhibition (**Figure 5.11**). Furthermore, these HEPIs were evaluated in the EB assay in order to investigate their EP inhibition activities. Among the three tested HEPIs, only two (**4.59a** and **4.60b**) inhibited EB efflux and displayed increase in fluorescence (**Figure 5.12**). These two analogues were further tested in combination with RIF and INH against intracellular *Mtb* to investigate their potentiating potential.

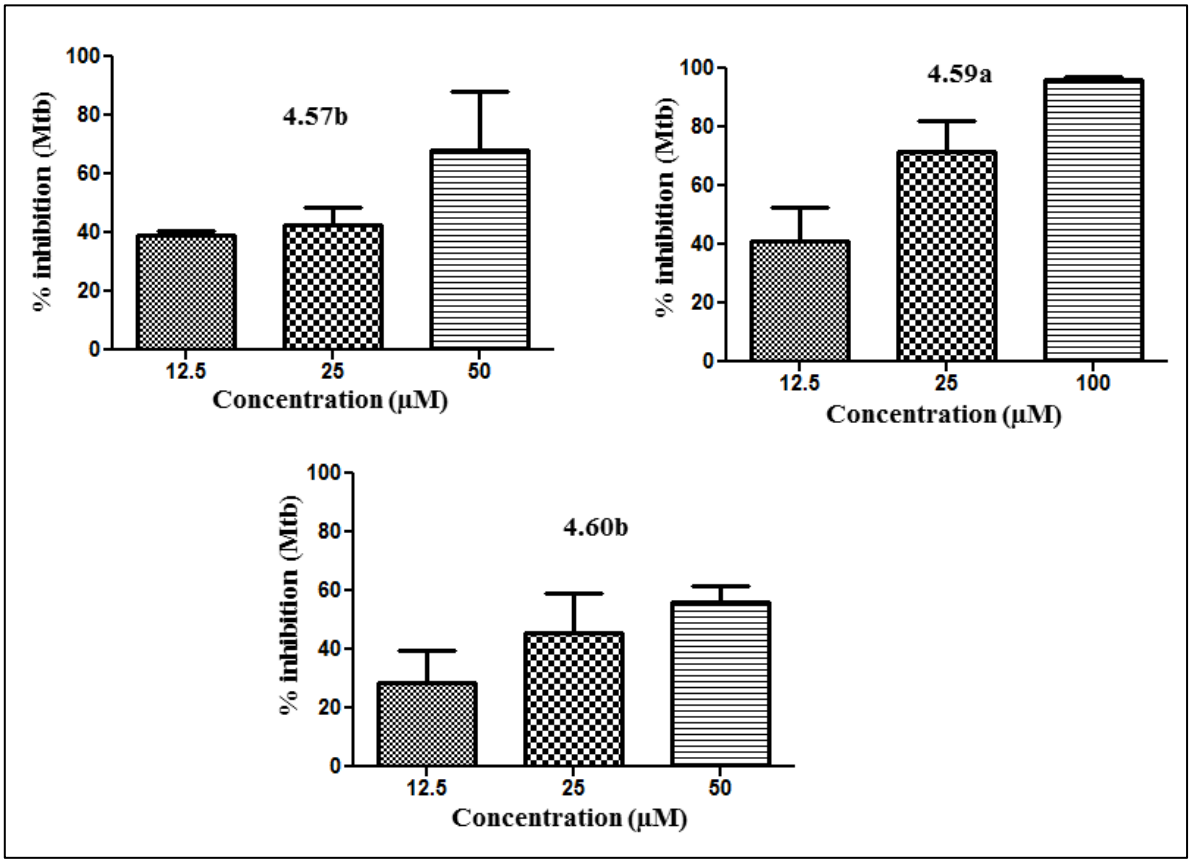

Figure 5.11: Antimycobacterial activity of selected HEPIs (**4.57b**, **4.59a**, and **4.60b**) against intracellular *Mtb* in macrophages at 12.5, 25, and 50 or 100 µM concentrations.

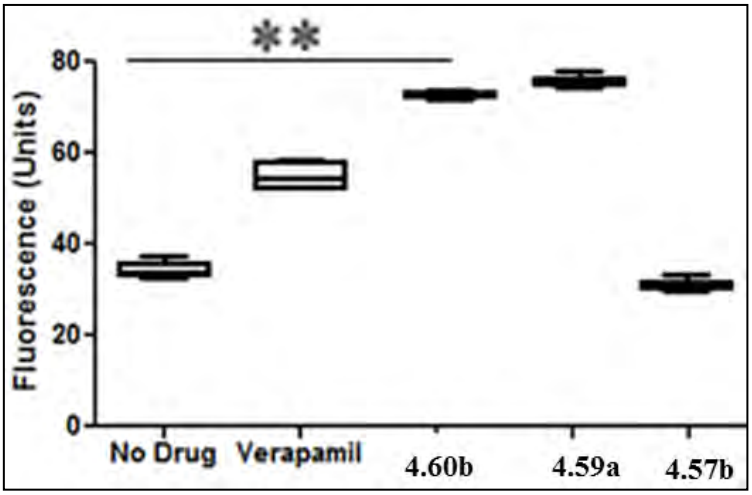

Figure 5.12: EP inhibitory indications of HEPIs (**4.60b, 4.59a** and **4.57b**).

5.6.2.2 Potentiating effect of HEPIs (4.59a and 4.60b) on RIF and INH against intracellular *Mtb*

The frontrunner HEPIs with the highest potency and ability to inhibit the efflux of EB where selected for evaluation in combination with RIF and INH against intracellular *Mtb*.

Various concentrations of INH and RIF (0.04, 0.008, 0.004 and 0.0008 µM) were first evaluated for individual potency against intracellular *Mtb*. A moderate potency (inhibition > 40%) was observed at 0.04 µM of INH and RIF while no significant inhibition was observed at other tested concentrations (**Figure 5.13** and **5.14**). These drugs were then tested in combination with **4.59a** and **4.60b** at concentrations of 3.125 and 6.25 µM respectively. Both HEPIs failed to show any significant potentiating effects on INH (**Figure 5.13**). However, a significant enhancement in the inhibitory activities of RIF was observed in combination with **4.59a** and **4.60b** at 3.125 and 6.25 µM concentrations, respectively (**Figure 5.14**).

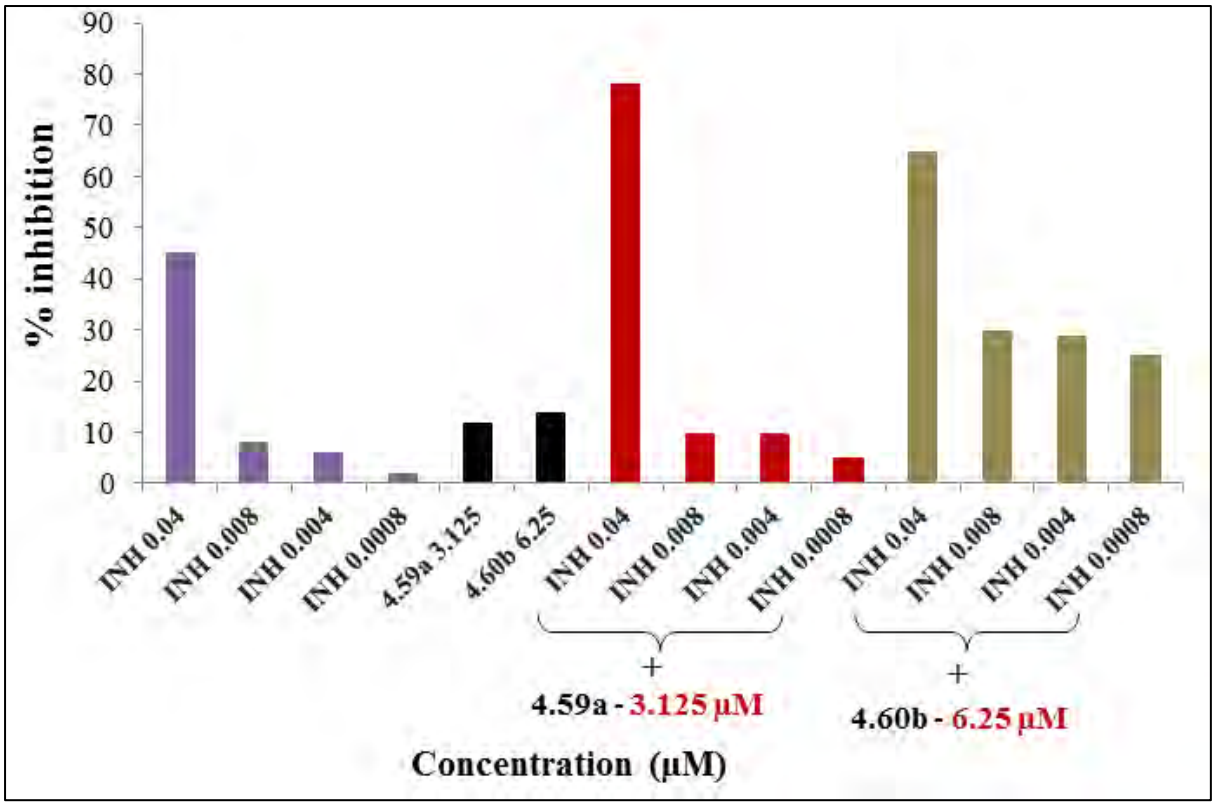

Figure 5.13: Potentiating effect of **4.59a** and **4.60b** on INH against *Mtb* in macrophages.

The specific potentiation of sub-inhibitory concentrations of RIF by HEPIs suggests that both **4.59a** and **4.60b** might be specifically inhibiting EPs implicated in RIF resistance and less effective against EPs responsible for the efflux of INH.

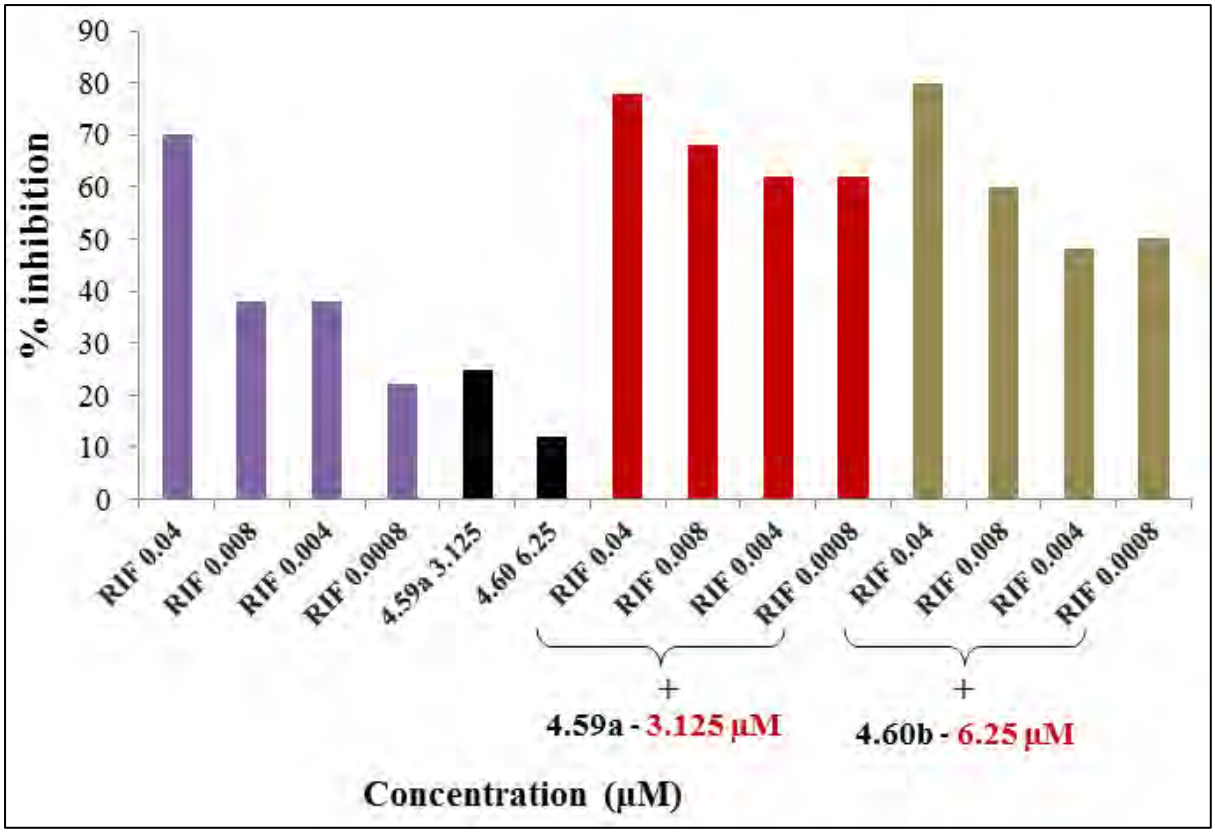

Figure 5.14: Potentiating effect of **4.59a** and **4.60b** on RIF against *Mtb* in macrophages.

5.6.3 Discussion and conclusion

A set of 11 HEPIs were synthesized and evaluated for cytotoxicity and antimycobacterial activity as individual agents and in combination with RIF (Table **5.13**).

Antimycobacterial activities revealed two HEPIs (**4.59a** and **4.60b**) as potential EPIs. These compounds increased the susceptibility of *Mtb* towards RIF when used in combination both *in vitro* (Table **5.13**) and *ex vivo* (Figure **5.13** and **5.14**). These two analogues also showed activity against *Mtb* ($MIC_{90} \leq 5$ µM) and a potentiating effect at a lower concentration ($MIC_{90} \leq 2.5$ µM) (Table **5.13**). The inhibition of EB efflux in the ethidium bromide assay confirmed the EP inhibition property of these two analogues (**Figure 5.12**).

In conclusion, the various results demonstrated that developing HEPIs around a VER template is a viable strategy and can be further explored to develop various dual acting EPIs and antimycobacterial agents with potentially enhanced pharmacological profiles.

References:

(1) Ramón-García, S.; Carol Ng.; Anderson, H.; Chao, J. D.; Zheng, X.; Pfeifer, T.; Av-Gay, Y.; Roberge, M.; Thompson, C. J. Synergistic Drug Combinations for Tuberculosis Therapy Identified by a Novel High-Throughput Screen. *Antimicrob. Agents Chemother.* **2011**, *55*, 3861–3869.

(2) Ramón-García, S.; Martín, C.; Aínsa, J. A; De Rossi, E. Characterization of Tetracycline Resistance Mediated by the Efflux Pump Tap from *Mycobacterium Fortuitum*. *J. Antimicrob. Chemother.* **2006**, *57*, 252–259.

(3) Odds, F. C. Synergy, Antagonism, and What the Chequerboard Puts between Them. *J. Antimicrob. Chemother.* **2003**, *52*, 1.

(4) Collins, L. A.; Franzblau, S. G. Microplate Alamar Blue Assay versus BACTEC 460 System for High-Throughput Screening of Compounds against *Mycobacterium tuberculosis* and Mycobacterium Avium. *Antimicrob. Agents Chemother.* **1997**, *41*, 1004–1009.

(5) Viveiros, M.; Martins, M.; Rodrigues, L.; Machado, D.; Couto, I.; Ainsa, J.; Amaral, L. Inhibitors of Mycobacterial Efflux Pumps as Potential Boosters for Anti-Tubercular Drugs. *Expert Rev. Anti. Infect. Ther.* **2012**, *10*, 983–998.

(6) Paixão, L.; Rodrigues, L.; Couto, I.; Martins, M.; Fernandes, P.; de Carvalho, C. CCR.; Monteiro, G. A; Sansonetty, F.; Amaral, L.; Viveiros, M. Fluorometric Determination of Ethidium Bromide Efflux Kinetics in Escherichia coli. *J. Biol. Eng.* **2009**, *3*, 18.

(7) Amaral, L.; Cerca, P.; Spengler, G.; Machado, L.; Martins, A.; Couto, I.; Viveiros, M.; Fanning, S.; Pagès, J.-M. Ethidium Bromide Efflux by Salmonella: Modulation by Metabolic Energy, pH, Ions and Phenothiazines. *Int. J. Antimicrob. Agents* **2011**, *38*, 140–145.

(8) Machado, D.; Couto, I.; Perdigão, J.; Rodrigues, L.; Portugal, I.; Baptista, P.; Veigas, B.; Amaral, L.; Viveiros, M. Contribution of Efflux to the Emergence of Isoniazid and Multidrug Resistance in *Mycobacterium tuberculosis*. *PLoS One* **2012**, *7*, e34538.

(9) Singh, K.; Kumar, M.; Pavadai, E.; Naran, K.; Warner, D. F.; Ruminski, P. G.; Chibale, K. Synthesis of New Verapamil Analogues and Their Evaluation in Combination with Rifampicin against *Mycobacterium tuberculosis* and Molecular Docking Studies in the Binding Site of Efflux Protein Rv1258c. *Bioorg. Med. Chem. Lett.* **2014**, *24*, 2985–2990.

(10) Torrea, G.; Coeck, N.; Desmaretz, C.; Van De Parre, T.; Van Poucke, T.; Lounis, N.; de Jong, B. C.; Rigouts, L. Bedaquiline Susceptibility Testing of *Mycobacterium tuberculosis* in an Automated Liquid Culture System. *J. Antimicrob. Chemother.* **2015**, 1–6.

(11) Shandil, R. K.; Jayaram, R.; Kaur, P.; Gaonkar, S.; Suresh, B. L.; Mahesh, B. N.;

Jayashree, R.; Nandi, V.; Bharath, S.; Balasubramanian, V. Moxifloxacin, Ofloxacin, Sparfloxacin, and Ciprofloxacin against *Mycobacterium tuberculosis*: Evaluation of in Vitro and Pharmacodynamic Indices That Best Predict in Vivo Efficacy. *Antimicrob. Agents Chemother.* **2007**, *51*, 576–582.

(12) Martins, M.; Viveiros, M.; Rodrigues, L. Phenothiazines , Bacterial Efflux Pumps and Targeting the Macrophage for Enhanced Killing of Intracellular XDRTB. *in vivo* **2010**, *424*, 409–424.

(13) Pereira, E.; Teodori, E.; Dei, S.; Gualtieri, F.; Garnier-Suillerot, A. Reversal of Multidrug Resistance by Verapamil Analogues. *Biochem. Pharmacol.* **1995**, *50*, 451–457.

(14) Demitto, F. D. O.; do Amaral, R. C. R.; Maltempe, F. G.; Siqueira, V. L. D.; Scodro, R. B. D. L.; Lopes, M. A.; Caleffi-Ferracioli, K. R.; Canezin, P. H.; Cardoso, R. F. In Vitro Activity of Rifampicin and Verapamil Combination in Multidrug-Resistant *Mycobacterium tuberculosis*. *PLoS One* **2015**, *10*, e0116545.

(15) Adams, K. N.; Szumowski, J. D.; Ramakrishnan, L. Verapamil, and Its Metabolite Norverapamil, Inhibit Macrophage-Induced, Bacterial Efflux Pump-Mediated Tolerance to Multiple Anti-Tubercular Drugs. *J. Infect. Dis.* **2014**, *210*, 456–466.

Chapter 6: Summary, conclusion and recommendations for future work

6.1 General

Efflux pumps (EPs) present in *Mtb* have been associated with drug resistance in this bacterium. EPs reduce the potency of anti-TB drugs and assist *Mtb* in overcoming the toxic and inhibitory effects of these drugs. One of the objectives of this study was to develop novel efflux pump inhibitors (EPIs) by structural modification of verapamil (VER) with attendant structure activity relationship (SAR) studies of resulting analogues, and synthesis of hybrid efflux pump inhibitors (HEPIs) by incorporation of various EPI moieties into the VER substructure. In addition, this study set out to identify reversed isoniazid (RINH) anti-TB agents by covalently linking isoniazid (INH) with various EPI moieties.

6.2 Verapamil analogues

As discussed in chapter **2**, verapamil is a compound well known for its calcium channel blocking properties and has been shown to inhibit efflux pump activity. Although a promising candidate for the development of EPIs, VER has liabilities that need to be considered. In particular, the cardiovascular antagonism and microsomal metabolic instability in the presence of cytochrome P450 (CYPs) are two major hurdles that need to be overcome.

The first objective was to design and synthesize analogues of VER able to potentiate the activity of various anti-TB drugs by efflux pump inhibition but potentially lacking undesired properties such as calcium channel antagonism and with *Mtb*-specific T-cells. Sets of compounds in four different series were designed and synthesized with various structural modifications as reflected in SAR 1, SAR 2, SAR 3 and SAR 4 (Chapter **3**). The chemistry mainly involved alkylation reactions using various bases including *n*-butyllithium and lithium diisopropyl amide. These syntheses were carried out *via* modified and relatively straight forward synthetic methods using affordable starting materials.

The next objective was to evaluate the synthesized analogues, both individually and in combination with the first line anti-TB drug rifampicin (RIF) *in vitro*. The initial screening showed that as expected, most of the analogues exhibited low potency ($MIC_{90} \geq 50$ μM). When tested in combination with RIF, some of the analogues (**3.13c**, **3.13d**, **3.13h**, **3.13k**, **3.13l** and **3.13n**) showed a 4-fold reduction in the MIC_{90} of RIF, which was comparable to VER. The encouraging potentiating potential of the benzyl analogues **3.13h** led to further

exploration of various substituents on the phenyl group of the benzyl moiety and identification of analogues **3.17a** with comparable potentiating effects as VER. The complete *in vitro* antimycobacterial and *ex vivo* cytotoxicity screening led to the identification of analogues with low cytotoxicity, good potentiating potential at low concentration, and which exhibited synergistic interactions with RIF, moxifloxacin (MOX) and bedaquiline (BDQ). The analogues **3.13h, 3.13n** (Table **5.1**) and **3.17a** (Table **5.3**) showed the most promising results as potential EPIs.

The final objective was to investigate the potentiating effect of frontrunner analogues on intracellular *Mtb* in macrophages as well as their cytotoxic effects on *Mtb*-specific T-cell proliferation. Analogues **3.13n** and **3.13h** showed no effect on *Mtb*-specific T-cells and displayed potency against intracellular *Mtb* comparable to VER. One of the analogues (**3.13n**) further potentiated the sub-inhibitory concentrations of RIF and INH in macrophages at a low concentration (2.5 μM). The ethidium bromide assay also demonstrated that EP inhibition is one of the plausible underlying mechanisms responsible for potentiation. The results concerning VER analogues from various assays revealed that structural modification is a viable strategy toward novel EPIs with improved pharmacological properties.

6.3 Reversed isoniazid (RINH) anti-TB agents

The first objective was to design and synthesize first generation reversed isoniazid (RINH) anti-TB agents. A total of 15 RINH agents (Table **5.9**) were designed and synthesized by covalently linking tricyclic and non-tricyclic moieties from known EPIs with INH using a three carbon alkyl chain linker. The chemistry involved a range of standardizations and modifications of various known reaction conditions, which were carried out with relative ease and using affordable starting materials.

Synthesized RINH agents were screened for antimycobacterial activity against drug sensitive (H37Rv), INH mono-resistant (R5401, R72 and R4965), and extremely drug resistant (X_60 and X_61) strains of *Mtb*. Generally, RINH agents exhibited good antimycobacterial activity ($MIC_{99} \leq 10$ μM) and selectivity (SI ≥ 10 μM) against the H37Rv strain of *Mtb*. In particular, phenothiazine-based RINH agents (**4.3a**, **4.3b**, **4.17b**, **4.23a**, and **4.23b**) along with iminodibenzyl **4.3c**, cyproheptadine **4.23c**, diphenylmethane **4.49**, and trityl **4.49** based RINH agents were the most potent ($MIC_{99} \leq 1.25$ μM; Table **5.9**). In some instances, RINH agents

(**4.17a**, **4.23a**, **4.23b**, **4.23c**, **4.46**, **4.49** and **4.53**) were potent against both low level INH mono-resistant strain (R5401; $MIC_{99} \leq 2.5$ μM; Table **5.9**) and XDR strains (X_60 and X_61; $MIC_{99} < 10$ μM; Table **5.9**). This suggests the absence of cross resistance in these RINH agents.

The poor ($MIC_{99} > 10$ μM) antimycobacterial activity of reversed anti-TB agents **4.28a** and **4.28b** (Table **5.9**) possessing a phenyl group in place of the pyridyl moiety of RINH agents **4.3a** and **4.3b (**Table **5.9**) demonstrated the importance of the latter for antimycobacterial activity. Generally speaking, the covalently linked hybrid of EPI precursors and INH demonstrated increased potency against drug sensitive (DS) and drug resistant (DR) strains of *Mtb* in comparison to the equimolar mixture (1:1) of the EPI precursor and INH which were ineffective against DR strains up to a maximum concentration of 10 μM. These results revealed the advantages of covalently linking an EPI or its precursors with an anti-TB drug rather than administering them as separate compounds in an equimolar mixture (1:1).

The third objective was to investigate the potency of selected RINH agents against intracellular *Mtb* in macrophages and EP inhibition using an ethidium bromide (EB) assay. Most of the tested RINH agents exhibited low *ex vivo* cytotoxicity (THP-1 cell line), good intracellular potency against *Mtb* in macrophages (Table **5.12**) and superior inhibition of EB efflux than the known EPI chlorpromazine (**Figure 5.9**). The limited SAR studies in both the macrophage and EB assays revealed that structural modifications on the phenothiazine nucleus is tolerated in respect of both antimycobacterial and EP inhibition activities, as well as the essentiality of the pyridyl moiety for antimycobacterial potency (Table **5.12**).

6.4 Hybrid efflux pump inhibitors

The first objective was to design and synthesize hybrid efflux pump inhibitors (HEPIs) in an attempt to develop novel EPIs. Structural modification of VER was achieved by replacing one of the dimethoxyphenyl groups of VER with various EPI moieties. A total of 11 HEPIs were synthesized *via* relatively straight forward synthetic methods using affordable starting materials.

Secondly, the potentiating potential of HEPIs with low cytotoxicity on various anti-TB drugs *in vitro* and in macrophages was investigated. Screening of HEPIs against the THP-1 cell

lines led to the identification of four compounds (**4.57a**, **4.57b**, **4.59a** and **4.60b**; Table **5.13**) with low toxicity ($IC_{20} \geq 25$ μM). *In vitro* evaluation of these HEPIs in combination with RIF revealed their potentiating potential at a lower concentration (≤ 65 μM) compared to that required for VER (125 μM). Two HEPIs (**4.59a** and **4.60b**) showed unexpectedly high antimycobacterial potency (MIC ≤ 5.0 μM) along with a good potentiating effect on RIF (4-fold reduction in the MIC_{90} of RIF) at a 100-fold lower concentration than VER.

Finally, selected HEPIs were investigated for their potency and potentiating effect on RIF and INH against intracellular *Mtb* in macrophages. One of the HEPIs, **4.59a**, increased the susceptibility of *Mtb* to the sub-inhibitory concentrations of RIF and INH in macrophages (**Figure 5.13** and **5.14**).

6.5 Recommendations for future work

Work undertaken in this PhD research study has demonstrated the potential for the future development of chemical compounds that can inhibit the functioning of efflux pumps in various strains of *Mtb* while displaying desired pharmacological profiles.

Structural modification of VER demonstrated the possibility of improving the pharmacological profile of new VER analogues. Further structural modifications may lead to the successful development of analogues devoid of liabilities associated with VER such as calcium channel blocking activity, microsomal instability in presence of CYPs, and interaction with *Mtb*-specific T-cells. The improved profile of compound exhibited by **3.13n**, which showed no interaction with *Mtb*-specific T-cells, as well as its excellent potentiating effect on RIF and INH both *in vitro* and in macrophages, provides a rationale basis for its further investigation in order to assess the cardiovascular properties as well as *in vivo* efficacy of these compounds. In addition to compound **3.13n**, further evaluation of analogues **3.15** and **3.17** in macrophages and on *Mtb*-specific T-cells may reveal additional potential EPIs superior to VER.

The generation of analogues with good microsomal metabolic stability will be important for future strategies to deliver novel EPIs which may be progressed to clinical stages of development. This is in view of the fact that the dimethoxyphenyl groups of VER (**Figure 6.1**) are metabolic hot spots, which make VER highly susceptible to CYP-mediated

metabolism. Therefore, SAR studies around the dimethoxyphenyl groups may lead to the generation of VER analogues with enhanced metabolic stability.

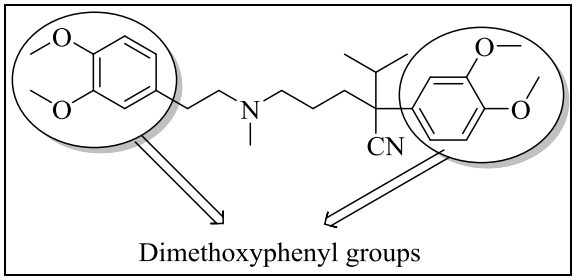

Figure 6.1: Dimethoxyphenyl groups of verapamil.

As mentioned previously, the first generation RINH agents led to the identification of various potent antimycobacterial agents, which showed *in vitro* potency against *Mtb* strains with low to high level drug resistant strains. Macrophage evaluation, microsomal metabolic stability and *in vivo* efficacy studies are required to demonstrate the lead potential of potent RINH agents. The encouraging *in vitro* results have shown that this approach can be explored further with other anti-TB drugs to develop antimycobacterial agents with superior efficacy against multi drug resistant strains of *Mtb*.

The identification of HEPIs with potential EPI properties holds promise for the future development of EPIs with potentially novel mechanisms of action. The *in vitro* and intracellular potentiation of RIF by **4.59a** warrants further investigation using *Mtb*-specific T-cell and cardiovascular assays. The various phenothiazine-, iminodibenzyl-, cyproheptadine-, dibenzosuberane-, and diphenylmethane-based EPI moieties used in the development of HEPIs are known to be associated with different undesirable properties such as anti-psychotic effects and cardiovascular antagonism. Therefore, it is essential that these liabilities are addressed as part of the future lead optimization campaign.

Chapter 7: Experimental

7.1 Chemistry

7.1.2 Reagents and solvents

All the commercially available chemicals and reagents used in this project were purchased either from Sigma Aldrich or Combi block in South Africa. Anhydrous solvents DMF, MeOH and dioxane were purchased from Sigma Aldrich, South Africa. Ethyl acetate, hexane, dichloromethane and acetone were purchased from Kimix Chemicals or Protea chemicals as Analytical Reagent (AR) grade solvents. The High Performance Liquid Chromatography (HPLC) grade solvents were bought from Sigma Aldrich (Ammonium Acetate and DMSO), Merck (glacial Acetic Acid) and Microsep (Acetonitrile and Methonol) for Chromatography and Mass spectrometry and HPLC usages.

7.1.3 Chromatography

Thin layer chromatographic (TLC) plates were purchased from Merck with specificity as F_{254} aluminium-backed pre-coated silica gel 60 plates. Detection and visualization of spots were done using (a) ultra violet (UV) lights (254/366 nm), (b) iodine vapours and (c) ninhydrin spray reagent. The purifications of products were done with column chromatography by using Merck kieselgel 60:70-230 mesh by gravity column chromatography and biotage flash chromatography.

7.1.4 Physical and Spectroscopic characterization

Melting points were determined on a Reichert-Jung Thermovar hot-stage microscope, and are uncorrected.

Reported compounds were characterized using ^{1}H-NMR whereas novel compounds were characterized using ^{1}H-NMR, ^{13}C-NMR as well as LC-MS.

HPLC: Compound peak purity of some compounds was determined by preparatory HPLC using a thermo separation system comprising of a Spectra series P200 pump, AS100 automated sampler and UV 100 variable wavelength detector. The UV detector was set to monitor the wavelength at 254 nm. The stationary phase used for Waters preparatory HPLC was a Waters® X-bridge C18 5.0 µm column (4.6 x 150 mm) (Phenomenex, Torrance, CA)

fitted with a Supelguard® Ascentis ™ guardcartidge C18 (2cm × 40 mm, 3um) (Supelco Analytical, Bellefonte, PA).

The mobile phase consisted of 0.4% acetic acid in 10 mM ammonium acetate in HPLC grade (Type 1) water; with flow rate = 1.20 mL/min; and acetonitrile (B) delivered at a flow rate 1.20 ml/min. detector: photo diode array (PDA) and all compounds were confirmed to have ≥ 95% purity.

Table 7.1: One of the gradients used for investigation of the purity of compounds with preparatory HPLC:

Time	%A	%B
Initial	75	25
9.00	0	100
14.00	0	100
14.10	75	25
20.00	75	25

Peak purity is reported as the integrated area of the compound peak as a percentage of total peak areas observed

LC-MS: Liquid chromatograph with mass spectrometer (LC-MS) analysis was performed using an Agilent® 1260 Infinity Binary Pump, Agilent® 1260 Infinity Diode Array Detector (DAD), Agilent® 1290 Infinity Column Compartment, Agilent® 1260 Infinity Standard Autosampler, and a Agilent® 6120 Quadrupole (Single) mass spectrometer, equipped with APCI and ESI multimode ionisation source. Purities were determined by Agilent® LC-MS using a Kinetex Core C18 2.6 µm column (50 x 3 mm); organic phase (Mobile Phase B): 0.4% acetic acid, 10 mM ammonium acetate in a 9:1 ratio of HPLC grade methanol and Type 1 water, aqueous phase (Mobile Phase A): 0.4% acetic acid in 10 mM ammonium acetate in HPLC grade (Type 1) water; with flow rate = 0.9 mL/min; detector: diode array (DAD) and all compounds were confirmed to have ≥ 95% purity.

Table 7.2: One of the gradients used for investigation of the purity and mass of compounds with LC-MS:

Time	%A	%B
Initial	75	25
1.00	75	25
3.00	0	100
4.50	0	100
5.20	75	25
6.00	75	25

All NMR spectra were recorded on Varian Mercury (^{1}H-300 MHz; ^{13}C-75 MHz), Varian Unity (^{1}H-400 MHz; ^{13}C-101 MHz), or Brucker Ultrashield-Plus Spectrometer (^{1}H-300 MHz; ^{13}C-75 MHz), and Brucker Ultrashield-Plus Spectrometer (^{1}H-600 MHz; ^{13}C-151 MHz). All the spectra were recorded in deuterated chloroform ($CDCl_3$) or deuterated dimethysulfoxide (DMSO-d_6) or deuterated methanol (MeOH-d_4) using tetramethylsilane as an internal standard. All the chemical shifts (δ) are recorded in ppm and are rounded off to two decimal place; coupling constants (*J*) are recorded in hertz (Hz) and rounded off to one decimal place. Abbreviations used in the assigning of ^{1}H-NMR signals are: br (broad), d (doublet or doublets), m (multiplets) s (singlet), t (triplet), dd (doublet of doublets), ddd (doublet of doublet of doublets) and td (triplet of doublets).

7.1.4.1 Verapamil Analogues

General method 1: Procedure for synthesis of 2-(3,4-dimethoxyphenyl)acetonitrile intermediates (3.7a-g)

n-Butyllithium (12.4 ml of a 2.5 M solution in hexane, 13.44 mmol) was added drop-wise to a stirred solution of 2-(3,4-dimethoxyphenyl)acetonitrile **3.8** (2.0 g, 11.2 mmol) in dry THF (25 ml) under an inert atmosphere of nitrogen at 0 °C. The reaction mixture was allowed to warm to room temperature (25 °C) and stirred for 30 minutes, then after again cooled to 0 °C and corresponding alky halide (16.96 mmol) dissolved in dry THF (15 ml) was added drop-wise to it over 5-7 minutes. The resulting reaction mixture was stirred at room temperature (25 °C) for 2 hours. Upon completion of reaction (TLC), cooled to 0 °C and quenched with saturated aqueous solution of NH_4Cl. The organic phase was extracted with ethyl acetate, dried over anhydrous Na_2SO_4 and concentrated *in vacuo*. The crude residue was purified by column chromatography to obtain **3.7**.

***2-(3,4-dimethoxyphenyl)-3-methylbutanenitrile* (3.7a)**[1]

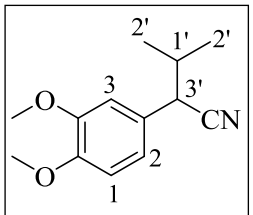

$C_{13}H_{18}NO_2$
Ex. Mass: 220.13

White solid (1.7 g, 69%); m.p. 50-52 ^oC; R_f 0.40 (25% EtOAc-Hexane); ^{1}H-NMR (400 MHz, $CDCl_3$) δ 6.87 (1H, dd, *J* = 8.0 and 2.0 Hz, H-2), 6.86 (1H, d, *J* = 8.0 Hz, H-1), 6.85 (1H, d, *J* = 2.0 Hz, H-3), 3.89 (3H, s, OC*H*$_3$), 3.87 (3H, s, OC*H*$_3$), 3.59 (1H, d, *J* = 6.4 Hz, H-3'), 2.10 (1H, m, H-1'), 1.05 (6H, d, *J* = 6.8 Hz, H-2').

***2-(3,4-dimethoxyphenyl)propanenitrile* (3.7c)**[2]

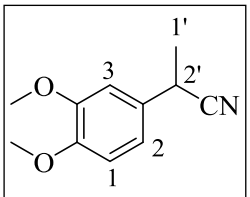

$C_{11}H_{13}NO_2$
Ex. Mass: 191.09

White solid (1.0 g, 46%); m.p. 72-74 °C; R_f 0.40 (20% EtOAc-Hexane); ^{1}H-NMR (400 MHz, $CDCl_3$) δ 6.83 (1H, dd, *J* = 8.0 and 2.0 Hz, H-2), 6.81 (1H, d, *J* = 8.0 Hz, H-1), 6.79 (1H, d, *J* = 2.0 Hz, H-3), 3.84 (3H, s, OC*H*$_3$), 3.82 (3H, s, OC*H*$_3$), 3.79 (1H, q, *J* = 7.2 Hz, H-2'), 1.57 (3H, d, *J* = 7.2 Hz, H-1').

***2-(3,4-dimethoxyphenyl)butanenitrile* (3.7d)**[2]

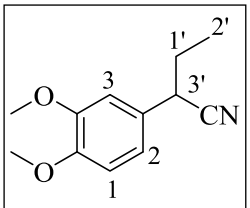

$C_{12}H_{16}NO_2$
Ex Mass: 206.12

Oil (1.1 g, 48%); R_f 0.35 (15% EtOAc-Hexane); ^{1}H-NMR (400 MHz, $CDCl_3$) δ 6.79 (1H, dd, *J* = 7.6 and 1.6 Hz, H-2), 6.79 (1H, d, *J* = 8.0 Hz, H-1), 6.75 (1H, m, H-3), 3.83 (3H, s, OCH_3), 3.81 (3H, s, OCH_3), 3.61 (1H, t, *J* = 6.8 Hz, H-3'), 1.86 (2H, m, H-1'), 1.0 (3H, t, *J* = 7.2 Hz, H-2').

***2-(3,4-dimethoxyphenyl)pentanenitrile* (3.7e)**[3]

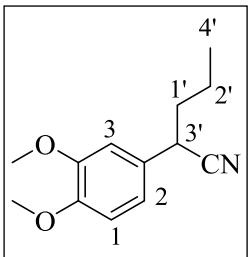

$C_{13}H_{18}NO_2$
Ex. Mass: 220.13

Oil (1.3 g, 53%); R_f 0.45 (20% EtOAc-Hexane); ^{1}H-NMR (400 MHz, $CDCl_3$) δ 6.76 (2H, m, H-1 and H-2), 6.73 (1H, d, *J* = 1.6 Hz, H-3), 3.80 (3H, s, OCH_3), 3.78 (3H, s, OCH_3), 3.64 (1H, dd, *J* = 8.4 and 6.4 Hz, H-3'), 1.75 (2H, m, H-1'), 1.41 (2H, m, H-2'), 0.87 (3H, t, *J* = 7.2 Hz, H-4').

***2-cyclopentyl-2-(3,4-dimethoxyphenyl)acetonitrile* (3.7f)**

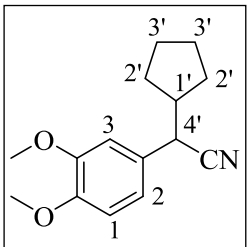

$C_{15}H_{21}NO_2$
Ext Mass: 247.16

White solid (1.66 g, 60%); m.p. 90-93 ^{o}C; R_f 0.50 (20% EtOAc-Hexane); ^{1}H-NMR (400 MHz, $CDCl_3$) δ 6.86 (2H, m, H-2 and H-1), 6.84 (1H, m, H-3), 3.91 (3H, s, OCH_3), 3.89 (3H, s, OCH_3), 3.66 (1H, d, *J* = 8.0 Hz, H-4'), 2.32-1.37 (9H, m, H-1', H-2' and H-3'); ^{13}C-NMR (101 MHz, $CDCl_3$) δ 149.3, 148.8, 128.3, 120.7, 119.9, 111.4, 110.7, 56.0, 55.9, 45.2, 42.1, 30.9, 30.3, 24.9 and 24.8.

***2-cyclohexyl-2-(3,4-dimethoxyphenyl)acetonitrile* (3.7g)**

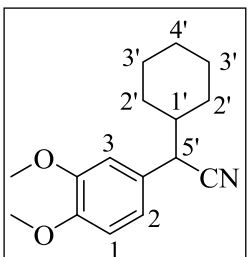

$C_{16}H_{24}NO_3$
Ex. Mass: 278.18

White solid (0.70 g, 50%); m.p. 84 - 86 ^{o}C; R_f 0.50 (25% EtOAc-Hexane); ^{1}H-NMR (400 MHz, $CDCl_3$) δ 6.85 (2H, m, H-2 and H-1), 6.80 (1H, m, H-3), 3.91 (3H, s, OCH_3), 3.89 (3H, s, OCH_3), 3.58 (1H, d, *J* = 6.8 Hz, H-5'), 1.89-1.19 (11H, m, H-1', H-2', H-3' and H-4'); ^{13}C-

NMR (101 MHz, $CDCl_3$) δ 149.2, 148.7, 127.1, 120.3, 120.2, 111.3, 111.0, 56.0, 55.9, 43.9, 42.8, 31.1, 29.7 (2C), 25.9 and 25.8.

General method 2: Synthesis intermediates 3.6y(a-g)

Diisopropylamine (0.68 ml, 4.6 mmol) in 20 ml of THF was cooled to -78 ^oC and 2.7N *n*-BuLi in hexanes (2.86 ml, 7.72 mmol) was introduced drop-wise using a syringe. After stirring the resulting mixture for 15 minutes, compound **3.7** (4.55 mmol) dissolved in anhydrous THF (5 ml) was added drop-wise over 8-10 min. The resulting reaction mixture was further stirred at -78 ^oC for 0.5 h before 1-bromo-3-chloropropane (4.8 g, 6.81 mmol) dissolved in THF (5 ml) was added drop-wise. The resulting reaction mixture was continued to be stirred at -78 ^oC for 20 min and then allowed to warm to room temperature (25 °C) and stirred for another 1 h. After completion of reaction (TLC), the reaction mixture was cooled to 0 ^oC and quenched with 20 ml of water added drop-wise, and extracted with ethyl acetate (3 × 20 ml). The extracts were dried over anhydrous $MgSO_4$ and evaporated *in vacuo*. The residue was purified by column chromatography to afford **3.6y**. To obtain **3.6x,** a solution of 1-2-dibromoethane in anhydrous THF (5 ml) was added instead of 1-bromo-3-chloropropane.

5-chloro-2-(3,4-dimethoxyphenyl)-2-isopropylpentanenitrile **(3.6ya)**[4]

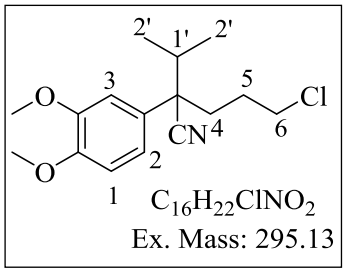

Oil (1.10 g, 81%); R_f 0.40 (25% EtOAc-Hexane); ^{1}H-NMR (400 MHz, $CDCl_3$) δ 6.92 (1H, dd, *J* = 8.0 and 2.0 Hz, H-2), 6.85 (1H, d, *J* = 8.0 Hz, H-1), 6.84 (1H, d, *J* = 2.0 Hz, H-3), 3.89 (3H, s, OC*H*$_3$), 3.88 (3H, s, OC*H*$_3$), 3.49 (2H, m, H-6), 2.22 (1H, m, H-4), 2.05 (2H, m, H-1' and H-4), 1.86 (1H, m, H-5), 1.46 (1H, m, H-5), 1.21 (3H, d, *J* = 6.8 Hz, H-2'), 0.80 (3H, d, *J* = 6.8 Hz, H-2').

5-chloro-2-(3,4-dimethoxyphenyl)pentanenitrile **(3.6yb)**

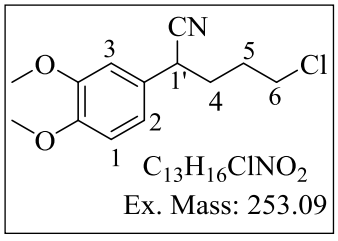

Oil (0.47 g, 41%); R_f 0.20 (20% EtOAc-Hexane); ^{1}H-MR (400 MHz, $CDCl_3$) δ 6.80 (1H, dd, *J* = 8.0 and 2.0 Hz, H-2), 6.76 (1H, d, *J* = 8.0 Hz, H-1), 6.74 (1H, d, *J* = 1.6 Hz, H-3), 3.81 (3H, s,

OCH_3), 3.79 (3H, s, OCH_3), 3.70 (1H, t, *J* = 7.2 Hz H-1'), 3.47 (2H, t, *J* = 6.0 Hz, H-6), 1.97 (2H, m, H-4), 1.85 (2H, m, H-5); ^{13}C-NMR (101 MHz, $CDCl_3$) δ 149.6, 148.7, 127.7(2C), 119.6, 112.0, 110.3, 56.1 9 (2C), 43.9, 36.3, 33.5, 29.7; LRMS (EI): *m/z* 253.31 $[M]^+$.

***5-chloro-2-(3,4-dimethoxyphenyl)-2-methylpentanenitrile* (3.6yc)**

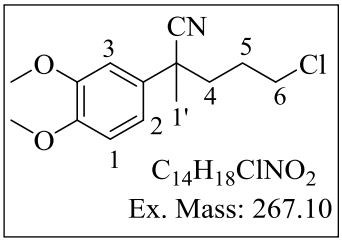

Oil (0.80 g, 66%); R_f 0.20 (20% EtOAc-Hexane); ^{1}H-NMR (400 MHz, $CDCl_3$) δ 6.92 (1H, dd, *J* = 8.0 and 2.4 Hz, H-2), 6.86 (1H, d, *J* = 1.6 Hz, H-3), 6.80 (1H, d, *J* = 8.0 Hz, H-1), 3.84 (3H, s, OCH_3), 3.82 (3H, s, OCH_3), 3.44 (2H, t, *J* = 6.2 Hz, H-6), 2.01 (2H, m, H-4), 1.90 (2H, m, H-5), 1.66 (3H, s, H-1'). ^{13}C-NMR (101 MHz, $CDCl_3$) δ 149.4, 148.8, 132.1, 123.2, 117.7, 111.5, 109.0, 56.1, 56.0, 44.4, 41.8, 39.3, 28.6 and 28.3; LRMS (EI): *m/z* 267.22 $[M]^+$.

***5-chloro-2-(3,4-dimethoxyphenyl)-2-ethylpentanenitrile* (3.6yd)**

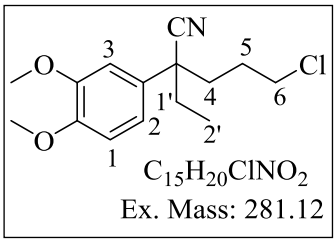

Oil (0.87 g, 68%); R_f 0.45 (20% EtOAc-Hexane); ^{1}H-NMR (400 MHz, $CDCl_3$) δ 6.85 (1H, dd, *J* = 8.0 and 2.0 Hz, H-2), 6.76 (1H, d, *J* = 2.0 Hz, H-3), 6.75 (1H, d, *J* = 8.0 Hz, H-1) 3.81 (3H, s, OCH_3), 3.79 (3H, s, OCH_3), 3.43 (2H, t, *J* = 6.4 Hz, H-6), 2.06 (2H, m, H-4), 1.85 (2H, m, H-1'), 1.55 (1H, m, H-5), 1.15 (1H, m, H-5), 0.82 (3H, t, *J* = 6.8 Hz, H-2'); ^{13}C-NMR (101 MHz, $CDCl_3$) δ 149.6, 149.1, 130.3, 121.8, 119.0, 112.2, 109.7, 56.1, 56.0, 44.5, 43.6 (2C), 38.2, 28.3 and 12.1; LRMS (EI): *m/z* 281.20 $[M]^+$.

***5-chloro-2-(3,4-dimethoxyphenyl)-2-propylpentanenitrile* (3.6ye)**[5]

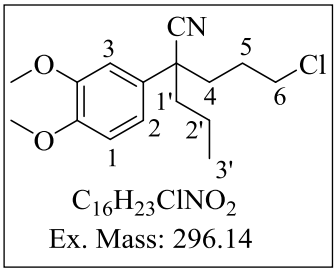

Oil (0.89 g, 66%); R_f 0.20 (20% EtOAc-Hexane); ^{1}H-NMR (400 MHz, $CDCl_3$) δ 6.88 (1H, dd, *J* = 8.4 and 2.4 Hz, H-2), 6.80 (1H, d, *J* = 2.0 Hz, H-3), 6.80 (1H, d, *J* = 8.0 Hz, H-1), 3.83 (3H, s, OCH_3), 3.81 (3H, s, OCH_3), 3.41 (2H, t, *J* = 6.4 Hz, H-6), 2.02 (2H, m, H-4), 1.87 (2H, m, H-1'), 1.75 (1H, m, H-2'), 1.53 (1H, m, H-5), 1.41 (1H, m, H-2'), 1.12 (1H, m, H-5), 0.82 (3H, t, *J* = 7.2 Hz, H-3').

***5-chloro-2-cyclopentyl-2-(3,4-dimethoxyphenyl)pentanenitrile* (3.6yf)**

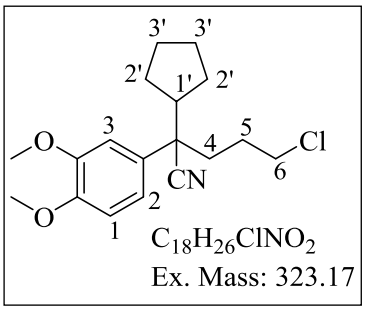

Oil (0.18 g, 46%); R_f 0.50 (20% EtOAc-Hexane); ^{1}H-NMR (400 MHz, $CDCl_3$) δ 6.97 (1H, dd, *J* = 8.4 and 2.4 Hz, H-2), 6.87 (2H, m, H-1 and H-3), 3.90 (3H, s, OC*H*$_3$), 3.89 (3H, s, OC*H*$_3$), 3.47 (2H, m, H-6), 2.30 (1H, m, H-1'), 2.13 (2H, m, H-4), 1.99-1.30 (10H, m, H-5, H-2' and H-3').

***5-chloro-2-cyclohexyl-2-(3,4-dimethoxyphenyl)pentanenitrile* (3.6yg)**

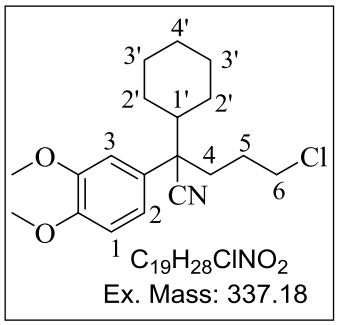

Oil (0.17 g, 43%); R_f 0.60 (25% EtOAc-Hexane); ^{1}H-NMR (400 MHz, $CDCl_3$) δ 6.92 (1H, dd, *J* = 8.4 and 2.4 Hz, H-2), 6.85 (2H, m, H-1 and H-3), 3.90 (3H, s, OC*H*$_3$), 3.89 (3H, s, OC*H*$_3$), 3.48 (2H, m, H-6), 2.26 (1H, m, H-1'), 2.05 (2H, m, H-4), 1.87-1.08 (12H, m, H-5, H-2', H-3' and H-4').

***4-bromo-2-(3,4-dimethoxyphenyl)-2-isopropylbutanenitrile* (3.6xa)**

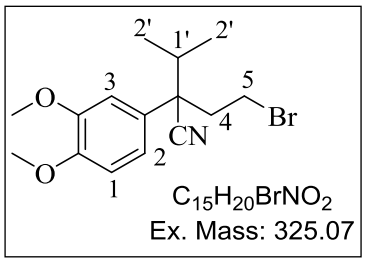

White solid (76%); m.p. 76-78 °C; R_f 0.60 (30% EtOAc-Hexane); ^{1}H-NMR (400 MHz, $CDCl_3$) δ 6.91 (1H, dd, *J* = 8.4 and 2.4 Hz, H-2), 6.86 (1H, d, *J* = 8.4 Hz, H-1), 6.84 (1H, d, *J* = 2.0 Hz, H-3), 3.88 (3H, s, OC*H*$_3$), 3.87 (3H, s, OC*H*$_3$), 3.31 (1H, m, H-5), 2.88 (1H, m, H-5), 2.66 (1H, m, H-4), 2.34 (1H, m, H-4), 2.31 (1H, m, H-1'), 1.21 (3H, d, *J* = 6.8 Hz, H-2'), 0.79 (3H, d, *J* = 6.8 Hz, H-2'). ^{13}C-NMR (101 MHz, $CDCl_3$) δ 149.5, 148.9, 128.9, 120.2, 118.6, 111.5, 109.5, 56.1, 55.9, 41.3, 38.1, 32.7, 27.2, 18.6 and 18.4.

General method 3: Boc protection and synthesis of intermediate 3.4 (a-c)

Et_3N (1.98 g, 2.73 ml, 19.6 mmol) was added to a solution of 3,4-dimethoxyamine **3.2** (13.1 mmol) in DCM (15 ml) at 0 °C. After 10 minutes, a solution of di-*tert*-butyl dicarbonate (3.39 g, 15.6 mmol) in DCM was added drop-wise to the reaction mixture. After completion

of reaction (TLC), DCM was removed under reduced pressure and the residue was taken in EtOAc (15 ml). The organic phase was washed with brine (3 × 10 ml), dried over anhydrous sodium sulphate and concentrated *in vacuo* to obtain desired compound **3.4**.

***tert-butyl (3,4-dimethoxyphenyl)carbamate* (3.4a)**[6]

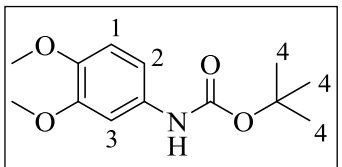

$C_{13}H_{19}NO_4$
Ex. Mass: 253.13

Grey solid (2.21 g**,** 67%); m.p. 84-86 °C; R_f 0.20 (20% EtOAc-Hexane); ^{1}H-NMR (400 MHz, $CDCl_3$) δ 6.76 (1H, d, *J* = 8.0 Hz, H-1), 6.72 (1H, m, H-3), 6.71 (1H, dd, *J* = 8.0 and 2.4 Hz, H-2), 3.86 (3H, s, OC*H*$_3$), 3.83 (3H, s, OC*H*$_3$), 1.51 (9H, s, H-4).

***tert-butyl (3,4-dimethoxybenzyl)carbamate* (3.4b)**[6]

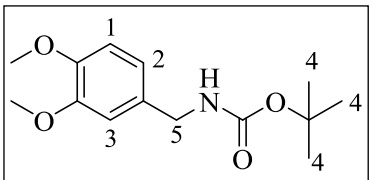

$C_{14}H_{21}NO_4$
Ex. Mass: 267.15

White solid (2.96 g, 85%); m.p. 55-58 °C; R_f 0.35 (20% EtOAc-Hexane); ^{1}H-NMR (400 MHz, $CDCl_3$) δ 6.83 (1H, d, *J* = 8.0 Hz, H-1), 6.81 (1H, d, *J* = 1.2 Hz, H-3), 6.71 (1H, m, H-2), 4.80 (1H, br s, NH), 4.23 (2H, br d, *J* = 6.0 Hz, H-5), 3.86 (3H, s, OC*H*$_3$), 3.84 (3H, s, OC*H*$_3$), 1.46 (9H, s, H-4).

***tert-butyl (3,4-dimethoxyphenethyl)carbamate* (3.4c)**[7]

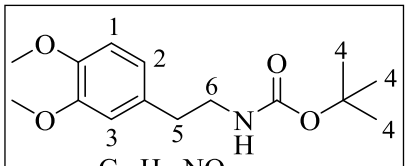

$C_{15}H_{23}NO_4$
Ex. Mass: 281.16

White solid (3.45 g, 94%); m.p. 64-66 °C; R_f 0.45 (20% EtOAc-Hexane); ^{1}H-NMR (400 MHz, $CDCl_3$) δ 6.80 (1H, d, *J* = 8.0 Hz, H-1), 6.73 (1H, d, *J* = 1.6 Hz, H-3), 6.73 (1H, dd, *J* = 8.0 and 1.6 Hz, H-2), 3.86 (3H, s, OC*H*$_3$), 3.85 (3H, s, OC*H*$_3$), 3.34 (2H, t, *J* = 6.8 Hz, H-6), 2.73 (2H, t, *J* = 6.8 Hz, H-5), 1.42 (9H, s, H-4).

General method 4: Synthesis of intermediates 3.3(a-d)

NaH (60% in mineral oil, 19.2 mmol) was added to a solution of compound **3.4** (7.6 mmol) in anhydrous DMF (6 ml) at 0 °C. After 15 minutes, reaction mixture was charged with corresponding bromoalkane (11.5 mmol). After completion of reaction (TLC), DMF was removed under reduced pressure and the residue was taken in EtOAc (20 ml), washed with brine (3 × 15 ml), dried over anhydrous $MgSO_4$ and concentrated *in vacuo* to obtain crude product. Purification by column chromatography afforded pure **3.3**.

***tert-butyl (3,4-dimethoxyphenyl)(methyl)carbamate* (3.3a)**

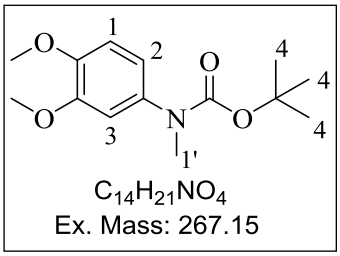

Oil (1.31 g 65%); R_f 0.20 (20% EtOAc-Hexane); ^{1}H-NMR (400 MHz, $CDCl_3$) δ 6.76 (1H, d, *J* = 2.4 Hz, H-3), 6.70 (1H, d, *J* = 8.0 Hz, H-1), 6.40 (1H, dd, *J* = 8.0 and 2.4 Hz, H-2), 3.75 (6H, s, 2 × OCH_3), 3.11 (3H, s, H-1'), 1.33 (9H, s, H-4).

***tert-butyl (3,4-dimethoxybenzyl)(methyl)carbamate* (3.3b)**

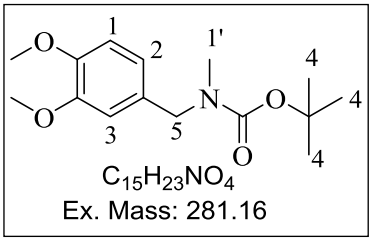

Oil (1.10 g, 51%); R_f 0.25 (20% EtOAc-Hexane); ^{1}H-NMR (400 MHz, $CDCl_3$) δ 6.78 (2H, m, H-2 and H-3), 6.75 (1H, d, *J* = 8.0 Hz, H-1), 4.34 (2H, s, H-5), 3.86 (6H, s, 2 × OCH_3), 2.78 (3H, s, H-1'), 1.48 (9H, s, H-4).

***tert-butyl (3,4-dimethoxyphenethyl)(ethyl)carbamate* (3.3c)**

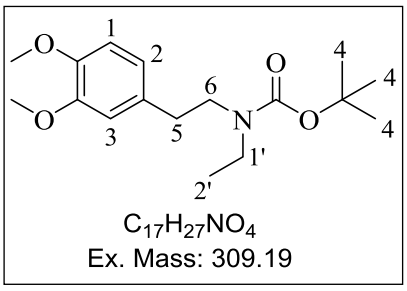

Oil (1.26 g, 54%); R_f 0.60 (20% EtOAc-Hexane); ^{1}H-NMR (400 MHz, $CDCl_3$) δ 6.72 (1H, d, *J* = 8.0 Hz, H-1), 6.65 (1H, d, *J* = 2.0 Hz, H-3), 6.65 (1H, dd, *J* = 8.0 and 2.0 Hz, H-2), 3.79 (3H, s, OCH_3), 3.78 (3H, s, OCH_3), 3.28 (2H, t, *J* = 6.4 Hz, H-6), 3.11 (2H, m, H-1'), 2.69 (2H, t, *J* = 6.4 Hz, H-5), 1.38 (9H, s, H-4), 1.01 (3H, t, *J* = 7.2 Hz, H-2').

***tert-butyl (3,4-dimethoxyphenethyl)(propyl)carbamate* (3.3d)**

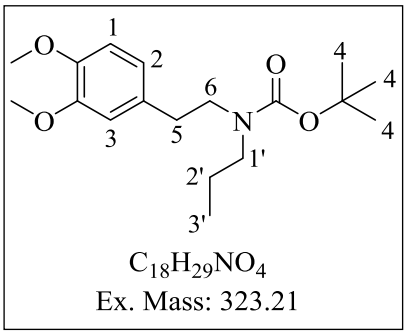

$C_{18}H_{29}NO_4$
Ex. Mass: 323.21

Oil (2.05 g, 84%); R_f 0.30 (10% EtOAc-Hexane); ^{1}H-NMR (400 MHz, $CDCl_3$) δ 6.79 (1H, d, *J* = 8.0 Hz, H-1), 6.65 (2H, m, H-2 and H-3), 3.87 (3H, s, OCH_3), 3.85 (3H, s, OCH_3), 3.35 (2H, t, *J* = 7.2 Hz, H-6), 3.10 (2H, t, *J* = 8.4 Hz, H-1'), 2.80 (2H, t, *J* = 7.6 Hz, H-5), 2.30 (2H, m, H-2'), 1.45 (9H, s, H-4), 0.86 (3H, t, *J* = 8.4 Hz, H-3').

General method 5: Boc deprotection and synthesis of intermediate 3.2(a-d)

A 10% solution TFA (3.69 g, 2.48 ml, 32.4 mmol) in DCM (v/v) was added to a solution of compound **3.3** (3.24 mmol) in DCM (10 ml), and stirred for 2 hour. After completion of the reaction (TLC), the solvent was removed *in vacuo* and the residue was dissolved in MeOH. The solution was charged with excess of Amberlyst A-21 for neutralisation and stirred for 30 minutes. After complete neutralisation (pH ≥ 7), the mixture was filtered, and filtrate was concentrated to obtain compound **3.2**.

***3,4-dimethoxy-N-methylaniline* (3.2a)**[8]

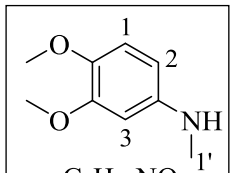

$C_9H_{13}NO_2$
Ex. Mass: 167.09

Oil (0.36 g, 67%); R_f 0.35 (20% EtOAc-Hexane); ^{1}H-NMR (400 MHz, $CDCl_3$) δ 6.70 (1H, d, *J* = 7.2 Hz, H-1), 6.16 (1H, d, *J* = 2.4 Hz, H-3), 6.10 (1H, dd, *J* = 8.0 and 2.4 Hz, H-2), 3.75 (3H, s, OCH_3), 3.72 (3H, s, OCH_3), 2.72 (3H, s, H-1').

***1-(3,4-dimethoxyphenyl)-N-methylmethylamine* (3.2b)**[8]

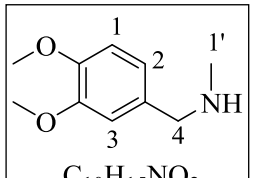

$C_{10}H_{15}NO_2$
Ex. Mass: 181.11

Oil (0.34 g, 58%); R_f 0.40 (20% EtOAc-Hexane); ^{1}H-NMR (400 MHz, $CDCl_3$) δ 6.83 (1H, d, *J* = 1.6 Hz, H-3), 6.78 (1H, dd, *J* = 8.0 and 1.6 Hz, H-2), 6.74 (1H, d, *J* = 8.0 Hz, H-1), 3.82 (3H, s, OCH_3), 3.80 (3H, s, OCH_3), 3.62 (2H, s, H-4), 2.39 (3H, s, H-1').

***2-(3,4-dimethoxyphenyl)-N-ethylethan-1-amine* (3.2c)**

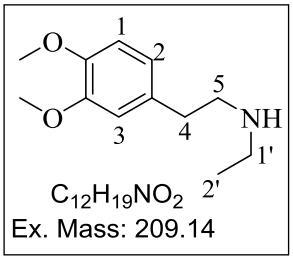

Oil (0.59 g, 87%); R_f 0.80 (20% EtOAc-Hexane); ^{1}H-NMR (400 MHz, $CDCl_3$) δ 6.72 (1H, d, *J* = 8.0 Hz, H-1), 6.72 (1H, d, *J* = 2.0 Hz, H-3), 6.72 (1H, dd, *J* = 8.0 and 2.0 Hz, H-2), 3.78 (3H, br s, OC*H*$_3$), 3.77 (3H, s, OC*H*$_3$), 3.0 (2H, t, *J* = 6.8 Hz, H-5), 2.87 (2H, t, *J* = 7.2 Hz, H-1'), 2.87 (2H, t, *J* = 6.4 Hz, H-4), 1.22 (3H, t, *J* = 7.2 Hz, H-2').

***N-(3,4-dimethoxyphenethyl)propan-1-amine* (3.2d)**

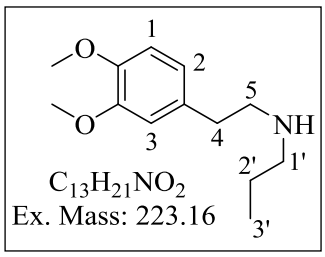

Yellow Solid (0.65 g, 90%); m.p. 89-92 °C; R_f 0.65 (20% EtOAc-Hexane); ^{1}H-NMR (400 MHz, $CDCl_3$) δ 9.38 (1H, s, NH), 6.72 (1H, d, *J* = 8.0 Hz, H-1), 6.64 (2H, m, H-2 and H-3), 3.75 (3H, s, OC*H*$_3$), 3.77 (3H, s, OC*H*$_3$), 3.07 (2H, t, *J* = 6.4 Hz, H-5), 2.87 (4H, m, H-4 and H-1'), 1.69 (2H, m, H-2'), 0.91 (3H, t, *J* = 7.2 Hz, H-3').

General method 6: Coupling of 3.6 and 3.2 to synthesise target compound 3.13

K_2CO_3 (0.53 g, 3.82 mmol) and **3.2** (1.50 mmol) were added to a solution of compound **3.6y** (2.0 mmol) in anhydrous DMF (5 ml). The reaction mixture was stirred at 80 ^oC for 12 h. After completion of reaction (TLC), DMF was removed under reduced pressure and the residue was taken in EtOAc (20 ml), washed with brine (3×15 ml), dried over anhydrous $MgSO_4$ and concentrated *in vacuo*. The residue was purified by flash chromatography on silica gel using DCM-MeOH to afford the product **3.13**.

***2-(3,4-dimethoxyphenyl)-5-((3,4-dimethoxyphenyl)(methyl)amino)-2-isopropylpentanenitrile* (3.13a)**

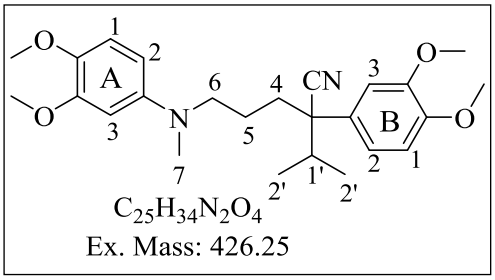

White solid (0.19 g, 29%); m.p. 115-117 °C; R_f 0.25 (5% MeOH-DCM); ^{1}H-NMR (400 MHz, $CDCl_3$) δ 6.85 (1H, dd, *J* = 8.4 and 2.4 Hz, H-2B), 6.75 (1H, d, *J* = 2.4 Hz, H-3B), 6.75 (1H, d, *J* = 8.4 Hz, H-1B), 6.68 (1H, d, *J* = 8.4 Hz, H-1A), 6.22 (1H,

d, *J* = 1.6 Hz, H-3A), 6.10 (1H, dd, *J* = 8.4 and 2.0 Hz, H-2A), 3.80 (3H, s, OC*H*$_3$), 3.78 (3H, s, OC*H*$_3$), 3.76 (3H, s, OC*H*$_3$), 3.73 (3H, s, OC*H*$_3$), 3.09 (2H, m, H-6), 2.68 (3H, s, H-7), 2.06 (1H, td, *J* = 12.4 and 4.4 Hz, H-4), 1.97 (1H, m, H-1'), 1.75 (1H, td, *J* = 12.8 and 4.4 Hz, H-4), 1.56 (1H, m, H-5), 1.25 (1H, m, H-5), 1.10 (3H, d, *J* = 6.8 Hz, H-2'), 0.72 (3H, d, *J* = 6.8 Hz, H-2'); ^{13}C-NMR (101 MHz, $CDCl_3$) δ 149.9, 149.2, 148.3, 147.2, 130.4, 129.3, 121.4, 118.7, 113.3, 111.3, 109.6, 105.0, 99.6, 56.7, 56.0 (3C), 53.5, 53.3, 38.9, 37.9, 35.3, 23.3, 18.9 and 18.4; LRMS (EI): *m/z* 426.23 $[M]^+$; HPLC purity 97% (t_r = 7.8 min) .

***5-((3,4-dimethoxybenzyl)(methyl)amino)-2-(3,4-dimethoxyphenyl)-2-isopropylpentanenitrile* (3.13b)**

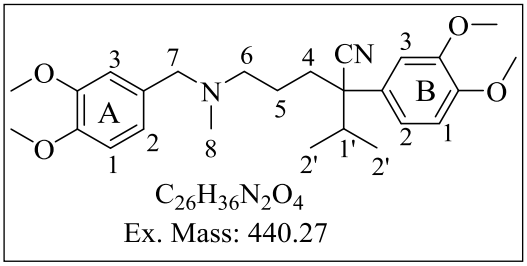

$C_{26}H_{36}N_2O_4$
Ex. Mass: 440.27

Oil (0.25 g, 34%); R_f 0.55 (10% MeOH-DCM); ^{1}H-NMR (400 MHz, $CDCl_3$) δ 6.86 (1H, dd, *J* = 7.6 and 2.0 Hz, H-2B), 6.78 (1H, d, *J* = 2.0 Hz, H-3B), 6.76 (1H, d, *J* = 8.0 Hz, H-1B), 6.74 (1H, d, *J* = 8.0 Hz, H-1A), 6.70 (1H, d, *J* = 1.6 Hz, H-3A), 6.70 (1H, dd, *J* = 8.0 and 1.6 Hz, H-2A), 3.81 (3H, s, OC*H*$_3$), 3.80 (3H, s, OC*H*$_3$), 3.79 (3H, s, OC*H*$_3$), 3.78 (3H, s, OC*H*$_3$), 3.28 (2H, s, H-7), 2.22 (2H, t, *J* = 8.4 Hz, H-6), 2.10 (1H, m, H-4), 2.03 (3H, s, H-8), 1.98 (1H, m, H-1'), 1.77 (1H, m, H-4), 1.52 (1H, m, H-5), 1.14 (1H, m, H-5), 1.14 (3H, d, *J* = 6.4 Hz, 3H, H-2'), 0.73 (3H, d, *J* = 6.8 Hz, H-2'); ^{13}C-NMR (101 MHz, $CDCl_3$) δ 150.2, 149.1, 148.9, 148.4, 130.7, 121.5, 121.0, 118.8 (2C), 112.1, 111.2, 110.9, 109.8, 61.9, 56.4, 56.1, 56.0 (3C), 53.3, 42.1, 38.0, 35.6, 23.4, 19.0 and 18.6; LRMS (EI): *m/z* 440.24 $[M]^+$; HPLC purity 98% (t_r = 10.2 min).

***4-((3,4-dimethoxybenzyl)(methyl)amino)-2-(3,4-dimethoxyphenyl)-2-isopropylbutanenitrile* (3.13c)**

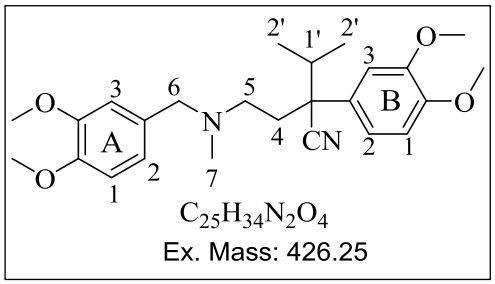

$C_{25}H_{34}N_2O_4$
Ex. Mass: 426.25

Oil (0.19 g, 29%); R_f 0.50 (10% MeOH-DCM); ^{1}H-NMR (400 MHz, $CDCl_3$) δ 6.91 (1H, dd, *J* = 8.4 and 2.4 Hz, H-2B), 6.86 (1H, m, H-3B), 6.83 (1H, d, *J* = 8.4 Hz, H-1B), 6.78 (1H, d, *J* = 8.8 Hz, H-1A), 6.74 (1H, d, *J* = 2.4 Hz, H-3A), 6.70 (1H, dd, *J* = 8.4 and 2.0 Hz, H-2A), 3.91 (6H, s, 2 × OC*H*$_3$),

3.89 (3H, s, OCH_3), 3.87 (3H, s, OCH_3), 3.34 (2H, m, H-6), 2.41 (2H, m, H-5), 2.18 (3H, s, H-7), 2.10 (2H, m, H-4), 2.01 (1H, m, H-1'), 1.21 (3H, d, J = 6.8 Hz, H-2'), 0.82 (3H, d, J = 6.8 Hz, H-2'). ^{13}C-NMR (101 MHz, $CDCl_3$) δ 149.1, 149.0, 148.4, 148.2, 131.3, 130.2, 121.1, 121.2, 118.6, 112.2, 111.2, 110.9, 109.7, 62.3, 56.0, 55.9, 55.8, 55.9, 53.8, 51.6, 42.2, 38.4, 35.4 and 18.2 (2C); LRMS (EI): *m/z* 426.22 $[M]^+$; HPLC purity 98% (t_r = 10.2 min).

***2-(3,4-Dimethoxy-phenyl)-2-(2-{[2-(3,4-dimethoxy-phenyl)-ethyl]-methyl-amino}-ethyl)-3-methyl-butyronitrile* (3.13d)**

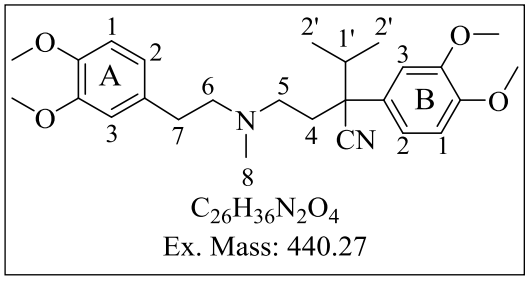

Oil (0.27 g, 40%); R_f 0.55 (10% MeOH-DCM); ^{1}H-NMR (400 MHz, $CDCl_3$) δ 6.96 (1H, dd, J = 8.4 and 2.4 Hz, H-2B), 6.90 (1H, d, J = 2.0 Hz, H-3B), 6.88 (1H, d, J = 8.4 Hz, H-1B), 6.80 (1H, d, J = 8.8 Hz, H-1A), 6.70 (2H, m, H-2A and H-3A), 3.91 (6H, s, 2 × OCH_3), 3.89 (3H, s, OCH_3), 3.87 (3H, s, OCH_3), 2.69 (2H, m, H-6), 2.57 (2H, m, H-7), 2.51 (1H, m, H-5), 2.40 (1H, m, H-5), 2.31 (3H, s, H-8), 2.10 (3H, m, H-4 and H-1'), 1.21 (3H, d, J = 6.4 Hz, H-2'), 0.84 (3H, d, J = 6.4 Hz, H-2'); ^{13}C-NMR (101 MHz, $CDCl_3$) δ 149.2, 149.0, 148.5, 147.5, 132.8, 130.2, 121.1, 120.5, 118.8, 112.2, 111.5, 111.2, 109.6, 59.72, 56.1, 56.0 (2C), 55.9 (2C), 53.9, 51.7, 42.2, 38.3, 35.2, 33.3 and 18.1; LRMS (EI): *m/z* 441.48 $[M+H]^+$; HPLC purity 98% (t_r = 10.3 min).

***5-((3,4-dimethoxyphenethyl)amino)-2-(3,4-dimethoxyphenyl)-2-isopropylpentanenitrile* (3.13e)**

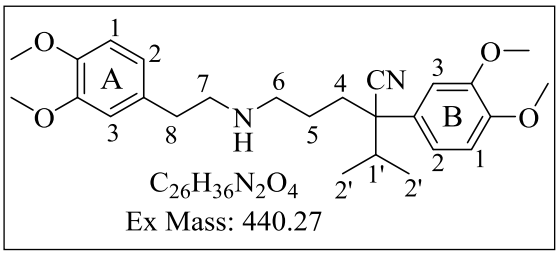

Oil (0.27 g, 37%); R_f 0.45 (10% MeOH-DCM); ^{1}H-NMR (400 MHz, $CDCl_3$) δ 6.89 (1H, dd, J = 8.0 and 2.0 Hz, H-2B), 6.83 (1H, d, J = 2.4 Hz, H-3B), 6.83 (1H, d, J = 8.0 Hz, H-1B), 6.78 (1H, d, J = 8.0 Hz, H-1A), 6.70 (1H, d, J = 2.0 Hz, H-3A), 6.70 (1H, dd, J = 8.0 and 2.0 Hz, H-2A), 3.84 (3H, s, OCH_3), 3.83 (3H, s, OCH_3), 3.81 (6H, s, 2 × OCH_3), 2.75 (2H, t, J = 6.4 Hz, H-7), 2.68 (2H, t, J = 6.4, H-8), 2.56 (2H, m, H-6), 2.05 (1H, m, J = 6.4, H-1'), 2.06 (1H, td, J = 12.0 and 4.4 Hz, H-4), 1.80 (1H, td, J =

8.8 and 4.4 Hz, H-4), 1.51 (1H, m, H-5), 1.15 (1H, m, H-5), 1.13 (3H, d, *J* = 6.79 Hz, H-2'), 0.75 (3H, d, *J* = 6.79 Hz, H-2'); ^{13}C-NMR (101 MHz, $CDCl_3$) δ 149.4, 149.1, 148.0, 147.1, 132.5, 130.6, 121.4, 120.6, 118.7, 112.1, 111.5, 111.3, 109.8, 56.1, 55.9 (3C), 53.3, 50.8, 49.2, 37.9, 35.6 (2C), 25.8, 18.9 and 18.6; LRMS (EI): *m/z* 441.28 $[M+H]^+$; HPLC purity 97% (t_r = 7.8 min).

***5-((3,4-dimethoxyphenethyl)(ethyl)amino)-2-(3,4-dimethoxyphenyl)-2-isopropylpentanenitrile* (3.13f)**

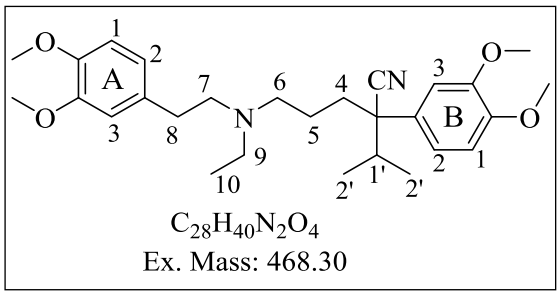

$C_{28}H_{40}N_2O_4$
Ex. Mass: 468.30

Oil (0.22 g, 33%); R_f 0.50 (10% MeOH-DCM); ^{1}H-NMR (400 MHz, $CDCl_3$) δ 6.84 (1H, dd, *J* = 8.0 and 2.0 Hz, H-2B), 6.81 (1H, d, *J* = 2.0 Hz, H-3B), 6.76 (1H, d, *J* = 8.0 Hz, H-1B), 6.71 (1H, d, *J* = 8.0, H-1A), 6.62 (1H, d, *J* = 2.0, H-3A), 6.60 (1H, dd, *J* = 8.0 and 2.0 Hz, H-2A), 3.83 (3H, s, OCH_3), 3.82 (3H, s, OCH_3), 3.81 (3H, s, OCH_3), 3.80 (3H, s, OCH_3), 2.55 (2H, t, *J* = 4.4 Hz, H-7), 2.50 (2H, t, *J* = 4.4 Hz, H-8), 2.43 (4H, m, H-6 and H-9), 2.05 (2H, m, H-1' and H-4), 1.78 (1H, m, H-4), 1.49 (1H, m, H-5), 1.13 (3H, d, *J* = 6.8 Hz, H-2'), 1.11 (1H, m, H-5), 0.94 (3H, t, *J* = 7.2 Hz, H-10), 0.75 (3H, d, *J* = 6.8 Hz, H-2'); ^{13}C-NMR (101 MHz, $CDCl_3$) δ 148.9, 148.3, 147.3, 146.5, 133.3, 130.8, 121.5, 120.5, 118.7, 112.2, 111.4, 111.2, 109.9, 56.0, 55.9 (2C), 55.3 (2C), 52.9, 47.3, 37.8, 35.7 (2C), 33.0, 23.4, 18.9, 18.6 and 11.7; LRMS (EI): *m/z* 469.31 $[M+H]^+$; HPLC purity 98% (t_r = 8.2 min).

***5-((3,4-dimethoxyphenethyl)(propyl)amino)-2-(3,4-dimethoxyphenyl)-2-isopropylpentanenitrile* (3.13g)**

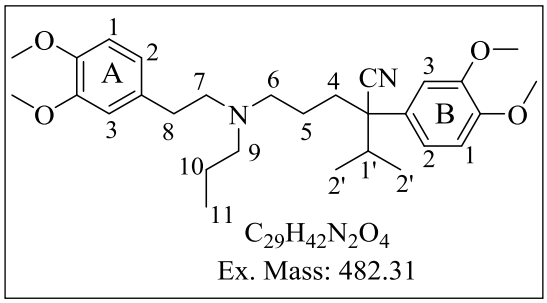

$C_{29}H_{42}N_2O_4$
Ex. Mass: 482.31

Oil (0.11 g, 17%); R_f 0.20 (70% EtOAc-Hexane); ^{1}H-NMR (400 MHz, $CDCl_3$) δ 6.90 (1H, dd, *J* = 8.0 and 2.4 Hz, H-2B), 6.86 (1H, d, *J* = 2.0 Hz, H-3B), 6.84 (1H, d, *J* = 8.0 Hz, H-1B), 6.79 (1H, d, *J* = 8.0 Hz, H-1A), 6.67 (1H, d, *J* = 2.0 Hz, H-3A), 6.67 (1H, dd, *J* = 8.0 and 2.0 Hz, H-2A), 3.84 (3H, s, OCH_3), 3.83 (3H, s, OCH_3), 3.82 (3H, s, OCH_3), 3.81 (3H, s, OCH_3), 2.54

(4H, m, H-7 and H-9), 2.39 (2H, t, *J* = 6.8 Hz, H-8), 2.30 (2H, t, *J* = 7.2 Hz, H-6), 2.10 (1H, td, *J* = 12.0 and 4.8 Hz, H-4)), 2.05 (1H, m, H-1'), 1.77 (1H, td, *J* = 4.8 and 2.0 Hz, H-4), 1.48 (1H, m, H-5), 1.37 (2H, m, H-10), 1.14 (3H, d, *J* = 6.8 Hz, H-2'), 1.08 (1H, m, H-5), 0.81 (3H, t, *J* = 7.2 Hz, H-11), 0.75 (3H, d, *J* = 6.72 Hz, H-2'); ^{13}C-NMR (101 MHz, $CDCl_3$) δ 150.1, 149.2, 148.9, 148.7, 133.8, 130.7, 121.5, 120.4, 118.7, 112.7, 111.3, 111.1, 109.8, 56.0 (3C), 55.9, 54.4, 53.5, 53.3, 41.1, 37.9, 35.8, 33.1, 23.4, 20.3, 18.9 (2C) and 11.9; HRMS (ESI): *m/z* 483.3221 $[M+H]^+$; HPLC purity 97% (t_r = 8.5 min).

***5-(benzyl(3,4-dimethoxyphenethyl)amino)-2-(3,4-dimethoxyphenyl)-2-isopropylpentanenitrile* (3.13h)**

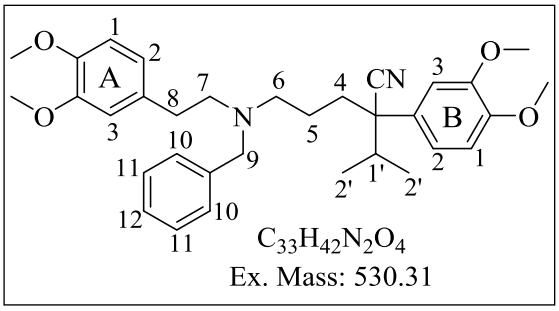

Oil (0.16 g, 26%); R_f 0.65 (10% MeOH-DCM); ^{1}H-NMR (400 MHz, $CDCl_3$) δ 7.21 (5H, m, H-10, H-11 and H-12), 6.86 (1H, dd, *J* = 8.4 and 2.0 Hz, H-2B), 6.81 (1H, d, *J* = 2.0 Hz, H-3B), 6.81 (1H, d, *J* = 8.0 Hz, H-1B), 6.76 (1H, d, *J* = 8.8 Hz, H-1A), 6.63 (1H, d, *J* = 2.4 Hz, H-3A), 6.63 (1H, dd, *J* = 8.0 and 2.4 Hz, H-2A), 3.82 (3H, s, OCH_3), 3.80 (3H, s, OCH_3), 3.77 (6H, s, 2 × OCH_3), 3.49 (2H, s, H-9), 2.60 (4H, m, H-8 and H-7), 2.40 (2H, t, *J* = 6.8 Hz, H-6), 2.00 (2H, m, H-1' and H-4), 1.72 (1H, m, H-4), 1.40 (2H, m, H-5), 1.11 (3H, d, *J* = 6.62 Hz, H-2'), 0.74 (3H, d, *J* = 6.69 Hz, H-2'); ^{13}C-NMR (101 MHz, $CDCl_3$) δ 149.1, 148.9, 148.4, 147.4, 137.8, 133.5, 133.0, 130.7, 128.9, 128.2, 127.0 (2C), 121.5, 120.6, 118.8, 112.2, 111.3, 111.2, 109.8, 58.3, 56.0 (2C), 55.9 (2C), 55.5, 53.3, 53.0, 38.0, 35.5, 32.9, 23.1, 18.9 and 18.6; LRMS (EI): *m/z* 531.32 $[M+H]^+$; HPLC purity 98% (t_r = 8.2 min).

***5-((3,4-dimethoxyphenethyl)(methyl)amino)-2-(3,4-dimethoxyphenyl)pentanenitrile* (3.13i)**

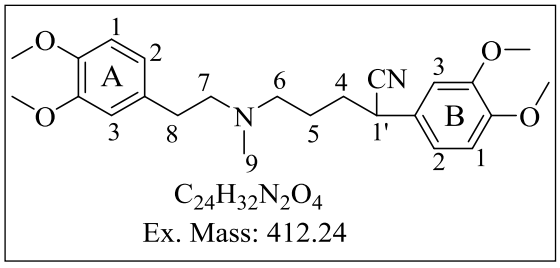

Oil (0.20 g, 32%); R_f 0.30 (10% MeOH-DCM); ^{1}H-NMR (400 MHz, $CDCl_3$) δ 6.82 (3H, m, H-1B, H-2B and H-3B), 6.77 (1H, d, *J* = 8.0 Hz, H-1A), 6.71 (2H, m, H-3A and H-2A), 3.88 (3H, s, OCH_3), 3.86 (3H, s, OCH_3), 3.85 (3H, s, OCH_3), 3.83 (3H, s, OCH_3), 3.75 (1H, dd, *J* = 14.8 and 6.8 Hz, H-1'), 2.69 (2H, t, *J* = 6.8 Hz,

H-7), 2.57 (2H, t, *J* = 6.8 Hz, H-8), 2.43 (2H, t, *J* = 7.6 Hz, H-6), 2.27 (3H, s, H-9), 1.90 (2H, m, H-5), 1.64 (2H, m, H-4); ^{13}C-NMR (101 MHz, $CDCl_3$) δ 149.5, 149.0, 148.9, 147.5, 133.1, 128.3, 121.0, 120.6, 119.6, 112.2, 111.4 (2C), 110.4, 59.7, 56.7, 56.1, 56.0, 55.9, 55.8, 42.1, 36.8, 33.8, 33.5 and 24.7; LRMS (EI): *m/z* 412.09 $[M]^+$; HPLC purity 96% (t_r = 6.8 min).

***5-((3,4-dimethoxyphenethyl)(methyl)amino)-2-(3,4-dimethoxyphenyl)-2-methylpentanenitrile* (3.13j)**

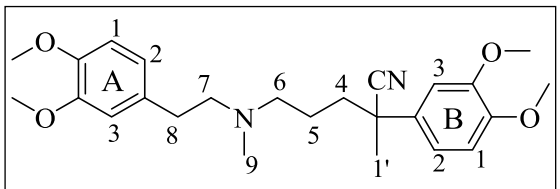

$C_{25}H_{34}N_2O_4$
Ex. Mass: 426.25

Oil (0.32 g, 49%); R_f 0.35 (10% MeOH-DCM); ^{1}H-NMR (400 MHz, $CDCl_3$) δ 7.00 (1H, dd, *J* = 8.0 and 2.4 Hz, H-2B), 6.98 (1H, d, *J* = 2.4 Hz, H-3B), 6.87 (1H, d, *J* = 8.0 Hz, H-1B), 6.82 (1H, d, *J* = 8.0 Hz, H-1A), 6.74 (1H, d, *J* = 2.0 Hz, H-3A), 6.82 (1H, dd, *J* = 8.0 and 2.0 Hz, H-2A), 3.93 (3H, s, OC*H*$_3$), 3.91 (3H, s, OC*H*$_3$), 3.89 (3H, s, OC*H*$_3$), 3.88 (3H, s, OC*H*$_3$), 2.74 (2H, t, *J* = 8 Hz, H-7), 2.61 (2H, t, *J* = 8 Hz, H-8), 2.45 (2H, t, *J* = 6.4 Hz, H-6), 2.29 (3H, s, H-9), 1.96 (2H, m, H-4), 1.72 (3H, s, H-1'), 1.68 (1H, m, H-5), 1.48 (1H, m, H-5); ^{13}C-NMR (101 MHz, $CDCl_3$) δ 149.2, 148.7, 147.5, 146.1, 132.7, 132.5, 123.5, 120.4, 117.7 (2C), 112.0, 111.4, 109.2, 59.2, 56.6, 56.1 (2C), 56.0 (2C), 42.1, 41.9, 39.5, 33.1, 27.9 and 23.0; LRMS (EI): *m/z* 427.26 $[M+H]^+$; HPLC purity 98% (t_r = 7.2 min).

5-((3,4-dimethoxyphenethyl)(methyl)amino)-2-(3,4-dimethoxyphenyl)-2-ethylpentanenitrile (3.13k)

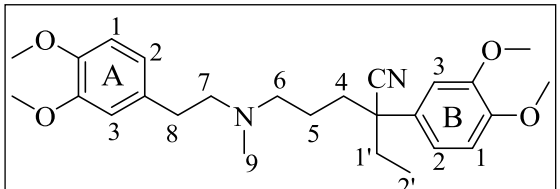

$C_{26}H_{36}N_2O_4$
Ex. Mass: 440.27

Oil (0.62 g, 49%); R_f 0.40 (10% MeOH-DCM); ^{1}H-NMR (400 MHz, $CDCl_3$) δ 6.91 (1H, dd, *J* = 8.0 and 2.0 Hz, H-2B), 6.87 (1H, d, *J* = 1.6 Hz, H-3B), 6.85 (1H, d, *J* = 8.0 Hz, H-1B), 6.78 (1H, d, *J* = 8.0 Hz, H-1A), 6.70 (1H, dd, *J* = 8.0 and 2.0 Hz, H-2A), 6.70 (1H, d, *J* = 2.0 Hz, H-3A), 3.89 (3H, s, OC*H*$_3$), 3.87 (3H, s, OC*H*$_3$), 3.86 (3H, s, OC*H*$_3$), 3.85 (3H, s, OC*H*$_3$), 2.68 (2H, t, *J* = 6.4 Hz, H-7), 2.54 (2H, t, *J* = 6.8 Hz, H-8), 2.38 (2H, t, *J* = 6.0 Hz, H-6), 2.22 (3H, s, H-9), 1.99 (2H, m, H-4), 1.88 (2H, m, H-1'),

1.65 (1H, m, H-5), 1.33 (1H, m, H-5), 0.91 (3H, t, *J* = 7.2 Hz, H-2'); ^{13}C-NMR (101 MHz, $CDCl_3$) δ 149.4, 148.9, 148.5, 147.4, 133.0, 130.7, 122.5, 120.6, 118.3 (2C), 112.2, 111.4, 109.5, 59.4, 56.8, 56.0, 55.9 (2C), 48.5, 41.9, 38.4, 34.4 (2C), 33.2, 23.1 and 9.7; HRMS (ESI): *m/z* 441.2761 $[M+H]^+$; HPLC purity 98% (t_r = 6.9 min).

***5-((3,4-dimethoxyphenethyl)(methyl)amino)-2-(3,4-dimethoxyphenyl)-2-propylpentanenitrile* (3.13l)**

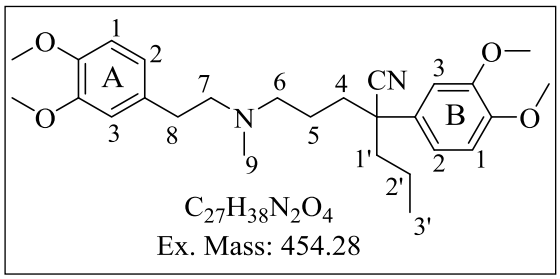

Oil (0.36 g, 53%); R_f 0.45 (10% MeOH-DCM); ^{1}H-NMR (400 MHz, $CDCl_3$) δ 6.87 (1H, dd, *J* = 8.0 and 1.6 Hz, H-2B), 6.87 (1H, d, *J* = 2.0 Hz, H-3B), 6.72 (1H, d, *J* = 8.0 Hz, H-1B), 6.70 (1H, d, *J* = 8.0 Hz, H-1A), 6.62 (2H, m, H-2A and H-3A), 3.92 (3H, s, OCH_3), 3.90 (3H, s, OCH_3), 3.89 (3H, s, OCH_3), 3.88 (3H, s, OCH_3), 2.71 (2H, t, *J* = 6.4 Hz, H-7), 2.57 (2H, t, *J* = 6.8 Hz, H-8), 2.40 (2H, t, *J* = 6.0 Hz, H-6), 2.25 (3H, s, H-9), 1.96 (2H, m, H-4), 1.83 (1H, m, H-5), 1.67 (2H, m, H-1'), 1.51 (1H, m, H-5), 1.35 (1H, m, H-2'), 1.20 (1H, m, H-2'), 0.92 (3H, t, *J* = 7.4 Hz, H-3'); ^{13}C-NMR (101 MHz) δ 150.1, 149.3, 148.9, 148.5, 135.5, 131.0, 122.7, 120.6, 118.2 (2C), 112.2, 111.4, 109.4, 59.4, 56.9, 56.1, 55.9 (2C), 47.8, 43.5, 41.9, 38.6, 33.2 (2C), 23.0, 18.4 and 13.9; HRMS (ESI): *m/z* 455.2910 $[M+H]^+$; HPLC purity 97% (t_r = 7.5 min).

***2-Cyclopentyl-5-((3,4-dimethoxyphenethyl)(methyl)amino)-2-(3,4-dimethoxyphenyl)pentanenitrile* (3.13m)**

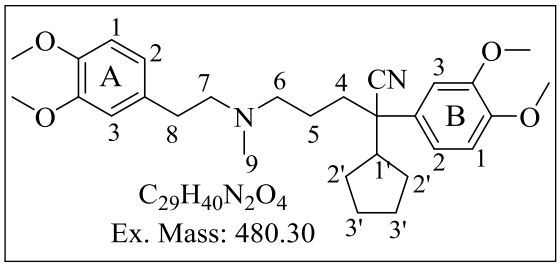

Oil (0.27 g, 36%); R_f 0.25 (5% MeOH-DCM); ^{1}H-NMR (400 MHz, $CDCl_3$) δ 6.90 (1H, dd, *J* = 8.4 and 2.4 Hz, H-2B), 6.85 (1H, d, *J* = 2.0 Hz, H-3B), 6.78 (1H, d, *J* = 8.0 Hz, H-1B), 6.74 (1H, dd, *J* = 7.2 and 1.6 Hz, H-2A), 6.65 (2H, m, H-3A and H-1A), 3.84 (3H, s, OCH_3), 3.83 (3H, s, OCH_3), 3.82 (3H, s, OCH_3), 3.81 (3H, s, OCH_3), 2.61 (2H, m, H-7), 2.45 (2H, m, H-8), 2.29 (2H, m, H-6), 2.22 (1H, m, H-1'), 2.14 (3H, s, H-9), 2.0 (1H, m, H-4), 1.92 (1H, m, H-2'), 1.83 (1H, m, H-4), 1.72 - 1.25 (8H, m, H-2', H-3'and H-5), 1.14 (1H, m, H-5); ^{13}C-NMR (101 MHz, $CDCl_3$) δ 149.9, 149.0, 148.5,

148.1, 133.1, 131.4, 121.8, 120.5, 118.4, 112.2, 111.3, 111.2, 109.6, 59.4, 56.9, 56.0, 55.9, 52.5 (2C), 50.1, 41.9, 37.2, 33.2, 29.5, 29.2, 25.4, 24.8 (2C) and 23.1; LRMS (EI): *m/z* 480.1 $[M]^+$; HPLC purity 98.5% (t_r = 12.47).

***2-Cyclohexyl-5-((3,4-dimethoxyphenethyl)(methyl)amino)-2-(3,4-dimethoxyphenyl)pentanenitrile* (3.13n)**

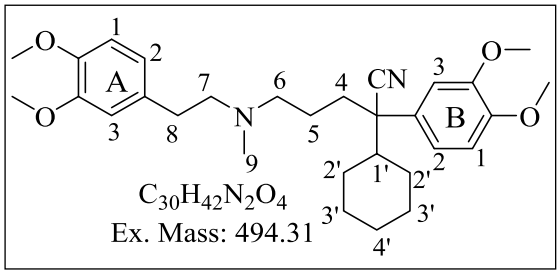

Oil (0.24 g, 32%); R_f 0.20 (50% EtOAc-Hexane); ^{1}H-NMR (400 MHz, $CDCl_3$) δ 6.84 (1H, dd, *J* = 8.4 and 2.4 Hz, H-2B), 6.81 (1H, d, *J* = 2.0 Hz, H-3B), 6.76 (2H, m, H-1B and H-3A), 6.66 (2H, dd, *J* = 6.4 and 2.0 Hz, H-2A and H-1A), 3.84 (3H, s, OC*H*$_3$), 3.83 (3H, s, OC*H*$_3$), 3.82 (s, 3H, OC*H*$_3$), 3.81 (3H, s, OC*H*$_3$), 2.62 (2H, m, H-7), 2.46 (2H, m, H-8), 2.30 (2H, m, H-6), 2.14 (3H, s, H-9), 2.07 (2H, m, H-4 and H-1'), 1.78-1.0 (13H, m, H-4, H-5, H-2', H-3' and H-4'); ^{13}C-NMR (101 MHz, $CDCl_3$) δ 149.6, 149.0, 148.1, 147.3, 133.1, 130.6, 121.9, 120.5, 118.7, 112.2, 111.3, 111.2, 109.9, 59.4 (2C), 56.9, 56.0, 55.9, 55.8, 52.7, 47.3, 42.0, 35.0, 33.2, 28.7, 26.3 (2C), 25.9 (2C) and 23.2; LRMS (EI): *m/z* 494.42 $[M]^+$; HPLC purity 99% (t_r = 13.11).

***5-(cyclopropyl(3,4-dimethoxyphenethyl)amino)-2-(3,4-dimethoxyphenyl)-2-isopropylpentanenitrile* (3.13o)**

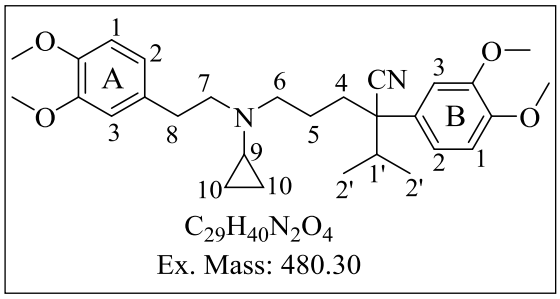

A stirred solution of **3.13o** (0.30 g, 1.2 mmol) in DCE was charged with cyclopropylboronic acid (0.2 g, 2.3 mmol), copper(II)acetate (0.23 g, 1.2 mmol), bipyridyl (0.18 g, 1.2 mmol) and sodium carbonate (0.24 g, 2.4 mmol). The reaction mixture was refluxed at 70 °C for 2 hours. After completion of reaction (TLC), water (10 ml) was added and organic layer was extracted with ethyl acetate (3 × 15) , dried over anhydrous $MgSO_4$ and concentrated to obtain **3.13o** as an oil (0.11 g, 19%); R_f 0.30 (10% MeOH-DCM); ^{1}H-NMR (400 MHz, $CDCl_3$) δ 6.82 (1H, dd, *J* = 8.4 and 2.0 Hz, H-2B), 6.79 (1H, d, *J* = 2.4 Hz, H-3B), 6.75 (1H, d, *J* = 8.0 Hz, H-1B), 6.70 (1H, d, *J* = 8.0 Hz, H-1A), 6.63 (1H, d, *J* = 2.4 Hz, H-3A), 6.63 (1H, dd, *J* = 8.0 and 2.4

Hz, H-2A), 3.80 (3H, s, OCH_3), 3.79 (3H, s, OCH_3), 3.78 (3H, s, OCH_3), 3.77 (3H, s, OCH_3), 2.60 (6H, m, H-7, H-8 and H-6), 2.01 (2H, m, H-1' and H-4), 1.71 (1H, m, H-4), 1.66 (1H, m, H-9), 1.53 (1H, m, H-5), 1.16 (1H, m, H-5), 1.11 (3H, d, J = 6.8 Hz, H-2'), 0.72 (3H, d, J = 6.8 Hz, H-2'), 0.36 (2H, d, J = 6.4 Hz, H-10), 0.27 (2H, s, H-10); ^{13}C-NMR (101 MHz, $CDCl_3$) δ 149.1, 148.9, 148.4, 147.3, 130.8, 121.5, 120.5, 118.7 (2C), 112.2, 111.4, 111.2, 109.9, 57.0, 56.0, 55.9 (2C), 54.9, 53.4, 37.8, 36.4, 36.0, 32.7 (2C), 23.1, 18.9, 18.6, 7.0 and 6.7; LRMS (EI): *m/z* 480.26 $[M]^+$; HPLC purity 98.5% (t_r = 6.8 min).

General method 7: Piperazinyl analogues of verapamil 3.15(a-l)

Potassium carbonate (5.0 mmol), and piperazine (2.0 mmol) was added to a solution of compound **3.6a** (2.4 mmol) in anhydrous DMF (5 ml). The reaction mixture was stirred at 80 ^oC for 12 h. After completion of reaction (TLC), DMF was removed under reduced pressure and the residue was taken in EtOAc (20 ml). The resulting solution was washed with brine (3×15 ml), dried over anhydrous $MgSO_4$ and concentrated *in vacuo*. The residue was purified by flash chromatography on silica gel using mixture DCM and MeOH as eluent to afford the product **3.15**.

2-(3,4-dimethoxyphenyl)-2-isopropyl-5-(4-methylpiperazin-1-yl)pentanenitrile **(3.15a)**

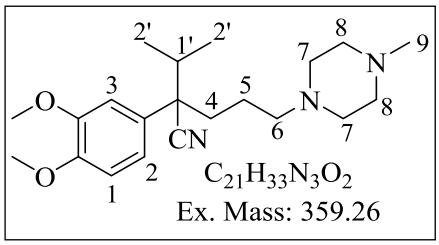

Oil (0.43 g, 60%); R_f 0.40 (10% MeOH-DCM); ^{1}H-NMR (400 MHz, $CDCl_3$) δ 6.93 (1H, dd, J = 8.4 and 2.0 Hz, H-2), 6.88 (2H, m, H-3 and H-1), 3.91 (3H, s, OCH_3), 3.90 (3H, s, OCH_3), 2.79 (4H, bs, H-7), 2.63 (4H, bs, H-8), 2.69 (3H, s, H-9), 2.51 (2H, t, J = 6.0 Hz, H-6), 2.18 (1H, m, H-4), 2.09 (1H, m, H-1'), 1.90 (1H, m, H-4), 1.58 (1H, m, H-5), 1.29 (1H, m, H-5), 1.19 (3H, d, J = 6.4 Hz, H-2'), 0.80 (3H, d, J = 6.4 Hz, H-2').^{13}C-NMR (101 MHz, $CDCl_3$) δ 149.2, 148.6, 130.2, 121.1, 118.7, 111.3, 109.9, 56.8, 56.2, 56.0, 53.3, 53.2 (2C), 49.9 (2C), 43.8, 38.0, 35.3, 22.5, 18.9 and 18.6. LRMS (EI): 359.30 $[M]^+$; HPLC purity 95% (t_r = 12.11 min).

***2-(3,4-Dimethoxyphenyl)-2-isopropyl-5-(4-phenylpiperazin-1-yl)pentanenitrile* (3.15b)**

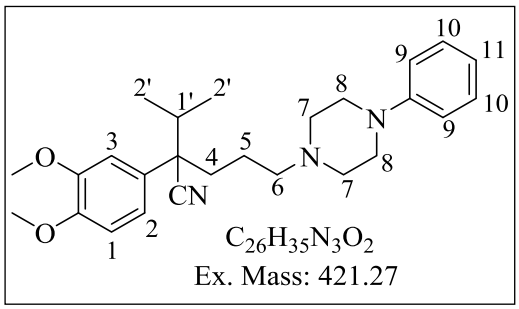

Oil (0.25 g, 49%); R_f 0.70 (10% MeOH-DCM); ^{1}H-NMR (400 MHz, $CDCl_3$) δ 7.20 (2H, m, H-1 and H-2), 6.85 (6H, m, H-3, H-9, H-10 and H-11), 3.86 (3H, s, OCH_3), 3.85 (3H, s, OCH_3), 3.12 (4H, t, *J* = 4.4 Hz, H-7), 2.45 (4H, t, *J* = 4.4 Hz, H-8), 2.30 (2H, m, H-6), 2.12 (1H, m, H-4), 2.04 (1H, m, H-1'), 1.85 (1H, m, H-4), 1.56 (1H, m, H-5), 1.22 (1H, m, H-5), 1.16 (3H, d, *J* = 6.80 Hz, H-2'), 0.76 (3H, d, *J* = 6.60 Hz, H-2'); ^{13}C-NMR (101 MHz, $CDCl_3$) δ 151.2, 149.1, 148.4, 130.7, 129.0, 121.3, 119.7 (2C), 118.7, 116.0 (2C), 111.2, 109.7, 57.8, 56.0, 55.9, 53.4, 53.0 (2C), 49.0 (2C), 37.8, 35.6, 22.8, 18.9 and 18.6; LRMS (EI): *m/z* 421.32 $[M]^+$; HPLC purity 98.5% (t_r = 12.47).

***2-(3,4-dimethoxyphenyl)-2-isopropyl-5-(4-(pyridin-4-yl)piperazin-1-yl)pentanenitrile* (3.15c)**

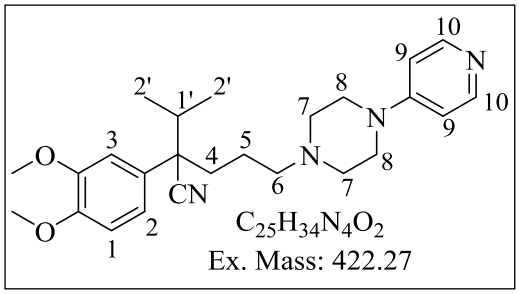

Oil (0.12 mg, 24%); R_f 0.40 (10% MeOH-DCM); ^{1}H-NMR (400 MHz, $CDCl_3$) δ 8.14 (2H, d, *J* = 7.2 Hz, H-10), 7.16 (2H, d, *J* = 6.8 Hz, H-9), 7.0 (3H, m, H-1, H-2 and H-3), 3.91 (3H, s, OCH_3), 3.90 (3H, s, OCH_3), 3.55 (4H, bs, H-7), 2.50 (4H, bs, H-8), 2.37 (2H, t, *J* = 5.2 Hz, H-6), 2.20 (1H, m, H-4), 2.10 (1H, m, H-1'), 1.90 (1H, m, H-4), 1.59 (1H, m, H-5), 1.27 (1H, m, H-5), 1.22 (3H, d, *J* = 6.4 Hz, H-2'), 0.80 (3H, d, *J* = 6.4 Hz, H-2'); ^{13}C-NMR (101 MHz, $CDCl_3$) δ 156.5, 149.2, 148.6, 141.6, 139.6, 130.5, 121.3, 118.7 (2C), 111.3, 109.9, 107.5, 57.4, 56.2, 56.0, 52.1 (2C), 46.1 (2C), 38.0, 35.4, 29.7, 22.9, 19.0 and 18.6; LRMS (EI): *m/z* 422.42 $[M]^+$; HPLC purity 96.7% (t_r = 12.10 min).

***2-(3,4-dimethoxyphenyl)-2-isopropyl-5-(4-(pyridin-2-yl)piperazin-1-yl)pentanenitrile* (3.15d)**

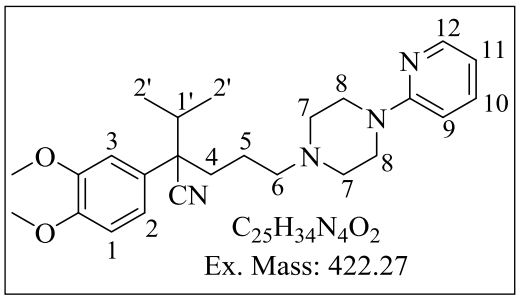

Oil (0.25 g, 58%); R_f 0.40 (10% MeOH-DCM); ^{1}H-NMR (400 MHz, $CDCl_3$) δ 8.20 (1H, ddd, *J* = 4.80, 2.0 and 1.10 Hz, H-12), 7.48 (1H, m, H-11), 6.96 (1H, dd, *J* = 8.0 and 2.4 Hz, H-2), 6.81 (2H, m, H-1 and H-3), 6.64 (2H, m, H-10 and H-9), 3.93 (3H, s, OC*H*$_3$), 3.92 (3H, s, OC*H*$_3$), 3.54 (4H, m, H-8), 2.48 (4H, t, *J* = 4.60 Hz, H-7), 2.38 (2H, m, H-6), 2.19 (1H, m, H-1'), 2.11 (1H, m, H-4), 1.93 (1H, m, H-4), 1.64 (1H, m, H-5), 1.27 (1H, m, H-5), 1.23 (3H, d, *J* = 6.80 Hz, H-2'), 0.84 (3H, d, *J* = 6.60 Hz, H-2'); ^{13}C-NMR (101 MHz, $CDCl_3$) δ 159.4, 149.1, 148.4, 147.9, 137.4, 130.6, 121.3, 118.7, 113.3, 111.2, 109.8, 107.0, 57.9, 56.0, 55.9, 52.8, 53.8, 45.0, 37.9, 35.6, 22.8, 18.9 and 18.6; LRMS (EI): *m/z* 422.38 $[M]^+$; HPLC purity 99% (t_r = 11.87).

***2-(3,4-dimethoxyphenyl)-2-isopropyl-5-(4-(3-methoxyphenyl)piperazin-1-yl)pentanenitrile* (3.15e)**

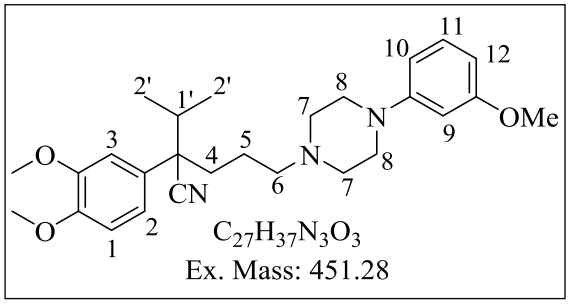

Oil (0.22 g, 47%); R_f 0.40 (10% MeOH-DCM); ^{1}H-NMR (400 MHz, $CDCl_3$) δ 7.17 (1H, t, *J* = 8.4 Hz, H-11), 6.97 (1H, dd, *J* = 8.4 and 2.4 Hz, H-2), 6.90 (1H, d, *J* = 2.0 Hz, H-3), 6.89 (1H, d, *J* = 7.6 Hz, H-1), 6.55 (1H, dd, *J* = 8.0 and 1.6 Hz, H-10), 6.47 (1H, t, *J* = 2.0 Hz, H-9), 6.43 (1H, dd, *J* = 8.0 and 2.0 Hz, H-12), 3.93 (3H, s, OC*H*$_3$), 3.92 (3H, s, OC*H*$_3$), 3.81 (3H, s, OC*H*$_3$), 3.20 (4H, bs, H-7), 2.52 (4H, bs, H-8), 2.38 (2H, t, *J* = 4.0 Hz, H-6), 2.31 (1H, m, H-4), 2.18 (1H, m, H-1'), 1.94 (1H, m, H-4), 1.63 (1H, m, H-5), 1.29 (1H, m, H-5), 1.23 (3H, d, *J* = 6.4 Hz, H-2'), 0.82 (3H, d, *J* = 6.0 Hz, H-2'); ^{13}C-NMR (101 MHz, $CDCl_3$) δ 160.6, 152.6, 149.2, 148.4, 130.6, 129.8, 121.4, 118.8, 111.3, 109.8, 108.9, 104.6, 102.6, 57.9, 56.1, 56.0, 55.2, 53.4, 53.0 (2C), 48.9 (2C), 37.9, 35.6, 22.9, 19.0 and 18.6; LRMS (EI): *m/z* 451.10 $[M]^+$; HPLC purity 95.2% (t_r = 13.55 min).

***2-(3,4-dimethoxyphenyl)-2-isopropyl-5-(4-(4-methoxyphenyl)piperazin-1-yl)pentanenitrile* (3.15f)**

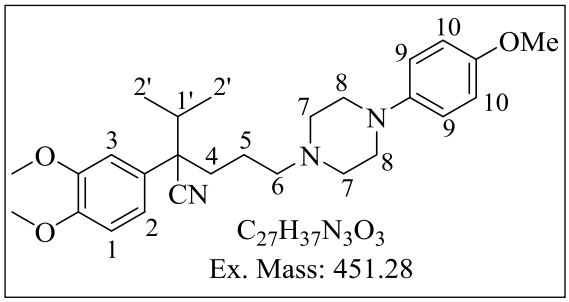

Oil (0.13 g, 28%); R_f 0.50 (10% MeOH-DCM); ^{1}H NMR (400 MHz, $CDCl_3$) δ 6.98 (1H, dd, *J* = 8.4 and 2.4 Hz, H-2), 6.90 (4H, m, H-1, H-3 and H-9), 6.96 (2H, m, H-10), 3.92 (3H, s, OCH_3), 3.91 (3H, s, OCH_3), 3.79 (3H, s, OCH_3), 3.10 (4H, t, *J* = 5.2 Hz, H-7), 2.53 (4H, t, *J* = 4.8 Hz, H-8), 2.37 (2H, t, *J* = 6.8 Hz, H-6), 2.20 (1H, m, H-4), 2.15 (1H, m, H-1'), 1.92 (1H, m, H-4), 1.63 (1H, m, H-5), 1.20 (1H, m, H-5), 1.24 (3H, d, *J* = 6.8 Hz, H-2'), 0.83 (3H, d, *J* = 6.4 Hz, H-2'); ^{13}C-NMR (101 MHz, $CDCl_3$) δ 153.9, 149.2, 148.4, 145.7, 130.7, 121.4, 118.8 (2C), 118.2, 114.4 (2C), 111.3, 109.8, 57.9, 56.1, 56.0, 55.6, 53.4, 53.2 (2C), 50.5 (2C), 37.8, 35.6, 22.9, 19.0 and 18.6; LRMS (EI): *m/z* 451.17 $[M]^+$; HPLC purity 95.2% (t_r = 12.98 min).

***2-(3,4-dimethoxyphenyl)-2-isopropyl-5-(4-(4-(trifluoromethyl)phenyl)piperazin-1-yl)pentanenitrile* (3.15g)**

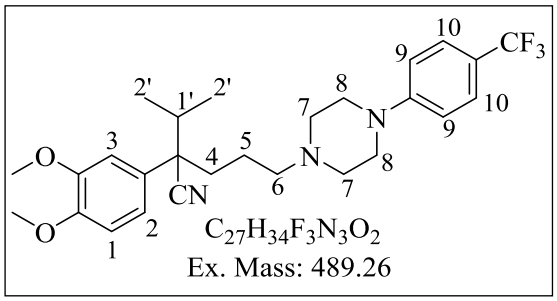

Oil (0.16 g, 37%); R_f 0.70 (10% MeOH-DCM); ^{1}H-NMR (400 MHz, $CDCl_3$) δ 7.45 (2H, d, *J* = 9.2 Hz, H-10), 6.97 (1H, dd, *J* = 8.4 and 2.4 Hz, H-2), 6.91 (3H, m, H-1 and H-9), 6.90 (1H, d, *J* = 2.0 Hz, H-3), 3.93 (3H, s, OCH_3), 3.90 (3H, s, OCH_3), 3.30 (4H, t, *J* = 5.2 Hz, H-7), 2.52 (4H, t, *J* = 4.8 Hz, H-8), 2.39 (2H, t, *J* = 6.0 Hz, H-6), 2.23 (1H, m, H-4), 2.12 (1H, m, H-1'), 1.92 (1H, m, H-4), 1.64 (1H, m, H-5), 1.27 (1H, m, H-5), 1.24 (3H, d, *J* = 6.4 Hz, H-2'), 0.83 (3H, d, *J* = 6.8 Hz, H-2'); ^{13}C-NMR (101 MHz, $CDCl_3$) δ 153.2, 149.2, 148.5, 130.7, 126.4 (2C), 121.4, 118.8, 114.5 (2C), 111.3 (2C), 109.6 (2C), 57.8, 56.1, 56.0, 53.4, 52.8 (2C), 47.8 (2C), 37.9, 35.6, 22.9, 19.0 and 18.6; LRMS (EI): *m/z* 489.13 $[M]^+$; HPLC purity 95% (t_r = 15.24 min).

***2-(3,4-dimethoxyphenyl)-5-(4-(2-fluorophenyl)piperazin-1-yl)-2-isopropylpentanenitrile* (3.15h)**

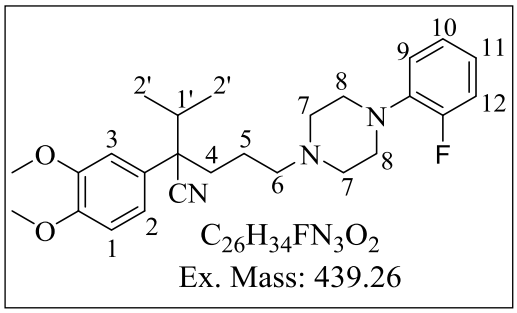

Oil (0.12 g, 37%); R_f (10% MeOH : DCM) 0.45; ^{1}H NMR (400 MHz, $CDCl_3$) 7.35 (1H, dd, *J* = 8.0 and 1.6 Hz, H-12), 7.20 (1H, ddd, *J* = 8.0, 7.2 and 1.6 Hz, H-11), 7.04 (1H, dd, *J* = 8.0 and 1.6 Hz, H-9), 6.96 (1H, ddd, *J* = 7.6, 7.2 and 1.2 Hz, H-10), 6.94 (1H, m, H-2), 6.88 (1H, d, *J* = 2.0 Hz, H-3), 6.84 (1H, d, *J* = 8.4 Hz, H-1), 3.90 (3H, s, OC*H*$_3$), 3.89 (3H, s, OC*H*$_3$), 3.07 (4H, bs, H-7), 2.57 (4H, bs, H-8), 2.42 (2H, t, *J* = 6.4 Hz, H-6), 2.21 (1H, m, H-4), 2.15 (1H, m, H-1'), 1.95 (1H, m, H-4), 1.63 (1H, m, H-5), 1.26 (1H, m, H-5), 1.20 (3H, d, *J* = 6.4 Hz, H-2'), 0.81 (3H, d, *J* = 6.8 Hz, H-2'); ^{13}C NMR (101 MHz, $CDCl_3$) δ 156.9, 149.1, 148.4, 130.6, 124.1, 122.3, 121.3, 118.9, 118.7, 116.1, 115.9, 111.2, 109, 57.9, 56.0, 55.9 (2C), 53.1 (2C), 50.3 (2C), 37.8, 35.6, 22.8, 18.9 and 18.6; LRMS: *m/z* 439.21 $[M]^+$; HPLC purity 98.5% (t_r = 12.78).

***5-(4-(4-acetylphenyl)piperazin-1-yl)-2-(3,4-dimethoxyphenyl)-2-isopropylpentanenitrile* (3.15i)**

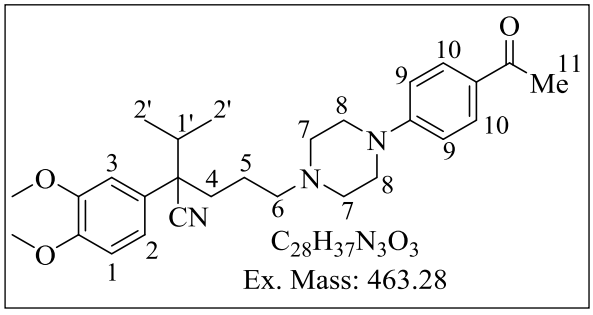

Oil (0.12 g, 28%); R_f 0.50 (10% MeOH-DCM); ^{1}H NMR (400 MHz, $CDCl_3$) δ 7.89 (2H, d, *J* = 9.2 Hz, H-10), 7.00 (1H, dd, *J* = 8.4 and 2.4 Hz, H-2), 6.91 (1H, d, *J* = 2.4 Hz, H-3), 6.88 (3H, m, H-1 and H-9), 3.93 (3H, s, OC*H*$_3$), 3.92 (3H, s, OC*H*$_3$), 3.37 (4H, t, *J* = 4.4 Hz, H-7), 2.53 (4H, t, *J* = 4.0 Hz, H-8), 2.54 (3H, s, H-11), 2.39 (2H, t, *J* = 8.0 Hz, H-6), 2.21 (1H, m, H-4), 2.12 (1H, m, H-1'), 1.93 (1H, m, H-4), 1.65 (1H, m, H-5), 1.28 (1H, m, H-5), 1.24 (3H, d, *J* = 6.8 Hz, H-2'), 0.83 (3H, d, *J* = 6.8 Hz, H-2'); ^{13}C NMR (101 MHz, $CDCl_3$) δ 196.3, 154.0, 149.2, 148.5, 130.6, 130.4 (2C), 121.4, 118.8 (2C), 113.4 (2C), 111.3, 109.8, 57.8, 56.1, 56.0, 53.4, 52.7 (2C), 47.2 (2C), 37.9, 35.6, 26.1, 22.9, 19.0 and 18.6; LRMS (EI): *m/z* 463.29 $[M]^+$; HPLC purity 95% (t_r = 13.37 min).

***5-(4-cyclohexylpiperazin-1-yl)-2-(3,4-dimethoxyphenyl)-2-isopropylpentanenitrile* (3.15j)**

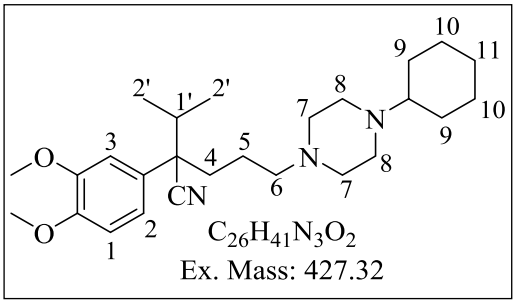

Oil (0.12 g, 32%); R_f 0.50 (10% MeOH- DCM); ^{1}H-NMR (400 MHz, $CDCl_3$) δ 6.95 (1H, dd, *J* = 8.0 and 2.4 Hz, H-2), 6.91 (1H, d, *J* = 8.4, H-1), 6.88 (1H, d, *J* = 2.4 Hz, H-3), 3.92 (3H, s, OC*H*$_3$), 3.91 (3H, s, OC*H*$_3$), 3.60 (4H, bs, H-7), 2.42 (4H, bs, H-10), 2.31 (2H, t, *J* = 7.2 Hz, H-6), 2.26 (1H, m, H-9), 2.13 (1H, m, H-4), 2.10 (1H, m, H-1'), 1.96-1.61 (8H, m, H-10 and H-11), 1.56 (1H, m, H-4), 1.30-1.03 (4H, m, H-12 and H-5), 1.20 (3H, d, *J* = 6.4 Hz, H-2'), 0.83 (3H, d, *J* = 6.4 Hz, H-2'); ^{13}C-NMR (101 MHz, $CDCl_3$) δ 149.1, 148.4, 130.7, 130.4, 118.8, 111.3, 109.8, 63.6, 58.0, 56.0, 55.9, 53.4 (3C), 48.9 (2C), 37.9, 35.7, 28.9 (2C), 26.3, 25.9 (2C), 23.0, 19.0 and 18.6; LRMS (EI): *m/z* 427.30 $[M]^+$; HPLC purity 98.5% (t_r = 12.77 min).

***2-(3,4-dimethoxyphenyl)-2-isopropyl-5-(4-(p-tolyl)piperazin-1-yl)pentanenitrile* (3.15k)**

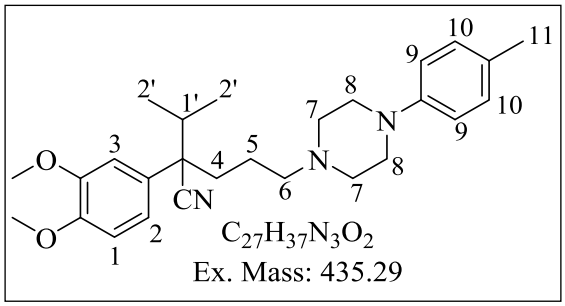

Oil (0.12 g, 35%); R_f 0.20 (10% MeOH-DCM); ^{1}H-NMR (400 MHz, $CDCl_3$) δ 7.01 (2H, d, *J* = 8.0 Hz, H-10), 6.97 (1H, dd, *J* = 8.4 and 2.0 Hz, H-2), 6.91 (1H, d, *J* = 2.0 Hz, H-3), 6.90 (1H, d, *J* = 8.4 Hz, H-1), 6.85 (2H, d, *J* = 8.8 Hz, H-9), 3.93 (3H, s, OC*H*$_3$), 3.92 (3H, s, OC*H*$_3$), 3.13 (4H, t, *J* = 4.0 Hz, H-7), 2.50 (4H, t, *J* = 4.4 Hz, H-8), 2.37 (2H, t, *J* = 6.4 Hz, H-6), 2.29 (3H, s, H-11), 2.21 (1H, m, H-4), 2.12 (1H, m, H-1'), 1.90 (1H, m, H-4), 1.64 (1H, m, H-5), 1.29 (1H, m, H-5), 1.23 (3H, d, *J* = 6.4 Hz, H-2'), 0.84 (3H, d, *J* = 6.8 Hz, H-2'); ^{13}C-NMR (101 MHz, $CDCl_3$) δ 149.3, 149.1, 148.4, 130.8, 129.6 (2C), 129.2, 121.4, 118.8, 116.4 (2C), 111.3, 109.8, 58.0, 56.1, 56.0, 53.4, 53.2 (2C), 49.7 (2C), 37.9, 35.7, 23.0, 20.4, 19.0 and 18.6; LRMS (EI): *m/z* 435.25 $[M]^+$; HPLC purity 98.6% (t_r = 13.91 min).

***4-(4-(4-cyano-4-(3,4-dimethoxyphenyl)-5-methylhexyl)piperazin-1-yl)benzonitrile* (3.15j)**

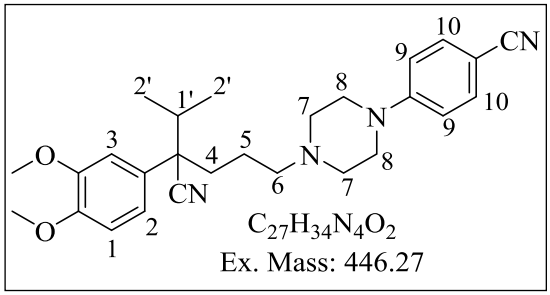

Oil (0.12 g, 30%); R_f 0.20 (10% MeOH-DCM); ^{1}H-NMR (400 MHz, $CDCl_3$) δ 7.51 (2H, d, *J* = 8.8 Hz, H-10), 6.96 (1H, dd, *J* = 8.4 and 2.4 Hz, H-2), 6.91 (1H, d, *J* = 2.0 Hz, H-3), 6.88 (1H, d, *J* = 8.4 Hz, H-1), 6.85 (2H, d, *J* = 9.2 Hz, H-9), 3.92 (3H, s, OC*H*$_3$), 3.91 (3H, s, OC*H*$_3$), 3.37 (4H, t, *J* = 4.0 Hz, H-7), 2.57 (4H, t, *J* = 4.4 Hz, H-8), 2.45 (2H, t, *J* = 6.4 Hz, H-6), 2.21 (1H, m, H-4), 2.11 (1H, m, H-1'), 1.95 (1H, m, H-4), 1.66 (1H, m, H-5), 1.31 (1H, m, H-5), 1.22 (3H, d, *J* = 6.4 Hz, H-2'), 0.82 (3H, d, *J* = 6.8 Hz, H-2'); ^{13}C-NMR (101 MHz, $CDCl_3$) δ 149.2, 149.1, 148.5, 133.5, 129.6 (2C), 129.2, 121.4, 118.8, 114.4 (2C), 111.3, 109.8, 58.0, 56.1, 56.0, 53.4, 53.2 (2C), 49.7 (2C), 37.9, 35.7, 23.0, 19.0 and 18.6; LRMS (EI): *m/z* 446.29 $[M]^+$; HPLC purity 98.6% (t_r = 13.80 min).

General procedure 8: Procedure for the synthesis of benzyl analogues of verapamil 3.17(a-l)

Potassium carbonate (0.094 g, 0.68 mmol), and benzyl bromide or benzyl chloride (0.51 mmol) were added to a solution of *Nor*-VER (**3.13e)** (0.15 g, 0.34 mmol) in anhydrous DMF (3 ml) and the reaction mixture was stirred at 80 ^oC for 10 h. After completion of reaction (TLC), DMF was removed under reduced pressure and the residue was taken in EtOAc (20 ml). The organic phase was washed with brine (3×15 ml), dried over anhydrous sodium sulphate and concentrated *in vacuo*. The residue was purified by flash chromatography on silica gel using DCM-MeOH to afford the product **3.17**.

***5-((3,4-dimethoxyphenethyl)(4-methylbenzyl)amino)-2-(3,4-dimethoxyphenyl)-2-isopropylpentanenitrile* (3.17a)**

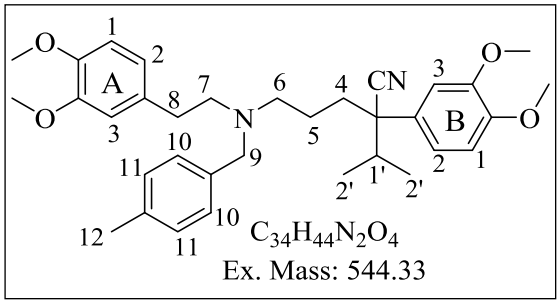

Oil (52 mg, 28%); R_f 0.30 (10% MeOH-DCM); ^{1}H-NMR (400 MHz, $CDCl_3$) δ 7.17 (2H, d, *J* = 8.0 Hz, H-11), 7.10 (2H, d, *J* = 8.0 Hz, H-10), 6.88 (1H, dd, *J* = 8.0 and 2.4 Hz, H-2B), 6.84 (2H, m, H-3A and H-3B), 6.78 (1H, d, *J* = 8.0 Hz, H-1B), 6.65 (2H, d, *J* = 8.0 Hz, H-2A and

H-1A), 3.89 (3H, s, OC*H*$_3$), 3.87 (3H, s, OC*H*$_3$), 3.86 (3H, s, OC*H*$_3$), 3.84 (3H, s, OC*H*$_3$), 3.53 (2H, s, H-9), 2.65 (4H, m, H-7 and H-8), 2.46 (2H, t, *J* = 4.2 Hz, H-6), 2.36 (3H, s, H-12), 2.14-1.97 (2H, m, H-1' and H-4), 1.79 (1H, m, H-4), 1.56 (1H, m, H-5), 1.20 (1H, m, H-5), 1.18 (3H, d, *J* = 6.6 Hz, H-2'), 0.80 (3H, d, *J* = 6.6 Hz, H-2'); ^{13}C-NMR (101 MHz, $CDCl_3$) δ 149.0 (2C), 148.8 (2C), 148.3 (2C), 147.3, 130.7, 128.8, 121.6, 120.5 (2C), 118.8 (2C), 112.2 (2C), 111.3, 111.1, 109.8, 57.9, 56.0, 55.9, 55.8, 55.7, 55.4, 53.3 (2C), 37.7 (2C), 35.4, 20.8 (2C), 18.9 and 18.6; LC-ESI-MS (+ve ion mode): *m/z* 545.20 $[M+H]^+$, purity 98.9% (t_r = 4.47 min).

***5-((4-chlorobenzyl)(3,4-dimethoxyphenethyl)amino)-2-(3,4-dimethoxyphenyl)-2-isopropylpentanenitrile* (3.17b)**

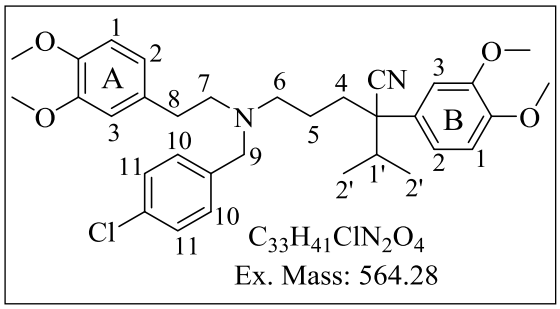

Oil (40 mg, 21%); R_f 0.40 (10% MeOH-DCM); ^{1}H-NMR (300 MHz, $CDCl_3$) δ 7.28 (2H, d, *J* = 9.0 Hz, H-11), 7.19 (2H, d, *J* = 8.1 Hz, H-10), 6.88 (1H, dd, *J* = 8.1 and 2.0 Hz, H-2B), 6.80 (2H, m, H-1B and H-3B), 6.79 (1H, d, *J* = 8.1 Hz, H-1A), 6.64 (2H, m, H-2A and H-3A), 3.89 (3H, s, OC*H*$_3$), 3.87 (3H, s, OC*H*$_3$), 3.86 (3H, s, OC*H*$_3$), 3.84 (3H, s, OC*H*$_3$), 3.51 (2H, s, H-9), 2.65 (4H, m, H-7 and H-8), 2.46 (2H, t, *J* = 5.7 Hz, H-6), 2.15-1.99 (2H, m, H-1' and H-4), 1.76 (1H, m, H-4), 1.56 (1H, m, H-5), 1.22 (1H, m, H-5), 1.19 (3H, d, *J* = 6.6 Hz, H-2'), 0.79 (3H, d, *J* = 6.6 Hz, H-2'); ^{13}C-NMR (101 MHz, $CDCl_3$) δ 149.1, 148.8, 148.3, 147.4, 130.6, 130.1 (2C), 128.3 (2C), 121.5 (2C), 120.6 (2C), 118.7 (2C), 112.1, 111.3, 111.1, 109.7, 57.7, 56.1, 56.0, 55.9, 55.8, 55.5, 53.0, 38.0 (2C), 35.6, 33.0, 23.1, 18.9 and 18.6; LC-ESI-MS (+ve ion mode): *m/z* 565.3 $[M+H]^+$, purity 99.9% (t_r = 4.91 min).

***2-(((4-cyano-4-(3,4-dimethoxyphenyl)-5-methylhexyl)(3,4-dimethoxyphenethyl)amino)methyl)benzonitrile* (3.17c)**

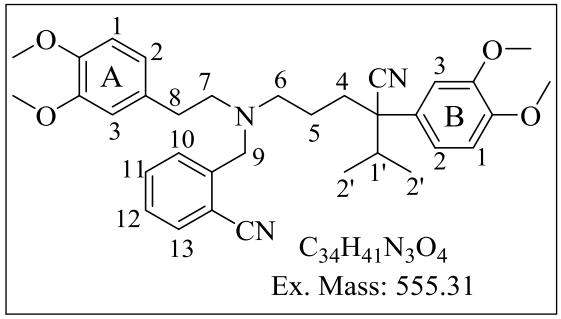

Oil (0.19 g, 58%); R_f 0.25 (10% MeOH-DCM); ^{1}H-NMR (300 MHz, $CDCl_3$) δ 7.62 (1H, dd, *J* = 8.7 and 0.9 Hz, H-13), 7.51 (1H, td, *J* = 7.8 and

1.2 Hz, H-12), 7.42 (1H, d, *J* = 7.5 Hz, H-10), 7.34 (1H, td, *J* = 7.5 and 1.2 Hz, H-11), 6.90 (1H, dd, *J* = 8.4 and 2.4 Hz, H-2B), 6.89 (1H, d, *J* = 2.1 Hz, H-3B), 6.81 (1H, d, *J* = 8.4 Hz, H-1B), 6.77 (1H, d, *J* = 8.7 Hz, H-1A), 6.63 (2H, m, H-2A and H-3A), 3.88 (3H, s, OC*H*$_3$), 3.86 (6H, s, 2 × OC*H*$_3$), 3.84 (3H, s, OC*H*$_3$), 3.76 (2H, s, H-9), 2.65 (4H, m, H-7 and H-8), 2.50 (2H, t, *J* = 6.0 Hz, H-6), 2.13-1.99 (2H, m, H-1' and H-4), 1.86 (1H, m, H-4), 1.53 (1H, m, H-5), 1.23 (1H, m, H-5), 1.16 (3H, d, *J* = 6.6 Hz, H-2'), 0.79 (3H, d, *J* = 6.6 Hz, H-2'); ^{13}C-NMR (75 MHz, $CDCl_3$) δ 149.0, 148.7, 148.3, 147.4, 132.9 (2C), 132.8, 130.6, 130.0 (2C), 127.3, 121.5, 120.6, 118.7, 117.9, 112.6, 112.2, 111.3, 111.1, 109.8, 57.7, 56.1, 56.0, 55.9, 55.8, 55.5, 53.0, 38.0 (2C), 35.6, 33.0, 23.1, 18.9 and 18.6; LC-ESI-MS (+ve ion mode): 556.3 $[M+H]^+$, purity 97.2% (t_r = 4.83 min).

***5-((3,4-dimethoxyphenethyl)(3-methoxybenzyl)amino)-2-(3,4-dimethoxyphenyl)-2-isopropylpentanenitrile* (3.17d)**

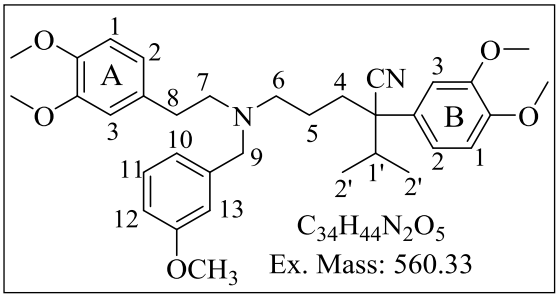

Oil (40 mg, 20%); R_f 0.50 (10 % MeOH-DCM); ^{1}H-NMR (400 MHz, $CDCl_3$) δ 7.10 (1H, t, *J* = 7.6 Hz, H-11), 6.77 (3H, m, H-10, H-12 and H-2B), 6.73 (1H, s, H-13), 6.72 (1H, d, *J* = 2.0 Hz, H-3B), 6.69 (1H, d, *J* = 8.0 Hz, H-1B), 6.67 (1H, d, *J* = 8.4 Hz, H-1A), 6.54 (2H, m, H-2A and H-3A), 3.76 (3H, s, OC*H*$_3$), 3.75 (3H, s, OC*H*$_3$), 3.73 (3H, s, OC*H*$_3$), 3.72 (3H, s, OC*H*$_3$), 3.68 (3H, s, OC*H*$_3$), 3.42 (2H, s, H-9), 2.54 (4H, m, H-7 and H-8), 2.34 (2H, t, *J* = 6.0 Hz, H-6), 2.02-1.88 (2H, m, H-1' and H-4), 1.78 (1H, m, H-4), 1.45 (1H, m, H-5), 1.06 (3H, d, *J* = 6.8 Hz, H-2'), 1.02 (1H, m, H-5), 0.70 (3H, d, *J* = 6.8 Hz, H-2'); ^{13}C-NMR (101 MHz, $CDCl_3$) δ 162.5, 151.9, 151.7, 151.1, 150.2, 144.3, 136.0, 133.5, 133.9, 124.3, 123.9, 123.4, 121.5,117.1, 115.1 (2C), 114.2, 114.0, 112.7, 61.2, 58.8 (2C), 58.7 (2C), 58.3, 58.0, 56.1, 56.0, 40.8, 38.4, 35.8, 26.1, 21.7 and 21.1; LC-ESI-MS (+ve ion mode): 561.2 $[M+H]^+$, purity 96.5% (t_r = 4.51 min).

***5-((3,4-dimethoxyphenethyl)(3-(trifluoromethyl)benzyl)amino)-2-(3,4-dimethoxyphenyl)-2-isopropylpentanenitrile* (3.17e)**

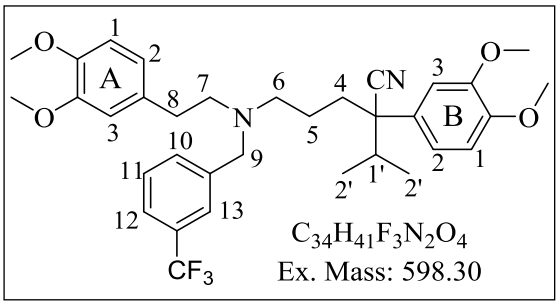

Oil (35 mg, 33%); R_f 0.50 (10% MeOH-DCM); ^{1}H-NMR (400 MHz, $CDCl_3$) δ 7.60 (1H, m, H-11), 7.51 (1H, m, H-12), 7.40 (2H, m, H-10 and H-13), 6.86 (2H, m, H-2B and H-3B), 6.82 (1H, d, *J* = 6.0 Hz, H-1B), 6.78 (1H, d, *J* = 6.4 Hz, H-1A), 6.48 (2H, m, H-2A and H-3A), 3.87 (3H, s, OC*H*$_3$), 3.86 (3H, s, OC*H*$_3$), 3.85 (3H, s, OC*H*$_3$), 3.84 (3H, s, OC*H*$_3$), 3.60 (2H, s, H-9), 2.66 (4H, m, H-7 and H-8), 2.45 (2H, t, *J* = 6.0 Hz, H-6), 2.16-1.96 (2H, m, H-1' and H-4), 1.77 (1H, m, H-4), 1.57 (1H, m, H-5), 1.17 (3H, d, *J* = 6.8 Hz, H-2'), 1.10 (1H, m, H-5), 0.81 (3H, d, *J* = 6.8 Hz, H-2'); ^{13}C-NMR (101 MHz, $CDCl_3$) δ 171.5, 149.01, 148.9, 148.3, 141.2, 133.0, 130.8, 130.7, 128.6, 124.1, 123.5, 123.6, 121.3,117.3, 116.2, 115.5 (2C), 114.5, 113.6, 112.1, 60.3, 58.0 (2C), 57.6 (2C), 56.0, 55.9, 55.9, 55.8, 37.9, 35.5, 33.1, 23.3, 21.0, 18.9 and 18.5; LC-ESI-MS (+ve ion mode): 599.3 $[M+H]^+$, purity 96.5% (t_r = 4.51 min).

***5-((3,4-dimethoxyphenethyl)(2-(trifluoromethoxy)benzyl)amino)-2-(3,4-dimethoxyphenyl)-2-isopropylpentanenitrile* (3.17f)**

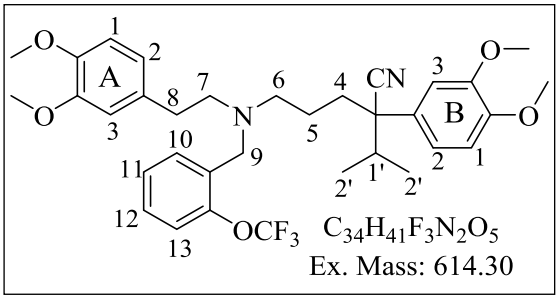

Oil (60 mg, 28%); R_f 0.70 (10% MeOH-DCM); ^{1}H-NMR (400 MHz, $CDCl_3$) δ 7.32 (1H, d, *J* = 6.0 Hz, H-13), 7.20-7.08 (3H, m, H-12, H-11 and H-10), 6.76 (1H, dd, *J* = 8.0 and 2.4 Hz, H-2B), 6.72 (1H, d, *J* = 2.0 Hz, H-3B), 6.68 (1H, d, *J* = 8.4 Hz, H-1B), 6.66 (1H, d, *J* = 8.4 Hz, H-1A), 6.54 (2H, m, H-2A and H-3A), 3.76 (3H, s, OC*H*$_3$), 3.75 (3H, s, OC*H*$_3$), 3.73 (3H, s, OC*H*$_3$), 3.72 (3H, s, OC*H*$_3$), 3.51 (2H, s, H-9), 2.53 (4H, m, H-7 and H-8), 2.37 (2H, t, *J* = 6.4 Hz, H-6), 2.01-1.90 (2H, m, H-1'and H-4), 1.68 (1H, m, H-4), 1.45 (1H, m, H-5), 1.10 (1H, m, H-5), 1.07 (3H, d, *J* = 6.8 Hz, H-2'), 0.69 (3H, d, *J* = 6.8 Hz, H-2'); ^{13}C-NMR (101 MHz, $CDCl_3$) δ 151.9, 151.7, 151.2, 150.5, 150.2, 135.9, 135.4, 133.6, 133.5 (2C), 130.1,129.4, 124.3, 123.3, 121.5, 115.0, 114.2, 114.0, 112.7, 58.8 (2C), 58.6 (3C), 56.3, 56.1,

54.8, 40.8, 38.4, 35.8, 26.3, 21.7 and 21.4; LC-ESI-MS (+ve ion mode): 615.1 $[M+H]^+$, purity 96.2% (t_r = 5.10 min).

***5-((3,4-dimethoxyphenethyl)(4-(trifluoromethoxy)benzyl)amino)-2-(3,4-dimethoxyphenyl)-2-isopropylpentanenitrile* (3.17g)**

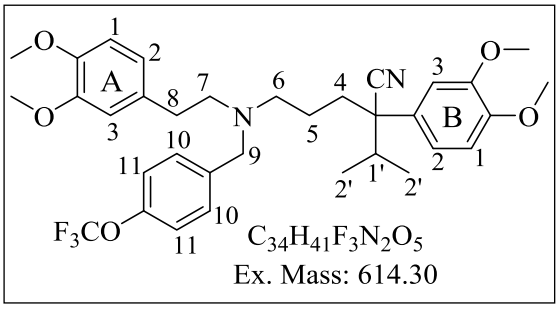

Oil (70 mg, 34%); R_f 0.80 (10% MeOH-DCM); ^{1}H-NMR (400 MHz, $CDCl_3$) δ 7.15 (2H, d, *J* = 8.4 Hz, H-11), 7.02 (2H, d, *J* = 8.0 Hz, H-10), 6.76 (1H, dd, *J* = 8.0 and 2.0 Hz, H-2B), 6.72 (2H, d, *J* = 2.0 Hz, H-3B), 6.70 (1H, d, *J* = 8.4 Hz, H-1B), 6.67 (1H, d, *J* = 8.0 Hz, H-1A), 6.52 (2H, m, H-3A and H-2A), 3.76 (3H, s, OCH_3), 3.75 (3H, s, OCH_3), 3.73 (3H, s, OCH_3), 3.72 (3H, s, OCH_3), 3.41 (2H, s, H-9), 2.54 (4H, m, H-7 and H-8), 2.35 (2H, t, *J* = 6.4 Hz, H-6), 2.02-1.90 (2H, m, H-1' andH-4), 1.65 (1H, m, H-4), 1.46 (1H, m, H-5) 1.10 (1H, m, H-5), 1.06 (3H, d, *J* = 6.8 Hz, H-2'), 0.70 (3H, d, *J* = 6.8 Hz, H-2'); ^{13}C-NMR (101 MHz, $CDCl_3$) δ 151.9, 151.7, 151.2, 150.2, 141.4 (2C), 135.8,133.5, 132.7 (2C),131.0, 124.3, 123.5 (3C), 121.5, 115.0, 114.2, 114.0, 112.0, 60.4, 58.8 (2C), 58.7 (2C), 58.4, 56.1, 56.0, 40.8, 38.4, 36.0, 26.1, 21.7 and 21.4; LC-ESI-MS (+ve ion mode): 615.3 $[M+H]^+$, purity 95.1% (t_r = 4.50 min).

***5-((3,4-dimethoxyphenethyl)(4-(methylthio)benzyl)amino)-2-(3,4-dimethoxyphenyl)-2-isopropylpentanenitrile* (3.17h)**

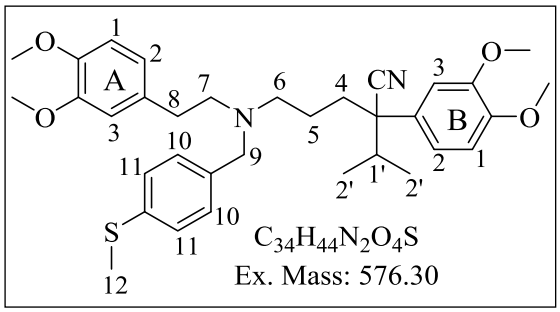

Oil (0.12 g, 61%); R_f 0.30 (10% MeOH-DCM); ^{1}H-NMR (400 MHz, $CDCl_3$); δ 7.08 (4H, m, H-10 and H-11), 6.77 (1H, dd, *J* = 8.4 and 2.0 Hz, H-2B), 6.73 (2H, d, *J* = 2.0 Hz, H-3B), 6.71 (1H, d, *J* = 7.6 Hz, H-1B), 6.67 (1H, d, *J* = 8.0 Hz, H-1A), 6.52 (2H, m, H-2A and H-3A), 3.77 (3H, s, OCH_3), 3.76 (3H, s, OCH_3), 3.74 (3H, s, OCH_3), 3.73 (3H, s, OCH_3), 3.40 (2H, s, H-9), 2.53 (4H, m, H-7 and H-8), 2.43 (3H, s, H-12), 2.34 (2H, t, *J* = 6.4 Hz, H-6), 2.02-1.89 (2H, m, H-1' and H-4), 1.66 (1H, m, H-4), 1.44 (1H, m, H-5), 1.12 (1H, m, H-5), 1.07 (3H, d,

J = 6.8 Hz, H-2'), 0.69 (3H, d, *J* = 6.8 Hz, H-2'); ^{13}C-NMR (101 MHz, $CDCl_3$) δ 151.9, 151.7, 151.2, 150.2, 139.5, 136.0, 133.5, 132.2 (2C), 129.5 (2C), 124.3, 123.4, 121.6, 115.0, 114.2, 114.0, 112.6; 61.0, 58.7, 58.8, 58.4 (2C), 58.5, 56.0, 55.90, 40.9, 38.2, 35.6, 29.7, 26.2, 21.3 21.5 and 15.1; LC-ESI-MS (+ve ion mode): 577.32 $[M+H]^+$, purity 97.6% (t_r = 4.57 min).

***4-(((4-cyano-4-(3,4-dimethoxyphenyl)-5-methylhexyl)(3,4 dimethoxyphenethyl)amino)methyl)benzonitrile* (3.17i)**

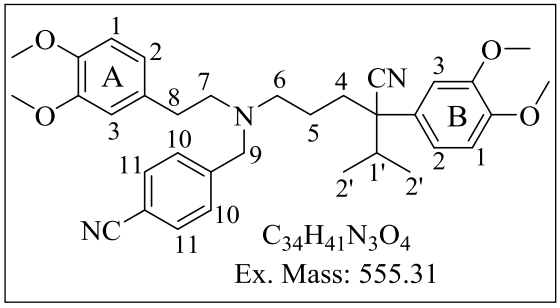

Oil (70 mg, 21%); R_f 0.6 (10% MeOH-DCM); ^{1}H-NMR (400 MHz, $CDCl_3$) δ 7.46 (2H, d, *J* = 8.0 Hz, H-11), 7.23 (2H, d, *J* = 7.6 Hz, H-10), 6.74 (1H, dd, *J* = 8.4 and 2.0 Hz, H-2B), 6.71 (2H, d, *J* = 2.0 Hz, H-3B), 6.70 (1H, d, *J* = 8.4 Hz, H-1B), 6.67 (1H, d, *J* = 8.0 Hz, H-1A), 6.50 (2H, m, H-3A and H-2A), 3.77 (3H, s, OC*H*$_3$), 3.75 (3H, s, OC*H*$_3$), 3.74 (3H, s, OC*H*$_3$), 3.72 (3H, s, OC*H*$_3$), 3.46 (2H, s, H-9), 2.51 (4H, m, H-7 and H-8), 2.34 (2H, t, *J* = 6.4 Hz, H-6), 2.02-1.88 (2H, m, H-1' and H-4), 1.78 (1H, m, H-4), 1.40 (1H, m, H-5), 1.06 (3H, d, *J* = 6.8 Hz, H-2'), 1.02 (1H, m, H-5), 0.80 (3H, d, *J* = 6.8 Hz, H-2'); ^{13}C-NMR (101 MHz, $CDCl_3$) δ 151.9, 151.7, 151.2, 150.3, 148.6, 135.6 (2C), 134.8, 133.4, 132.0 (2C), 124.2, 123.4, 121.7, 121.5, 115.0, 1114.2, 114.0, 113.5, 112.7, 61.0, 58.9, 58.8, 58.7, 58.6, 56.2 (2C), 56.1, 40.8, 38.4, 36.0, 26.1, 21.7 and 21.5; LC-ESI-MS (+ve ion mode): 556.2 $[M+H]^+$, purity 95.1% (t_r = 4.73 min).

***5-((3-acetylbenzyl)(3,4-dimethoxyphenethyl)amino)-2-(3,4-dimethoxyphenyl)-2-isopropylpentanenitrile* (3.17j)**

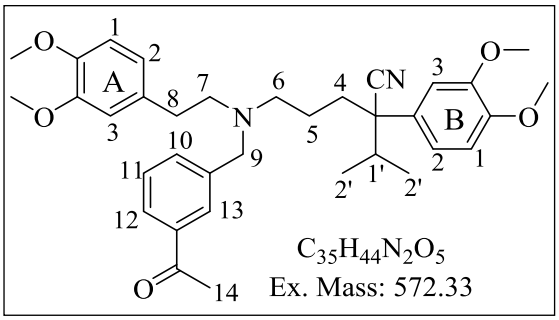

Oil (50 mg, 27%); R_f 0.30 (10% MeOH-DCM); ^{1}H-NMR (400 MHz, $CDCl_3$) δ 7.76 (1H, s, H-13), 7.71 (1H, d, *J* = 7.6 Hz, H-12), 7.33 (1H, d, *J* = 6.8 Hz, H-10), 7.27 (1H, t, *J* = 7.6 Hz, H-11), 6.77 (1H, dd, *J* = 8.4 and 2.0 Hz, H-2B), 6.73 (1H, d, *J* = 2.0 Hz, H-3B), 6.69 (1H, d, *J* =

8.2 Hz, H-1B), 6.66 (1H, d, *J* = 8.0 Hz, H-1A), 6.51 (2H, m, H-2A and H-3A), 3.76 (3H, s, OC*H*$_3$), 3.74 (3H, s, OC*H*$_3$), 3.73 (3H, s, OC*H*$_3$), 3.71 (3H, s, OC*H*$_3$), 3.48 (2H, s, H-9), 2.53 (4H, m, H-7 and H-8), 2.48 (3H, s, H-14), 2.35 (2H, t, *J* = 6.4 Hz, H-6), 2.02-1.89 (2H, m, H-1' and H-4), 1.70 (1H, m, H-4), 1.45 (1H, m, H-5), 1.10 (1H, m, H-5), 1.05 (3H, d, *J* = 6.8 Hz, H-2'), 0.69 (3H, d, *J* = 6.8 Hz, H-2'); ^{13}C-NMR (101 MHz, $CDCl_3$) δ 200.9, 151.9, 151.7, 151.2, 150.2, 143.4, 140.0, 136.2, 135.9, 133.5, 131.2, 129.8, 124.3, 123.4, 121.5, 115.0, 114.2, 114.0, 112.7, 61.0, 58.8, 58.7, 58.6 (2C), 58.3, 56.1, 56.0, 40.8, 38.4, 35.9, 29.4, 26.1, 21.7 and 21.4; LC-ESI-MS (+ve ion mode): 573.1 $[M+H]^+$, purity 98.3% (t_r = 4.37 min).

***4-Cyano-4-(3,4-dimethoxy-phenyl)-heptanedioic acid dimethyl ester* (3.18)**

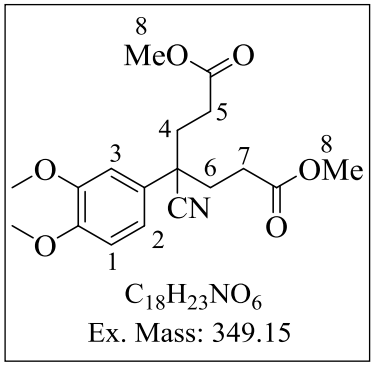

$C_{18}H_{23}NO_6$
Ex. Mass: 349.15

A solution of 40% methanolic Triton B (0.8 mL) was rapidly added to a stirred boiling solution of the commercially available 2-(3,4-dimethoxyphenyl)acetonitrile (1.5 g, 8.5 mmol) and methyl acrylate (2.27 g, 27.0 mmol) in *tert*-butyl alcohol (20 mL). The resulting reaction mixture was refluxed for 18 h. After completion of reaction (TLC), solvent was distilled off under reduced pressure and residue was dissolved in DCM (40 ml). The solution was washed with dilute HCl and water, dried with anhydrous sodium sulphate and concentrated *in vacuo* to obtain crude product as yellow solid. Purification by column chromatography (20% EtOAc-Hexane) afforded a white solid 2.1 g (72%). m.p. 60-62 °C; R_f 0.30 (40% EtOAc-Hexane); ^{1}H-NMR (400 MHz, $CDCl_3$) δ 6.93 (1H, dd, *J* = 8.4 and 2.4 Hz, H-2), 6.85 (1H, d, *J* = 8.4 Hz, H-1), 6.83 (1H, d, *J* = 2.4 Hz, H-3), 3.88 (3H, s, OC*H*$_3$), 3.86 (3H, s, OC*H*$_3$), 3.60 (6H, s, H-8), 2.47 (2H, m, H-4 and H-5), 2.31 (2H, m, H-6 and H-7), 2.27 (2H, m, H-6 and H-7), 2.34 (2H, m, H-4 and H-5).

***5-Cyano-5-(3,4-dimethoxy-phenyl)-2-oxocyclohexanecarboxylic acid methyl ester* (3.19)**

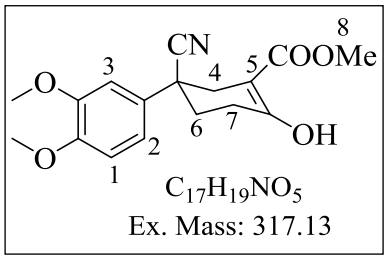

$C_{17}H_{19}NO_5$
Ex. Mass: 317.13

A solution of compound **3.18** (1.0 gram, 2.87 mmol) in dry DME was added to the suspension of NaH (60% in oil, 105 mg, 4.29 mmol) in dry DME (20 ml) under an atmosphere of nitrogen. The reaction mixture was stirred at 60 °C for one hour. After completion of reaction (TLC), cooled to room temperature (25 °C), quenched with 1M HCl (aq) solution and concentrated under reduced pressure. The crude was taken in water and acidified to pH = 3, extracted with DCM, dried over sodium sulphate and concentrated under reduced pressure. Purification was done by column chromatography at (20% EtOAc-Hexane) to obtain a white solid 0.6 g (65%). m.p 118-120 °C; R_f 0.30 (30% EtOAc-Hexane); ^{1}H-NMR (400 MHz, $CDCl_3$) δ 12.40 (1H, s, OH), 7.04 (1H, dd, *J* = 5.6 and 2.4 Hz, H-2), 7.0 (1H, d, *J* = 2.4 Hz, H-3), 6.91 (1H, m, H-1), 3.95 (3H, s, OC*H*$_3$), 3.92 (3H, s, OC*H*$_3$), 3.81 (3H, s, H-8), 3.03 (1H, d, *J* = 16.0 Hz, H-4), 2.90 (1H, m, H-6), 2.69 (1H, d, *J* = 16.0 Hz, H-4), 2.52 (1H, m, H-6), 2.31 (1H, m, H-7), 2.21 (1H, m, H-7).

***1-(3,4-Dimethoxy-phenyl)-4-oxo-cyclohexanecarbonitrile* (3.20)**

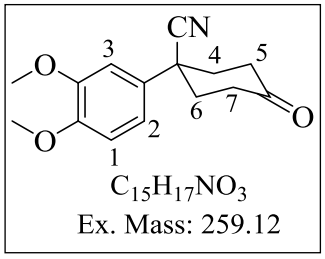

$C_{15}H_{17}NO_3$
Ex. Mass: 259.12

A suspension of **3.19** (0.3 g, 0.96 mmol) in mixture acetic acid (6.5 mL) and 10% sulphuric acid (3.5 mL**)** were heated to reflux for 5 h. After completion of reaction (TLC), the mixture was extracted with toluene. The extracts were washed with saturated Na_2CO_3 solution, water and dried over anhydrous sodium sulphate. Removal of the organic solvent *in vacuo* afforded a white solid, which was recrystallized from ethanol. Yield 0.15 g (60%); m.p. 109-112 °C; R_f 0.4 (40% EtOAc-Hexane); ^{1}H-NMR (400 MHz, $CDCl_3$) δ 7.08 (2H, m, H-2 and H-3), 6.91 (1H, d, *J* = 8.4 Hz, H-1), 3.94 (3H, s, OC*H*$_3$), 3.92 (3H, s, OC*H*$_3$), 2.95 (2H, td, *J* = 14.8 and 6.0 Hz, H-4 and H-5), 2.61 (2H, m, H-6 and H-7), 2.51 (2H, m, H-6 and H-7), 2.28 (2H, td, *J* = 14.8 and 6.0 Hz, H-4 and H-5).

***1-(3,4-Dimethoxy-phenyl)-4-[2-(3,4-dimethoxy-phenyl)-ethylamino] cyclohexanecarbonitrile* (3.22)**

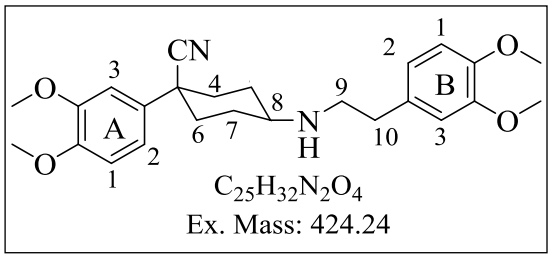

A toluene (50 ml) solution of **3.20** (0.5 g, 1.93 mmol), homoveratrylamine (0.39 g, 2.13 mmol), and *p*-toluene sulfonic acid monohydrate (0.06 g) was reflux for 45 h. The water was removed from the reaction with the aid of a Dean-Stark trap. After completion of reaction (TLC), solvent was removed *in vacuo* and residue was dissolved in ethyl acetate, washed with water, and dried over anhydrous sodium sulphate. Evaporation of the solvent *in vacuo* afforded 0.75 g of **3.21** as an oil that was quite unstable and was used as such in the next reaction.

$NaBH_4$ (70 mg) was cautiously added to a solution of immine **3.21** (0.7 g) in hot methanol (15 ml) over 0.5 h and reflux for 2 h. After completion of reduction (TLC), reaction mixture was cooled to 0 °C, treated with a few drops of water and excess of solvent was removed *in vacuo*. The residue was dissolved in chloroform, washed with water, and dried over anhydrous sodium sulphate. Removal of solvent *in vacuo* afforded 0.5 g of crude as an oil, which was purified by column chromatography (10% MeOH-DCM) to afford **3.22** as a white solid. Yield 0.15 g (22%); m.p. 59-61 °C; R_f 0.46 (10% MeOH-DCM); ^{1}H-NMR (400 MHz, $CDCl_3$) δ 7.02 (2H, m, H-2B and H-3B), 6.88 (1H, m, H-1B), 6.85 (1H, m, H-1A) 6.81 (2H, m, H-2A and H-3A), 3.93 (3H, s, OCH_3), 3.91 (3H, s, OCH_3), 3.90 (3H, s, OCH_3), 3.89 (3H, s, OCH_3), 2.97 (2H, t, J = 8.0 Hz, H-9), 2.82 (2H, t, J = 7.2 Hz, H-10), 2.60 (1H, tt, J = 11.2 and 3.4 Hz, H-8), 2.26 (2H, m, H-4 and H-6), 2.15 (2H, m, H-5 and H-7), 1.84 (2H, m, H-4 and H-6), 1.73 (2H, m, H-5 and H-7); ^{13}C-NMR (101 MHz, $CDCl_3$) δ 149.2, 149.1, 148.2, 147.7, 133.2, 132.4, 122.4, 120.6, 117.4, 112.2, 111.6, 111.4, 109.4, 56.1, 56.0, 55.9 (2C), 55.8, 48.2, 43.7, 36.5 (2C), 36.2 and 30.6 (2C). LC-ESI-MS (+ve ion mode): *m/z* 425.2 $[M+H]^+$, 447.1 $[M+Na]^+$, 463.1 $[M+K]^+$, purity 99.1% (t_r = 9.97 min).

***6,7-dimethoxy-1,2,3,4-tetrahydronaphthalen-1-ol* (3.24)**[9,10]

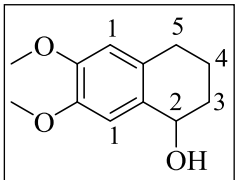

$C_{12}H_{16}O_3$
Ex. Mass: 208.11

$NaBH_4$ (0.46 g, 12.12 mmol) was added to a stirred solution of **3.23** (1.25 g, 6.06 mmol) in portions over ten minutes at room temperature (25 °C). The resulting reaction mixture was stirred for another 6 hours and monitored by TLC. After completion of reaction, ethanol was removed *in vacuo* and excess of $NaBH_4$ was quenched with saturated solution of ammonium chloride. The extraction was done with DCM (3×15 ml), dried over sodium sulphate and concentrated *in vacuo* to obtain **3.24** in 95% yields as white solid. m.p. 173-175 °C; R_f 0.30 (30% EtOAc-Hexane); ^{1}H-NMR (300 MHz, $CDCl_3$) δ 6.95 (1H, s, H-1), 6.59 (1H, s, H-1), 4.72 (1H, t, *J* = 4.8 Hz, H-2), 3.88 (3H, s, OC*H*$_3$), 3.86 (3H, s, OC*H*$_3$), 2.82-2.59 (2H, m, H-5), 2.06-1.68 (4H, m, H-3 and H-4).

***6,7-dimethoxy-1,2-dihydronaphthalene* (3.25)**[9]

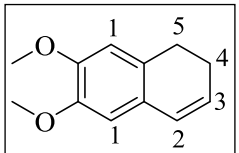

$C_{12}H_{14}O_2$
Ex. Mass: 190.10

A mixture of **3.24** (1.2 g, 5.76 mmol) in toluene was heated to reflux and a few crystals of *p*-toluene sulfonic acid (10 mg, 0.057 mmol) was added. The resulting reaction mixture was refluxed for 1.5 hours. After completion of reaction (TLC), solvent was removed *in vacuo* and residue was dissolved in ethyl acetate. The solution was washed with saturated solution of sodium bicarbonate and brine. The combined extract was dried over sodium sulphate and concentrated to obtain crude product. Purification by column chromatography afforded **3.25** as an oil, yield 1.0 gram (90%). R_f 0.3 (50% EtOAc-Hexane); ^{1}H-NMR (300 MHz, $CDCl_3$) δ 6.76 (1H, s, H-1), 6.66 (1H, s, H-1), 6.40 (1H, d, *J* = 9.6 Hz, H-2), 5.93 (1H, dt, *J* = 9.6 and 4.8 Hz, H-3), 3.89 (3H, s, OC*H*$_3$), 3.87 (3H, s, OC*H*$_3$), 2.99 (2H, t, *J* = 6.9 Hz, H-5), 2.60-2.51 (2H, m, H-4).

***1-hydroxy-6,7-dimethoxy-1,2,3,4-tetrahydronaphthalen-2-yl 3-chlorobenzoate* (3.26)**[9]

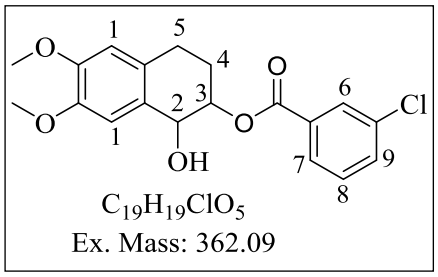

$C_{19}H_{19}ClO_5$
Ex. Mass: 362.09

*m*CPBA (1.0 g, 5.79 mmol) was added to a solution of **3.25** (1.0 g, 5.26 mmol) in DCM and saturated solution of $NaHCO_3$ at 0 °C over 10 minutes in portions. The resulting reaction mixture was stirred at 0 °C for another 10 minutes, and then transferred to room temperature (25 °C) and stirred for another 2.5 hours. After completion of reaction (TLC), DCM layer was washed with saturated solution of sodium carbonated, dried over sodium sulphate and concentrated to obtain **3.26** as yellow solid in 75% yield. R_f 0.50 (50% EtOAc-Hexane); ^{1}H-NMR (300 MHz, $CDCl_3$) δ 8.04 (1H, m, H-6), 7.97 (1H, m, H-7), 7.55 (1H, m, H-9), 7.41 (1H, m, H-8), 6.67 (2H, m, H-1), 4.23 (1H, m, H-3), 3.89 (3H, s, OCH_3), 3.84 (3H, s, OCH_3), 3.10-2.76 (2H, m, H-5), 2.31-1.90 (2H, m, H-4).

***6,7-dimethoxy-3,4-dihydronaphthalen-2(1H)-one* (3.28)**[9]

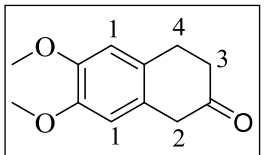

$C_{12}H_{14}O_3$
Ex. Mass: 206.09

A mixture of solutions of **3.26** in methanol and excess of aqueous NaOH (2M) was refluxed for 10 hour. After completion of reaction (TLC), methanol was removed *in vacuo* and organic content were extracted with ethyl acetate. The combined EtOAc extracts were dried over sodium sulphate and concentrated *in vacuo* to obtain **3.27**. The crude product was used in next step without further purification.

Boron(III) fluoride etherate (2 drops) was added to a solution of diol **3.27** in ether (3 mL). The solution was stirred at 30 °C for 20 min, washed with water and dried over magnesium sulphate and concentrated. Purification by column chromatography afforded **3.28** (55%); ^{1}H-NMR (300 MHz, $CDCl_3$) δ 6.76 (1H, s, H-1), 6.64 (1H, s, H-1), 3.90 (3H, s, OCH_3), 3.88 (3H, s, OCH_3), 3.53 (2H, s, H-2), 3.03 (2H, t, J = 6.6 Hz, H-4), 2.58 (2H, t, J = 6.3 Hz, H-3).

***6,7-dimethoxy-N-methyl-1,2,3,4-tetrahydronaphthalen-2-amine* (3.29)**

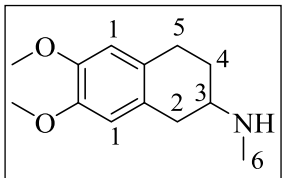

$C_{13}H_{19}NO_2$
Ex. Mass: 221.14

Compounds **3.29** was added to a solution of methyl amine in methonal and acetic acid. The reaction mixture was stirred for 15 minute followed with the addition of Sodium cyanotrihydroborate in portions under an atmosphere of nitrogen. After completion of addition, reaction was further stirred at room temperature (25 °C) for 16 hours. After completion of reaction (TLC), solvent was removed *in vacuo* and residue was acidified with 1M HCl and extracted with diethyl ether. The aqueous layer was basified with Na_2CO_3 and extracted with DCM. The combined DCM layers were dried over sodium sulphate and concentrated to obtain **3.29** as an oil (0.30 g, 55%); .R_f 0.30 (10% MeOH-DCM); ^{1}H-NMR (300 MHz, $CDCl_3$) δ 6.61 (1H, s, H-1), 6.54 (1H, s, H-1), 3.83 (3H, s, OCH_3), 3.82 (3H, s, OCH_3), 2.92 (3H, s, H-6), 2.80-1.80 (7H, m, H-2, H-3, H-4 and H-5).

***2-(3,4-dimethoxyphenyl)-2-isopropylpent-4-ynenitrile* (3.30)**[11]

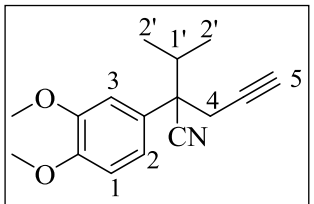

$C_{16}H_{19}NO_2$
Ex. Mass: 257.14

The general method 1 was adopted using **3.7a** (0.5 g, 2.28 mmol) and propargyl bromide (0.5 ml of 80% in toluene, 2.28 mmol) to obtain **3.30** as an oil (0.35 g, 60%). R_f 0.20 (10% EtOAc-Hexane); ^{1}H-NMR (300 MHz, $CDCl_3$) δ 7.05 (1H, dd, *J* = 8.0 and 2.0 Hz, H-2), 6.84 (2H, m, H-1 and H-3), 3.91 (3H, br s, OCH_3), 3.89 (3H, s, OCH_3), 2.91 (1H, m, H-5), 2.38 (1H, m, H-1'), 2.08 (2H, m, H-4), 1.21 (3H, d, *J* = 6.6 Hz, H-2'), 0.89 (3H, d, *J* = 6.6 Hz, H-2').

***6-((6,7-dimethoxy-1,2,3,4-tetrahydronaphthalen-2-yl)(methyl)amino)-2-(3,4-dimethoxyphenyl)-2-isopropylhex-4-ynenitrile* (EDP42)**[11]

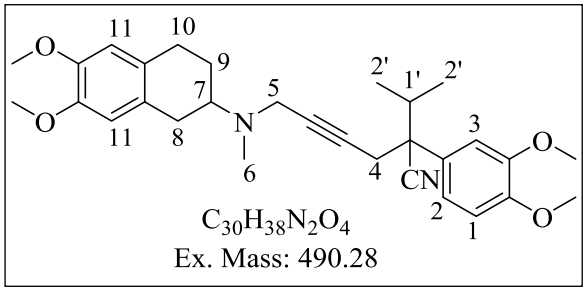

$C_{30}H_{38}N_2O_4$
Ex. Mass: 490.28

A solution of formaldehyde (0.035 ml of 40% in water, 0.46 mmol), **3.30** (0.11 g, 0.42 mmol) and $CuSO_4$ (0.01 g) was added to a

solution of **3.29** (0.12 g, 0.53 mmol) in mixture of ethanol and water (1:1). The pH of the solution was adjusted to 8 with 50% sulphuric acid. The resulting reaction mixture was refluxed for 24 hours. After completion of reaction (TLC), quenched with 5 ml of saturated NH_4OH and extracted with DCM. The combined DCM layer were dried over sodium sulphate and concentrated to afford crude **EDP42**. Purification was done by column chromatography at 1-2% MeOH-DCM to obtain **EDP42** as an oil. Yield (40 mg, 20%); R_f 0.60 (10% MeOH-Hexane); ^{1}H-NMR (400 MHz, $CDCl_3$) δ 7.05 (1H, m, H-1), 6.84 (1H, d, *J* = 2.0 Hz, H-3), 6.73 (1H, dd, *J* = 8.0 and 2.4 Hz, H-2), 6.60 (2H, two doublets, *J* = 2.0 Hz, H-11), 3.89 (3H, s, OCH_3), 3.87 (3H, s, OCH_3), 3.86 (3H, s, OCH_3), 3.83 (3H, s, OCH_3), 3.45 (2H, s, H-5), 3.10-2.51 (7H, H-8, H-7 and H-4 and H-10), 2.31 (3H, d, *J* = 14.0, H-6), 2.27 (1H, m, H-1'), 2.06 (1H, m, H-9), 1.55 (1H, m, H-9), 1.20 (3H, *J* = 6.8 Hz, H-2'), 0.84 (3H, *J* = 6.4 Hz, H-2'); ^{13}C-NMR (101 MHz, $CDCl_3$) δ 149.0, 148.7, 147.3, 147.2, 130.1, 127.9, 126.9, 120.9, 119.1, 112.3, 111.5, 111.0, 110.8, 80.7, 78.9, 57.6, 56.0, 55.9, 55.8, 52.7, 43.4, 38.8, 38.7, 36.5, 32.9, 29.7, 29.2, 28.1, 26.6, 18.8 and 18.5; LC-ESI-MS (+ve ion mode): *m/z* 491.3 $[M+H]^+$, purity 98.2% (t_r = 4.078 min).

7.1.4.2 Reversed anti-TB agents

General procedure 9: Procedure for the synthesis of compound 4.2(a and b)

1-bromo-3-chloropropane (30.15 mmol) and NaH (30.15 mmol) was added to a solution of compound **4.1** (25.1 mmol) in anhydrous DMF (10 ml). The resulting reaction mixture was stirred at room temperature (25 °C) for 12 hours. After completion of reaction (TLC), DMF was removed *in vacuo* and the residue was taken in EtOAc (30 ml). The organic phase was washed with brine (3×20 ml), dried over anhydrous sodium sulphate and concentrated *in vacuo*. Purification by flash chromatography on silica gel using EtOAc-Hexane as eluent afforded product **4.2a** and **4.2b**.

***10-(3-chloropropyl)-10H-phenothiazine* (4.2a)**[12]

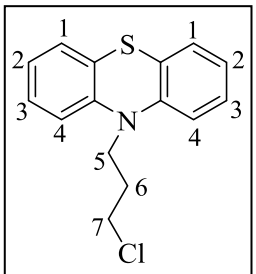

$C_{15}H_{14}ClNS$
Ex. Mass: 275.05

White solid (4.5 g, 63%); m.p. 61-63 °C; R_f 0.60 (10% EtOAc-Hexane); ^{1}H-NMR (400 MHz, $CDCl_3$) δ 7.20 (4H, m, H-2 and H-3), 6.98 (2H, dd, *J* = 7.2 and 1.2 Hz, H-4), 6.94 (2H, dd, *J* = 7.2 and 1.2 Hz, H-1), 4.12 (2H, t, *J* = 6.8 Hz, H-5), 3.70 (2H, t, *J* = 6.8 Hz, H-7), 2.27 (2H, quin, *J* = 6.4 Hz, H-6).

***2-chloro-10-(3-chloropropyl)-10H-phenothiazine* (4.2b)**[12]

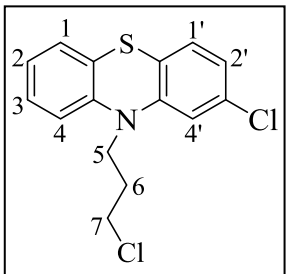

$C_{15}H_{13}Cl_2NS$
Ex. Mass: 309.01

White solid (4.95 g, 75%); m.p. 66-68 °C; R_f 0.50 (10% EtOAc-Hexane); ^{1}H-NMR (400 MHz, $CDCl_3$) δ 7.20 (2H, m, H-1 and H-3), 7.07 (1H, d, *J* = 8.0 Hz, H-1'), 6.99 (1H, td, *J* = 7.6 and 0.8 Hz, H-2), 6.93 (2H, dd, *J* = 8.4 and 2.4 Hz, H-4 and H-2'), 6.85 (1H, d, *J* = 2.0 Hz, H-4'), 4.08 (2H, t, *J* = 6.4 Hz, H-5), 3.69 (2H, t, *J* = 6.0 Hz, H-7), 2.27 (2H, quin, *J* = 6.4 Hz, H-6).

***5-(3-chloropropyl)-10,11-dihydro-5H-dibenzo[b,f]azepine.*(4.2c)**[12]

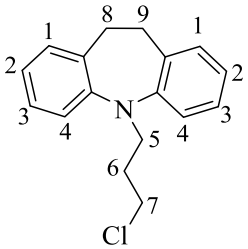

$C_{17}H_{18}ClN$
Ex. Mass: 271.11

A solution of azapine (1.0 g, 5.12 mmol) in dry toluene was added to the suspension of sodium amide (0.5 g, 12.80 mmol) in dry toluene. After stirring at room temprature (25 °C) for 30 minutes, 1-bromo-3-chloropropane (0.94 g, 1.23 ml, 10.14 mmol) was added drop-wise to the reaction mixture. The resulting reaction mixture was further stirred for another 24 hours at room temprature (25 °C). After completion of reaction (TLC), cooled to 0 °C, quenced with brine and extracted with ethyl acetate (3 × 15 ml). The combined ethylacetate extracts were dried over sodium sulphate and concentrated *in vacuo* to obtain **4.2c** as an oil (0.83 g, 60%). R_f 0.65 (5% EtOAc-Hexane); ^{1}H-NMR (400 MHz, $CDCl_3$) δ 7.22-7.10 (6H, m, H-1, H-3 and H-4), 6.99 (2H, td, *J* = 7.6 and 1.2 Hz, H-2), 3.96 (2H, t, *J* = 6.4 Hz, H-5), 3.62 (2H, t, *J* = 6.4 Hz, H-7), 3.21 (4H, s, H-8 and H-9), 2.27 (2H, quin, *J* = 6.4 Hz, H-6).

General procedure 10: Procedure for the synthesis of target compound 4.3

NaH (3.87 mmol) was added to a cooled solution (0 °C) of compound **4.2** (3.22 mmol) and isoniazid (3.87 mmol) in anhydrous DMF (3 ml). The resulting reaction mixture was stirred at room temperature (25 °C) for 24 h. After completion of reaction (TLC), DMF was removed *in vacuo* and the residue was taken in EtOAc (25 ml). The organic phase was washed with brine (3×15 ml), dried over anhydrous sodium sulphate and concentrated *in vacuo*. Purification by flash chromatography on silica gel using MeOH-DCM as eluent afforded product **4.3**.

***N'-(3-(10H-phenothiazin-10-yl)propyl)isonicotinohydrazide* (4.3a)**

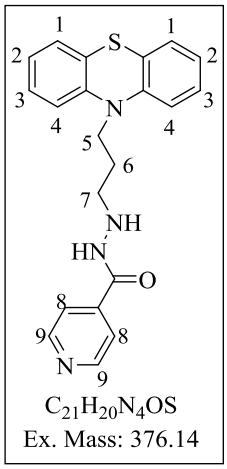

$C_{21}H_{20}N_4OS$
Ex. Mass: 376.14

Oil (0.24 g, 18%); R_f 0.20 (5% MeOH-DCM); ^{1}H-NMR (400 MHz, $CDCl_3$) δ 8.71 (2H, d, *J* = 6.0 Hz, H-9), 7.45 (2H, d, *J* = 6.4 Hz, H-8), 7.19 (4H, m, H-2 and H-3), 6.98 (2H, dd, *J* = 7.2 and 1.2 Hz, H-1), 6.94 (2H, dd, *J* = 7.2 and 1.2 Hz, H-4), 4.08 (2H, t, *J* = 6.4 Hz, H-5), 3.13 (2H, t, *J* = 6.4 Hz, H-7), 2.06 (2H, m, H-6); ^{13}C-NMR (101 MHz, $CDCl_3$) δ 165.2, 150.2 (2C), 145.2 (2C), 140.1, 127.7 (2C), 127.4 (2C),

125.5 (2C), 122.8 (2C), 120.8 (2C), 115.7 (2C), 49.6, 44.7 and 25.3; LRMS (EI): *m/z* 377.32 $[M+H]^+$; HPLC purity 96% (t_r = 13.77).

***N'-(3-(2-chloro-10H-phenothiazin-10-yl)propyl)isonicotinohydrazide* (4.3b)**

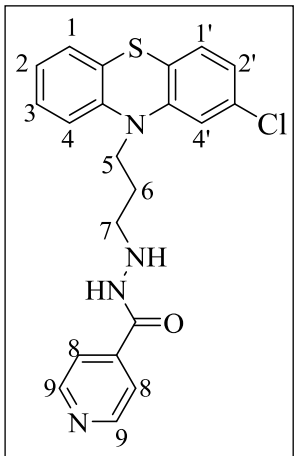

$C_{21}H_{19}ClN_4OS$
Ex. Mass: 410.10

Oil (0.32 g, 24%); R_f 0.20 (5% MeOH-DCM); ^{1}H-NMR (400 MHz, $CDCl_3$) δ 8.70 (2H, d, *J* = 6.0 Hz, H-9), 7.44 (2H, d, *J* = 6.0 Hz, H-8), 7.16 (2H, m, H-1 and H-3), 7.02 (1H, d, *J* = 8.0 Hz, H-1'), 6.92 (1H, td, *J* = 7.6 and 0.8 Hz, H-2), 6.89 (2H, dd, *J* = 8.4 and 2.4 Hz, H-4 and H-2'), 6.83 (1H, d, *J* = 2.0 Hz, H-4'), 4.01 (2H, t, *J* = 6.4 Hz, H-5), 3.09 (2H, t, *J* = 6.4 Hz, H-7), 2.03 (2H, quin, *J* = 6.4 Hz, H-6). ^{13}C-NMR (101 MHz, $CDCl_3$) δ 165.1, 150.5 (2C), 144.9 (2C), 142.1, 133.4, 128.5, 127.9 (2C), 125.9, 123.8 (2C), 120.8 (3C), 115.6 (2C), 49.5, 44.6 and 25.1; LRMS (EI): *m/z* 411.54 $[M+H]^+$; HPLC purity 96% (t_r = 17.00).

***N'-(3-(10,11-dihydro-5H-dibenzo[b,f]azepin-5-yl)propyl)isonicotinohydrazide* (4.3c)**

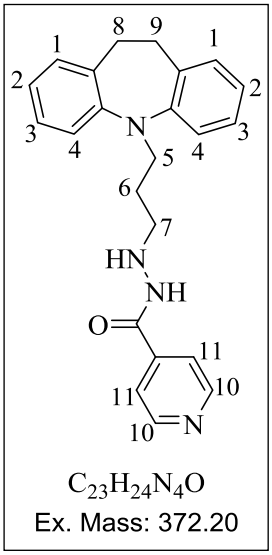

$C_{23}H_{24}N_4O$
Ex. Mass: 372.20

Oil (0.11 g, 15%); R_f 0.65 (5% EtOAc-Hexane); ^{1}H-NMR (400 MHz, $CDCl_3$) δ 7.16 - 7.08 (4H, m, H-2 and H-3), 7.60 (2H, d, *J* = 7.2 Hz, H-1), 6.99 (2H, m, H-4), 3.88 (2H, t, *J* = 6.8 Hz, H-5), 2.99 (2H, t, *J* = 6.4 Hz, H-7), 3.12 (4H, s, H-8 and H-9), 2.27 (2H, quin, *J* = 6.8, Hz, H-6); ^{13}C-NMR (101 MHz, $CDCl_3$) δ 165.1, 149.4 (2C), 147.3, 140.6, 134.1, 129.4, 126.1, 122.2, 121.4, 119.6, 49.0 (2C), 31.9 (2C), 26.0; LC-ESI-MS (+ve ion mode): *m/z* 373.1 $[M+H]^+$, purity 95.1% (t_r = 4.73 min).

N',N'-bis(3-(10H-phenothiazin-10-yl)propyl)isonicotinohydrazide **(4.4a)**

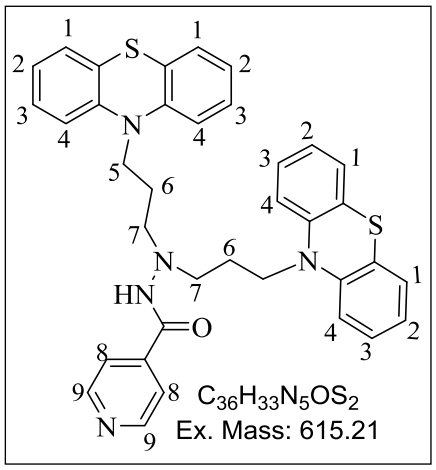

Oil (0.30 g, 27%); R_f 0.45 (5% MeOH-DCM); ^{1}H NMR (400 MHz, $CDCl_3$) δ 8.64 (2H, d, *J* = 6.0 Hz, H-9), 7.30 (2H, d, *J* = 6.4 Hz, H-8), 7.11 (8H, m, H-2 and H-3), 6.87 (2H, dd, *J* = 7.2 and 1.2 Hz, H-1), 6.83 (4H, dd, *J* = 7.2 and 1.2 Hz, H-4), 4.08 (4H, t, *J* = 6.4 Hz, H-5), 3.13 (4H, t, *J* = 6.4 Hz, H-7), 2.06 (4H, m, H-6); ^{13}C-NMR (101 MHz, $CDCl_3$) δ 165.0, 150.1 (2C), 145.2 (4C), 140.8 (2C), 127.7 (4C), 127.3 (4C), 125.1 (4C), 122.5 (4C), 120.9 (2C), 115.9 (2C), 55.6 (2C), 44.4 (2C) and 24.5 (2C); LRMS: *m/z* 615.90 $[M]^+$; HPLC purity 94.3% (t_r = 13.18).

N',N'-bis(3-(2-chloro-10H-phenothiazin-10-yl)propyl)isonicotinohydrazide **(4.4b)**

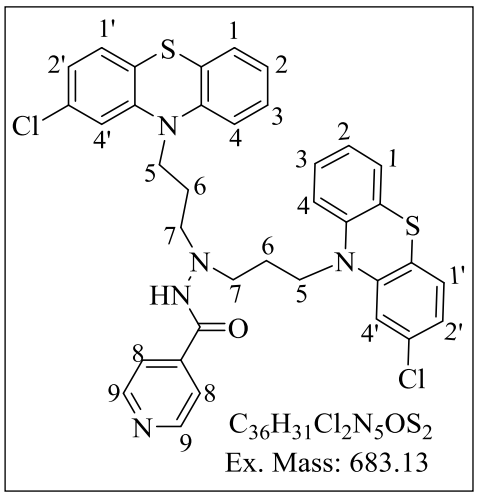

Oil (0.14 g, 26%); R_f 0.20 (5% MeOH-DCM); ^{1}H NMR (400 MHz, $CDCl_3$) δ 8.64 (2H, d, *J* = 6.0 Hz, H-9), 7.38 (2H, d, *J* = 6.0 Hz, H-8), 7.13 (4H, m, H-1 and H-3), 6.95 (2H, d, *J* = 8.0 Hz, H-1'), 6.90 (2H, td, *J* = 7.6 and 0.8 Hz, H-2), 6.87 (4H, dd, *J* = 8.4 and 2.4 Hz, H-4 and H-2'), 6.80 (2H, d, *J* = 2.0 Hz, H-4'), 3.91 (4H, t, *J* = 6.4 Hz, H-5), 2.99 (4H, t, *J* = 6.4 Hz, H-7), 1.88 (4H, m, H-6); ^{13}C NMR (101 MHz, $CDCl_3$) δ 164.8, 149.9 (2C), 146.4 (4C), 144.5 (2C), 140.9 (2C), 133.3 (2C), 127.9 (4C), 127.6 (2C), 125.9 (2C), 123.8 (4C), 120.8 (2C), 115.6 (2C), 55.4 (2C), 44.4 (2C) and 24.5 (2C); LRMS: *m/z* 684.1 $[M]^+$; HPLC purity 98.2% (t_r = 15.65).

General Procedure 11: Procedure for the synthesis of 4.5

1-Amino-3-propanol (4.77 mmol) was added to a solution of **4.2** (3.21 mmol) and potassium carbonate (4.26 mmol) in DMF (5 ml). The reaction mixture was stirred at 80 °C for 10 hours. After completion of reaction (TLC), DMF was evaporated under reduced pressure and residue was taken in ethyl acetate. The organic layer was washed with water (20 ml × 5),

dried over sodium sulphate and concentrated. The crude product was purified by biotage flash column chromatography using 1-10% methanol in DCM as eluent to afford **4.5.**

***3-((3-(10H-phenothiazin-10-yl)propyl)amino)propan-1-ol* (4.5a)**

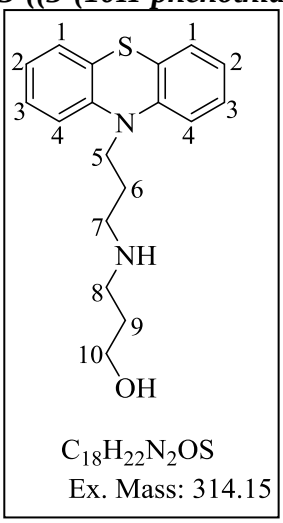

$C_{18}H_{22}N_2OS$
Ex. Mass: 314.15

White solid (0.64 g, 65%); m.p. 100-103 °C; R_f 0.20 (10% MeOH-DCM); ^{1}H-NMR (400 MHz, $CDCl_3$) δ 7.19 (4H, m, H-1 and H-3), 6.95 (2H, td, *J* = 7.6 and 1.2 Hz, H-2), 6.91 (2H, dd, *J* = 8.4 and 1.2 Hz, H-4), 3.98 (2H, t, *J* = 6.8 Hz, H-5), 3.73 (2H, t, *J* = 5.2 Hz, H-10), 2.84 (2H, t, *J* = 5.6 Hz, H-8), 2.81 (2H, t, *J* = 6.8 Hz, H-7), 2.04 (2H, quin, *J* = 6.8 Hz, H-6), 1.70 (2H, quin, *J* = 5.6 Hz, H-9); ^{13}C-NMR (101 MHz, $CDCl_3$) δ 145.0 (2C), 127.6 (2C), 127.4 (2C), 125.6 (2C), 122.7 (2C), 115.7 (2C), 63.3, 49.2, 47.1, 45.9, 30.3 and 26.4; LC-ESI-MS (+ve ion mode): *m/z* 315.1 $[M+H]^+$.

***3-((3-(2-chloro-10H-phenothiazin-10-yl)propyl)amino)propan-1-ol* (4.5b)**

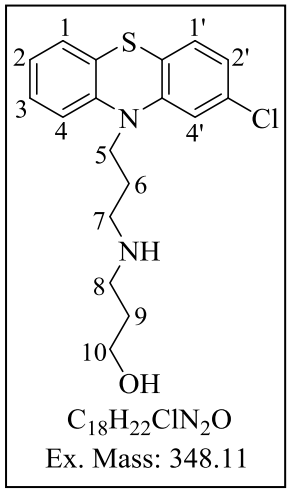

$C_{18}H_{22}ClN_2O$
Ex. Mass: 348.11

White solid (0.77 g, 68%); m.p. 61-64 °C; R_f 0.20 (10% MeOH-DCM); ^{1}H-NMR (400 MHz, $CDCl_3$) δ 7.15 (2H, m, H-1 and H-3), 7.05 (1H, d, *J* = 8.4 Hz, H-1'), 6.95 (1H, td, *J* = 7.6 and 1.2 Hz, H-2), 6.90 (1H, dd, *J* = 8.4 and 2.0 Hz, H-4), 6.88 (1H, dd, *J* = 8.4 and 1.2 Hz, H-2'), 6.85 (1H, d, *J* = 2.0 Hz, H-4'), 3.93 (2H, t, *J* = 6.8 Hz, H-5), 3.73 (2H, t, *J* = 5.6 Hz, H-10), 2.82 (2H, t, *J* = 6.0 Hz, H-8), 2.81 (2H, t, *J* = 6.8 Hz, H-7), 2.04 (2H, quin, *J* = 6.0 Hz, H-6), 1.70 (2H, quin, *J* = 5.6 Hz, H-9). ^{13}C NMR (101 MHz, $CDCl_3$) δ 146.6, 144.5, 133.2, 128.1, 127.7 (2C), 127.6, 125.2, 124.1, 123.1, 122.5, 116.0, 63.5, 49.4, 47.0, 45.3, 30.5 and 26.5; LC-ESI-MS (+ve ion mode): *m/z* 349.4 $[M+H]^+$, 350.1 $[M+1+H]^+$ and 351.1 $[M+2+H]^+$.

General Procedure 12: Procedure for the synthesis of 4.6

Di-*tert*-butyl dicarbonate anhydride (1.83 mmol) was added in portions over 3-5 minute to a solution of compound **4.5** (1.44 mmol) and triethylamine (1.73 mmol) in DCM at 0 °C. After

completion of addition, the reaction mixture was stirred at room temperature (25 °C) and monitored by TLC. After completion of reaction, quenched with water and extracted with ethyl acetate, dried over sodium sulphate and concentrated to obtain **4.6**.

***tert-butyl (3-(10H-phenothiazin-10-yl)propyl)(3-hydroxypropyl)carbamate* (4.6a)**

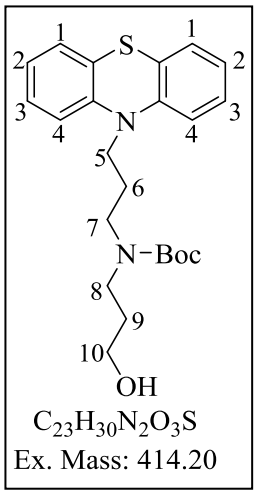

$C_{23}H_{30}N_2O_3S$
Ex. Mass: 414.20

Oil (0.75 g, 95%); R_f 0.60 (10% MeOH-DCM); ^{1}H-NMR (400 MHz, $CDCl_3$) δ 7.17 (4H, m, H-1 and H-3), 6.93 (2H, m, H-2), 6.91 (2H, d, *J* = 8.0 Hz, H-4), 3.90 (2H, t, *J* = 7.2 Hz, H-5), 3.73 (2H, t, *J* = 5.6 Hz, H-10), 3.25 (4H, m, H-8 and H-7), 2.04 (2H, quin, *J* = 6.8 Hz, H-6), 1.57 (2H, m, H-9), 1.41 (9H, s, Boc). ^{13}C-NMR (101 MHz, $CDCl_3$) δ 156.8, 145.2 (2C), 127.7 (2C), 127.2 (2C), 126.2 (2C), 122.1 (2C), 115.7 (2C), 80.1, 58.3, 44.6 (2C), 43.1, 30.5, 28.3 (3C) and 25.8; LC-ESI-MS (+ve ion mode): *m/z* 415.2 $[M+H]^+$.

***tert-butyl (3-(2-chloro-10H-phenothiazin-10-yl)propyl)(3-hydroxypropyl)carbamate* (4.6b)**

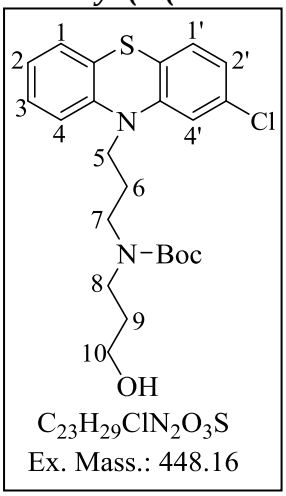

$C_{23}H_{29}ClN_2O_3S$
Ex. Mass.: 448.16

Oil (60.0 g, 93%); R_f 0.60 (10% MeOH-DCM); ^{1}H-NMR (400 MHz, CD_3OD) δ 7.26 (1H, td, *J* = 8.0 and 1.6 Hz, H-3), 7.20 (1H, dd, *J* = 7.6 and 1.6 Hz, H-1), 7.11 (1H, d, *J* = 8.0 Hz, H-1'), 7.0 (3H, m, H-2, H-4 and H-4'), 6.97 (1H, dd, *J* = 8.4 and 1.2 Hz, H-2'), 3.94 (2H, t, *J* = 6.8 Hz, H-5), 3.50 (2H, t, *J* = 6.4 Hz, H-10), 3.32 (2H, t, *J* = 6.4 Hz, H-8), 3.23 (2H, t, *J* = 7.2 Hz, H-7), 2.04 (2H, quin, *J* = 7.2 Hz, H-6), 1.70 (2H, quin, *J* = 6.8 Hz, H-9), 1.41 (s, 9H, Boc). ^{13}C-NMR (101 MHz, CD_3OD) δ 154.4, 145.6, 143.4, 131.8, 126.3 (2C), 125.9 (2C), 125.7, 121.5, 120.7, 114.6, 114.3, 78.3, 57.6, 43.3, 42.9 (2C), 28.3, 25.9 (3C) and 25.8; LC-ESI-MS (+ve ion mode): *m/z* 449.2 $[M+H]^+$, 450.2 $[M+1+H]^+$ and 451.2 $[M+2+H]^+$.

General Procedure 13: Procedure for the synthesis of 4.7

A solution of **4.6** (1.23 mmol) in DCM was charged with triphenyl phosphine (1.84 mmol) and carbon tetrabromomethane (1.84 mmol). The reaction mixture was stirred at room temperature (25 °C) for 6 hour. After completion of reaction (TLC), quenched with water and

extracted with DCM. The combine DCM layer was dried over anhydrous sodium sulphate and concentred *in vacuo*. The crude product was purified by column chromatography using 20-40% ethyl acetate in hexane as eluent.

***tert-butyl (3-(10H-phenothiazin-10-yl)propyl)(3-bromopropyl)carbamate* (4.7a)**

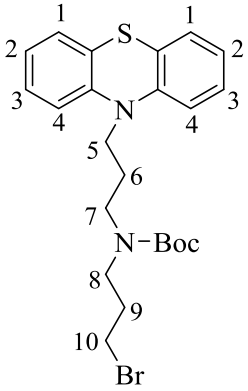

$C_{23}H_{29}BrN_2O_2S$
Ex. Mass.: 476.11

Oil (0.53 g, 83%); R_f 0.6 (10% MeOH-DCM); ^{1}H-NMR (400 MHz, $CDCl_3$) δ 7.17 (4H, m, H-1 and H-3), 6.93 (2H, m, H-2), 6.91 (2H, d, *J* = 8.0 Hz, H-4), 3.91 (2H, t, *J* = 6.8 Hz, H-5), 3.31 (4H, m, H-8 and H-10), 3.21 (2H, t, *J* = 6.8 Hz, H-7), 2.06 (2H, quin, *J* = 6.8 Hz, H-6), 1.57 (2H, quin, *J* = 6.8 Hz, H-9), 1.43 (9H, s, Boc). ^{13}C-NMR (101 MHz, $CDCl_3$) δ 156.6, 144.6 (2C), 127.6 (2C), 127.3 (2C), 125.7 (2C), 122.8 (2C), 115.8 (2C), 79.7, 46.3, 45.1, 44.7, 31.6, 30.6, 28.4 (3C) and 25.9; LC-ESI-MS (+ve ion mode): *m/z* 477.5 $[M+H]^+$.

***tert-butyl(3-bromopropyl)(3-(2-chloro-10H-phenothiazin-10-yl)propyl)carbamate* (4.7b)**

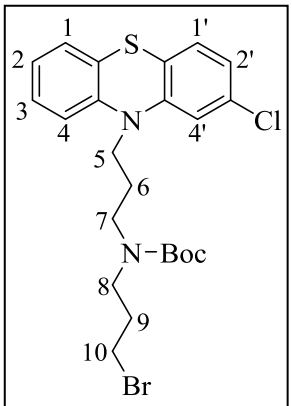

$C_{23}H_{28}BrClN_2O_2S$
Ex.Mass.: 510.07

Oil (0.55 g, 88%); R_f 0.6 (10% MeOH-DCM); ^{1}H-NMR (400 MHz, CD_3OD) δ 7.20 (1H, td, *J* = 8.0 and 1.6 Hz, H-3), 7.19 (1H, dd, *J* = 7.6 and 1.6 Hz, H-1), 7.11 (1H, d, *J* = 8.0 Hz, H-1'), 7.0 (3H, m, H-2, H-4 and H-4'), 6.97 (1H, dd, *J* = 8.4 and 1.2 Hz, H-2'), 3.94 (2H, t, *J* = 6.4 Hz, H-5), 3.50 (2H, t, *J* = 6.4 Hz, H-10), 3.32 (2H, t, *J* = 6.4 Hz, H-8), 3.23 (2H, t, *J* = 7.2 Hz, H-7), 2.04 (2H, quin, *J* = 7.2 Hz, H-6), 1.70 (2H, quin, *J* = 6.8 Hz, H-9), 1.41 (9H, s, Boc); ^{13}C-NMR (101 MHz, CD_3OD) δ 154.4, 145.6, 143.4, 131.8, 126.3 (2C), 125.9 (2C), 125.7, 121.5, 120.7, 114.6, 114.3, 78.3, 57.6, 43.3, 42.9 (2C), 28.3, 25.9 (3C) and 25.8; LC-ESI-MS (+ve ion mode): *m/z* 511.1 $[M+H]^+$.

General Procedure 14: Procedure for the synthesis of 4.8

A solution of compound **4.7** (0.3 g, 0.628 mmol) in DMF (1 ml) was added to a mixture of isoniazid and triethylamine under an atmosphere of nitrogen at room temperature (25 °C). The reaction mixture was continuously stirred for an additional hour, after which it was

heated to 55 °C and stirred for another 6 hours. After completion of reaction (TLC), DMF was removed *in vacuo*, dried pver sodium sulphate and concentrated *in vacuo*. The crude product was purified by biotage flash chromatography.

***tert-butyl (3-(10H-phenothiazin-10-yl)propyl)(3-isonicotinoylhydrazinyl)propyl) carbamate* (4.8a)**

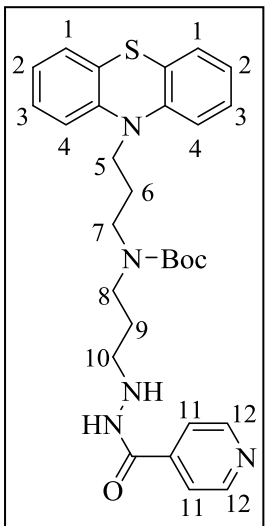

$C_{29}H_{35}N_5O_3S$
Ex. Mass: 533.25

White solid (0.18 g, 35%); m.p. 55-58 °C; R_f 0.35 (10% MeOH-DCM); ^{1}H-NMR (400 MHz, CD_3OD) δ 8.67 (2H, d, *J* = 6.0 Hz, H-12), 7.73 (2H, d, *J* = 6.4 Hz, H-11), 7.18 (2H, td, *J* = 7.2 and 1.6 Hz, H-3), 7.12 (2H, dd, *J* = 7.6 and 1.2 Hz, H-1), 6.96 (2H, dd, *J* = 7.6 and 0.8 Hz, H-4), 6.95 (2H, td, *J* = 7.2 and 1.2 Hz, H-2), 3.90 (2H, t, *J* = 6.4 Hz, H-5), 3.35 (2H, t, *J* = 7.2 Hz, H-8), 2.81 (2H, t, *J* = 7.2 Hz, H-7), 2.78 (2H, t, *J* = 6.8 Hz, H-10), 2.01 (2H, quin, *J* = 6.4 Hz, H-6), 1.80 (2H, quin, *J* = 7.2 Hz, H-9), 1.40 (9H, bs, Boc); ^{13}C-NMR (101 MHz, CD_3OD) δ 164.5 (2C), 156.1, 149.6 (2C), 145.4, 141.3, 127.1 (2C), 126.9 (2C), 122.6 (2C), 121.7 (2C), 121.4, 115.7 (2C), 79.8, 48.5, 44.6 (2C), 44.0, 27.3 (3C), 26.5 and 26.4; LC-ESI-MS (+ve ion mode): *m/z* 534.2 $[M+H]^+$.

***tert-butyl(3-(2-chloro-10H-phenothiazin-10-yl)propyl)(3-(2-isonicotinoylhydrazinyl)propyl)carbamate* (4.8b)**

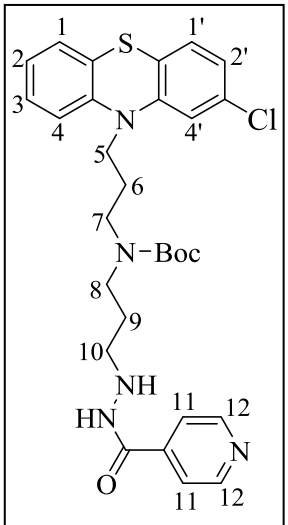

$C_{29}H_{34}ClN_5O_3S$
Ex. Mass.: 567.21

White solid (0.15 g, 30%); m.p. 62-64 °C; R_f 0.40 (10% MeOH-DCM); ^{1}H-NMR (400 MHz, CD_3OD) δ 7.20 (1H, td, *J* = 7.6 and 2.0 Hz, H-3), 7.18 (1H, dd, *J* = 8.0 and 1.6 Hz, H-1), 7.13 (1H, d, *J* = 8.0 Hz, H-1'), 7.01 (3H, m, H-2, H-4 and H-3'), 6.99 (1H, dd, *J* = 8.0 and 1.6 Hz, H-2'), 3.93 (2H, t, *J* = 6.8 Hz, H-5), 3.33 (2H, t, *J* = 7.2 Hz, H-7), 2.84 (2H, t, *J* = 7.2 Hz, H-8), 2.80 (2H, t, *J* = 6.4 Hz, H-10), 2.07 (2H, quin, *J* = 6.4 Hz, H-6), 1.70 (2H, quin, *J* = 7.2 Hz, H-9), 1.36 (9H, bs, Boc); ^{13}C-NMR (101 MHz, CD_3OD) δ 165.2, 156.5 148.3 (2C), 145.3 142.9, 139.1, 132.1, 126.2, 126.1, 126.0, 124.1,

123.3, 121.8, 121.0, 120.1 (2C), 114.8 and 114.7, 79.5, 48.4, 44.2 (2C), 44.0, 27.1 (3C), 26.5 and 26.4; LC-ESI-MS (+ve ion mode): *m/z* 568.1 $[M+H]^+$ and 570.1 $[M+2+H]^+$.

General Procedure 15: Procedure for the synthesis of 4.10

10 ml of a 10% mixture of TFA in DCM by volume was added to compound **4.8** (0.94 mmol) in a round bottom flask and stirred at room temperature (25 °C) for one hour. After completion of reaction (TLC), excess of TFA was removed *in vacuo* and residue was dissolved in 10% MeOH in DCM. The amberlyst A-21 was added to scavenger the residual TFA and stirred for one hour, after which reaction mixture was filtered through the bed of celite silica and washed with a 20% mixture of methanol in DCM. The combined organic layer was concentrated under reduced pressure to obtain **4.10.**

***N'-(3-((3-(10H-phenothiazin-10-yl)propyl)amino)propyl)isonicotinohydrazide* (4.10a)**

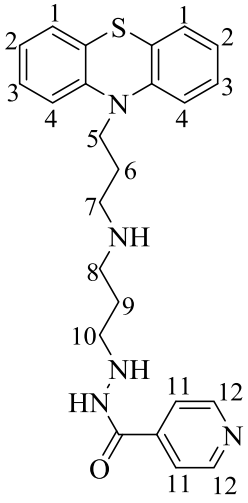

$C_{24}H_{27}N_5OS$
Ex. Mass: 433.19

White solid (0.40 g, 66%); m.p. 48-50 °C; R_f 0.50 (10% MeOH-DCM); ^{1}H-NMR (400 MHz, DMSO-d_6) δ 10.30 (1H, s, NH), 8.70 (2H, d, *J* = 5.2 Hz, H-12), 7.73 (2H, d, *J* = 6.0 Hz, H-11), 7.18 (4H, m, H-1 and H-3), 6.96 (2H, d, *J* = 8.0 Hz, H-4), 6.95 (2H, t, *J* = 6.8 Hz, H-2), 3.91 (2H, t, *J* = 6.8 Hz, H-5), 3.01 (4H, m, H-7 and H-8), 2.89 (2H, t, *J* = 6.0 Hz, H-10), 2.04 (2H, quin, *J* = 7.2 Hz, H-6), 1.70 (2H, quin, *J* = 6.8 Hz, H-9); ^{13}C-NMR (101 MHz, DMSO-d_6) δ 164.3, 150.2 (2C), 144.5 (2C), 140.0, 127.6 (2C), 127.2 (2C), 124.2 (2C), 122.7 (2C), 121.2 (2C), 115.9 (2C), 48.4, 45.8, 44.7, 43.6, 23.7 and 23.3; LC-ESI-MS (+ve ion mode): *m/z* 434.2 $[M+H]^+$, purity 99% (t_r = 3.969 min).

***N'-(3-((3-(2-chloro-10H-phenothiazin-10-yl)propyl)amino)propyl)isonicotinohydrazide* (4.10b)**

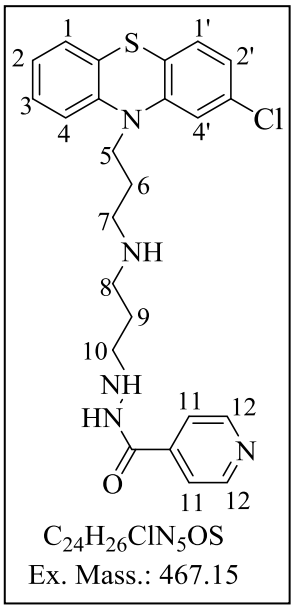

$C_{24}H_{26}ClN_5OS$
Ex. Mass.: 467.15

White solid (0.37 g, 83%); m.p. 61-64 °C; R_f 0.20 (10% MeOH-DCM); ^{1}H-NMR (400 MHz, CD_3OD) δ 8.74 (2H, dd, *J* = 6.4 and 2.0 Hz, H-12), 7.74 (2H, dd, *J* = 6.4 and 1.6 Hz, H-11), 7.15 (2H, m, H-1 and H-3), 7.05 (1H, d, *J* = 8.0 Hz, H-1'), 6.90 (2H, m, H-4 and H-4'), 6.95 (1H, td, *J* = 7.6 and 1.2 Hz, H-2), 6.88 (1H, dd, *J* = 8.4 and 2.0 Hz, H-2'), 4.18 (2H, t, *J* = 6.4 Hz, H-5), 3.22 (4H, m, H-7 and H-8), 3.09 (2H, t, *J* = 6.0 Hz, H-10), 2.04 (2H, quin, *J* = 6.4 Hz, H-6), 1.70 (2H, quin, *J* = 6.0 Hz, H-9); ^{13}C-NMR (101 MHz, CD_3OD) δ 165.1, 148.3 (2C), 145.7, 142.9, 139.2, 132.1, 126.5, 126.1, 125.9, 124.4, 123.3, 121.9, 121.0, 120.1 (2C), 114.8, 114.7, 49.3, 44.1, 42.4 (2C), 22.9 and 21.9; LC-ESI-MS (+ve ion mode): *m/z* 468.1 $[M+H]^+$, 469.1 $[M+1+H]^+$ and 470.1 $[M+2+H]^+$, purity 97.1% (t_r = 3.545 min.).

***tert-butyl 4-((methylsulfonyl)oxy)piperidine-1-carboxylate* (4.13)**

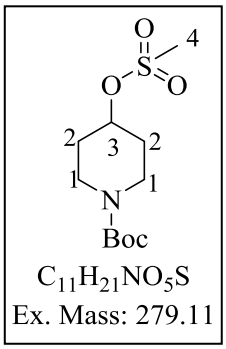

$C_{11}H_{21}NO_5S$
Ex. Mass: 279.11

Di-tert-butyl dicarbonate anhydride (12.83 mmol) was added in portions to a solution of triethylamine (1.30 g, 1.80 ml, 12.83 mmol) and 4-hydroxypiperidine **4.11** (9.88 mmol) in DCM (15 ml) at 0 °C. After completion of addition, the reaction mixture was warmed to room temperature (25 °C) and stirred for one hour. After completion of reaction (TLC), quenched with water and extracted with dichloromethane, dried over sodium sulphate and concentrated under reduced pressure to obtain **4.12** as white solid which was used in the next step without further purification.

Methanesulfonyl chloride (0.85 g, 0.58 ml, 7.44 mmol) was added drop-wise to a solution of *tert*-Butyl 4-hydroxylpiperidine-1-carboxylate **4.12** (1.25 g, 6.21 mmol) and triethylamine (0.75 g, 1.10 ml, 7.41 mmol) in DCM at 0 °C. After completion of addition, the reaction mixture was stirred at room temperature (25 °C) for 1 hour. After completion of reaction

(TLC), the reaction was quenched with water and extracted with DCM. The combined DCM layer was washed with brine, dried over sodium sulphate and concentrated *in vacuo* to obtain **4.13** as light yellow solid (1.34 g, 97%). R_f 0.70 (5% MeOH-DCM), m.p. 193-195 °C; ^{1}H-NMR (400 MHz, CD_3OD) δ 4.80 (1H, m, H-3), 3.62-3.23 (4H, m, H-1), 2.96 (3H, s, H-4), 1.88-1.39 (4H, m, H-2), 1.39 (9H, s, Boc).

General procedure 16: Procedure for the synthesis of 4.14

Phenothiazine **4.1 (**6.54 mmol) was added to the suspension of NaH (7.21 mmol) in DMSO under an atmosphere of nitrogen. The mixture was stirred at room temperature (25 °C) for ten minutes, then at 70 °C for 50 minutes. A solution of compound **4.13** (7.21 mmol) in DMSO (5 ml) was added to the reaction mixture at 70 °C. The resulting reaction mixture was then stirred at 100 °C under an atmosphere of nitrogen for 18 hours, however reaction did not go to completion. After 18 hours, the reaction mixture was diluted with DCM, washed with 1*N* NaOH (2 × 5ml), dried over sodium sulphate and concentrated *in vacuo*. Purification was done by column chromatography at 2% DCM in Hexane as eluent to afford **4.14**.

***tert-butyl 4-(10H-phenothiazin-10-yl)piperidine-1-carboxylate* (4.14a)**

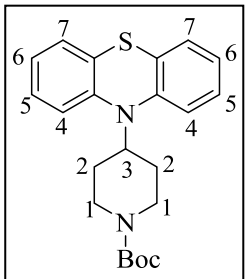

$C_{22}H_{26}N_2O_2S$
Ex. Mass: 382.17

Pink solid (0.75 g, 30%); m.p. 120-122 °C; R_f 0.50 (20% EtOAc-Hexane); ^{1}H-NMR (400 MHz, CD_3OD) δ 7.19 (2H, dd, *J* = 1.6 and 6.8 Hz, H-7), 7.18 (2H, m, H-6), 7.15 (2H, m, H-5), 7.03 (2H, m, H-4), 4.08 (2H, dt, *J* = 12.8 and 4.4 Hz, H_e-1), 4.90 (1H, tt, *J* = 11.2 and 3.6 Hz, H-3), 2.90 (2H, m, H_a-1), 2.09 (2H, bd, *J* = 12.8 Hz, H_e-2), 1.98 (2H, qd, *J* = 12.8 and 4.4 Hz, H_a-2), 1.91 (9H, s, Boc). ^{13}C-NMR (101 MHz, CD_3OD) δ 153.9, 144.4 (2C), 128.1 (2C), 125.4 (4C), 122.0 (2C), 120.8 (2C), 78.0, 61.5, 41.3 (2C), 30.5 (3C) and 30.0 (2C); LC-ESI-MS (+ve ion mode): *m/z* 383.2 $[M+H]^+$ and 283.2 [M-Boc+ H].

***tert-butyl 4-(2-chloro-10H-phenothiazin-10-yl)piperidine-1-carboxylate* (4.14b)**

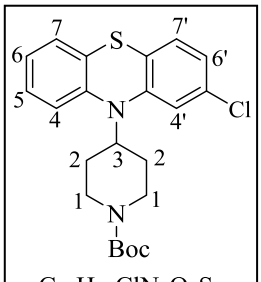

$C_{22}H_{25}ClN_2O_2S$
Ex Mass.: 416.13

White Solid (0.90 g, 32%); m.p. 157-158 °C; R_f 0.20 (10% DCM-Hexane); ^{1}H-NMR (400 MHz, $CDCl_3$) δ 7.21 (1H, d, *J* = 8.0 Hz, H-7'), 7.04 (2H, m, H-7 and H-5), 7.15 (1H, d, *J* = 2.0 Hz, H-4'), 7.09

(1H, d, *J* = 7.6 Hz, H-4), 7.00 (1H, m, H-6), 6.95 (1H, dd, *J* = 8.4 and 2.0 Hz, H-6'), 4.20 (2H, d, *J* = 12.8 Hz, H_e-1), 3.83 (1H, t, *J* = 8.8 Hz, H-3), 2.84 (2H, m, H_a-1), 2.08 (4H, m, H-2), 1.49 (9H, s, Boc). ^{13}C-NMR (101 MHz, $CDCl_3$) δ 154.7, 146.0, 143.5, 132.7, 129.7, 128.5, 127.9, 127.5, 127.3, 124.4, 124.0, 122.1, 121.9, 79.8, 63.7, 43.6, (2C), 32.12 (2C) and 28.4 (3C); LC-ESI-MS (+ve ion mode): *m/z* 417.1 $[M+1]^+$, 318.1 $[M\text{-Boc }+1+H]^+$ and 319.1 $[M\text{-Boc }+2+H]^+$.

General Procedure 17: Procedure for the synthesis of 4.15

Compound **4.14** (1.83 mmol) was dissolved in 2 ml of a mixture 10% TFA in DCM (v/v) and stirred for one hour. After completion of reaction (TLC), solvent was removed under reduced pressure. The residue was dissolved in DCM, basified with 1*N* NaOH. The combined DCM layers were dried over anhydrous sodium sulphate and concentrated to afford **4.15**.

***10-(piperidin-4-yl)-10H-phenothiazine* (4.15a)**

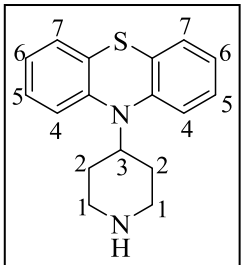

$C_{17}H_{18}N_2S$
Ex. Mass: 282.12

Grey solid (0.45 g, 87%); m.p. 100-103 °C; R_f 0.10 (10% MeOH-DCM); ^{1}H-NMR (400 MHz, CD_3OD) δ 7.20 (2H, m, H-6), 7.19 (2H, m, 2H, H-5), 7.15 (2H, ddd, *J* = 7.6, 1.2 and 0.4 Hz, H-7), 7.03 (2 H, dd, *J* = 7.6 and 0.8 Hz, H-4), 4.90 (1H, m, H-3), 4.08 (2H, dt, *J* = 12.8 and 2.8 Hz, H_e-1), 2.90 (2H, ddd, *J* = 16.0, 12.4 and 4.0 Hz, H_a-1), 2.13 (4H, m, H-2). ^{13}C-NMR (101 MHz, CD_3OD) δ 143.8 (2C), 128.3 (2C), 125.4 (4C), 122.1 (2C), 120.3 (2C), 61.3, 43.8 (2C) and 30.9 (2C); LC-ESI-MS (+ve ion mode): *m/z* 283.1 $[M+H]^+$.

***2-chloro-10-(piperidin-4-yl)-10H-phenothiazine* (4.15b)**

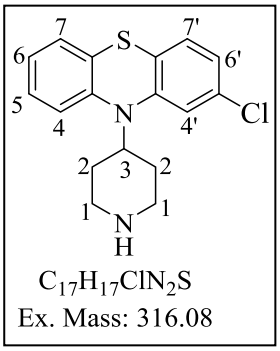

$C_{17}H_{17}ClN_2S$
Ex. Mass: 316.08

White solid (0.51 g, 95%); 131-133 °C R_f 0.15 (10% MeOH-DCM); ^{1}H-NMR (400 MHz, DMSO-d_6) δ 7.23 (2H, m, H-7 and H-5), 7.16 (3H, m, H-6, H-7' and H-4'), 7.05 (1H, dd, *J* = 8.4 and 2.4 Hz, H-6'), 7.01 (1H, m, H-4), 3.80 (1H, m, H-3), 3.03 (2H, d, *J* = 12.8 Hz, H_e-1), 2.59 (2H, m, H_a-1), 2.00 (4H, m, H-2); ^{13}C-NMR (101 MHz, $CDCl_3$) δ 146.9, 144.7, 132.4, 128.5, 128.0, 127.6, 127.3, 126.7, 124.2, 123.4, 120.8, 120.0, 63.6, 46.5 and 33.6; LC-ES-MS(+ve ion mode): *m/z* 317.1 $[M+H]^+$, 318.1 $[M+1+H]^+$ and 319.1 $[M+2+H]^+$.

General procedure 17: Procedure for reaction of various intermediates with 1-bromo-3-chloropropane

A solution of piperazine or piperidine intermediate (1 equivalent), triethylamine (2.5 equivalent) and 1-bromo-3-chloropropane (2.0 equivalent) was stirred at 68 °C for 6 hour. After completion of reaction (TLC), toluene was removed *in vacuo* and residue was dissolved in DCM. The DCM layer was washed with water (3 × 15 ml), dried over sodium sulphate and concentrated. The crude product was purified by column chromatography.

***10-(1-(3-chloropropyl)piperidin-4-yl)-10H-phenothiazine* (4.16a)**

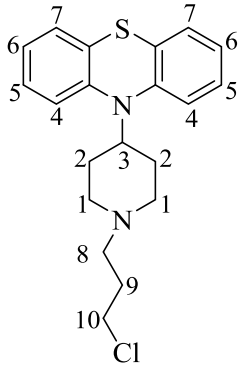

$C_{20}H_{23}ClN_2S$
Ex. Mass.: 358.13

The general method **17** was adopted and 1.13 mmol of **4.15a** was used to obtain **4.16a** as an oil (0.48 g, 75%); R_f 0.80 (10% MeOH-DCM); ^{1}H-NMR (400 MHz, CD_3OD) δ 7.20 (2H, m, H-6), 7.19 (2H, m, H-5), 7.15 (2H, dd, *J* = 7.0 and 0.8 Hz, H-7), 7.03 (2H, m, H-6), 3.74 (1H, m, H-3), 3.61 (2H, t, *J* = 6.4 Hz, H-10), 3.0 (2H, m, H_e-1), 2.55 (2H, t, *J* = 7.2 Hz, H-8), 2.90 (2H, d, *J* = 11.2 Hz, H_a-1), 2.17 (6H, m, H_e-1 and H-2), 1.96 (2H, quin, *J* = 6.8 Hz, H-9); ^{13}C-NMR (101 MHz, CD_3OD) δ 145.2 (2C), 129.8 (2C), 126.8 (4C), 123.4 (2C), 121.6 (2C), 62.6, 58.5, 55.2, 53.0 (2C), 42.5 and 31.4 (2C); LC-ESI-MS (+ve ion mode): *m/z* 359.1 $[M+H]^+$, 360.1 $[M+1+H]^+$ and 361.1 $[M+2+H]^+$.

***2-chloro-10-(1-(3-chloropropyl)piperidin-4-yl)-10H-phenothiazine* (4.16b)**

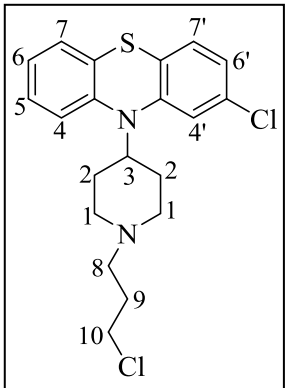

$C_{20}H_{22}Cl_2N_2S$
Ex. Mass: 392.09

The general method **17** was adopted and 1.02 mmol of **4.15b** was used to obtain **4.16b** as an oil (0.41 g, 72%), R_f 0.60 (10% DCM-Hexane); ^{1}H-NMR (400 MHz, DMSO-d_6) δ 7.19 (2H, m, H-7 and H-5), 7.16 (1H, dd, *J* = 8.0 and 2.4 Hz, H-4), 7.09 (2H, m, H-7' and H-4'), 7.02 (1H, m, H-6), 6.99 (1H, dd, *J* = 8.4 and 2.4 Hz, H-6'), 3.78 (1H, m, H-3), 3.63 (2H, t, *J* = 6.4 Hz, H-10), 3.01 (2H, bd, *J* = 8.0 Hz, H_e-1), 2.61 (2H, t, *J* = 6.4 Hz, H-8), 2.32 (4H, m, H_a-1 and H_e-2), 2.05 (4H, m, H_a-2), 2.05 (2H, quin, *J* = 6.8 Hz, H-9); ^{13}C-NMR (101 MHz, $CDCl_3$) δ 146.6, 144.3,

132.9, 128.3, 128.0, 127.9, 127.6, 127.3, 123.9, 123.6, 121.6, 121.2, 55.4, 53.0 (2C), 43.0, 31.4 (2C) and 29.7 (2C); LC-ESI-MS (+ve ion mode): *m/z* 393.1 $[M+H]^+$, 394.1 $[M+1+H]^+$ and 395.1 $[M+2+H]^+$.

General Procedure 18: Procedure for the synthesis of target compound by reaction of corresponding chloro-intermediate and isoniazid.

Triethylamine (4 equivalent) was added to a solution of isoniazid (4 equivalent) and chloro-intermediate (1 equivalent) in isopropanol, and resulting mixture was refluxed for 24 hourss. After completion of reaction (TLC), *iso* propanol was removed *in vacuo* and residue was taken in DCM (40 ml), and washed with water (5 x 15 mL). The aqueous layer was extracted with DCM (5 x 10 mL) and the combined DCM extracts was washed with brine (1 x 20 ml), dried over sodium sulphate and concentrated *in vacuo*. The crude was purified by column chromatography to afford the target compound.

***N'-(3-(4-(10H-phenothiazin-10-yl)piperidin-1-yl)propyl)isonicotinohydrazide* (4.17a)**

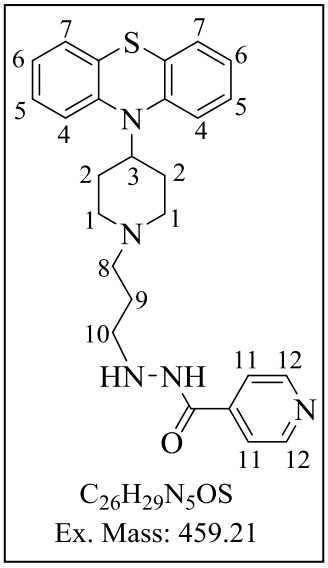

$C_{26}H_{29}N_5OS$
Ex. Mass: 459.21

The general method **18** was adopted and 0.726 mmol of **4.16a** was used to obtain **4.17a** as white solid (0.136 g, 30%); m.p. 54-56 °C; R_f 0.20 (10% MeOH-DCM), only distinguished after 3 runs of TLC; ^{1}H-NMR (400 MHz, DMSO-d_6) δ 8.74 (2H, d, J = 6.0 Hz, H-12), 7.75 (2H, d, J = 6.0 Hz, H-11), 7.20 (2H, m, H-6), 7.19 (2H, m, H-5), 7.15 (2H, d, J = 7.0 Hz, H-7), 7.03 (2H, m, H-4), 3.75 (1H, t, J = 12.8 Hz, H-3), 3.00 (2H, bd, J = 9.2 Hz, H_e-1), 2.87 (2H, t, J = 6.8 Hz, H-10), 2.44 (2H, t, J = 7.2 Hz, H-8), 2.18 (4H, m, H_e-1 and H_a-2), 2.1 (2H, bd, J = 10.0 Hz, H_e-2), 1.65 (2H, quin, J = 6.8 Hz, H-9); ^{13}C-NMR (101 MHz, DMSO-d_6) δ 163.8, 150.4 (2C), 145.3 (2C), 140.7, 130.0 (2C), 127.8 (2C), 127.5 (2C), 123.8 (2C), 121.5 (2C), 120.8 (2C), 62.5, 56.2, 53.2 (2C), 50.2, 31.6 (2C) and 25.4; LC-ESI-MS (+ve ion mode): *m/z* 460.2 $[M+H]^+$, purity 99.8% (t_r = 4.032 min).

***N'-(3-(4-(2-chloro-10H-phenothiazin-10-yl)piperidin-1-yl)propyl)isonicotinohydrazide* (4.17b)**

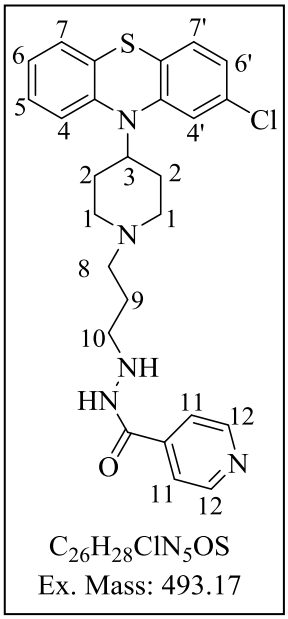

$C_{26}H_{28}ClN_5OS$
Ex. Mass: 493.17

The general method **18** was adopted and 0.791 mmol of **4.16b** was used to obtain **4.17b** as white solid (0.17 g, 30%), m.p. 85-87 °C; R_f 0.20 (10% DCM-Hexane); ^{1}H-NMR (400 MHz, CD_3OD) δ 8.74 (2H, d, *J* = 6.4 Hz, H-12), 7.75 (2H, d, *J* = 6.0 Hz, H-11), 7.19 (2H, m, H-7 and H-5), 7.17 (1H, d, *J* = 2.0 Hz, H-4'), 7.13 (1H, d, *J* = 7.2 Hz, H-7'), 7.09 (1H, d, *J* = 7.6 Hz, H-4), 7.02 (1H, m, H-6), 6.99 (1H, dd, *J* = 8.4 and 2.4 Hz, H-6'), 3.79 (1H, m, H-3), 3.10 (2H, bd, *J* = 10.0 Hz, H_e-1), 3.00 (2H, t, *J* = 6.4 Hz, H-10), 2.61 (2H, t, *J* = 6.8 Hz, H-8), 2.32 (4H, m, H_a-1 and H_e-2), 2.05 (4H, m, H-2), 2.05 (2H, quin, *J* = 7.2 Hz, H-9); ^{13}C-NMR (101 MHz, CD_3OD) δ 164.5, 149.6 (2C), 146.3, 144.6, 141.3, 132.5, 129.0, 128.4, 127.6, 127.1, 126.9, 123.7, 123.2, 121.4 (2C), 121.3, 121.0, 62.5, 56.1, 52.8 (2C), 50.0, 31.1 (2C) and 24.5; LC-ES-MS (+ve ion mode): *m/z* 494.1 $[M+H]^+$, 495.1 $[M+1+H]^+$, 496.1 $[M+2+H]^+$, and 516.1 $[M+Na]^+$, purity 99.5% (t_r = 3.772).

***tert-butyl 4-oxopiperidine-1-carboxylate* (4.19)**

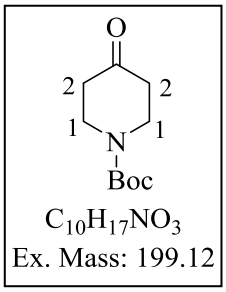

$C_{10}H_{17}NO_3$
Ex. Mass: 199.12

Triethylamine was added to a stirring solution of 4-piperidone monohydrochloride **4.18** (2.0 g, 13.09 mmol) in methanol and continued stirred for 5 minutes. Boc_2O (3.5 g, 17.29 mmol) was added in portions over a period of 5 minutes, followed by addition of DMAP (40 mg, 1.32 mmol). The resulting reaction mixture was stirred at ambient temperature (25 °C) for 20 hour. After completion of reaction (TLC), the methanol was removed *in vacuo* and crude was dissolved in DCM, washed with 2M HCl (2 × 10 ml), sat. $NaHCO_3$ and sat. NaCl (l 5 m × 2), respectively. The combined DCM layer was dried over sodium sulphate and concentrated to afford **4.18** as a white solid (3.9 g, 97 %), R_f 0.50 (30% EtOAc-Hexane); ^{1}H-NMR (400 MHz, $CDCl_3$) δ 3.74 (4H, t, *J* = 6.0 Hz, 4Hz, H-1), 2.46 (4H, t, *J* = 6.4 Hz, 2Hz, H-2), 1.52 (9H, s, Boc).

General Procedure 19: Procedure for the synthesis of 4.21

Titanium tetrachloride (1.84 g, 9.7 ml, 9.70 mmol, 1M in toluene) was added drop-wise to the suspension of zinc (1.43 g, 21.86 mmol) under nitrogen atmosphere. The resulting reaction mixture was stirred for one hour at 40 °C and then cooled to 0 °C, followed by the drop wise addition of a solution of **4.19** (1.26 g, 6.33 mmol) and **4.20** (4.8497 mmol). After completion of addition, the reaction mixture was the refluxed for 12 hours. After completion of reaction (TLC), crude was filtered through celite silica. The dioxane was removed *in vacuo*, residue was dissolved in ethyl acetate and washed with 2M HCl, dried over sodium sulphate and concentrated to obtain crude condensed alkene **4.21**. Purification was done by column chromatography.

***4-(9H-thioxanthen-9-ylidene)piperidine* (4.21a)**

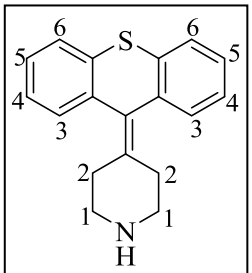

$C_{18}H_{17}NS$
Ex. Mass: 279.11

White solid (0.54 g, 40%); m.p. 188-190 °C; R_f 0.10 (5% MeOH-DCM); ^{1}H-NMR (400 MHz, DMSO-d_6) δ 9.10 (1H, s, NH), 7.90 (2H, dd, J = 7.6 and 1.2 Hz, H-6), 7.46 (2H, dd, J = 7.6 and 1.2 Hz, H-3), 7.32 (2H, td, J = 7.6 and 1.6 Hz, H-4), 7.30 2H, (2H, td, J = 7.6 and 16 Hz, H-5), 3.30 (2H, m, H_e-1), 2.96 (2H, m, H_a-1), 2.88 (2H, m, H_e-2), 2.62 (2H, m, H_a-2); ^{13}C-NMR (101 MHz, DMSO-d_6) δ 137.0, 136.9 (2C), 134.9 (2C), 129.5, 129.3 (2C), 127.63 (2C), 126.9 (2C), 126.6 (2C), 48.0 (2C) and 31.8 (2C); LC-ESI-MS (+ve ion mode): *m/z* 280.1 $[M+H]^+$.

***4-(2-chloro-9H-thioxanthen-9-ylidene)piperidine* (4.21b)**

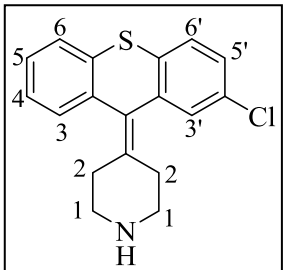

$C_{18}H_{16}ClNS$
Ex. Mass: 313.07

White solid (0.54 g, 40%); m.p. 216-218 °C; R_f 0.30 (5% MeOH-DCM); ^{1}H-NMR (400 MHz, CD_3OD) δ 7.55 (1H, dd, J = 7.6, and 1.2 Hz, H-6), 7.51 (1H, d, J = 8.0 Hz, H-6'), 7.42 (2H, m, H-5' and H-3'), 7.37 (2H, td, J = 7.6 and 1.2 Hz, H-4), 7.30 (2H, td, J = 7.6 and 1.2 Hz, H-5), 7.28 (1H, dd, J = 7.6 and 1.2 Hz, H-3), 3.44 (2H, m, H_e-1), 2.99 (2H, m, H_a-1), 2.92 (2H, m, H_e-2), 2.88 (2H, m, H_a-2); ^{13}C-NMR (101 MHz, DMSO-d_6) δ 137.9, 135.5, 134.5, 134.0, 132.6, 131.7, 130.7, 129.4 (2C), 128.6, 127.8, 127.6, 127.3,

127.1, 44.7 (2C) and 27.5 (2C); LC-ESI-MS (+ve ion mode): *m/z* 314.1 $[M+H]^+$, 315.1 $[M+1+H]^+$ and 316.1 $[M+2+H]^+$.

***4-(5H-dibenzo[a,d][7]annulen-5-ylidene)piperidine* (4.21c)**

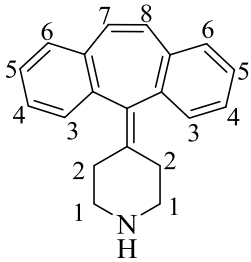

$C_{20}H_{19}N$
Ex. Mass: 273.15

White solid (0.73 g, 55%); m.p. 250-252 °C; R_f 0.10 (10% MeOH-DCM); ^{1}H-NMR (400 MHz, CD_3OD) δ 7.42 (2H, m, H-5 and H-4), 7.40 (2H, m, H-3), 7.28 (2H, dd, *J* = 8.4 and 1.6 Hz, H-6), 6.99 (2H, s, H-7 and H-8), 3.30 (2H, m, H_e-1), 2.93 (2H, m, H_a-1), 2.60 (2H, m, H_e-2), 2.38 (2H, m, H_a-2); LC-ESI-MS (+ve ion mode): *m/z* 274.2 $[M+H]^+$.

***1-(3-chloropropyl)-4-(5H-dibenzo[a,d][7]annulen-5-ylidene)piperidine* (4.22a)**

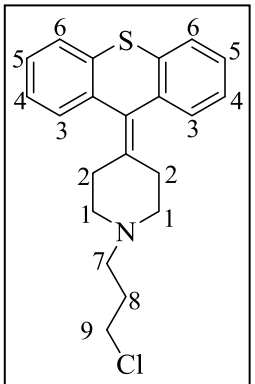

$C_{21}H_{22}ClNS$
Ex. Mass: 355.12

The general method **17** was adopted and 0.621 mmol of **4.21b** was used to obtain **4.22b** as yellow solid (0.15 g, 65%); m.p. 136-138 °C; R_f 0.65 (10% MeOH-DCM); ^{1}H-NMR (400 MHz, $CDCl_3$) δ 7.52 (2H, ddd, *J* = 8.0, 1.2 and 0.4 Hz, H-3), 7.34 (2H, ddd, *J* = 8.4, 1.6 and 0.8 Hz, H-6), 7.27 (2H, td, *J* = 7.2 and 1.2 Hz, H-4), 7.20 (2H, td, *J* = 7.6 and 1.6 Hz, H-5), 3.63 (2H, t, *J* = 6.8 Hz, H-9), 2.76 (2H, m, H_e-1), 2.72 (2H, m, H_a-1), 2.70 (2H, m, H_e-2), 2.51 (2H, t, *J* = 6.8 Hz, H-7), 2.17 (2H, m, H_a-2), 1.99 (2H, m, H-8); ^{13}C-NMR (101 MHz, $CDCl_3$) δ 137.0 (2C), 135.5, 135.4 (2C), 130.4, 128.8 (2C), 127.2 (2C), 126.2 (2C), 125.8 (2C), 55.3, 55.0 (2C), 43.3, 30.6 (2C) and 30.1; LC-ESI-MS (+ve ion mode): *m/z* 356.1 $[M+H]^+$.

***4-(2-chloro-9H-thioxanthen-9-ylidene)-1-(3-chloropropyl)piperidine* (4.22b)**

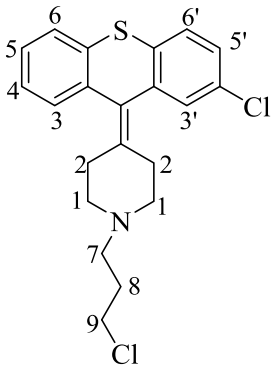

$C_{21}H_{21}Cl_2NS$
Ex. Mass: 389.08

The general method **17** was adopted and 0.958 mmol of **4.21c** was used to obtain **4.22c** as oil (0.22 g, 60%), R_f 0.7 (10% MeOH-DCM); ^{1}H-NMR (400 MHz, $CDCl_3$) δ 7.50 (1H, dd, *J* = 8.0 and 1.2 Hz, H-6), 7.43 (1H, d, *J* = 8.4 Hz, H-6'), 7.30 (2H, m, H-5' and H-4'), 7.29 (1H, td, *J* = 7.6 and 1.2 Hz, H-4), 7.21 (1H, td, *J* = 8.0 and 1.6 Hz, H-5), 7.28 (1H, dd, *J* = 8.0 and 2.4 Hz, H-3), 3.63 (2H, t, *J* = 6.8 Hz, H-9), 2.88 (2H, m, H_e-1), 2.71 (4H, m, H_a-1 and H_e-2), 2.51 (2H, t, *J* = 6.8 Hz, H-7), 2.16 (2H, m, H_a-2), 1.99 (2H, quin, *J* = 6.8 Hz, H-8); ^{13}C-NMR (101 MHz, $CDCl_3$) δ 138.6, 136.5, 135.1, 134.0, 131.8, 129.6, 129.0, 128.6, 128.3, 127.3 (2C), 126.4, 126.2, 126.0, 55.2, 54.9 (2C), 54.8, 43.0, and 30.5 (2C); LC-ESI-MS (+ve ion mode): *m/z* 390.0 $[M+H]^+$, 391.1 $[M+1+H]^+$ and 392.0 $[M+2+H]^+$.

***1-(3-chloropropyl)-4-(5H-dibenzo[a,d][7]annulen-5-ylidene)piperidine* (4.22c)**

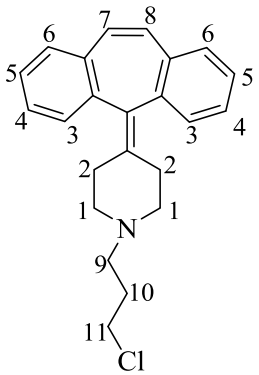

$C_{23}H_{24}ClN$
Ex. Mass: 349.16

The general method **17** was adopted and 1.13 mmol of **4.21a** was used to obtain **4.22a** as an oil (0.22 g, 55%); R_f 0.6 (10% MeOH-DCM); ^{1}H-NMR (400 MHz, $CDCl_3$) δ 7.33-7.37 (4H, m, H-5 and H-4), 7.25-7.29 (2H, m, H-3), 7.21 (2H, dd, *J* = 8.4 and 1.2 Hz, H-6), 6.95 (2H, s, H-7 and H-8), 3.61 (2H, t, *J* = 6.4 Hz, H-11), 2.70 (2H, m, H_e-1), 2.55 (2H, t, *J* = 6.8 Hz, H-9), 2.12-2.27 (4H, m, H_a-1 and H_e-2), 2.20 (2H, m, H_a-2), 2.02 (2H, quin, *J* = 6.4 Hz, H-10); ^{13}C-NMR (101 MHz, $CDCl_3$) δ 139.0 (2C), 134.8 (2C), 131.0 (2C), 128.4 (2C), 128.2 (2C), 127.8 (4C), 126.4 (2C), 55.4, 55.1 (2C), 43.1 and 29.6 (3C); LC-ESI-MS (+ve ion mode): *m/z* 350.2 $[M+H]^+$, 351.2 $[M+1+H]^+$ and 352.2 $[M+2+H]^+$.

***N'-(3-(4-(9H-thioxanthen-9-ylidene)piperidin-1 yl)propyl)isonicotinohydrazide* (4.23a)**

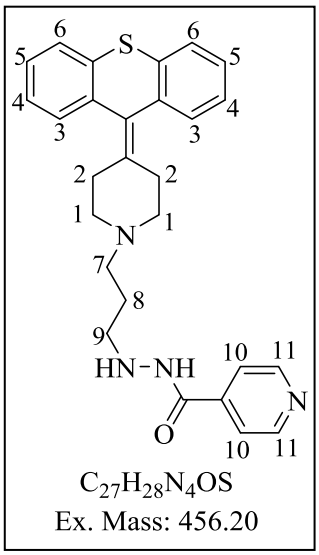

The general method **18** was adopted and 0.421 mmol of **4.22a** was used to obtain **4.23a** as white solid (70 mg, 37%); m.p. 105-107 °C; R_f 0.30 (10% MeOH-DCM); ^{1}H-NMR (400 MHz, DMSO-d_6) δ 8.76 (2H, bs, H-11), 7.67 (2H, d, *J* = 5.6 Hz, H-10), 7.49 (2H, dd, *J* = 7.6 and 1.2 Hz, H-3), 7.29 (2H, dd, *J* = 7.6 and 1.6 Hz, H-6), 7.25 (2H, td, *J* = 7.6 and 1.6 Hz, H-4), 7.18 (2H, td, *J* = 7.6 and 1.6 Hz, H-5), 3.02 (2H, *J* = 5.6 Hz, H-9), 2.92 (2H, m, H_e-1), 2.82-2.60 (4H, m, H_a -1 and H_e -2), 2.55 (2H, t, *J* = 5.6 Hz, H-7), 2.18 (2H, m, H_a-2), 1.80 (2H, quin, *J* = 6.4 Hz, H-8); ^{13}C-NMR (101 MHz, $CDCl_3$) δ 164.2, 150.6 (2C), 140.5, 136.6 (2C), 135.3 (2C), 134.1, 130.9, 128.7 (2C), 127.3 (2C), 126.3 (2C), 125.9 (2C), 121.0 (2C), 56.6, 54.7 (2C), 51.1, 30.1 (2C) and 25.5; LC-ESI-MS (+ve ion mode): *m/z* 457.2 $[M+H]^+$, purity 96.5% (t_r = 4.12 min).

***N'-(3-(4-(2-chloro-9H-thioxanthen-9-ylidene)piperidin-1-yl)propyl)isonicotinohydrazide* (4.23b)**

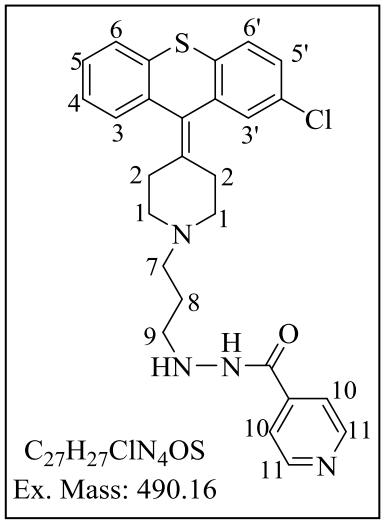

The general method **18** was adopted and 0.384 mmol of **4.22b** was used to obtain **4.23b** as white solid (0.06 g, 32%); m.p. 99-102 °C; R_f 0.30 (10% MeOH-DCM); ^{1}H-NMR (400 MHz, $CDCl_3$) δ 8.50 (2H, d, *J* = 5.2 Hz, H-11), 7.70 (2H, d, *J* = 5.6 Hz, H-10), δ 7.48 (1H, d, *J* = 8.0 Hz, H-6), 7.43 (1H, d, *J* = 8.4 Hz, H-6'), 7.30 (3H, m, H-5', H-3' and H-4), 7.21 (1H, m, H-5), 7.28 (1H, dd, *J* = 8.4 and 2.0 Hz, H-3), 3.02 (2H, t, *J* = 6.0 Hz, H-9), 2.97 (2H, m, H_e-1), 2.76 (4H, m, H_a-1 and H_e-2), 2.62 (2H, t, *J* = 6.4 Hz, H-7), 2.23 (1H, m, H_a-2), 1.82 (2H, quin, *J* = 6.4 Hz, H-8); ^{13}C-NMR (101 MHz, $CDCl_3$) δ 164.5, 150.6 (2C), 140.3, 138.2, 136.0, 135.0, 134.6, 133.9, 131.9, 130.4, 128.8, 128.5, 128.4, 127.3, 126.7, 126.4, 126.2, 121.0 (2C), 56.3, 54.6, 54.4, 52.0, 50.7, 29.8 and 22.0; LC-ESI-MS (+ ve ion mode): 491.2 $[M+H]^+$, 492.2 $[M+1+H]^+$ and 493.2 $[M+2+H]^+$, purity 96.8% (t_r = 4.248 min).

***N'-(3-(4-(5H-dibenzo[a,d][7]annulen-5-ylidene)piperidin-1 yl)propyl)isonicotinohydrazide* (4.23c)**

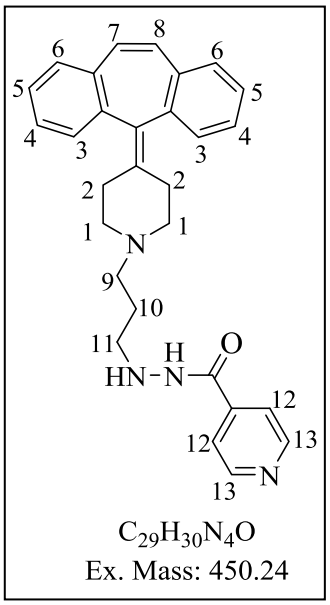

The general method **18** was adopted and 0.515 mmol of **4.22c** was used to obtain **4.23c** as white solid (90 mg, 40%), m.p. 120-122 °C; R_f 0.20 (10% MeOH-DCM); ^{1}H-NMR (400 MHz, CD_3OD) δ 8.70 (2H, dd, *J* = 6.0 and 1.6 Hz, H-13), 7.66 (2H, dd, *J* = 6.4 and 1.6 Hz, H-12), 7.34-7.39 (4H, m, H-5 and H-4), 7.27-7.30 (2H, m, H-3), 7.22 (2H, dd, *J* = 8.0 and 1.2 Hz, H-6), 6.95 (2H, s, H-7 and H-8), 2.99 (2H, t, *J* = 6.8 Hz, H-11), 2.80 (2H, m, H_e-1), 2.59 (2H, t, *J* = 6.8 Hz, H-9), 2.45 (4H, m, H_a-1 and H_e-2), 2.23 (1H, m, H_a-2), 1.82 (2H, quin, *J* = 6.8Hz, H-10); ^{13}C-NMR (101 MHz, $CDCl_3$) δ 164.2, 150.5 (2C), 140.3, 138.7 (2C), 134.7 (2C), 134.3, 134.1, 131.0 (2C), 128.3 (4C), 127.6 (2C), 126.4 (2C), 121.0 (2C), 56.4, 55.0 (2C), 50.8, 29.4 (2C) and 25.3; LC-ESI-MS (+ve ion mode): *m/z* 451.2 $[M+H]^+$, purity 95.5% (t_r = 4.257 min).

***1-(10,11-Dihydro-5H-dibenzo[a,d]cyclohepten-5-yl)-piperazine* (4.25)**

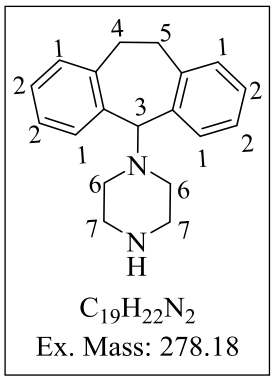

A solution of piperazine (37.6 mg, 2.19 mmol) in dry toluene (6 mL) was drop-wise added to a mixture of dibenzosuberanyl chloride **4.24** (0.5 g, 0.437 mmol) and MS-4A° in dry toluene (5 mL), under argon at 0 °C. Then DBU (0.082 ml, 0.55 mmol) was added and the reaction mixture was stirred for 10 hours. After completion of reaction (TLC), the reaction mixture was filtered through a pad of celite. The solvent was evaporated *in vacuo* and the residue was dissolved in MeOH. The by product was insoluble in the methanol and filtered off. The filtrate was evaporated to dryness to yield **4.25** as a yellow solid (0.4 mg, 67%); m.p. 246-246.5 °C; R_f 0.30 (15% MeOH-DCM); ^{1}H-NMR (400 MHz, $CDCl_3$,) δ 7.09 (4H, t, *J* = 7.2 Hz, H-2), 7.01 (4H, m, H-1), 3.96 (2H, m, H-4 and H-5), 3.89 (1H, s, H-3), 2.73 (6H, bm, H-4, H-5 and H-7), 2.03 (4H, bs, H-6).

***1-(3-Chloro-propyl)-4-(10,11-dihydro-5H-dibenzo[a,d]cyclohepten-5-yl)-piperazine* (4.26)**

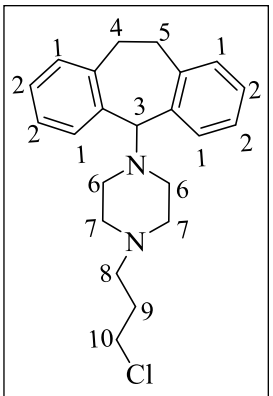

$C_{22}H_{27}ClN_2$
Ex. Mass: 354.19

The general method **17** was adopted and 0.0.72 mmol of **4.25** was used to obtain **4.26** as oil (0.185 g, 72%); R_f 0.6 (8% MeOH-DCM); ^{1}H-NMR (400 MHz, $CDCl_3$,) δ 7.19 (4H, td, *J* = 7.6 and 1.6 Hz, H-2), 7.11 (4H, m, H-1), 4.03 (2H, m, H-4 and H-5), 4.0 (1H, s, H-3), 3.60 (2H, t, *J* = 6.8 Hz, H-10), 2.82 (2H, m, H-4 and H-5), 2.43 (2H, t, *J* = 7.2 Hz, H-8), 2.42-2.36 (8H, two br s, H-6 and H-7), 1.95 (2H, quin, *J* = 7.2 Hz, H-9).

***Isonicotinic acid N'-{3-[4-(10,11-dihydro-5H-dibenzo[a,d]cyclohepten-5-yl)-piperazin-1-yl]-propyl}-hydrazide* (4.27)**

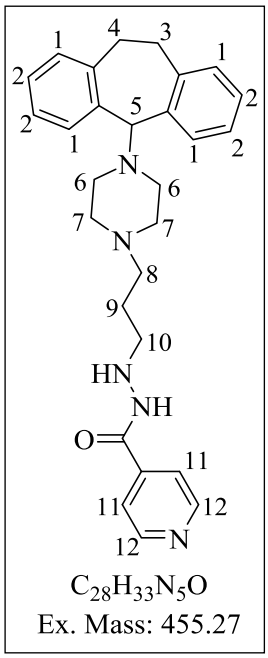

$C_{28}H_{33}N_5O$
Ex. Mass: 455.27

The general method **18** was adopted and 0.31 mmol of **4.26** was used to obtain **4.27** as white solid (0.2 g, 42%); m.p. 155-157 °C; R_f 0.60 (10% MeOH-DCM); ^{1}H-NMR (400 MHz, $CDCl_3$) δ 8.68 (2H, d, *J* = 5.6 Hz, H-12), 7.67 (2H, d, *J* = 5.6 Hz, H-11), 7.02 (8H, m, H-1 and H-2), 3.87 (1H, s, H-5), 3.85 (2H, m, H-3 and H-4), 2.91 (2H, t, *J* = 5.6 Hz, H-10), 2.68 (2H, m, H-3 and H-4), 2.65-2.49 (8H, two br s, H-6 and H-7), 2.65 (2H, t, *J* = 6.4 Hz, H-8), 1.76 (1H, quin, *J* = 6.4 Hz, H-9); ^{13}C-NMR (101 MHz, $CDCl_3$) δ 164.3, 150.5 (2C), 140.5, 139.6, 138.5, 130.9 (2C), 130.8 (3C), 128.10 (3C), 125.7 (2C), 121.2 (2C), 56.1, 53.3 (2C), 50.6 (2C), 50.2, 31.8 (2C), 29.6 and 25.0; LRMS (EI) *m/z* 456.20 $[M+H]^+$; HPLC purity 99.8% (t_r = 11.52 min).

***N'-(3-(10H-phenothiazin-10-yl)propyl)benzohydrazide* (4.28a)**

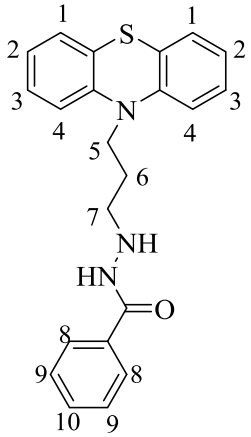

$C_{22}H_{21}N_3OS$
Ex. Mass: 375.14

The general method **18** was adopted and 0.25 mmol of **4.3a** was used to obtain **4.28a** as an oil (80 mg, 20%); R_f 0.6 (10% MeOH-DCM); ^{1}H-NMR (400 MHz, $CDCl_3$) δ 7.72 (2H, d, *J* = 8.4 Hz, H-8), 7.52 (1H, tt, *J* = 7.6 and 1.6 Hz, H-10), 7.43 (2H, t, *J* = 8.0 Hz, H-9), 7.15 (2H, m, H-3), 7.10 (2H, dd, *J* = 7.6 and 1.2 Hz, H-1), 6.99 (2H, dd, *J* = 7.6 and 1.2 Hz, H-4), 6.90 (2H, td, *J* = 7.2 and 1.2 Hz, H-2), 4.05 (2H, t, *J* = 6.4 Hz, H-5), 3.04 (2H, t, *J* = 6.4 Hz, H-7), 2.02 (2H, quin, *J* = 6.8 Hz, H-6); ^{13}C-NMR (101 MHz, $CDCl_3$) δ 167.8, 145.4 (2C), 132.9, 131.3 (2C), 128.2 (2C), 127.1 (2C), 126.9 (2C), 126.8 (2C), 125.3, 122.2 (2C), 115.6 (2C), 48.8, 44.4 and 25.0; LC-ESI-MS (+ve ion mode): 376.1 $[M+H]^+$, purity 96.8% (t_r = 4.672 min).

***N'-(3-(2-chloro-10H-phenothiazin-10-yl)propyl)benzohydrazide* (4.28b)**

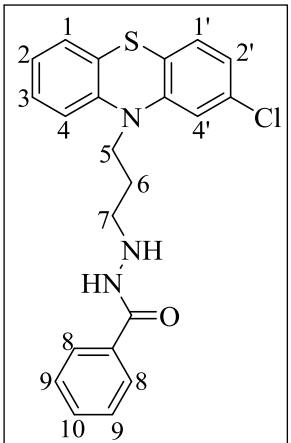

$C_{22}H_{20}ClN_3OS$
Ex. Mass: 409.10

The general method **18** was adopted and 0.31 mmol of **4.3b** was used to obtain **4.28b** as an oil (75 mg, 25%); R_f 0.2 (5% MeOH-DCM); ^{1}H-NMR (400 MHz, $CDCl_3$) δ 7.72 (2H, d, *J* = 7.2 Hz, H-8), 7.52 (1H, t, *J* = 7.6 Hz, H-10), 7.43 (2H, t, *J* = 7.2 Hz, H-9), 7.12 (1H, td, *J* = 8.0 and 1.6 Hz, H-3), 7.11 (1H, dd, *J* = 8.0 and 1.6 Hz, H-1), 7.05-7.01 (2H, m, H-1' and H-4), 7.00 (2H, d, *J* = 2.0, H-4'), 6.95 (1H, td, *J* = 7.6 and 1.2 Hz, H-2), 6.90 (1H, dd, *J* = 8.4 and 2.4 Hz, H-2'), 4.04 (2H, t, *J* = 6.4 Hz, H-5), 3.05 (2H, t, *J* = 6.4 Hz, H-7), 2.02 (2H, quin, *J* = 6.8 Hz, H-6); ^{13}C-NMR (101 MHz, $CDCl_3$) δ 167.8, 146.8, 144.6, 133.1, 132.9, 131.4, 128.1 (2C), 127.6, 127.2, 126.9, 126.8 (2C), 125.0, 124.1, 122.7, 121.9, 116.0, 115.7, 48.7, 44.6 and 24.9; LC-ESI-MS (+ve ion mode): 410.1 $[M+H]^+$, 411.1 $[M+1+H]^+$, 412.1 $[M+2+H]^+$, purity 97% (t_r = 4.543 min).

***diethyl 2,6-dimethyl-4-(3-nitrophenyl)-1,4-dihydropyridine-3,5-dicarboxylate* (4.32)**[13]

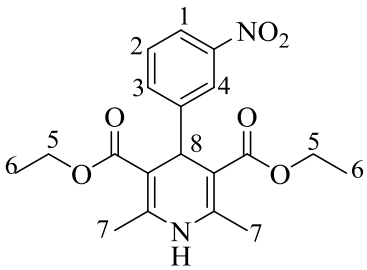

$C_{19}H_{22}N_2O_6$
Ex. Mass: 374.15

A solution of ethyl 3-oxobutanoate (2.0 g, 18.24 mmol) and ammonium acetate (8.0 g, 100 mmol) was stirred for 10 hour at room temperature (25 °C). After completion of reaction (TLC), methanol was distilled of and the residue was dissolved in ethyl acetate and washed with water, dried over sodium sulphate and concentrated to obtain **4.30** (2.4 g, 75%) as yellow solid**.** This compound was used in next step without further purification.

A catalytic amount of acetic acid was added to a solution of ethyl 3-oxobutanoate (1.8 g, 14.0 mmol), benzaldehyde (1.96 g, 13.92 mmol) and **4.30** (1.6 g, 12.4 mmol) in ethanol. The reaction mixture was refluxed (85 °C) for 24 hours. After completion of reaction (TLC), solvent was removed under reduced pressure and the residue was dissolved in ethyl acetate, washed with water, dried over sodium sulphate and concentrated to obtain **4.32** as yellow solid. The crude was recrystallized from mixture of DCM/Hexane to afford a yellow solid (3.0 g, 65%); m.p. 160-162 °C; R_f 0.30 (30% EtOAc-Hexane); ^{1}H-NMR (400 MHz, $CDCl_3$) δ 8.0 (1H, dd, *J* = 2.3 and 1.8 Hz, H-4), 7.98 (1H, ddd, *J* = 8.2, 2.3 and 1.1 Hz, H-1), 7.58 (1H, m, H-3), 7.36 (1H, m, H-2), 5.17 (1H, s, H-8), 4.15 (4H, m, H-5), 2.54 (6H, s, H-7), 1.20 (6H, t, *J* = 7.0 Hz, H-6).

***diethyl 1-(2-ethoxy-2-oxoethyl)-2,6-dimethyl-4-(3-nitrophenyl)-1,4-dihydropyridine-3,5-dicarboxylate* (4.33)**[14]

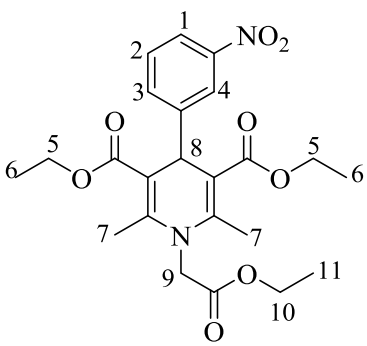

$C_{23}H_{28}N_2O_8$
Ex. Mass: 460.18

A solution of compound **4.32** (3.2 g, 8.6 mmol) in anhydrous THF (15 ml) was added to a suspension of NaH (0.29 g, 13.0 mmol) in anhydrous THF (20 ml) under a nitrogen atmosphere at 0 ^{o}C and stirred for 30 minutes at room temperature (25 °C). Reaction mixture was cooled to 0 ^{o}C and solution of chloromethyl ethyl ether (1.22 g, 13.0 mmol) in THF (10 ml) was added drop-wise to the reaction mixture and stirred at

room temperature (25 °C) for 2 h. After completion of reaction (TLC), quenched with water (10 ml) at 0 °C and extracted with EtOAc (3×15). The organic extracts were dried over anhydrous $MgSO_4$ and removed under reduced pressure. Purification through column chromatography afforded a yellow solid (2.5 g, 68%); m.p. 188-189 °C; R_f 0.5 (40% EtOAc-Hexane); ^{1}H-NMR (400 MHz, $CDCl_3$) δ 8.07 (1H, dd, *J* = 2.3 and 1.8 Hz, H-4), 7.99 (1H, ddd, *J* = 8.2, 2.3 and 1.1 Hz, H-1), 7.58 (1H, m, H-3), 7.36 (1H, m, H-2), 5.17 (1H, s, H-8), 4.86 (2H, s, H-9), 4.15 (4H, m, H-5), 3.48 (2H, q, *J* = 7.0 Hz, H-10), 2.54 (6H, s, H-7), 1.25 (9H, m, H-6 and H-11).

***1-(2-ethoxy-2-oxoethyl)-5-(ethoxycarbonyl)-2,6-dimethyl-4-(3-nitrophenyl)-1,4-dihydropyridine-3-carboxylic acid* (4.34)**[14]

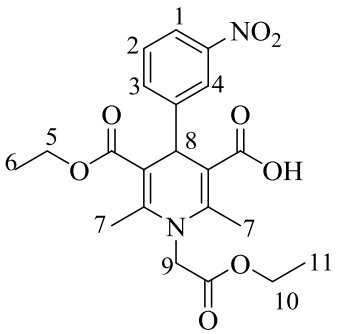

$C_{21}H_{24}N_2O_8$
Ex. Mass: 432.15

Sodium (Na) (0.86g) was added to 1-dimethylamino-2-propanol (10 ml) and reaction mixture was stirred for 1 h at room temperature (25 °C). A solution of H_2O (0.25 ml) in 1-dimethylamino-2-propanol (2.7 ml) was added drop-wise to the mixture. The resulting reaction mixture was stirred until Na was completely dissolved with warming. Solution of compound **4.32** (2.5 g) in benzene (12.5 ml) was added to the reaction mixture under cooling in an ice bath and the reaction mixture was stirred at room temperature (25 °C) for 3 h. The solvent was then evaporated off and residue acidified to pH 2 by careful addition of 3*N* HCl under cooling. The aqueous solution was extracted with DCM. The extracts were washed with water and dried over anhydrous $MgSO_4$. The solvent was removed under reduced pressure and purification by column chromatography afforded a yellow solid (0.65 g, 28%); m.p. 175-176 °C; R_f 0.25 (40% EtOAc-Hexane); ^{1}H-NMR (400 MHz, $CDCl_3$) δ 8.04 (1H, m, H-4), 7.99 (1H, ddd, *J* = 8.0, 2.4 and 1.2 Hz, H-1), 7.61 (1H, m, H-3), 7.35 (1H, ddd, *J* = 9.0, 7.7 and 1.1 Hz, H-2), 5.19 (1H, s, H-8), 4.86 (2H, s, H-9), 4.17 (2H, m, H-10), 3.47 (2H, q, *J* = 6.96 Hz, H-5), 2.58 (3H, s, H-7), 2.54 (3H, s, H-7), 1.25 (6H, m, H-6 and H-11).

***5-(Ethoxycarbonyl)-2,6-dimethyl-4-(3-nitrophenyl)-1,4-dihydropyridine-3-carboxylic acid* (4.35)**

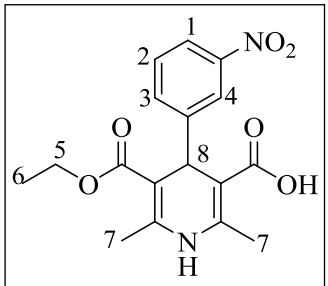

$C_{17}H_{18}N_2O_6$
Ex. Mass: 346.12

1*N* HCl (4 ml) was added to a solution of compound **4.34** (0.65g) in acetone (15 ml) and the solution was stirred at room temperature (25 °C) for 2 h. After completion of reaction (TLC), acetone was removed *in vacuo*, dissolved in EtOAc (30 ml) and washed with water (3 ×10 ml). The organic extract was dried over anhydrous $MgSO_4$ and concentrated to obtain **4.35** as a yellow solid (0.13 g, 23%); m.p. 157-159 ^oC; R_f 0.40 (50% EtOAc-Hexane); ^{1}H-NMR (400 MHz, DMSO-d_6) δ 8.96 (1H, s, NH), 8.00 (2H, m, H-1 and H-4), 7.61 (1H, m, H-3), 7.55 (1H, t, *J* = 7.70 Hz, H-2), 4.99 (1H, s, H-8), 4.02 (2H, m, H-5), 2.30 (3H, s, H-7), 2.29 (3H, s, H-7), 1.15 (3H, m, H-6).

***ethyl 5-(2-isonicotinoylhydrazine-1-carbonyl)-2,6-dimethyl-4-(3-nitrophenyl)-1,4-dihydropyridine-3-carboxylate* (4.36)**

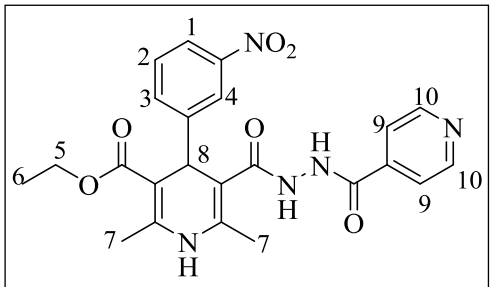

$C_{23}H_{23}N_5O_6$
Ex. Mass: 465.16

HOBt (0.049 g, 0.36 mmol), EDCI (0.069g, 0.36 mmol) and isoniazid (0.02g, 0.144 mmol) were added to a solution of compound **4.35** (0.05g, 0.144 mmol) in DMF (5 ml) and reaction mixture was stirred at room temperature (25 °C) for 24 h. After completion of reaction (TLC), solvent was removed under reduced pressure and residue was taken in EtOAc (15 ml) and washed with brine (2×10). The organic extract was dried over anhydrous $MgSO_4$, concentrated under reduced pressure and purification by column chromatography afforded a yellow solid (25 mg, 36%); m.p. 172-174 ^oC; R_f 0.5 (20% MeOH-DCM); ^{1}H-NMR (400 MHz, DMSO-d_6) δ 10.51 (1H, br s, NH), 9.71 (1H, br s, NH), 8.74 (2H, dd, 6.0 Hz, H-10), 8.68 (1H, br s, NH), 8.05 (1H, t, *J* = 2.0 Hz, H-4), 8.02 (1H, ddd, J = 11.6, 3.6 and 1.2 Hz), 7.76 (2H, d, *J* = 6.0 Hz, H-9), 7.70 (1H, d, *J* = 8.0 Hz, H-3), 7.57 (1H, t, *J* = 8.4 Hz, H-2), 4.99 (1H, s, H-8), 4.01 (2H, m, H-5), 2.30 (3H, s, H-7), 2.24 (3H, s, H-7), 1.15 (3H, t, *J* = 7.2 Hz, H-6); ^{13}C-NMR (101 MHz, DMSO-d_6) δ 167.9, 167.1, 164.6, 150.8, 150.1, 148.1(2C), 148.3, 147.5, 147.8, 140.0, 138.4, 134.7, 129.9, 122.4, 121.7 (2C), 121.5, 105.8,

99.1, 59.4, 19.0, 17.6, and 14.6; LRMS (EI): *m/z* 466.15 $[M+H]^+$; HPLC purity 96% (t_r = 11.05).

2-bromo-1,1-diphenylethan-1-ol **(4.43)**

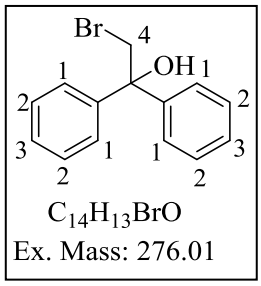

$C_{14}H_{13}BrO$
Ex. Mass: 276.01

Compound **4.42** (3.08 g, 11.11 mmol) and NBS (2.17 g, 12.19 mmol) were stirred in acetone-H_2O (10 mL; 5:1) at room temperature (25 °C). After completion of reaction (TLC), acetone was removed *in vacuo* and residue was dissolved in ethyl acetate. The organic layer was washed with water (2 × 20 ml), dried over sodium sulphate and concentrated. The crude was purified by column chromatography using 10% ethyl acetate in hexane as eluent to obtain **4.43** as a yellow solid (3.0 g, 90%); m.p. 70-72 °C; R_f 0.50 (10% EtOAc-Hexane); ^{1}H-NMR (400 MHz, CD_3OD) δ 7.50 (4H, d, *J* = 7.2 Hz, H-1), 7.38 (4H, t, *J* = 7.2 Hz, H-2), 7.33 (2H, t, *J* = 6.8 Hz, H-3), 4.18 (2H, s, H-4), 3.16 (1H, s, OH);

tert-butyl 4-(2-hydroxy-2,2-diphenylethyl)piperazine-1-carboxylate **(4.44)**

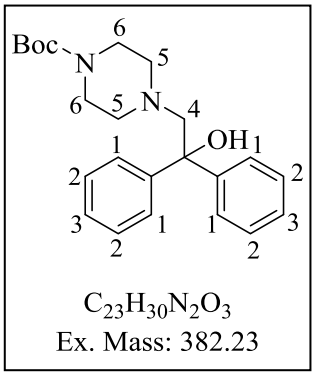

$C_{23}H_{30}N_2O_3$
Ex. Mass: 382.23

The compound **4.43** (1.0 g, 3.37 mmol) was added to a solution of 1-boc-piperazine (0.7 g, 3.76 mmol) and cesium carbonate in 3 ml DMSO and stirred at 80 °C for 8 hour. Reaction did not go to completion (TLC), the reaction was quenched with water and extracted with ethyl acetate. The organic layer was dried over sodium sulphate and concentrated to obtain crude product which was purified by column chromatography using 15% ethyl acetate in hexane as eluent to obtain **4.44** as a white solid (0.45 g, 40%); m.p. 100-102 °C; R_f 0.60 (40% EtOAc-Hexane); ^{1}H-NMR (400 MHz, CD_3OD) δ 7.53 (4H, d, *J* = 7.6 Hz, H-1), 7.33 (4H, t, *J* = 7.2 Hz, H-2), 7.33 (2H, t, *J* = 7.6 Hz, H-3), 5.15 (1H, s, OH), 3.33 (6H, bs, H-4 and H-6), 2.37 (4H, bs, H-5), 1.46 (9H, s, Boc); ^{13}C-NMR (101 MHz, $CDCl_3$) δ 154.6, 146.8, 128.2 (4C), 126.8 (2C), 125.6, 128.2 (4C), 79.8, 74.2, 67.5, 54.2 (2C), 43.5 (2C), 28.4 (3C).

***1,1-diphenyl-2-(piperazin-1-yl)ethan-1-ol* (4.41)**

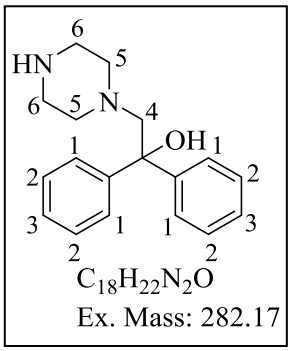

A 10 ml of 10% mixture of TFA in DCM by volume was added to compound **4.44** in a round bottom flask and stirred at room temperature (25 °C) for one hour. After completion of reaction (TLC), remaining of TFA was *vacc off* and residue was redissolved in DCM followed by the addition of a saturated solution of sodium bicarbonate to basify until the pH 8. The DCM layer was separated, dried over sodium sulphate and concentrated to obtain **4.41** as a white solid (0.25 g, 97%); m.p. 66 °C; R_f 0.10 (10% MeOH-DCM); ^{1}H-NMR (400 MHz, CD_3OD) δ 7.50 (4H, d, *J* = 7.6 Hz, H-1), 7.32 (4H, t, *J* = 7.2 Hz, H-2), 7.23 (2H, t, *J* = 7.6 Hz, H-3), 3.33 (2H, s, H-4), 3.03 (4H, bs, H-6), 2.65 (4H, bs, H-5); ^{13}C-NMR (101 MHz, $CDCl_3$) δ 146.5 (2C), 127.6 (4C), 126.5 (2C), 126.0 (4C), 76.6, 66.9, 51.5 (2C), 43.8 (2C).

2-*(4-(3-chloropropyl)piperazin-1-yl)-1,1-diphenylethan-1-ol* (4.45)

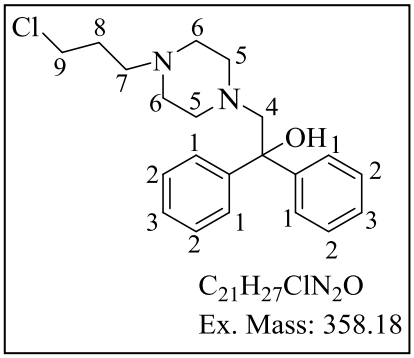

The general method **17** was adopted and 0.88 mmol of **4.41** was used to obtain **4.45** as a yellow solid (0.23 g, 72%); m.p.77-79 °C; R_f 0.30 (5 % MeOH-DCM); ^{1}H-NMR (400 MHz, CD_3OD) δ 7.50 (4H, dd, *J* = 7.6 and 1.2 Hz, H-1), 7.32 (4H, td, *J* = 7.2 and 1.2 Hz, H-2), 7.23 (2H, tt, *J* = 7.6 and 1.2 Hz, H-3), 5.25 (1H, s, OH), 3.58 (2H, t, *J* = 6.8 Hz, H-9), 3.30 (2H, s, H-4), 2.45 (6H, m, H-6 and H-7) 2.39 (4H, bs, H-5), 1.92 (2H, quin, *J* = 7.2 Hz, H-8); ^{13}C-NMR (101 MHz, $CDCl_3$) δ 147.9 (2C), 128.2 (4C), 126.7 (2C), 125.4 (4C), 73.8, 67.5, 55.2, 54.4 (2C), 53.2 (2C), 42.9, 29.8.

***N'-(3-(4-(2-hydroxy-2,2-diphenylethyl)piperazin-1-yl)propyl)isonicotinohydrazide* (4.46)**

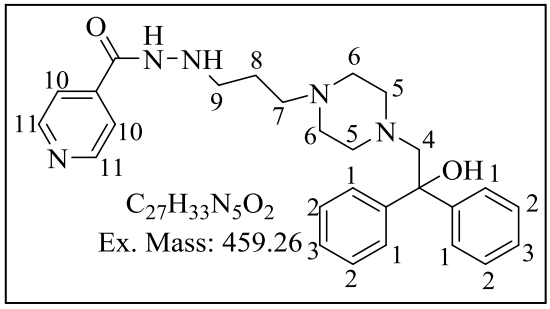

The general method **18** was adopted and 0.56 mmol of **4.45** was used to obtain **4.46** as a white solid (0.1 g, 35%); m.p.115-117 °C; R_f (10% MeOH-DCM) 0.20; ^{1}H-NMR (400 MHz, $CDCl_3$) δ 8.75 (2H, dd, *J* = 6.0 and 1.6 Hz, H-11), 7.52 (2H, dd, *J* = 6.4 and 1.6 Hz, H-10), 7.50 (4H, dd, *J* = 7.2 and 1.2 Hz, H-1), 7.32 (4H, td, *J* = 6.4 and 1.2 Hz, H-2), 7.23 (2H, tt, *J* = 7.6 and 1.2 Hz, H-3), 5.14 (1H, s, OH), 3.29 (2H, s, H-4), 2.99 (2H, t, *J* = 6.0 Hz, H-9), 2.52 (2H, t, *J* = 6.8 Hz, H-7), 2.40-2.54 (8H, m, H-5 and H-6) 1.76 (2H, quin, *J* = 6.4 Hz, H-8); ^{13}C-NMR (101 MHz, $CDCl_3$) δ 164.3, 150.6 (2C), 146.8 (2C), 140.3, 128.0 (4C), 126.7 (2C), 125.3 (4C), 120.9 (2C), 74.3, 67.5, 56.6, 54.0 (2C), 53.1 (2C), 51.0 and 25.2; LC-ESI-MS (+ ve ion mode): 460.3 $[M+H]^+$, purity 99.8% (t_r = 4.03 min).

***1-tritylpiperazine* (4.48)**

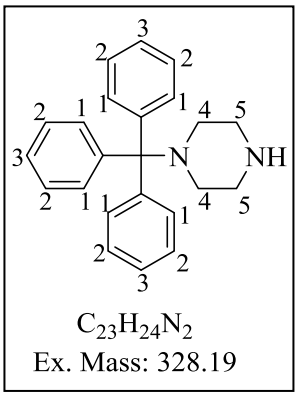

A solution of trityl bromide (1.0 g.3.10 mmol) in 6 ml of mixture of toluene and methanol (5:1 toluene/methanol (v/v)) was added drop-wise to a cooled solution of piperazine (2.67 g, 30.96 mmol) in 13 ml of mixture of toluene and methanol (5:1 toluene/methanol (v/v)) at 0 °C. After completion of addition, the reaction mixture was stirred at ambient temperature (25 °C) for one hour. After completion of reaction (TLC), reaction mixture was washed with water (5 ×20 ml) to remove excess of piperazine. The organic layer was dried over sodium sulphate and concentrated under reduced pressure to obtain white solid (0.75 g, 73.5%); m.p. 94-96 °C; R_f 0.45 (10% MeOH-DCM); ^{1}H-NMR (300 MHz, $CDCl_3$) δ 7.47 (6H, m, H-1), 7.29 (6H, t, *J* = 7.8 Hz, H-2), 7.18 (3H, t, *J* = 7.2 Hz, H-3), 3.23–2.95 (6H, bm, Pip-H), 1.90-1.43 (2H, bm, Pip-H).

***1-(3-chloropropyl)-4-tritylpiperazine* (4.49)**

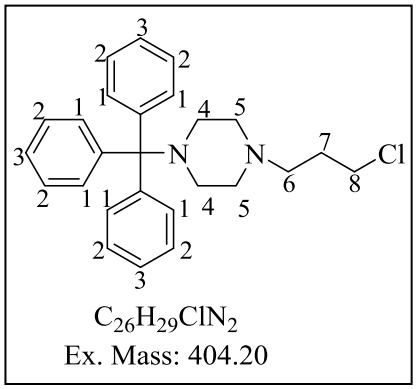

The general method **17** was adopted and 2.44 mmol of **4.48** was used to obtain **4.49** as white solid (0.65 g, 66%); m.p. 114-116 °C; R_f 0.80 (10% MeOH-DCM); δ 7.51 (6H, m, H-1), 7.29 (6H, t, *J* = 7.2 Hz, H-2), 7.18 (3H, t, *J* = 7.8 Hz, H-3), 3.56 (2H, t, *J* = 6.6 Hz, H-8), 3.23 – 2.95 (6H, bm, Pip-H), 3.56 (2H, t, *J* = 7.2 Hz, H-6), 1.95 (2H, quin, *J* = 6.6 Hz, H-7), 1.90-1.43 (2H, bm, Pip-H).

***N'-(3-(4-tritylpiperazin-1-yl)propyl)isonicotinohydrazide* (4.50)**

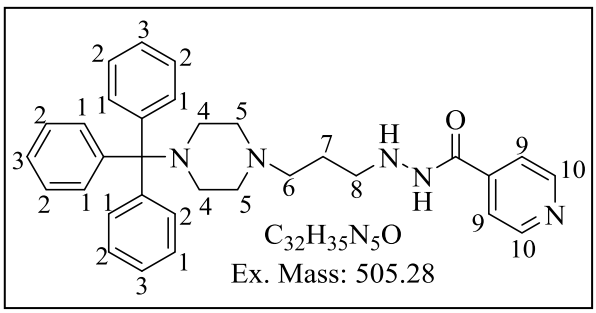

The general method **18** was adopted and 0.89 mmol of **4.49** was used to obtain **4.50** as white solid (0.2 g, 40%); m.p. 199-200 °C; R_f 0.20 (10% MeOH-DCM); ^{1}H-NMR (400 MHz, $CDCl_3$) δ 8.65 (2H, dd, *J* = 6.0 and 1.6 Hz, H-10), 7.52 (8H, m, H-9 and H-1), 7.27 (6H, t, *J* = 7.2 Hz, H-2), 7.16 (3H, t, *J* = 7.2 Hz, H-3), 3.37 – 2.27 (8H, bm, Pip-H), 2.96 (2H, t, *J* = 6.0 Hz, H-8), 2.64 (2H, t, *J* = 6.4 Hz, H-6), 1.82 (2H, quin, *J* = 6.4 Hz, H-7), ^{13}C-NMR (101 MHz, $CDCl_3$) δ 163.8, 150.4 (3C), 148.7, 140.3 (3C), 129.2 (6C), 127.6 (6C), 126.4 (2C), 120.9 (2C), 76.8, 57.1 (2C), 53.9 51.0 (2C), 47.0 and 25.6; LRMS (EI): *m/z* 505.07 $[M]^+$.

***1-Benzhydrylpiperazine* (4.52)**

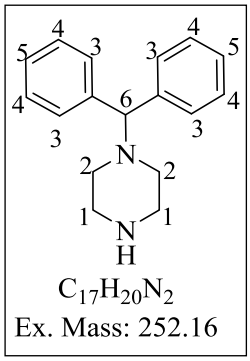

Solid potassium carbonate (0.56 g, 4.04 mmol) and catalytic NaI (0.12 g, 0.81 mmol) was added to a solution of piperazine (0.7 g, 8.1 mmol) in acetonitrile and stirred with heating until all the solids were dissolved. Bromodiphenylmethane **4.51** was added and the reaction mixture was heated at reflux at 90 °C for 8 hour. After completion of

the reaction (TLC), the reaction was quenched with water (10 ml), extracted with ethyl acetate (2 × 15 ml), dried over anhydrous sodium sulphate and evaporated to afford a crude yellow solid. Purification was performed by column chromatography at 2.5% MeOH-DCM to afford **4.52** as white solid (0.65 g, 65%); m.p.: 70-72 °C; R_f 0.30 (20% MeOH-DCM); ^{1}H-NMR (400 MHz, $CDCl_3$) δ 7.35 (4H, dd, *J* = 8.4 and 1.2 Hz, H-3), 7.19 (4H, t, *J* = 7.6 Hz, H-4), 7.10 (2H, tt, *J* = 7.6 and 1.2 Hz, H-5), 4.15 (1H, s, H-6), 2.82 (4H, t, *J* = 4.8 Hz, H-1), 2.30 (4H, bs, H-2), 1.80 (1H, bs, NH).

***1-Benzhydryl-4-(3-chloro-propyl)-piperazine* (4.53)**

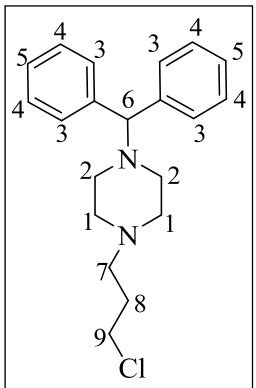

$C_{20}H_{25}ClN_2$
Ex. Mass: 328.17

The general method **17** was adopted and 2.34mmol of **4.51** was used to obtain **4.53** as oil (0.70 g, 90%); R_f 0.30 (20% MeOH-DCM); δ ^{1}H-NMR (400 MHz, $CDCl_3$) 7.35 (4H, dd, *J* = 7.6 and 1.2 Hz, H-3), 7.20 (4H, t, *J* = 7.6 Hz, H-4), 7.11 (2H, tt, *J* = 7.2 Hz and 1.2 Hz, H-5), 4.16 (1H, s, H-6), 3.51 (2H, t, *J* = 6.8 Hz, H-9), 2.42 (2H, t, *J* = 6.8 Hz, H-7), 2.37 (8H, bs, H-1 and H-2), 1.87 (2H, quin, *J* = 6.8 Hz, H-8).

***Isonicotinic acid N'-[3-(4-benzhydryl-piperazin-1-yl)-propyl]-hydrazide* (4.54)**

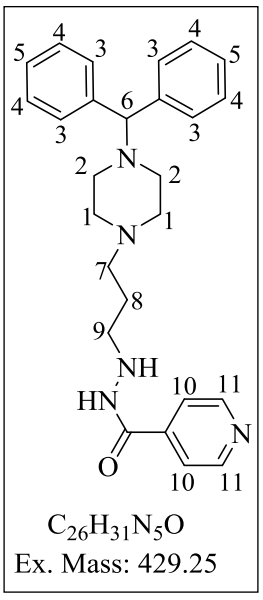

$C_{26}H_{31}N_5O$
Ex. Mass: 429.25

The general method **18** was adopted and 2.34 mmol of **4.53** was used to obtain **4.54** as white solid (0.2 g, 42%); m.p. 55-57 °C; R_f 0.60 (10% MeOH-DCM); ^{1}H-NMR (400 MHz, $CDCl_3$) δ 8.75 (2H, d, *J* = 4.0 Hz, H-11), 7.65 (2H, d, *J* = 5.6 Hz, H-10), 7.35 (4H, d, *J* = 7.6 Hz, H-3), 7.30 (4H, t, *J* = 7.2 Hz, H-4), 7.11 (2H, t, *J* = 7.2 Hz, H-5), 4.21 (1H, s, H-6), 3.01 (2H, t, *J* = 6.0 Hz, H-9), 2.64 (4H, bs, H-1), 2.47 (4H, bs, H-2), 2.65 (2H, t, *J* = 6.4 Hz, H-7), 1.83 (2H, quin, *J* = 6.4 Hz, H-8); ^{13}C-NMR (101 MHz, $CDCl_3$) δ 164.1, 150.5 (2C), 142.3 (2C), 140.5, 128.5 (4C), 127.9 (4C), 127.1 (2C), 121.1 (2C), 76.0, 56.4, 53.6(2C), 51.0 (2C), 50.07, and 25.6; LRMS (EI): *m/z* 430.20 $[M+H]^+$; HPLC purity 98.8% (t_r = 13.91 min).

7.1.4.3 Hybrid Efflux Pump inhibitors

***2-(3,4-Dimethoxyphenyl)-5-((2-hydroxyethyl)(methyl)amino)-2-isopropylpentanenitrile* (4.55)**

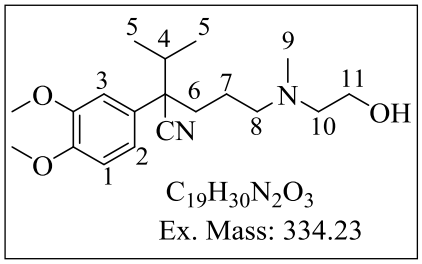

2-(Methylamino)ethan-1-ol (0.21 g, 3.38 mol) and K_2CO_3 (0.78 g, 5.64 mol) were added to a solution of compound **3.6c** (1.0 g, 3.38 mol) in anhydrous DMF (10 ml) and stirred at 80 ^oC for 12 h. After completion of reaction (TLC), DMF was removed *in vacuo* and the residue was dissolved in EtOAc (25 ml). The organic phase was washed with brine (3×15 ml), dried over anhydrous $MgSO_4$ and concentrated *in vacuo*. Purification was done by column chromatography to afford **4.55** as an oil (0.35 g, 31%); R_f 0.30 (5% MeOH-DCM); ^{1}H-NMR (400 MHz, $CDCl_3$) δ 6.89 (1H, dd, *J* = 8.4 and 2.0 Hz, H-2), 6.81 (2H, m, H-1 and H-3), 3.86 (3H, s, OC*H*$_3$), 3.85 (3H, s, OC*H*$_3$), 3.59 (2H, m, H-11), 2.48 (2H, m, H-10), 2.41 (2H, m, H-8), 2.18 (3H, s, H-9), 2.10 (2H, H-4 and H-6), 1.90 (m, 1H, H-6), 1.57 (1H, m, H-7), 1.13 (1H, m, H-7), 1.14 (3H, d, *J* = 6.6 Hz, H-5), 0.75 (3H, d, *J* = 6.80 Hz, H-5); ^{13}C-NMR (101 MHz, $CDCl_3$) δ 149.1, 148.4, 130.5, 121.3, 118.7, 111.2, 109.6, 58.7, 58.2, 57.1, 56.0, 55.9, 53.3, 41.2, 37.9, 35.4, 23.2, 18.9 and 18.5; LRMS (EI): *m/z* 334.20 $[M]^+$.

***5-((2-Chloroethyl)(methyl)amino)-2-(3,4-dimethoxyphenyl)-2-isopropylpentanenitrile* (4.56)**

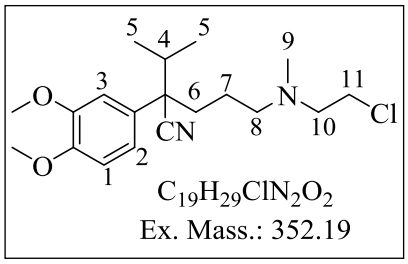

Solution of compound **4.55** (0.80 g, 2.39 mmol) in DCM (10 ml) was cooled to 0 ^oC and $SOCl_2$ (2.85 g, 23.95 mmol) was added drop-wise to it. The reaction mixture was stirred at room temperature (25 °C) for 14 h and then washed with water. The organic layer was dried over anhydrous $MgSO_4$ and concentrated *in vacuo*. Purification by flash chromatography on silica gel using DCM-MeOH as eluent afforded product **4.56** as an oil (0.70 g, 83%); R_f 0.50 (5% MeOH-DCM); ^{1}H-NMR (400 MHz, $CDCl_3$) δ 6.87 (1H, dd, *J* = 8.4 and 2.2 Hz, H-2), 6.81 (2H, m, H-1 and H-3), 3.84 (3H, s, OC*H*$_3$), 3.83 (3H, s, OC*H*$_3$), 3.46 (2H, t, *J* = 6.8 Hz, H-11), 2.59 (2H, m, H-10), 2.34 (2H, m, H-8), 2.13 (3H, s, H-9), 2.02 (2H, m, H-4 and H-6),

1.85 (1H, m, H-6) 1.47 (1H, m, H-7), 1.11 (1H, m, H-7), 1.12 (3H, d, *J* = 6.4 Hz, H-5), 0.75 (3H, d, *J* = 6.4 Hz, H-5); ^{13}C-NMR (101 MHz, $CDCl_3$) δ 149.5, 148.8, 129.4, 121.0, 118.9, 111.3, 109.5, 56.4 (2C), 55.9 (2C), 53.2, 46.8, 38.1, 36.7, 34.8, 20.4, 18.8 and 18.7; LRMS (EI): *m/z* 352.13 $[M]^+$.

General 19: Procedure for the synthesis of compound 4.57 (a and b)

To a solution of compound **4.56** (1.0 equiv) in anhydrous DMF (5 ml), phenothiazine **4.1** (1.0 equiv) and NaH (2.5 equiv) were added and the reaction mixture was stirred at room temperature (25 °C) for 48 h. After completion of reaction (TLC), DMF was removed *in vacuo* and the residue was taken in EtOAc (25 ml). The organic phase was washed with brine (3 × 15 ml), dried over anhydrous $MgSO_4$ and concentrated *in vacuo*. Purification by flash chromatography on silica gel using MeOH-DCM as eluent afforded product **4.57**.

5-((2-(10H-phenothiazin-10-yl)ethyl)(methyl)amino)-2-(3,4-dimethoxyphenyl)-2-isopropylpentanenitrile **(4.57a)**

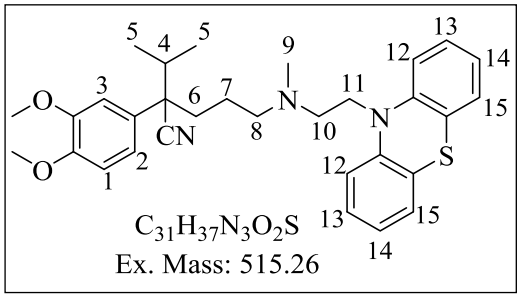

Oil (0.12 g, 16%); R_f 0.40 (5% MeOH-DCM); ^{1}H-NMR (400 MHz, CD_3OD) δ 7.13 (4H, m, H-14 and H-15), 6.95 (1H, d, *J* = 1.2 Hz, H-3), 6.92 (2H, d, *J* = 8.0 Hz, H-12), 6.90 (4H, m, H-13, H-2 and H-1), 3.96 (2H, t, *J* = 6.4 Hz, H-11), 3.80 (3H, s, OCH_3), 3.76 (3H, s, OCH_3), 2.66 (2H, m, H-10), 2.35 (2H, m, H-8), 2.14 (3H, s, H-9), 2.05 (2H, m, H-4 and H-6), 1.91 (1H, m, H-6), 1.41 (1H, m, H-7), 1.12 (3H, d, *J* = 6.8 Hz, H-5), 1.06 (1H, m, H-7), 0.73 (3H, d, *J* = 6.6.8 Hz, H-5); ^{13}C-NMR (101 MHz, CD_3OD) δ 149.2, 148.5, 145.0 (2C), 130.6, 127.1 (2C), 126.9 (2C), 125.0 (2C), 122.3 (2C), 121.1, 119.0, 115.3 (2C), 111.5, 109.9, 56.7, 55.3, 55.1, 53.8, 53.3, 45.0, 41.3, 37.3, 34.9, 23.2, 17.9 and 17.5; LRMS (EI): *m/z* 515.35 $[M]^+$; HPLC purity 97% (t_r = 15.48).

***5-((2-(2-chloro-10H-phenothiazin-10-yl)ethyl)(methyl)amino)-2-(3,4-dimethoxyphenyl)-2-isopropylpentanenitrile* (4.57b)**

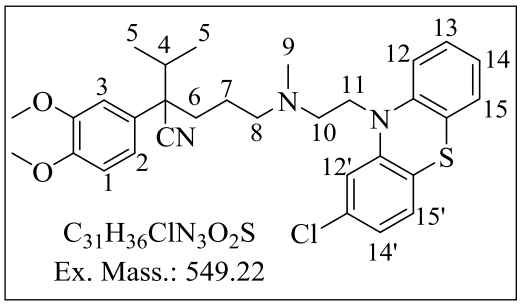

Oil (0.23 g, 29%); R_f 0.50 (5% MeOH-DCM); ^{1}H-NMR (400 MHz, CD_3OD) δ 7.13 (1H, m, H-13), 7.07 (1H, dd, *J* = 8.0 and 2.0 Hz, H-14'), 7.00 (1H, d, *J* = 8.4 Hz, H-15'), 6.98 (1H, d, *J* = 2.0 Hz, H-12'), 6.90 (6H, m, H-12, H-14, H-15, H-1, H-2 and H-3), 3.90 (2H, t, *J* = 6.0 Hz, H-11), 3.79 (3H, s, OC*H*$_3$), 3.76 (3H, s, OC*H*$_3$), 2.60 (2H, t, *J* = 6.0 Hz, H-10), 2.31 (2H, t, *J* = 6.8 Hz, H-8), 2.10 (3H, s, H-9), 2.04 (2H, m, H-4 and H-6), 1.90 (1H, m, H-6), 1.41 (1H, m, H-7), 1.11 (3H, d, *J* = 6.8 Hz, H-5), 1.05 (1H, m, H-7), 0.72 (3H, d, *J* = 6.8 Hz, H-5); ^{13}C-NMR (101 MHz, CD_3OD) δ 149.3, 148.6, 146.4 (2C), 133.1, 130.8, 127.6, 127.3, 127.0, 124.4, 123.4, 122.8, 122.0, 121.0, 119.0, 115.7, 115.5, 111.5, 109.9, 56.8, 55.3, 55.1, 54.0, 53.3, 45.5, 41.2, 37.3, 34.9, 23.3, 18.0 and 17.6; LRMS (EI): *m/z* 549.20 $[M]^+$; HPLC purity 97% (t_r = 16.70).

***5-{[2-(10,11-Dihydro-dibenzo[b,f]azepin-5-yl)-ethyl]-methyl-amino}-2-(3,4-dimethoxy-phenyl)-2-isopropyl-pentanenitrile* (4.57c)**

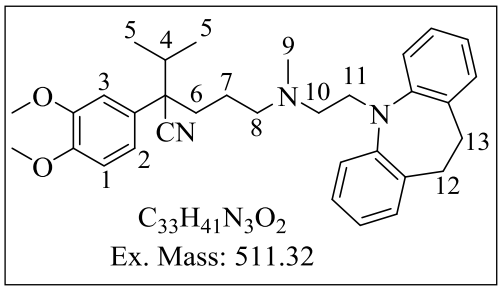

Compound **4.56** (0.164 g, 0.85 mmol) and **4.1c** (0.25 g, 0.71 mmol) were dissolved in benzene and charged with sodium amide. The reaction mixture was refluxed for 24 hour but the reaction did not go to completion. The solvent was evaporated *in vacuo* and purification was done by column chromatography at 0-1% MeOH-DCM to afford an oil (80 mg, 24%); R_f 0.6 (5% MeOH-DCM); ^{1}H NMR (400 MHz, $CDCl_3$) δ 7.12 (1H, dd, *J* = 8.0 and 1.6 Hz, H-2), 7.10 (5H, m, ArH), 6.94 (5H, m, ArH), 3.91 (3H, s, OC*H*$_3$), 3.90 (3H, s, OC*H*$_3$), 3.86 (2H, t, *J* = 7.6 Hz, H-11), 3.17 (4H, s, H-12 and H-13), 2.48 (2H, t, *J* = 6.0 Hz, H-10), 2.28 (2H, m, H-8), 2.13 (3H, s, H-9), 2.06 (2H, m, H-4 and H-6), 1.92 (1H, m, H-6), 1.55 (1H, m, H-7), 1.19 (3H, d, *J* = 6.4 Hz, H-5), 1.16 (1H, m, H-7), 0.83 (3H, d, *J* = 6.80 Hz, H-5). ^{13}C-NMR (101 MHz, $CDCl_3$) δ 149.1, 148.3, 146.1, 134.4, 129.7 (3C), 126.4 (3C), 122.5 (3C), 120.1 (3C), 118.8, 111.2, 109.9, 57.6, 56.1, 55.9 (2C), 49.2, 42.2, 37.9, 35.5, 32.2 (3C), 23.6, 19.0 and 18.6;

LRMS (EI) *m/z* 511.69 $[M]^+$; HPLC purity 97.9% (t_r = 3.83 min).

General method 20: Procedure for the synthesis of 4.58-4.61

Potassium carbonate (2.0 equivalent), and **4.56** (1.5 equivalent) were added to a solution of piperazine or piperidine containing intermediates (1 equivalent) in anhydrous DMF (5 ml). The resulting reaction mixture was stirred at 80 ^oC for 12 h. After completion of reaction (TLC), DMF was removed under reduced pressure and the residue was taken in EtOAc (20 ml). The organic phase was washed with brine (3×15 ml), dried over anhydrous $MgSO_4$ and concentrated *in vacuo*. Purification by column chromatography afforded the target compounds.

***5-{[2-(4-Benzhydryl-piperazin-1-yl)-ethyl]-methyl-amino}-2-(3,4-dimethoxy-phenyl)-2-isopropyl-pentanenitrile* (4.58)**

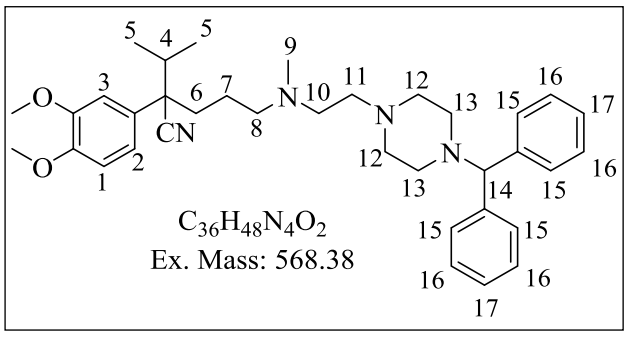

The general method **20** was adopted and 1.23 mmol of **4.51** was used to obtain **4.58** as an oil (0.25 g, 57%); R_f 0.60 (10% MeOH-DCM); ^{1}H-NMR (400 MHz, $CDCl_3$) δ 7.42 (4H, d, *J* = 6.8 Hz, H-15), 7.29 (4H, t, *J* = 7.2 Hz, H-16), 7.19 (2H, tt, *J* = 7.2 and 1.2 Hz, H-17), 6.94 (1H, dd, *J* = 8.4 and 1.6 Hz, H-2), 6.88 (1H, d, *J* = 2.0 Hz, H-3), 6.85 (1H, d, *J* = 8.4 Hz, H-1), 4.23 (1H, s, H-14), 3.91 (3H, s, OC*H*$_3$), 3.87 (3H, s, OC*H*$_3$), 2.65-2.42 (11H, bm, H-6, H-11, H-12 and H-13), 2.38 (2H, m, H-10), 2.26 (2H, m, H-8), 2.18 (3H, s, H-9), 2.09 (2H, m, H-4 and H-6), 1.92 (1H, m, H-6), 1.55 (1H, m, H-7), 1.19 (3H, d, *J* = 6.4 Hz, H-5), 1.16 (1H, m, H-7), 0.83 (3H, d, *J* = 6.8 Hz, H-5); ^{13}C-NMR (101 MHz, $CDCl_3$) δ 149.1, 148.4, 142.7, 130.7, 128.5 (5C), 128.0 (4C), 127.0 (2C), 121.5, 118.8, 111.2, 109.8, 76.2, 57.5, 56.1, 55.9 (2C), 54.5, 53.9 (2C), 53.4, 51.6 (2C), 42.2, 37.9, 35.6, 23.2, 19.0 and 18.6; LRMS (EI) *m/z* 568.31 $[M]^+$; purity 96.5% (t_r = 3.78 min).

***5-((2-(4-(5H-dibenzo[a,d][7]annulen-5-ylidene)piperidin-1-yl)ethyl)(methyl)amino)-2-(3,4-dimethoxyphenyl)-2-isopropylpentanenitrile* (4.59a)**

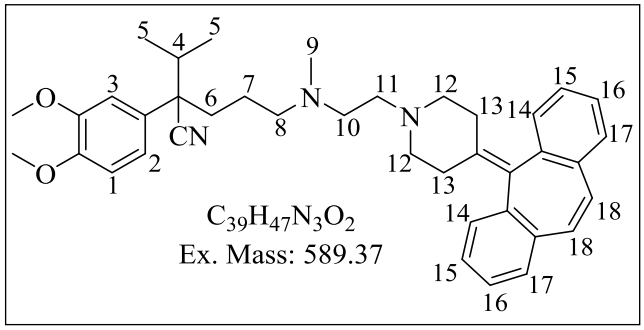

The general method **20** was adopted and 0.0.274 mmol of **4.21c** was used to obtain **4.59a** as white solid (80 mg, 24%), m.p. 70-72 °C; R_f 0.50 (10% MeOH-DCM); ^{1}H-NMR (400 MHz, CD_3OD) δ 7.37 (2H, m, H-14), 7.40 (2H, m, H-16), 7.28 (2H, td, *J* = 8.4 and 1.6 Hz, H-15), 7.21 (2H, dd, *J* = 7.6 and 1.6 Hz, H-17), 7.00 (1H, dd, *J* = 8.4 and 2.0 Hz, H-2), 6.98-6.93 (2H, m, H-1 and H-3), 6.95 (2H, s, H-18), 3.30 (2H, m, H_e-1), 2.93 (2H, m, H_a-1), 2.60 (2H, m, H_e-2), 2.38 (2H, m, H_a-2), 3.91 (3H, s, OCH_3), 3.90 (3H, s, OCH_3), 2.68 (2H, t, *J* = 6.0 Hz, H-11), 2.52 (2H, m, H-10), 2.38 (2H, m, H-8), 2.14 (3H, s, H-9), 2.12 (1H, m, H-6), 2.03 (1H, m, H-4), 1.92 (1H, m, H-6) 1.56 (1H, m, H-7), 1.20 (1H, m, H-7), 1.19 (3H, d, *J* = 6.4 Hz, H-5), 0.75 (3H, d, *J* = 6.8 Hz, H-5); ^{13}C-NMR (101 MHz, CD_3OD) δ 149.5 (2C), 148.41 (2C), 138.7 (2C), 134.5, 134.1, 130.4 (2C), 128.0 (4C), 127.5 (2C), 126.1 (2C), 121.1, 119.1 (2C), 111.6, 110.0, 56.8, 55.4, 55.1, 54.9, 54.8, 54.3, 53.4 (2C), 41.8, 37.3, 35.0, 29.1 (2C), 22.7, 17.9 and 17.5; LC-ESI-MS (+ve ion mode): *m/z* 590.3 $[M+H]^+$, purity 98.4% (t_r = 4.632 min).

***5-((2-(4-(9H-thioxanthen-9-ylidene)piperidin-1-yl)ethyl)(methyl)amino)-2-(3,4-dimethoxyphenyl)-2-isopropylpentanenitrile* (4.59b)**

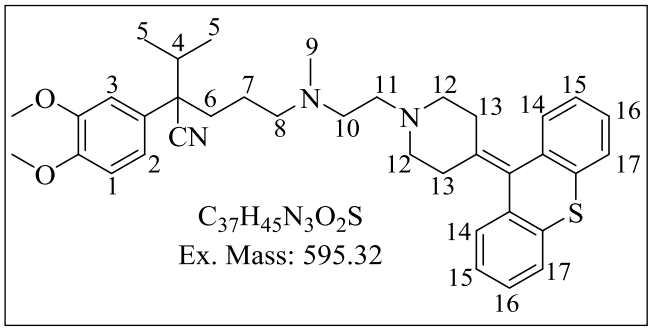

The general method **20** was adopted and 0.358 mmol of **4.21a** was used to obtain **4.59b** as white solid (40 mg, 20%), m.p. 60-62 °C; R_f 0.65 (10% MeOH-DCM); ^{1}H-NMR (400 MHz, CD_3OD) δ 7.48 (2H, dd, *J* = 7.6 and 1.2 Hz, H-17), 7.34 (2H, dd, *J* = 7.6 and 1.2 Hz, H-14), 7.29 (2H, m, H-16), 7.22 (2H, td, *J* = 7.2 and 1.6 Hz, H-15), 7.00 (1H, dd, *J* = 8.4 and 1.2 Hz, H-2), 6.95 (1H, d, *J* = 8.4 Hz, H-1), 6.94 (1H, d, *J* = 2.0 Hz, H-3), 3.83 (3H, s, OCH_3), 3.79 (3H, s, OCH_3), 2.79 (2H, m, H-11), 2.65 (6H, m, H-10, H-8 and H_e-12), 2.52 (4H, m, H_a-12 and H_e-13), 2.33 (3H, s, H-9), 2.18 (5H, m, H-4, H-6 and H_a-13),

1.56 (1H, m, H-7), 1.20 (3H, d, *J* = 6.6 Hz, H-5), 1.16 (1H, m, H-7), 0.79 (3H, d, *J* = 6.6 Hz, H-5); ^{13}C-NMR (101 MHz, CD_3OD) δ 149.6 (2C), 148.8 (2C), 136.8 (2C), 135.3, 130.4, 128.5 (2C), 126.8 (2C), 126.2 (2C), 125.7 (2C), 121.3, 119.2 (2C), 111.7, 111.0, 56.6, 55.4, 55.2, 54.6, 54.5, 53.8, 53.4, 53.2, 41.1, 37.3, 34.9, 29.7 (2C), 22.3, 18.0 and 17.5; LC-ESI-MS (+ve ion mode): *m/z* 596.2 $[M+H]^+$, purity 95.1% (t_r = 4.672 min).

5-((2-(4-(2-chloro-10H-phenothiazin-10-yl)piperidin-1-yl)ethyl)(methyl)amino)-2-(3,4-dimethoxyphenyl)-2-isopropylpentanenitrile **(4.59c)**

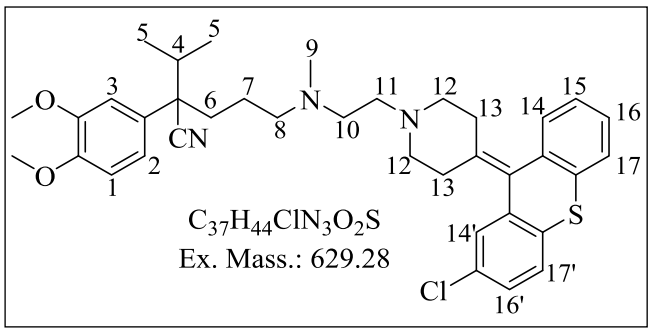

The general method **20** was adopted and 0.447 mmol of **4.21b** was used to obtain **4.59c** as white solid (0.10 g, 36%); m.p. 85-87 °C; R_f 0.65 (10% MeOH-DCM); ^{1}H-NMR (400 MHz, $CDCl_3$) δ 7.49 (1H, d, *J* = 7.8 Hz, H-17), 7.46 (1H, d, *J* = 8.4 Hz, H-17'), 7.33 (3H, m, H-14, H-14' and H-16'), 7.24 (2H, t, *J* = 7.8 Hz, H-15 and H-16), 7.02 (1H, d, *J* = 7.8 Hz, H-2), 7.00 (2H, m, H-1 and H-3), 3.84 (3H, s, OCH_3), 3.08 (3H, s, OCH_3), 2.76 (2H, m, H-8), 2.64 (4H, m, H-10 and H-11), 2.50 (2H, m, H_e-12), 2.42 (4H, m, H_a-12 and H_e-13), 2.21 (3H, s, H-9), 2.16 (2H, m, H_a-13), 2.05 (2H, m, H-6 and H-4), 1.94 (1H, m, H-6), 1.53 (1H, m, H-7), 1.20 (3H, d, *J* = 6.6 Hz, H-5), 1.16 (1H, m, H-7), 0.79 (3H, d, *J* = 6.6 Hz, H-5); ^{13}C-NMR (101 MHz, CD_3OD) δ 149.5 (2C), 148.8 (2C), 138.5 (2C), 136.2, 135.8 (2C), 134.8, 134.1, 131.5, 130.8, 129.8, 128.7, 128.1, 128.0, 126.8, 126.4, 126.1, 126.0, 56.8, 55.3, 55.1, 54.6 (3C), 53.7, 53.4, 41.3, 37.3, 35.1, 29.8 (2C), 22.8, 18.0 and 17.6; LC-ESI-MS (+ve ion mode): 630.2 $[M+H]^+$, 631.2 $[M+1+H]^+$, 632.2 $[M+2+H]^+$; purity 95.2% (t_r = 4.895 min).

5-(4-(9H-thioxanthen-9-yl)piperidin-1-yl)-2-(3,4-dimethoxyphenyl)-2-isopropylpentanenitrile **(4.60a)**

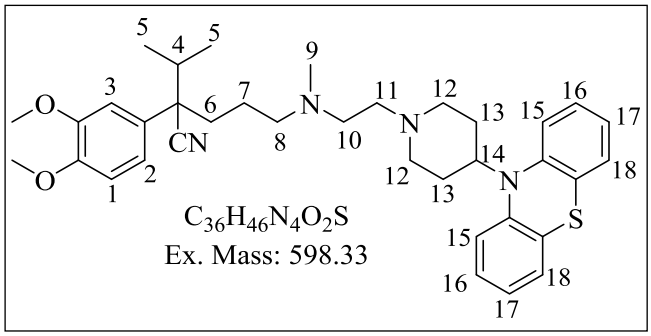

The general method **20** was adopted and 0.319 mmol of **4.15a** was used to obtain **4.60a** as white solid (90 mg, 25%); m.p.

35-37 °C; R_f 0.40 (10% MeOH-DCM); ^{1}H-NMR (400 MHz, CD_3OD) δ 7.21 (1H, dd, *J* = 8.0 and 1.6 Hz, H-2), 7.18 (3H, m, H-3 and H-15), 7.17 (2H, dd, *J* = 8.4 and 1.2 Hz, H-18), 6.96 - 7.03 (5H, m, H-17, H-16 and H-1), 3.86 (3H, s, OC*H*$_3$), 3.83 (3H, s, OC*H*$_3$), 3.76 (1H, m, H-14), 2.95 (2H, t, *J* = 7.2 Hz, H-8), 2.38-2.54 (6H, m, H-10, H-11 and H_e-12), 2.23 (3H, s, H-9), 2.18 (6H, m, H_a-12, H_e-13 and H_a-13), 2.09 (2H, m, H-4 and H-6), 1.96 (1H, m, H-6), 1.55 (1H, m, H-7), 1.21 (3H, d, *J* = 6.4 Hz, H-5), 1.16 (1H, m, H-7), 0.80 (3H, d, *J* = 6.4 Hz, H-5); ^{13}C-NMR (101 MHz, $CDCl_3$) δ 149.5, 148.8 (2C), 145.3, 130.8 (2C), 129.9 (2C), 126.8 (4C), 123.4 (2C), 121.7 (2C), 119.2, 111.4, 110.0, 62.38, 56.8, 55.4, 55.1, 54.5, 53.7, 53.1, 53.0 (2C), 41.3, 37.3, 35.1, 31.2 (2C), 22.8, 18.0, 17.5; LC-ESI-MS (+ve ion mode): 599.3 [M+H]+, purity 96.6% (t_r = 4.473 min).

5-((2-(4-(2-chloro-10H-phenothiazin-10-yl)piperidin-1-yl)ethyl)(methyl)amino)-2-(3,4-dimethoxyphenyl)-2-isopropylpentanenitrile **(4.60b)**

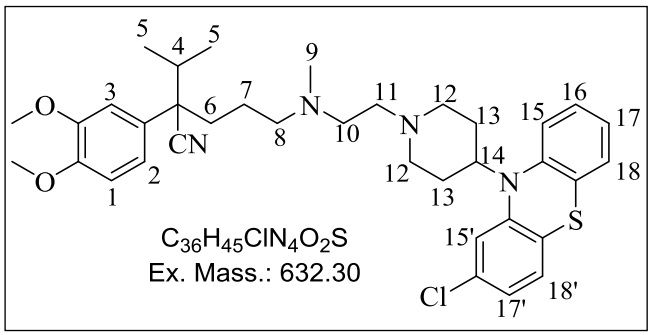

The general method **20** was adopted and 0.379 mmol of **4.15b** was used to obtain **4.60b** as white solid (60 mg, 21%), m.p. 50-52 °C; R_f 0.60 (10% MeOH-DCM); ^{1}H-NMR (400 MHz, CD_3OD) δ 7.21 (1H, dd, *J* = 8.4 and 1.6 Hz, H-2), 7.12-7.18 (3H, m, H-3, H-15' and H-15), 7.09 (1H, d, *J* = 8.4 Hz, H-1), 7.03-7.00 (2H, m, H-17' and H-17), 6.96 (2H, m, H-18 and H-18'), 3.86 (3H, s, OC*H*$_3$), 3.83 (3H, s, OC*H*$_3$), 3.73 (m, 1H, H-14), 2.95 (2H, m, H-8), 2.50-2.42 (6H, m, H-10, H-11 and H_e-12), 2.22 (3H, s, H-9), 2.16 (5H, m, H_a-12, H_e-13 and H-7), 2.07 (2H, m, H_a-13), 1.96 (1H, m, H-6), 1.55 (1H, m, H-7), 1.21 (3H, d, *J* = 6.4 Hz, H-5), 1.16 (1H, m, H-7), 0.80 (3H, d, *J* = 6.4 Hz, H-5); ^{13}C-NMR (101 MHz, $CDCl_3$) δ 149.4, 148.8, 146.4, 144.7. 132..5, 130.7, 129.1, 128.3, 127.6, 127.1, 126.9, 123.8, 123.2, 121.3, 121.1, 121.0, 119.2, 111.6, 111.0, 60.5, 56.8, 55.4, 55.2, 54.5, 53.6, 53.4, 53.1, 53.0, 41.3, 37.3, 35.1, 31.1 (2C), 22.8, 18.0 and 17.6; LC-ESI-MS (+ve ion mode): 633.3 $[M+H]^+$, 634.3 $[M+1+H]^+$ and 635.3 $[M+2+H]^+$, purity 96.2 (t_r = 4.631 min).

5-({2-[4-(10,11-Dihydro-5H-dibenzo[a,d]cycloheptен-5-yl)-piperazin-1-yl]-ethyl}-methyl-amino)-2-(3,4-dimethoxy-phenyl)-2-isopropyl-pentanenitrile **(4.61)**

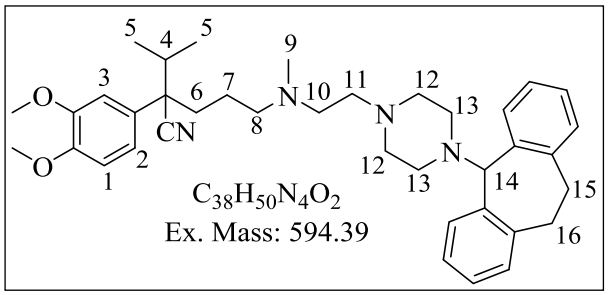

The general method **20** was adopted and 0.360 mmol of **4.25** was used to obtain **4.61** as yellow solid (0.70 g, 34%); R_f 0.25 (10% MeOH-DCM); m.p. 60-61 °C; ^{1}H-NMR (400 MHz, $CDCl_3$) δ 7.25-7.00 (8H, m, ArH), 6.94 (1H, dd, *J* = 8.0 and 2.8 Hz, H-2), 6.89 (1H, d, *J* = 2.4 Hz, H-3), 6.84 (1H, d, *J* = 8.4 Hz, H-1), 4.01 (1H, s, H-14), 4.0 (4H, m, H-15 and H-16), 3.91 (3H, s, OC*H*$_3$), 3.87 (3H, s, OC*H*$_3$), 2.81 (2H, m, H-8), 2.70-2.25 (12H, bm, H-10, H-11, H-12 and H-13), 2.18 (3H, s, H-9), 2.09 (2H, m, H-4 and H-6), 1.89 (1H, m, H-6), 1.54 (1H, m, H-7), 1.23 (1H, m, H-7), 1.19 (3H, d, *J* = 6.4 Hz, H-5), 0.82 (3H, d, *J* = 6.8 Hz, H-5). ^{13}C-NMR (101 MHz, $CDCl_3$) δ 149.1, 148.4, 139.7 (2C), 139.2 (2C), 130.8 (2C), 130.7 (2C), 130.6, 127.7 (2C), 125.5 (2C), 121.4, 118.8, 111.2, 109.8, 57.4, 56.1, 55.9 (2C), 55.7, 54.4, 54.0 (2C), 53.4, 51.5 (2C), 42.1, 37.9, 35.5, 31.8 (2C), 23.2, 19.0 and 18.6; LRMS (EI) *m/z* 595.3 $[M+H]^+$; HPLC purity 93.5% (t_r = 4.04 min).

5-{[2-(Benzhydryl-amino)-ethyl]-methyl-amino}-2-(3,4-dimethoxy-phenyl)-2-isopropyl-pentanenitrile **(4.63)**

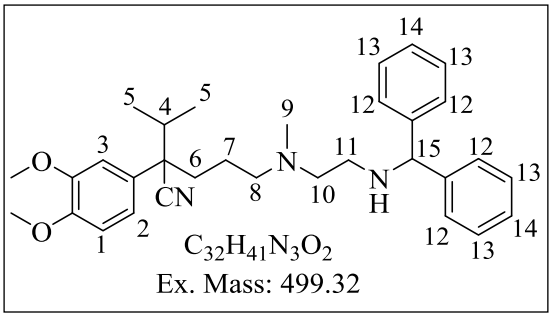

A suspension of **4.56** (1.0 g, 2.84 mmol), benzylhydrylamine **4.62** (0.57 g, 3.12 mmol) and potassium carbonate (1.18 g, 2.8401 mmol) in ethanol 30 ml was heated to reflux for 48 hour. The reaction mixture was cooled to room temperature (25 °C) and filtered. The filtrate was reduced *in vacuo* and residue was purified by column chromatography at 1% MeOH-DCM to get **4.63** as an oil (0.42 g, 30%); R_f 0.45 (5% MeOH-DCM); ^{1}H-NMR (400 MHz, $CDCl_3$) δ 7.43 (4H, m, H-12), 7.30 (4H, t, *J* = 8.0 Hz, H-13), 7.23 (2H, t, *J* = 7.2 Hz, H-14), 6.95 (1H, dd, *J* = 8.4 and 2.0 Hz, H-2), 6.88 (1H, d, *J* = 2.4 Hz, H-3), 6.87 (1H, d, *J* = 8.4 Hz, H-1), 5.32 (1H, s, H-15), 3.91 (3H, s, OC*H*$_3$), 3.90 (3H, s, OC*H*$_3$), 2.68 (2H, t, *J* = 6.0 Hz, H-11), 2.52 (2H, m, H-10), 2.38 (2H, m, H-8), 2.14 (3H, s, H-9), 2.12 (1H, m, H-6), 2.03 (1H, m, H-

4), 1.92 (1H, m, H-6) 1.56 (1H, m, H-7), 1.20 (1H, m, H-7), 1.19 (3H, d, *J* = 6.4 Hz, H-5), 0.75 (3H, d, *J* = 6.8 Hz, H-5). ^{13}C-NMR (101 MHz, $CDCl_3$) δ 149.2, 148.4, 144.1, 128.5 (5C), 127.8 (5C), 127.0 (3C), 118.9, 111.2, 109.8, 67.7, 57.0, 56.7, 56.1, 55.9 (2C), 45.1, 41.5, 38.0, 35.4, 23.0, 18.9 and 18.6; LRMS (EI): *m/z* 500.2 $[M+H]^+$; HPLC purity 94.5% (t_r = 11.52 min).

7.2 Procedures for Biological assays

7.2.1 Antibodies, media and reagents

Ethidium bromide, 3-(4,5-Dimethylthiazol-2-yl)-2,5-diphenyltetrazolium bromide (MTT), saponin, human AB (HAB) serum, fetal calf serum (FCS), tween-80 and apoptosis detection kit were purchased from Sigma (Saint Louis, USA). Components of mycobacteria growth media such as Middlebrook 7H9, Middlebrook7H10, and supplements [albumin, dextraose, catalase (ADC) and oleic acid with ADC (OADC)] were purchased from Becton-Dickinson. [^{3}H]-uridine was obtained from Perkin-Elmer, Inc USA. Carboxyfluorescein diacetate succinimidyl ester (CFSE) was purchased from Life Technologies. IL-1β, TNF-α, IFN-γ primary and secondary antibodies for ELISA were obtained from R&D.

Antibiotic-free RPMI 1640 (Gibco 11875) supplemented with 10% heat-inactivated human AB serum and 200 mM L-glutamine (Lonza BioWhittaker) was used for cell culture. MTT working solutions were prepared in phosphate buffer saline (PBS). MTT is converted into a blue formazan in the presence of live cells. A 10% sodium dodecyl sulphate in a 40% aqueous solution of dimethyl formamide was used as a formazan solubilisation buffer.

7.2.2 Chequerboard synergy assay for combination Antimycobacterial screening

The fractional inhibitory concentration index (FICI) was determined in a 96-well plate format using the microplate alamar blue assay (MABA).[15–17] Briefly, a 10 ml culture of *Mycobacterium tuberculosis* MA[12] was grown to an OD_{600} of 0.6 - 0.7. The culture was then diluted 1:500 in liquid 7H9 medium. Rifampicin (RIF) was prepared to a working concentration of 0.2μM (25x MIC) and Verapamil (VER) and subsequent derivatives were diluted to a working concentration of 3mM (6x MIC).

In two 96-well microtitre plates (plate A and plate B), 50 μl of 7H9 medium was added to all

wells. In plate A, VER (or derivatives) was serially diluted down the plate (B-H) using a multichannel pipette. Similarly, in plate B, Rif was serially diluted across the plate (2-12). Using a multichannel pipette, all 50µl of row 2 in plate B was transferred to row 2 in plate A. This was done for all the rows from plate B to plate A bringing the final volume in plate A to 100µl (chequerboard synergy assay plate). Finally, 50 µl of the 1:500 diluted *M. tuberculosis* cultures was added to all wells. Each chequerboard synergy assay plate included 3 controls: Rif only control in A2-A12; VER/derivatives only in 1B-1H and a media only control in well A1.

The microtitre plates were sealed in a ziplock bag and incubated at 37 °C with a humidifier to prevent evaporation of liquid, for 14 days. On day 14 alamar blue was added to each well (10% of the final volume in each well, thus, 15µl) and the plate was further incubated at 37 °C for 24H, after which observations were made. The lowest concentration of drug that inhibits growth of more than 99% of the bacterial population is considered to be the MIC_{99} (blue well).

The fractional inhibitory concentration (FIC) for each compound was calculated as follows[10] FIC_{RIF} (MIC of RIF in the presence of VER/Derivative)/(MIC of RIF alone). Similarly, the FIC_{VER} for VER/derivative was calculated. The FICI was calculated as FIC_{RIF} plus FIC_{VER}. Synergy was defined by FICI values of ≤ 0.5, antagonism by FICI values of ≥ 4.0, and no interaction by FICI values from 0.5 to 4.0 according to the recommended classification.[18]

7.2.3 MGIT BACTEC 960 assay: For MIC determination against sensitive and resistant strains of *Mtb*.

For drug-resistant strains from South Africa, mycobacterial growth was measured by using mycobacterial growth indicator tubes (MGIT).Mycobacterial inocula were prepared from cultures of all strains grown on Lowenstein Jensen (LJ) slants. Cell suspensions were prepared in saline and the turbidity adjusted to 0.5 McFarland units. A 1:5 dilution of the bacterial suspension was prepared, and 0.5 ml of the suspension was inoculated into MGIT tubes containing test and control compounds. For *mycobacterial* growth evaluation, the MGIT 960 system (Becton Dickinson, Sparks, MD) was used, where *M. tuberculosis* growth is observed through fluorescent changes due to oxygen consumption during mycobacterial growth[19] (Becton Dickinson and Company 1999. Bactec MGIT 960 system user's manual,

catalog number 445876. Becton Dickinson and Company, Franklin Lakes, NJ). One-tenth milliliter of serially diluted compound was added to the MGIT tube containing 7H9 culture medium, with the final DMSO concentration not exceeding 1.2%. Incubation at 37°C was continued in the MGIT system, and the growth units (GU) were monitored daily. For MIC_{99} evaluations, a 1% bacterial control culture was prepared in a drug-free MGIT tube and the MIC_{99} of the compound determined relative to the growth units of the control (GU_400). When the GU of the growth control were 400 and the GU of the drug-containing tube were more than 100, the results were defined as showing resistance, and when the GU of the drug-containing tube were equal to or less than 100, the results were considered to show susceptibility.

7.2.4 Monocytes and bacterial cultures for macrophage evaluations (THP-1 cell line, BCG, Erdman and *Mtb*)

Mycobacterium bovis BCG Connaught strain (ATCC 35745) and *M. tuberculosis* Erdman (ATCC 35801) were grown in suspension with constant gentle rotation in roller bottles containing Middlebrook 7H9 broth supplemented with 10% ADC enrichment and 0.05% Tween 80 (Sigma-Aldrich). Stock vials of BCG and Mtb were prepared from 2 week logarithmic phase cultures and aliquots were frozen at -80 ^{o}C until needed for the different experiments. The number of bacteria (CFU/ml) in the frozen vials was quantified by plating samples on 7H10 Middlebrook agar supplemented with OADC. On the day of macrophage infection, bacteria were thawed and sonicated for l min in a water bath sonicator (W385; Heat Systems Ultrasonics, Farmingdale, NY) to obtain a single-cell suspension and diluted appropriately in complete RPMI 1640 medium.

A leukemic monocyte line (THP-1) obtained from the ATCC (TIB-202) was cultured in RPMI medium supplemented with 200 mM L-glutamine and 10 % FCS and used for cytotoxicity assays.

Human peripheral blood mononuclear cells (PBMCs) stored in liquid nitrogen were used to generate monocyte cultures and to study the effects of drugs on Mtb-specific immunity. These PBMC were obtained from six healthy purified protein derivative (PPD) skin test positive donors following a protocol approved by the Saint Louis University Institutional Review Board. Monocytes were purified from PBMCs by plastic adherence based on the

unique adhesion properties of monocytes/macrophages.[20] Briefly, 1.5×10^5 cells were plated in each well of 96-well round-bottom microtiter plates (Corning Inc., USA). Non-adherent cells were washed off with complete RMPI medium after overnight incubation at 37 °C and 5% CO_2. In general, approximately 10% of the initial number of PBMCs plated were retained as adherent monocytes (>90% $CD14^+$ [data not shown]), which were then cultured for 2-4 days before infection with *M. bovis* BCG or *Mtb* (Erdman).

7.2.5 Method to determine cytotoxicity against THP-1 cell line

THP-1 cells in RPMI with L-glutamine were cultured in round-bottom 96-well plates at a concentration of 1.5 $x10^4$/well. Drugs were added at different concentrations and cultures were incubated at 37 ^oC. After 24 h, MTT assay was performed as described previously. The amount of formazan formation was quantified by measuring the absorbance at 570 nm using an SLT Rainbow plate reader (Tecan, U.S., Inc). Percent cytotoxicity was calculated using relative optical densities as follows: 100 – {100 X [OD with drug/OD without drug]}.

7.2.6 Measuring effects of verapamil, norverapamil and analogs on intracellular *Mtb*

Adherent monocytes were infected with BCG or Mtb for 4 hours at an MOI of 3. Unphagocytosed bacteria were removed by washing three times with warm serum-free RPMI. Infected monocytes were cultured in complete RPMI media with and without drugs for 72h, and then lysed with a 0.2% saponin (Sigma) in RPMI 1640 medium. After cell lysis, residual bacteria were quantified by culturing aliquots on 7H10 media and counting colony forming units (CFU) every week for 3 weeks or using an [^{3}H]-uridine incorporation assay as described previously.[21] Briefly, the uridine incorporation assay was performed by adding 1 μCi [^{3}H]-uridine in 7H9 Middlebrook broth into each well, and incubating plates for another 72 h at 37 °C and 5% CO_2. Bacteria were then harvested on glass fiber filtermats (PerkinElmer Wallac Inc), using a Tomtec Mach III cell harvester 96 (Tomtec Inc., Hamden, CT). Filtermats were air dried, scintillation fluid added, and mycobacterial incorporation of tritiated uridine was quantified using a Microbeta scintillation counter (PerkinElmer Wallac Inc.). Mycobacterial growth inhibition was determined using the following formula: percent inhibition = 100 − [100 × (dpm or CFU in the drug-treated cultures/dpm or CFU in the untreated cultures)].

7.2.6 CFSE-based flow cytometry assay

A CFSE-based flow cytometry assay was performed as described previously using *Mtb*-whole cell lysate (WL) at a final concentration of 10 μg/ml to stimulate *Mtb*-specific T cells during 7 days of culture.[21,22] Flow-cytometric acquisition was performed by use of a FACSCalibur (BD) instrument, and analyses were done using CellQuest (version 3.3; BD) and FlowJo (version 6.2.1; Tree Star) softwares. A minimum of 10,000 $CD3^+$ events were acquired. The proliferating cells were identified as populations with decreased mean FL1 fluorescence intensity and are labeled as CFSE-low ($CFSE^{lo}$). The total number of viable cells recovered was determined by counting cell aliquots resuspended in trypan blue using hemocytometer and light microscope.

7.2.7 Ethidium bromide assay

Efflux pump activity was measured based on methods described previously.[23] Conditions for this assay were first optimized using in vitro BCG cultures. Briefly, the turbidity of logarithmic phase cultures of BCG in 7H9 Middlebrook broth was adjusted to the standard turbidity of McFarland 0.5. Aliquots of 100 μl were transferred into three sets of 2 ml sarstedt tubes. Ethidium bromide and verapamil were added (1ug/ml and 250 μg/ml, respectively) and cultures were incubated at room temperature (25 °C) for 1h. Bacteria were pelleted by centrifugation, washed once with 1 ml PBS, and resuspended in PBS with 0.4% glucose with and without various efflux pump inhibitors or analogs. These cultures were incubated at 37 ^oC for 1 hour. Bacteria suspensions were sonicated for 15 seconds in a water bath sonicator and aliquots were transferred to a round-bottom 96-well plate. Flow-cytometric acquisition was performed using a Guava easy Cyte instrument (Guava Technology, Hayward, CA), and analyses were done using FlowJo (version 6.2.1; Tree Star) software. A minimum of 5,000 events were acquired.

References

(1) Zhongxu Ren, Bo-Liang Deng, Jennifer Riggs-Sauthier, M. H. Oligomer-Calcium Channel Blocker Conjugates. PCT/ US 2008/ 010385.

(2) Falk, A.; Göderz, A.-L.; Schmalz, H.-G. Enantioselective Nickel-Catalyzed Hydrocyanation of Vinylarenes Using Chiral Phosphine-Phosphite Ligands and TMS-CN as a Source of HCN. *Angew. Chem. Int. Ed. Engl.* **2013**, *52*, 1576–1580.

(3) Jo, M.; Palma, P. N. Catechol- O -Methyltransferase and Its Inhibitors in Parkinson ' S Disease. *CNS Drug Reviews* **2007**, *13*, 352–379.

(4) Wang, C.; Wang, T.; Zhou, N.; Pan, X.-Y.; He, H.-Z. Design, Synthesis and Evaluation of 9-Hydroxy-7H-furo[3,2-G]chromen-7-One Derivatives as New Potential Vasodilatory Agents. *J. Asian Nat. Prod. Res.* **2014**, *16*, 304–311.

(5) Guin, J.; Varseev, G.; List, B. Catalytic Asymmetric Protonation of Silyl Ketene Imines. *J. Am. Chem. Soc.* **2013**, *135,* 2100−2103

(6) Redko, B.; Albeck, A.; Gellerman, G. Facile Synthesis and Antitumor Activity of Novel N(9) Methylated AHMA Analogs. *New J. Chem.* **2012**, *36*, 2188.

(7) Sawant, R. T.; Waghmode, S. B. Synthesis of N -Boc-C1 Vinyl Tetrahydroisoquinoline via Zn-Mediated Intramolecular Cyclization of N -Boc Protected Iodo Acetonide. *Synth. Commun.* **2011**, *41*, 2385–2391.

(8) Chen, M.; Ren, Z.-H.; Wang, Y.-Y.; Guan, Z.-H. Palladium-Catalyzed Oxidative Carbonylation of Aromatic C-H Bonds of N-Alkylanilines with CO and Alcohols for the Synthesis of O-Aminobenzoates. *J. Org. Chem.* **2015**, *80*, 1258–1263.

(9) Jensen, B. L.; Slobodzian, S. V. A Concise Synthesis of 1-Substituted-2-Tetralones by Selective Diol Dehydration Leading to Ketone Transposition. *Tetrahedron Lett.* **2000**, *41*, 6029–6033.

(10) Prasomsri, T.; Galiasso Tailleur, R. E.; Alvarez, W. E.; Sooknoi, T.; Resasco, D. E. Conversion of 1- and 2-Tetralone Over HY Zeolite. *Catal. Letters* **2010**, *135*, 226–232.

(11) Teodori, E.; Dei, S.; Romanelli, M.; Scapecchi, S.; Gualtieri, F.; Budriesi, R.; Chiarini, A.; Lemoine, H.; Mannhold, R. Synthesis and Pharmacological Evaluation of Verapamil Analogs with Restricted Molecular Flexibility. *Eur. J. Med. Chem.* **1994**, *29*, 139–148.

(12) Kubota, K.; Kurebayashi, H.; Miyachi, H.; Tobe, M.; Onishi, M.; Isobe, Y. Synthesis and Structure-Activity Relationships of Phenothiazine Carboxylic Acids Having Pyrimidine-Dione as Novel Histamine H(1) Antagonists. *Bioorg. Med. Chem. Lett.* **2009**, *19*, 2766–2771.

(13) Niaz, H.; Kashtoh, H.; Khan, J.; Khan, A.; Wahab, A.-T.-; Alam, M. T.; Khan, K. M.; Perveen, S.; Choudhary, M. I. Synthesis of Diethyl 4-Substituted-2,6-Dimethyl-1,4-

Dihydropyridine-3,5-Dicarboxylates as a New Series of Inhibitors against Yeast A-Glucosidase. *Eur. J. Med. Chem.* **2015**, *95*, 199–209.

(14) Iwanami, M.; Shibanuma, T.; Fujimoto, M.; Kawai, R.; Tamazawa, K.; Takenaka, T.; Takahashi, K.; Murakami, M. Synthesis of New Water-Soluble Dihydropyridine Vasodilators. *Chem. Pharm. Bull. (Tokyo).* **1979**, *27*, 1426–1440.

(15) Ramón-García, S.; Ng, C.; Anderson, H.; Chao, J. D.; Zheng, X.; Pfeifer, T.; Av-Gay, Y.; Roberge, M.; Thompson, C. J. Synergistic Drug Combinations for Tuberculosis Therapy Identified by a Novel High-Throughput Screen. *Antimicrob. Agents Chemother.* **2011**, *55*, 3861–3869.

(16) Collins, L. A.; Franzblau, S. G. Microplate Alamar Blue Assay versus BACTEC 460 System for High-Throughput Screening of Compounds against *Mycobacterium tuberculosis* and Mycobacterium Avium. *Antimicrob. Agents Chemother.* **1997**, *41*, 1004–1009.

(17) Collins, L. A.; Torrero, M. N.; Franzblau, S. G. Green Fluorescent Protein Reporter Microplate Assay for High-Throughput Screening of Compounds against *Mycobacterium tuberculosis*. *Antimicrob. Agents Chemother.***1998**, *42*, 344–347.

(18) Odds, F. C. Synergy, Antagonism, and What the Chequerboard Puts between Them. *J. Antimicrob. Chemother.* **2003**, *52*, 1.

(19) Ru, S.; Pfyffer, G. E.; Casal, M.; Chadwick, M.; Siddiqi, S. Multicenter Laboratory Validation of the BACTEC MGIT 960 Technique for Testing Susceptibilities of *Mycobacterium tuberculosis* to Classical Second-Line Drugs and Newer Antimicrobials. *J. Clin. Microbiol.* **2006**, *44*, 688–692.

(20) Worku, S.; Hoft, D. F. Differential Effects of Control and Antigen-Specific T Cells on Intracellular Mycobacterial Growth. *Infection and immunity* **2003**, *71*, 1763–1773.

(21) Hoft, D. F.; Blazevic, A.; Abate, G.; Hanekom, W. A.; Kaplan, G.; Soler, H.; Weichold, F.; Geiter, L.; Sadoff, J. C.; Horwitz, M. A. A New Recombinant BCG Vaccine Safely Induces Significantly Enhanced TB-Specific Immunity in Human Volunteers. *J. Infect. Dis.* **2009**, *198*, 1491–1501.

(22) Abate, G.; Eslick, J.; Newman, F. K.; Frey, S. E.; Belshe, R. B.; Monath, T. P.; Hoft, D. F. Flow-Cytometric Detection of Vaccinia-Induced T Cells Capable of Antigen-Specific Expansion and Effector Functions. *J. Infect. Dis.* **2005**, *63110*.

(23) Paixão, L.; Rodrigues, L.; Couto, I.; Martins, M.; Fernandes, P.; de Carvalho, C. R.; Monteiro, G. A; Sansonetty, F.; Amaral, L.; Viveiros, M. Fluorometric Determination of Ethidium Bromide Efflux Kinetics in Escherichia Coli. *J. Biol. Eng.* **2009**, *3*, 18.